JOURNAL OF CHROMATOGRAPHY

INTERNATIONAL JOURNAL ON CHROMATOGRAPHY, ELECTROPHORESIS AND RELATED METHODS

ELSEVIER

CONTENTS

Contents (continued)

(Continued overleaf)

Contents (continued)

Quantitative Gas Chromatography for Laboratory Analyses and On-line Process Control

by G. GUIOCHON and C.L. GUILLEMIN

(Journal of Chromatography Library, 42)

This is a book which no chemical analyst should be without!

It explains how quantitative gas chromatography can - or should - be used for accurate and precise analysis. All the problems involved in the achievement of quantitative analysis by GC are covered, whether in the research lab, the routine analysis lab or in process control.

The discussion of the theoretical background is restricted to essentials. It is presented in a way that is simple enough to be understood by all analytical chemists, while being complete and up-to-date.

Extensive and detailed descriptions are given of the various steps involved in the derivation of precise and accurate data. This starts with the selection of the instrumentation and column, continues with the choice of optimum experimental conditions, then calibration and ends with the use of correct procedures for data acquisition and calculations.

Finally, there is almost always a way to reduce errors and an entire chapter deals with this single issue. Numerous examples are provided.

A lexicon explaining the most important chromatographic terms and a detailed index complete the book.

This is a book which should be on the library shelf of all universities, instrument companies and any laboratory and plant where gas chromatography is used.

A brochure describing the contents of this book in detail is available on request from the publisher

JOURNAL

of

CHROMATOGRAPHY

EFFECT OF RANDOM NOISE AND PEAK ASYMMETRY ON THE PRECISION AND ACCURACY OF MEASUREMENTS OF THE COLUMN EFFICIENCY IN CHROMATOGRAPHY

JENNIFER V. H. SCHUDEL and GEORGES GUIOCHON*

Department of Chemistry, University of Tennessee, 575 Buehler Hall, Knoxville, TN 37996-1600 (U.S.A.)
and Oak Ridge National Laboratory, Analytical Chemistry Division, Oak Ridge, TN 37831-6120 (U.S.A.)
(First received May 16th, 1988; revised manuscript received August 22nd, 1988)

SUMMARY

The reproducibility and bias of the measurement of column efficiency from chromatographic peaks were studied. Peaks of various signal-to-noise and τ/σ ratios, a measure of the asymmetry of a peak, were generated by computer simulation. A range of experimental peaks were also analyzed. Column efficiencies for a variety of peaks were computer calculated, using eight commonly employed methods. The results are compared.

The moment method gave the best results in almost all instances of noisy or skewed peaks, except in the simulated noisy cases with a signal-to-noise ratio of less than 40, and seems to be the most accurate method for the measurement of column efficiency for those with access to a computer for calculations. The most common method, the half-height method, surprisingly seems fairly sensitive to noise fluctuations, and did not perform as well as some of the other methods, including the 3σ, 4σ and 5σ methods, in the most noisy instances.

INTRODUCTION

There has been a considerable amount of research reported during the last 10 years regarding column efficiency in high-performance liquid chromatography (HPLC) and the influence of many experimental parameters on column performance. It is therefore remarkable that the literature contains so few reports on the precision or accuracy of these determinations, and that only a small number of publications contain any figures on the reproducibility of the data reported[1]. The few discussions published that do deal with the advantages and inconveniences of the various methods of determining column efficiency and height equivalent to a theoretical plate (HETP), contain almost no reference to the precision of the methods considered.

This is not a very good sign of the importance placed on these investigations by the scientific community; only important, relevant data have to be precise and accurate. We decided, although belatedly, that it would be useful to study the error generation process in the determination of the plate number and HETP.

The reproducibility and bias of calculated column efficiency values are the result of the influence of many variables, such as pump or temperature fluctuations, detector response and the choice of the calculation or measurement method; the last parameter is one that is very often overlooked. The effect that this choice has on the calculated efficiency values obtained from peaks deviating from the ideal Gaussian profile or those having noisy baselines, as commonly occurs in chromatography, will be discussed here.

Historically[2-4], the calculation of column efficiencies has involved the manual measurement of retention times and peak widths at various peak heights. The analyst, manually analyzing peaks, unconsciously applies averaging procedures in order to find the average signal for the baseline and use it for making determinations. However, these procedures are usually not understood, not reported and probably not linear. The systematic or indeterminate errors introduced by the manual measurement of peak efficiencies have been discussed previously[5]. More recently[6-8], however, very sophisticated electronic integrators and procedures of data acquisition and handling by computers have begun to replace the manual methods. However, with skewed peak profiles or noisy baselines, there is still a possibility of errors in these measurements that may introduce biases into the calculation of the column efficiency. Also, in some earlier work the effects of sampling parameters on the calculation of peak areas and retention times were studied[9-12].

In this work, the effect of the choice of the measurement method on the value of the column efficiency was investigated. The reproducibility and bias of efficiency values obtained by computer simulation using eight different methods were studied for a wide variety of experimental conditions. The results obtained with some experimental chromatographic peaks are compared.

THEORETICAL

The origin and definition of the concept of theoretical plates in chromatography are related to the assumption of a Gaussian profile for the elution band of a very small, narrow, sample plug. A Gaussian profile can be obtained from either the derivation of the elution profile by means of the Craig model, for a large number of plates, or the integration of the mass balance of chromatography, assuming a linear isotherm. The elution profile is then given by

$$y = \frac{A}{\sigma} \exp \left[\frac{-(t - t_R)^2}{2\sigma^2} \right] \tag{1}$$

where y is the solute concentration in the mobile phase at time t, t_R is the retention time (elution time of the peak maximum), A is the peak area and σ is the standard deviation of the peak.

Although the elution peaks observed experimentally are rarely truly Gaussian, this model is the most convenient and remains very useful in discussing problems related to column performance. Most studies of column efficiency use this model while making some minor corrections to account for moderate band asymmetry. The column efficiency is related to the relative thickness of the peak, i.e., to the ratio of the retention time to the standard deviation. The theoretical plate number is the most popular parameter characterizing the column efficiency and is defined as

$$N = \frac{t_R^2}{\sigma^2} \tag{2}$$

Measuring the column efficiency hence requires an estimate of the band variance (σ^2). This can be done by relating the standard deviation of the peak either to its width at some intermediate height, or to its area, using eqn. 1 in both instances.

The band width at a fraction x of the peak height is given by

$$W_x = 2\sigma\sqrt{2\log(1/x)} \tag{3}$$

Depending on whether one is interested in the properties of the nearly symmetrical top part of the band or in those of its tail, one will choose a large or a small value for x.

There are two other methods for estimating the band variance which are not dependent on any part of the profile. The first determines the peak area and the other uses the second central moment of the peak.

If y_0 is the peak height, the peak area is given by

$$A = \sigma y_0 \sqrt{2\pi} \tag{4}$$

The peak area is conveniently measured with an electronic integrator. This method has been extended to non-Gaussian profiles. It then becomes incorrect, however, as its basis is the Gaussian profile defined by eqn. 1.

The second method employs an alternative method for the determination of the variance, which is based on the statistical properties of distributions. The peak profile is the distribution of the residence times of the sample molecules in the column. As the signal rapidly becomes very small at times far from the retention time, the following integrals are finite:

$$\mu_0 = \int_0^\infty f(t)\, dt \tag{5}$$

$$\mu_1 = \int_0^\infty tf(t)\, dt \tag{6}$$

$$\mu_2 = \int_0^\infty (t - \mu_1)^2 f(t)\, dt \tag{7}$$

where μ_0, μ_1 and μ_2 are the zeroth, first and second central moments of the residence time distribution, respectively. The peak area is equal to the zeroth moment and the retention time or time of the signal mass center is directly related to the first moment. The second central moment is proportional to the variance of the distribution. Between these moments and the classical parameters of chromatography, we have the following relationships:

TABLE I

VARIOUS PEAK HEIGHTS AND CONSTANTS FOR COLUMN EFFICIENCY CALCULATIONS

Method	Peak height (%)	a
2σ (inflection)	60.7	4
Half-height	50.0	5.54
3σ	32.4	9
4σ	13.4	16
5σ	4.4	25

$$t_R = \frac{\mu_1}{\mu_0} \tag{8}$$

$$\sigma^2 = \frac{\mu_2}{\mu_0} \tag{9}$$

thus providing an independent method of determining the retention time and the variance of the distribution. This definition is valid for any distribution, *i.e.*, also for asymmetric peaks. The definition of the plate number still remains based on the assumption that the peak profile is Gaussian, however, and its extension to non-symmetrical peaks is merely empirical.

METHODS OF CALCULATION

We used eight different methods for the determination of the plate number, which we found described and used in the literature. Some of these methods have been used very frequently, others only exceptionally.

Five of these methods are based on the use of the band width measured at different relative heights to estimate the variance of the peak (see eqn. 3), namely the width at half-height and the widths at the relative heights where the band width of a Gaussian peak would be equal to 2σ, 3σ, 4σ and 5σ, respectively. The corresponding values of the relative peak heights are reported in Table I. All of these methods use the retention time of the peak maximum. The sixth method is based on the use of the peak area (see eqn. 4) to derive the standard deviation. Although they may be used, and indeed are used by many workers to account for the column efficiencies obtained with asymmetric bands, these six definitions assume that the bands are Gaussian and, therefore, should not be used when the peak asymmetry is significant.

The seventh method used to determine the column efficiency is based on the ratio of the first and second moments. The last method is asymmetry-based[8,13], obtained from the Foley–Dorsey equation[14]. A perpendicular is dropped from the apex of the peak to the baseline and the base width at 10% of the peak height, *i.e.*, $W_{0.1}$, is measured, A/B is the ratio of the distances from the perpendicular to the rear side and the front side of the peak, along the 10% horizontal line (see Fig. 1). The ratio of the retention time of the peak maximum to the width at 10% of the peak height and the ratio A/B are combined in a semi-empirical expression for the plate number:

$$N = \frac{41.7 \, (t_R/W_{0.1})^2}{(A/B) + 1.25} \tag{10}$$
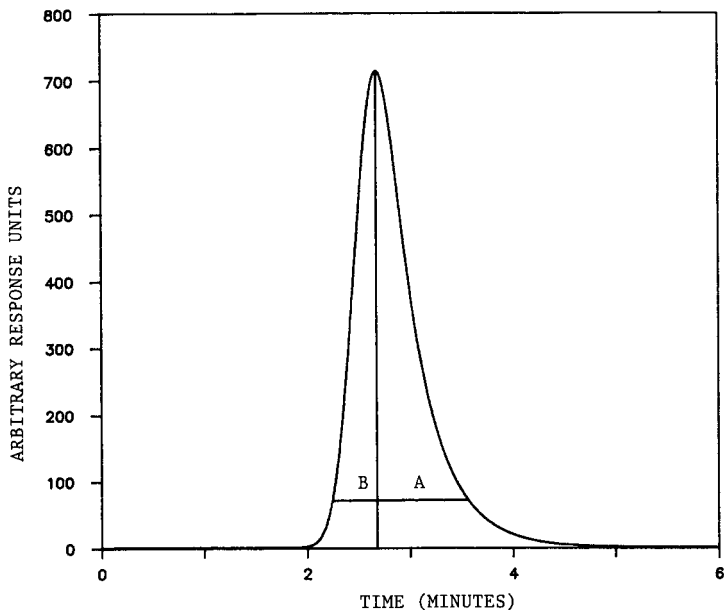
Fig. 1. Determination of peak asymmetry (A/B) at 10% of the peak height for the asymmetry-based method.

A comparison between the results obtained using these eight different methods, and between the errors made in these determinations, permits us to rank their performances.

THE SIMULATION

We simulated the procedure of data acquisition and handling used to determine the column efficiency with these different methods. A signal is generated and a noisy or drifting sequence is added to it to simulate a chromatogram. Then the various algorithms are applied for digital signal acquisition, storage and processing in order to determine the retention time, peak areas and band widths at different heights. The end results are compared to the known values incorporated in the original signal. The repetition of the entire procedure, with the same original signal but different noise sequences, gives the reproducibility of the procedure. Thus, an average bias and a standard deviation can be derived to characterize the performance of a method of column efficiency measurement. The procedure is repeated with the same signal characteristics, using the different methods.

The analog-to-digital (A/D) conversion of the signal is done by selecting the value of the signal generated, at a certain frequency, usually 5 Hz. This duplicates the operation of the most common A/D converters used in HPLC. The analog signal is thus replaced with the set of signal values at the edges of a time grid, kdt. It is important that this time grid be shifted randomly with respect to the true signal maximum, in order to avoid the systematic reproduction of artifacts[3,10]. There is no reason for a measurement of the signal to occur systematically at the peak maximum, or at the same time away from it. To perform a random shift, the initial time value of each

simulated peak is randomly shifted from the origin of the function by an interval equal to the product of 0.01, the standard deviation and a random integer between − 10 and + 10 (ref. 10). As the interval between points is constant on each chromatogram, this shift in the time of the origin of the signal results in a shift of the calculated peak points along the curve.

The retention times, which are required by all methods except the moment method, are obtained as follows. The upper 2–4% of the peak points, around the peak maximum, are fitted to a second-order polynomial. The coordinates of the maximum of this parabola yield the best estimates of the retention time and the peak height. As even strongly tailing peaks are usually fairly symmetrical near the peak maximum[15], the results should not be significantly altered for an asymmetric peak, except in extreme cases. This procedure permits the elimination of noise spikes or other fluctuations from being considered as potential maxima.

The many types of chromatographic peaks analyzed were computer generated using a PASCAL program. The peak definitions, which include the retention time, the standard deviation, the peak area, the length of the chromatogram, the signal-to-noise ratio (S/N), the random grid shift value, the time constant for the exponentially modified Gaussian[16,17], τ, and the data acquisition rate are read from an input file. The ordinate values of the peak are then calculated at the regularly spaced intervals of the time grid. In order not to insert a bias into the calculations, we chose a sufficiently high point density of approximately 20 points per standard deviation[10]. Noise is generated randomly by the program and added to each data point. Various retention times were used in order to show if any bias was introduced by increasing retention times.

The peak simulation and evaluation programs were run on a VAX cluster running VAX/VMS version 4.6. Each chromatogram is generated ten times and the same calculation program is run on all of them. The mean value of the column efficiencies is calculated for all measurement methods. The reproducibility is defined as the relative standard deviation of the ten measurements and the bias is the difference between the mean and true values. It should be emphasized that each peak is completely defined by the program user and, hence, the true value of the column efficiency is known. The reproducibility and bias of the calculations were determined using the Lotus Symphony spreadsheet program.

EXPERIMENTAL

Some experimental data were collected and analyzed. The system included a 10 cm × 4.6 mm I.D. HPLC column packed with 10-μm ODS particles and the mobile phase was methanol–water (70:30, v/v). The sample used was based on a standard HPLC test mixture and included uracil, ethylbenzene, toluene and benzaldehyde.

Peaks obtained under a variety of experimental conditions were acquired using a Spectra-Physics 4270 computing integrator connected to an IBM PC-AT running Autolab software. The experimental data were then uploaded to the UTCC VAX cluster for use by the efficiency calculation program.

RESULTS AND DISCUSSION

The eight methods were compared by computer evaluation of a series of noisy

TABLE II

PEAK DEFINITION SUMMARY

Case	Retention time (s)	σ (s)	S/N	τ	Peak area
A	200	5–15	$25-10^6$	0–25	30 000
B	1000	5–15	$25-10^6$	0	30 000
C	2500	5–15	$25-10^6$	0	30 000

Gaussian or EMG peaks generated for the analysis. The aim was to use band profiles that are representative of experimentally observed chromatographic peaks. The definitions of the simulated profiles are summarized in Table II.

The primary objective of the comparison was the determination of the accuracy of each method, relative to the "true" or "correct" efficiency value, as defined above, and the reproducibility in the presence of increasing noise or peak asymmetry.

When dealing with noisy Gaussian peaks, the true efficiency value is derived from eqn. 1, as both the retention time and the peak variance are well defined. With tailing peaks, on the other hand, the result of the moment method, applied to noiseless peaks, is assumed to be the correct value.

A systematic study of simulated noisy peaks was conducted. For the entire range of noise values and retention times, the moment method proves to have the lowest bias and the best reproducibility of the eight methods. At S/N in excess of 100, the bias and
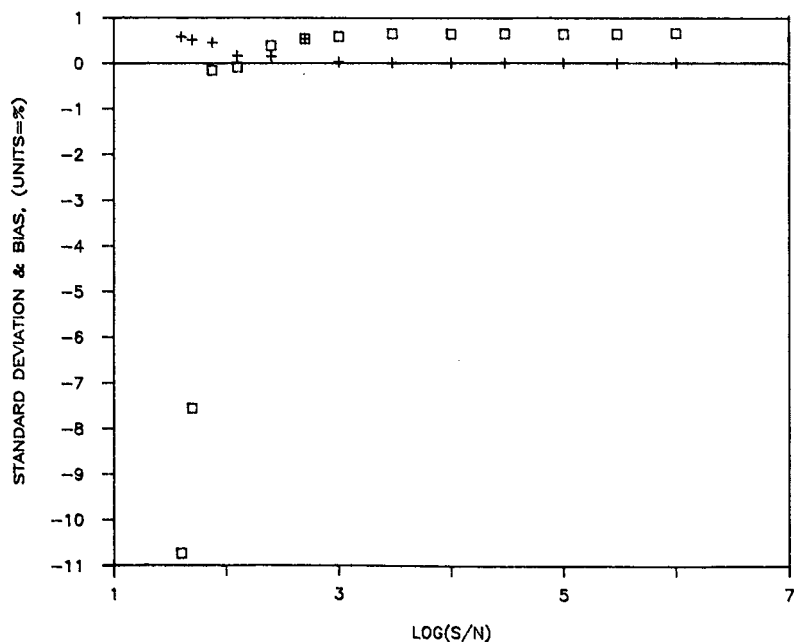
Fig. 2. Standard deviation (+) and bias ($\square$) vs. log (S/N) using the moment method, $\sigma = 15$, $t_r = 200$ s.
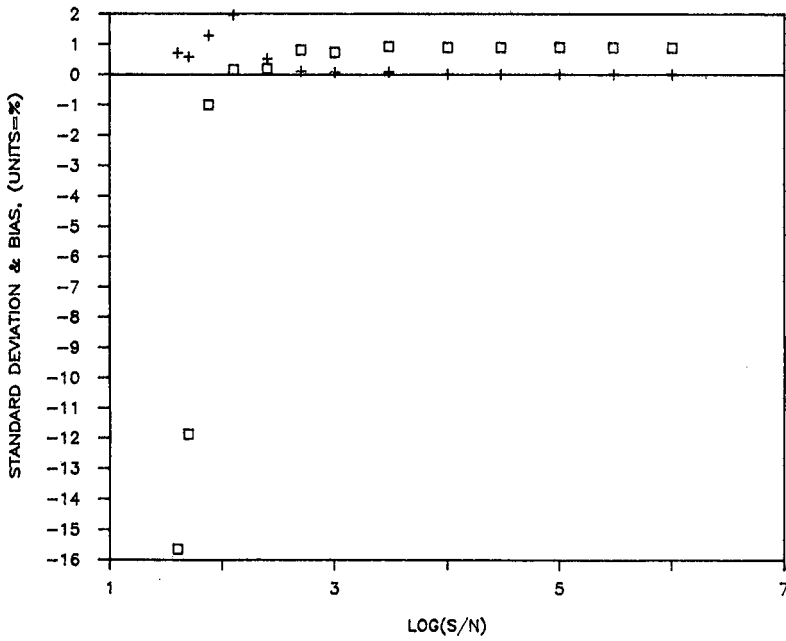
Fig. 3. Standard deviation ($+$) and bias ($\square$) *vs.* log (S/N) using the moment method, $\sigma = 10$, $t_r = 200$ s.
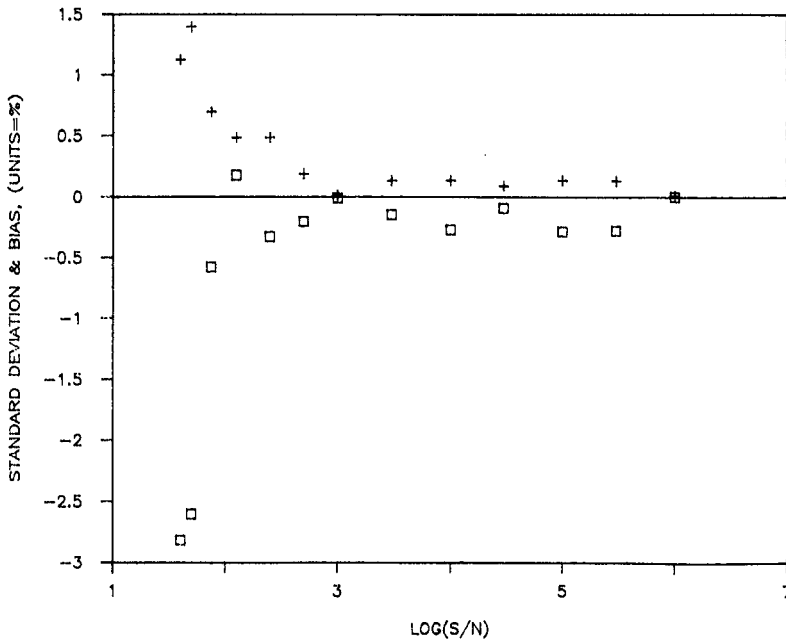
Fig. 4. Standard deviation ($+$) and bias ($\square$) *vs.* log (S/N) using the 3σ method, $\sigma = 15$, $t_r = 200$ s.

standard deviation for this method are independent of the noise and remain close to 0.5% (bias) and less than 0.1% (precision), as shown in Figs. 2 and 3. Only at S/N less than 500 does the standard deviation begin to increase slightly. The bias is low and consistent over the entire range of retention times and peak sigma values. Some slight negative deviations in the bias appear at an S/N of 50. This is probably the result of increased difficulty in the determination of the peak thresholds.

The other calculation methods, with the exception of the peak height–area method, give poorer reproducibility and larger bias, even in the least noisy instances, when the peaks are defined to be very narrow. This may be the result of using too few data points per peak sigma value for the calculation of the polynomial fits. However, the moment method seems to be unaffected by this.

For the wider peaks, the general trend is that the 2σ and the half-height methods give consistent results, fairly low standard deviations of the plate number and bias until an S/N of *ca.* 1000, whereas the 3σ, 4σ and 5σ methods give results that are just about indistinguishable at S/N of 500 or larger. For lower S/N values, the standard deviation of the 5σ method increases rapidly whereas the 3σ method seems to follow the results of the moment most closely (see Fig. 4).

In some instances, when S/N is less than 50, the subroutine of the computer program which implements the 5σ method is no longer able to compute an efficiency value, owing to the increased difficulty in determining the peak widths at very low peak heights in the presence of a large amount of noise. Surprisingly, the half-height method seems sensitive to noise fluctuations. This method shows consistently higher and less consistent standard deviations of the plate number and biases when compared with the moment or even the 3σ method, as shown in Fig. 5.
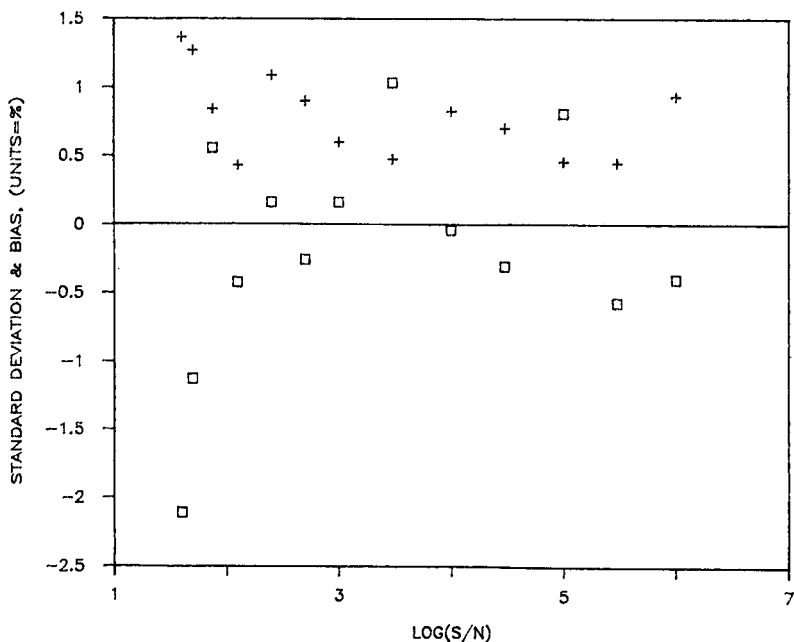
Fig. 5. Standard deviation (+) and bias (□) *vs.* log (S/N) using the half-height method, $\sigma = 15$, $t_r = 200$ s.
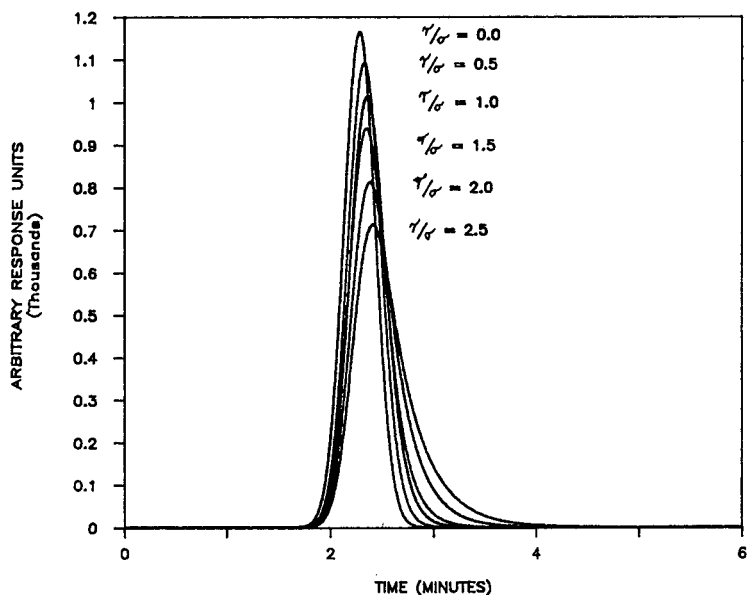
Fig. 6. Variation of peak shape with various τ/σ ratios.

In the study of the asymmetric profiles, the τ/σ ratio is varied from 0.0 to 2.5 (see Fig. 6). The peak standard deviation is held constant at 10 s while the value of τ is varied. In the least skewed case, $\tau = 0$. Increasing the value of τ result in an increase in the amount of tailing in the simulated peaks. The range of τ/σ valves investigated seems to reveal the marked difference between the results of the different calculation methods very well. It is generally observed that the methods that use peak width measurements from the upper portion of the peak profiles give efficiency values that are much higher than those obtained by the moment method[8]. The values obtained by the 5σ and the asymmetry-based methods seem to follow the results of the moment method most closely (see Fig. 7 and ref. 8). This is normal as they can take into account the effect of a larger band width closer to the baseline.

For the computer evaluation of skewed chromatographic peaks, the moment method of calculation is, consistently, the best method. However, as it is not always

TABLE III

EXPERIMENTAL RESULTS

S/N	Relative standard deviation (%)	Method
3000–200	0.25–1.60	Moment
3000–200	1.28–2.71	3σ
3000–200	1.76–3.40	Half-height
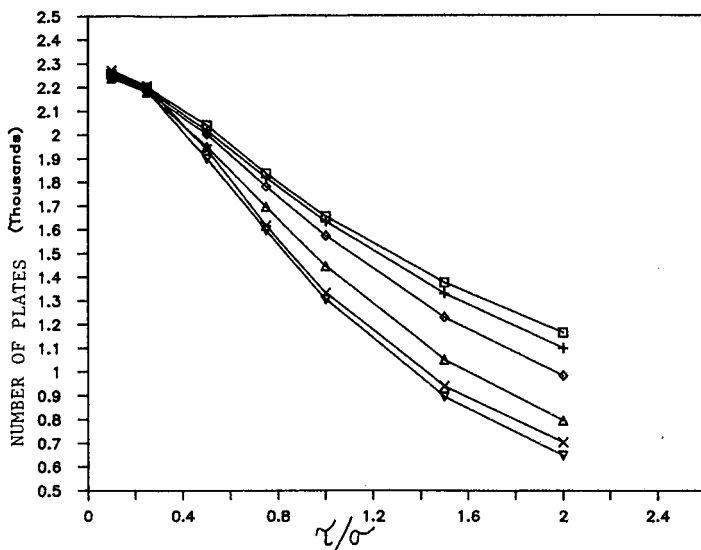
Fig. 7. Effect of the peak asymmetry on calculated column efficiency (number of theoretical plates *vs.* τ/σ). Method: □, inflection; +, half-height; ◇, 3σ; △, 5σ; ×, asymmetry; ▽, moment.

possible to use a computer for data acquisition, and as the method of choice for manual methods needs to be sensitive to peak asymmetry, the 5σ or the asymmetry-based methods seem to be the best suited for this application.

The results of the efficiency calculation program for the experimentally generated peaks followed the same trends as were shown for the study of simulated chromatographic peaks. A summary of the results is given in Table III. Again, the moment method proves to be the best efficiency calculation method. The 3σ, 4σ and 5σ methods give very similar results down to the lowest S/N values. For this set of experimental peaks, the 5σ method ceased to compute efficiency values at S/N = 200. The half-height method, again, was found to be consistently less precise than the 3σ, 4σ and 5σ methods at higher S/N but it was able to continue computing even when S/N became small.

CONCLUSION

Because the occurrence of peak tailing and random noise is a reality for chromatographers, it is critical that a measurement method gives an accurate value for the column efficiency. This study has determined that the choice of the measurement or calculation method has a major impact on the precision and accuracy of the values obtained. As a result, it is important that all efficiency values be accompanied by a statement of the conditions under which the value is obtained, and the relative accuracy of the calculation method used.

Throughout this work there has been a common result for both the skewed and the noisy profiles; the moment method of calculating column efficiencies from

chromatographic peaks gives the best precision and accuracy. This is not a difficult method to employ with a small computer or even a computing integrator for the calculations. However, if the measurement must be made manually, the 4σ or 5σ method seems to give adequate values for peaks with a moderate to high S/N ratio and skew. Peaks with very high noise levels should probably be measured by the 3σ method or, perhaps, continue to be measured by the standby, half-height method. Worse reproducibility and accuracy should be expected from efficiency determinations when using these methods with noisy peaks.

Finally, it should be emphasized that the determination of column efficiency from signals acquired by a computer is precise and accurate only if proper programs are used. These programs should average out the noise contributions in the calculation of the retention times, the standard deviations and the peak moments. These programs should not simply mimic the behavior of the analyst working on the chromatogram. In that event they do not make good use of the computer possibilities and replicate human errors needlessly.

REFERENCES

1 B. L. Karger, H. Barth, E. Dallmeier, G. Courtois and E. Keller, *J. Chromatogr.*, 83 (1973) 289.
2 D. Ball, W. Harris and H. Habgood, *Anal. Chem.*, 40 (1968) 1113.
3 M. Delaney, *Analyst (London)*, 107 (1982) 606.
4 D. Ball, W. Harris and H. Habgood, *Anal. Chem.*, 40 (1968) 129.
5 D. Ball, W. Harris and H. Habgood, *Sep. Sci.*, 2 (1967) 81.
6 S. Chesler and S. Cram, *Anal. Chem.*, 43 (1971) 1922.
7 E. Grushka, M. Myers, P. Schettler and J. C. Giddings, *Anal. Chem.*, 41 (1969) 889.
8 B. Bidlingmeyer and F. V. Warren, Jr., *Anal. Chem.*, 56 (1984) 1583A.
9 M. Goedert and G. Guiochon, *Anal. Chem.*, 42 (1970) 962.
10 M. Goedert and G. Guiochon, *Chromatographia*, 6 (1973) 76.
11 M. Goedert and G. Guiochon, *J. Chromatogr. Sci.*, 2 (1973) 326.
12 B. Rodgers and J. Oberholtzer, *Anal. Chem.*, 41 (1969) 1234.
13 J. Foley and J. Dorsey, *Anal. Chem.*, 55 (1983) 730.
14 J. Foley and J. Dorsey, *J. Chromatogr. Sci.*, 22 (1973) 40.
15 M. Goedert and G. Guiochon, *Chromatographia*, 6 (1973) 39.
16 H. Yau, *Anal. Chem.*, 49 (1977) 395.
17 A. Anderson, T. Gibb and A. Littlewood, *J. Chromatogr. Sci.*, 8 (1970) 640.

CHROM. 20 940

CO-OPERATIVE CLUSTER MODEL FOR MULTIVALENT AFFINITY INTERACTIONS INVOLVING RIGID MATRICES

ROBERT J. YON

School of Biological Sciences and Environmental Health, Thames Polytechnic, Wellington Street, London SE18 6PF (U.K.)

SUMMARY

A rapid-equilibrium model of affinity partitioning of multi-site proteins is described, that applies when long-range translatory movement of matrix-ligand groups is prevented by a rigid matrix. Two essential postulates are made: (1) the matrix ligands are distributed singly or in clusters within spherical bounds of the size of the protein molecule, and may be treated as a Poisson distribution; (2) due to the proximity of matrix ligands, binding of a protein molecule to a cluster is highly co-operative. Equations are derived that allow the predicted partitioning and chromatographic behaviour of this model to be examined and its properties described. Published data on the interaction of aldolase and phosphocellulose are re-interpreted in terms of the new theory.

INTRODUCTION

Early theoretical treatments of affinity chromatography were formulated on the assumption of a single interaction between protein and matrix-ligand, and were consequently applicable only to monomeric proteins or when the matrix-ligand was highly diluted[1–4]. Since then the theory has been adapted to the case of multivalency, *i.e.* where an N-site (*i.e.* presumably oligomeric) protein molecule can establish from 1 to N contacts with matrix-ligands[5–11]. Theory appropriate to oligomeric proteins is of particular importance, for several reasons, including: (1) the great majority of functional proteins, including many important enzymes, are oligomeric in structure; (2) current practice is to use highly-substituted column matrices (*e.g.* dye-ligand matrices) for protein purification, with the consequent increased likelihood of multivalent contacts; (3) since the Gibbs energy of binding is additive with respect to individual occupied sites, extremely tight binding to the matrix is possible in principle without loss in specificity; (4) quantitative affinity chromatography has been recommended for measuring protein–ligand binding constants, and it is important to ensure that the theoretical basis of such use is secure in the case of oligomeric proteins.

In relation to a protein with identical sites, most of the afore-mentioned theoretical treatments of the multivalent case assume, explicitly or implicitly, one or both of the following postulates: (1) a single microscopic equilibrium binding constant

may be used for each successive interaction of a protein molecule with matrix-ligand; (2) all sites on the protein have access to the same concentration of matrix-ligand. Although they are valid for interactions of soluble ligand with protein, conceptual difficulties arise when these postulates are applied to ligands immobilised on rigid matrices. One difficulty arises from the uneven distribution of matrix-ligand groups at the molecular level, and their inability to diffuse. This uneven distribution and the size of the protein molecule set a limit on the number of matrix-ligand groups that can be bound by any individual protein molecule at a particular locus within the matrix. The equal-access assumption, discussed above, clearly is inappropriate for this situation. A second difficulty is the intuitive expectation that, while the probability of a first contact by a protein molecule within a static cluster of matrix-ligands will be the same as for contact with an isolated matrix-ligand, subsequent contacts within the cluster by the same molecule ought to have a higher probability due to proximity; in other words successive contacts within a cluster should show cooperativity. Of existing theoretical models, only that of Kyprianou and Yon[7] implies such co-operativity. This model, however, is deficient in assuming a single uniform type of cluster. In a recent paper, Hubble[12] discusses the different but related problem of affinity chromatography of proteins with intrinsic co-operative binding properties, e.g. allosteric enzymes.

A multivalency model that makes simple assumptions about the clustering of matrix-ligands, and about cooperativity in binding to the matrix, will now be described.

THEORY

Symbols

$[P_t]$	Total concentration of protein
$[P_s]$	Concentration of all soluble protein forms
R	Partitioning ratio, defined as $[P_t]/[P_s]$
$[S]$	Total concentration of soluble ligand
$[M]$	Total concentration of accessible matrix-ligand
N	Number of identical ligand-binding sites per protein molecule
r	Radius (nm) of protein molecule
K_S	Microscopic (site) association constant for the binding of soluble ligand
K_M	Microscopic (site) constant for binding of matrix-ligand
$[X_1], [X_2],...[X_N]$	Concentrations of clusters containing 1,2,...N matrix-ligands, respectively
$K_1, K_2,...K_N$	Stoichiometric (cluster) association constants for concerted binding of protein to clusters of 1,2,...N matrix-ligands, respectively

All concentrations are in mol/l. Microscopic (site) constants and stoichiometric constants are defined according to Klotz[13]. Other symbols will be defined as required.

General description

The present model is an extension of an earlier model[7] in which the concept of concerted binding of a protein to a single type of matrix-ligand cluster was implicitly

proposed. The major present innovation is the assumption that the non-diffusible matrix groups are randomly distributed, thereby enabling the concentrations of "effective clusters" within this distribution to be computed by statistical means. An effective cluster is defined as a group of accessible matrix-ligands within the volume of space (assumed spherical) equivalent to that occupied by a protein molecule. Strictly, the matrix-ligands capable of binding to a protein molecule should be a subgroup within the cluster that satisfies steric requirements imposed by the protein, *e.g.* location at the apices of a tetrahedron. To simplify the mathematics, this restriction will be relaxed in the present treatment. The implications of this relaxation will be discussed later (see Discussion).

Let X_i denote a cluster containing i accessible matrix-ligands, where i takes values from 1 to N. For any one of these cluster-types, protein–ligand complexes involving fewer than i matrix-ligands are neglected. This implies a concerted binding of all i matrix-ligands, *i.e.* a high degree of cooperativity. The justification for this assumption will be discussed later. By reasoning entirely analogous to that described by Nichol *et al.*[3] and Kyprianou and Yon[7] it may be shown that, in an equilibrium batch experiment, the protein will partition between soluble and matrix phases according to the relationship:

$$R = 1 + \sum_{i=1}^{N} \frac{K_i[X_i]}{K_i[P_t] + (1 + K_S[S])^i} \tag{1}$$

This equation may be adapted to frontal-elution chromatography by use of the relationship[10,14] $R = V/V_0$, in which V is the (variable) elution volume of the protein, given by the centroid of the advancing protein front, and V_0 is the elution volume in the absence of any interaction with the matrix, provided that V_0 can be estimated.

Eqn. 1 contains N cluster concentrations $[X_i]$ and N stoichiometric association constants K_i. Expressions for $[X_i]$ and K_i will now be derived.

The cluster-concentrations [X_i]

The cluster concentrations may be related to the overall concentration of matrix-ligand, [M], and the dimensions of the protein molecule, as shown next. For mathematical simplicity (see earlier discussion) the protein will be treated as a sphere, and all matrix-ligands "within" this sphere assumed to be capable of binding. This simplification allows the cluster concentrations to be calculated by assuming a Poisson distribution of matrix-ligand groups (see *e.g.* ref. 15), *i.e.* the probability $p(i)$ of finding exactly i groups in a sphere whose average content is m is given by:

$$p(i) = \frac{e^{-m} \cdot m^i}{i!} \tag{2}$$

For a protein of radius r (in nm), and a concentration [M] (in mol/l) of accessible matrix-ligands, the average number of groups contained within the equivalent sphere is readily shown to be:

$$m = 2.52[M]r^3 \tag{3}$$

where the numerical factor 2.52 arises from a combination of the formula for spherical volume (radius in nm) and Avogadro's number. It should be noted that clusters with more than N groups are in theory included in this distribution, *i.e.*, i can take all positive integral values. However, as will be shown later, higher-order clusters are negligible at the accessible matrix-ligand concentrations encountered in practice, therefore clusters with more than N groups are conveniently neglected. The concentrations of effective clusters X_i (eqn. 1) are related to the probabilities $p(i)$ as follows:

$$\frac{i[X_i]}{[M]} = \frac{p(i)}{1 - p(0)} = \frac{[\text{matrix-ligand in } i\text{-clusters}]}{[\text{total matrix ligand}]} \tag{4}$$

Combining eqns. 2 and 4 gives the cluster concentration as:

$$[X_i] = \frac{m^i[M]}{i \cdot i!(e^m - 1)} \tag{5}$$

In practice $[M]$ rarely exceeds 0.1 mM, therefore m is of the order 0.01 for a protein of ordinary radius (say 4 nm). To a good approximation, therefore, the expansion $e^m = 1 + m$ may be used for the exponential term in eqn. 5. Together with eqn. 3 and some rearrangement, this enables eqn. 5 to be written as:

$$[X_i] = \frac{(2.52r^3)^{i-1} [M]^i}{i \cdot i!} \tag{6}$$

The stoichiometric constants K_i

    For isolated matrix-ligand groups (*i.e.* "clusters" of 1) the stoichiometric association constant is given by

$$K_1 = NK_M \tag{7}$$

where K_M is the intrinsic (site) association constant for binding matrix-ligand. This is the constant measured by standard monovalent methods[2,3] *i.e.* when the concentration of matrix-ligand $[M]$ is sufficiently small for bivalent and higher-order interactions to be ignored. For clusters of 2 or more, the cluster concentration $[X_i]$, and the value of K_M, govern the first contact of the N-valent protein with the cluster. Succeeding contacts within the cluster are governed by the much higher "local" concentration of matrix-groups. It is proposed, therefore, to treat each of the successive constants K_i (where $i > 1$) as the product of K_M^i, a statistical factor ^NC_i (as in the free-solution case, see ref. 13) and an "enhanced concentration factor" E, defined as

$$E = \frac{\text{apparent matrix-ligand concn. "inside" the cluster}}{\text{cluster concentration}}$$

Since i groups in a sphere of radius r (in nm) is equivalent to a concentration of $i/(2.52r^3)$ mol/l, and the cluster concentration is given by eqn. 6 above, it may be shown that

$$E = \frac{i^2 \cdot i!}{(2.52r^3 \, [\text{M}])^i} \tag{8}$$

Hence the association constants K_i are given by

$$K_i = {}^N C_i \cdot K_{\text{M}}^i \cdot \frac{i^2 \cdot i!}{(2.52r^3 \, [\text{M}])^i} \tag{9}$$

where ${}^N C_i = N!/[(N - i)!i!]$.

Finally, substitution of eqns. 6, 7 and 9 into 1 yields, as the partitioning equation:

$$R = 1 + \frac{NK_{\text{M}}[\text{M}]}{NK_{\text{M}}[\text{P}_t] + 1 + K_{\text{S}}[\text{S}]} +$$

$$\sum_{i=2}^{N} \frac{N!i(2.52r^3)^{i-1}(K_{\text{M}}[\text{M}])^i}{i!\{N!K_{\text{M}}^i i^2 [\text{P}_t] + (2.52r^3[\text{M}])^i (N - i)!(1 + K_{\text{S}}[\text{S}])^i\}} \tag{10}$$

This equation implies protein adsorption into a set of mutually-independent adsorption sites.

RESULTS

The following aspects of the predicted behaviour of the theoretical model presented above have been examined by computer modelling.

Effect of protein radius

A novel aspect of the present theory is its introduction of protein size as a determinant of partitioning behaviour through the calculation of cluster concentrations $[X_i]$, and not, as is more often the case, through gel-filtration effects. This size-dependence is quite sensitive; as shown in eqn. 6, $[X_i]$ varies as the $(i-1)$th power of r^3, thus a 2.1-fold increase in the radius increases $[X_2]$ by 10-fold, and $[X_3]$ by 100-fold. The remaining discussion will focus on a four-site protein of radius 4 nm, typical of several glycolytic and other roughly spherical enzymes *e.g.* aldolase and lactate dehydrogenase.

Predicted cluster concentrations for a typical multi-site protein

The predicted cluster distribution has been examined for a four-site protein of radius 4 nm. Fig. 1 shows the computed cluster concentrations $[X_i]$ as a function of total accessible matrix-ligand concentration [M], based on use of eqn. 5 with the exponential term unchanged. It has been assumed that matrix-clusters with more than four groups (significant only at very high, and probably unrealistic, values of [M]) are "seen" by the protein as clusters of four. In Fig. 1a the absolute values of $[X_i]$ are given (note log–log scales) and in (b) $[X_i]$ is expressed as a fraction of all clusters.

The total concentration of immobilised ligand in an affinity matrix is usually readily measurable, and experience has shown that, using present-day immobilisation
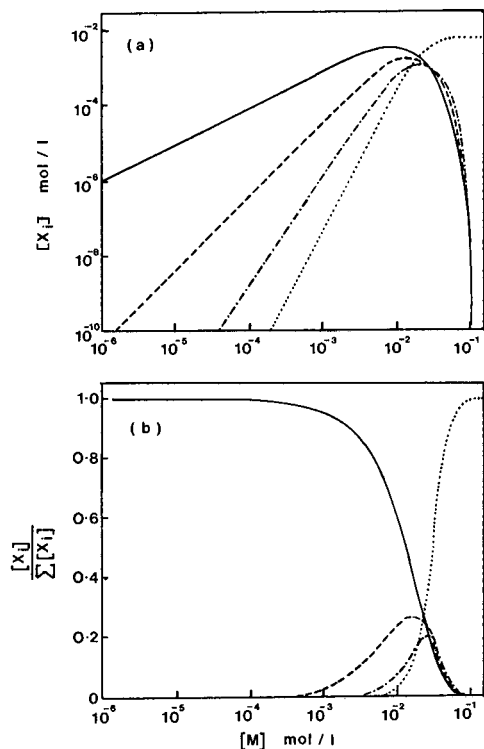
Fig. 1. Dependence of cluster concentrations $[X_i]$ on the total concentration of accessible matrix-ligand groups, $[M]$, for a four-site protein molecule of radius 4 nm. The calculations are based on eqn. 5 in the text; clusters with more than four groups are included with four-clusters. (a) Absolute values of $[X_i]$ (note log–log scale). (b) $[X_i]$ relative to total of all clusters. Key: X_1, ———; X_2, – – –; X_3, ·—·—·—·; X_4, ·····.

technology, values greater than 10^{-2} M are rarely, if ever, encountered. The fraction of these groups that are accessible constitutes $[M]$; attempts to estimate its value have invariably indicated that, at most, a few percent of the total may be involved. It seems reasonable, therefore, to take 10^{-3} M as a practical upper limit for $[M]$. Fig. 1 shows that even at the top end of this range, a protein of radius 4 nm "sees" over 95% of all the accessible matrix-ligand as isolated, single ligand-groups. At lower, more realistic $[M]$-values, single matrix-ligands are overwhelmingly predominant (Fig. 1b). The small concentrations of two-clusters and three-clusters may have significant effects depending on protein concentration (see next paragraph), but clusters of four are nearly always of no practical effect, their concentrations never exceeding about 10^{-10} M.

Effect of protein concentration

Inspection of the summated term in eqn. 1 shows that, for clusters of i matrix-ligands, this term becomes negligible when the cluster concentration $[X_i]$ is very much smaller than the protein concentration $[P_t]$. That is, only clusters whose concentrations approach or exceed that of the protein are expected to affect the partitioning ratio (or elution volume). Moreover, to be effective cluster concentrations
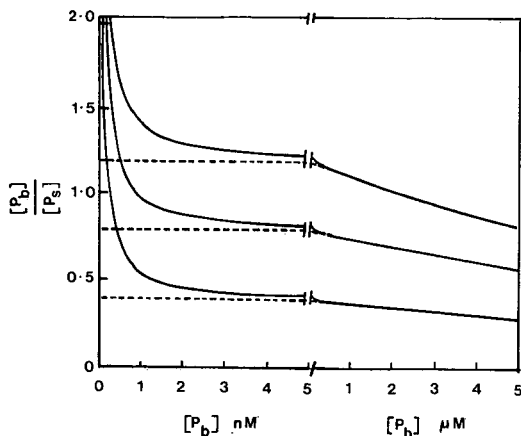
Fig. 2. Scatchard-type partitioning plots for concerted-cluster and monovalent models using the same model parameters. Continuous lines are used for the concerted-cluster model which models a four-site protein of 4 nm radius. Dashed lines are used for the monovalent model, for which the single stoichiometric constant was taken as $4K_M$. The two sets of lines coincide over the right-hand half of the diagram. Parameters for both plots were: $[M] = 3 \mu M$, $K_M = 10^5 M^{-1}$, $K_S = 10^6 M^{-1}$, $[S] = 0$ (top curves), $[S] = 0.5 \mu M$ (middle curves) and $[S] = 2 \mu M$ (bottom curves). $[P_b]$ = adsorbed protein; $[P_s]$ = protein in solution phase.

must be substantially higher than this when in competition with soluble ligand S, $i.e.$ when the soluble ligand concentration is such that $K_S[S]$ makes a substantial contribution to the denominator of eqn. 1. At the assumed upper limit for $[M]$ (about $10^{-3} M$), the sum of the cluster concentrations $[X_2]$ and $[X_3]$ is in the micromolar range, so partitioning or chromatography experiments that use protein concentrations in the micromolar range (as many do) are likely to show the effects of such higher-order clusters. The corollary to this is, of course, that in most cases $[M]$ is expected to be well below $10^{-3} M$, so that unless $[P_t]$ is well below the micromolar range, the effects of higher-order clusters will pass unnoticed, $i.e.$ the partitioning will appear effectively monovalent. This point is well illustrated in the Scatchard plots of Fig. 2, which show that, above a certain value of $[P_t]$, predictions of the present theory and of monovalent theory[3] are indistinguishable.

Predicted values of stoichiometric association constants

Fig. 3a shows the dependence of the stoichiometric constants K_i on $[M]$, for $K_M = 10^4 M^{-1}$, $K_M = 10^6 M^{-1}$ (a fairly typical value and about the minimum for K_M consistent with effective affinity chromatography[16,17]), and $K_M = 10^8 M^{-1}$. Note the log–log scales used. The most striking feature of this prediction is the relatively enormous increase on going from K_{i-1} to K_i, compared to what one would expect from purely statistical considerations[13]. The difference is due to the postulated "enhanced concentration factor", E (see Theory), the corresponding values of which, for $i = 2$, 3 and 4, are given in Fig. 3b (note log–log scales). Under conditions least favourable to large E ($i.e.$ $[M]$ approaching $10^{-3} M$), its size is several hundreds for two-clusters, and tens of thousands for three-clusters. More likely conditions (higher K_M and/or lower $[M]$) both lead to enormously increased values of E.

Two consequences flow from these predictions: (1) Since, for $i > 1$, each K_i is at
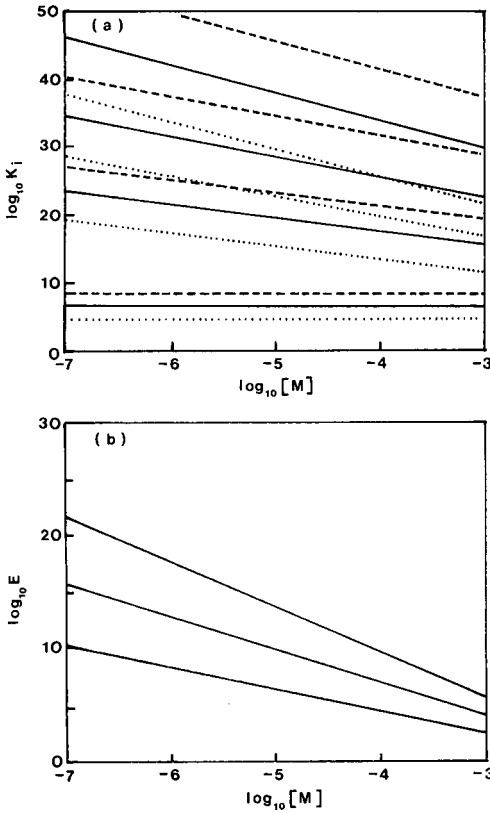
Fig. 3. Dependence of (a) stoichiometric cluster constants K_i and (b) "enhanced concentration" factor, E, on the total concentration of accessible matrix-ligand groups, [M]. The calculations are based on eqns. 7–9 in the text, applied to a four-site protein of radius 4 nm, with K_M set to $10^4 \, M^{-1}$ ($\cdots$), $10^6 \, M^{-1}$ (———) or 10^8 M^{-1} (– – –). Reading upwards for each K_M set, the lines are for K_1, K_2, K_3 and K_4 respectively. Note log–log scales.

least E times greater than the corresponding K_{i-1}, we are justified in neglecting protein molecules interacting by fewer than i contacts with a cluster of i matrix-ligands, a basic assumption of the present model. That is, cluster interactions are indeed highly concerted. (2) The enormous K_i values suggest that one should expect "irreversible" binding to clusters to be quite common. This will likely arise from extremely small "off" rate constants for protein-cluster interactions, since the chance of all i contacts being simultaneously severed is small. "Irreversible" cluster interactions permit a major simplification of eqn. 10. Since other terms in the numerator of eqn. 1 are negligible compared to $K_i[P_t]$, one may cancel K_i so that the summated term becomes $[X_i]/[P_t]$, for $i > 1$. For most reasonable values of [M] only two-clusters are likely to be significant (see Fig. 1), so the partitioning ratio turns out as

$$R = 1 + \frac{NK_M[M]}{NK_M[P_t] + 1 + K_S[S]} + \frac{2.52r^3[M]^2}{4[P_t]} \tag{11}$$

In attempts to fit experimental data to the cluster model by the least-squares method, it has been found in several cases that this simpler equation gives as good a fit to the data, and generates the same parameter values as the more complex eqn. 10. This was the case for a re-interpretation of published data on the interaction of aldolase and phosphocellulose[20].

DISCUSSION

The equations presented above rest mainly on two assumptions: (1) interactions within a cluster are highly cooperative; (2) cluster concentrations follow a Poisson-type distribution. The idea that proximity leads to highly cooperative interactions is not new in biochemistry; it occurs for example in quantitative treatments of DNA annealing and of the helix-coil transition in proteins, and is here extended to multivalent affinity interactions. Invoking the Poisson distribution, *i.e.* assuming a truly random distribution of matrix-ligand groups is a more uncertain proposition, as a number of factors may operate to produce non-random distributions. For example, if the matrix-ligand is a dye, there is evidence that stacking of dye molecules may occur at high dye concentrations[19]. Moreover, the assumption that all matrix-ligands within the bounds of a cluster can bind to protein ignores the restrictive requirements of the spatial distribution (*e.g.* tetrahedral) of protein binding-sites. Strictly, the model as currently formulated applies to matrix-ligands that lack long-range translatory motion, but have considerable local freedom (short-range translation and rotation). Conceivably, more elaborate models of geometrical probability will be found to replace the Poisson distribution for other cases. Notwithstanding these difficulties, the concerted-cluster model represents the first attempt to address the problem of restricted mobility in an affinity matrix. A need for some such model is likely to arise soon, as modern trends in affinity chromatography (in particular the development of high-density, high-performance columns) will inevitably call for greater use of rigid, high-flow matrices (silica, controlled-pore glass, etc.) with consequent limitations in matrix-ligand mobility.
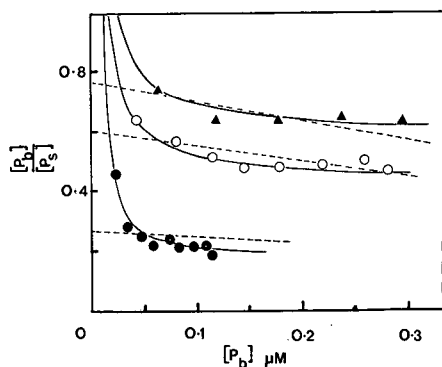
Fig. 4. Scatchard-type plots of the interaction of aldolase and phosphocellulose, with phosphate as soluble ligand. The data are from Table II of ref. 6. Concentrations of phosphate were: ▲, 0.3 mM; ○, 1.0 mM; ◑, 5.0 mM. Fitted curves are for the concerted cluster model (————) and the reacted-site-probability model (− −). For other details, see ref. 20. Diagram by permission of the Biochemical Society.

In a search for experimental evidence to support co-operativity and clustering in affinity partitioning, published data on the interaction of aldolase and phosphocellulose have been re-examined; a communication on this work has been published[20]. These data were originally cited in support of a theory of multivalency based on reacted site probability[6]. In the re-examination, the values of K_M and [M] were estimated by non-linear regression of the data in Table II of ref. 6, using both the concerted-cluster and the reacted-site-probability models. Fig. 4 shows the results plotted in the same format as Fig. 2. By the criterion of the smaller sum-of-squares of residual errors, the fit to the concerted-cluster model was better by an order of magnitude. For other details see ref. 20. Of several published sets of data examined, the aldolase–phosphocellulose data have shown the most pronounced upwards curvature at low protein concentrations, in Scatchard-type graphs. This behaviour is predicted by the cluster model, but not by the monovalent or reacted-site-probability models. While experimental data which show a steep increase in [bound protein]/[free protein] at low total protein concentrations clearly fit the cluster model better, data which follow a more near-linear relationship tend to fit all three (monovalent, cluster, reacted-site probability) models about equally well (by the least-squares criterion). In such cases, the cluster model approximates the monovalent model in predicted behaviour (see Fig. 2), *i.e.* clusters are predicted to be negligible. Upon examination, several other sets of published data on affinity interactions appear to exhibit this near-linear relationship. Before it can be decided whether or not the concerted-cluster theory is applicable to these systems, the experiments should be repeated with the emphasis on a considerably lower range of protein concentrations, where the steep increase in Scatchard-type graphs, denoting significant concentrations of high-affinity adsorption sites, may be evident.

ACKNOWLEDGEMENTS

REFERENCES

1 P. Andrews, B. J. Kitchen and D. J. Winzor, *Biochem. J.*, 135 (1973) 897.
2 B. M. Dunn and I. M. Chaiken, *Proc. Natl. Acad. Sci. U.S.A.*, 71 (1974) 2382.
3 L. W. Nichol, A. G. Ogston, D. J. Winzor and W. H. Sawyer, *Biochem. J.*, 143 (1974) 435.
4 K.-I. Kasai and S.-I. Ishii, *J. Biochem. (Tokyo)*, 77 (1975) 261.
5 I. M. Chaiken, *Anal. Biochem.*, 97 (1979) 1.
6 L. W. Nichol, L. D. Ward and D. J. Winzor, *Biochemistry*, 20 (1981) 4856.
7 P. Kyprianou and R. J. Yon, *Biochem. J.*, 207 (1982) 549.
8 H. W. Hethcote and C. DeLisi, in I. M. Chaiken, M. Wilchek and I. Parikh (Editors), *Affinity Chromatography and Biological Recognition*, Academic Press, New York, 1983, p. 119.
9 D. J. Winzor, in P. D. G. Dean, W. S. Johnson and F. A. Middle (Editors), *Affinity Chromatography: A Practical Approach*, IRL Press, Oxford, 1985, Ch. 6, p. 149.
10 P. J. Hogg and D. J. Winzor, *Arch. Biochem. Biophys.*, 234 (1984) 55.
11 H. E. Swaisgood and I. M. Chaiken, *Biochemistry*, 25 (1986) 4148.
12 J. Hubble, (1987), *Biotech. Bioeng.*, 30 (1987) 208.
13 I. M. Klotz, *Acc. Chem. Res.*, 7 (1974) 162.

14 G. A. Gilbert, *Nature (London)*, 212 (1966) 296.
15 C. Chatfield, *Statistics for Technology*, Chapman & Hall, London, 2nd edn., 1978, p. 69.
16 R. J. Yon, *Biochem. J.*, 185 (1980) 211.
17 R. K. Scopes, *Anal. Biochem.*, 165 (1987) 235.
18 R. J. Yon, *Biochem. Soc. Trans.*, 16 (1988) 542.
19 Y-C. Liu, R. Ledger and E. Stellwagen, *J. Biol. Chem.*, 259 (1984) 3796.
20 R. J. Yon, *Biochem. Soc. Trans.*, 16 (1988) 543.
21 P. J. Hogg and D. J. Winzor, *Arch. Biochem. Biophys.*, 240 (1985) 70.

CHROM. 20 935

EXPERT SYSTEM FOR THE SELECTION OF HIGH-PERFORMANCE LIQUID CHROMATOGRAPHIC METHODS IN PHARMACEUTICAL ANALYSIS

VALIDATION OF THE RULES FOR THE SELECTION OF THE MOBILE PHASE

M. DE SMET, A. PEETERS, L. BUYDENS and D. L. MASSART*

Vrije Universiteit Brussel, Farmaceutisch Instituut, Laarbeeklaan 103, B-1090 Brussels (Belgium)

SUMMARY

The rules for the selection of the mobile phase and the validation performed on 44 pharmaceutical preparations, containing one to five active compounds, are described. These rules are incorporated into an expert system, called LABEL, for the selection of high-performance liquid chromatographic methods in pharmaceutical analysis. A single stationary phase type is used, namely a nitrile or cyanopropyl (CN) column, which can be used in both normal-phase (NP) and reversed-phase (RP) chromatography. Three mobile phase systems were evaluated on this column type: NP, RP with water and RP with buffer. LABEL selects one of these three systems on the basis of the rules incorporated for the mobile phase selection, checks if the addition of ion-suppressing agents to the eluting agent is necessary and finally gives the starting composition of the mobile phase in each of the three systems. For this selection the number of compounds in the sample, the acid–base properties and the hydrophobicity of the solutes are the more important factors. The validation of the rules on 44 pharmaceutical preparations resulted in an immediate success in 82% of all cases. In half of the remaining cases, the system proposed can be adapted with a minor change in conditions, so that it can also be used in practice.

INTRODUCTION

In the last few years, many efforts have been made to develop systematic optimization strategies for high-performance liquid chromatographic (HPLC) methods. Usually, these strategies deal with the optimization of mobile phase parameters such as solvent strength, solvent selectivity, pH and flow-rate. Excellent overviews were given by Berridge[1] and Schoenmakers[2]. Most HPLC separations are performed in the reversed-phase (RP) mode and the different optimization strategies developed have been mainly applied in this mode. However, for some separation problems, normal-phase (NP) chromatography is more suitable[3].

In our laboratory, a general approach for the separation of pharmaceutical compounds was developed with the use of a single stationary phase type, namely a cyanopropyl or nitrile (CN) column, which can be applied in both the RP and NP modes owing to its intermediate polarity properties[4–6]. A separation strategy applied with success in many instances consists in carrying out a gradient elution from which a suitable solvent strength is determined for isocratic elution. Afterwards the solvent selectivity is changed to enhance the resolution between peaks while keeping the solvent strength constant. In the RP mode, one can use eluting agents with water as the basis solvent but it is also possible to replace it by a buffer solution. A systematic study of the parameters influencing the retention of basic, acidic and neutral drugs with mobile phases containing buffers was carried out on a CN column[7]. In this way, it is possible to chromatograph drugs on a CN column with three different mobile phase systems: NP, RP with water and RP with buffer. In the first two mobile phase systems, ion-suppressing agents can be added to the eluting agent to improve the peak shape. The nature of this factor depends on the acid–base properties of the pharmaceutical compounds being chromatographed.

The selection of a single column type offers the advantage that a more manageable number of possible combinations of stationary phase with mobile phases is obtained with which successful separations are possible in most instances. As one can now choose from three mobile phase systems, the problem to be solved is which mobile phase system to select for a certain separation problem. Until now, not much attention has been paid to this point in the literature and it is usually treated by most chromatographers by habit or by trial-and-error experiments. This selection can be incorporated into an expert system. Expert systems are software products that can offer intelligent advice on problems requiring some expertise. The existing optimization strategies can then be coupled to an expert system since the software is available. In our laboratory, the feasibility of the integration of experimental optimization methods into an expert system has been demonstrated[8]. In this way, one could obtain an expert system that gives advice about the different steps in the development of an HPLC method, starting with the initial selection of the chromatographic mode and finishing with the optimized separation of the compounds of interest.

In a previous paper, the knowledge base of the expert system LABEL was described[9]. LABEL is an expert system that selects suitable HPLC systems for the label claim analysis of pharmaceutical preparations. For a certain separation problem, the system gives advice about the detection mode (UV detection at fixed or variable wavelength and electrochemical detection in the oxidative mode), the chromatographic mode and the starting mobile phase composition to use in the selected mode so that a "first guess" system for an HPLC analysis is obtained. In this way, one has two strategies for selecting suitable starting mobile phase compositions for pharmaceutical analysis, *viz.*, the strategy incorporated in the expert system and the strategy with the gradient elution, and both have advantages and limitations.

In this paper, the rules incorporated in the expert system for the selection of the chromatographic mode and the starting mobile phase will be described and validated; those for detection will be considered elsewhere[10]. For all the samples examined in this study, UV detection was always used. The validation of the rules was performed on commercially available pharmaceutical formulations.

EXPERIMENTAL

Apparatus

The HPLC instrumentation included two Varian 5060 liquid chromatographs equipped with a Rheodyne loop injector (loop volumes used, 10, 50 and 100 μl). One chromatograph was equipped with a variable-wavelength UV detector (Varian UV-100 detector, a.u.f.s. 0.05) and the other with a Varian fixed-wavelength UV detector (254 nm, a.u.f.s. 0.08). The chromatograms were recorded with a Varian Vista CDS 401 chromatographic data system. Two HPLC instruments were used for practical reasons, one for the RP and the other for the NP mode; if we had used only one instrument, much time would have been spent in switching from the one chromatographic mode to the other by rinsing with solvents that are compatible with the two systems.

The columns used were 250 $\times$ 4 mm I.D. stainless-steel columns packed with LiChrosorb CN of particle size 5 μm and obtained from Merck (Darmstadt, F.R.G.). The flow-rate was 1 ml/min in the RP and 2 ml/min in the NP mode. All experiments were carried out at ambient temperature. For the determination of the dead time of the chromatographic system, methanol in the RP and *n*-hexane in the NP mode were injected.

Standards and reagents

All drugs were of pharmaceutical purity, methanol, dichloromethane and *n*-hexane were all of liquid chromatographic grade and glacial acetic acid and chloroform were of analytical-reagent grade, all obtained from Merck. Doubly distilled water which was further purified with a Water-I system (Gelman Sciences, Ann Arbor, MI, U.S.A.) was used for the mobile phase. Propylamine of analytical-reagent grade was purchased from Fluka (Buchs, Switzerland). In the RP with buffer mode, a phosphate buffer was used with a pH of 3 and an ionic strength of 0.05 or 0.02 for the mobile phase. The buffer solution used for the extraction of basic drugs was also a phosphate buffer of pH 3 with an ionic strength of 0.4, which contained sodium octylsulphate ($5 \cdot 10^{-2}$ M) as counter ion (Merck). For the preparation of the buffer solutions, phosphoric acid (H_3PO_4) (1 M) and sodium dihydrogenphosphate ($NaH_2PO_4 \cdot H_2O$) of analytical-reagent grade (Merck) were used. The buffer solution used for the extraction of acidic drugs was a phosphate buffer of pH 5.5 prepared from $NaH_2PO_4 \cdot H_2O$ and disodium hydrogenphosphate ($Na_2HPO_4 \cdot 2H_2O$) (Merck). Tri-*n*-octylamine (0.1 M), used as a counter ion in the ion-pair extraction of acidic drugs, was of analytical-reagent grade from Janssen Chimica (Beerse, Belgium).

Sample preparation

Table I lists the pharmaceutical preparations analysed. For the tablets and the coated tablets, a number of tablets were pulverized and homogeneously mixed and an aliquot of the resulting powder was suspended in a suitable solvent. After ultra-sonification for 20 min and centrifugation, the clear supernatant was diluted and the diluted solution was injected into the HPLC system. In the RP mode, the solvent for dissolution was methanol and the supernatant was diluted with water. In the NP mode, dichloromethane was used to dissolve the active compounds and *n*-hexane for dilution of the supernatant. The supernatant was diluted until peaks were obtained that fell

TABLE I

LIST OF THE DIFFERENT PHARMACEUTICAL FORMULATIONS

No.	Name	Active compounds	Amount or concentration	Dosage form
1	Aacicortisol	Hydrocortisone sodium succinate	133.7 mg	Ampoules
2	Acid A Vit	Tretinoine	0.5 mg/ml	Lotio
3	Afebryl	Acetylsalicylic acid	300 mg	Effervescent tablets
		Ascorbic acid	300 mg	
		Paracetamol	200 mg	
4	Algotropyl	Promethazine hydrochloride	5 mg	Suppository
		Paracetamol	200 mg	
5	Androcur	Cyproterone acetate	50 mg	Tablets
6	Arovit	Retinol	50 000 IU	Coated tablets
7	Asept'acqua	Merbromin	20 mg/ml	Solution
8	Atropine Cusi	Atropine sulphate	5 mg/ml	Ophthalmic solution
9	Beneurol	Thiamine hydrochloride	300 mg	Coated tablets
10	Buscopan	Hyoscine butylbromide	10 mg	Tablets
11	Buscopan Compositum	Metamizol	250 mg	Ampoules
		Hyoscine butylbromide	20 mg	
12	Cibalgine	Allobarbital	30 mg	Tablets
		Propyphenazone	220 mg	
13	Desclidium	Viquidil hydrochloride	100 mg	Capsules
14	Exidol	Glafenine	200 mg	Tablets
15	Flagyl	Metronidazole	500 mg	Suppository
16	Frisium	Clobazam	10 mg	Tablets
17	Haldol	Haloperidol	5 mg/ml	Ampoules
18	Hoofd- en zenuwpijn poeders	Acetylsalicylic acid	350 mg	Powder
		Caffeine	50 mg	
		Phenacetin	200 mg	
19	Inderal	Propranolol hydrochloride	10 mg	Tablets
20	Insidon	Opipramol hydrochloride	50 mg	Coated tablets
21	Isoptine	Verapamil hydrochloride	40 mg	Coated tablets
22	Kevopril	Quinupramine	2.5 mg	Tablets
23	Largactil	Chlorpromazine	40 mg/ml	Solution
24	Masteron	Drostanolone propionate	100 mg/ml	Ampoules
25	Migrane Kranit	Caffeine	85 mg	Tablets
		Phenobarbital	30 mg	
		Paracetamol	200 mg	
		Propyphenazone	150 mg	
		Ethaverine hydrochloride	20 mg	
26	Minidiab	Glipizide	5 mg	Tablets
27	Monazone	Mofebutazon	250 mg	Coated tablets
28	Monotrean	Papaverine	40 mg	Coated tablets
		Quinine hydrochloride	100 mg	
29	Negram	Nalidixic acid	500 mg	Tablets
30	Nitrobaat	Nitroglyerin	1 mg	Tablets
31	Noscaphan	Dextromethorphan hydrobromide	3.5 mg per 5 ml	Syrup
		Guaifenesin	35 mg per 5 ml	
		Noscapine hydrochloride	3.5 mg per 5 ml	
32	Polistine-T-Caps	Carbinoxamine maleate	12 mg	Capsules
33	Priamide	Isopropamide iodide	5 mg	Coated tablets
34	Primperan	Metoclopramide hydrochloride	10 mg	Tablets
35	Prolopa	Levodopa	100 mg	Capsules
		Benserazide	25 mg	

TABLE I *(continued)*

No.	Name	Active compounds	Amount or concentration	Dosage form
36	Sedergine	Acetylsalicylic acid	330 mg	Effervescent tablets
		Ascorbic acid	200 mg	
37	Solubacter	Triclocarban	10 mg/g	Solution
38	Tagamet	Cimetidine	200 mg	Tablets
39	Torecan	Thiethylperazine dimaleate	10 mg	Coated tablets
40	Trinitrine Cafeinee	Nitroglycerin	0.5 mg	Coated tablets
		Caffeine	30 mg	
41	Trinitrine Papaverine	Nitroglycerin	0.3 mg	Coated tablets
		Papaverine hydrochoride	5 mg	
42	Uro-S3	Phenazopyridine hydrochloride	50 mg	Coated tablets
		Sulphadiazine	67 mg	
		Sulphamerazine	67 mg	
		Sulphathiazole	67 mg	
43	Vascoril	Cinepazet maleate	300 mg	Tablets
44	Vesalium	Haloperidol	0.3 mg	Coated tablets
		Isopropamide iodide	2 mg	

within scale at the detector attenuation stated. The following pharmaceutical preparations were treated in this way: Androcur, Arovit, Beneurol, Cibalgine, Exidol, Frisium, Inderal, Migraine Kranit, Monazone, Monotrean, Negram, Nitrobaat, Priamide, Primperan, Tagamet, Trinitrine Caffeinee, Trinitrine Papaverine, Uro-S$_3$ and Vesalium. For some tablets and coated tablets, the mobile phase was used to dilute the clear supernatant. This was the case with following pharmaceutical preparations: Buscopan, Isoptine, Kevopril, Minidiab and Vascoril.

For Insidon and Torecan, which are determined in the NP mode, an ion-pair extraction for basic drugs was carried out. A number of tablets were pulverized and homogeneously mixed. An aliquot of the resulting powder, equivalent with the mean weight of one tablet, was suspended in 50 ml of water for Insidon and in 50 ml of 0.2 M hydrochloric acid for Torecan. After ultrasonification and centrifugation, 5 ml of the clear supernatant were transferred into a centrifuge tube and 10 ml of phosphate buffer containing sodium octylsulphate ($5 \cdot 10^{-2}$ M) and 5 ml of chloroform were added. After gently shaking for 30 min in a shaking bath and centrifugation, the chloroform phase was diluted with the mobile phase.

For the determination of active compounds in capsules, the capsules were opened and the contents homogeneously mixed. Then the same sample preparation procedure was followed as for the tablets and the coated tablets. Desclidium was diluted with the mobile phase while Polistine-T-Caps and Prolopa were diluted with water.

Powders (Hoofdpijn en Zenuwpijn poeders) were treated in the same way as capsules, after homogeneously mixing.

The effervescent tablets Afebryl and Sedergine were both treated in the same way. One tablet was dissolved in 25 ml of water and shaken for 10 min. To 5 ml of this

solution, 5 ml of phosphate buffer (pH 5.5 and ionic strength 0.1) and 10 ml of chloroform containing tri-n-octylamine (0.1 M) were added and the mixture was shaken for 30 min. After centrifugation, the chloroform phase was diluted with the mobile phase and injected into the HPLC system

In the set of pharmaceutical formulations, two dosage forms as suppositories were included, namely Algotropyl and Flagyl. One Algotropyl suppository was placed in a centrifuge tube, 50 ml of methanol were added and the mixture was shaken for 30 min at 40°C. After centrifugation, the clear supernatant was diluted with methanol. For Flagyl, the same procedure was carried out but the suppository was dissolved in water and the supernatant diluted with water.

Ampoules, solutions and ophthalmic solutions were treated in an analogous manner for the sample pretreatment. Asept'acqua, Atropine Cusi, Buscopan Compositum and Largactil were diluted with water. Solubacter was diluted with methanol. A Masteron ampoule was diluted with dichloromethane. The pharmaceutical preparation Aacicortisol contains ampoules with the active compound, hydrocortisone sodium succinate, as powder and ampoules with the dissolution solvent for injection. An aliqout of the powder was dissolved in chloroform and further diluted with the mobile phase used in the NP mode. For Haldol, an ion-pair extraction for basic drugs was carried out. The contents of one ampoule were placed in a 50-ml volumetric flask and diluted to volume with 10^{-2} M hydrochloric acid. To 5 ml of this solution, 10 ml of phosphate buffer (pH 3 and ionic strength 0.4) containing $5 \cdot 10^{-2}$ M sodium octylsulphate and 5 ml of chloroform were added and further treated as for Insidon and Torecan.

Acid-A-Vit lotion was diluted with dichloromethane before injection. Noscaphan syrup was diluted with water before injection.

Detection

UV detection was used for all the samples and the wavelength was 254 nm except for Atropine Cusi, Nitrobaat, Noscaphan, Prolopa, Trinitrine Papaverine (220 nm) and Buscopan, Trinitrine Caffeinee (235 nm).

Software and hardware

The expert system, LABEL, is implemented in a software tool called KES (Knowledge Engineering System, Software Architecture & Engineering, Arlington, VA, U.S.A.; release 2.3). It runs on Apollo, Vax and IBM/AT computers.

RESULTS AND DISCUSSION

Description of the rules for mobile phase selection

The different decisions that have to be taken for the selection of the mobile phase on a CN column are represented in a decision tree (Fig. 1). The parameters determining the direction followed in the decision tree are primarily the number of compounds to be separated in the sample, the acid–base properties and the hydrophobicity of the compounds of interest. The hydrophobicity of a compound is expressed in this paper as the number of carbon atoms present in the molecule. We are aware that this parameter is not the only important factor for determining the hydrophobic character of a compound but, as will be shown later, it seems to be sufficient for the purposes of this system.
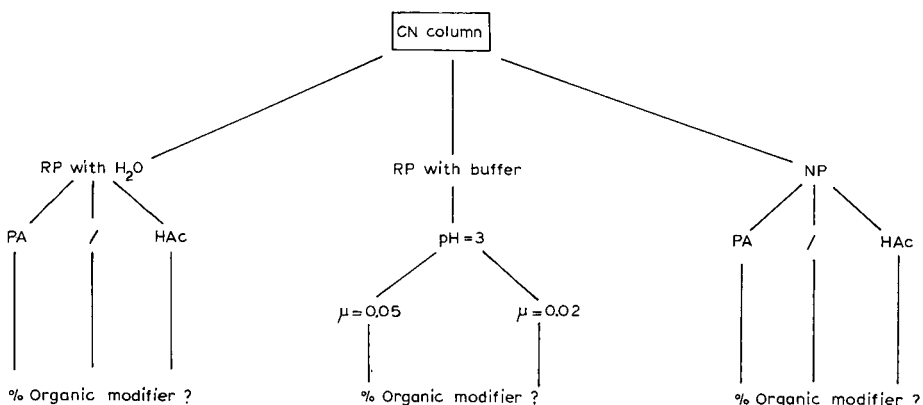
Fig 1. Decision tree for the selection of the mobile phase on a CN column. RP = reversed phase; NP = normal phase; /, no ion-suppressing agent; μ = ionic strength of the buffer.

The number of compounds in the sample and the hydrophobicity of the compounds determine if the RP or the NP mode should be used. For samples with one compound with a carbon number larger than 20 the NP mode is advised, otherwise the RP mode with water is used. For samples containing two or more compounds, the RP mode with water is advised, except when there are two or more compounds with a carbon number smaller than 10, then the NP mode is used.

The addition of ion-suppressing agents to the mobile phase depends on the
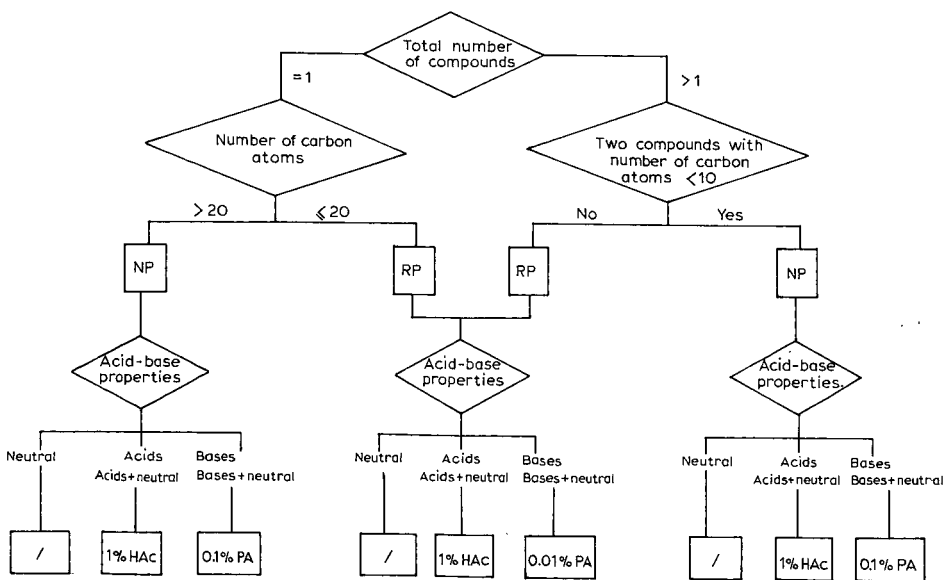
Fig. 2. Pathway followed by the expert system for the selection of the chromatographic mode and the kind of ion-suppressing agent to use in the mobile phase. RP = reversed phase with water; NP = normal phase; /, no ion-suppressing agent.

acid–base status of the compounds to be analysed. Propylamine (PA) is added to the eluting agent when basic drugs or a mixture of basic and neutral compounds are chromatographed (0.01% in the RP mode with water and 0.1% in the NP mode). Acetic acid (HAc) is added to the mobile phase for the chromatography of acidic drugs or mixtures of acidic and neutral compounds (1% HAc in the NP mode and the RP mode with water). The parameters that are important for the mobile phase selection and the relationship between them are outlined in Fig. 2.

All the rules formulated so far are abrogated when the following situations occur: when the use of electrochemical detection is necessary (which is never the case in this study), when basic and acidic drugs have to be determined in one mixture, when amphoteric compounds are present in the sample and when the sample contains fat-soluble vitamins. The chromatographic mode to use in the first three situations is RP with buffer. When the sample contains fat-soluble vitamins, the chromatographic mode advised is NP. More details are given in ref. 9.

For the determination of the acid–base status of a compound, the expert system can give some advice if the end user does not know it. The acid–base status of a compound can be determined by the expert system in three different ways. First, a list of different classes of drugs is available, wherein the compounds are classified as acidic, basic or neutral drugs. Second, the acid–base status of a compound is determined by the expert system by considering the anion or the cation accompanying the active compound[11]. Finally, it is also possible to know the acid–base status of a drug by considering the presence of functional groups in the molecule. There is a list available wherein different functional groups are classified as strongly basic, weakly basic, strongly acidic and weakly acidic[11]. Depending on the presence of these groups in the chemical structure, a compound can be classified as basic or acidic. More details of the determination of the acid–base status are given in ref. 9. The expert system LABEL also gives the starting mobile phase composition in the chromatographic mode selected. This mobile phase composition is not the optimal one for the sample being chromatographed. The main condition required of the starting mobile phase composition is that the solutes are chromatographed in a suitable capacity factor range. For the determination of the optimal mobile phase composition, the existing optimization strategies can be coupled to the expert system. These optimization strategies can then take the starting mobile phase composition as a starting point.

In all the chromatographic modes, the number of carbon atoms of a compound is also an important parameter for the selection of the starting mobile phase composition. The mean of all the carbon atoms in a sample is calculated and this value determines the volume percentage of organic modifier to use in the starting mobile phase composition. In the RP mode, methanol is used as organic modifier and in the NP mode, dichloromethane. An overview of the rules in the different chromatographic modes is presented in Table II. In the RP with buffer mode the volume percentage of organic modifier is restricted to 70% in order to avoid solubility problems with the buffer solution. From Table II, one observes that in the RP with water mode, two sets of rules determining the starting mobile phase composition are formulated: a distinction is made when basic drugs on the one hand and acidic or neutral drugs on the other have to be analysed. A larger volume percentage of organic modifier in the mobile phase is necessary for the chromatography of basic drugs in order to obtain suitable capacity factors for the solutes chromatographed because of the stronger interaction

of the basic compounds with the residual silanol groups. In the RP with buffer mode three classes of rules are distinguished depending on the kind of drugs to be analysed: the first is applied when basic, neutral or mixtures of both are chromatographed, the second for acidic and mixtures of acidic and neutral drugs and the third for mixtures of basic, acidic and neutral compounds. In this last class of rules, a subdivision is made depending on the number of acidic and basic drugs present in the sample. A larger volume percentage of organic modifier is needed when the number of basic drugs is larger than the number of acidic compounds[7]. The first two classes of rules in the RP with buffer mode are usually applied when electrochemical detection is necessary or when the samples contain amphoteric compounds, which are then considered as neutral compounds for the selection of the starting mobile phase composition (see also Table II).

For the buffer solution, one usually applies a pH of 3 and an ionic strength of 0.05 (ref. 7). An exception is made when electrochemical detection in the oxidative mode is used for solutes with a number of carbon atoms smaller than 10. In this instance an ionic strength of 0.02 is used for the buffer solution.

The expert system also contains rules to determine if a gradient elution is suitable for a certain separation problem. When the difference in the number of carbon atoms between two solutes in a mixture is larger than 15, the expert system advises, in addition to an isocratic mobile phase composition, also a gradient elution.

Validation of the rules for mobile phase selection

Initially, 50 pharmaceutical formulations were selected at random from the Belgian Drug repertory 1987. For the different formulations, LABEL was consulted to obtain an HPLC system. For six pharmaceutical formulations, no mobile phase was advised as these samples contain compounds that cannot be determined by UV or electrochemical detection in the oxidative mode. The validation was then performed on the 44 remaining pharmaceutical formulations. In this set, there are thirty formulations with one active compound, nine with two, three with three, one with four and one with five. In the pharmaceutical formulations containing acetylsalicylic acid a supplementary compound, namely salicylic acid, is taken into account to establish the mobile phase composition, as the latter is a known major degradation product of the former.

Two criteria have to be fulfilled in order to be able to conclude that the recommended chromatographic mode and the starting mobile phase composition are suitable for the pharmaceutical formulation being analysed. The first is that the compounds have to elute with a capacity factor (k') between 0.5 and 10 and the second is that the asymmetry factor (a_S) calculated at 10% of the peak height should not exceed 2. These limits take into account that the mobile phase composition given by the expert system is considered as a starting point, a first guess, and not as an optimal one. In the latter instance, the range for the criteria would have been more restricted.

Table III shows the k' and a_S values obtained in the recommended HPLC systems for all the drugs in the pharmaceutical formulations. For 36 pharmaceutical preparations, the two criteria are fulfilled. For Afebryl, Sedergine and Hoofdpijn- en Zenuwpijn poeders, all containing acetylsalicylic acid, different k' values, situated in the required range, are obtained although the same mobile phase composition is used. This is due to the fact that different CN columns were used. For Migraine Kranit

TABLE II

RULES FOR THE DETERMINATION OF THE STARTING MOBILE PHASE COMPOSITION IN THE DIFFERENT CHROMATOGRAPHIC MODES

$$C_i = \frac{C_1 + C_2 + \ldots + C_n}{n}$$

where C_i is the mean of the number of carbon atoms of all the compounds in the sample, $C_1, C_2, \ldots, C_n$ are the number of carbon atoms in compound $1, 2, \ldots, n$ and n is the number of compounds in the sample.

Mode*	C_i	Mobile phase
NP (with PA, HAc and /)	$C_i < 5 \rightarrow 70\%$	dichloromethane
	$5 \leqslant C_i < 10 \rightarrow 65\%$	dichloromethane
	$10 \leqslant C_i < 15 \rightarrow 60\%$	dichloromethane
	$15 \leqslant C_i < 20 \rightarrow 55\%$	dichloromethane
	$20 \leqslant C_i < 25 \rightarrow 50\%$	dichloromethane
	$25 \leqslant C_i < 30 \rightarrow 45\%$	dichloromethane
	$30 \leqslant C_i < 35 \rightarrow 40\%$	dichloromethane
	$35 \leqslant C_i < 40 \rightarrow 35\%$	dichloromethane
	$40 \leqslant C_i < 45 \rightarrow 30\%$	dichloromethane
	$C_i \geqslant 45 \rightarrow 25\%$	dichloromethane
RP with water (with HAc or /)	$C_i < 5 \rightarrow 5\%$	methanol
	$5 \leqslant C_i < 10 \rightarrow 10\%$	methanol
	$10 \leqslant C_i < 15 \rightarrow 25\%$	methanol
	$15 \leqslant C_i < 20 \rightarrow 40\%$	methanol
	$20 \leqslant C_i < 25 \rightarrow 55\%$	methanol
	$25 \leqslant C_i < 30 \rightarrow 70\%$	methanol
	$30 \leqslant C_i < 35 \rightarrow 85\%$	methanol
	$C_i \geqslant 35 \rightarrow 100\%$	methanol
RP with water (with PA)	$C_i < 5 \rightarrow 35\%$	methanol
	$5 \leqslant C_i < 10 \rightarrow 45\%$	methanol
	$10 \leqslant C_i < 15 \rightarrow 55\%$	methanol
	$15 \leqslant C_i < 20 \rightarrow 65\%$	methanol
	$20 \leqslant C_i < 25 \rightarrow 75\%$	methanol
	$25 \leqslant C_i < 30 \rightarrow 85\%$	methanol
	$30 \leqslant C_i < 35 \rightarrow 95\%$	methanol
	$C_i \geqslant 35 \rightarrow 100\%$	methanol
RP with buffer (the sample contains basic, neutral or basic + neutral drugs)**	$C_i < 5 \rightarrow 5\%$	methanol
	$5 \leqslant C_i < 10 \rightarrow 10\%$	methanol
	$10 \leqslant C_i < 15 \rightarrow 20\%$	methanol
	$15 \leqslant C_i < 20 \rightarrow 30\%$	methanol
	$20 \leqslant C_i < 25 \rightarrow 40\%$	methanol
	$25 \leqslant C_i < 30 \rightarrow 50\%$	methanol
	$30 \leqslant C_i < 35 \rightarrow 60\%$	methanol
	$C_i \geqslant 35 \rightarrow 70\%$	methanol
RP with buffer (the sample contains acidic or acidic + neutral drugs)**	$C_i < 5 \rightarrow 3\%$	methanol
	$5 \leqslant C_i < 10 \rightarrow 5\%$	methanol
	$10 \leqslant C_i < 15 \rightarrow 10\%$	methanol
	$15 \leqslant C_i < 20 \rightarrow 15\%$	methanol
	$20 \leqslant C_i < 25 \rightarrow 20\%$	methanol
	$25 \leqslant C_i < 30 \rightarrow 25\%$	methanol
	$30 \leqslant C_i < 35 \rightarrow 30\%$	methanol
	$35 \leqslant C_i < 40 \rightarrow 35\%$	methanol
	$C_i \geqslant 40 \rightarrow 40\%$	methanol

TABLE II *(continued)*

Mode*	C_i	Mobile phase	
RP with buffer [the sample	$C_i < 5 \rightarrow 5\%$	methanol	
contains basic + acidic or	$5 \leqslant C_i < 10 \rightarrow 10\%$	methanol	
basic + acidic + neutral drugs	$10 \leqslant C_i < 15 \rightarrow 20\%$	methanol	
and the number of acidic	$15 \leqslant C_i < 20 \rightarrow 30\%$	methanol	
drugs < the number of (basic	$20 \leqslant C_i < 25 \rightarrow 40\%$	methanol	
+ neutral drugs)]	$25 \leqslant C_i < 30 \rightarrow 50\%$	methanol	
	$30 \leqslant C_i < 35 \rightarrow 60\%$	methanol	
	$C_i \geqslant 35 \rightarrow 70\%$	methanol	
RP with buffer [the sample	$C_i < 5 \rightarrow 5\%$	methanol	
contains basic + acidic or	$5 \leqslant C_i < 10 \rightarrow 10\%$	methanol	
basic + acidic + neutral drugs	$10 \leqslant C_i < 15 \rightarrow 15\%$	methanol	
and the number of acids $\geqslant$	$15 \leqslant C_i < 20 \rightarrow 20\%$	methanol	
the number of (basic +	$20 \leqslant C_i < 25 \rightarrow 25\%$	methanol	
neutral drugs)]	$25 \leqslant C_i < 30 \rightarrow 30\%$	methanol	
	$30 \leqslant C_i < 35 \rightarrow 35\%$	methanol	
	$35 \leqslant C_i < 40 \rightarrow 40\%$	methanol	
	$C_i \geqslant 40 \rightarrow 45\%$	methanol	

* NP = normal phase; RP = reversed phase; PA = propylamine; HAc = acetic acid; / = no ion-suppressing agent.
** For the selection of the starting mobile phase composition, the amphoteric drugs have been considered as neutral compounds.

tablets, the expert system advises an isocratic mobile phase composition and a gradient elution as this formulation contains solutes for which the difference in the number of carbon atoms is larger than 15 [caffeine (C_8), paracetamol (C_8) and ethaverine hydrochloride (C_{24})]. Both chromatographic systems give suitable results for this particular case and one would prefer the isocratic one for analysis.

For eight formulations the criteria are not fulfilled: Atropine Cusi, Buscopan, Desclidium, Masteron, Noscaphan, Priamide, Prolopa and Vesalium. For these formulations, the separation strategy with the gradient elution, developed in our laboratory[4-6], has then been carried out as an alternative, to check if the selected chromatographic mode is not suitable or if the advised starting mobile phase composition for these samples is not appropriate. The separation strategy consists in carrying out a gradient elution from which an isocratic mobile phase composition with a suitable solvent strength is determined so that the drugs elute within a suitable k' range. To obtain the isocratic mobile phase composition from the gradient elution, the geometric mean of the volume percentages of organic modifier at which each drug elutes in the gradient elution is calculated and multiplied with an experimentally determined factor, 3/4 (refs. 4-6).

For Atropine Cusi, the mobile phase composition calculated from the gradient elution was methanol–water–PA (75:25:0.01) and resulted in $k' = 11.7$ and $a_S = 2.5$. Neither of the two strategies gives an acceptable solution. A mobile phase composed of methanol–PA (100:0.01) did result in a k' value of 6.3 but the a_S value was still 2.1. This suggests that the advised RP with water mode is not suitable for this compound. The same conclusion can be drawn for Buscopan because in the NP mode the active

TABLE III

k' VALUES AND a_S VALUES OF THE COMPOUNDS IN THE MOBILE PHASE SYSTEM RECOMMENDED BY THE EXPERT SYSTEM.

No.[*]	Active compounds	Recommended mobile phase system[**]	k'	a_S
1	Hydrocortisone sodium succinate	NP with HAc CH_2Cl_2–Hex–HAc (45:55:1)	2.0	1.2
2	Tretinoine	NP with HAc CH_2Cl_2–Hex–HAc (50:50:1)	1.0	1.1
3	Acetylsalicylic acid Ascorbic acid Paracetamol (Salicylic acid)	NP with HAc CH_2Cl_2–Hex–HAc (65:35:1)	2.0 8.4 2.3 2.5	1.1 1.5 1.1 1.1
4	Paracetamol Promethazine hydrochloride	RP with buffer CH_3OH–B (15:85)	0.6 5.5	1.0 1.5
5	Cyproteronacetate	NP with / CH_2Cl_2–Hex (45:55)	4.7	1.4
6	Retinol	NP with / CH_2Cl_2–Hex (50:50)	1.7	1.0
7	Merbromin	RP with HAc CH_3OH–H_2O–HAc (55:45:1)	0.7	1.0
8	Atropine sulphate	RP with PA CH_3OH–H_2O–PA (65:35:0.01)	17.0	3.0
9	Thiamine hydrochloride	RP with PA CH_3OH–H_2O–PA (55:45:0.01)	0.7	1.0
10	Hyoscine butylbromide	NP with PA CH_2Cl_2–Hex–PA (50:50:0.1)	>20	/
11	Metamizol Hyoscine butylbromide	RP with buffer CH_3OH–B (20:80)	0.5 1.3	1.0 1.1
12	Allobarbital Propyphenazone	RP with HAc CH_3OH–H_2O–HAc (25:75:1)	0.6 1.2	1.2 1.3
13	Viquidil hydrochloride	RP with PA CH_3OH–H_2O–PA (75:25:0.01)	17.5	1.6
14	Glafenine	RP with PA CH_3OH–H_2O–PA (65:35:0.01)	0.6	1.1
15	Metronidazole	RP with / CH_3OH–H_2O (10:90)	0.8	1.1
16	Clobazam	RP with / CH_3OH–H_2O (40:60)	1.2	1.0

TABLE III *(continued)*

No.[*]	Active compounds	Recommended mobile phase system[**]	k'	a_S
17	Haloperidol	NP with PA CH$_2$Cl$_2$–Hex–PA (50:50:0.1)	1.8	1.0
18	Acetylsalicylic acid	NP with HAc	1.2	1.1
	Phenacetin	CH$_2$Cl$_2$–Hex–HAc	3.9	1.3
	Caffeine	(65:35:1)	4.6	1.4
	(Salicylic acid)		1.9	1.1
19	Propanolol hydrochloride	RP with PA CH$_3$OH–H$_2$O–PA (65:35:0.01)	7.6	1.8
20	Opipramol hydrochloride	NP with PA CH$_2$Cl$_2$–Hex–PA (50:50:0.1)	4.9	1.5
21	Verapamil hydrochloride	NP with PA CH$_2$Cl$_2$–Hex–PA (45:55:0.1)	0.9	1.0
22	Quinupramine	NP with PA CH$_2$Cl$_2$–Hex–PA (50:50:0.1)	9.7	1.2
23	Chlorpromazine	RP with PA CH$_3$OH–H$_2$O–PA (65:35:0.01)	5.9	1.1
24	Drostanolone propionate	NP with / CH$_2$Cl$_2$–Hex (50:50)	>20	/
25	Caffeine	RP with Buffer	0.8	1.0
	Phenobarbital	CH$_3$OH–B	1.1	1.0
	Paracetamol	(20:80)	0.6	1.0
	Propyphenazone		1.9	1.2
	Ethaverine hydrochoride		5.0	1.5
25	Caffeine	Gradient elution	1.3	1.0
	Phenobarbital	CH$_3$OH–B (0:100)	1.9	1.0
	Paracetamol	⌈ 20 min	0.9	1.0
	Propyphenazone	⌊	4.1	1.1
	Ethaverine hydrochloride	CH$_3$OH–B (50:50)	6.6	1.1
26	Glipizide	NP with HAc CH$_2$Cl$_2$–Hex–HAc (50:50:1)	10.7	1.9
27	Mofebutazon	RP with HAc CH$_3$OH–H$_2$O–HAc (25:75:1)	1.1	1.1
28	Papaverine	RP with PA	0.6	1.0
	Quinine hydrochoride	CH$_3$OH–H$_2$O–PA (75:25:0.01)	2.1	1.0
29	Nalidixic acid	RP with HAc CH$_3$OH–H$_2$O–HAc (25:75:1)	1.3	1.9
30	Nitroglycerin	RP with HAc CH$_3$OH–H$_2$O–HAc (5:95:1)	2.3	1.3

TABLE III (continued)

No.[*]	Active compounds	Recommended mobile phase system[**]	k'	a_S
31	Guaifenesin	RP with PA	0	/
	Dextromethorphan hydrobromide	CH$_3$OH–H$_2$O–PA (65:35:0.01)	0.3	1.0
	Noscapine hydrochloride		0.5	1.0
32	Carbinoxamine maleate	RP with PA CH$_3$OH–H$_2$O–PA (65:35:0.01)	5.9	1.3
33	Isopropamide iodide	NP with PA CH$_2$Cl$_2$–Hex–PA (50:50:0.1)	>20	/
34	Metoclopramide hydrochloride	RP with PA CH$_3$OH–H$_2$O–PA (55:45:0.01)	10.2	1.5
35	Levodopa	RP with buffer	0.3	1.0
	Benserazide	CH$_3$OH–B (10:90)	0.5	1.0
36	Acetylsalicylic acid	NP wih HAc	2.0	1.1
	Ascorbic acid	CH$_2$Cl$_2$–Hex–HAc	8.4	1.5
	(Salicylic acid)	(65:35:1)	2.5	1.1
37	Triclocarban	RP with / CH$_3$OH–H$_2$O (25:75)	10.0	1.6
38	Cimetidine	RP with PA CH$_3$OH–H$_2$O–PA (55:45:0.01)	0.7	1.0
39	Thiethylperazine dimaleate	NP with PA CH$_2$Cl$_2$–Hex–PA (50:50:0.1)	2.5	1.3
40	Nitroglycerin	NP with HAc	2.0	1.2
	Caffeine	CH$_2$Cl$_2$–Hex–HAc (65:35:1)	3.8	1.8
41	Nitroglycerin	RP with buffer	2.2	1.0
	Papaverine hydrochloride	CH$_3$OH–B (15:85)	2.7	1.4
42	Sulphadiazine	RP with buffer	1.0	1.0
	Sulphamerazine	CH$_3$OH–B	1.0	1.0
	Sulphathiazole	(15:85)	1.2	1.0
	Phenazopyridine hydrochloride		1.3	1.2
43	Cinepazet maleate	NP with PA CH$_2$Cl$_2$–Hex–PA (50:50:0.1)	2.2	1.2
44	Isopropamide iodide	RP with PA	0	/
	Haloperidol	CH$_3$OH–H$_2$O–PA (75:25:0.01)	1.0	1.0

  [*] The numbers correspond to the pharmaceutical formulations in Table I.
  [**] RP = reversed phase; NP = normal phase; B = buffer solution (see Experimental); HAc = acetic acid; Hex = n-hexane; PA = propylamine; / (in the recommended mobile phase system) = no ion-suppressing agent).

compound, hyoscine butylbromide, does not elute, even with the gradient elution. However, it is possible to chromatograph it in the RP with buffer mode (see Buscopan Compositum).

For Desclidium, the condition of the asymmetry factor is fulfilled but the mobile phase composition given by the expert system and that determined from the gradient elution resulted in too strong a retention. When 100% methanol (containing 0.01% of PA) is used a k' value of 8.5 is recorded. The same phenomenon is observed for Masteron. The expert system advises a mobile phase composition of methanol–water–PA (50:50:0.01), with which the drug is not eluted. The isocratic composition calculated from the gradient elution is methanol–water–PA (75:25:0.01), resulting in $k' = 17.5$ and $a_S = 1.8$. By increasing the proportion of methanol, the k' value obtained falls within the required range.

For two of the three drugs present in the Noscaphan syrup, the proposed mobile phase composition (methanol–water–PA; 65:35:0.01) gives too small a retention. With the separation strategy, a mobile phase composed of methanol–water–PA (30:70:0.01) is used and both criteria are fulfilled for two of the three drugs. The other drug, guaiphenesin, possesses ten carbon atoms, which is a limiting value for exhibiting retention on a CN column in the RP mode. To obtain a smaller k' value for isopropamide iodide in Priamide, 100% dichloromethane (containing 0.1% of PA) was used, but even then a k' value of 15 and an a_S value of 1.3 were recorded. These results suggest that the NP mode is not to be recommended, but this compound has also been chromatographed in the RP mode (see Vesalium) without success as it exhibits no retention. Isopropamide iodide is a quaternary ammonium derivative and ion-pair chromatography would perhaps offer a suitable solution[12]. Prolopa capsules contain levodopa, which does not exhibit sufficient retention on a CN column in the RP mode, even without an organic modifier in the mobile phase. Levodopa belongs to the group of the catecholamines, for which ion-par chromatography has been used in many studies.

A possible solution for the exceptions revealed by carrying out the validation step is to put them in a database that could be coupled to the expert system. This database could then be continuously updated when more pharmaceutical preparations are analysed.

Sample preparation

As the set of pharmaceutical preparations contain different dosage forms, different approaches for the sample preparation were applied. In the RP mode, usually methanol was applied for the dissolution of the active compounds and the dilution was performed with water. In the NP mode, dichloromethane was the solvent for dissolution and *n*-hexane for dilution. In some instances, problems of solubility occurred when water in the RP or *n*-hexane in the NP mode was used for the dilution. The dilution was then performed with the mobile phase rather than with the solvents for dissolution. When the solvent in which the compounds are dissolved possesses a stronger solvent strength than the mobile phase, the compounds are chromato-graphed with a bad peak shape[13]. This phenomenon is illustrated in Fig. 3, where cinepazet maleate, the active compound of Vascoril tablets was diluted with different solvents. The sample preparation was carried out in the first instance as described under Experimental for the determination in the NP mode, *viz.*, dissolution in
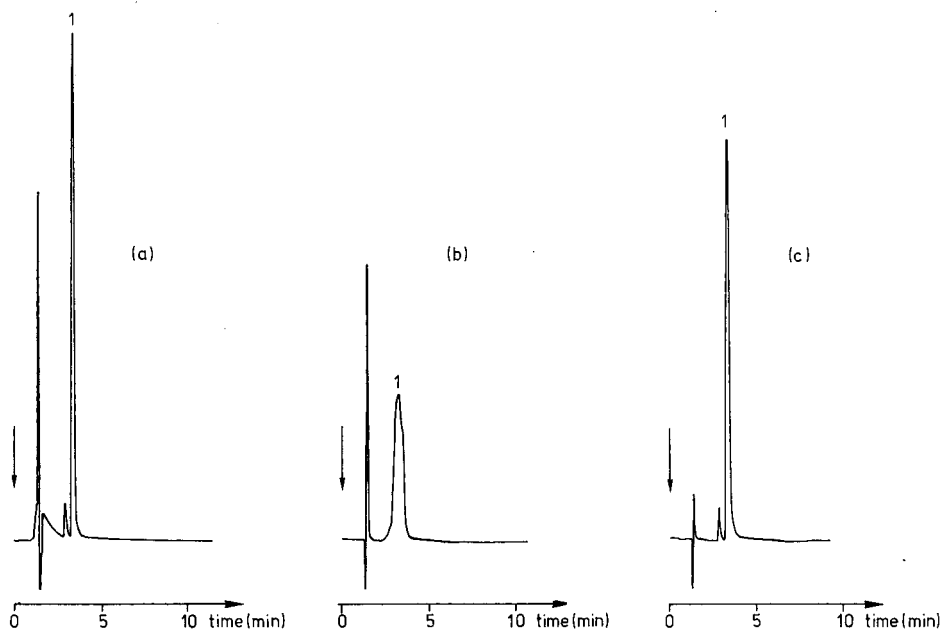
Fig. 3. Chromatograms obtained after injection of cinepazet maleate in different solution solvents: (a) *n*-hexane; (b) dichloromethane; (c) the mobile phase. The same concentration was injected. Mobile phase: dichloromethane–*n*-hexane–PA (50:50:0.1).

dichloromethane and dilution with *n*-hexane (Fig. 3a). A good peak shape was observed for this drug. However, after a certain time, problems arose because cinepazet maleate was only sparingly soluble in *n*-hexane. Therefore, the dilution was performed with dichloromethane and the chromatogram obtained (Fig. 3b) had a bad peak shape. Fig. 3c shows the chromatogram obtained when the dilution was performed with the mobile phase, which gave an acceptable result. This phenomenon was not observed for all compounds (see Experimental). For example, Acid A Vit lotio, containing tretinoine, is an ethanolic solution that has been diluted with dichloromethane and a good peak shape is obtained although the solvent strength of the injected solvent is stronger than that of the mobile phase. For Algotropyl suppositories, the supernatant was injected in a methanolic solution without problems of peak shape.

For some pharmaceutical preparations, an ion-pair extraction, which has been used in our laboratory for the determination of basic drugs in pharmaceutical preparations and in biological materials[14,15], was necessary to permit the determination of the active compounds in the chromatographic mode selected. This applied, for example, to Insidon and Torecan tablets, containing opipramol hydrochloride and thiethylperazine dimaleate, respectively. The expert system advises the NP mode, but these compounds are not soluble in dichloromethane. Dissolution in methanol and dilution with dichloromethane resulted in a broad solvent peak and a bad peak shape. This problem was solved by carrying out an ion-pair extraction with sodium octylsulphate as counter ion. The chloroform phase was then diluted with the mobile

phase. The same procedure also has to be applied to Haldol ampoules, as they contain an aqueous solution of haloperidol which was not compatible with the NP system selected. For Masteron ampoules, dilution with dichloromethane was possible as these ampoules contain an oil solution of drostanolone propionate.

The expert system advises the NP mode for both of the effervescent tablets, although the tablets must first be dissolved in water. In this way, it was necessary to carry out an extraction with a solvent that was miscible with the mobile phase. With a classical liquid–liquid extraction, it was not possible to extract the compounds of interest into the organic phase. Then, an ion-pair extraction with tri-*n*-octylamine, which has been applied in our laboratory for the extraction of colour additives[16], was used with success.

CONCLUSION

The rules incorporated in an expert system for the selection of suitable mobile phase systems for the chromatography of drugs in pharmaceutical preparations on a CN column were validated. It is possible to formulate these rules using a fairly rough parameter for the determination of the hydrophobic character of a compound, namely the number of carbon atoms in a molecule. The selection of one of the three chromatographic modes which can be used on a CN column was performed in addition to the determination of a starting mobile phase composition. In 82% of all instances, success was achieved in a manner that probably could not have been done better by a human chromatographic expert. In three of the eight remaining instances, simple adaptation of the volume ratio of the mobile phase solvents was sufficient. For the other five pharmaceutical formulations, it can be concluded that the selected chromatographic mode was not appropriate, which was also confirmed by the results obtained with the separation strategy involving gradient elution.

The use of an expert system for HPLC methods in a laboratory has the advantage that technicians or other workers with less chromatographic experience are able to start an analysis without the help or intervention of the chromatographic expert. The expert system can always be updated with new knowledge and rules. LABEL was developed for use with the CN column only. However, this column type is very interesting as it can be applied in different chromatographic modes. If one had chosen different stationary phase types to apply in the RP and NP modes, the number of rules would have been larger because, in that event, supplementary rules would be necessary to decide between the column types to use.

The rules formulated in this paper were developed for the chromatography of drugs on a certain type of CN column, namely a LiChrosorb CN column. Probably, if the rules were to be transferred to another type of CN column from a different manufacturer different results would be obtained. It is well known that even different columns from the same manufacturer, packed with the same type of stationary phase but emanating from different batches, can provide different results. It is then not possible, for a certain separation problem, to transfer unchanged the chromatographic system developed on one column to another. However, the results given in this paper were obtained on four different LiChrosorb CN columns so that the problem of column reproducibility has been taken into account in this validation. It can be stated that this problem does not influence the success of finding a suitable HPLC system

with the two criteria used and their range premised. It should be suitable for the rules developed for this kind of CN column to be transferred to the same type of columns emanating from a different manufacturer by carrying out only small modifications. This study is now under investigation.

In this paper, rules were also validated for the selection of the starting mobile phase composition for a certain separation problem. In previous papers, a separation strategy was described in which a suitable solvent strength for isocratic elution was determined from a gradient elution. This strategy was also applied in this paper to samples for which the expert system does not give a suitable solution and, in most instances, does not give an appropriate solution either. Comparing the two strategies, one can state that with the expert system it is possible to find a suitable mobile phase composition by carrying out one experiment. This is certainly not valid for the separation strategy, as one has first to perform a gradient elution and afterwards an isocratic elution, resulting in a minimum of two experiments. When some compounds coelute in the gradient elution, the position of each compound has to be determined as one has to know the volume percentage at which each compound elutes for the determination of the mobile phase composition in the isocratic elution. At the other hand, the separation strategy can be carried out on CN columns emanating from any manufacturer or even on another column type, whereas this is not true for the expert system. In this way, one would more quickly obtain a suitable HPLC system with the separation strategy.

Some attention has also been paid to the sample preparation of the pharmaceutical preparations. Despite the fact that no general approach has been formulated in LABEL until now, one can state that for some formulations, one can certainly incorporate in the expert system some more general rules about the dissolution and dilution of the samples in relation to the chromatographic mode used. This aspect will be incorporated in the expert system and further validated.

ACKNOWLEDGEMENTS

REFERENCES

1 J. C. Berridge, *Techniques for the Automated Optimization of HPLC Separations*, Wiley-Interscience, New York, 1985.
2 P. J. Schoenmakers, *Optimization of Chromatograhic Selectivity*, Elsevier, Amsterdam, 1986.
3 S. R. Abboth, *J. Chromatogr. Sci.*, 18 (1980) 540.
4 M. De Smet, G. Hoogewijs, M. Puttemans and D. L. Massart, *Anal. Chem.*, 56 (1984) 2662.
5 M. De Smet and D. L. Massart, *J. Pharm. Biomed. Anal.*, 6 (1988) 277.
6 M. De Smet and D. L. Massart, *J. Liq. Chromatogr.*, in press.
7 M. De Smet and D. L. Massart, *J. Chromatogr.*, 410 (1987) 77.
8 Y. Z. Hu, A. Peeters, G. Musch and D. L. Massart, *Anal. Chim. Acta*, in press.
9 M. De Smet, G. Musch, A. Peeters, L. Buydens and D. L. Massart, *Anal. Chem.*, in press.
10 G. Musch and D. L. Massart, in preparation.
11 M. R. De Taevernier, Y. Michotte, L. Buydens, M. P. Derde, M. De Smet, L. Kaufman, G. Musch, J. Smeyers-Verbeke, A. Thielemans, L. Dryon and D. L. Massart, *J. Pharm. Biomed. Anal.*, 4 (1986) 297.
12 J. A. De Schutter and P. De Moerloose, *J. Chromatogr.*, 437 (1988) 83.
13 L. R. Snyder and J. J. Kirkland, *Introduction to Modern Liquid Chromatography*, Wiley-Interscience, New York, 1979, Ch. 19.
14 G. Hoogewijs and D. L. Massart, *J. Pharm. Biomed. Anal.*, 2 (1984) 449.
15 G. Hoogewijs and D. L. Massart, *J. Pharm. Biomed. Anal.*, 3 (1985) 165.
16 M. Puttemans, L. Dryon and D.L. Massart, *Anal. Chim. Acta*, 165 (1984) 245.

CHROM. 20 950

NUMERICAL SIMULATION OF COLUMN PERFORMANCE IN ION-EXCLUSION CHROMATOGRAPHY

BRONISŁAW K. GŁÓD*, ANDRZEJ PIASECKI and JANUSZ STAFIEJ

Polish Academy of Sciences, Institute of Physical Chemistry, Kasprzaka 44/52, 01-224 Warsaw (Poland)

SUMMARY

The separation mechanism of acidic compounds in ion-exclusion chromatography has been described using two approaches. The first one is based on the global thermodynamic and chromatographic relationships, the other on a computer simulation of the column performance. Strong acids leave the column unseparated, within its dead volume, and weak acids appear at the end of the chromatogram also unseparated. It was found that the addition of an acidic compound eliminates the dependence of the retention volume on the sample concentration. By use of the computer simulations, the evolution of the chromatographic peaks with time and the peak shape for the sample analyzed have been studied. The results compare favourably with the experimental data available in the literature.

INTRODUCTION

Ion-exclusion chromatography (IEC) has been described as an efficient method for the separation of ionic species[1–8]. Qualitatively, the primary mechanism of separation is based on the following phenomenon: neutral molecules penetrate the cation exchange resin while anions are repulsed — in other words excluded from it[1]. This has been confirmed by Tanaka *et al.*[9] who have shown that the dependence of the distribution coefficient, K_d, on the pK_a values of various acidic compounds is analogous to the dependence of K_d on the logarithm of the molecular weight in size exclusion chromatography.

A more quantitative description of these findings has been attempted[10] and the following formula was derived:

$$K_d = [1 + 2c/K_a - (1 + 8c/K_a)^{1/2}]/(2c/K_a - 2) \tag{1}$$

where K_a is the dissociation constant of the acid analyzed and c is the maximum peak concentration of the sample. The latter quantity can be evaluated only approximately or has to be determined experimentally.

In this work we have developed a more accurate approach towards the quantitative description of the separation mechanism in IEC. In this approach some simplifying assumptions used when deriving eqn. 1 are abandoned; K_d cannot be

expressed in a closed form as in eqn. 1 and has to be evaluated numerically as a function of the parameters characterizing the sample, the column, the mobile and the stationary phases. The influence of these parameters on K_d is the subject of the present study. The use of an acidic compound to buffer the mobile phase is advantageous in IEC in some instances because it eliminates the dependence of the distribution coefficient on the sample concentration. A numerical simulation of the column performance using the finite element method has also been performed. This method provides additional information on the influence of the above parameters on the peak shape.

For convenience all symbols used in this work are listed below:

c Overall concentration of the sample in the peak volume
c_i Sample concentration injected
c_b Buffer concentration
c_{bM} Buffer concentration in the mobile phase
c_{bS} Buffer concentration in the stationary phase
c_f Functional group concentration in the support
c_M Sample concentration in the mobile phase
c_S Sample concentration in the stationary phase
K_a Dissociation constant of compound analyzed
K_b Dissociation constant of buffering compound
K_d Global distribution coefficient
k_d Local distribution coefficient
K_f Dissociation constant of resin functional group
m Sample mass corresponding to a theoretical plate
m_b Buffer mass corresponding to a theoretical plate
N Number of theoretical plates of the column
V_i Sample volume injected
V_M Column dead volume
v_M V_M/N
V_P Peak volume
V_R Retention volume
V_S Inner volume of the column
v_S V_S/N

FORMULATION OF THE MODEL

The following assumptions are involved in our model.

(1) Homogeneity of the column, implying that the ratio of the volume of the mobile phase to the volume of the stationary phase, as well as the mobile phase flow-rate, are constant along the column length.

(2) The influence of the axial diffusion of the sample and kinetic effects can be neglected.

(3) The separation in IEC is dominated by a Donnan membrane equilibrium mechanism and can be described by the following set of equations [cf., eqns. 3–7 of ref. 10]

$$[H^+]_M[R^-]_M[HR]_M = [H^+]_S[R^-]_S[HR]_S \tag{2}$$

$$[H^+]_M[B^-]_M[HB]_M = [H^+]_S[B^-]_S[HB]_S \tag{3}$$

$$K_a = [H^+]_M[R^-]_M/[HR]_M \tag{4}$$

$$K_b = [H^+]_M[B^-]_M/[HB]_M \tag{5}$$

$$K_f = [H^+]_S[F^-]_S/[HF]_S \tag{6}$$

$$[H^+]_M = [R^-]_M + [B^-]_M \tag{7}$$

$$[H^+]_S = [F^-]_S + [R^-]_S + [B^-]_S \tag{8}$$

$$[HR]_M = [HR]_S \tag{9}$$

$$[HB]_M = [HB]_S \tag{10}$$

where HR, HB and HF are the formulae of the sample acidic compound, of the acid used as a buffer and of the acidic functional group of the resin respectively. The subscripts M and S refer to the mobile phase and to the stationary phase respectively. In the above equations it is assumed that the properties of the solvent in the stationary phase are the same as those in the mobile phase.

The overall buffer and functional group concentrations can be expressed as

$$c_b = [B^-]_M + [HB]_M \tag{11}$$

$$c_f = [F^-]_S + [HF]_S \tag{12}$$

For a specified amount of the acidic sample, its equilibrium concentration in specified volumes of the mobile and the stationary phases can be calculated on the basis of eqns. 2–12 together with an additional equation expressing the mass conservation for the amount of sample.

In what we call the global approach, it is assumed that the equilibrium conditions apply to the peak volume of the sample:

$$V_P = V_R(2\pi/N)^{1/2} \tag{13}$$

Therefore the sample is distributed between the volumes of the two phases corresponding to the sample peak volume, as expressed by:

$$c_i V_i = \{V_S([R^-]_S + [HR]_S) + V_M([R^-]_M + [HR]_M)\} V_P/(V_M + V_S) \tag{14}$$

The analogous equation in ref. 10 is based on the implicit assumption that the volumes of the mobile and the stationary phases are equal. Eqn. 14 is the mass conservation equation, but the retention volume is not yet specified. In the global approach this can be done by considering the definition of the distribution coefficient and its relationship with the retention volume:

$$K_d = ([R^-]_S + [HR]_S)/([R^-]_M + [HR]_M) \tag{15}$$

$$K_d = (V_R - V_M)/V_S \tag{16}$$

The set of eqns. 2–16 can be solved with respect to the distribution coefficient, K_d, retention volume, V_R, peak volume, V_P, and the twelve concentrations: $[H^+]_M$, $[H^+]_S$, $[R^-]_M$, $[R^-]_S$, $[B^-]_S$, $[B^-]_M$, $[F^-]_S$, $[HR]_M$, $[HR]_S$, $[HB]_M$, $[HB]_S$, $[HF]_S$. The solution is in the form of functions of the parameters K_a, K_b, K_f, c_i, c_b, c_f, V_i, V_M, V_S and N. These functions cannot be obtained in a closed form and a numerical procedure is required. It is fairly simple for pure water as a mobile phase, and assuming complete dissociation of the functional groups in the stationary phase: $c_b = [HF]_S = 0$. If $c = c_i V_i/V_P$ denotes the overall concentration of the sample in the peak volume, then eqn. 14 can be rewritten as:

$$c = \{V_S([R^-]_S + [HR]_S) + V_M([R^-]_M + [HR]_M)\}/(V_M + V_S) \tag{17}$$

After some elementary algebra, eqns. 2–6, 11, 12 and 15–17) yield:

$$c = c_i V_i (N/2\pi)^{1/2}/(K_d V_S + V_M) \tag{18}$$

$$[R^-]_S = (cV_M - [R^-]_M V_M - [R^-]_M^2 V_M/K_a + cV_S - [R^-]_M^2 V_S/K_a)/V_S \tag{19}$$

$$[R^-]_M = \,^1\!/_2 K_a [1 + (4c/K_a)(V_M/V_{S+1})/(K_d + V_M/V_S)]^{1/2} - 1 \tag{20}$$

$$K_d = (V_M/V_S)(c - [R^-]_M - [R^-]_M^2/K_a) + c/([R^-]_M + [R^-]_M^2/K_a) \tag{21}$$

The above equations provide the necessary relations to determine the four unknown quantities: the distribution coefficient, peak concentration, c, and the concentrations $[R^-]_S$ and $[R^-]_M$, as functions of the other parameters. The numerical method adopted is as follows. An arbitrary value, say $1/2$, is ascribed to K_d. On the basis of this value, c and the other unknowns are calculated (eqns. 18–20) as well as the next value of K_d (eqn. 21). The procedure is then repeated until self consistency is reached. The case of the buffered mobile phase can be treated in a similar fashion.

The global approach is inconsistent in that eqns. 2–10 generally determine a non-linear distribution isotherm, while the use of eqns. 13, 15 and 16 is justified only in the linear case. To eliminate this inconsistency a numerical simulation method has been devised in which eqns. 2–10 are applied locally to small fragments of the column corresponding roughly to theoretical plates. The portion of the mobile phase at such a plate is "equilibrated" with the portion of the stationary phase and then "moved" to the next plate simulating the passage of the sample. The "equilibration" amounts to a calculation of the distribution of the amount of the sample compound brought by the incoming portion of the mobile phase plus what remained in the stationary phase. This involves a recurrent procedure implying that the set of eqns. 2–10 and

$$c_S(i,j) = [R^-]_S + [HR]_S \tag{22}$$

$$c_M(i,j) = [R^-]_M + [HR]_M \tag{23}$$

$$m(i,j) = c_S(i - 1, j)v_S + c_M(i - 1, j - 1)v_M \tag{24}$$

$$k_d(i,j) = c_S(i,j)/c_M(i,j) \tag{25}$$

$$c_{bM}(i,j) = [B^-]_M + [HB]_M \tag{26}$$

$$c_{bS}(i,j) = [B^-]_S + [HB]_S \tag{27}$$

$$m_b(i,j) = c_{bM}(i - 1, j)v_M + c_{bS}(i - 1, j - 1)v_S \tag{28}$$

are solved at ith time step and jth plate with the following initial and boundary conditions

$$c_S(0,j) = c_M(0,j) = 0 \text{ for } j = 1, ..., N \tag{29}$$

$$c_{bM}(0,j) = c_b \text{ for } j = 1, ..., N \tag{30}$$

$$c_{bS}(0,j) = c_{bS}{}^0 \tag{31}$$

where $c_{bS}{}^0$ is the buffer concentration in the stationary phase at equilibrium with the mobile phase buffer at a concentration c_b. It can be calculated on the basis of eqns. 2–10 assuming the absence of the sample in the mobile phase:

$$c_M(i,0) = c_i \text{ for } i = 1, ..., V_i/v_m \tag{32}$$

$$c_M(i,0) = 0 \text{ for } i > V_i/v_m \tag{33}$$

$$c_{bM}(i,0) = c_b \text{ for all time steps} \tag{34}$$

The method is suitable for studying the peak evolution with time and its final shape.

RESULTS

Global approach, unbuffered mobile phase

At first we considered the influence of such parameters as c_i, K_a and c_f on the distribution coefficient. We assumed the following values[10]: $V_M = 800 \mu l$, $V_S = 2000$ μl, $V_i = 5 \mu l$, $N = 1000$ and the complete functional group dissociation.

The dependence of the distribution coefficient on the sample concentration for several values of the acid dissociation constant and for the concentration of the functional groups, $c_f = 10^{-3} M$, is presented in Fig. 1. The distribution coefficient is a growing, S-shaped function of the sample concentration. For low and high sample concentrations, K_d is practically constant with the sample concentration. The K_d vs. c_i curves for values of K_a much less than c_f form a set of parallel curves, as is presented in Fig. 2 for several values of K_a and $c_f = 10^3 M$. Also K_d is hardly dependent on c_f for K_a
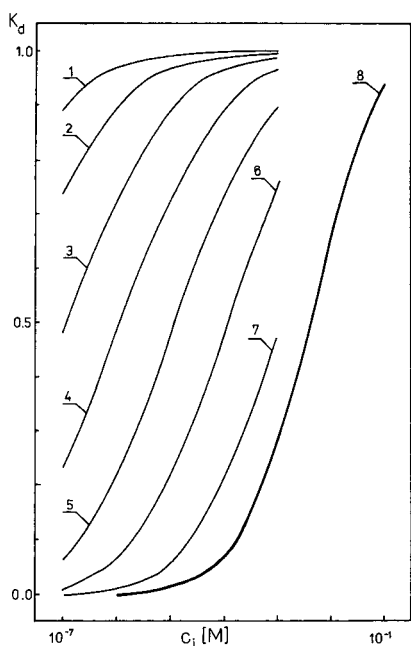
Fig. 1. Dependence of the distribution coefficient, K_d, on sample concentration, c_i, for a concentration of functional groups, $c_f = 10^{-3}$ M, and for several values of the acid dissociation constant, K_a: 1, 10^{-10}; 2, 10^{-9}; 3, 10^{-8}; 4, 10^{-7}; 5, 10^{-6}; 6, 10^{-5}; 7, 10^{-4}; 8, $\geq 10^{-3}$ M. $V_M = 800$ μl, $V_S = 2000$ μl, $V_i = 5$ μl, $N = 1000$.
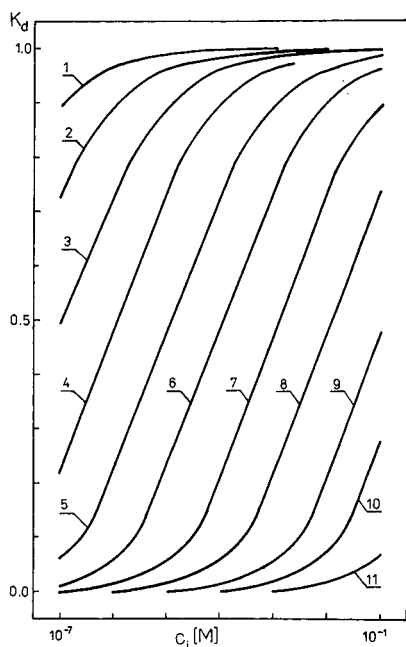
Fig. 2. Dependence of K_d, on c_i for $c_f = 10^3$ M, and for several values of the acid dissociation constant, K_a: 1, 10^{-10}; 2, 10^{-9}; 3, 10^{-8}; 4, 10^{-7}; 5, 10^{-6}; 6, 10^{-5}; 7, 10^{-4}; 8, 10^{-3}; 9, 10^{-2}; 10, 10^{-1}; 11, 10^0 M. Other conditions as in Fig. 1.

much less than c_f. When K_a is greater than c_f then the distribution coefficient is practically independent of the value of K_a up to the limit of a completely dissociated acid corresponding to the rightmost curve in Fig. 1. A set of these curves, *i.e.*, K_d *vs.* c_i curves for a completely dissociated acid, corresponding to different concentrations of the functional groups is presented in Fig. 3. The lower the c_f value the more pronounced and growing function is such a curve. However, K_a greater than c_f is rather a theoretical case since under normal chromatographic conditions c_i and K_a are much less than c_f.

The dependence of the distribution coefficient on the logarithm of the dissociation constant for various concentrations of the injected sample and the functional group concentration, $c_f = 10^{-3}$ M is presented in Fig. 4. If K_a is much less than c_f then K_d is a decreasing function of K_a (the leftmost part of Fig. 4). For higher values of the dissociation constant the distribution coefficient becomes a constant independent of K_a but dependent on c_i. It is worth noting that an increase in the sample concentration and a decrease in the dissociation constant have a similar effect — an increase of the K_d value. It is consistent with the fact that neutral molecules can penetrate the resin and in this way contribute to the increase in K_d.

The influence of the functional group concentration on the distribution coefficient has also been considered. For K_a and c_i much greater than c_f the distribution
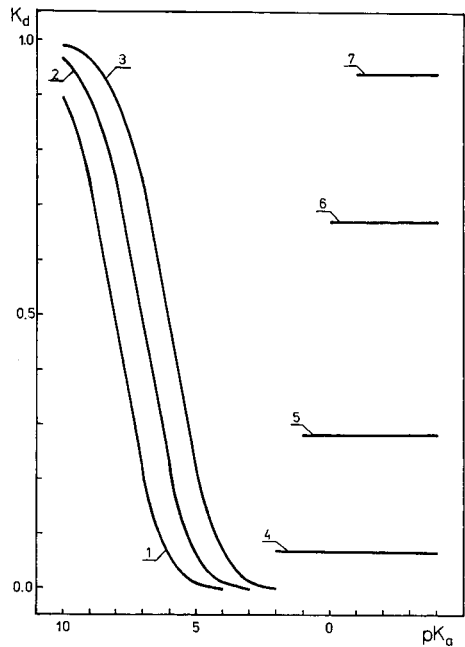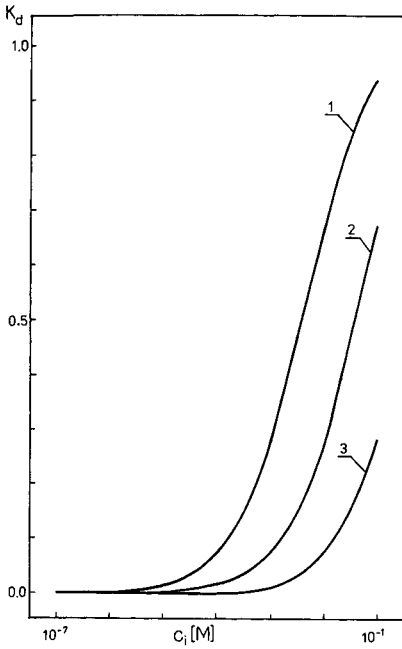
Fig. 3. Dependence of K_d on c_i for an acid dissociation constant, $K_a = 10^{-3}$ M and for several values of c_f: 1, 10^{-3}; 2, 10^{-2}; 3, 10^{-1} M. Other conditions as in Fig. 1.

Fig. 4. Dependence of K_d on the logarithm of the acid dissociation constant, pK_a for $c_f = 10^{-3}$ M, and for several values of the sample concentration, c_i: 1, 10^{-7}; 2, 10^{-6}; 3, 10^{-5}; 4, 10^{-4}; 5, 10^{-3}; 6, 10^{-2}; 7, 10^{-1} M. Other conditions as in Fig. 1.

coefficient is a decreasing function of c_f and K_d does not depend on K_a. However, for a normal chromatographic condition, K_a and c_i are much less than c_f, the distribution coefficient is independent of c_f and depends only on the ratio c_i/K_a. Therefore it is convenient to use reduced variables, c_i/K_a and c_f/K_a, instead of c_i, K_a and c_f, because the distribution coefficient depends only on two independent variables. The dependence of
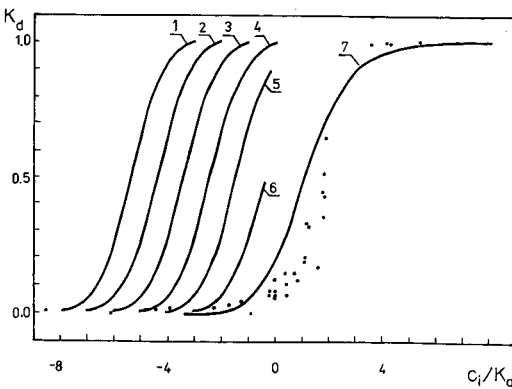
Fig. 5. Dependence of K_d on the quotient c_i/K_a for various values of c_f/K_a: 1, 10^{-6}; 2, 10^{-5}; 3, 10^{-4}; 4, 10^{-3}; 5, 10^{-2}; 6, 10^{-1}; 7, $\geqslant 10^0$. Points represent experimental values. Other conditions as in Fig. 1.

the distribution coefficient on c_i/K_a for various c_f/K_a is presented in Fig. 5. It is seen that K_d is a growing function of the quotient c_i/K_a. If we consider the usual chromatographic conditions when c_i is much greater than K_a then the decreasing function reduces to a constant one and the distribution coefficient depends only on c_i/K_a. This result is worth emphasizing since little effort is required to calculate the retention volume of any acid provided the parameters describing the column are known. The points in Fig. 5 correspond to the experimental data[10]. A good agreement with the theoretical calculations is observed. Analogous results were obtained for data presented in ref. 9.

The dependences of the distribution coefficient on the ratio c_f/K_a for several values of c_i/K_a are presented in Fig. 6. The distribution coefficient is a decreasing function of the ratio and it is practically zero when c_i is of the order of c_f or greater.

We have also considered the influence of the other experimental parameters on the distribution coefficient. An increase in the number of the theoretical plates, N, while keeping constant both V_S and V_M (and assuming that $c_f \gg c_i$ and $c_f \gg K_a$) results in a parallel shift of the K_d vs. c_i/K_a curve towards the stronger and more dilute acids. An increase in the ratio V_M/V_S while keeping constant N and $V_M + V_S$ results in a change of the slope of the curves K_d vs. c_i/K_a. In other words a change of the pK_a range of the separable acids is observed. An uniform increase in N, V_M and V_S (increase of the column length), i.e., keeping $N/(V_M + V_S)$ and V_M/V_S constant, results in better separations over wider ranges of pK_a values of the acids analyzed.

Global approach, buffered mobile phase

The dependence of the distribution coefficient and the retention volume of the analyzed sample on the sample concentration injected is inconvenient from the analytical point of view. We have tried to eliminate it by the addition of a strongly acidic buffer to the mobile phase. Most important, from the practical point of view, is the dependence of the distribution coefficient on c_i and K_a. The dependence of the distribution coefficient on the sample concentration injected is presented in Fig. 7. The curves K_d vs. c_i or K_d vs. K_a are shifted towards more dilute and/or stronger acids when the buffering acidic compound is added to the mobile phase. It follows that the pK_a range of separable acids is also shifted in the same way. Therefore a change in the
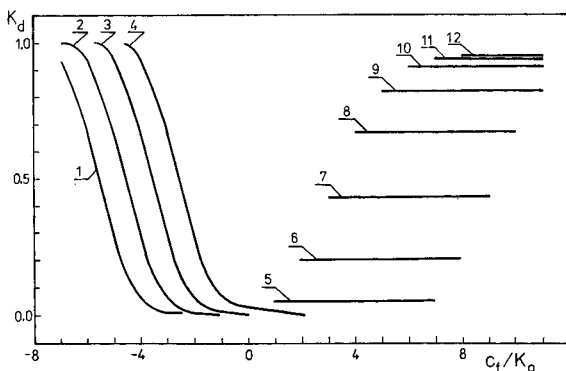
Fig. 6. Dependence of K_d on c_f/K_a for various values of c_i/K_a: 1, 10^{-5}; 2, 10^{-4}; 3, 10^{-3}; 4, 10^{-2}; 5, 10^{-1}; 6, 10^0; 7, 10^1; 8, 10^2; 9, 10^3; 10, 10^4; 11, 10^5; 12, 10^6. Other conditions as in Fig. 1.
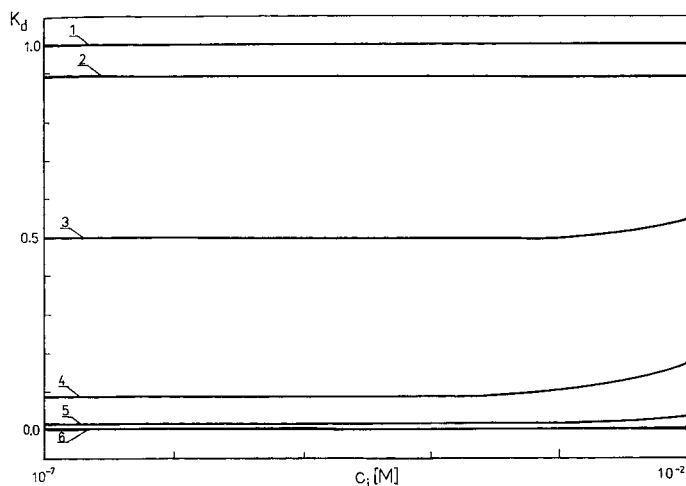
Fig. 7. Dependence of K_d on c_i for several values of K_a: 1, 10^{-5}; 2, 10^{-4}; 3, 10^{-3}; 4, 10^{-2}; 5, 10^{-1}; 6 = 10^0. $c_b = 10^{-3}$ M, $K_b = 10^3$, $c_f = 1$ M, $V_M = 800$ μl, $N = 1000$, $V_S = 2000$ μl, $V_i = 5$ μl.

buffer concentration or its dissociation constant can be used to control the retention volume, and consequently the separation, of the sample analyzed. Acids unseparated in pure water used as a mobile phase can be separated when a buffer is added. As is also seen in Fig. 7, the distribution coefficient is hardly dependent on the concentration of the sample injected when this concentration is lower than or approximately equal to the buffer concentration. This is advantageous from the analytical point of view.

The dependence of the distribution coefficient on the buffer concentration is a growing function as is seen in Fig. 8, for various values of K_a and for $c_i = 10^{-3}$ M. It can also be deduced from the figure that c_B, as well as K_b, can be used to control the range of pK_a of the acids analyzed. This behaviour is a result of the drawback of the dissociation of the analyzed sample caused by the addition of the buffer. The dependences of K_d on the other parameters are analogous to those for the unbuffered mobile phase.
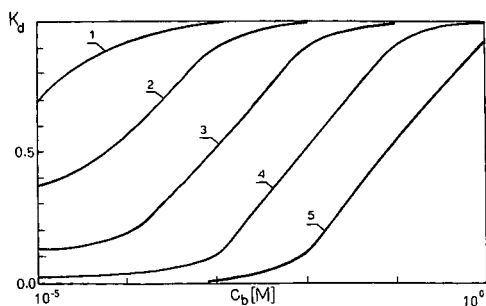
Fig. 8. Dependence of K_d on the buffer concentration, c_b, for several values of K_a: 1, 10^{-5}; 2, 10^{-4}; 3, 10^{-3}; 4, 10^{-2}; 5, 10^{-1} M. $c_i = 10^{-3}$ M. Other conditions as in Fig. 7.
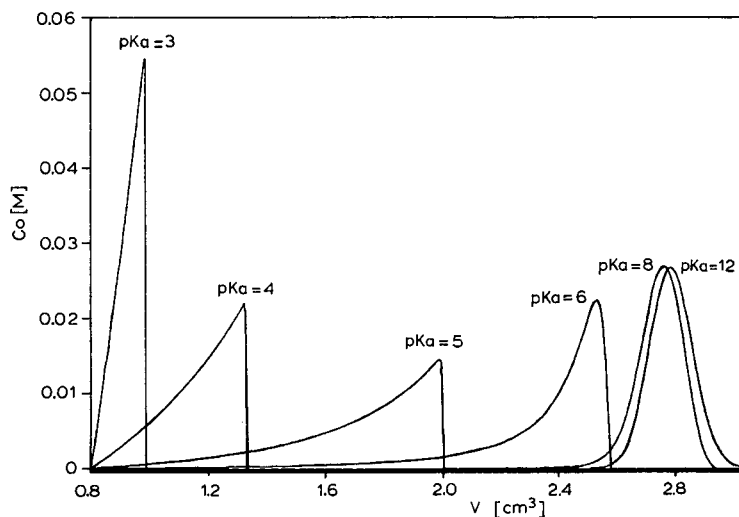
Fig. 9. Chromatograms of several acidic compounds (unbuffered mobile phase). $c_i = 10^{-3}$ M. Other conditions as in Fig. 1. $c_0 = c_M(i,N+1)$ —output concentration; $V = i \cdot v_M$ —elution volume.

Computer column modelling

The results of the computer simulation are presented in the form of calculated concentration profiles in Figs. 9 and 10 for unbuffered and buffered mobile phases respectively and for several values of pK_a of the acids analyzed. In the case of an unbuffered mobile phase the concentration profiles assume the form of leading peaks, except for the strongest and the weakest acids which form fairly symmetrical peaks. As was mentioned in the previous paragraph, after addition of a buffer the stronger acids
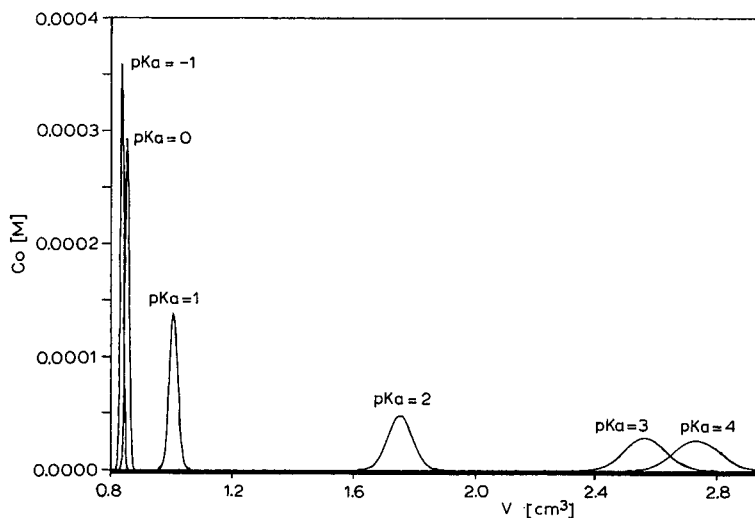
Fig. 10. Chromatograms of several acidic compounds (buffered mobile phase). $c_i = 10^{-3}$ M. Other conditions as in Fig. 7.
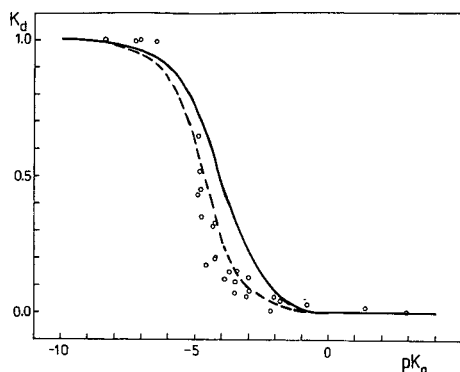
Fig. 11. Dependence of K_d on the logarithm of the acid dissociation constant, pK_a. Solid line: global approach; dashed line: computer modelling; points: experimental values (see Table I, ref. 10). $c_i = 10^{-3}$ M. Other conditions as in Fig. 1.

were separated. In the presence of a sufficiently strong and concentrated buffer, all peaks become fairly symmetrical, as has been observed experimentally. The concentration profiles of the sample in the two phases can also be calculated at the time steps of the sample passage down the column. The sample concentration in the stationary phase is never higher than it is in the mobile phase.

We expect the computer simulation to be more accurate and physically correct than the global approach. Therefore it is pleasing that the results obtained in this way are closer to the experimental values as is seen in Fig. 11. The good agreement of the model predictions and the experiment provides support to our ion-exclusion model explaining the primary mechanism of separation of acidic compounds. In real systems however other mechanisms play a role as was described in our previous paper (ref. 10, p. 41).

CONCLUSIONS

Despite its inconsistencies, the global approach describes the experimental facts fairly well. Computer simulations which eliminate these inconsistencies describe the facts even better and provide reasonable predictions on how the addition of the buffer influences the peak shape.

REFERENCES

1 R. H. Wheaton and W. C. Bauman, *Ind. Eng. Chem.*, 45 (1953) 238.
2 G. A. Harlow and D. H. Morman, *Anal. Chem.*, 36 (1964) 2438.
3 P. Jandera and J. Churácek, *J. Chromatogr.*, 86 (1973) 351.
4 H. F. Walton, *Anal. Chem.*, 48 (1976) 52R.
5 W. Czerwiński, *Chem. Anal. (Warsaw)*, 12 (1967) 597.
6 E. Rajakylä, *J. Chromatogr.*, 218 (1981) 695.
7 V. T. Turkelson and M. Richards, *Anal. Chem.*, 50 (1978) 1420.
8 J. Lehotay and M. Traiter, *J. Chromatogr.*, 91 (1974) 261.
9 K. Tanaka, T. Ishizuka and H. Sunahara, *J. Chromatogr.*, 174 (1979) 153.
10 B. K. Głód and W. Kemula, *J. Chromatogr.*, 366 (1986) 39.

CHROM. 20 949

SOLUBILITY PARAMETERS OF GAS CHROMATOGRAPHIC MIXED STATIONARY PHASES

E. FERNÁNDEZ-SÁNCHEZ, A. FERNÁNDEZ-TORRES, J. A. GARCÍA-DOMÍNGUEZ* and J. M. SANTIUSTE

Instituto de Quimica Física "Rocasolano" CSIC, Serrano 119, 28006 Madrid (Spain)

and

E. PERTIERRA-RIMADA

Departamento de Bioquimica, Facultad de Veterinaria, Universidad Complutense, 28040 Madrid (Spain)

(First received June 7th, 1988; revised manuscript received September 1st, 1988)

SUMMARY

Gas chromatography was used to measure activity coefficients, Ω^∞, partial molar free energies of mixing, $\Delta \bar{G}_1^\infty$, Flory–Huggins interaction parameters, χ^∞, and its enthalpic and entropic contributions, of a number of solutes on five single and fourteen mixed stationary phases at 120°C. Solubility parameters of the stationary phases, δ_2, were deduced by the method of DiPaola-Baranyi and Guillet for the different solute–stationary phase combinations. The polymer–polymer interaction parameter, $\chi'_{2,3}$, was also calculated for the various mixed systems.

INTRODUCTION

One of the problems with which the chromatographer is faced is to find a column with an appropriate selectivity for separating the components of the mixture to be analysed. Basically there are three procedures that can be used to modify the selectivity of the chromatographic column if no commercial stationary phase that can perform the separation is available: to synthesize new stationary phases with functional groups capable of producing the desired effect, to use columns coupled in series or to use mixtures of stationary phases in the same chromatographic column. Mixed stationary phases are particularly useful in connection with work with open-tubular columns, bearing in mind that there are few stationary phases with the necessary characteristics of stability, wettability, etc., which are needed if a long-lasting and efficient column is to be obtained. Some workers think that mixed stationary phase behaviour might easily be predicted from the characteristics of the liquids that are mixed[1-5]. Others, however consider that there is great uncertainty in this matter[1,6-12]. In our opinion, any attempt to predict the chromatographic behaviour of mixed stationary phases must be based on a good knowledge of their thermodynamic properties.

The most popular stationary phases in gas chromatography (GC) are polymers of high molecular weight, often unknown. Thermodynamic characterization of

polymers is possible with the use of GC[13] and has been greatly facilitated after the work of Patterson *et al.*[14], who showed that this characterization is possible with the molecular weight of the polymer being ignored. Many papers based on these ideas have been published[15-22]. One such important thermodynamic parameter is the solubility parameter of the stationary phase. Many physical properties are related to this parameter, and it is a general impression that its knowledge may lead to approximate estimates of the chromatographic behaviour of mixed stationary phases.

In this work, solubility parameters at 120°C were calculated for three sets of stationary phases using partial molar free energies of mixing following the procedure described by Price *et al.*[20]. The Flory–Huggins interaction parameter χ^∞ was also calculated, as together with its enthalpic and entropic contributions, χ_H^∞ and χ_S^∞. The polymer–polymer interaction parameter $\chi'_{2,3}$ was evaluated for different mixed stationary phases.

EXPERIMENTAL

The apparatus, stationary phases, columns and chromatographic procedures have been described previously[12]. The same mixtures of OV-101–OV-25, OV-101–Carbowax 20M and OV-225–SP-2340 were used.

RESULTS AND DISCUSSION

Activity coefficients

Activity coefficients at infinite dilution based on the weight fraction, Ω_1^∞, were calculated[14,20] using the equation

$$\ln \Omega_1^\infty \equiv \ln \frac{a_1}{w_1} = \ln \left(\frac{273.15 \, R}{P_1^0 \, V_g^0 \, M_1} \right) - \frac{P_1^0}{RT} (B_{11} - V_1^0) \tag{1}$$

which has the advantage of ignoring the molecular weight of the polymer. In this equation, a_1 and w_1 are the activity and weight fraction of the solute in the polymer, respectively, and M_1, P_1^0, B_{11}, V_1^0 and V_g^0 are the molecular weight, saturated vapour pressure, second virial coefficient, molar volume and specific retention volume of the solute at the column temperature T, respectively.

Vapour pressures were deduced using Antoine coefficients from various sources[23,24]. The second virial coefficients of *n*-nonane, *n*-decane and *n*-dodecane were calculated by the procedure of O'Connell and Prausnitz[25]; for other solutes, values were extrapolated from literature values corresponding to other temperatures[26]. Densities at 393 K were calculated according to the pertinent equation[27]. No data were found for six of the ten solutes used by McReynolds to characterize stationary phases[28]. Molar volumes were calculated from molecular weight and density values. Molar enthalpies of vaporization were deduced from data published at various temperatures[7,23,29,30]. Values at 393 K are shown in Table I.

Activity coefficients of the various solutes in the different stationary phases (single and mixed) found according to eqn. 1 are shown in Table II.

TABLE I

PHYSICAL PROPERTIES OF SOLUTES AT 393 K

Solute	P_1^0 (Torr)	$-B_{11}$ (l mol^{-1})	ρ_1 (g ml^{-1})	V_1^0 (ml mol^{-1})	ΔH_v (cal mol^{-1})	δ_1 [(cal ml^{-1})$^{\frac{1}{2}}$]
n-Hexane	2984.49	0.895	0.5450	158.13	6125	5.81
n-Heptane	1373.88	1.285	0.5924	169.16	7263	6.19
n-Octane	647.74	1.785	0.6170	185.14	8327	6.38
n-Nonane	310.89	2.439	0.6368	201.43	9465	6.57
n-Decane	151.27	3.106	0.6536	217.70	10610	6.72
n-Undecane	74.34	3.935	0.6660	234.71	11750	6.84
n-Dodecane	36.89	5.102	0.6761	251.96	12650	6.86
n-Tridecane	18.25	6.362	0.6861	268.72	13750	6.95
n-Tetradecane	9.17		0.6940	285.88	14800	7.00
n-Pentadecane	4.59		0.6988	303.98	16010	7.08
Benzene	2249.31	0.74	0.7681	101.71	6950	7.79
1-Butanol	823.27	1.055	0.7354	100.79	10255	9.69
2-Pentanone	1259.22	1.29	0.7043	122.30	7720	7.53
Pyridine	870.96	0.97	0.8873	89.15	8323	9.21

The solute–polymer interaction parameter

The Flory–Huggins solute–polymer interaction parameter may be calculated from activity coefficients[14,20,*]. In the case of pure solvents the equation is

$$\chi_{1,2}^\infty = \ln \Omega_1^\infty + \ln \frac{\rho_1}{\rho_2} - \left(1 - \frac{V_1^0}{V_2^0}\right) \qquad (2)$$

where ρ_1 and ρ_2 are the densities of the solute (1) and the polymer (2) and V_1^0 and V_2^0 the corresponding molar volumes. When the polymer is in fact a mixture of two polymers (mixed stationary phases) the equation becomes[15,31,32].

$$\chi_{1,(2,3)}^\infty = \ln \Omega_1^\infty + \ln \frac{\rho_1}{\rho_m} - \left(1 - \frac{V_1^0}{V_2^0}\right)\varphi_2 - \left(1 - \frac{V_1^0}{V_3^0}\right)\varphi_3 \qquad (3)$$

where ρ_m is the density of the mixture of polymers, V_2^0 and V_3^0 are the molar volumes of the two polymers and φ_2 and φ_3 the corresponding volume fractions in the mixture. As V_2^0 and V_3^0 are much larger than V_1^0, the use of both equations is greatly simplified.

Values of the solute–polymer interaction parameters corresponding to the different solutes in the various stationary phases are presented in Table III. Comparing values of χ^∞ corresponding to n-alkanes with the corresponding values of the partition coefficients (K_R) for the same mixtures[12], it may be observed that even in the set of mixtures where values of K_R may be said to show a "quasi"-linear behaviour with mixture composition (OV-101–OV-25), the same type of behaviour may not be observed in the case of the χ^∞ values.

---

* There is a transcription error in eqn. 3 in ref. 20. The authors used the correct equation in their calculations.

TABLE II

ACTIVITY COEFFICIENTS AT 393 K ON DIFFERENT STATIONARY PHASES

Mixtures of OV-101–OV-25

Compound	φ_{OV-101}							
	1	*0.831*	*0.589*	*0.410*	*0.397*	*0.268*	*0.084*	*0*
n-Hexane	4.70	5.18	6.30	7.70	7.70	8.40	10.90	11.57
n-Heptane	5.10	5.63	6.85	8.39	8.37	9.17	11.89	12.68
n-Octane	5.43	5.95	7.35	9.02	8.99	9.86	12.85	13.73
n-Nonane	5.76	6.32	7.78	9.54	9.56	10.52	13.71	14.68
n-Decane	6.05	6.67	8.20	10.11	10.12	11.17	14.54	15.75
n-Undecane	6.38	7.01	8.66	10.72	10.68	11.82	15.41	16.74
n-Dodecane	6.70	7.34	9.13	11.31	11.27	12.49	16.26	17.77
Benzene	4.69	4.62	4.63	4.74	4.85	4.82	5.02	4.85
1-Butanol	14.62	14.48	15.48	16.06	16.65	16.64	18.09	17.14
2-Pentanone	7.04	6.64	6.96	7.14	7.45	7.00	7.52	7.33
Pyridine	6.85	7.18	5.81	5.56	6.03	5.68	5.52	5.24

Mixtures of OV-101–Carbowax 20M

Compound	φ_{OV-101}				
	1	*0.757*	*0.509*	*0.257*	*0*
n-Hexane	4.70	6.54	9.61	14.95	25.77
n-Heptane	5.10	7.11	10.53	16.61	31.01
n-Octane	5.43	7.68	11.29	18.06	34.93
n-Nonane	5.76	8.18	12.15	19.57	40.09
n-Decane	6.05	8.68	13.02	21.08	45.48
n-Undecane	6.38	9.17	13.85	22.81	51.91
n-Dodecane	6.70	9.69	14.68	24.51	58.68
Benzene	4.69	5.54	5.69	6.05	5.58
1-Butanol	14.62	12.94	9.74	7.83	6.54
2-Pentanone	7.04	8.24	7.92	7.53	6.68

Mixtures of OV-225–SP-2340

Compound	φ_{OV-225}						
	1	*0.781*	*0.508*	*0.363*	*0.327*	*0.103*	*0*
n-Hexane	11.46	12.61	15.94	24.85	25.28	41.30	59.95
n-Heptane	13.03	14.35	18.45	29.06	29.29	50.10	74.39
n-Octane	14.52	15.99	21.22	33.46	33.96	60.11	91.68
n-Nonane	16.09	17.90	23.87	38.10	39.19	71.59	110.99
n-Decane	17.71	19.94	26.91	43.69	44.70	85.44	134.53
n-Undecane	19.51	21.87	30.08	48.99	50.87	100.69	162.91
n-Dodecane	21.37	24.09	33.67	55.88	57.81	117.12	196.58
n-Tridecane	23.56	26.69	37.89	63.51	65.77	140.88	237.91
n-Tetradecane*	25.71	29.24	42.29	71.50	74.42	166.16	285.56
n-Pentadecane*	28.53	32.59	47.87	81.77	85.51	198.80	346.19
Benzene	4.12	4.08	4.01	5.20	4.50	5.68	6.98
1-Butanol	8.00	7.35	6.59	7.95	6.97	7.91	9.69
2-Pentanone	4.23	4.18	4.10	6.19	4.57	6.60	8.22
Pyridine	3.72	3.37	3.02	3.80	3.18	3.58	4.37

* Values calculated without second virial coefficient correction.

TABLE III

SOLUTE–POLYMER INTERACTION PARAMETERS (χ^∞) AT 393 K

Mixtures of OV-101–OV-25

Compound	φ_{OV-101}							
	1	*0.831*	*0.589*	*0.410*	*0.397*	*0.268*	*0.084*	*0*
n-Hexane	0.044	0.102	0.248	0.412	0.409	0.471	0.696	0.741
n-Heptane	0.208	0.269	0.415	0.581	0.577	0.643	0.867	0.915
n-Octane	0.313	0.365	0.526	0.694	0.688	0.755	0.985	1.036
n-Nonane	0.401	0.458	0.614	0.782	0.781	0.852	1.082	1.134
n-Decane	0.477	0.538	0.693	0.866	0.864	0.938	1.167	1.231
n-Undecane	0.550	0.606	0.766	0.943	0.937	1.014	1.243	1.310
n-Dodecane	0.613	0.666	0.834	1.012	1.006	1.083	1.312	1.386
Benzene	0.385	0.332	0.282	0.269	0.290	0.258	0.263	0.214
1-Butanol	1.478	1.430	1.446	1.446	1.480	1.454	1.503	1.433
2-Pentanone	0.704	0.607	0.604	0.592	0.633	0.546	0.582	0.540
Pyridine	0.908	0.917	0.654	0.574	0.652	0.567	0.504	0.436

Mixtures of OV-101–Carbowax 20M

Compound	φ_{OV-101}				
	1	*0.757*	*0.509*	*0.257*	*0*
n-Hexane	0.044	0.321	0.655	1.048	1.544
n-Heptane	0.208	0.487	0.829	1.237	1.813
n-Octane	0.312	0.606	0.940	1.361	1.973
n-Nonane	0.401	0.700	1.045	1.473	2.142
n-Decane	0.476	0.786	1.141	1.573	2.294
n-Undecane	0.550	0.860	1.221	1.671	2.445
n-Dodecane	0.613	0.930	1.294	1.758	2.583
Benzene	0.385	0.498	0.474	0.487	0.358
1-Butanol	1.478	1.303	0.968	0.700	0.472
2-Pentanone	0.704	0.809	0.718	0.618	0.451

Mixtures of OV-225–SP-2340

Compound	φ_{OV-225}						
	1	*0.781*	*0.508*	*0.363*	*0.327*	*0.103*	*0*
n-Hexane	0.776	0.865	1.089	1.529	1.544	2.028	2.397
n-Heptane	0.988	1.077	1.319	1.769	1.775	2.304	2.696
n-Octane	1.137	1.226	1.499	1.950	1.964	2.527	2.946
n-Nonane	1.272	1.370	1.649	2.112	2.139	2.734	3.169
n-Decane	1.394	1.504	1.795	2.275	2.296	2.937	3.387
n-Undecane	1.509	1.615	1.925	2.408	2.444	3.120	3.597
n-Dodecane	1.615	1.727	2.053	2.555	2.587	3.286	3.800
n-Tridecane	1.727	1.844	2.186	2.697	2.731	3.485	4.006
n-Tetradecane*	1.826	1.947	2.307	2.827	2.866	3.662	4.200
n-Pentadecane*	1.937	2.063	2.438	2.968	3.012	3.848	4.399
Benzene	0.096	0.080	0.053	0.307	0.163	0.387	0.590
1-Butanol	0.716	0.624	0.507	0.689	0.556	0.674	0.874
2-Pentanone	0.035	0.016	−0.013	0.395	0.089	0.451	0.666
Pyridine	0.137	0.031	−0.086	0.139	−0.040	0.069	0.265

* Values calculated without second virial coefficient correction.

The solubility parameter

According to the Hildebrand–Scatchard theory, the solubility parameter of a substance is defined as the square root of the cohesive energy density, defined as the ratio of the energy of vaporization to the molar volume, both at the same temperature:

$$\delta \equiv (\Delta E_v / V_1^0)^{\frac{1}{2}} \tag{4}$$

When two liquids are mixed the difference between the two solubility parameters (δ_1 and δ_2) is given[29] by the expression

$$\delta_1 - \delta_2 = (\Delta E_m / \varphi_1 \varphi_2 V_m)^{\frac{1}{2}} \tag{5}$$

where ΔE_m is the energy of mixing of the two liquids at constant volume, φ_1 and φ_2 are the volume fractions of the components and V_m is the average molar volume based on molar fraction. Solubility parameters have been useful in describing the thermodynamic properties of dilute solutions and have been shown to be related to a number of physical properties of polymers such as surface tension, wettability and glass transition temperature. Solubility parameters of substances at a given temperature T may be calculated with the expression

$$\delta_1 = \left(\frac{\Delta H_v - RT}{V_1^0} \right)^{\frac{1}{2}} \tag{6}$$

where ΔH_v is the molar enthalpy of vaporization of the substance at temperature T and R is the universal gas constant. In this way δ values at 120°C were calculated for the various solutes used in this work and are shown in the last column in Table I.

Polymers have very low vapour pressures and therefore it is not possible to calculate δ_2 directly using eqn. 6. However, Guillet[13] has shown that gas–liquid chromatography is ideal for determining this parameter at a given temperature. Two methods[29] were used in this work to calculate values of δ_2 for the different mixtures of the three sets of stationary phases studied. One is based on the molar partial free energy of mixing, $\Delta \bar{G}_1^\infty$, and the other on the Flory–Huggins interaction parameter, χ^∞. Assuming zero volume change on mixing, eqn. 5 may be written in terms of the partial molar heat of mixing ($\Delta \bar{H}_1^\infty$)[29]:

$$\Delta \bar{H}_1^\infty = V_1^0 (\delta_1 - \delta_2)^2 \tag{7}$$

At constant pressure, it is the free energy and not the heat of mixing that is given directly by the solubility parameters[29,33], and eqn. 7 therefore becomes

$$\Delta \bar{G}_1^\infty = V_1^0 (\delta_1 - \delta_2)^2 \tag{8}$$

The partial molar free energy of mixing was evaluated[29] from the expression

$$\Delta \bar{G}_1 = RT \ln \Omega_1^\infty \tag{9}$$

TABLE IV

PARTIAL MOLAR FREE ENERGIES OF MIXING ($\Delta \bar{G}_1^\infty$, cal mol^{-1}) AT 393 K

Mixtures of OV-101–OV-25

Compound	φ_{OV-101}							
	1	0.831	0.589	0.410	0.397	0.268	0.084	0
n-Hexane	1209	1284	1438	1595	1595	1663	1866	1913
n-Heptane	1273	1350	1503	1662	1660	1732	1934	1984
n-Octane	1323	1393	1558	1718	1716	1788	1995	2047
n-Nonane	1367	1441	1602	1762	1764	1839	2046	2099
n-Decane	1406	1483	1644	1807	1808	1885	2091	2154
n-Undecane	1448	1521	1686	1853	1850	1930	2137	2201
n-Dodecane	1486	1557	1728	1895	1892	1973	2179	2248
Benzene	1208	1196	1197	1215	1234	1228	1260	1234
1-Butanol	2096	2088	2140	2169	2197	2197	2262	2220
2-Pentanone	1525	1479	1516	1535	1569	1521	1576	1556
Pyridine	1504	1540	1375	1341	1404	1357	1335	1294

Mixtures of OV-101–Carbowax 20M

Compound	φ_{OV-101}				
	1	0.757	0.509	0.257	0
n-Hexane	1209	1467	1768	2113	2538
n-Heptane	1273	1532	1839	2195	2683
n-Octane	1322	1593	1894	2261	2776
n-Nonane	1367	1642	1951	2323	2884
n-Decane	1406	1689	2005	2382	2982
n-Undecane	1448	1732	2053	2443	3086
n-Dodecane	1486	1775	2099	2499	3181
Benzene	1208	1338	1358	1407	1344
1-Butanol	2096	2000	1779	1608	1467
2-Pentanone	1525	1648	1617	1577	1484

Mixtures of OV-225–SP-2340

Compound	φ_{OV-225}						
	1	0.781	0.508	0.363	0.327	0.103	0
n-Hexane	1906	1980	2163	2510	2523	2907	3198
n-Heptane	2006	2081	2277	2632	2638	3058	3367
n-Octane	2090	2166	2387	2742	2754	3200	3530
n-Nonane	2171	2254	2479	2844	2866	3337	3679
n-Decane	2246	2338	2572	2951	2969	3475	3830
n-Undecane	2321	2410	2659	3040	3070	3603	3979
n-Dodecane	2392	2486	2747	3143	3170	3721	4126
n-Tridecane	2469	2566	2840	3243	3270	3866	4275
n-Tetradecane*	2537	2637	2926	3336	3367	3995	4418
n-Pentadecane*	2618	2722	3022	3441	3476	4135	4568
Benzene	1106	1099	1085	1287	1176	1357	1518
1-Butanol	1624	1558	1474	1620	1517	1615	1774
2-Pentanone	1126	1117	1102	1424	1186	1475	1645
Pyridine	1025	948	864	1044	905	996	1152

* Values calculated without second virial coefficient correction.

Values of $\Delta \bar{G}_1^\infty$ for the different solutes and mixtures are presented in Table IV. Rearranging eqn. 8, values of $[\delta_1^2 - (\Delta \bar{G}_1^\infty / V_1^0)]$ may be plotted *versus* δ_1. The slope of the straight line obtained is twice the solubility parameter of the polymer, δ_2.

A second method, based on the procedure developed by Guillet and co-workers[20,29], was used to evaluate solubility parameters of the various stationary phases at 120°C. Combining the Flory treatment[34] with Hildebrand–Scatchard theory and bearing in mind that the interaction parameter has free energy characteristics with enthalpic (χ_H^∞) and entropic (χ_S^∞) contribution terms, the following expression may be written[20]:

$$\chi^\infty = \frac{V_1^0 (\delta_1 - \delta_2)^2}{RT} + \chi_S^\infty \tag{10}$$

This equation may be rewritten as

$$\frac{\delta_1^2}{RT} - \frac{\chi^\infty}{V_1^0} = \frac{2\,\delta_2}{RT} \cdot \delta_1 - \left(\frac{\delta_2^2}{RT} + \frac{\chi_S^\infty}{V_1^0} \right) \tag{11}$$

Representation of the term in the left-hand side of eqn. 11 *versus* δ_1 will yield a straight line whose slope will allow an estimation of δ_2. Fig. 1 shows such plots for a few mixed stationary phases. In all instances (20 stationary phases) an excellent linear correlation was found (regression coefficients > 0.99). Values of the solubility parameter of the stationary phases at 120°C calculated according to eqns. 8 and 11 are given in Table V for the different mixtures investigated. The value obtained with eqn. 11 is slightly higher than that corresponding to eqn. 8 in all instances. Representation of the rearranged eqn. 8 allows the estimation of the solubility parameter of the stationary phase from the intercept of the straight line. The values so deduced are much closer to those obtained with eqn. 11. Comparing their results with literature values,
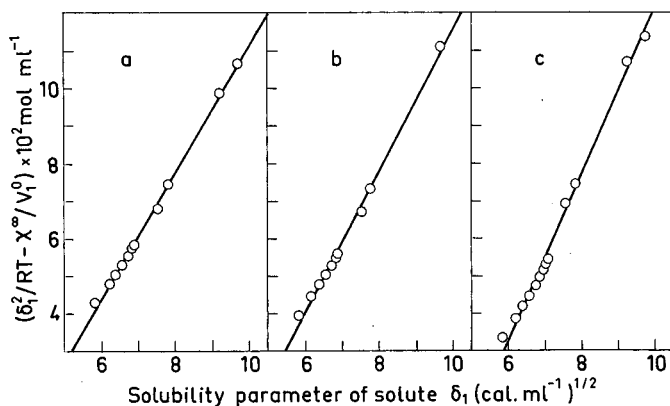
Fig. 1. Estimation of solubility parameter (δ_2) of mixed stationary phases from χ (eqn. 11). (a) OV-101/OV-25 = 0.831:0.169; (b) OV-101/Carbowax 20M = 0.509:0.491; (c) OV-225/SP-2340 = 0.363:0.637.

DiPaola-Baranyi and Guillet[29] arrived at the conclusion that in their case the procedure based on χ gave better results. In the present instance there are no reported values to compare at 120°C, so we cannot say that one of the methods is better than the other. In any event, the values are sufficiently close to each other to make us think that the values are not far from correct.

Fig. 2 shows the variation of the solubility parameter δ_2 of the various stationary phases in the three systems studied, as deduced with the help of eqn. 11. For curves a and b the values corresponding to a volume fraction of 1 (polymer OV-101 in both instances) are slightly different because the number of solutes used to calculate it is not the same (see Tables III and IV). The general shape of the curves resembles that of the partition coefficients of n-alkanes corresponding to the same mixed systems[12]. Except perhaps for curve a, it may be said that solubility parameters of mixtures of polymers may not be deduced as a linear combination of those corresponding to the pure components.

Enthalpic and entropic contributions to the solute–polymer interaction parameter

Once the solubility parameter of the stationary phase has been found, eqn. 10 may be used to calculate the enthalpic and entropic contributions to the solute–polymer interaction parameter ($\chi^{\infty} = \chi_H^{\infty} + \chi_S^{\infty}$). χ_S^{∞} can also be found from the intercept of the straight line defined by eqn. 11. Table VI presents the values obtained for χ_H^{∞} for the various solutes on the different stationary phases. The values of χ_S^{∞} deduced from the representation of eqn. 11 (Fig. 1) are given in Table VII. The value of χ_S^{∞} obtained by difference between the values shown in Tables III and VI is generally higher than that obtained from eqn. 11 (Table VII). As an example, Table VIII shows the differences corresponding to one mixed stationary phase (OV-101/OV-25 = 0.397/0.603). All three systems of mixed stationary phases show similar
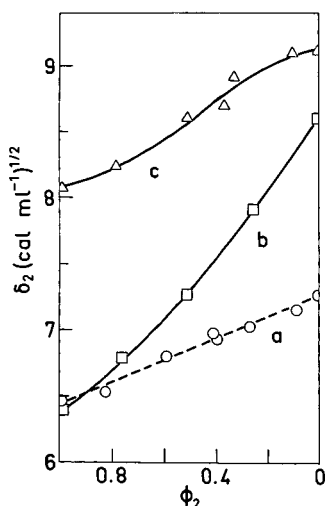
Fig. 2. Variation of the solubility parameter δ_2 (eqn. 11) of the stationary phase with mixture composition. (a) OV-101–OV-25; (b) OV-101–Carbowax 20M; (c) OV-225–SP-2340. φ_2 represents the volume fraction of the first polymer in each instance.

TABLE V

SOLUBILITY PARAMETERS OF STATIONARY PHASES, δ_2 [(cal mol^{-1})$^{\frac{1}{2}}$], AT 393 K

Mixtures of OV-101–OV-25

Equation	$\varphi_{OV\text{-}101}$							
	1	0.831	0.589	0.410	0.397	0.268	0.084	0
Eqn. 8 ($\Delta\bar{G}_1^\infty$)	5.92 ± 0.19	5.98 ± 0.17	6.21 ± 0.18	6.35 ± 0.18	6.28 ± 0.18	6.39 ± 0.18	6.53 ± 0.20	6.65 ± 0.19
Eqn. 11 (χ_1^∞)	6.46 ± 0.12	6.54 ± 0.10	6.80 ± 0.14	6.97 ± 0.16	6.90 ± 0.15	7.02 ± 0.16	7.19 ± 0.19	7.32 ± 0.21

Mixtures of OV-101–Carbowax 20M

Equation	$\varphi_{OV\text{-}101}$				
	1	0.757	0.509	0.257	0
Eqn. 8 ($\Delta\bar{G}_1^\infty$)	5.85 ± 0.24	6.16 ± 0.26	6.73 ± 0.23	7.29 ± 0.20	7.99 ± 0.09
Eqn. 11 (χ_1^∞)	6.37 ± 0.14	6.72 ± 0.16	7.32 ± 0.17	7.90 ± 0.18	8.63 ± 0.27

Mixtures of OV-225–SP-2340

Equation	$\varphi_{OV\text{-}225}$						
	1	0.781	0.508	0.363	0.327	0.103	0
Eqn. 8 ($\Delta\bar{G}_1^\infty$)	7.40 ± 0.11	7.59 ± 0.11	7.93 ± 0.12	7.95 ± 0.11	8.19 ± 0.13	8.41 ± 0.13	8.43 ± 0.13
Eqn. 11 (χ_1^∞)	8.10 ± 0.23	8.30 ± 0.25	8.64 ± 0.29	8.66 ± 0.24	8.91 ± 0.30	9.13 ± 0.30	9.15 ± 0.29

TABLE VI

ENTHALPIC CONTRIBUTIONS (χ_H^∞) TO THE SOLUTE–POLYMER INTERACTION PARAMETERS AT 393 K

Mixtures of OV-101–OV-25

Compound	$\varphi_{OV\text{-}101}$							
	1	0.831	0.589	0.410	0.397	0.268	0.084	0
n-Hexane	0.085	0.107	0.197	0.272	0.238	0.296	0.385	0.461
n-Heptane	0.016	0.027	0.081	0.133	0.109	0.151	0.218	0.279
n-Octane	0.001	0.006	0.041	0.082	0.063	0.097	0.155	0.209
n-Nonane	0.003	0.000	0.014	0.043	0.028	0.054	0.101	0.148
n-Decane	0.019	0.009	0.002	0.018	0.009	0.026	0.063	0.102
n-Undecane	0.042	0.026	0.000	0.006	0.001	0.011	0.038	0.071
n-Dodecane	0.052	0.033	0.001	0.004	0.000	0.008	0.035	0.068
Benzene	0.229	0.202	0.127	0.087	0.103	0.076	0.046	0.028
1-Butanol	1.349	1.283	1.081	0.956	1.009	0.921	0.807	0.726
2-Pentanone	0.180	0.154	0.084	0.049	0.063	0.041	0.018	0.007
Pyridine	0.858	0.809	0.659	0.568	0.606	0.542	0.461	0.404

Mixtures of OV-101–Carbowax 20M

Compound	$\varphi_{OV\text{-}101}$				
	1	0.757	0.509	0.257	0
n-Hexane	0.063	0.165	0.456	0.880	1.605
n-Heptane	0.007	0.060	0.275	0.633	1.290
n-Octane	0.000	0.026	0.205	0.543	1.194
n-Nonane	0.010	0.006	0.145	0.458	1.098
n-Decane	0.034	0.000	0.099	0.388	1.017
n-Undecane	0.065	0.004	0.069	0.339	0.966
n-Dodecane	0.078	0.007	0.066	0.346	1.007
Benzene	0.261	0.150	0.029	0.002	0.092
1-Butanol	1.424	1.145	0.731	0.416	0.146
2-Pentanone	0.211	0.104	0.007	0.021	0.189

Mixtures of OV-225–SP-2340

Compound	$\varphi_{OV\text{-}225}$						
	1	0.781	0.508	0.363	0.327	0.103	0
n-Hexane	1.058	1.246	1.614	1.641	1.937	2.221	2.249
n-Heptane	0.791	0.960	1.298	1.324	1.600	1.869	1.895
n-Octane	0.698	0.865	1.202	1.228	1.507	1.781	1.808
n-Nonane	0.607	0.771	1.106	1.132	1.413	1.690	1.717
n-Decane	0.532	0.692	1.025	1.051	1.334	1.615	1.643
n-Undecane	0.480	0.639	0.975	1.001	1.288	1.576	1.604
n-Dodecane	0.494	0.662	1.016	1.044	1.348	1.653	1.683
n-Tridecane	0.458	0.625	0.983	1.011	1.321	1.634	1.664
n-Tetradecane*	0.441	0.612	0.978	1.007	1.328	1.651	1.683
n-Pentadecane*	0.407	0.577	0.947	0.976	1.302	1.634	1.666
Benzene	0.013	0.034	0.094	0.099	0.163	0.233	0.240
1-Butanol	0.328	0.253	0.144	0.138	0.080	0.042	0.039
2-Pentanone	0.051	0.091	0.191	0.200	0.296	0.398	0.408
Pyridine	0.139	0.094	0.037	0.034	0.010	0.001	0.000

* Values calculated without second virial coefficient correction.

TABLE VII

ENTROPIC CONTRIBUTION (χ_S^∞) TO THE SOLUTE–POLYMER INTERACTION PARAMETERS CALCULATED FROM EQN. 11

Mixtures of OV-101–OV-25

Compound	φ_{OV-101}							
	1	*0.831*	*0.589*	*0.410*	*0.397*	*0.268*	*0.084*	*0*
n-Hexane	0.268	0.297	0.388	0.483	0.497	0.514	0.640	0.635
n-Heptane	0.287	0.318	0.415	0.516	0.532	0.550	0.685	0.679
n-Octane	0.314	0.348	0.454	0.565	0.582	0.602	0.750	0.743
n-Nonane	0.342	0.379	0.494	0.615	0.633	0.655	0.816	0.809
n-Decane	0.370	0.409	0.534	0.664	0.684	0.708	0.882	0.874
n-Undecane	0.398	0.441	0.576	0.716	0.738	0.763	0.951	0.942
n-Dodecane	0.428	0.474	0.618	0.769	0.792	0.819	1.021	1.012
Benzene	0.173	0.191	0.249	0.310	0.320	0.331	0.412	0.408
1-Butanol	0.171	0.190	0.247	0.308	0.317	0.328	0.408	0.405
2-Pentanone	0.208	0.230	0.300	0.373	0.384	0.397	0.495	0.491
Pyridine	0.151	0.167	0.218	0.272	0.280	0.289	0.361	0.357

Mixtures of OV-101–Carbowax 20M

Compound	φ_{OV-101}				
	1	*0.757*	*0.509*	*0.257*	*0*
n-Hexane	0.264	0.502	0.634	0.684	0.609
n-Heptane	0.283	0.538	0.678	0.732	0.652
n-Octane	0.309	0.588	0.742	0.801	0.713
n-Nonane	0.336	0.640	0.807	0.872	0.776
n-Decane	0.364	0.692	0.873	0.942	0.839
n-Undecane	0.392	0.746	0.941	1.016	0.904
n-Dodecane	0.421	0.801	1.010	1.091	0.971
Benzene	0.170	0.323	0.408	0.440	0.392
1-Butanol	0.168	0.320	0.404	0.436	0.388
2-Pentanone	0.204	0.389	0.490	0.529	0.471

Mixtures of OV-225–SP-2340

Compound	φ_{OV-225}						
	1	*0.781*	*0.508*	*0.363*	*0.327*	*0.103*	*0*
n-Hexane	0.418	0.364	0.305	0.653	0.425	0.676	0.985
n-Heptane	0.447	0.390	0.326	0.698	0.454	0.724	1.055
n-Octane	0.489	0.426	0.357	0.764	0.497	0.792	1.154
n-Nonane	0.532	0.464	0.388	0.831	0.541	0.862	1.255
n-Decane	0.575	0.501	0.420	0.899	0.585	0.931	1.357
n-Undecane	0.620	0.540	0.452	0.969	0.630	1.004	1.463
n-Dodecane	0.665	0.580	0.486	1.040	0.677	1.078	1.571
n-Tridecane	0.710	0.619	0.518	1.109	0.722	1.149	1.675
n-Tetradecane*	0.755	0.658	0.551	1.180	0.768	1.223	1.782
n-Pentadecane*	0.803	0.700	0.586	1.255	0.816	1.300	1.895
Benzene	0.269	0.234	0.196	0.420	0.273	0.435	0.634
1-Butanol	0.266	0.232	0.194	0.416	0.271	0.431	0.628
2-Pentanone	0.323	0.282	0.236	0.505	0.328	0.523	0.762
Pyridine	0.235	0.205	0.172	0.367	0.239	0.381	0.555

* Values calculated without second virial coefficient correction.

TABLE VIII

ENTROPIC CONTRIBUTION TO THE SOLUTE–POLYMER INTERACTION PARAMETER
FOUND WITH EQNS. 10 AND 11 FOR OV-101/OV-25 = 0.397:0.603

Solute	χ_H^∞	χ_S^∞	
		Eqn. 10	Eqn. 11
n-Hexane	0.238	0.171	0.497
n-Heptane	0.109	0.468	0.532
n-Octane	0.063	0.626	0.582
n-Nonane	0.028	0.753	0.633
n-Decane	0.009	0.855	0.684
n-Undecane	0.001	0.936	0.738
n-Dodecane	0.0004	1.006	0.792
Benzene	0.103	0.187	0.320
1-Butanol	1.009	0.472	0.317
2-Pentanone	0.063	0.570	0.384
Pyridine	0.606	0.046	0.280

differences between the values found for χ_S^∞ by the two procedures. Perhaps values derived from the intercept of eqn. 11 (Table VII) are less reliable than those found from eqn. 10. The reason might be that the range of values of solubility parameters of solutes, δ_1, used is small (5.8–9.7) and extrapolation to $\delta_1 = 0$ is not very precise.

As predicted by Flory[35], it may be found that $\chi_H^\infty < \chi_S^\infty$ with values of χ_H^∞ that are small for solutes and polymers of similar chemical structure (values of the solubility parameters of the same order). From the results shown in Table VI it may be observed that, as expected, χ_H^∞ values for n-alkanes in OV-101 are rather small, increasing as the mixed stationary phase becomes more and more polar (the proportion of the polar component increases in the mixed stationary phase). On polar polymers, polar substances show small values of the enthalpic contribution to the interaction parameter (benzene in OV-225 or OV-25; pyridine in SP-2340). When the "polarities" of the solute and polymer are dissimilar, the value of the enthalpic contribution becomes more important. Thus it may be observed that χ_H^∞ values are larger than χ_S^∞ values for the polar solutes in apolar stationary phases or n-alkanes in systems such as that of the cyanosilicones. In all instances of solute–polymer similarity, χ_S^∞ should be more important than χ_H^∞, and the contrary should be expected in instances of dissimilarity. The values of δ_1 and δ_2 may give an idea of the relative values of χ_H^∞ and χ_S^∞. However, the prediction of the value of the solute–polymer interaction parameter, χ^∞, does not seem possible from a knowledge of the two solubility parameters.

The concept of χ_S^∞ is ambiguous and it probably indicates the importance of the interaction of the solute molecule with the polymer in the ordering of the system[36]. It must be considered as a correction factor and probably should be further corrected to take into account pressure–volume effects[20]:

$$\chi^\infty = \chi_H^\infty + \chi_S^\infty + \chi_{PV}^\infty \tag{12}$$

TABLE IX

POLYMER-POLYMER INTERACTION PARAMETER, $\chi'_{2,3}$, AT 393 K

Mixtures of OV-101–OV-25

Compound	$\varphi_{OV\text{-}101}$					
	0.831	0.589	0.410	0.397	0.268	0.084
n-Hexane	0.423	0.340	0.180	0.230	0.423	−0.182
n-Heptane	0.417	0.348	0.184	0.243	0.425	−0.146
n-Octane	0.495	0.348	0.189	0.254	0.444	−0.131
n-Nonane	0.479	0.367	0.214	0.260	0.437	−0.120
n-Decane	0.474	0.385	0.232	0.280	0.464	0.014
n-Undecane	0.517	0.398	0.229	0.298	0.474	0.042
n-Dodecane	0.548	0.399	0.234	0.304	0.486	0.110
Benzene	0.175	0.136	0.061	−0.035	0.009	−0.453
1-Butanol	0.285	0.054	0.021	−0.123	−0.046	−0.856
2-Pentanone	0.489	0.133	0.062	−0.117	0.196	−0.358
Pyridine	−0.637	0.247	0.226	−0.122	−0.024	−0.371

Mixtures of OV-101–Carbowax 20M

Compound	$\varphi_{OV\text{-}101}$		
	0.757	0.509	0.257
n-Hexane	0.476	0.503	0.582
n-Heptane	0.603	0.667	0.859
n-Octane	0.600	0.751	0.969
n-Nonane	0.675	0.845	1.163
n-Decane	0.718	0.914	1.330
n-Undecane	0.817	1.039	1.506
n-Dodecane	0.877	1.144	1.670
Benzene	−0.651	−0.409	−0.636
1-Butanol	−0.378	0.063	0.159
2-Pentanone	−0.906	−0.555	−0.534

Mixtures of OV-225–SP-2340

Compound	$\varphi_{OV\text{-}225}$				
	0.781	0.508	0.363	0.327	0.103
n-Hexane	1.559	1.939	1.212	1.466	2.189
n-Heptane	1.666	2.037	1.330	1.647	2.336
n-Octane	1.796	2.111	1.467	1.775	2.514
n-Nonane	1.851	2.225	1.593	1.862	2.593
n-Decane	1.905	2.319	1.681	1.995	2.654
n-Undecane	2.052	2.447	1.866	2.136	2.843
n-Dodecane	2.141	2.550	1.957	2.265	3.132
n-Tridecane	2.234	2.652	2.082	2.408	3.094
n-Tetradecane*	2.331	2.749	2.210	2.534	3.178
n-Pentadecane*	2.418	2.844	2.323	2.646	3.222
Benzene	0.729	1.146	0.449	1.207	1.646
1-Butanol	0.744	1.151	0.555	1.214	1.990
2-Pentanone	0.918	1.433	0.182	1.683	1.624
Pyridine	0.786	1.145	0.344	1.197	1.979

* Values calculated without second virial coefficient correction.

The polymer–polymer interaction parameter

The polymer–polymer interaction parameters have been presented previously[12] for the three systems studied here. The values, deduced according to Perry and Tiley[7], are mean values for all *n*-alkanes and stationary phase compositions, including single stationary phases. The value corresponding to each solute on every mixed stationary phase may be deduced according to the expression[15,16,37]

$$\chi^{\infty}_{1,(2,3)} = \chi^{\infty}_{1,2}\varphi_2 + \chi^{\infty}_{1,3}\varphi_3 - \chi'_{2,3}\varphi_2\varphi_3 \tag{13}$$

where all the symbols have the usual meanings and $\chi'_{2,3}$ is the polymer–polymer interaction parameter normalized for the size of the solute molecule ($\chi'_{2,3} = V^0_1\chi_{2,3}/V^0_2$). In this way, values of $\chi'_{2,3}$ are obtained for each probe and mixture composition. Table IX presents the results obtained. It may be observed that the value of $\chi'_{2,3}$ depends on both the solute and mixture composition. This effect has been observed in the past[37].

The dependence of the value of the polymer–polymer interaction parameter on the chemical structure of the solute is a common phenomenon, although not allowed by theory[32]. It has been interpreted as arising from the preferential interaction with one of the two types of polymer segments[38]. Olabisi[39] attributed this to the non-random distribution of the solute in the stationary phase owing to its preferential affinity for one of the components. Selective solutes do not "sense" the three varieties of intramolecular contacts in the polymer mixture (A–A, A–B, B–B) in proportion to concentration. Instead, they detect a relatively low concentration of the chains for which they are non-solvents. This modifies the retention volume (and $\chi'_{2,3}$) values relative to those which would be obtained by a truly random mixing of the solute with the polymer[38]. Less selective solvents, on the other hand, exhibit a more random "sampling" of the molecular environment of the stationary phase owing to the equal affinities they have for both. It is therefore expected that a better measure of the polymer–polymer interaction will be likely with less selective solvents. According to these ideas, solutes with different chemical structure should behave differently in a mixture of two "different" polymers, *i.e.*, polymers of very different "polarity". Accordingly, one type of solute may behave in such a way that they show a "linear behaviour with mixture composition" when specific retention volumes are considered, whereas other types of solutes might not show the same type of linear dependence on mixture composition, when the same mixture is considered in both instances.

TABLE X

MEAN VALUES OF $\chi'_{2,3}/V^0_1$ FOR *n*-ALKANES AT 393 K

System	a^*	b^{**}
OV-101–OV-25	1.59	1.42
OV-101–Carbowax 20M	4.39	4.33
OV-225–SP-2340	9.02	9.79

* Values obtained according to Perry and Tiley[7,12].
** This work.

In order to compare the values of the polymer–polymer interaction parameter obtained in this paper based only on mixed stationary phases with those found previously for the same systems using both single and mixed stationary phases, we calculated the average value of $\chi'_{2,3}/V_1^0$ corresponding to all n-alkanes in all mixed stationary phases. The values are compared with those obtained previously[12] in Table X. The figures corresponding to each system are not exactly the same because in the present instance only mixed stationary phases could be considered.

ACKNOWLEDGEMENTS

REFERENCES

1 G. W. Pilgrim and R. A. Keller, *J. Chromatogr. Sci.*, 11 (1973) 206.
2 J. H. Purnell and J. M. Vargas de Andrade, *J. Am. Chem. Soc.*, 97 (1975) 3585 and 3590.
3 R. J. Laub and J. H. Purnell, *J. Chromatogr.*, 112 (1975) 71.
4 R. J. Laub and J. H. Purnell, *J. Am. Chem. Soc.*, 98 (1976) 30 and 35.
5 A. Gröbler and G. Bálizs, *J. Chromatogr. Sci.*, 19 (1981) 46.
6 J. F. K. Huber, E. Kenndler and H. Markens, *J. Chromatogr.*, 167 (1978) 291.
7 R. W. Perry and P. F. Tiley, *J. Chem. Soc., Faraday Trans. I*, 74 (1978) 1655.
8 P. F. Tiley, *J. Chromatogr.*, 179 (1979) 247.
9 A. J. Ashworth, T. M. Letcher and G. J. Price, *J. Chromatogr.*, 262 (1983) 33.
10 A. J. Ashworth and G. J. Price, *J. Chromatogr.*, 324 (1985) 231.
11 A. J. Ashworth and T. M. Letcher, *J. Chromatogr.*, 362 (1986) 1.
12 E. Fernández-Sánchez, A. Fernández-Torres, J. A. García-Domínguez, J. García-Muñoz, V. Menéndez, M. J. Molera, J. M. Santiuste and E. Pertierra-Rimada, *J. Chromatogr.*, 410 (1987) 13.
13 J. E. Guillet, *J. Macromol. Sci. Chem.*, 4 (1970) 1669.
14 D. Patterson, Y. B. Tewari, H. P. Schreiber and J. E. Guillet, *Macromolecules*, 4 (1971) 356.
15 D. D. Deshpande, D. Patterson, H. P. Schreiber and C. S. Su, *Macromolecules*, 7 (1974) 530.
16 C. S. Su, D. Patterson and H. P. Schreiber, *J. Appl. Polym. Sci.*, 20 (1976) 1025.
17 G. DiPaola-Baranyi and P. Degré, *Macromolecules*, 14 (1981) 1456.
18 K. S. Siow, S. H. Goh and K. S. Yap, *J. Chromatogr.*, 354 (1986) 75.
19 A. C. Su and J. R. Freid, *J. Polym. Sci., Polym. Lett.*, 24 (1986) 343.
20 G. J. Price, J. E. Guillet and J. H. Purnell, *J. Chromatogr.*, 369 (1986) 273.
21 K. G. Furton and C. F. Poole, *J. Chromatogr.*, 399 (1987) 47.
22 J. M. Barrales-Rienda and J. Vidal Gancedo, *Macromolecules*, 21 (1988) 220.
23 R. C. Wilhoit and B. J. Zwolinski, *Handbook of Vapour Pressures and Heats of Vaporization of Hydrocarbons and Related Compounds*, Thermodynamics Research Centre, Texas A&M University, College Station, TX, 1971.
24 T. Boublík, V. Fried and E. Hála, *The Vapour Pressures of Pure Substances*, Elsevier, Amsterdam, 1975.
25 J. P. O'Connell and J. M. Prausnitz, *Ind. Eng. Chem., Process Des. Dev.*, 6 (1976) 245.
26 J. H. Dymond and E. B. Smith, *The Virial Coefficients of Pure Gases and Mixtures. A Critical Compilation*, Clarendon Press, Oxford, 1980.
27 National Research Council of the U.S.A., *International Critical Tables of Numerical Data, Physics, Chemistry and Technology*, Vol. III, McGraw-Hill, New York, 1928.
28 W. O. McReynolds, *J. Chromatogr. Sci.*, 8 (1970) 685.
29 G. DiPaola-Baranyi and J. E. Guillet, *Macromolecules*, 11 (1978) 228.
30 V. Majer and V. Svoboda, *Enthalpies of Vaporization of Organic Compounds. A Critical Review and Data Compilation*, Chemical Data Series No. 32, Blackwell, Oxford, 1985.
31 J. M. Braun and J. E. Guillet, *Adv. Polym. Sci.*, 21 (1976) 107.
32 A. K. Nandi, B. M. Mandal and S. N. Bhattacharyya, *Macromolecules*, 18 (1985) 1454.

33 D. Patterson, *Rubber Chem. Technol.*, 40 (1967) 1.
34 P. J. Flory, *Principles of Polymer Chemistry*, Cornell University Press, Ithaca, NY, 1953.
35 P. J. Flory, *Discuss. Faraday Soc.*, 49 (1970) 7.
36 J. E. G. Lipson and J. E. Guillet, in R. B. Seymour and G. Stahl (Editors), *Solvent–Property Relations in Polymers*, Pergamon Press, New York, 1982, p. 235.
37 G. DiPaola-Baranyi, S. J. Fletcher and P. Degré, *Macromolecules*, 15 (1982) 885.
38 T. C. Ward, D. P. Sheehy, J. S. Riffle and J. E. McGrath, *Macromolecules*, 14 (1981) 1791.
39 O. Olabisi, *Macromolecules*, 8 (1975) 316.

.

CHROM. 20 951

INFLUENCE OF EXPERIMENTAL CONDITIONS UPON POLARITY PARAMETERS AS MEASURED BY GAS CHROMATOGRAPHY

ADAM VOELKEL

Poznań Technical University, Institute of Chemical Technology and Engineering, Pl. M. Sklodowskiej-Curie 2, 60-965 Poznań (Poland)

(First received May 19th, 1988; revised manuscript received August 15th, 1988)

SUMMARY

The influence of different chromatographic experimental parameters upon empirical, thermodynamic and dispersive force polarity parameters is examined for unusual stationary phases. The parameters considered were found to be sensitive to the column temperature, solute sample size and stationary phase loading.

INTRODUCTION

Polarity parameters have been reported in studies of groups of surfactants, etc., used as the stationary phases in packed chromatographic columns[1–11]. In recent papers the main interest has been in the influence of the structure of these compounds upon their polarities, although some relationships between various polarity parameters were also presented.

The aim of this paper is to explore the influence of different experimental parameters such as the temperature, gas flow-rate, column loading, probe sample size and composition upon some polarity parameters. The results with the present unusual stationary phases should be in conformity with results obtained for more commonly used phases.

EXPERIMENTAL

Experiments were carried out using a Chrom-5 gas chromatograph (Kovo, Czechoslovakia) with flame ionization detection (FID) and an IT2 Integrator (Kovo), or a GCHF 18.3 (Gide, G.D.R.) gas chromatograph with thermal conductivity detection (TCD) or FID. The conditions were: column (1 m × 3 mm I.D.), with stationary phase liquid loadings of 10, 15, 20 or 25% (w/w); support, Porolith (mesh size 0.2–0.5 mm); column temperature, isothermal 50–100°C; carrier gas, helium or nitrogen, 40 ml/min; solute probes, methanol, ethanol, 1-propanol, 1-butanol, 2-butanone, 2-pentanone, benzene, pyridine, 1-nitropropane and C_5–C_{11} *n*-alkanes; time for column stabilization, overnight; sample sizes both for *n*-alkanes and polar solutes, 0.1, 0.2 and 0.3 μl. Each measurement was repeated five times and averaged.

The following polarity parameters were considered: retention index, I_R, of

methanol and ethanol; polarity index, PI, of methanol and ethanol, PI $=$ 100 log $(C - 4.7) + 60$ (ref. 12), where C is the apparent number of carbon atoms in a standard n-alkane having the same retention time as that of the alcohol; coefficient ρ, defined as the ratio of the adjusted retention time of an alcohol to that of n-hexane; partial molal free energies of solution of an hydroxyl, $\Delta G_s^m(OH)$, or carbonyl group, $\Delta G_s^m(C=O)$, calculated as described by Risby and co-workers[13–16]; the sum of the differences between the retention indices for the first five McReynolds solutes, $\sum_{i=1}^{5} \Delta I_i$, on a given stationary phase and on squalane; and Criterion A for n-alkanes calculated according to Ševčik and Löwentap[17]

$$A = \frac{t_{R,n+1} - t_{R,n}}{t_{R,n} - t_{R,n-1}}$$

and the partial molar Gibbs free energy of solution per methylene group, $\Delta G^E(CH_2)$, as demonstrated by Roth and Novák[19].

Stationary phases

Surfactant of different structures described in previous papers[1–11] and indicated in Table I were used for temperature studies. The influence of the solute sample size, methods of retention time and of dead time estimation upon the polarity parameters were estimated for the following stationary phases used at 70 and 90°C:

(1) $C_6H_{13}OCH_2CH(OH)CH_2OCH_2CH_2OC_6H_{13}$;
(2) $C_4H_9O(CH_2CH_2O)_2CH_2CH(OH)CH_2(OCH_2CH_2)_4C_4H_9$;
(3) $C_8H_{17}S(CH_2CH_2O)_4H$;
(4) $C_8H_{17}O(CH_2CH_2O)_2H$;
(5) $C_8H_{17}OCH_2CH(OH)CH_2OCH_2CH_2OC_8H_{17}$;
(6) $C_{10}H_{21}NH(CH_2CH_2O)_3H$. These were used in Tables II–IV.

Dead time measurements

The dead time was calculated from retention times of C_5–C_9 n-alkanes by using the Grobler and Balizs[19] method. When TCD was used the air peak time was considered as the dead time. For comparison, the method of Ševčik and Löwentap[20] was considered.

Retention time measurements

The retention times of solute probes were measured at the peak maxima for symmetrical peaks. When an asymmetric peak was obtained for alcohols or pyridine, three different retention times, corresponding to the peak maximum (max), centre of gravity of the peak (CG) and the median of the peak (MED) were calculated. The elution time of the CG was calculated as

$$t_{R(CG)} = m_1 = \frac{\int_0^\infty tc(t)\,dt}{\int_0^\infty c(t)\,dt} \tag{1}$$

where m_1 denotes the first statistical moment of the peak, t the elution time of each point of the peak and $c(t)$ its concentration[21]. The elution time corresponding to the MED was computed according to the definition of Jönsson[22]. The retention time of the peak maximum was recorded by the integrator.

Statistical calculations

For comparison of polarity parameters calculated from the three retention times estimated by different methods for asymmetrical peaks and for different methods of dead time estimation, a goodness of fit test for the average values was performed according to the F-test and to the Students' t-test.

RESULTS AND DISCUSSION

The results are presented in Tables I–IV and Figs. 1–3. Previous papers[1-11] have shown that, generally, polarity parameters decrease with increasing column temperature. This is supported by the present results for stationary phases comprising some oligooxyethylene derivatives of alcohols, thioalcohols and alkylamines (Table I). In all cases, the retention index, polarity index, coefficient ρ and criterium A decrease with increasing temperature from 50 to 100°C.

Petrowski and Vanatta[23] confirmed the temperature dependence of coefficient ρ and found a linear relationship between ln ρ and the column temperature. The coefficient ρ is, in fact, the retention of the polar solute (alcohol) relative to non-polar n-hexane, and this should change both with the polarity of the stationary phase and with temperature. It is well known that variations in the retention index increase with increasing stationary phase polarity[24].

The influence of carrier gases upon the performance of packed columns was examined by Rohrschneider and Pelster[25]. At temperatures above 70°C they found hydrogen to be the most suitable carrier gas, while below 70°C nitrogen was most suitable. Here, no significant influence of carrier gas upon the polarity parameters considered was observed using helium or nitrogen.

Increase in the column length also did not change the values of any polarity parameters. However, for longer (2 m) columns, longer analysis times, peak broadening and skewing and higher pressure drops increasing the risk of loss of stationary phase were observed. To prevent this one should use, at least for stationary phase–surfactant polarity measurements, relatively short columns, with relatively large support particles, low gas flow-rates and temperatures above the melting point of the stationary phase used, but not so high as to cause bleeding!

The sensitivity of the retention index of two alcohols (methanol and ethanol), the polarity index and the coefficient ρ to the sample size and the stationary phase content is presented in Figs. 1 and 2. These polarity parameters may be sensitive to the sample size of the polar alcohol solute(s), particularly methanol. If they change, their absolute values generally decrease as the sample size of the polar probe increases. The measured I_R of methanol decreases with increasing ratio of the polar probe/standard n-alkanes. The influence of a change in the sample size of n-alkanes is much weaker.

The data presented for dispersive force parameters show that they are sensitive to the sample size of the solute used for their estimation (Table IV). Criterion A increases with increasing sample size of n-alkanes at lower stationary phase loadings.

TABLE I

TEMPERATURE DEPENDENCE OF POLARITY PARAMETERS USING SOME OLIGOOXYETHYLENE DERIVATIVES OF ALCOHOLS, THIO-ALCOHOLS AND ALKYLAMINES AS STATIONARY PHASES

Stationary phase*	Temp. (°C)	Retention index		Polarity index		Coefficient ρ		Criterion A
		Methanol	Ethanol	Methanol	Ethanol	Methanol	Ethanol	Alkanes
$C_9H_{17}O(EO)_2H$**	50	665	719	88.7	101.0	1.89	2.93	3.580
	60	656	713	86.6	99.0	1.69	2.74	2.475
	70	644	709	83.6	97.6	1.42	2.63	2.310
	80	636	705	82.4	95.1	1.37	2.33	2.680
	90	629	700	79.2	93.2	1.12	2.11	2.220
	100	621	697	73.4	91.2	1.10	1.99	2.143
$C_8H_{17}NH(EO)_2H$	50	764	813	108.2	115.2	4.78	6.33	2.682
	60	756	807	107.7	113.7	4.42	5.97	2.428
	70	753	800	106.3	112.1	4.00	5.63	2.295
	80	744	793	103.2	105.5	3.54	5.07	2.192
	90	742	788	101.1	102.1	3.04	4.80	2.101
	100	738	783	99.5	101.2	2.65	4.73	2.068
$C_8H_{17}S(EO)_3H$	50	703	753	96.2	106.8	2.19	4.12	2.460
	60	694	739	94.7	104.0	2.02	3.87	2.349
	70	689	723	91.3	99.6	1.88	3.55	2.224
	80	655	699	86.8	94.7	1.63	2.49	2.167
	90	648	680	85.6	92.7	1.50	1.93	2.099
	100	635	670	84.0	90.5	1.43	1.66	2.044

* 25% column loading.
** $EO = -CH_2CH_2O-$.

TABLE II

INFLUENCE OF SOLUTE SAMPLE SIZE AND STATIONARY PHASE LOADING ON DISPERSIVE FORCE PARAMETERS AT 90°C

Stationary phase	Loading (%)	Solute sample size (μl)	Criterion A Alkanes	$\Delta G^E (CH_2)$ (J/mol)		
				Alkanes	Alcohols	Ketones
1	10	0.1	2.318	254	103	596
		0.2	2.327	261	102	592
		0.3	2.346	240	99	590
	15	0.1	2.327	265	101	594
		0.2	2.310	233	100	593
		0.3	2.302	218	99	590
	20	0.1	2.328	194	102	592
		0.2	2.329	189	100	590
		0.3	2.335	178	99	588
	25	0.1	2.330	172	99	587
		0.2	2.330	173	99	587
		0.3	2.332	172	99	586
2	10	0.1	2.122	273	196	811
		0.2	2.124	271	195	808
		0.3	2.127	268	193	803
	15	0.1	2.127	268	195	808
		0.2	2.129	264	193	806
		0.3	2.131	262	192	803
	20	0.1	2.131	262	193	806
		0.2	2.134	263	192	804
		0.3	2.136	265	191	800
	25	0.1	2.135	267	192	800
		0.2	2.136	266	191	800
		0.3	2.136	267	191	801
4	10	0.1	2.289	199	103	589
		0.2	2.292	192	102	588
		0.3	2.301	187	100	580
	15	0.1	2.293	192	101	582
		0.2	2.298	189	100	580
		0.3	2.297	183	99	577
	20	0.1	2.296	188	102	582
		0.2	2.298	184	101	580
		0.3	2.303	179	99	576
	25	0.1	2.310	174	97	575
		0.2	2.311	175	97	576
		0.3	2.311	174	96	576

The partial molar excess Gibbs free energy of solution per methylene group, $\Delta G^E(CH_2)$, decreases significantly with increasing sample size when n-alkanes are used as the solutes and when estimated at high stationary phase loadings. This parameter generally decreases also when the amount of the stationary phase increases. The

TABLE III

VARIATION OF RETENTION INDEX WITH INCREASING PROBE SAMPLE SIZE FROM 0.1 μl (STEP 0.1 μl) TO $\Delta I_i/0.1$ μl FOR THE FIRST FIVE McREYNOLDS SOLUTES AND THEIR SUM

$\sum_{i=1}^{5} \Delta I_i - \Delta\left(\sum_{i=1}^{5} \Delta I_i\right)$. Sample size of alkanes: 0.1 μl. Temperature: 90°C.

Phase	Loading (%)	Probe					$\sum_{i=1}^{5} \Delta I_i$
		X' Benzene	Y' 1-Butanol	Z' 2-Pentanone	U' 1-Nitropropane	S' Pyridine	
2	10	+0.5	−0.5	+1.0	+1.2	−12.5	−10.3
	15	0.0	+0.6	+1.0	+1.3	−11.6	− 8.7
	20	+2.3	−0.7	−1.0	+2.0	− 8.6	− 1.0
	25	+0.2	−0.1	+1.0	+0.7	− 2.5	− 0.7
3	10	+1.3	+0.3	0.0	+0.6	− 5.8	− 3.6
	15	0.0	0.0	0.0	0.0	− 3.0	− 3.0
	20	−0.3	−0.6	+0.3	+0.6	− 3.0	− 3.0
	25	0.0	0.0	0.0	0.0	− 0.3	− 0.3
4	10	0.0	+1.0	0.0	+0.3	−21.0	−19.7
	15	+1.0	−1.0	−0.3	+0.3	− 7.7	− 7.7
	20	−0.6	0.0	0.0	0.0	− 2.7	− 3.3
	25	+0.2	0.0	0.0	+0.3	− 0.8	− 0.3

sample size dependence is much weaker when alcohols and ketones are used as the probe solutes and is insignificant for higher liquid loadings of stationary phase.

The sensitivity of the retention index to variations in column liquid loading, support activity and sample size has been examined by several workers[24,26–31]. Vernon and Suratman[24] have pointed out that the sample size and sample composition influence the retention index. These effects were much stronger on a polar than on a non-polar phase. The present work suggests they are stronger with non-polar solute probes.

Jönsson and Mathiasson[29] have concluded that in the presence of surface adsorption, both on the surface of the support and on the surface of the liquid phase, the retention volume usually varies with sample size. Accurate measurements of retention data thus require the retention volume to be corrected for adsorption[27–30]. It was found[30] that the contribution from adsorption varies strongly with sample size. Adsorption effects, of course, decrease significantly with increasing stationary phase loadings as possibly shown in Table III. Both column loadings and sample size ought to be high in order to keep the variation in retention index as small as possible[31]. The effect of the sample size of polar probes depends significantly upon the column loading (Figs. 1–3). Increasing the amount of the stationary phase decreases the influence of the sample size, and usually 25% loadings gave the most consistent results for each polarity parameter.

Observed variations may be attributed both to the adsorption effects of polar probes (see Mathiasson et al.[31]) and of n-alkane reference compounds. These results
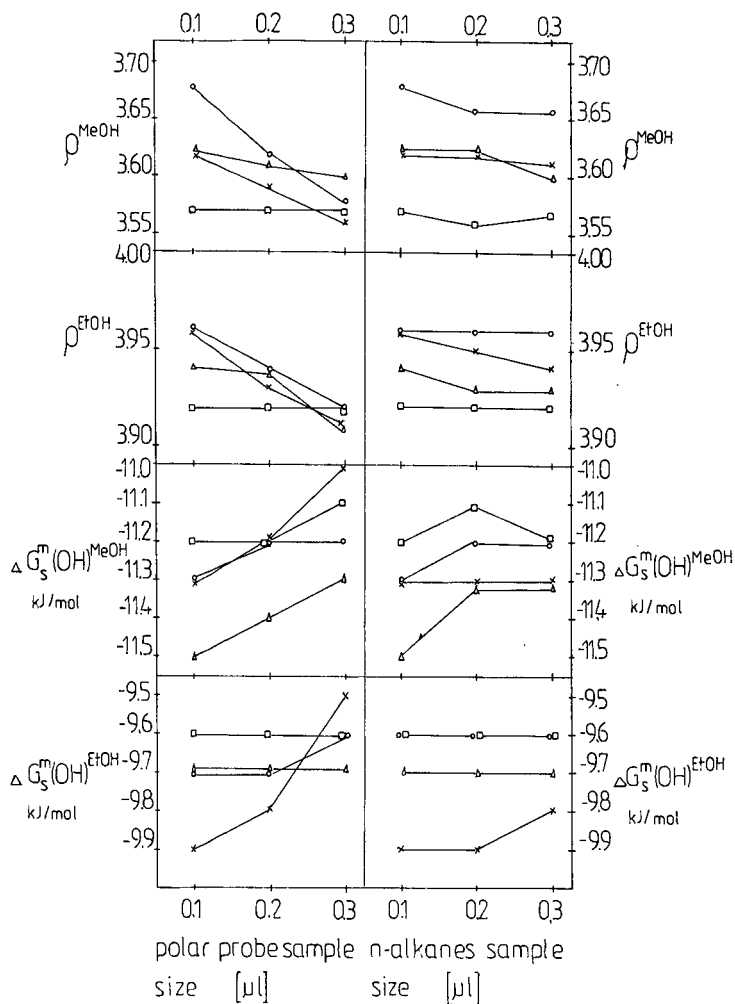
Fig. 1. The influence of the sample size of the solute probe on the polarity parameters considered. Stationary phase: $C_8H_{17}O(CH_2CH_2O)_2H$. Liquid phase loading (%): $\times$, 10; $\bigcirc$, 15; $\triangle$, 20; $\square$, 25. Sample sizes of reference n-alkanes and polar probes were 0.1 μl for both halves of the figure.

justify the standard liquid loading of 25% used in previous works[1-11] where the sample size varied between 0.2 and 0.3 μl.

A significant variation consequent upon the sample size of polar probes is observed (for lower liquid loadings) for the sums of the first five McReynolds probes, $\sum_{i=1}^{5} \Delta I_i$ (Fig. 3), particularly due to the retention index of pyridine (Table III). Vernon and Rayakorn[26] have found pyridine and butanol to show exceptionally high solute–support interactions but this was not found here for butanol.

In several cases, chromatographic peaks were broadened and skewed, especially those of pyridine and to a minor degree methanol and ethanol. What is the proper

TABLE IV

POLARITY PARAMETERS CALCULATED FROM RETENTION TIMES OF POLAR SOLUTES ESTIMATED BY DIFFERENT METHODS*

MeOH = methanol; EtOH = ethanol; BuOH = butanol; Py = pyridine.

Phase	PI^{MeOH} calc. from**			ρ^{EtOH} calc. from			I_R^{BuOH} calc. from			I_R^{Py} calc. from		
	$t'_{R,max}$	$t'_{R,MED}$	$t'_{R,CG}$	$t'_{R,max}$	$t'_{R,MED}$	$t'_{R,CG}$	$t'_{R,max}$	$t'_{R,MED}$	$t'_{R,CG}$	$t'_{R,max}$	$t'_{R,MED}$	$t'_{R,CG}$
1	89.4	89.2	89.1	1.77	1.76	1.76	855	853	852	929	911	903
2	107.2	107.0	106.8	3.96	3.94	3.90	1008	1003	1000	1100	1084	1072
3	97.2	97.1	96.9	4.10	4.10	4.09	839	837	836	960	955	948
4	83.6	83.5	83.5	2.63	2.60	2.57	918	917	916	1035	1030	1026
5	72.5	72.4	72.3	1.34	1.33	1.30	836	834	833	892	890	887
6	103.6	103.6	103.5	5.06	5.05	5.03	935	934	932	909	902	898

* Stationary phase loading 25%; probe sample size 0.1 μl; temperature 70°C for PI and ρ, and 90°C for I_R.

** t'_{max}, t'_{MED}, t'_{CG} = retention times for the maximum, median or centre of the peak, respectively.
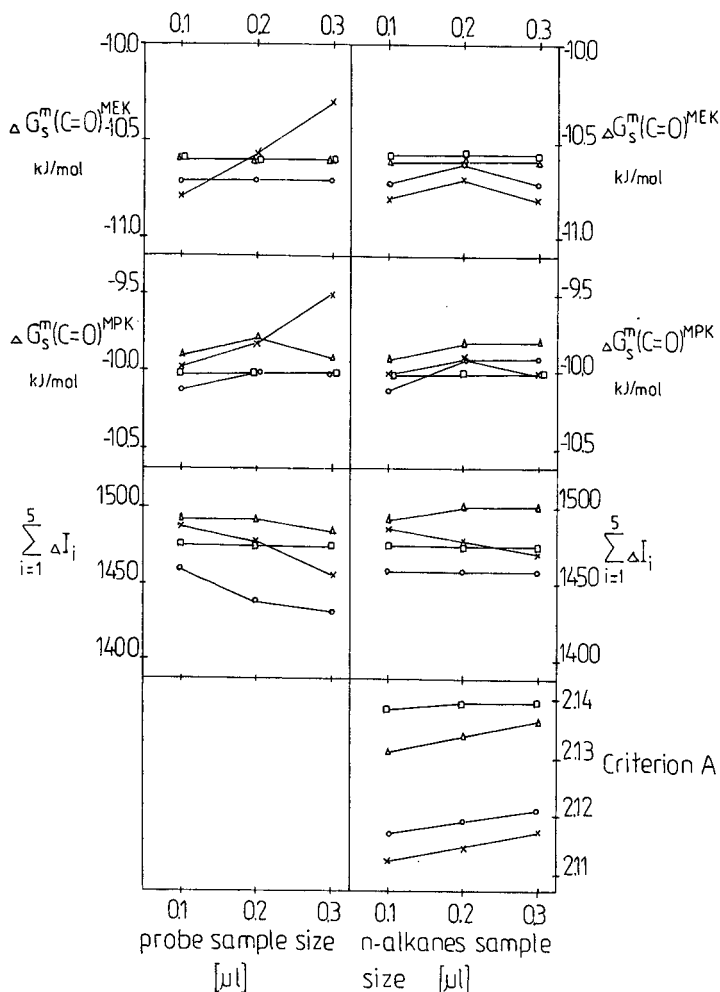
Fig. 2. The influence of the sample size of the solute probe on the polarity parameters. Stationary phase: $C_4H_9O(CH_2CH_2O)_2CH_2CH(OH)CH_2(OCH_2CH_2)_4OC_4H_9$. Other details as in Fig. 1.

measure of the retention time of non-symmetrical chromatographic peaks? The characterization of the elution profiles was extensively examined[32-37], Jönsson in a series of papers[22,38-40] studied the problem of the correct measure of retention time in linear, non-ideal elution chromatography. He examined relationships between three different retention measures (the maximum of the peak, the median and the centre of gravity) and the skew and the width of the elution peak observed. For symmetric peaks these three measures of retention time (or retention volume) would be identical, but the elution peak is generally skewed and the degree of skewness depends on the nature of the peak broadening mechanisms[22,39]. Generally, the correct measure of the retention time is the median, while the maximum and the centre of gravity are different from the true retention time.
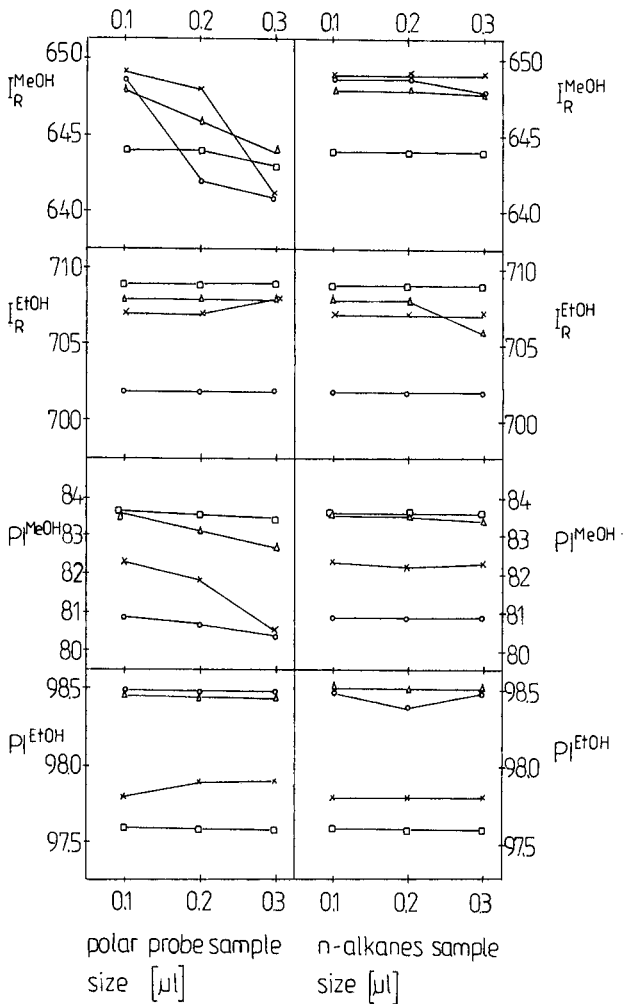
Fig. 3. The influence of the solute sample size on the polarity parameters. Stationary phase: $C_4H_9O(CH_2CH_2O)_2CH_2CH(OH)CH_2(OCH_2CH_2)_4OC_4H_9$. $\Delta G_s^m(C=O)^{MEK}$ and $\Delta G_s^m(C=O)^{MPK}$ = partial molal Gibbs free energies of solution of the carbonyl group for 2-butanone and 2-pentanone, respectively. Other details as in Fig. 1.

Using three different measures for retention time for some solute probes, three sets of polarity parameters were determined (Table IV). Different retention times were obtained by measuring to the median (MED), centre of gravity (CG) or maximum of the peak. The polarity parameters calculated from three sets of retention times are generally close to each other for alcohols as the observed differences are random and statistically insignificant. However, differences in the retention time and retention index of pyridine are high, systematic and significant on all six stationary phases examined.

Another factor which might influence the polarity parameters is the method of

the dead time estimation. Many workers have extensively examined the problem of dead time estimation[41-52]. Wainwright and Haken[52] reviewed the methods of presentation of retention data, measurement and calculation of column dead time, and presented procedures for its calculation. They pointed out that the dead time can be determined most accurately by using at least four *n*-alkanes and the calculation method of Grobler and Balizs[19]. The methods using three consecutive *n*-alkanes and the direct calculation methods of Peterson and Hirsch[53], Sevčik[45] or Sevčik and Löwentap[20] were also recommended[51]. Whilst different values of the dead time were obtained here, the values of the polarity parameters were not influenced by the method of dead time estimation as the observed differences are random and statistically insignificant.

In the case of stationary phases with significantly low molecular masses, one should take into account possible bleeding. The differences in the amounts of liquid phase, weighed before and after the experiment (after extraction from the support), confirmed that no significant loss of the liquid phase took place during the polarity measurements at the standard temperature.

CONCLUSIONS

The column temperature significantly influences all the polarity parameters considered. They decrease with increasing temperature (Table I), although not always due to a decrease in the stationary phase polarity.

An increase in the amount of liquid stationary phase decreases the sensitivity of the polarity parameters to changes in the sample size, both of the polar probes and the reference *n*-alkanes (Figs. 1 and 2). An increase in the sample size of the polar probe decreases (for liquid loadings below 20%) the values of the retention index, polarity index and coefficient p, while the partial molal free energies of solution of hydroxyl, $\Delta G_s^m(OH)$, and carbonyl, $\Delta G_s^m(C=O)$, groups were sometimes increased. Dispersive force parameters, such as criterion A, slightly increase with increasing sample size of the *n*-alkanes. The partial molar excess Gibbs free energy of solution per methylene group, $\Delta G^E(CH_2)$, slightly decreases with increasing solute sample size if the stationary phase loading is less than 25%. This may be attributed to support activity and could be reduced by blocking the active sites on the support surface by using a silanized support.

The influence of the carrier gas, the column length and the method of dead time estimation upon the polarity parameters is statistically insignificant.

It was found that the skewness of alcohols' peaks is small and differences between the polarity parameters calculated from different retention times are random and insignificant. The peaks for pyridine are highly skewed and the retention indices calculated from different retention times are quite different. They may be arranged in the following order: $I_{R,max} > I_{R,MED} > I_{R,CG}$.

No significant loss of the stationary phase during polarity measurement has been observed. Differences between the amount of the liquid phase before and after chromatographic measurements were generally below 0.2%.

ACKNOWLEDGEMENT

REFERENCES

1   J. Szymanowski, A. Voelkel, J. Beger and H. Merkwitz, *J. Chromatogr.*, 330 (1985) 61.
2   J. Beger, H. Merkwitz, J. Szymanowski and A. Voelkel, *J. Chromatogr.*, 333 (1985) 319.
3   A. Voelkel, J. Szymanowski, J. Beger and K. Ebert, *J. Chromatogr.*, 391 (1987) 373.
4   A. Voelkel, J. Szymanowski, J. Beger and K. Ebert, *J. Chromatogr.*, 398 (1987) 31.
5   A. Voelkel, J. Szymanowski, J. Beger and K. Ebert, *J. Chromatogr.*, 409 (1987) 29.
6   J. Szymanowski, A. Voelkel, J. Beger and H.-J. Binte, *J. Prakt. Chem.*, 327 (1985) 353.
7   A. Voelkel, *Chromatographia*, 23 (1987) 195.
8   A. Voelkel, *Chromatographia*, 25 (1988) 95.
9   A. Voelkel, *J. Chromatogr.*, 435 (1988) 29.
10 A. Voelkel, *J. Chromatogr.*, 450 (1988) 291.
11 J. Szymanowski, A. Voelkel and Z. A. Rashid, *J. Chromatogr.*, 402 (1987) 55.
12 V. R. Huebner, *Anal. Chem.*, 34 (1962) 488.
13 T. H. Risby, P. C. Jurs and B. L. Reinbold, *J. Chromatogr.*, 99 (1974) 173.
14 B. L. Reinbold and T. H. Risby, *J. Chromatogr. Sci.*, 13 (1975) 372.
15 C. E. Figgins, T. H. Risby and P. C. Jurs, *J. Chromatogr. Sci.*, 14 (1976) 453.
16 C. E. Figgins, B. L. Reinbold and T. H. Risby, *J. Chromatogr. Sci.*, 15 (1977) 208.
17 J. Ševčik and M. S. H. Löwentap, *J. Chromatogr.*, 217 (1981) 139.
18 M. Roth and J. Novák, *J. Chromatogr.*, 234 (1982) 337.
19 A. Grobler and G. Balizs, *J. Chromatogr. Sci.*, 12 (1974) 57.
20 J. Ševčik and M. S. H. Löwentap, *J. Chromatogr.*, 147 (1978) 75.
21 J. R. Conder and C. L. Young, *Physicochemical Measurement by Gas Chromatography*, Wiley, New York, 1979, p. 69.
22 J. A. Jönsson, *Chromatographia*, 14 (1981) 653.
23 G. E. Petrowski and J. R. Vanatta, *J. Am. Oil Chem. Soc.*, 50 (1973) 284.
24 F. Vernon and J. B. Suratman, *Chromatographia*, 17 (1983) 597.
25 L. Rohrschneider and E. Pelster, *J. Chromatogr.*, 186 (1980) 249.
26 F. Vernon and M. Rayakorn, *Chromatographia*, 13 (1980) 611.
27 R. L. Pecsok and B. H. Gump, *J. Phys. Chem.*, 71 (1967) 2202.
28 F. Riedo and E. sz. Kováts, *J. Chromatogr.*, 186 (1980) 47.
29 J. A. Jönsson and L. Mathiasson, *J. Chromatogr.*, 179 (1979) 1.
30 L. Mathiasson and J. A. Jönsson, *J. Chromatogr.*, 179 (1979) 7.
31 L. Mathiasson, J. A. Jönsson, A. M. Olsson and L. Haraldson, *J. Chromatogr.*, 152 (1978) 11.
32 M. Goedert and G. Guiochon, *Anal. Chem.* 42 (1970) 962.
33 M. Goedert and G. Guiochon, *Anal. Chem.*, 45 (1973) 1188.
34 S. Huang, J. W. Wilson, D. J. Wilson and K. A. Overholser, *J. Chromatogr.*, 89 (1974) 119.
35 P. R. Rony and J. E. Funk, *J. Chromatogr. Sci.*, 9 (1971) 215.
36 T. S. Sørensen, *J. Chromatogr.*, 88 (1974) 197.
37 C. V. Madjar and G. Guiochon, *J. Chromatogr.*, 142 (1977) 61.
38 J. A. Jönsson, *Chromatographia*, 13 (1980) 273.
39 J. A. Jönsson, *J. Chromatogr.*, 150 (1978) 11.
40 J. A. Jönsson, *Chromatographia*, 13 (1980) 729.
41 J. Guberska, *Chem. Anal. (Warsaw)*, 19 (1974) 161.
42 J. A. Jönsson and R. Jönsson, *J. Chromatogr.*, 111 (1975) 265.
43 J. A. Jönsson, *J. Chromatogr.*, 139 (1977) 156.
44 J. K. Haken, M. S. Wainwright and R. J. Smith, *J. Chromatogr.*, 133 (1977) 1.
45 J. Ševčik, *J. Chromatogr.*, 135 (1977) 183.
46 R. J. Smith, J. K. Haken and M. S. Wainwright, *J. Chromatogr.*, 147 (1978) 65.
47 W. E. Sharpless and F. Vernon, *J. Chromatogr.*, 161 (1978) 83.
48 J. R. Ashes, S. C. Mills and J. K. Haken, *J. Chromatogr.*, 166 (1978) 391.
49 W. K. Al-Thamir, J. H. Purnell, C. A. Wellington and R. J. Laub, *J. Chromatogr.*, 173 (1979) 388.
50 N. S. Wainwright, J. K. Haken and D. Srisukh, *J. Chromatogr.*, 179 (1979) 160.
51 L. S. Ettre, *Chromatographia*, 13 (1980) 73.
52 M. S. Wainwright and J. K. Haken, *J. Chromatogr.*, 184 (1980) 1.
53 M. L. Peterson and J. Hirsch, *J. Lipid Res.*, 1 (1959) 132.

CHROM. 20 917

RETENTION IN REVERSED-PHASE LIQUID CHROMATOGRAPHY: SOLVATOCHROMIC INVESTIGATION OF HOMOLOGOUS ALCOHOL–WATER BINARY MOBILE PHASES

JAMES J. MICHELS and JOHN G. DORSEY*

Department of Chemistry, University of Florida, Gainesville, FL 32611 (U.S.A.)

(First received March 3rd, 1988; revised manuscript received August 12th, 1988)

SUMMARY

The mechanism of retention in reversed-phase liquid chromatography (RPLC) has been further investigated using the $E_T(30)$ solvatochromic solvent polarity scale. The retention behavior of a variety of solutes was measured using a homologous series of normal alcohols as the organic modifiers in hydroorganic mobile phases. The results imply that a systematic change in the extent of solvation of the stationary phase occurs with respect to the size of the organic modifier. It was also found that a linear extrapolation of the log k' *versus* $E_T(30)$ plots for different mobile phases using methanol, ethanol and acetonitrile (but not *n*-propanol) as modifiers, intersected at approximately the $E_T(30)$ value of pure water. This intersection is further evidence that the $E_T(30)$ model of solute retention is a useful tool with which to study the mechanism of retention in RPLC. The extrapolated retention value in water, log k'_w, from the $E_T(30)$ plots should then prove to be a more reliable means of estimating solute lipophilicity using RPLC than the percent organic modifier model.

INTRODUCTION

Many approaches have been taken to study the effects of the mobile phase in reversed-phase liquid chromatography (RPLC)[1–9]. The most commonly used mobile phases in RPLC are binary solutions of water with an organic solvent modifier such as methanol, acetonitrile or tetrahydrofuran. Retention in RPLC is primarily controlled by the chromatographic strength of the mobile phase, with the strength frequently denoted as the percent of the organic modifier in the binary aqueous solution[10]. It has been shown both experimentally[11] and theoretically[5] that a quadratic function best describes plots of log k' *versus* percent organic modifier.

We have previously developed a method of modeling retention that relates the strength of the mobile phase to a measured polarity of the solvent[9]. An independent examination of the effect of changing mobile phase polarity on chromatographic retention has been performed using $E_T(30)$ solvatochromic solvent polarity measurements. Solvatochromism is a phenomenon that relates changes in the spectral behavior (intensity, position or shape) of a probe molecule to changes in its environment.

The $E_T(30)$ scale relates changes in position of the λ_{max} for the electronic absorption of the molecule 2,6-diphenyl-4-(2,4,6-triphenyl-N-pyridinio) phenolate (ET-30) to changes in the polarity of the solvent. ET-30 signifies the acronym for the probe molecule itself while $E_T(30)$ stands for the measured polarity value calculated by the equation:

$$E_T(30)(\text{kcal/mole}) = 28\ 592/\lambda_{max}(\text{nm}) \tag{1}$$

It was shown that by plotting $\log k'$ *versus* the $E_T(30)$ polarity of the mobile phase, a linear relationship was found. The regression analysis of 332 data sets revealed a higher degree of linearity for the $E_T(30)$ model over the percent organic modifier model[9].

A review of the use of solvatochromism to study retention in RPLC and other forms of chromatography has recently been published[12]. There are two solvatochromic scales that have been used to investigate retention processes in reversed-phase chromatography. The $E_T(30)$ scale, the single parameter scale used here, and the multiparameter $\pi^\star$ scale of solvent dipolarity/polarizability developed by Kamlet *et al.*[13]. The $\pi^\star$ scale is intended to represent the solute–solvent interactions in the absence of strong forces such as hydrogen-bonding or ion–dipole interactions. Additionally, both α and β scales of solvent hydrogen-bond donor or acceptor interactions have been derived which independently account for these strong forces. The Kamlet and Taft methods are essentially more rigorous than the single-parameter scales in that they separate the three interactions into individual terms, however, they are also only empirical measures. While the $E_T(30)$ scale is a single parameter scale, it has been shown to be sensitive to both solvent dipolarity/polarizability as well as solvent hydrogen-bond donor ability. This sensitivity to hydrogen bonding effects makes this solvent scale useful for studying aqueous reversed-phase mobile phases.

An interesting perspective on the "meaning" of single and multiparameter solvent scales is found in a paper by Sjöström and Wold[14] and a reply by Kamlet and Taft[15]. Sjöström and Wold argue that instead of the classical interpretation of linear free energy relationships expressing a combination of "fundamental" effects that they should be viewed strictly as locally valid linearizations of complicated relationships. It is perhaps best at this point in the solvatochromic studies of chromatographic retention mechanisms, whether with single or multi-parameter scales, to keep this view in mind. While perhaps useful for predictive purposes, it is yet to be determined if they are providing a "fundamental" measure of the retention process: they may merely be providing a convenient linearization of more complicated phenomena.

The most rigorous approach to understanding the retention mechanism of reversed-phase chromatography is that recently developed by Dill[5] using a lattice statistical thermodynamic approach. He proposed that two driving forces dominate retention; (i) the difference in the chemistry of the contacts of the solute with surrounding molecular neighbors in the stationary and mobile phase, and (ii) the partial ordering of the grafted stationary phase chains which, at sufficiently high bonding density, leads to an entropic expulsion of solute from the stationary phase relative to that which would be expected in a simpler amorphous oil phase–water partitioning process. We have tested (i) against an extensive data base of almost 350 sets of experiments and in agreement with theory have found that the mobile phase contri-

bution to retention can be described by the binary interaction constants of solutes with solvents[16]. From this extensive data base it was also found that the $E_T(30)$ solvent polarity appears to provide a direct measure of the binary interaction constants. While this is almost certainly a "convenient linearization of more complicated phenomena", it still provides a useful means of probing mobile phase effects on the retention process. We have also tested (ii) by synthesizing monomeric octadecyl stationary phases over a range of 1.5–4.0 μmol/m^2, and have found, in agreement with theory, that partition coefficients go through a maximum at approximately 3.0 μmol/m^2 (ref. 17). Above this density chain packing constraints become significant, and creation of a solute sized cavity in the stationary phase becomes entropically expensive.

If the measured $E_T(30)$ polarity is truly a good descriptor of mobile phase strength, then by correlating retention *versus* the $E_T(30)$ polarity of the solvent for a given solute on a given column, the retention behavior of the solute in all solvent systems on that particular column should be the same. Retention behavior is characterized by the slope of the log k' *versus* $E_T(30)$ plots and defined here as the sensitivity of the change in retention of a solute to changes in the mobile phase polarity. This is similar to Snyder's "S" value, which is the slope of log k' *versus* percent organic modifier[18]. Inspection of the regression coefficients for 89 of the 332 data sets revealed that the retention behavior of these systems are not normalized as expected[9]. Data taken from the literature on columns ranging in chain length from C_2 to C_{18} show that, for a given solute and column, the methanol slope is greater than the acetonitrile slope by an average ratio of 1.4[9].

One interpretation of this 1.4 methanol–acetonitrile slope ratio is the active role of the stationary phase in RPLC. If the stationary phase were truly a passive entity, as is said to be true by the solvophobic theory[3], the slopes of the $E_T(30)$ plots should be the same for a solute in any solvent system. The $E_T(30)$ scale has previously been shown to accurately measure solution properties, as evidenced by correlations of $E_T(30)$ polarity with reaction rate constants[19] and heats of solution at infinite dilution[20]. Retention is a result of the free energy change as a solute transfers between the mobile and stationary phases. As iso-$E_T(30)$ values of two mobile phases suggest that they are energetically equivalent, at least as seen by the ET-30 molecule, then the different slopes suggest that the solute is experiencing a different environment in the stationary phase with methanol–water as compared to acetonitrile–water. While it can be argued that the local environment of the ET-30 molecule is very different between methanol and acetonitrile, similar slope ratio differences are seen between methanol and ethanol, where the local environment of the ET-30 molecule would be more similar. This must primarily result from differences in the extent of solvation of the alkyl chains bonded to the silica as the organic modifier is changed. These differences in extent of solvation have also been shown by others[21–24].

To further clarify the meaning of the slope of the log k' *vs.* $E_T(30)$ plots we attemped to induce systematic changes in the retention behavior for a given system by using a homologous series of organic modifiers. The series chosen was that of the *n*-alcohols (methanol, ethanol and *n*-propanol) because they are readily available, non-toxic, have low wavelength UV cutoffs and their distribution behavior in an RPLC system has been previously characterized[25]. The extent of solvation of the stationary phase was expected to change in direct proportion to the molecular size of

the modifier, resulting in a systematic change in the slopes of the $E_T(30)$ plots for each solute. Therefore, the aim of this study was to provide further evidence that the change in the log k' *versus* $E_T(30)$ slopes is indeed due to changes in the nature of the stationary phase and to also characterize ethanol and *n*-propanol mobile phases for RPLC by the $E_T(30)$ solvatochromic solvent polarity scale.

EXPERIMENTAL

Solvatochromic measurements

All solvatochromic measurements were made using ET-30 (Reichardt's Dye) (Aldrich, Milwaukee, WI, U.S.A.). Binary solvents were prepared by mixing additive volumes of ET-30 in pure organic solvent, pure organic solvent and water to the desired solvent compositions with the final concentration of ET-30 being approximately 200 mg/l. Samples were placed into a 1-cm path length quartz cell and spectra obtained with a Hewlett-Packard (Palo Alto, CA, U.S.A.) Model 8450A diode-array spectrophotometer or an IBM Instruments (Danbury, CT, U.S.A.) Model 9420/9430 UV–VIS spectrophotometer. Maximum absorbance wavelengths were determined using a peak-picking algorithm on each instrument. Three spectra were acquired for each sample and the $E_T(30)$ values for each sample were averaged. The $E_T(30)$ data produced were fit to the appropriate degree polynomial using the Interactive Microware (State College, PA, U.S.A.) program CURVE FITTER run on an Apple (Cupertino, CA, U.S.A.) II + 48K microcomputer, and any unmeasured $E_T(30)$ values were determined by interpolation.

Retention measurements

All retention measurements were obtained with a Beckman (San Ramon, CA, U.S.A.) Model 100A isocratic LC pump, a Beckman Model 153 fixed wavelength (254 nm) UV detector, a Valco (Houston, TX, U.S.A.) C6W injector with a 10-μl sample loop, a Fisher (Austin, TX, U.S.A.) Recordall Series 5000 strip chart recorder and a Hamilton (Reno, NV, U.S.A.) 705 SNR LC syringe. A Beckman Ultrasphere ODS (5μm), 15 cm $\times$ 4.6 mm I.D. column and a DuPont (Wilmington, DE, U.S.A.) Zorbax TMS (6 μm), 15 cm $\times$ 4.6 mm I.D. column were used. The columns and solvents were thermostated at 30°C with a Brinkmann Lauda (Westbury, NY, U.S.A.) Model MT heater/circulator. Fisher HPLC-grade methanol and acetonitrile, certified 1-propanol and Florida Distillers (Lake Alfred, FL, U.S.A.) absolute ethyl alcohol (200 proof) were used as received. Water was first purified with a Barnstead (Milford, MA, U.S.A.) Nanopure system, irradiated with UV light in a Photronix (Medway, MA, U.S.A.) Model 816 HPLC reservoir for at least 24 h and then filtered through a Rainin (Woburn, MA, U.S.A.) 0.45-μm Nylon-66 membrane filter prior to use. Pure solutes were used as received and stock solutions made in HPLC grade methanol: Eastman Kodak (Rochester, NY, U.S.A.) reagent ACS spectro grade toluene, butylbenzene, naphthalene, *p*-nitroanisole and benzylamine, Fisher certified ethylbenzene and nitrobenzene, Mallinckrodt (St. Louis, MO, U.S.A.) organic reagent benzophenone, MCB (Norwood, OH, U.S.A.) *p*-nitrophenol and Alfa (Danvers, MA, U.S.A.) *n*-propylbenzene. Retention times were determined manually and the breakthrough time (t_o) used to calculate capacity factors found by the elution of an injection of HPLC-grade methanol.

Linear regression

Regression calculations were done by using the Interactive Microware program CURVE FITTER run on an Apple II + 48K microcomputer.

RESULTS AND DISCUSSION

Solvatochromic polarity measurements

The results of the $E_T(30)$ solvent polarity measurements for binary aqueous solutions of ethanol and of *n*-propanol are illustrated in Fig. 1. $E_T(30)$ measurements for methanol and acetonitrile aqueous solutions have previously been discussed[9,26,27]. As previously evidenced with methanol–water and acetonitrile–water solutions, the $E_T(30)$ polarity values for aqueous ethanol and *n*-propanol solutions show non-linear behavior when related to either mole fraction or volume percent of organic modifier. Fig. 1a–d show the change in $E_T(30)$ values for ethanol and *n*-propanol *versus* both volume percent and mole fraction. As has been previously discussed about the organic-rich region of the acetonitrile–water system[9,28], the ET-30 probe molecule may be sensing a breakdown in the hydrogen-bonding network of the solutions in the high organic content ranges. Unlike the acetonitrile–water system, the $E_T(30)$ changes shown here are not as great because ethanol and *n*-propanol are stronger hydrogen-bond donors than acetonitrile. From entropy and enthalpy of mixing data it has been hypothesized for dilute aqueous solutions of a non-electrolyte that a collective stabilization of the hydrogen-bond lattice of water occurs due to an increase in the energy of water–water hydrogen-bonds or in their number[29]. Therefore, it could be that a change in the hydrogen-bonding network of the solution is being sensed by the ET-30 probe in the dilute alcohol concentration
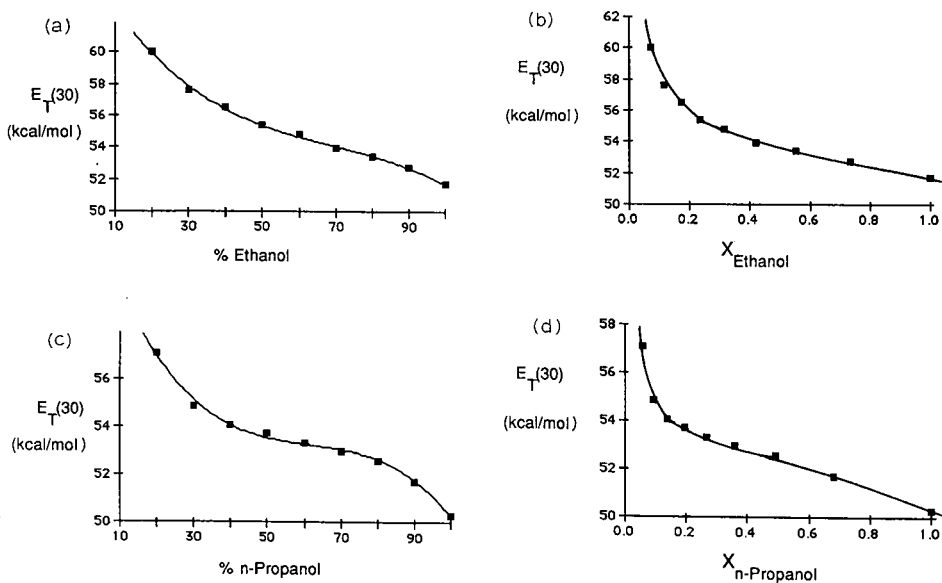
Fig. 1. The $E_T(30)$ polarity of binary hydroorganic mobile phases as it varies with (a) percent ethanol; (b) mole fraction ethanol; (c) percent *n*-propanol and (d) mole fraction *n*-propanol.

region as well. Furthermore, the random mixing approximation is not expected to be generally viable in the limits of extreme composition[11], less than a few percent of either mobile phase component. In these regions, the ET-30 probe molecules or the minor component of the binary solvent may associate to form non-random mixtures.

Chromatographic retention measurements

Retention data was gathered for ten solutes on an octadecylsilane (C_{18}) reversed-phase column using aqueous methanol, ethanol, n-propanol and acetonitrile solutions as the mobile phases. The test solutes were chosen so that a variety of compound types would be used. Acetonitrile was used as a reference organic modifier from which the homologous alcohols could be compared in the form of log k' vs. $E_T(30)$ slope ratios. It was expected that upon going from methanol to ethanol to n-propanol mobile phases, the slopes of the log k' vs. $E_T(30)$ plots for any of the test solutes would decrease by an amount linearly related to the carbon number of the alcohol modifier; this is a consequence of the displacement model of reversed-phase retention[30]. This was believed since it has been shown that for alcohol–water mobile phases on a C_{18} column, the extent of solvation of the surface by the alcohol over the water increases with carbon chain length of the alcohol[25].

An example of the data generated in this study is the log k' *versus* $E_T(30)$ plots for naphthalene in all four solvent systems shown in Fig. 2. The average correlation coefficient (r) for a total of forty different data sets (similar to Fig. 2 but unreported) is 0.997 ± 0.002. By observing the positioning of each of the data sets along the $E_T(30)$ axis, it is obvious that not all of the polarities for all the different solvents overlap. The weakest n-propanol solvent used (30%) was about 1050 cal/mol less polar than the strongest methanol solvent used (90%). It is also obvious that there are no iso-E_T (30) values in reasonable isocratic retention ranges among the four solvent systems. In other words, there are no points of identical retention at one particular $E_T(30)$ value. If the $E_T(30)$ values are giving a useful measure of mobile phase strength, then one possible explanation is a continued change in the solvation structure of the sta-

Fig. 2. Retention of naphthalene on an Ultrasphere ODS column at 30°C as a function of $E_T(30)$ polarity with binary hydroorganic mobile phases.

tionary phase even for organic modifiers of the same functionality differing only in size.

From Fig. 2 and the $E_T(30)$ slopes and Snyder S values for all ten solutes in Table I, a few trends can be observed. First, as seen previously with aqueous methanol and acetonitrile mobile phases[9], the slopes of the log k' versus $E_T(30)$ plots for the ethanol and n-propanol mobile phases increase with increasing solute size. The addition of methylene groups in the alkylbenzene homologous series (toluene to n-butylbenzene) produces a linear relationship with respect to the log k' versus $E_T(30)$ slopes ($r = 0.998$ for ethanol and 0.999 for n-propanol). Second, the log k' versus $E_T(30)$ plots for methanol, ethanol and acetonitrile appear to extend to a common point. In fact, all three extrapolate to an average $E_T(30)$ value of 62.5 $\pm$ 2.9 kcal/mol ($n = 27$) which is approximately the $E_T(30)$ value for pure water of 63.1 kcal/mol[31]. The n-propanol plots, however, do not approach the other plots near 63.1 kcal/mol at all, which suggests that a different mechanism of retention may be occurring with the aqueous n-propanol mobile phases in contrast to the other three. Third, the expected results of a decrease in the log k' versus $E_T(30)$ slopes with increasing carbon number of the alcohol solvent modifiers did not occur. As seen in Table I, the $E_T(30)$ slopes for each test solute decreased when going from methanol–water to ethanol–water, but upon going from ethanol–water to n-propanol–water the slopes increase. None of the solutes, however, showed intersections near 0% modifier when volume-% was used as the organic-concentration descriptor.

If the slope of a log k' versus $E_T(30)$ plot for a test solute in an alcohol-modified solvent is ratioed to that in acetonitrile-modified solvent for all three alcohols, the retention behavior for each alcohol–water system can be compared to the others for all ten solutes. The average methanol–acetonitrile ratio for all ten solutes came to be 1.13 $\pm$ 0.09, for ethanol–acetonitrile 0.84 $\pm$ 0.05 and for n-propanol–acetonitrile 1.14 $\pm$ 0.06. The methanol–acetonitrile slope ratio was within experimental error of the previously determined average value of 1.18 $\pm$ 0.05 for C_{18} at 40°C[9]. The larger the slope or slope ratio, the greater the change in retention per unit of polarity change. Methanol slope ratios are greater than those for ethanol due to the fact that in a binary alcohol–water mobile phase, methanol does not selectively solvate the stationary phase to as large a degree as ethanol. When comparing one chromatographic system using methanol to another using ethanol, the stationary phase will be less polar (contain less alcohol) for the methanol system when the mobile phases for both are equal in alcohol composition. If an equivalent increase in mobile phase polarity as measured by $E_T(30)$ is performed in each system, retention will change to a greater extent in the methanol system than the ethanol system due to the greater difference in the polarity of the mobile and stationary phases. For n-propanol–water mobile phases, however, the stationary phase may be saturated by n-propanol when using solutions of 30% or more. It was calculated that when using a 9% n-propanol–water solvent, the C_{18} chains on the surface have already taken up 95% of the maximum uptake by n-propanol[25]. Therefore, for the concentrations of n-propanol used (30–70%), increasing the amount of n-propanol in the solvent may not produce changes at the stationary phase in the same manner as with methanol and ethanol.

Another consideration is the chemical information obtained from $E_T(30)$ measurements. The ET-30 molecule is sensitive to solvent dipolarity/polarizability and hydrogen bond acidity. According to Kamlet et al.[32], the $E_T(30)$ polarity of a given

TABLE I

SLOPES OF THE LOG k' VERSUS $E_T(30)$ PLOTS AND SNYDER S VALUES FOR THE HOMOLOGOUS SOLVENTS AND ACETONITRILE ON ALTEX ULTRASPHERE ODS COLUMN AT 30°C

Solute	Methanol-water		Ethanol-water		n-Propanol-water		Acetonitrile-water	
	$E_T(30)$ slope	$-S$	$E_T(30)$ slope	$-S$	$E_T(30)$ slope	$-S$	$E_T(30)$ slope	$-S$
Toluene	0.504	3.11	0.381	2.92	0.543	2.46	0.464	2.72
Ethylbenzene	0.581	3.59	0.442	3.38	0.598	2.70	0.519	3.04
n-Propylbenzene	0.690	4.12	0.509	3.44	0.667	3.01	0.578	3.38
n-Butylbenzene	0.835	4.63	0.559	3.78	0.728	3.28	0.636	3.72
Naphthalene	0.594	3.66	0.423	3.23	0.598	2.70	0.516	3.02
Benzophenone	0.607	3.73	0.394	2.99	0.546	2.42	0.513	3.00
Nitrobenzene	0.354	2.52	0.287	2.63	0.413	1.83	0.332	2.24
p-Nitroanisole	0.409	2.41	0.347	3.15	0.418	1.85	0.398	2.71
p-Nitrophenol	0.338	2.41	0.260	2.38	0.403	2.22	0.350	2.38
Benzylamine	0.321	2.29	0.240	2.19	0.298	1.66	0.274	1.88

solvent can be related to the dipolarity/polarizability (π^*) and hydrogen bond acidity (α) scales by the regression equation[33,34]:

$$E_T(30) = 28.21 + 12.40\pi^* + 14.40\alpha \tag{2}$$

For water, methanol, ethanol, n-propanol and acetonitrile, respectively, the values of π^* are 1.09, 0.60, 0.54, 0.52 and 0.75 and the values of α are 1.17, 0.93, 0.83, 0.78 and 0.19[33]. These π^* and α values show only small differences among the three pure alcohols. If the trends seen in the log k' *versus* $E_T(30)$ plots among the various organic modifiers were not due to differences in the solvation structure of the stationary phase, then the trends should be due to the solvent parameters measured by π^* and α. Cheong and Carr have examined the π^* and α properties of aqueous solutions of methanol, 2-propanol and tetrahydrofuran[34] and attribute decreases in hydrogen bond acidity for methanol–water mixtures from that of the pure solvents to the formation of less hydrogen bond acidic complexes. These effects between the different mobile phases, however, are normalized by the $E_T(30)$ scale and should not show up as differences in the log k' *versus* $E_T(30)$ plots.

It was necessary to see if the hypothesis of n-propanol saturation at the C_{18} surface was possibly occurring. Retention measurements were made for benzylamine and p-nitrophenol, the two least retained solutes, at n-propanol in water compositions below 30% (10–25%). The previously determined n-propanol-acetonitrile slope ratio for benzylamine was 1.09 while that for p-nitrophenol was 1.15. When the retention measurements were observed from 35 to 10% n-propanol, the new slope ratios for n-propanol–acetonitrile came to 0.57 for benzylamine and 0.23 for p-nitrophenol. It is interesting to note that these slope ratios are less than the average ethanol–acetonitrile value of 0.84 $\pm$ 0.05. The p-nitrophenol value is questionable because the log k' *versus* $E_T(30)$ plot was not as linear as desired ($r = 0.969$). Fig. 3 shows the log k' *versus* $E_T(30)$ plot for benzylamine from 10 to 50% n-propanol in water. The linear region of the plot extends from 10 to about 35% with an apparent break occurring between 35 and 40%. It is also interesting to note that when the point of intersection of the 10 to 35% n-propanol plots with the other three modifiers was calculated for both benzylamine and p-nitrophenol, the average $E_T(30)$ intersection point was 58.70 $\pm$ 1.06 kcal/mol ($n = 6$), which is close to the $E_T(30)$ value of pure water. Based on the resulting n-propanol–acetonitrile slope ratios and the intersection of the n-propanol plots with those of the other three modifiers, it would appear that
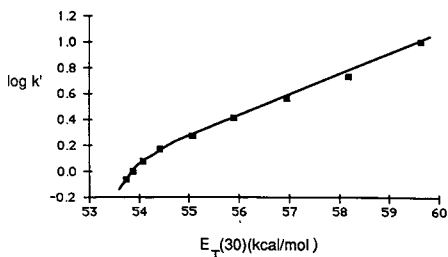
Fig. 3. Retention of benzylamine on an Ultrasphere ODS column at 30°C as a function of $E_T(30)$ polarity with mobile phases ranging from 10 to 50% n-propanol in water.
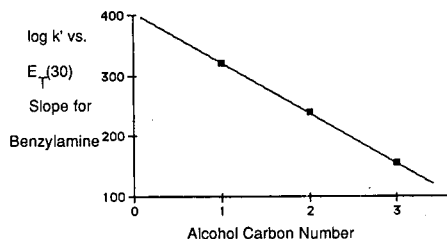
Fig. 4. The relationship between the retention behavior of benzylamine [using the $E_T(30)$ model] on an Ultrasphere ODS column at 30°C and the carbon number of the modifier alcohol in a binary hydroorganic mobile phase.

for *n*-propanol compositions at or below 30% the mechanism of retention is similar to that when using the other modifiers. Above 30% *n*-propanol, the C_{18} stationary phase may be saturated by *n*-propanol and a different mechanism of retention is operative. While only two data sets were measured due to the extremely long retention times and poor peak shapes in this mobile phase range, the implications are encouraging.

If the slopes of the log k' *versus* $E_T(30)$ plot for benzylamine are plotted against the carbon number of the alcohol modifier, a linear relationship is found ($r = 0.999$), as illustrated in Fig. 4. The same trend is seen for *p*-nitrophenol but the linearity is slightly worse ($r = 0.979$). When the *n*-propanol slope of the 30 to 50% solvents was used, no linear correlation was found between the $E_T(30)$ slope and alcohol carbon number. Thus, a systematic change in retention may occur when using modifier compositions in a range where no surface saturation occurs.

In order to see if the solvation differences of the stationary phase between solvent systems could be minimized, retention measurements for the ten test solutes were made on a trimethylsilane (C_1) column. By using a C_1 column, it was hoped that specific solvation interactions between the solvent modifier and the bonded phase would be minimized. Normalization of the retention behavior of a solute in various solvent systems should then be reflected in all alcohol–acetonitrile ratios of log k' *versus* $E_T(30)$ slopes approaching unity.

No conclusive results could be found in the C_1 retention data, however. One of the problems encountered when using C_1 columns in RPLC is the impreciseness of the chemistry of the surface. The polarity of the reversed-phase surface increases as the bonded carbon chain is shortened since the residual silanol groups are left less shielded from the solute and mobile phase and are freer to interact in the retention process[35]. Silanol interactions can affect results in the form of irreproducible retention times and tailed peak shapes. Furthermore, a C_1 column likely exhibits an adsorption type mechanism rather than partitioning because of the shallow "depth" of the stationary phase. A representative plot of the data gathered is shown for naphthalene in Fig. 5. The linearity for all data sets deteriorated in contrast to the C_{18} data as expressed in a lower and more scattered average r value of 0.991 ± 0.016 ($n = 40$). A slight degree of curvature was evident with most of the plots. No surprising trends are noticeable from the $E_T(30)$ slopes and S values shown in Table II. When slope ratios were calculated, methanol–acetonitrile remained about the same (1.16 ± 0.15), *n*-
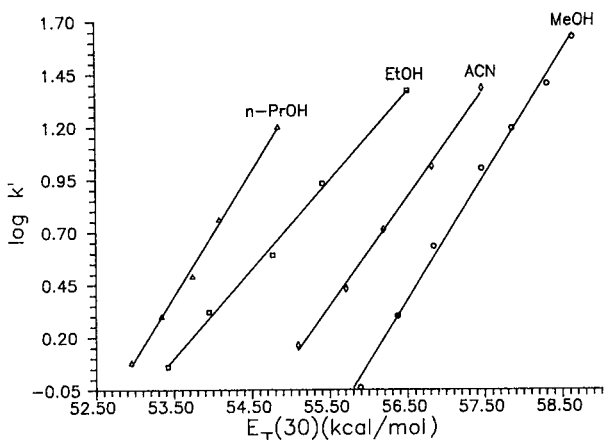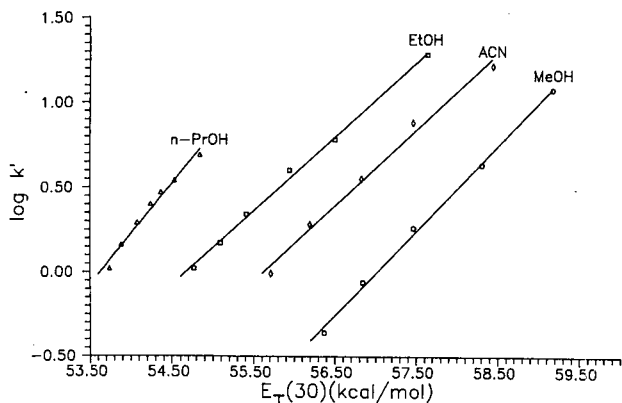
Fig. 5. Retention of naphthalene on a Zorbax TMS column at 30°C as a function of $E_T(30)$ polarity with binary hydroorganic mobile phases.

propanol–acetonitrile increased slightly (1.22 ± 0.20), and ethanol–acetonitrile came to unity (1.00 ± 0.10). The uncertainty in each average slope ratio, though, is too great to make any generalizations with respect to the solvation behavior of each solvent system on the C_1 surface.

A beneficial aspect of this work is the intersection of the C_{18} log k' versus $E_T(30)$ plots for different modifiers (except n-propanol) at the $E_T(30)$ value of pure water. This intersection is further evidence that $E_T(30)$ plots are monitoring the correct partitioning processes under different equilibrium conditions. A problem often associated with the evaluation of solute lipophilicity by high-performance liquid chromatography (HPLC) is the extrapolation of log k' versus % organic plots to 0% organic concentration in the mobile phase[36]. The reproducibility of the retention value in pure water (log k'_w) is affected by the magnitude and direction of curvature in a log k' versus percentage plot[37]. Reymond et al.[38] have recently shown that linear extrapolations of methanol–water retention data yielded practically identical log k'_w values as parabolic extrapolations of acetonitrile–water mixtures. Schoenmakers et al.[39], however, reported that the quadratic fit of log k' versus percent organic modifier does not hold at >90% water, and they recommend adding an empirical (percent modifier)$^{1/2}$ term for that range. Since more than one binary solvent system can be used to determine the log k'_w value, it would be desirable to have as low of an uncertainty between log k'_w values as possible. An average and standard deviation of log k'_w values for each test solute in the different mobile phases was determined. The data sets used were those for methanol, ethanol and acetonitrile. Due to the previously discussed problem of stationary phase saturation, n-propanol was not considered. Calculation of log k'_w for all ten test solutes used in this study at 0% modifier by linearization of percent organic plots for thirty data sets gave an average deviation of 0.32. Subsequent calculation of log k'_w at 63.1 kcal/mole [the $E_T(30)$ value of pure water] for $E_T(30)$ plots gave an average deviation of 0.19; an improvement of about 40%. In addition, preliminary work has shown that log k' versus $E_T(30)$ plots for different modifiers converge toward the $E_T(30)$ value of water, as seen in Fig. 6. Plots of log k' versus percentage for different modifiers do not converge to 0% organic at all

TABLE II

SLOPES OF THE LOG k' VERSUS $E_T(30)$ PLOTS AND SNYDER S VALUES FOR THE HOMOLOGOUS SOLVENTS AND ACETONITRILE ON ZORBAX TMS COLUMN AT 30°C

Solute	Methanol–water		Ethanol–water		n-Propanol–water		Acetonitrile–water	
	$E_T(30)$ slope	$-S$	$E_T(30)$ slope	$-S$	$E_T(30)$ slope	$-S$	$E_T(30)$ slope	$-S$
Toluene	0.390	2.78	0.379	3.29	0.530	2.90	0.370	2.54
Ethylbenzene	0.468	3.33	0.444	3.85	0.611	3.33	0.433	2.96
n-Propylbenzene	0.556	3.97	0.515	4.47	0.687	3.73	0.502	3.42
n-Butylbenzene	0.653	4.64	0.597	5.17	0.750	4.07	0.567	3.85
Naphthalene	0.500	3.55	0.435	4.24	0.598	3.25	0.446	3.04
Benzophenone	0.579	4.10	0.474	4.60	0.580	3.25	0.448	3.05
Nitrobenzene	0.357	2.72	0.296	2.89	0.367	2.37	0.331	2.28
p-Nitroanisole	0.412	3.14	0.332	3.24	0.375	2.41	0.361	2.48
p-Nitrophenol	0.329	2.51	0.264	2.76	0.276	2.05	0.323	2.23
Benzylamine	0.321	2.44	0.248	2.59	0.213	1.62	0.208	1.57
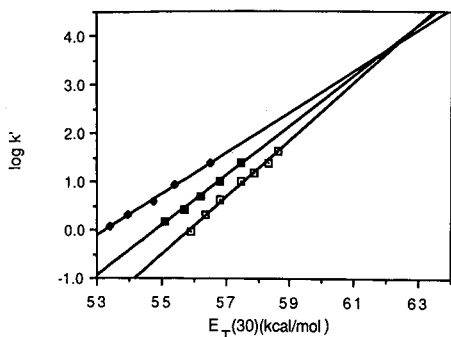
Fig. 6. Convergence of $E_T(30)$ retention plots for naphthalene to the $E_T(30)$ value of pure water (63.1 kcal/mol). ($\square$) Methanol; ($\blacksquare$) acetonitrile; ($\blacklozenge$) ethanol.

but diverge[40]. The use of log k'_w values from $E_T(30)$ plots has also been demonstrated for the successful calculation of solvent–solvent contact free energies of binary organic–water mixtures[16]. Since the scatter of the values appears to be decreased from those found using the percentage model and the $E_T(30)$ plots for different solvents converge to a common point instead of diverging, the $E_T(30)$ solvatochromic polarity scale should be a reliable means of estimating log k'_w values for the evaluation of lipophilicity. Further investigations of this possibility are underway.

CONCLUSION

The $E_T(30)$ solvatochromic solvent polarity scale has been used to further study the effects of the mobile phase in reversed-phase liquid chromatography. Retention measurements were made on a variety of test solutes using a homologous series of alcohols (methanol, ethanol and n-propanol) as organic modifiers to determine whether a systematic change in the solvation of a C_{18} surface could be observed. We infer from the results and our model that a systematic change in the solvation structure of the stationary phase occurs with respect to the carbon number of the modifying alcohol. This relationship is hypothesized to exist, however, only if the alcohol component in the binary mobile phase is used in a concentration range such that saturation of the stationary phase does not occur. Retention measurements were also made on a C_1 column using the same solutes and mobile phases to determine if solvation effects could be normalized for all solvents, but no conclusive judgements can presently be made. The applicability of using the log k' versus $E_T(30)$ plots of various solvent systems for the estimation of solute lipophilicity has also been shown to be quite promising.

ACKNOWLEDGEMENT

REFERENCES

1 B. L. Karger, L. R. Snyder and C. Eon, *Anal. Chem.*, 50 (1978) 2126–2136.
2 P. J. Schoenmakers, H. A. H. Billiet and L. de Galan, *Chromatographia*, 15 (1982) 205–214.
3 C. Horváth, W. Melander and I. Molnár, *J. Chromatogr.*, 125 (1976) 129–156.
4 D. E. Martire and R. E. Boehm, *J. Phys. Chem.*, 87 (1983) 1045–1062.
5 K. A. Dill, *J. Phys. Chem.*, 91 (1987) 1980–1988.
6 P. Jandera, H. Colin and G. Guiochon, *Anal. Chem.*, 54 (1982) 435–441.
7 P. C. Sadek, P. W. Carr, R. M. Doherty, M. J. Kamlet, R. W. Taft and M. H. Abraham, *Anal. Chem.*, 57 (1985) 2971–2978.
8 P. W. Carr, R. M. Doherty, M. J. Kamlet, R. W. Taft, W. Melander and Cs. Horváth, *Anal. Chem.*, 58 (1986) 2674–2680.
9 B. P. Johnson, M. G. Khaledi and J. G. Dorsey, *Anal. Chem.*, 58 (1986) 2354–2365.
10 J. R. Gant, J. W. Dolan and L. R. Snyder, *J. Chromatogr.*, 185 (1979) 153–177.
11 P. J. Schoenmakers, H. A. H. Billiet, R. Tijssen and L. de Galan, *J. Chromatogr.*, 149 (1978) 519–537.
12 J. G. Dorsey, *Chromatography*, 2(5) (1987) 37–41.
13 M. J. Kamlet, J. L. M. Abboud and R. W. Taft, *J. Am. Chem. Soc.*, 99 (1977) 6027–6038.
14 M. Sjöström and S. Wold, *Acta Chem. Scand. B*, 35 (1981) 537–554.
15 M. J. Kamlet and R. W. Taft, *Acta Chem. Scand. B*, 39 (1985) 611–628.
16 P. T. Ying, J. G. Dorsey and K. A. Dill, *Anal. Chem.*, submitted for publication.
17 K. B. Sentell and J. G. Dorsey, *Anal. Chem.*, submitted for publication.
18 L. R. Snyder, J. W. Dolan and J. R. Gant, *J. Chromatogr.*, 165 (1979) 3–30.
19 H. Elias, G. Gumbel, S. Neitzel and H. Volz, *Fresenius' Z. Anal. Chem.*, 306 (1981) 240–244.
20 Z. Ilic, Z. Maksimovic and C. Reichardt, *Glas. Hem. Drus. Beograd.*, 49 (1984) 17–23.
21 R. M. McCormick and B. L. Karger, *Anal. Chem.*, 52 (1980) 2249–2257.
22 R. M. McCormick and B. L. Karger, *J. Chromatogr.*, 199 (1980) 259–273.
23 C. R. Yonker, T. A. Zwier and M. F. Burke, *J. Chromatogr.*, 241 (1982) 257–268.
24 C. R. Yonker, T. A. Zwier and M. F. Burke, *J. Chromatogr.*, 241 (1982) 269–280.
25 R. P. W. Scott and C. F. Simpson, *Faraday Symp. Chem. Soc.*, 15 (1980) 69–82.
26 B. P. Johnson, M. G. Khaledi and J. G. Dorsey, *J. Chromatogr.*, 384 (1987) 221–230.
27 J. G. Dorsey and B. P. Johnson, *J. Liq. Chromatogr.*, 10 (1987) 2695–2706.
28 S. Balakrishnan and A. J. Easteal, *Aust. J. Chem.*, 34 (1981) 943–947.
29 Y. I. Naberuklin and V. A. Rogov, *Russ. Chem. Rev.*, 40 (1971) 207–215.
30 X. Geng and F. E. Regnier, *J. Chromatogr.*, 332 (1985) 147–168.
31 C. Reichardt and E. Harbusch-Gornert, *Liebigs Ann. Chem.*, (1983) 721–743.
32 M. J. Kamlet, J. L. M. Abboud and R. W. Taft, in R. W. Taft (Editor), *Progress in Physical Organic Chemistry*, Vol. 13, Wiley, New York, NY, 1981.
33 M. J. Kamlet, J. L. M. Abboud, M. H. Abrahams and R. W. Taft, *J. Org. Chem.*, 48 (1983) 2877–2887.
34 W. J. Cheong and P. W. Carr, *Anal. Chem.*, 60 (1988) 820–826.
35 P. E. Antle, A. P. Goldberg and L. R. Snyder, *J. Chromatogr.*, 321 (1985) 1–32.
36 J. E. Garst and W. C. Wilson, *J. Pharm. Sci.*, 73 (1984) 1616–1623.
37 J. E. Garst, *J. Pharm. Sci.*, 73 (1984) 1623–1629.
38 D. Reymond, G. N. Chung, J. M. Mayer and B. Testa, *J. Chromatogr.*, 391 (1987) 97–109.
39 P. J. Schoenmakers, H. A. H. Billiet and L. de Galan, *J. Chromatogr.*, 282 (1983) 107–121.
40 J. J. Michels and J. G. Dorsey, unpublished results.

CHROM. 20 938

REVERSED-PHASE HIGH-PERFORMANCE THIN-LAYER CHROMATOGRAPHY AND COLUMN LIQUID CHROMATOGRAPHY OF METAL COMPLEXES OF PHEOPHORBIDE *a*

KYOKO ADACHI*, KOICHI SAITOH and NOBUO SUZUKI*

Department of Chemistry, Faculty of Science, Tohoku University, Sendai, Miyagi 980 (Japan)
(First received July 27th, 1988; revised manuscript received August 25th, 1988)

SUMMARY

The thin-layer chromatographic mobilities of pheophorbide *a* (Phor-a) and six metal–Phor-a complexes were measured on an octadecyl-bonded silica gel (C_{18} silica) thin layer with various polar developing solvents, such as methanol, ethanol, acetonitrile and their mixtures with an aqueous solution containing an electrolyte such as sodium chloride. The mobility of the metal complex decreases in the following order of complexed metal ions: $Co^{III} > Fe^{III} > Zn^{II} > Phor$-a $> Ni^{II} \approx Pd^{II} > Cu^{II}$, although the Fe^{III} complex shows an exceptionally smaller mobility than the Zn^{II} complex when pure acetonitrile or the water–acetonitrile containing sodium chloride is used as the developing solvent. The mobility of a metal–Phor-a complex is generally smaller than that of the pheophorbide *b* complex of the same metal. A successful reversed-phase high-performance liquid chromatographic separation was achieved for a mixture of Phor-a and its Fe^{III}, Co^{III}, Cu^{II} and Zn^{II} complexes by using ethanol–phosphate buffer (pH 3) (85:15, v/v) as the mobile phase.

INTRODUCTION

Pheophorbide is one of the significant degradation products of chlorophyll and is found in natural waters[1], marine sediments[2] and brined green vegetables[3]. Pheophorbide contains in its molecular structure a chlorin macrocycle which has complexing ability with metal ions. The formation of pheophorbide complexes with Cu^{II} or Zn^{II} is utilized to enhance the green colour of stored and processed vegetables[4,5].

The usefulness of chromatography for the separation and detection of the Cu^{II} and Zn^{II} complexes of pheophorbide has been reported[6]. However, the chromatographic characteristics of complexes with other metals have hardly been studied. In previous work, the retention behaviour of pheophorbides, including both *a* and *b* forms (Phor-a and Phor-b), was investigated in comparison with that of chlorophylls

---

* Present address: Department of Chemistry, Hamamatsu University School of Medicine, Hamamatsu, 431-31 Japan.

and pheophytins in reversed-phase high-performance thin-layer chromatography (HPTLC) and high-performance liquid chromatography (HPLC)[7].

In this paper we describe the reversed-phase HPTLC and HPLC behaviour of the metal complexes of Phor-a, which is one of the predominant derivatives from chlorophyll-a, the most common type of chlorophyll. The complexes with Fe^{III}, Co^{II}, Co^{III}, Ni^{II}, Cu^{II}, Zn^{II} and Pd^{II} were studied. In addition, the chromatographic mobility of each metal–Phor-a complex was compared with that of the corresponding metal complex of Phor-b.

This work was carried out as part of a series of studies on the chromatography of porphyrins, metalloporphyrins and related compounds. Porphine[8], tetraphenyl-porphine[9,10], tetratolylporphine[11], etioporphyrin[12], haematoporphyrin[13] and their metal complexes have been investigated so far.

EXPERIMENTAL

Materials

All procedures for the preparation of pheophorbides and their metal complexes (see Fig. 1) were carried out in the dark.
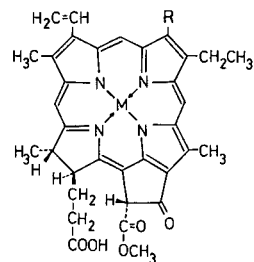
Fig. 1. Formula of a typical complex of Phor-a or Phor-b with a divalent metal M. $R = CH_3$ for Phor-a and CHO for Phor-b.

Phor-a was prepared from spinach leaves as described previously[7]. The metal complexes of Phor-a were prepared by the procedure detailed below, which were similar to those used for the Phor-a complexes of Cu^{II} ans Zn^{II} by Jones *et al.*[14].

In the first step of the preparation, 10 mg of a metal compound (see below) and a few small crystals of ascorbic acid were added to an acetone solution (2 ml) containing about 1 mg of Phor-a. The mixture was warmed at 40°C in an atmosphere of nitrogen in order to prevent undesirable oxidation of the Phor-a structure in the reaction procedure. The chlorides of Fe^{II} and Pd^{II} and acetates of Co^{II}, Ni^{II}, Cu^{II} and Zn^{II} were used as the metal compounds. In preparing both Ni and Co complexes, acetic acid was used as the reaction solvent instead of acetone. The reaction time was 2 h for each reaction, except for the Ni complex, which required 10 h. In each reaction process, a small portion of the reaction mixture was regularly sampled in order to check the Phor-a consumption and the formation of the desired complex by monitoring the changes in the visible absorption spectra and the disappearance of the fluorescence of Phor-a under UV radiation, and also by HPTLC.

In the second step of the preparation, the crude metal–Phor-a complex was extracted with 6 ml of diethyl ether from the reaction mixture that had preliminarily been cooled and then diluted with 10 ml of water. The ether phase, after separation from aqueous phase, was washed with 3 ml of 6 *M* hydrochloric acid to remove unreacted Phor-a (this procedure was omitted with of Zn^{II} complex, because undesirable demetallation occurred). The ether phase was then washed repeatedly with 2-ml portions of water until the pH of the aqueous phase became higher than about 5. After removal of the ether by evaporation, the solid product was dried *in vacuo* and then stored in a phosphorus pentoxide desiccator in an atmosphere of nitrogen at $-20°C$.

In the washing step with 6 *M* hydrochloric acid, the metal complexes other than the Co complex did not transfer from their ether solutions to the acid, whereas part of Co complex was back-extracted into the acid. The fraction of Co complex that had been transferred from the ether solution to the 6 *M* hydrochloric acid was so stable that it was no longer re-extracted with a new portion of diethyl ether. This fraction of the Co complex is hereafter denoted Co(Phor-a)$_{acid}$ in order to distinguish it from the fraction that is non-extractable into 6 *M* hydrochloric acid; the latter fraction is denoted Co(Phor-a)$_{ether}$. The Co(Phor-a)$_{acid}$ complex was almost completely transferred into diethyl ether after 10-fold dilution of the acidic solution with water. It was solidified, dried and stored as for Co(Phor-a)$_{ether}$.

The final product of each methal–Phor-a complex was checked by fast atom bombardment mass spectrometry. A significant signal appeared at the *m/z* value corresponding to the molecular ion $(M + 1)^+$ of the desired metal complex. The mass spectrometric results for Co(Phor-a)$_{ether}$ are considered under Results and Discussion.

Phor-b and its metal complexes were prepared by using similar procedures to those used for Phor-a and its metal complexes. The purity of each product was checked by HPTLC and HPLC. Contamination with a small amount of unreacted Phor-b was unavoidable in the procedures used, because both Phor-b and its metal complexes were so soluble in 6 *M* hydrochloric acid that the contaminating Phor-b could not be removed selectively from the metal complex product by washing with the acidic solution.

HPTLC

RP-18 F$_{254s}$ HPTLC plates (10 × 10 cm) coated with C$_{18}$-silica were obtained from Merck (Darmstadt, F.R.G.). A frontal portion of the thin-layer coating was scraped off the plate so that the development would automatically stop when the solvent front had run 75 mm from the sample origin.

Sample solutions of Phor-a and its metal complexes in diethyl ether were prepared in the concentration range 0.1–1 m*M*. A 0.5-µl portion of the sample solution was spotted at the origin and development was carried out horizontally in a Model 28510 chamber (Camag, Muttenz, Switzerland) in a thermostated room at 25°C until the migration of the solvent front had automatically stopped after 75 mm.

The compounds in the chromatogram were detected spectrophotometrically with a Shimadzu (Kyoto, Japan) CS-920 densitometer at a detection wavelength 410 nm for Phor-a and its metal complexes, except for the Fe^{III} complex (390 nm), and at 430 nm for Phor-b and its metal complexes.

HPLC

A Twincle solvent-delivery pump and a VL-611 sample injection valve (Jasco, Tokyo, Japan), a TSK ODS-80TM column (particle diameter 5 μm, packed in a 150 mm × 4.6 mm I.D. stainless-steel tube) (Toyo Soda, Tokyo, Japan) and a rapid-scanning UV–visible multi-wavelength spectrophotometric detector of our original design[15] were assembled into a liquid chromatograph system. A mixture of alcohol (methanol or ethanol) and an aqueous solution (pH buffered solution or unbuffered aqueous sodium chloride solution) was used as the mobile phase at a flow-rate of 0.78 ml/min.

Sample solutions of Phor-a and its metal complexes were prepared at a 0.1 mM concentration in acetone and a 2-μl aliquot of each solution was injected into the column. Spectrophotometric detection was carried out at 410 nm, except for Fe (Phor-a), which was detected at 390 nm. In-flow recording of UV–visible absorption spectra of the column effluent was continued through every HPLC experiment by using the rapid-scanning UV–visible spectrophotometric detector in order to identify the substance eluted from the column.

Spectroscopy

Visible absorption spectra were recorded with a Hitachi (Tokyo, Japan) U-3200 spectrophotometer. The bandpass was set at 1 nm.

Mass spectra were obtained by using a JEOL JMS-HX100 mass spectrometer equipped with a fast atom bombardment ionization system (JEOL, Tokyo, Japan). The sample, which had been preliminarily dissolved in dimethyl sulphoxide, was added to a glycerol–triglycerol (1:1) mixture used as a matrix. They were coated on the ionization target, followed by bombardment with a xenon atom beam (at 6 kV and 20 mA) under $5.0 \cdot 10^{-6}$ Torr pressure.

Electron spin resonance (ESR) spectra were recorded at 77 K with a JEOL JES-FE2XG ESR spectrometer.

RESULTS AND DISCUSSION

Spectral characteristics

Phor-a has two major absorption bands in the visible region, which shifted on metal complex formation. The wavelengths of maximum absorption and relative absorptivities measured for Phor-a and its metal complexes are summarized in Table I. The metal complexes other than those of Ni^{II} and Pd^{II} have two absorption maxima in common with Phor-a, one in the blue region and the other in the red. The complexes of Ni^{II} and Pd^{II} have two maxima with comparable absorptivities in the blue region. The absorption bands of the Fe^{III} and Co^{III} complexes were broad in comparison with the others. According to the relative absorptivities shown in Table I, the absorption bands in the blue, rather than those in the red region, are suitable for the sensitive spectrophotometric detection of Phor-a and its metal complexes by HPTLC and HPLC, although exceptions are found for the complexes of Ni^{II} and Pd^{II}.

Table I indicates that the absorption spectra observed for Co(Phor-a)$_{ether}$ and Co(Phor-a)$_{acid}$ are different from each other, implying that these types of Co complex have different chemical forms. In order to clarify the oxidation state of the cobalt in these complexed forms with Phor-a, their ESR characteristics were examined. It is

TABLE I

VISIBLE ABSORPTION SPECTRAL CHARACTERISTICS FOR PHEOPHORBIDE *a* AND ITS METAL COMPLEXES IN DIETHYL ETHER AT 25 °C

Substance	Wavelength of maximum absorption, blue/red (nm)	Relative absorptivity (blue/red)
Phor-a	409/667	2.00
Fe(Phor-a)Cl	387/623	2.27
Co(Phor-a)$_{ether}$*	411/652	1.63
Co(Phor-a)$_{acid}$*	430/662	1.41
Ni(Phor-a)	393, 417/648	0.95**
Cu(Phor-a)	422/650	1.37
Zn(Phor-a)	426/655	1.37
Pd(Phor-a)	390, 418/638	0.67**

 * A fraction of the product.
 ** The absorbance at the longer wavelength of the two peaks in blue region was taken for the calculation.

predicted, in principle, that an ESR signal should be observed for the complex of Co^{II} (d^7), but not for Co^{III} (d^6) species. The ESR parameters determined for Co(Phor-a)$_{ether}$ and Co(Phor-a)$_{acid}$ are compared with those for the Co complexes of protoporphyrin IX dimethyl ester (P$_p$DME)[16] in Table II. Although the samples to be applied in ESR were prepared at nearly the same concentrations, a strong ESR signal was recorded for the Co(Phor-a)$_{ether}$ sample, whereas only a faint response was obtained for the Co(Phor-a)$_{acid}$ sample. The intensity of the ESR signal (peak-to-peak height) for the latter sample was smaller than 1/15th of that for the former. It was found that the ESR parameters determined for the Co(Phor-a)$_{ether}$ sample were close to those for the oxygen adduct of the Co^{II}–P$_p$DME complex rather than the simple Co^{II}–P$_p$DME complex, as shown in Table II. Accordingly, it is considered that Co(Phor-a)$_{ether}$ contains Co(Phor-a)O$_2$. In the mass spectrum recorded for the Co(Phor-a)$_{ether}$ sample, significant peaks appeared at *m/z ca.* 682 and 650, which

TABLE II

ESR PARAMETERS FOR THE COBALT COMPLEXES OF PHEOPHORBIDE *a* AND PROTOPORPHYRIN IX DIMETHYL ESTER (P$_p$DME) AT 77 K

No.	Sample or known complex	Solvent	$g_\perp$	$g_{//}$	$|A_\perp|$ $\cdot 10^4$ cm^{-1}	$|A_{//}|$ $\cdot 10^4$ cm^{-1}	Ref.
1	Co(Phor-a)$_{ether}$*	DEE*	1.992	2.076	14.9	20.9	This work
2	Co(Phor-a)$_{acid}$**	DEE	1.992	2.084	14.2	19.3	This work
3	Co(P$_p$DME)–MTE*	Toluene	2.360	2.016	37.7	90.1	16
4	Co(P$_p$DME)–MTE–O$_2$	Toluene	2.002	2.072	21	12	16
5	Co(P$_p$DME)–ME*	Toluene	2.384	2.018	54.4	93.2	16
6	Co(P$_p$DME)–ME–O$_2$	Toluene	2.003	2.059	19.2	14	16

 * DEE = diethyl ether; MTE = 2-(methylthio)ethanol; ME = mercaptoethanol.
 ** Very weak response.

TABLE III

R_F VALUES OF PHEOPHORBIDE a AND ITS METAL COMPLEXES ON A C_{18}-BONDED SILICA GEL THIN LAYER AT 25°C

RP-18 F_{254s} HPTLC plate (Merck No. 13724).

Developing solvent	$R_F \cdot 100$						
	Phor-a	Fe^{III}	Co^{III}	Ni^{II}	Cu^{II}	Zn^{II}	Pd^{II}
Methanol	42	47–62*	81–92*	31	30	73	32
Methanol–water (95:5)**	19	28–40*	87	14	13	47	13
Methanol–water (95:5) containing 0.01 M NaCl	19	75	91	14	13	50	14
Ethanol	80	100	100	73	72	92	73
Ethanol–water (87.5:12.5)	42	46–54*	62–71*	36	31	68	35
Ethanol–water (87.5:12.5) containing 0.01 M NaCl	42	85	92	35	30	67	34
Acetonitrile	32	65	1–9*	25	23	72	24
Acenotrile–water (95:5)	31	61	86–97*	24	24	73	25
Acenotrile–water (95:5) containing 0.01 M NaCl	31	61	100	27	24	76	25

* Broadened spot.
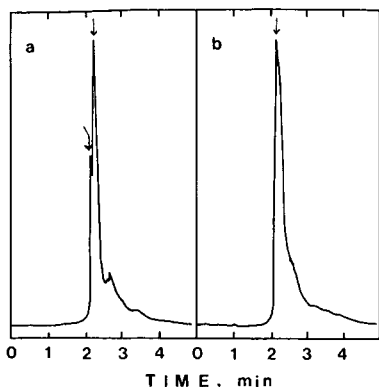
Fig. 2. HPLC traces of (a) Co(Phor-a)$_{ether}$ and (b) Co(Phor-a)$_{acid}$. Mobile phase: methanol–(0.02 *M* NaH$_2$PO$_4$–0.02 *M* H$_3$PO$_4$, pH 3) (95:5, v/v); flow-rate, 0.78 ml/min. Detection at 415 nm.

could be assigned to the molecular ions of Co(Phor-a)O$_2$ [(M + 1)$^+$] and its deoxygenated form, Co(Phor-a) [(M − 32) + 1)$^+$], respectively. It was confirmed by HPLC (see Fig. 2) that Co(Phor-a)$_{acid}$ apparently contained one particular form of the complex (eluted at retention time, t_R, 2.18 min) and that Co(Phor-a)$_{ether}$ contained at least two components (t_R 2.17 and 2.28 min, respectively).

From the above results, it was concluded that the material obtained in the Co(Phor-a)$_{acid}$ fraction was a complex of Co^{III}, such as Co(Phor-a)Cl, with considerable purity, and that obtained in the Co(Phor-a)$_{ether}$ fraction was a mixture of the Co^{III} complex, Co^{II} complex–O$_2$ adduct and others. It was considered that the complex first synthesized from Co^{II} under reductive conditions had been converted into its oxygen adduct or a Co^{III} in the subsequent washing, extraction and other steps.

To the following chromatographic studies were aplied the Co^{III} complex obtained as Co(Phor-a)$_{acid}$.

HPTLC of Phor-a and its metal complexes

The HPTLC mobility was measured for Phor-a and its metal complexes with different developing solvents, including pure methanol, ethanol and acetonitrile and their mixtures with aqueous solutions. Three examples of chromatograms are illustrated in Fig. 3 and the R_F values determined are summarized in Table III.
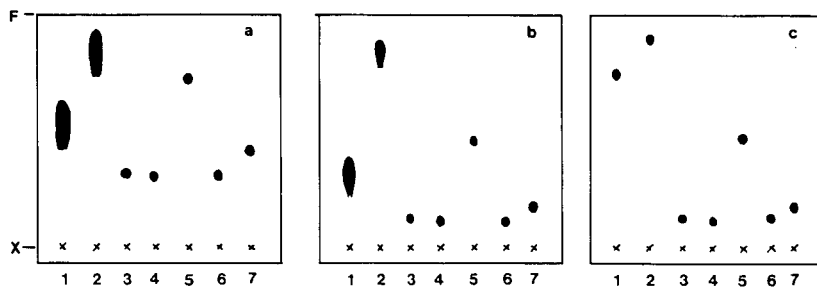
Fig. 3. HPTLC traces of pheophorbide and its metal complexes on RP-18 F$_{254s}$ plates. Developing solvents: (a) methanol; (b) methanol–water (95:5, v/v); (c) 0.01 *M* sodium chloride in methanol–water (95:5, v/v). Compounds: Pheo-a complexes of (1) Fe^{III}, (2) Co^{III}, (3) Ni^{II}, (4) Cu^{II}, (5) Zn^{II}, (6) Pd^{II}; (7) Phor-a. ×, Sample origin; F = solvent front.

When a pure organic solvent or its mixture with water was used as the developing solvent, the complexes of trivalent metals, such as Fe^{III} and Co^{III}, gave diffuse spots on the chromatogram (see in Fig. 3a and b). When an electrolyte such as sodium chloride was added to the developing solvent, the chromatograms of both the Fe^{III} and Co^{III} complexes were improved to sharp spots with enhanced mobilities (R_F values), as shown in Fig. 3c. In contrast, the complexes of divalent metals, such as Ni^{II}, Cu^{II}, Zn^{II} and Pd^{II}, always gave sharp spots on the chromatograms obtained with different solvents, and the mobilities of the complexes were almost independent of the presence of an electrolyte in the developing solvent. These results imply that dissociation or exchange of the anion (Cl^-) bonded with the central metal ion (Fe^{III} or Co^{III}) of the complex occurred during the migration process on the chromatogram developed with the pure water-containing organic solvent, and that the metal complex was stabilized when sodium chloride was added to the developing solvent.

The variation of the mobility of each metal–(Phor-a) complex with the concentration of the organic component in the developing solvent was examined by using ethanol–water and acetonitrile–water mixtures. The results are shown in Figs. 4 and 5, respectively. With both solvent systems, the R_M values [$R_M = \log(1/R_F - 1)$] of Phor-a and its divalent metal complexes decrease linearly with increase in the volume percentage (φ) of the organic component in the developing solvent, and the R_M vs. φ plots for these complexes are parallel to each other. The R_M values of Fe^{III} and Co^{III} complexes were so small in the methanol–water that a reliable relationship between R_M and the ethanol content of the developing solvent could not be confirmed. In the acetonitrile–water binary solvent Co^{III} was not retarded (R_M values smaller than -1.5), but the Fe^{III} complex exhibited moderate mobility, thus being smaller than Phor-a and larger than the Zn^{II} complex. It is considered that acetonitrile does not solvate the Fe^{III}–(Phor-a) complex as strongly as methanol.
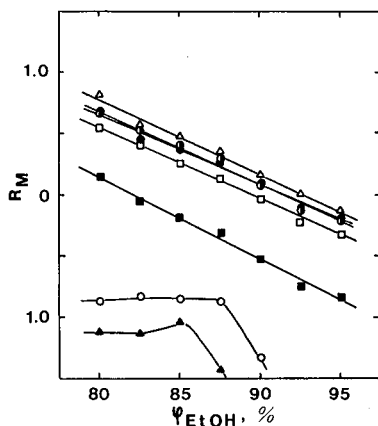
Fig. 4. R_M values of Phor-a and its metal complexes as a function of the ethanol content (φ_{EtOH}) of the ethanol–water containing 0.01 M sodium chloride used as the developing solvent. Compounds: ($\square$) Phor-a and its ($\bigcirc$) Fe^{III}, ($\blacktriangle$) Co^{III}, ($\bullet$) Ni^{II}, ($\triangle$) Cu^{II}, ($\blacksquare$) Zn^{II} and ($\varhexagon$) Pd^{II} complexes.
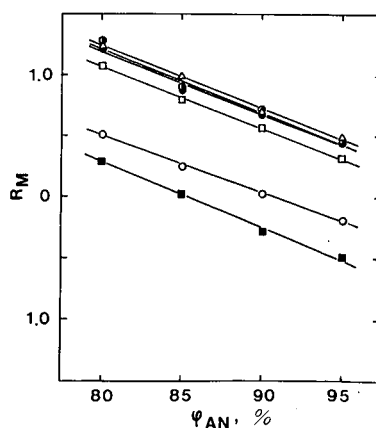
Fig. 5. R_M values of Phor-a and its metal complexes as a function of the acetonitrile content (φ_{AN}) of the acetonitrile–water containing 0.01 M sodium chloride used as the developing solvent. Symbols as in Fig. 3. The plots for the Co^{III} complex are omitted because of the extremely small R_M values.
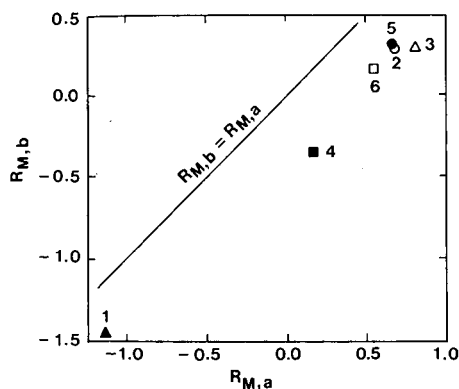
Fig. 6. Correlation between the R_M values of metal complexes of Phor-a ($R_{M,a}$) and -b ($R_{M,b}$). Developing solvent: 0.01 M sodium chloride in ethanol–water (80:20, v/v). Compounds: 1 = Co^{III}; 2 = Ni^{II}; 3 = Cu^{II}; 4 = Zn^{II}; 5 = Pd^{II}; 6 = metal-free Phor.

The mobility order for the divalent metal complexes is the same for both the methanol–water and acetonitrile–water binary developing solvents: Zn(Phor-a) > Phor-a > Ni(Phor-a) $\approx$ Pd(Phor-a) > Cu(Phor-a). This order is consistent with those for metal complexes of porphyrins, such as porphine[8] and its *meso*-tetraphenyl[9,10] and *meso*-tetratolyl[11] derivatives and haematoporphyrin[13], in reversed-phase HPTLC on an octadecyl-bonded silica gel plate.

Comparison with the HPTLC behaviour of Phor-b and its metal complexes

In order to examine the difference in the chromatographic behaviour between the metal complexes of Phor-a and Phor-b, the R_M values of these complexes are compared in Fig. 6. The R_M value of a metal complex of Phor-b is about 0.4 R_M unit smaller than that of the corresponding Phor-a complex. The replacement of the non-polar CH_3 group bonded to the chlorin macrocycle (in a Phor-a molecule) with a polar CHO group (in a Phor-b molecule) results in a decrease in the retention, (that is, a decrease in R_M) in the reversed-phase liquid chromatographic mode.

HPLC behaviour of metal complexes of Phor-a

It was pointed out in the HPTLC study that the addition of a salt to the developing solvent was effective in achieving non-diffuse spots on the chromatograms, particularly for the complexes of trivalent metals. In this HPLC study, three mobile phases containing different salts were used for comparison, consisting of 85:15 (v/v) mixtures of ethanol and aqueous solutions of (a) 0.067 M sodium chloride, (b) 0.02 M sodium acetate adjusted to pH 3 with hydrochloric acid and (c) 0.02 M sodium dihydrogenphosphate adjusted to pH 3 with phosphoric acid.

In order to examine the effects of a metal (stainless steel) coming into contact with the. liquid at the column wall and tubing, the UV–visible absorption spectrum was recorded for each metal complex in the column effluent by using a rapid-scanning spectrophotometric detector, and it was compared with that recorded for the same metal complexes in comparable solutions prepared in glassware. These spectra were comparable to each other in every instance. It was concluded that the metal parts of

the column and tubing had little effect on the metal complexes chromatographed in the instrument used.

It was found that both the peak shape and the retention time of the Fe^{III}–Phor-a complex depended considerably on the salt added to the mobile phase, whereas such a salt effect was not significant for the Phor-a complexes with divalent metals. The elution curves recorded for Phor-a and its Fe^{III}, Co^{III} and Zn^{II} complexes with these mobile phases are shown in Fig. 7. The Fe^{III} complex gave two poorly resolved peaks with the mobile phase containing sodium chloride (Fig. 7a), whereas it gave sharp peaks with the other mobile phases (Fig. 7b and c).

Taking account that the Fe^{III} complex injected into the column was prepared in the form Fe(Phor-a)Cl, it is considered that the anion (Cl^-) bonded to the iron was exchanged during the chromatographic process with a different anion present in the mobile phase used. The chemical species assigned to the poorly resolved peaks obtained for the Fe^{III} complex with the mobile phase containing sodium chloride (Fig. 7a) had not yet been clarified.

According to the chromatograms shown in Fig. 7, the mobile phase containing sodium dihydrogenphosphate–phosphoric acid at pH 3 is effective in separating the Fe^{III} complex from the Co^{III} complex. By using this mobile phase, the separation of several metal complexes was tested. Phor-a and its Fe^{III}, Co^{III}, Cu^{II} and Zn^{II} complexes
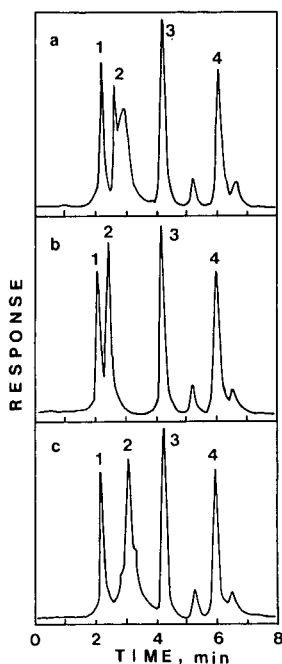
Fig. 7. HPLC elution curves for Phor-a and its Fe^{III}, Co^{III} and Zn^{II} complexes recorded by using 85:15 (v/v) mixtures of ethanol and aqueous solutions containing different salts. Aqueous solutions: (a) 0.067 M sodium chloride; (b) 0.02 M sodium acetate adjusted to pH 3 with hydrochloric acid; (c) 0.02 M sodium dihydrogenphosphate–0.02 M phosphoric acid (pH 3). Flow-rate, 0.78 ml/min. Detection at 390 nm for the Fe^{III} complex and 410 nm for the others. Peaks: 1 = Co^{III}; 2 = Fe^{III}; 3 = Zn^{II}; 4 = Phor-a.
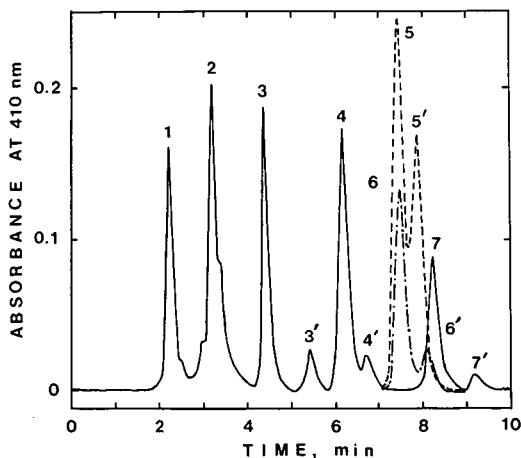
Fig. 8. HPLC separation of Phor-a and its metal complexes. Mobile phase: ethanol–(0.02 *M* sodium dihydrogen phosphate–0.02 *M* phosphoric acid, pH 3) (85:15, v/v); flow-rate, 0.78 ml/min. Peaks: 1 = Co^{III}; 2 = Fe^{III}; 3 = Zn^{II}; 4 = Phor-a; 5 = Ni^{II}; 6 = Pd^{II}; 7 = Cu^{II}.

were successfully separated from each other, as shown in Fig. 8. The complexes of Ni^{II} and Pd^{II} were hardly resolved, as shown by the superimposed broken curves in Fig. 8. A small peak (or a shoulder in some instances) appeared behind every major peak in the chromatogram. From the real-time monitoring of absorption spectra with the aid of a rapid scanning spectrophotometric detector, the column effluents assigned to every minor peak and its preceding major peak gave the same absorption spectra in the UV–visible region (350–700 nm). The small peak is assigned to the isomer or allomer of the substance that gives the preceding major peak on the chromatogram.

ACKNOWLEDGEMENTS

REFERENCES

1 R. R. Bidigare, M. C. Kennicutt, II, and J. M. Brooks, *Limnol. Oceanogr.*, 30 (1985) 432.
2 K. Hata, N. Handa and K. Ohta, *Chikyu Kagaku*, 14 (1980) 23.
3 I. D. Jones, R. C. White and E. Gibbs, *J. Food. Sci.*, 28 (1963) 437.
4 H. Fishbach and S. H. Newburger, *J. Assoc. Off. Agric. Chem.*, 26 (1943) 134.
5 S. H. Schanderl, G. L. Marsh and C. O. Chichester, *J. Food. Sci.*, 30 (1965) 312.
6 I. D. Jones, L. S. Butler, E. Gibbs and R. C. White, *J. Chromatogr.*, 70 (1972) 206.
7 N. Suzuki, K. Saitoh and K. Adachi, *J. Chromatogr.*, 408 (1987) 181.
8 Y. Wakui, K. Saitoh and N. Suzuki, *Chromatographia*, 22 (1986) 160.
9 K. Saitoh, M. Kobayashi and N. Suzuki, *Anal. Chem.*, 53 (1981) 2309.

10 K. Saitoh, M. Kobayashi and N. Suzuki, *J. Chromatogr.*, 243 (1982) 291.
11 M. Kobayashi, K. Saitoh and N. Suzuki, *Chromatographia*, 18 (1984) 441.
12 S. Miyake, K. Saitoh and N. Suzuki, *Chromatographia*, 20 (1985) 417.
13 N. Suzuki, K. Saitoh and Y. Sugiyama, *Chromatographia*, 22 (1986) 132.
14 I. D. Jones, R. C. White, E. Gibbs and C. D. Denard, *J. Agric. Food Chem.*, 16 (1968) 80.
15 K. Saitoh and N. Suzuki, *Anal. Chem.*, 51 (1979) 1683.
16 L. C. Dickinson and J. C. W. Chien, *Inorg. Chem.*, 15 (1976) 1111.

CHROM. 20 942

SEPARATION OF HYDROPHILIC THIOLS USING REVERSED-PHASE CHROMATOGRAPHY WITH TRIHALOACETATE BUFFERS

W. A. MacCREHAN* and D. SHEA★

Organic Analytical Research Division, Center for Analytical Chemistry, National Institute of Standards and Technology, Gaithersburg, MD 20899 (U.S.A.)

(First received January 19th, 1988; revised manuscript received May 17th, 1988)

SUMMARY

The reversed-phase retention behavior of several neutral and cationic hydrophilic thiols using trihaloacetic acid pairing agents is studied. Retention of cationic compounds increases with the size of the halogen substituent in the order: trifluoro- < trichloro- < tribromoacetic acid. The effect of pH, ionic strength, pairing ion and counter ion concentration on retention of cysteine and other thiols is measured. The formation of mobile phase ionic interactions is proposed as the mechanism of retention enhancement.

INTRODUCTION

Hydrophilic thiols of low molecular weight are involved in a variety of physiological and environmental processes. Clinical applications include heavy metal detoxification[1], the treatment of rheumatoid arthritis[2], and Wilson's disease[3]. Thiols are also important in the transport and bioavailability of metals in aquatic ecosystems[4]. Because of the significance of hydrophilic thiols, methods for their selective determination are needed. Compounds of interest in our work on marine sediment porewater are listed in Table I. Liquid chromatography (LC) is a technique well suited to the task of determining these water-soluble compounds in complex matrices.

Retention and separation of multicomponent mixtures of these thiols by LC are strongly influenced by their hydrophilic and ionic properties. For example, cysteine may be anionic, zwitterionic, or cationic depending on mobile phase pH; whereas methanethiol is neutral over most of the pH range (below pH 10). Various approaches have been used for the separation of mixtures of some of these compounds. The conjugate anions have been separated on a strong anion-exchange column[8], but with relatively low efficiency. Cation exchange has been used at low pH for the determination of cysteine, glutathione and penicillamine[9], but the neutral thiols were not well retained. Reversed-phase columns may be used directly, however, the more hydro-

---

* Permanent address: Department of Chemistry, Southeastern Massachusetts University, North Dartmouth, MA 02747, U.S.A.

TABLE I

pK_a VALUES OF THIOLS IN THIS STUDY

Analyte	Structure	Speciation category	pK_a value(s)[5-7]			
			pK_1	pK_2	pK_3	pK_4
Methanethiol	CH$_3$ – SH	Type A	10.33			
Ethanethiol	CH$_3$CH$_2$ – SH	Type A	10.61			
1-Propanethiol	CH$_3$CH$_2$CH$_2$ – SH	Type A	–			
2-Propanethiol	CH$_3$CHCH$_3$ SH	Type A	10.06			
2-Mercaptoethanol	CH$_2$CH$_2$ – SH OH	Type A	9.4			
1-Mercaptoglycerol	CH$_2$CHCH$_2$ – SH OH OH	Type A	9.28			
2-Mercaptopropanoic acid	CH$_3$CH – COOH SH	Type B	3.5	10.1		
3-Mercaptopropanoic acid	CH$_2$CH$_2$ – COOH SH	Type B	4.27	10.54		
Mercaptopyruvic acid	HS – CH$_2$C – COOH O	Type B	(2.49)*	–		
N-Acetylcysteine	HS – CH$_2$CH – COOH HN – C – CH$_3$ O	Type B	3.2	9.7		
Cysteine	HS – CH$_2$CH – COOH NH$_2$	Type C	1.9	8.15	10.3	
Penicillamine	(CH$_3$)$_2$C – CH – COOH SH NH$_2$	Type C	1.9	7.9	10.6	
Glutathione	HOOC – CHCH$_2$ – C – NHCH – C – NHCH$_2$COOH NH CH$_2$SH	Type D	2.1	3.5	8.7	9.5

* Pyruvic acid.

philic compounds (*e.g.* cysteine) show relatively little retention. Alkyl sulfate/sulfo-nate pairing agents have been used to increase the reversed-phase retention of three cationic thiols at pH 3[9]. However, the use of these long alkyl chain pairing agents requires long mobile/stationary phase equilibration time[10,11] and often results in nearly irreversible adsorption of the agent to the chromatographic column[11-13]. In addition, the retention of neutral compounds is decreased by the adsorption of the pairing agent to the stationary phase[10,11,14], which may complicate optimization of the separation of mixtures of ionic and neutral compounds.

    Another approach to LC thiol determination is to derivatise the thiol moiety with orthophthalaldehyde (OPA) in the presence of excess amine to yield a fluorescent product that is easily separated by reversed-phase LC[15]. However, these OPA adducts exhibit poor stability and interferences may occur in samples that contain both primary amines and thiols, because OPA reacts with both moieties. Furthermore, cysteine and glutathione may undergo cyclization[16] in the OPA reaction and may not be determined by this approach. Because of these drawbacks, other LC approaches to the determination of thiols are needed.

    In our study of the use of electrochemical detection for the LC determination of thiols[17], we observed increased retention of the cationic compounds on a reversed-phase column with the use of trihaloacetate (THA) buffers compared to inorganic

buffers such as phosphate. Retention also increased with increasing concentration and size of the THA halogen (Br > Cl > F). Other investigators have also noted buffer effects on the LC retention of ionic compounds[18-20]. In particular, the reversed-phase retention of cationic catecholamines was increased when a trichloroacetic acid buffer (TCA) was used[18]. Increases in retention similar to that obtained with octylsulfate were found with 0.1 mol/l TCA for these compounds. The authors suggested that increased retention of the cations resulted from the formation of ion pairs with the trichloroacetate anion.

In this paper, we describe a detailed examination of the reversed-phase retention of cationic and neutral thiols using trifluoro-, trichloro- and tribromoacetate buffers (TFA, TCA, and TBA respectively). The chromatographic variables that were investigated include pH, ionic strength, stationary phase material, counter cation size, and the concentration and size of the THA anion. A scheme for the isocratic separation of 12 low-molecular-weight, hydrophilic thiols is presented.

EXPERIMENTAL*

Chromatography

A liquid chromatograph consisting of two reciprocating dual-piston pumps with gradient controller was used to mix various mobile phase compositions during the isocratic separations (1 ml/min flow-rate). For all studies, 1% methanol was added to the mobile phase so that a catalytic oxygen-scrubber could be used to remove oxygen[21] which otherwise may oxidize the thiols[17]. The mobile phase was also sparged with nitrogen for 30 min and blanketed with helium to reduce the level of dissolved oxygen. Three commercial, octadecylsilyl-modified silica (C_{18}) columns with 5-μm particle size and 250 $\times$ 4.6 mm I.D. bed dimensions were used: Zorbax ODS (DuPont, Wilmington, DE, U.S.A.) and Vydac 201HS and Vydac 201TP (The Separations Group, Hesperia, CA, U.S.A.). Thiols were detected using a thin-layer electrochemical cell and is detailed elsewhere[17]. Briefly the detection conditions were: 1.0 mm gold–mercury thin-film working electrode; +200 mV applied potential (*vs.* Ag/AgCl, 3 mol/l KCl); 2-s time constant.

Reagents

Mobile phases were prepared with Burdick and Jackson Labs. distilled-in-glass grade methanol (Muskegon, MI, U.S.A.) and distilled water that was further purified with an ion-exchange/carbon adsorption system (Milli-Q, Millipore, Bedford, MA, U.S.A.). Buffers were prepared by addition of the conjugate acid followed by base titration to obtain the desired pH (measured *versus* standard buffers with a glass electrode). The acids/buffers included: phosphoric and perchloric acids (reagent grade, Mallinckrodt, Paris, KY, U.S.A.), monochloroacetic and monochloropropanoic acids (Alfa Products, Danvers, MA, U.S.A.), trifluoroacetic acid (Sequinal quality, Pierce, Rockford, IL, U.S.A.), trichloroacetic acid (ACS certified grade, Fisher

Scientific, Springfield, NJ, U.S.A.) and were used without further purification. Tribromoacetic acid (purum grade, Fluka, Ronkonkoma, NY, U.S.A.) was recrystallized from benzene before use and was limited to 0.05 mol/l concentration by its aqueous solubility. Buffers were prepared with bases of various counter cation size: lithium and ammonium hydroxides (Suprapur, Merck, Darmstadt, F.R.G.) and sodium and potassium hydroxides (analytical reagent, Mallinckrodt, Paris, KY, U.S.A.). The buffers served not only to control the pH of the mobile phase but also acted as supporting electrolyte for the electrochemical detector.

Thiols used in this study included cysteine, glutathione, N-acetylcysteine, mercaptoethanol, 2- and 3-mercaptopropanoic acid, 1-mercaptoglycerol and penicillamine (Sigma, St. Louis, MO, U.S.A.), methanethiol (Aldrich, Milwaukee, WI, U.S.A.), and mercaptopyruvate, 1- and 2-propanethiol, and ethanethiol (Fluka) and were stored under nitrogen at 4°C. Aqueous thiol stock solutions were prepared in a nitrogen-filled glove box using deoxygenated (1 h nitrogen sparge) mobile phase, standardized by iodometric titration[22], and stored with refrigeration ($\approx$ 4°C) under a nitrogen atmosphere. It was necessary to prepare dilute standard solutions ($\approx$ μmol/l) daily[17].

RESULTS AND DISCUSSION

The retention of ionic compounds in reversed-phase systems may be enhanced by the addition of oppositely charged, hydrophobic pairing ions to the mobile phase, often termed "ion-pair" chromatography. Three basic mechanisms have been proposed to model the observed increase in retention: (1) an ion pair forms in the mobile phase, increasing the lipophilicity of the ion followed by partitioning into the stationary phase[23], (2) the stationary phase is modified by the adsorbed pairing agent to form a "dynamic ion exchanger"[10,24] and (3) modification of the stationary–mobile phase interface with non-stoichiometric interaction of the pairing ion and analyte[25,26]. It is often very difficult to prove the dominance of one of the three mechanisms for any given separation system. As noted by Knox and Hartwick[10], the chromatographic retention factor k' is a thermodynamically derived quantity, and its measurement does not *directly* shed any light on the kinetics or mechanism of the retention process. In this work, the increased retention of cationic thiols by the use of trihaloacetate buffers as pairing agents was investigated.

Effect of chromatographic variables on the retention of thiols

Strategies for the separation of biogenic thiols must take the proton equilibria of the compounds into account. Fig. 1 illustrates the four classes of equilibria exhibited by the thiols used for this study, containing combinations of carboxylate (pK_a $\approx$ 2–4), amine (pK_a $\approx$ 8–9), as well as the thiol (pK_a $\approx$ 9–11) functionalities. Note that at the lowest pH normally used for silica-based column materials, pH = 2, type A and B are neutral, and type C and D are about half zwitterionic and half cationic. We will refer to these latter types as "net-cationic", since they show retention behavior expected for cationic species in the presence of oppositely charged pairing agent, *vide infra*.

We initially tested the addition of four commonly-used pairing agents for the separation of cations: pentane- and heptanesulfonate, as well as octane- and dodeca-
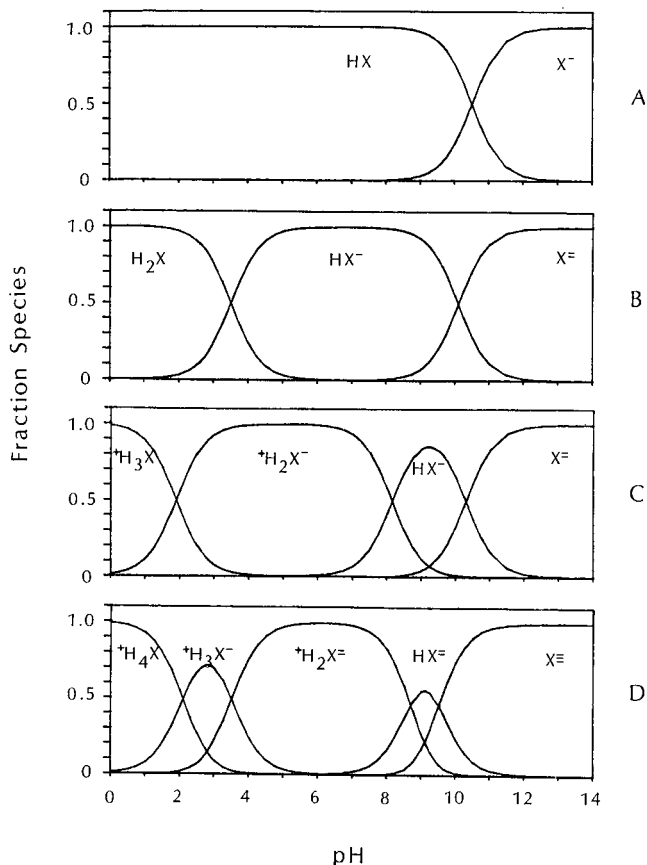
Fig. 1. Protic equilibria of the four classes of thiols from Table I.

nesulfate all in 0.1 mol/l monochloroacetate buffer with a pH of 3. Although the retention of the net-cationic thiols was increased by the addition of these reagents, the retention of the neutral components was decreased. This effect has been observed by others[10]. For example in our system, k' for cysteine was increased from 0.1 to 0.9 by the addition of 1 mmol/l dodecanesulfate at pH 3; whereas, the retention of neutral 3-mercaptopropanoic acid was decreased from a k' of 5 to 2.1. This made the simultaneous multicomponent separation of the net-cationic thiols from the hydrophilic neutral thiols more difficult. Employing alkyl sulfate/sulfonate pairing agents resulted in co-elution of thiols at low k' values.

We also examined the reversed-phase retention of the thiols as a function of mobile phase pH and buffer-type without the addition of alkyl sulfate/sulfonate pairing agents. The acid form of the buffers are listed in Table II and were neutralized with lithium hydroxide to achieve the desired pH. We found that the reversed-phase retention of cysteine was higher at pH 2 than at pH 3 for a given buffer, as shown in Table III. According to Fig. 1, cysteine (type C) is net-cationic at pH 2 and primarily zwitterionic at pH 3. The anionic salt of the buffer apparently acts as a pairing agent

TABLE II

pK_a VALUES OF BUFFERS EMPLOYED[6,27]

Acid	pK_a value
Acetic	4.76
Monochloroacetic (MCA)	2.86
2-Chloropropanoic (MPA)	2.88
Trifluoroacetic (TFA)	0.23
Trichloroacetic (TCA)	0.63
Tribromoacetic (TBA)	0.66

with the net-cationic cysteine (pH 2), thus increasing hydrophobicity and retention over the zwitter-ionic form (pH 3). The buffer anions used here only enhance the retention of the net-cationic form, not the zwitterion form.

At a mobile phase pH of 3, there was no difference in the retention of cysteine when different buffers were used, but retention was influenced by the nature of the buffer at pH 2. These results are shown in Table III. Given the pK_a values for MCA and MCP (Table II), these buffers will be largely protonated at pH 2. Thus it is surprising to see the retention of cysteine increase significantly from pH 3 to pH 2 for these buffers. The protonation of the thiol to the net-cationic form appears to be much more important than deprotonation of the pairing agent in enhancing reversed-phase retention. Although the hydrophobicity of the pairing agent should increase by using MCP instead of MCA, substituting a single methyl group on the monochloro-acetic acid resulted in only a modest increase in the retention of the net-cationic cysteine. This contrasts results obtained with 4–10 carbon alkyl sulfates, where increasing the carbon length of the alkyl chain substantially increases cation retention[23]. An additional disparity between these two types of pairing agents is that alkyl sulfonates/sulfates were found to enhance the retention of the zwitterion form of cysteine as well. This has also been observed by others for cysteine[9] and longer chain peptides[10].

The higher retention of the net-cationic cysteine with the TCA buffer prompted further investigation of the pairing agent properties of this buffer anion. The effect of the mobile phase pH on the retention of 4 thiols (cysteine, glutathione, 2-mercaptopropanoic acid and methanethiol) over the range of 1.25 to 5.0 using the trihaloace-tate TCA, is shown in Fig. 2. The maximum k' value was achieved at pH values near 1.8, although in solution, half of cysteine and glutathione are still in the zwitterion

TABLE III

CYSTEINE RETENTION WITH DIFFERENT BUFFERS

Mobile phase pH	k' for cysteine with acid (0.05 mol/l)			
	Unbuffered HClO$_4$	MCA	MCP	TCA
3	0.14	0.13	0.12	0.12
2	0.36	0.39	0.44	0.71
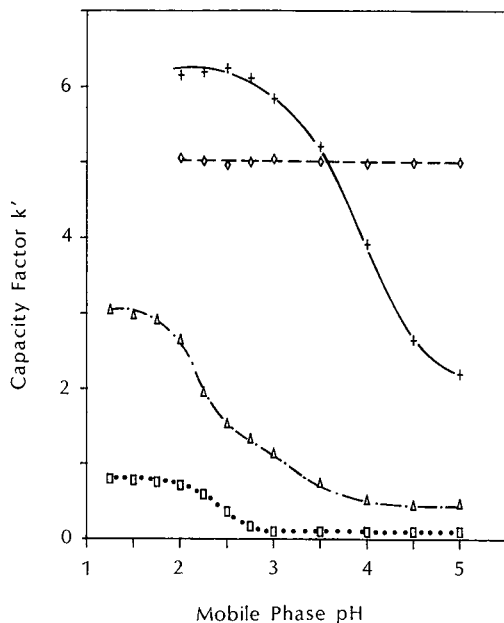
Fig. 2. Effect of pH on the reversed-phase retention of four thiols. Compounds: (□) cysteine, (+) 2-mercaptopropanoic acid, (◇) methanethiol, (△) glutathione. Mobile phase: 0.05 mol/l TCA buffer.

form. However, since the additional LC partition equilibria favors the more neutral form, the effective "chromatographic pK_a" (pK_a') may be shifted substantially from the solution value[24,28]. These pK_a' values were higher than the solution pK_a (at μ = 0.1) values for cysteine (2.4 vs. 1.9) and 2-mercaptopropanoic acid (3.9 vs. 3.5) but were similar for glutathione (2.1 for both). In the case of glutathione the retention behavior and hence the pK_a' measurement is complicated by a second proton equilibrium with pK_a = 3.5. As expected, methanethiol, which is neutral over this pH range shows no dependance of retention on mobile phase pH.

We also compared three commercially available C_{18} columns for their retention of the net-cation cysteine with the pH 2 TCA mobile phase, the results are listed in Table IV. Although the Zorbax ODS column did not have the largest silica surface area, the high % C loading produced the highest k' values for cysteine. Since reten-

TABLE IV

REVERSED-PHASE C_{18} COLUMNS TESTED FOR CYSTEINE RETENTION

All data are from manufacturer's specifications.

Column	% C	Pore size (Å)	End capped	Surface area (m²/g)	Particle size (μm)	k' k'
Vydac TP	9	300	No	100	5	0.36
Vydac HS	13	80	Yes	500	5	0.42
Zorbax ODS	16	60	No	330	5–6	1.09

Mobile Phase TCA Concentration P_m (mol/l)
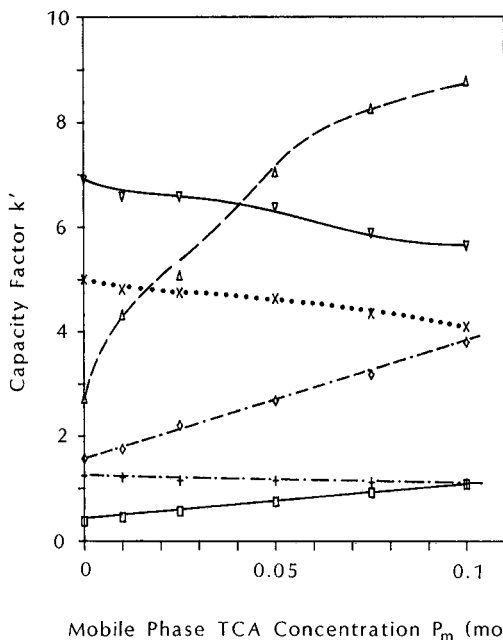
Fig. 3. Effect of P_m of TCA on retention of thiols at constant pH 2 buffer concentration. Compounds: (□) cysteine, (+) 1-mercaptoglycerol, (◇) glutathione, (△) penicillamine, (×) 3-mercaptopropanoic acid, (▽) 2-mercaptopropanoic acid.

tion of this compound was essential to our work, all further studies were performed on the Zorbax ODS column.

To investigate further the possibility of buffer ion–analyte interactions, retention of the thiols was measured as a function of TCA mobile phase concentration (P_m) at a constant pH of 2.0. To minimize the effect of ionic strength, test amounts of TCA were substituted for equal amounts of perchlorate. Fig. 3 shows the change in k' with the mobile phase concentration of pairing agent. A marked increased retention is observed for the net-cationic analytes (cysteine, glutathione, penicillamine) with increasing P_m, with a slight decrease in retention observed for the thiols that are neutral at this pH (1-mercaptoglycerol, 2- and 3-mercaptopropanoic acid). Since the pH and ionic strength remain constant in this experiment, the increased retention of the net-cations with P_m must be a result of solvophobic ion interactions between the TCA anions and the analytes. The slightly decreased retention of the neutral compounds with increasing P_m must be primarily a result of displacement by the increased adsorbed pairing agent on the stationary phase[10,11] or by lowering of the surface tension of the stationary phase by the adsorbed surfactant[14,29]. However, the slight decrease in retention for polar neutral compounds using TCA is much less than that observed for alkyl sulfates/sulfonates[10] and is consistent with the low surface coverages found for the THA in these experiments (*vide infra*).

The effect of increasing ionic strength at constant P_m using TCA on the retention of 3 net-cationic and 1 neutral thiol is presented in Fig. 4. For the net-cations, the
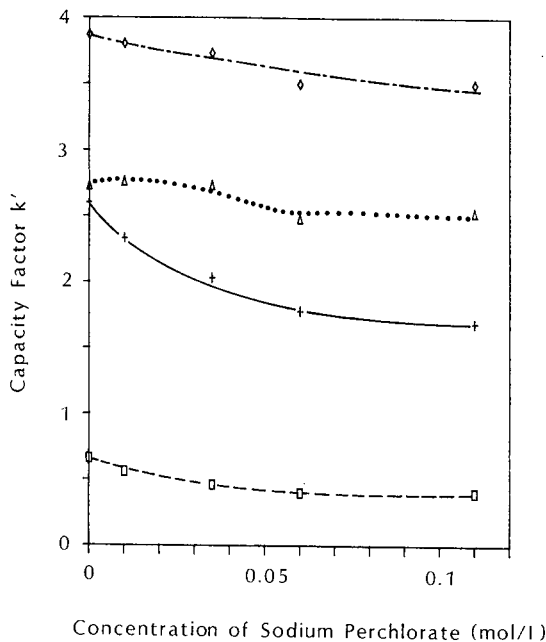
Fig. 4. Ionic strength effect on the retention of four thiols. Compounds: ($\square$) cysteine, ($+$) glutathione, ($\diamond$) 3-mercaptopropanoic acid, ($\triangle$) N-acetylcysteine, Mobile phase: 0.05 mol/l TCA with added NaClO$_4$.

slight decrease in k' must result from competition of the added cation for interaction with the TCA buffer anion. Little change is noted for the retention of 3-mercaptopropanoic acid, a neutral compound at this pH.

We also examined the effect of changing the charge density of the counter cation used to prepare the TCA buffer on the retention of the net-cation cysteine. Any ionic interaction between the counter cation and the buffer anion should cause a decrease in retention of the net-cation thiols, by decreasing the "free" anion available for cysteine pairing. Using a 0.01 mol/l TCA buffer at pH 2, cysteine retention was highest for the counter cations with the lowest charge density, in the order K$^+$ > NH$_4^+$ $\approx$ Na$^+$ > Li$^+$. This order is expected based on the predicted strength of the interaction of the counter cations with the TCA anion, with Li$^+$ possessing a high charge density and forming stronger ionic interactions than Na$^+$ and the other cations (in order of decreasing charge density).

Effect of the halogen substituents of the trihaloacetic acid

Since increased retention of the net-cations was found using trichloroacetic acid over monochloroacetic acid, we decided to investigate the pairing agent properties of the series of trifluoro-, trichloro- and tribromoacetic acid buffers, all at pH 2.

The adsorption of the three pairing agents to the reversed-phase stationary phase was studied by breakthrough experiments using a minimum dead-volume solvent switch and ultraviolet absorbance detection at 235 nm. The concentration of the pairing agent adsorbed to the stationary phase (P_s) was calculated using the method of Knox and Hartwick[10]. A plot of P_s as a function of P_m for the three THAs is
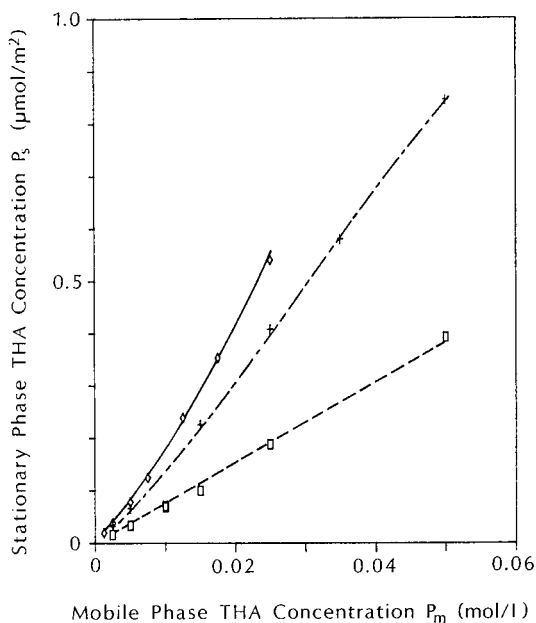
Fig. 5. P_s as a function of P_m for the THA pH 2 buffers. ($\square$) TFA, ($+$) TCA, ($\diamond$) TBA.

presented in Fig. 5. Adsorption of all three compounds is in the linear region of the adsorption isotherm. The comparitively low reversed-phase adsorption of these pairing agents is expected since the haloacetic acids are nearly 100% ionized at this pH and have small hydrophobic R groups. In the THA systems, the P_s values found are all at least one order of magnitude lower than for octylsulfate, which shows a curvilinear isotherm with stationary phase saturation occurring at P_m above 0.02 mol/l[10]. The adsorption of the THA occurs in the order TBA > TCA > TFA, as expected from the relative sizes of the hydrophobic trihalomethyl moiety. Rapid reversibility of the adsorption of all of the THA buffers was observed upon switching the mobile phase to pure phosphate buffer, requiring elution of 2–5 column volumes. This is in sharp contrast to the unfavored reversed-phase desorption observed for alkyl sulfate/sulfonate pairing agents, especially the longer chain C_8–C_{12} compounds, which may require elution of up to 20 l of aqueous solution to return the column to the original condition[11].

A comparison of TFA, TCA, and TBA buffers was made on the retention of the net-cation cysteine. Since retention was maximized at low pH, pH $=$ 2 was chosen for the study. A plot of the capacity factor of cysteine as a function of P_m, at constant ionic strength, is shown in Fig. 6. For all three buffers the retention increases with P_m, but the increase was most dramatic for the larger THAs. The reversed-phase retention of cysteine is plotted as a function of the stationary-phase pairing agent concentration (P_s) in Fig. 7. Equal net-cation retention is not obtained for the three THAs at any given P_s. This contrasts results found for alkyl sulfate/sulfonates, where cation retention is equivalent for equal stationary phase concentrations, independent of the size of the hydrophobic moiety of the pairing ion, and depends only on the surface con-
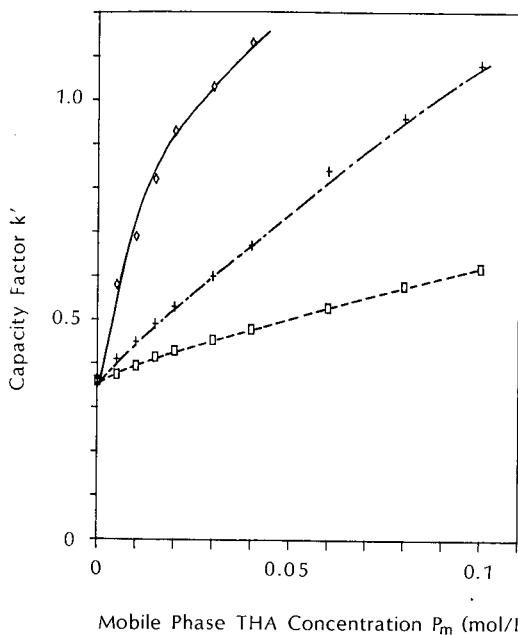
Fig. 6. Effect of P_m of the THA pH 2 buffers on cysteine reversed-phase retention. ($\square$) TFA, (+) TCA, ($\diamond$) TBA.

centration of adsorbed pairing ions[10]. In the THA pairing system, the surface concentration of adsorbed pairing agent is not the dominant parameter in net-cation retention.

Since the retention enhancement appeared to be a strong function of the size of
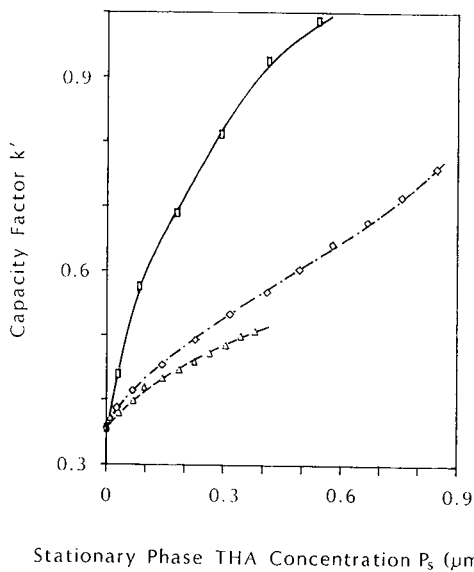
Fig. 7. Cysteine retention as a function of P_s. ($\triangle$) TFA, ($\diamond$) TCA, ($\square$) TBA.

TFA   TCA   TBA

101 $\overset{\circ}{A}^2$ 131 $\overset{\circ}{A}^2$ 154 $\overset{\circ}{A}^2$
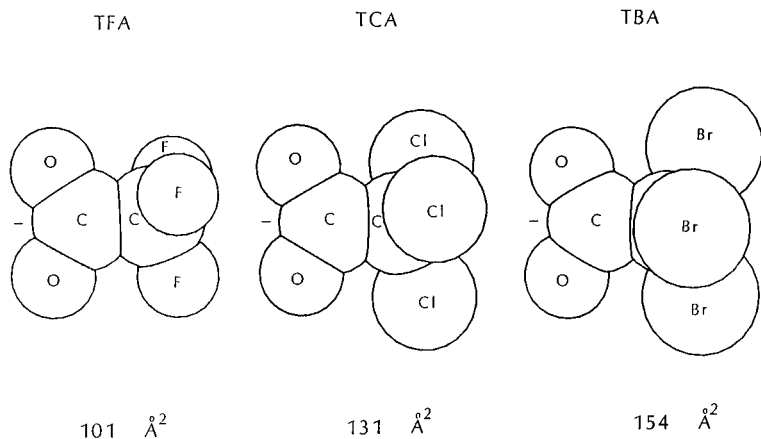
Fig. 8. Space filling models of THA anions.

the halogen moiety of the THA, we decided to examine this relationship. The size differences of the three anions are graphically represented by the space filling models shown in Fig. 8. A plot of the log of the retention enhancement factor[30] *versus* the molecular surface area of the three THA (calculated from known bond lengths and Van der Waals' radii) shows an excellent linear relationship (Fig. 9). This retention behavior is most consistent with solvophobic ionic interactions with the pairing agent that enhance reversed-phase partitioning[30]. It is also possible that hydrogen bonding
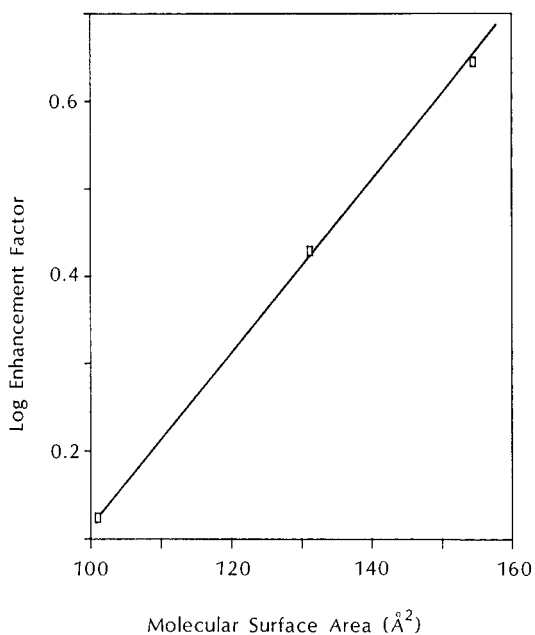
Fig. 9. Retention enhancement factor for cysteine as a function of pairing agent surface area.

between the pairing anion and the protonated primary amine of the cysteine may enhance the tendency to form structure-specific ionic interactions.

Although an excellent correlation of the retention enhancement factor and the surface area of the THA was found, differences in ionic interactions between the three anions, resulting from inductive effects of the halogens on the electron density at the carboxylate anion, are not accounted for. The interaction formation constants of the THA anions with the net-cation cysteine may be calculated[30]. Although a number of tenuous assumptions need to be made about the retention mechanism with this approach, the following values were calculated for the THA–cysteine interaction formation constants: 30 ± 2 for TFA, 39 ± 2 for TCA and 41 ± 5 for TBA (± 1 S.D., n = 9). The trend of these chromatographically-derived formation constants is consistent with the intuitively expected inductive effect that the halogens have on the electron density of the carboxylate anion; *i.e.*, the trifluoride is most electronegative, withdrawing electron density from the anion, and it has the lowest interaction constant with the net-cation. Note that the tendency of the THAs to form ionic interactions may also reflect the effect of the hydrophobicity of the THA anions as expected from solvophobic theory[30]. Since the inductive and solvophobic effects both favor the tendency to form ionic interactions in the order TBA > TCA > TFA >, it is impossible to sort out which is the more important parameter. Nevertheless, the linear relationship between the retention enhancement factor and the molecular size of the THAs is most consistent with the solvophobic effect being the more dominant factor in the retention of the net-cations in this system.

For the application of the reversed-phase THA pairing separation system to the determination of the biogenic thiols in marine sediment pore-water samples[17], we chose to use TCA buffer rather than the more retentive TBA buffer because of the noise-generating, electroactive impurities in the commercial TBA and because of its limited aqueous solubility. Development of an analytical reversed-phase separation of the neutral thiols (mercaptopyruvic acid, 2-mercaptoethanol, 1-mercaptoglycerol,
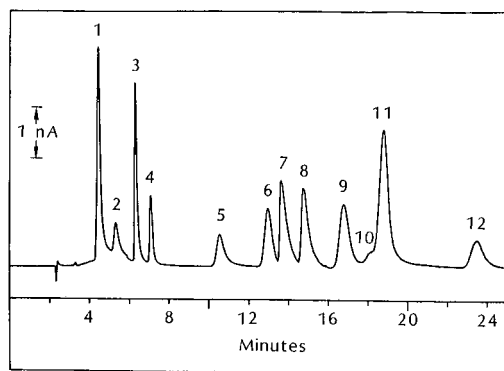
Fig. 10. Separation of several biogenic thiols. Mobile phase: 0.05 mol/l TCA buffer– methanol (99:1) (pH 2). Compounds: 1 = cysteine (0.55 nmol), 2 = mercaptopyruvic acid (0.07 nmol), 3 = 2-mercaptoethanol (0.05 nmol), 4 = 1-mercaptoglycerol (0.16 nmol), 5 = glutathione (0.65 nmol), 6 = 3-mercaptopropanoic acid (0.11 nmol), 7 = methanethiol (0.19 nmol), 8 = ethanethiol (0.16 nmol), 9 = 2-mercaptopropanoic acid (0.12 nmol), 10 = 2-propanethiol (0.05 nmol), 11 = 1-propanethiol (0.25 nmol), 12 = penicillamine (0.10 nmol).

2- and 3-mercaptopropanoic acid, methanethiol, ethanethiol, 1- and 2-propanethiol, was simply a case of choosing a mobile phase pH low enough to ensure that all ionizable functional groups were protonated. At pH 2, using the methanol–water (1:99) mobile phase, all of these components could be baseline separated. Adjustment of the concentration of TCA to 0.05 mol/l (see Fig. 3) provided the appropriate retention of the net-cations cysteine, penicillamine and glutathione for resolution from the other thiols of interest. This optimization process was greatly facilitated by the lack of appreciable change in retention of the neutral components with changing TCA concentration. The TCA concentration required for optimum selectivity of compounds not studied here could easily be obtained from a plot of k' vs. P_m like shown in Fig. 3. Fig. 10 shows the simultaneous separation of twelve biogenic thiols using the TCA buffer system. One advantage of the TCA mobile phase was in the qualitative identification of the thiols in sediment pore-water samples. The retention of the net-cationic thiols could be easily varied by a change in the mobile phase concentration of TCA; whereas neutral thiols showed no change in retention. These experiments were facilitated by the rapid system response to mobile phase changes, where elution of only 2–5 column volumes was required for column–mobile phase equilibration. Using this separation, twelve biogenic thiols were identified and determined at the nanomolar level in sediment pore-water samples[17].

ACKNOWLEDGEMENT

REFERENCES

1 S. Selander, K. Kramer and L. Hallberg, *Br. J. Ind. Med.*, 23 (1966) 282.
2 J. M. Walshe, *Am. J. Med.*, 21 (1956) 487.
3 Multicenter Trial Group, *Lancet*, (1973) 257.
4 D. Shea and W. A. MacCrehan, *Sci. Total Environ.*, 73 (1988) 135–141.
5 E. P. Serjeant and B. Dempsey, *Ionization Constants of Organic Acids In Aqueous Solution*, Pergamon Press, New York, 1979.
6 A. E. Martell and R. M. Smith, *Critical Stability Constants*, Plenum Press, New York, 1974.
7 L. G. Sillen and A. E. Martell, *Stability Constants of Metal Ion Complexes: Supplement No. 1*, Royal Society of Chemistry, London, (1971).
8 H. Nakamura and Z. Tamura, *Anal. Chem*, 53 (1981) 2190–2193.
9 L. A. Allison, J. Keddington and R. E. Shoup, *J. Liq. Chromatogr.*, 6 (1983) 1785–1798.
10 J. H. Knox and R. A. Hartwick, *J. Chromatogr.*, 204 (1981) 3–21.
11 I. Girard and C. Gonnet, *J. Liq. Chromatogr.*, 8 (1985) 2035–2046.
12 J. H. Knox and J. Jurand, *J. Chromatogr.*, 149 (1978) 297–312.
13 A. Bartha, G. Vigh, H. Billiet and L. de Galan, *Chromatographia*, 20 (1985) 587–590.
14 J. J. Stranahan and S. N. Deming, *Anal. Chem.*, 54 (1982) 2251–2256.
15 K. Mopper and D. Delmas, *Anal. Chem.*, 56 (1984) 2557–2560.
16 L. A. Allison, G. S. Mayer and R. E. Shoup, *Anal. Chem.*, 56 (1984) 1089–1096.
17 D. Shea and W. A. MacCrehan, *Anal. Chem.*, 60 (1988) 1449–1454.
18 P. A. Asmus and C. R. Freed, *J. Chromatogr.*, 169 (1979) 303–311.
19 W. R. Melander, J. Stoveken and Cs. Horváth, *J. Chromatogr.*, 185 (1979) 111–127.
20 M. Otto and W. Wegscheider, *J. Liq. Chromatogr.*, 6 (1983) 685–704.
21 W. A. MacCrehan, S. D. Yang and B. A. Benner, *Anal. Chem.*, 60 (1988) 284–286.

22 D. A. Skoog and D. M. West, *Fundamentals of Analytical Chemistry*, Holt, Rinehart and Winston, New York, 1976.

23 W. R. Melander and C. Horvath, in M. T. W. Hearn (Editor) *Ion-Pair Chromatography*, Marcel Dekker, New York, 1985, pp. 42–71.

24 J. L. M. van de Venne, J. L. H. M. Hendrikx and R. S. Deelder, *J. Chromatogr.*, 167 (1978) 1–16.

25 J. Ståhlberg, *J. Chromatogr.*, 356 (1986) 231–245.

26 B. A. Bidlingmeyer, S. N. Deming, W. P. Price Jr., B. Sachok and M. Petrusek, *J. Chromatogr.*, 186 (1979) 419–434.

27 Z. Rappoport (Editor), *Handbook of Tables for Organic Compound Identification*, CRC Press, Cleveland, OH, 1967, p. 429.

28 K. C. Kong, B. Sachok and S. N. Deming, *J. Chromatogr.*, 199 (1980) 307–316.

29 C.-G. Wu and S. N. Deming, *J. Chromatogr.*, 302 (1984) 79–88.

30 G. Horváth, W. Melander, I. Molnár and P. Molnár, *Anal. Chem.*, 49 (1977) 2295–2305.

CHROM. 20 945

SEPARATION OF *CIS–CIS, CIS–TRANS* AND *TRANS–TRANS* ISOMERS OF (±)-ATRACURIUM BESYLATE AND *CIS* AND *TRANS* ISOMERS OF ITS MAJOR QUATERNARY DECOMPOSITION PRODUCTS AND RELATED IMPURITY BY REVERSED-PHASE HIGH-PERFORMANCE LIQUID CHROMATOGRAPHY

ULRICH NEHMER

Analytical Department, Chemical-Pharmaceutical Research Institute, Boul. "Kl. Ochridski" 3, 1156 Sofia (Bulgaria)

SUMMARY

The separation and determination of isomer ratios of *cis–cis, cis–trans* and *trans–trans* isomers of (±)-atracurium besylate and *cis* and *trans* isomers of its major quaternary decomposition products and related impurity using an octadecylsilica column and acetonitrile–phosphate buffer mobile phases were studied. The influence of the acetonitrile and buffer concentration and the pH of the mobile phase on the capacity factor (k'), selectivity (α), resolution (R_s) and peak symmetry factor (S) of the atracurium isomers was investigated. It was found that the acetonitrile concentration influenced α, whereas the buffer concentration and the pH of the mobile phase affected only k', S and R_s. Hydrophobic and silanophilic interactions were factors in the retention mechanism of the isomers under the conditions investigated.

INTRODUCTION

Atracurium besylate is a highly selective, competitive (non-depolarizing) neuromuscular blocking agent[1]. In a previous paper[2] the simultaneous determination of atracurium besylate and its major decomposition products and related impurities by reversed-phase high-performance liquid chromatography (RP-HPLC) was reported. Atracurium has four chiral centres at C-1 and N-2 in the two tetrahydropapaverine units (Fig. 1). Because of molecular symmetry, the sixteen isomers that are
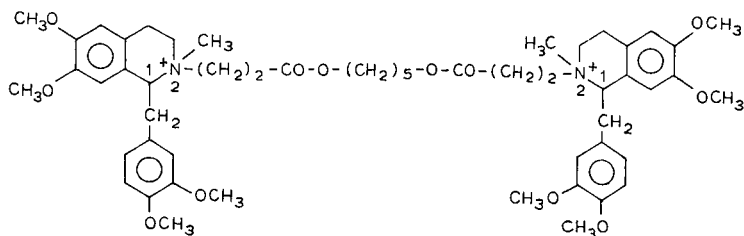
Fig. 1. Structure of atracurium.
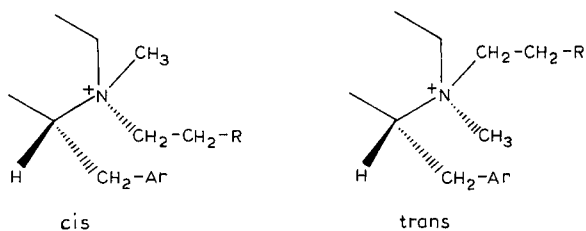
Fig. 2. Structures of *cis* and *trans* isomers.

theoretically possibly reduce to ten. These may be arbitrarily reduced by consideration of the relative configuration about the two C-1–N-2 bonds. The *cis* configuration is defined arbitrarily as that in which the two bulky substituents [1-(3,4-dimethoxyl-benzyl) and 2-alkylene-ester groups] are *cis* (Fig. 2). Three configurations are possible for the molecule when considering the orientation of the groups at either end of the molecule, *cis–cis*, *cis–trans* and *trans–trans*. In the major decomposition products and related impurity of atracurium containing only one quaternary amino group, *cis* or *trans* configurations are possible. Stenlake *et al.*[3] had found that the atracurium isomers show different relative molar neuromuscular blocking potencies in anaesthetized cats. Therefore, analysis of atracurium for manufacturing and quality control purposes requires the ability to separate components similar in structure. HPLC with a silica stationary phase has been used to determine the total isomer content and *cis–cis*, *cis–trans* and *trans–trans* isomer ratios of atracurium[3,4]. The mobile phase used for the separation of the atracurium isomers contained hydrobromic acid and had a very low pH (below 2). This is a very aggressive mobile phase both for the silica stationary phase and the stainless-steel parts of the chromatographic system. The reported chromatographic conditions[3,4] can separate the *cis–cis*, *cis–trans* and *trans–trans* isomers of atracurium in about 10 min, but cannot separate the major decomposition products of atracurium from each other and the related impurity (monoquaternary analogue of atracurium; V) was not always clearly resolved from the peak of the *cis–cis* isomers of atracurium.

This paper describes an RP-HPLC method for the separation of the *cis–cis*, *cis–trans* and *trans–trans* isomers of atracurium and the *cis* and *trans* isomers of its major quaternary decomposition products and related impurity using isocratic and gradient elution.

EXPERIMENTAL

Chemicals

Atracurium besylate and its major decomposition products and related impurity were described in a previous paper[2]. The compounds studied for separating isomers are listed in Table I.

Acetonitrile (HPLC grade) and dibasic potassium phosphate trihydrate were obtained from Merck (Darmstadt, F.R.G.) and orthophosphoric acid from Fluka (Buchs, Switzerland).

TABLE I

COMPOUNDS STUDIED FOR THE SEPARATION OF STEREOISOMERS

No.	Compound
I	Atracurium
II	2-(2-Carboxyethyl)-2-methyl-1,2,3,4-tetrahydropapaverinium
III	2-(9-Hydroxy-3-oxo-4-oxanoyl)-2-methyl-1,2,3,4-tetrahydropapaverinium
IV	2-(3,11-Dioxo-4,10-dioxatridec-12-enyl)-2-methyl-1,2,3,4-tetrahydropapaverinium
V	2-Methyl-2,2'-(3,11-dioxo-4,10-dioxatridecamethylene)bis(1,2,3,4-tetra-hydropapaverinium)

Equipment
    A Waters Assoc. (Milford, MA, U.S.A.) HPLC system consisting of two Model 501 pumps, a Model 440 ultraviolet detector equipped with a 280-nm filter and a 740 Data Module was employed. A Rheodyne (Berkeley, CA, U.S.A.) 7120 injection valve (10-μl sample loop) was used. A Nova-Pak C_{18} Radial-Pak cartridge (10 cm $\times$ 8 mm I.D.), particle size 5 μm, in a Radial Compression Module RCM-100 from Waters Assoc. and a Radelkis (Budapest, Hungary) Model OP-211/1 pH meter equipped with a glass electrode and a calomel reference electrode were used. The mobile phases and sample preparation were described in a previous paper[2].
    The retention time of an unretained compound, t_0, was determined using sodium nitrate. The resolution of peaks, R_s, was calculated as

$$R_s = 2(t_2 - t_1)/(w_1 + w_2)$$

where t_1 and t_2 are the retention times and w_1 and w_2 are the base peak widths of the two peaks. Retention times were determined automatically by the integrator and peak widths at the base were measured manually from the integrator trace.

RESULTS AND DISCUSSION

    The effect of mobile phase conditions (concentration of organic component and buffer and pH) on the capacity factor (k'), selectivity (α), R_s and peak symmetry factor (S) of the *cis–cis*, *cis–trans* and *trans–trans* isomers of atracurium was investigated. The peak symmetry factor was calculated as the ratio of the rear part to the front part of the peak at 10% of the peak height.

Effect of acetonitrile content in the mobile phase
    Table II gives selected HPLC data for the three atracurium isomers to show the influence of the acetonitrile content in the mobile phase on k', α and R_s. A constant buffer concentration in the aqueous component of the mobile phase (0.1 mol/l) was maintained. It can be seen that a reduction in the percentage of the organic modifier in the mobile phase improves the isomer resolution. The α values in Table II show that they depend strongly on the acetonitrile content, but there is no significant difference in the influence of the acetonitrile content in the mobile phase on the column selectivity at different mobile phase pH (pH 5 and 3). With 28% acetonitrile in the mobile phase

TABLE II

EFFECT OF ACETONITRILE CONTENT IN THE MOBILE PHASE ON THE CAPACITY FACTOR (k'), SELECTIVITY (α) AND RESOLUTION (R_s) OF THE *CIS–CIS, CIS–TRANS* AND *TRANS–TRANS* ISOMERS OF ATRACURIUM AT DIFFERENT MOBILE PHASE pH AND 0.1 *M* PHOSPHATE BUFFER CONCENTRATION IN THE AQUEOUS COMPONENT OF THE MOBILE PHASE

The subscripts 1, 2 and 3 to k', α and R_s denote the *trans–trans, cis–trans* and *cis–cis* isomers of atracurium, respectively.

pH	Acetonitrile (%)	k'_1	k'_2	k'_3	α_{21}	α_{31}	α_{32}	$R_{s_{21}}$	$R_{s_{31}}$	$R_{s_{32}}$
5.0	28	10.06	11.44	12.56	1.13	1.25	1.10	2.09	3.48	1.29
	30	4.88	5.38	5.75	1.10	1.18	1.08	1.56	2.07	0.84
	35	1.94	2.06	2.19	1.06	1.11	1.05	0.86	1.54	0.64
	40	1.12	1.12	1.12	1.00	1.00	1.00	0.74	1.24	0.45
3.0	28	9.41	10.68	11.77	1.13	1.25	1.10	2.36	3.88	1.50
	35	1.81	2.00	2.12	1.10	1.14	1.06	1.08	1.79	0.80
	40	0.75	0.75	0.75	1.00	1.00	1.00	–	–	–

a good separation of the *cis–cis, cis–trans* and *trans–trans* isomers of atracurium for determining isomer ratios was obtained.

Effect of pH of the mobile phase

Fig. 3 shows the pH dependence of the peak symmetry factor S of the *cis–cis, cis–trans* and *trans–trans* isomers of atracurium when using 28% acetonitrile and 0.1 *M* phosphate buffer solution. It is clear that the peak symmetry is affected by the

Fig. 3. pH depencence of the peak symmetry factor, S, of the (■) *cis–cis*, (▲) *cis–trans* and (△) *trans–trans* isomers of atracurium.

TABLE III

EFFECT OF MOBILE PHASE pH ON THE CAPACITY FACTOR (k'), SELECTIVITY (α) AND RESOLUTION (R_s) OF THE CIS-CIS, CIS-TRANS AND TRANS-TRANS ISOMERS OF ATRACURIUM AT 28% ACETONITRILE AND 0.1 M PHOSPHATE BUFFER CONCENTRATION IN THE AQUEOUS COMPONENT OF THE MOBILE PHASE

Subscripts 1, 2 and 3 as in Table II.

pH	k'_1	k'_2	k'_3	α_{21}	α_{31}	α_{32}	$R_{s_{21}}$	$R_{s_{31}}$	$R_{s_{32}}$
3	9.41	10.68	11.77	1.13	1.25	1.10	2.36	3.88	1.50
4	9.61	10.88	11.97	1.13	1.24	1.10	2.28	3.82	1.45
5	10.06	11.44	12.56	1.13	1.25	1.10	2.09	3.48	1.29
6	10.49	11.84	12.96	1.13	1.24	1.10	1.67	2.81	1.16

mobile phase pH. This effect can be explained by the dual retention mechanism[5] for the atracurium isomers and the other compounds investigated, in which both hydrophobic and silanophilic interactions on the surface of the reversed-phase octadecylsilica stationary phase dictate the chromatographic behaviour of solutes. The silanophilic interaction can include ionic interaction (ion exchange) between the quaternary amino groups or protonated amines and the dissociated surface silanol groups of octadecylsilica. Silanophilic interaction can have undesirable effects, for example excessive peak tailing (low S values). The cation-exchange behaviour of surface silanol groups in a chromatographic system will depend primarily on the pK_a of the silanols, the mobile phase pH, ionic strength and composition. The pK_a of surface silanol groups has been reported to be in the range 5–7[6]. At lower mobile phase pH the silanol group dissociation will be suppressed and the silanophilic interaction between the residual silanol groups and the amines decrease. This weaker silanophilic interaction leads to a better peak shape and a decrease in the k' values (Table III) of the atracurium isomers.

Table III illustrates that variation of the mobile phase pH over the range examined has no significant effect on the selectivity. It can be concluded that the increase in R_s values with decreasing mobile phase pH is caused by the better peak shape (higher S values) at lower mobile phase pH, i.e., the column efficiency is improved.

TABLE IV

EFFECT OF BUFFER CONCENTRATION ON THE CAPACITY FACTOR (k'), SELECTIVITY (α) AND RESOLUTION (R_s) OF THE CIS-CIS, CIS-TRANS AND TRANS-TRANS ISOMERS OF ATRACURIUM AT 28% ACETONITRILE AND MOBILE PHASE pH 5.0

Subscripts 1, 2 and 3 as in Table II.

C_{buf} (M)	k'_1	k'_2	k'_3	α_{21}	α_{31}	α_{32}	$R_{s_{21}}$	$R_{s_{31}}$	$R_{s_{32}}$
0.025	11.50	13.25	14.69	1.15	1.28	1.11	1.83	3.00	1.10
0.050	11.12	12.50	13.75	1.12	1.24	1.10	1.87	3.23	1.25
0.100	10.06	11.44	12.56	1.13	1.25	1.10	2.09	3.48	1.29
0.150	7.88	9.00	9.76	1.14	1.24	1.08	1.80	2.73	1.09

Effect of buffer concentration in the mobile phase

Capacity factors were determined for the three atracurium isomers using mobile phases consisting of 28% acetonitrile and 72% aqueous solutions of potassium phosphate of concentration 0.025, 0.05, 0.1 and 0.15 mol/l. The mobile phase pH was maintained at 5.0.

The results are shown in Table IV. Over the range examined, k' decreased with increasing buffer concentration in the mobile phase. The α values in Table IV are not significantly affected by variations of the ionic strength of the mobile phase. The data in Table IV illustrate that the R_s values pass through a maximum at a buffer concentration about 0.1 mol/l.

Fig. 4 shows the effect of potassium phosphate concentration (C_{buf}) on the peak symmetry factor S. It can be seen that S increases with increasing buffer concentration in the mobile phase. The R_s values are affected by a combined effect of the variation of the buffer concentration in the mobile phase. With increasing buffer concentration in the mobile phase the peak shape is improved, which contributes to higher R_s values. On the other hand, the differences in the retention times of the isomers are decreased, which leads to lower R_s values. At buffer concentrations higher than 0.1 mol/l the second effect seems to be greater than the first, so that the R_s values effectively decrease. The potassium cations compete with the positivily charged solute for interaction on ion-exchange sites of the octadecylsilica[7,8]. The increase in the buffer concentration in the mobile phase will cause a decrease in the silanophilic interactions between the solute and the surface silanol groups of the stationary phase. Decreasing the silanophilic interactions will decrease the retention of the atracurium isomers (and the other compounds investigated) and contribute to increase the peak symmetry factors S.

Determination of isomer ratios

Fig. 5 shows a typical chromatogram for the determination of atracurium isomer
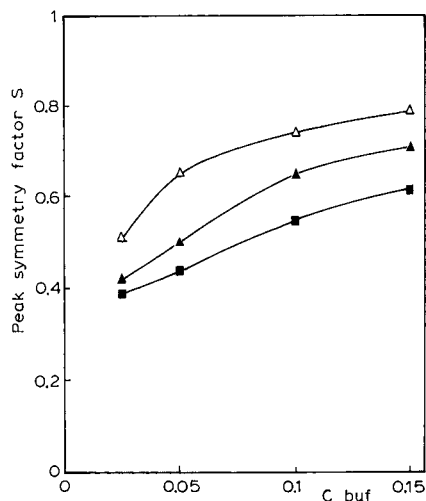
Fig. 4. Effect of buffer concentration on S values of *cis–cis*, *cis–trans* and *trans–trans* isomers of atracurium. Symbols as in Fig. 3.
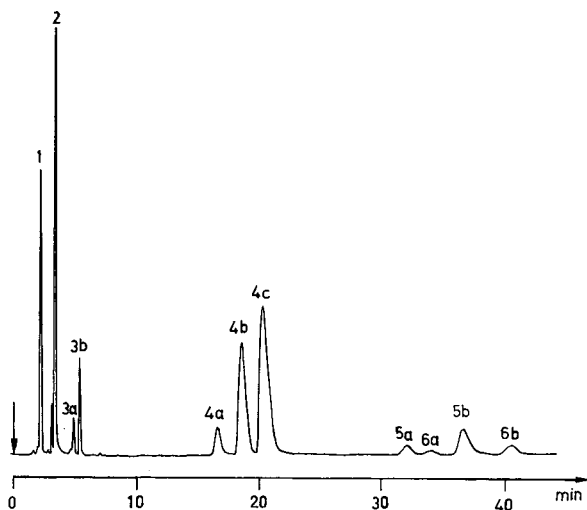
Fig. 5. Reversed-phase HPLC trace of partially decomposed ($\pm$)-atracurium besylate spiked with compound V showing the separation of the *cis–cis*, *cis–trans* and *trans–trans* isomers of atracurium. Column, Nova-Pak C_{18} Radial-Pak (10 cm × 8 mm I.D.; particle size, 5 μm). Mobile phase, acetonitrile–0.1 M potassium phosphate buffer (28:72), pH 5.0; flow-rate, 1.5 ml/min; detection, 280 nm (0.1 a.u.f.s.). Peaks: 1 = II; 2 = laudanosin; 3a, 3b = *trans* and *cis* isomers of III, respectively; 4a, 4b, 4c = *trans–trans*, *cis–trans* and *cis–cis* isomers of atracurium, respectively; 5a, 5b = *trans* and *cis* isomers of V, respectively; 6a, 6b = *trans* and *cis* isomers of IV, respectively.

ratios in the presence of its major decomposition products and related impurity using isocratic elution. It can be seen that it is possible to determine the isomer ratio of atracurium and its major quaternary decomposition products with the exception of compound II.

To determine the isomer ratio of compound II and the other compounds studied in the same run a gradient technique was applied. A representative chromatogram obtained by gradient elution of a mixture containing atracurium and its major decomposition products and related impurity is shown in Fig. 6. A mobile phase of pH 5.0 (about 5.5 in gradient elution) was chosen to avoid interference of the two peaks of compound V with those of atracurium or compound IV[2]. In the absence of compound V it is possible to use a mobile phase of pH 3 to improve the peak shape of the isomers.

As the pure *cis–cis*, *cis–trans* and *trans–trans* isomers of atracurium were not available, the identity of the peaks was deduced from literature results[4]. It is known[4] that the ratio of the *cis–cis*, *cis–trans* and *trans–trans* isomers of atracurium is approximately 10:6:1 (corresponding to about 59% *cis–cis*, 35% *cis–trans* and 6% *trans–trans* isomers, respectively). Because the *cis* isomer of the quaternary decomposition products of atracurium can be obtained from its *cis–cis* and *cis–trans* isomers, which show much higher percentages in atracurium than the *trans–trans* isomer, based on the overall *cis:trans* ratio in atracurium (approximately 3:1), the *cis* and *trans* isomers of the decomposition products should occur in a ratio of 3:1. This means that the larger of the two isomer peaks of a corresponding quaternary decomposition product of atracurium is associated with its *cis* isomers.
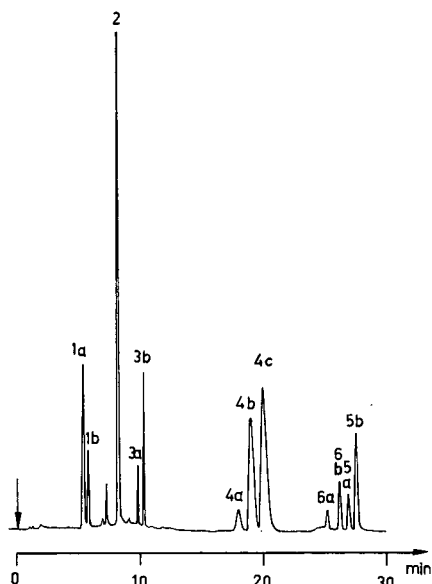
Fig. 6. Chromatogram obtained by gradient elution of partially decomposed ($\pm$)-atracurium besylate spiked with compound V (same sample as in Fig. 5). Column, Nova-Pak C_{18} Radial-Pak (10 cm × 8 mm I.D., particle size, 5 μm). Eluent: (A) acetonitrile; (B) acetonitrile–0.1 M phosphate buffer (1:10), pH 5.0; solvent programme, 2 min 7% A, 5 min linear gradient from 7% A to 21% A, 14 min isocratic at 21% A, 1 min linear gradient from 21% A to 30% A; flow-rate, 2.5 ml/min; detection, 280 nm (0.1 a.u.f.s.). Peaks: 1a, 1b = *cis* and *trans* isomers of II, respectively; other peaks as in Fig. 5.

For compound V the identities of the peaks were deduced by analogy with the results for atracurium (the larger peak should be associated with the *cis* isomer). In addition to these considerations, fractions containing the *cis–cis* isomer of atracurium were collected, which was degraded in acidic and basic media to obtain its quaternary decomposition products (*cis* isomers). Reinjection of these fractions containing the degraded *cis–cis* isomers of atracurium made possible the peak identification of the *cis* isomers of the quaternary decomposition products of atracurium based on retention times. For atracurium the *trans–trans* isomer is eluted before the *cis–trans* and *cis–cis* isomers. Comparision with literature results[4], for which silica (Partisil) was used as the stationary phase, illustrates the converse elution order of the atracurium isomers studied. For the quaternary decomposition products and related impurity of atracurium the *trans* isomer is eluted before the *cis* isomer, except for compound II, where the opposite occurs. It is difficult to explain this reversed retention order of compound II. The free carboxylic acid group of compound II and its smaller molecular size could make changes in the interactions between the isomers and the stationary and/or mobile phase possible. The results obtained in this work and those in ref. 4 indicate that hydrophobic and silanophilic interactions contribute to the retention of the compounds investigated.

Peak areas were measured and the isomer ratios were expressed as a percentage of the sum of the areas found for the three atracurium isomers. From the chromatograms showed in Figs. 5 and 6 the following results were obtained: 7.0%

trans–trans, 38.3% *cis–trans* and 54.7% *cis–cis* isomers with isocratic elution and 7.0% *trans–trans*, 38.0% *cis–trans* and 55.0% *cis–cis* isomers with gradient elution. The reproducibility (coefficient of variation; $n = 5$) of the isomer percentage for the same solution was 0.71% for the *trans–trans*, 0.50% for the *cis–trans* and 0.14% for the *cis–cis* isomer. By analogy with atracurium, the isomer percentage of its major quaternary decomposition products can be determined with similar reproducibility. From the chromatogram shown in Fig. 6 the following results for the *trans* isomers of the quaternary decomposition products and related impurity of atracurium were determined: 29.1% for II, 26.9% for III, 25.3% for IV and 24.4% for V. In this way it is possible to study the decomposition of atracurium with respect to its isomer rarios and that of the quaternary decomposition products obtained. The samples can also be successfully analysed on a LiChrosorb RP-18 column (25 cm × 4 mm I.D., particle size 5 μm) (Merck).

The results demonstrate that RP-HPLC is an efficient and rapid method for the simultaneous determination of isomer ratios of atracurium and its quaternary decomposition products and related impurity.

REFERENCES

1 R. Hughes and D. J. Chapple, *Br. J. Anaesth.*, 53 (1981) 45.
2 U. Nehmer, *J. Chromatogr.*, 435 (1988) 425.
3 J. B. Stenlake, R. G. Waigh, G. H. Dewar, N. C. Dhar, R. Hughes, D. J. Chapple, J. C. Lindon, A. G. Ferrige and P. H. Cobb, *Eur. J. Med. Chem. Chim. Ther.*, 19 (1984) 441.
4 B. Carthy and G. T. Hill, *Anal. Proc.*, 20 (1983) 177.
5 A. Nahum and Cs. Horváth, *J. Chromatogr.*, 203 (1981) 53.
6 B. L. Karger, J. N. Lepage and N. Tanaka, in Cs. Horváth (Editor), *High-Performance Liquid Chromatography — Advances and Perspectives*, Vol. 2, Academic Press, New York, 1980, p. 133.
7 E. Papp and G. Vigh, *J. Chromatogr.*, 259 (1983) 49.
8 E. Papp and G. Vigh, *J. Chromatogr.*, 282 (1983) 59.

AUTOMATED RECYCLING FREE FLUID ISOTACHOPHORESIS

PRINCIPLE, INSTRUMENTATION AND FIRST RESULTS

JEFFREY E. SLOAN*, WOLFGANG THORMANN*,**, GARLAND E. TWITTY and MILAN BIER

Center for Separation Science, University of Arizona, Bldg. 20, Tucson, AZ 85721 (U.S.A.)

(Received August 4th, 1988)

SUMMARY

Most investigations involving preparative isotachophoresis report the use of solid support media in which sample loads of up to 1 g are fractionated within several hours. Larger throughputs and simpler recovery of purified proteins have been achieved by continuous flow isotachophoresis. This method is based on a thin film of fluid flowing between two parallel plates with the electric field applied perpendicular to flow direction. Both the leading and the terminating electrolytes, as well as the sample, are continuously admitted to one end of the electrophoretic chamber and are collected through an array of outlet tubes at the other. In recycling isotachophoresis the effluent from each channel is reinjected into the cell through a corresponding influent port. The development of automated recycling isotachophoresis with a computer controlled counterflow of leading electrolyte is described together with its prospective use as a downstream processing unit operation in biotechnology.

INTRODUCTION

In isotachophoresis (ITP), separation is based upon differences in electrophoretic mobilities and carried out in a discontinuous background buffer system. The buffers are chosen so that there is a distinct mobility difference between the two buffers, the leading constituent having a higher electrophoretic mobility than the terminating one. The sample components of interest must have mobilities intermediate between those of the two electrolyte constituents in order to migrate isotachophoretically between the leader and terminator. The completion of a separation based upon ITP is characterized by a migrating steady state consisting of adjacent sample zones[1-8]. Complex protein samples are typically subfractionated by adding suitable

---

* Present address: Applied Biosystems Inc., 850 Lincoln Center Drive, Foster City, CA 94404, U.S.A.
** Present address: Department of Clinical Pharmacology, University of Bern, Murtenstrasse 35, CH-3010 Bern, Switzerland.

spacer components (simple buffer constituents or synthetic ampholyte mixtures such as Ampholine[7,8]). In addition, a small amount of a dye is often included for the visualization of the leading edge of the ITP stack. The purification problems of the modern biotechnology industry have prompted in recent years a renewed interest in preparative electrophoresis[9]. Among the various electrophoretic methods, preparative ITP is the least explored. Nevertheless, it constitutes an attractive purification methodology because of (i) its high resolution coupled with high protein concentration, (ii) the achievement of high throughput, (iii) the control over the fractionation pH which is important in order to minimize protein precipitation and denaturation, problems which are specific for isoelectric focusing (IEF), (iv) the high efficiency of the process in terms of utilizing the power for separation, and (v) minimum consumption of inexpensive buffer solutions relative to the amount of protein processed[10-14]. Factors (iv) and (v) guarantee economical operation. Analytical ITP is complementary and essential to preparative scale ITP. It was used to predict the order of the individual components in the stack, whether a given pair of spacers will indeed bracket the protein in the stack and whether the choice of leading and terminating electrolytes is appropriate for the system under consideration[10,15]. The advantage of the analytical system is that the scale of the experiment is on the micro- to nanogram scale and that the analysis may be performed within a few minutes if a capillary-type instrument with on-line detection is used.

Most investigations involving preparative ITP report the use of solid support media. Vertical columns filled with polyacrylamide, agarose or granulated gels (Sephadex[10]), and procedures using horizontal gel slabs of about 3 mm thickness, are the favorite approaches[11]. Columns are equipped with an elution chamber at the end permitting transportation of the emerging sample components through a detector and into the fraction collector. Gel slabs are cut with an array of parallel blades, followed by elution of the sample constituents from each gel segment. Small scale preparative ITP in polyacrylamide gel filled glass tubes of 5 to 6 mm I.D. and procedures using annular gels wrapped arround a glass tube (hollow cylinder technique[14]), are alternative and less popular methods. When fractionating proteins in solid support media, sample loads of typically 1 g are applied yielding < 50 mg quantities of specific components in a matter of several hours. Further scale up is very difficult. Removal of the heat produced, the laborious set up of the column or slab, as well as the tedious recovery after separation, are the major obstacles.

Continuous flow electrophoretic methods[16-18], in particular continuous flow isotachophoresis (CFITP)[18-29], with the electric field applied perpendicular to the flow direction, appear to possess the capacity required for downstream processing of fermentation products in biotechnology (> 10 g protein/day). Both the leader and the terminator, as well as the sample, are continuously admitted to one end of the electrophoretic chamber and are fractionated at the other. Early versions utilized filter-paper, membrane compartmentation or density gradients for fluid stabilization[19,20]. More recent setups comprise a thin film of fluid flowing between two parallel plates[21-30]. An example of the latter type of instrument is the Elphor VaP 21 continuous flow electrophoresis apparatus of Bender and Hobein (Munich, F.R.G.) for which a maximum processing rate of 5 g protein per hour was reported in the CFITP mode[28]. CFITP represents an elegant method for the continuous concentration of dilute protein solutions. The positions of the sample zones at the exit are

dependent on the electric field strength, temperature, flow-rate, sample and buffer composition. In the case of small mobility differences, considerable separation distances are needed. To overcome this problem fractionation can be carried out under counter current conditions comprised of a continuous introduction of leading electrolyte on the leading side and withdrawal of an equal amount of fluid on the terminating side. By suitable adjustment of the electric field strength, the mixture being separated travels through the center of the cell with the leading boundary virtually immobilized. To obtain long term stability and proper control with this technique, appropriate automatic feedback devices would need to be incorporated as suggested many years ago by Fawcett[23]. The optical monitor at the bottom of the VaP 21 chamber, consisting of a scanning light beam together with a photosensor, comprises a first approach for on-line detection.

In another approach the principle of recycling electrophoresis, where the effluent from each channel is continuously reinjected into the cell through the corresponding influent port[9,15,31–35], was applied to IEF[9,31–33] and to zone electrophoresis[9,33], and was recently proposed for ITP[34,35]. Similarly, Ivory and co-workers[36–38] described a recycling zone electrophoresis approach where the effluent from each channel is not reinjected into the corresponding influent port but backshifted by a specified number of input channels. The development of automated ITP in a recycling mode (RITP) is the objective of the research endeavor reported here.

MATERIALS AND METHODS

A recycling free flow focusing apparatus (RF3) has recently been designed and constructed in our laboratory in which fluid flows through a narrow channel (0.75 mm) between two flat plates[9]. The fluid residence time in the apparatus is only a few seconds. This impacts a remarkable stability due to fluid dynamics[39]. On the other hand, the short residence time prevents complete separation in a single pass through the separation chamber thus recycling is essential to achieve steady state focusing. This apparatus has been modified for use in the RITP mode. A schematic representation of the entire RITP set up is shown in Fig. 1a and that of the separation chamber in Fig. 1b. ITP takes place within a thin flowing stream in a 35 cm long rectangular chamber having a width of 5.5 cm (volume 14.44 ml). Arrays of 48 inlet and outlet ports define the bottom and top respectively, and dialysis membranes isolate the separation chamber from the electrode compartments. The two channels at the extreme edges represent the fluid between the membrane and the electrophoretic chamber (Fig. 2). Fluid of 44 channels flows through the 5.5 cm wide chamber. The system developed (Fig. 1) consists of the separation chamber along with accessory components [recirculating pump, heat exchanger, flow stabilizing equipment and power supply (EC 600; EC Apparatus Corp., St. Petersburg, FL, U.S.A.)], a UV sensor (2138 Uvicord S; LKB, Bromma, Sweden) for determining the position of the interface between the leading electrolyte and the sample components (front), a method of sample injection, a method of applying a bulk counterflow of leading electrolyte (syringe pump No. 351; Sage Instruments, Orion, Cambridge, MA, U.S.A.) and a computer system for data gathering/data treatment/data storage and control [Commodore 64 (C-64)].

The separation chamber is the most complex portion of the device. It consists of
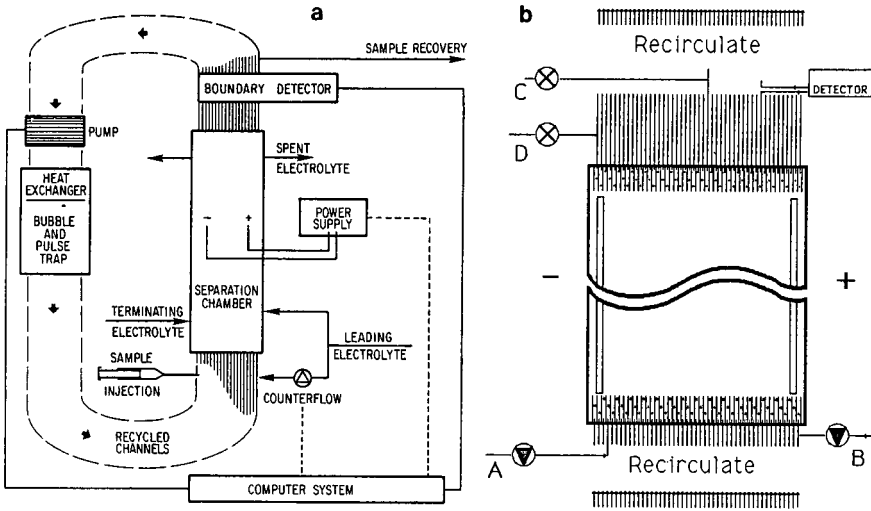
Fig. 1. Schematic representation of the RF3 configured for RITP (a) and the RITP separation chamber (b). A = Sample inlet; B = counterflow inlet; C = center drain valve; D = counterflow drain valve.

a securely braced piece of 3.8 cm plexiglass into which has been machined a cavity to a depth of 0.75 mm; at both ends of this cavity are 1.25 to 1.90 cm partitions (0.25 mm thick, 1.25 mm center to center distance) which serve the purpose of stabilizing the flow prior to entrance into the cell. Each channel formed by these partitions is connected to one tube from the manifold matrix. The electrodes are mounted in chambers on the front of the separation chamber and are connected to the flowing fluid via a thin slot (0.75 mm) running the length of the chamber (Fig. 2). The cell was attached
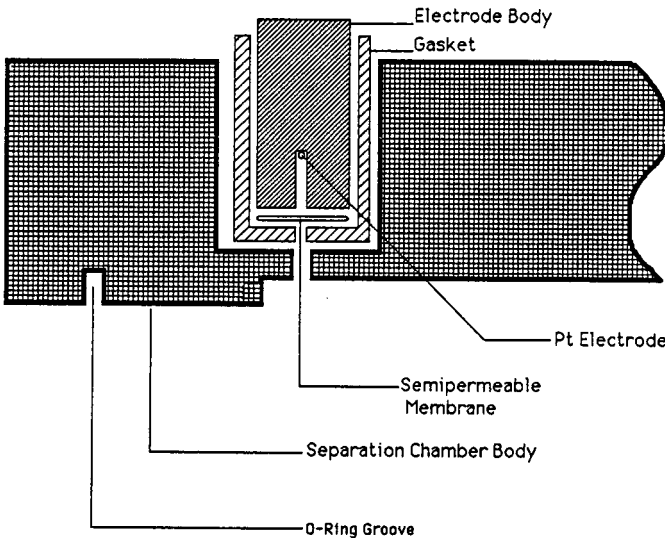
Fig. 2. Cut-away view of the separation chamber detailing the electrode mounting chambers.

to a thermostated cooling plate and sealed using a pair of O rings. Recirculation of the process fluid is provided by a 52-channel peristaltic pump accurate to within 10% per channel. The pump has an adjustable shoe so that the amount of pressure on the tubing may be carefully adjusted to provide minimum pulsing at the inlet and outlet. The flow-rate of process fluid through the pump may be above 500 ml/min (> 12 ml/min per channel). The third major portion of the system is the combined array of heat exchangers/bubble and pulse traps. Serving as the primary fluid reservoir of the system they provide for the most straightforward modification of the process volume. These reservoirs maintain the separation of all 48 fractions (about 4.5 ml each in the current model) of the process volume while providing uniform cooling and storage.

In its simplest implementation, RITP constitutes a batch process. A typical experiment proceeds as follows. The terminator is used as the electrode solution on the side opposite to the detector (Fig. 1b), whereas leading electrolyte with a two to ten-fold higher concentration than employed in the separation chamber is in the other electrode compartment. The electrophoresis chamber, the tubing loops and the channel reservoirs are filled with leading electrolyte (about 250 ml in the current model) which is recirculated until the fluid has thermally equilibrated. The sample is then injected into tube No. 4 (A) and the power (50 to 200 W; constant current of 50 to 100 mA) is applied. As soon as the front is detected (typically around channel 40), the center drain tube (C) is closed and a drain tube on the terminator side (channel 1, D) is opened. When the absorbance at the detector has reached some preset value, the syringe pump (B) is toggled on or off to control the position of the stack. The volume drained from the cell exits via channel 1 (D) and a net movement of fluid is established in a direction opposite to that of electromigration. Upon completion of the separation, the power is switched off and all pumps are stopped. A fraction collector is attached and 48 individual fractions are collected and analyzed separately for pH, conductivity, absorbance and specific activity. Selected fractions were also analyzed by capillary ITP using the Tachophor 2127 analyzer (LKB) featuring a 0.5 mm I.D. PTFE capillary and UV and conductivity detection at the column end.

Monitoring of the sample stack is based on flow through UV absorbance using the LKB 2138 Uvicord S. The C-64 was interfaced to the system employing a modified commercially available analog to digital/digital to analog (A/D, D/A) converter (MW-611; Microworld R&D, Lakewood, CO, U.S.A.)[35]. This board also has sixteen single ended discrete outputs (solid state darlington relays) capable of switching 30 V.d.c. at approximately 100 mA. A 12-V d.c. power supply was built into the interface box and a separate relay box was built to hold up to sixteen 12-V d.c. relays (DPDT) with contacts rated at 1000 V. These relays were chosen to withstand voltages associated with conductivity detection (not yet implemented). A relay was employed to toggle the syringe pump in response to the UV absorbance measurement. The interface between the Uvicord and the A/D converter required the construction of a 50-fold linear operational amplifier with overvoltage and reverse polarity protection. This amplifier converted the 0–100 mV Uvicord signal to the 0–5 V signal required by the A/D converter. The computer provides for measurements to be taken of the order of one per second and the logging of all data every fifteen clock seconds. Three computer programs were written for the data collection and manipulation. Fig. 3 displays an example of the three programs in operation. The dotted line in Fig. 3a is the set control absorbance maintained by the computer and the solid line is the actual

a)

time (1 tic = 5 minutes)

b)

time (1 tic = 5 minutes)
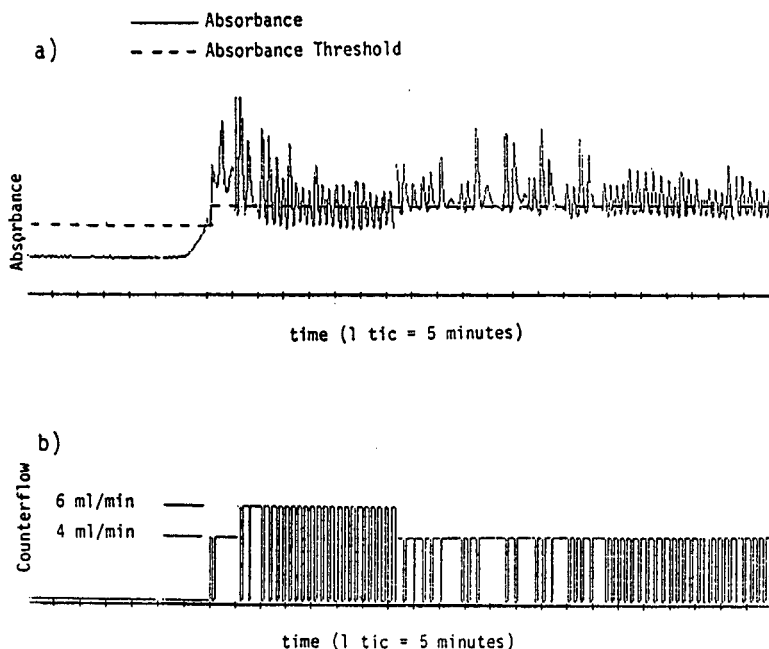
Fig. 3. Example of tracing of UV absorbance *vs.* time (a) and of counterflow *vs.* time (b) during RITP.

absorbance recorded by the computer. Fig. 3b is a record of the counterflow of leading electrolyte (4 to 6 ml/min) applied to the system by the syringe pump.

RESULTS AND DISCUSSION

Adjacent sample components may overlap in the steady state if the quantity is insufficient to form ITP plateaus[40]. Separation, however, can be achieved (i) by using spacer components[7,8] and (ii) by the employment of leading/terminating buffers which selectively stack the component of interest. Fig. 4a shows RITP data of two anionic dyes, amaranth red and fluorescein, with acetate as a spacing constituent. Amaranth red absorbs at 525 nm, fluorescein at 450 nm and the two sample components are detected at 254 nm. The data of Fig. 4a were gathered after 180 min of current flow (current density = 0.021 A/cm^2). Counterflow was applied for 94 min at a rate of about 3 ml/min. Selected fractions from these experiments were analyzed by capillary ITP using the Tachophor 2127 (Fig. 4b). These measurements confirmed the separation of the two dyes shown with the absorbance data of Fig. 4. Resolution in RITP in a 0.75-mm thin fluid film, however, is somewhat lower compared to that in the 0.5 mm I.D. capillary. Nevertheless, the system behaves in ITP manner in two respects, (i) the distinct step gradients in pH and conductivity and (ii) the relative spacing of the two dyes by addition of varying amounts of acetate (data not shown). Also, the zone structure could be immobilized by application of a pulsed counterflow (Fig. 3b).

An anionic protein separation is presented in Fig. 5. A 5 m*M* solution hydro-
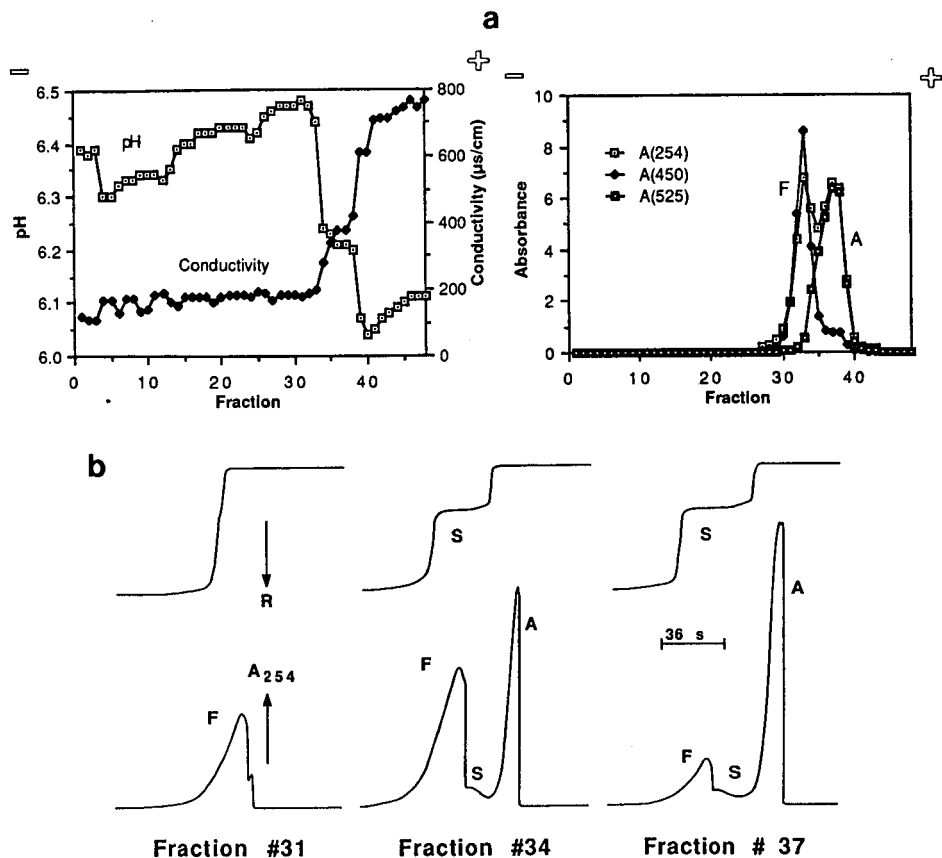
Fig. 4. (a) Anionic RITP of amaranth red (A), acetate (S) and fluorescein (F) using 10 mM hydrochloric acid-histidine (pH 6) as the leading electrolyte. A 20 mM solution of the same electrolyte was the anolyte. A 20 mM solution of 2-(4-morpholino)ethanesulfonic acid (MES) adjusted with histidine to pH 6 was employed as the catholyte. A constant current of 55 mA was applied (power level 60 W). A 2-ml sample containing 5 mM of each dye and 150 mM acetate was injected. (b) Anionic capillary ITP analyses of fractions 31, 34 and 37 of this RITP run using a 22-cm PTFE capillary of 0.5 mm I.D. The same electrolyte system was employed. A 5-μl volume of each fraction was injected and the experiments were performed at a constant 150 μA. The time of analysis was about 5 min. The measured conductivity is given as resistance (R).

chloric acid adjusted with ammediol to pH 9.5 was employed as a leader whereas ε-aminocaproic acid (EACA) was the terminating constituent. Bovine serum albumin was separated from canine hemoglobin by use of glycine as a spacer. Such low-molecular-weight spacers have the particular advantage of being easily removed from the final purified product. The two proteins were assayed spectrophotometrically at 415 nm (hemoglobin) and 602 nm (blue stained albumin). The data shown are corrected for the absorption of hemoglobin at 602 nm and blue stained albumin at 415 nm. The data shown in Fig. 6 illustrate the loading capacity of the RITP apparatus described. A 2.88-g amount of bovine albumin was processed employing 5 mM hydrochloric acid with ammediol (pH 9.17) as the leading electrolyte and EACA as the terminating constituent. The fractions were collected after 39 min of current flow at a
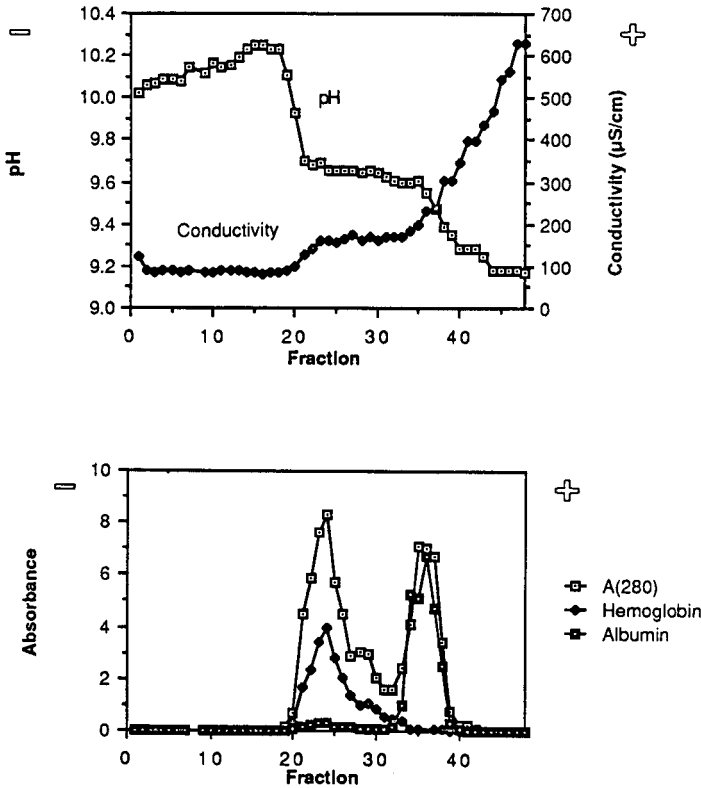
Fig. 5. Anionic RITP of 345 mg bovine albumin and 350 mg canine hemoglobin with 38 mg of glycine as a spacing constituent. A solution of 5 mM hydrochloric acid adjusted with ammediol to pH 9.54 was used as the leading electrolyte. A 60 mM solution of EACA with ammediol at pH 10.47 was the catholyte and 15 mM hydrochloric acid with ammediol was the anolyte. Profiles for total protein (280 nm), albumin and hemoglobin are shown.

current density of 0.038 A/cm^2 (counterflow for 9 min). An albumin recovery of 83% was obtained. The steady state protein concentration under these conditions was found to be about 8 mg/ml (0.8%, w/v), a value which compares well with computer simulation data and experimental values obtained with other electrophoretic instrumentation[41]. The total protein load for the RITP apparatus used is in excess of 3 g, the separation of which could be achieved in the order of 30 min leading to a protein processing rate of 6 g/h.

Cationic RITP data depicting the stacking of prepurified lectins from lentils (lens culinaris) are shown in Fig. 7. A 2.5-ml volume of a lentil extract which was prepurified with the Biostream separator in a recycling mode[42] was injected into 10 mM potassium acetate, processed at a constant current density of 0.038 A/cm^2, and held around channel 39 by counterflow. The presence of the lectins LcH-A and LcH-B, as well as a complex formed by the two proteins (middle band[42]) in the stack is documented by polyacrylamide gel (PAG) IEF analysis (Fig. 7b).

We have shown during this preliminary investigation of automated RITP that the application of counterflow to the moving steady state system has the capacity to
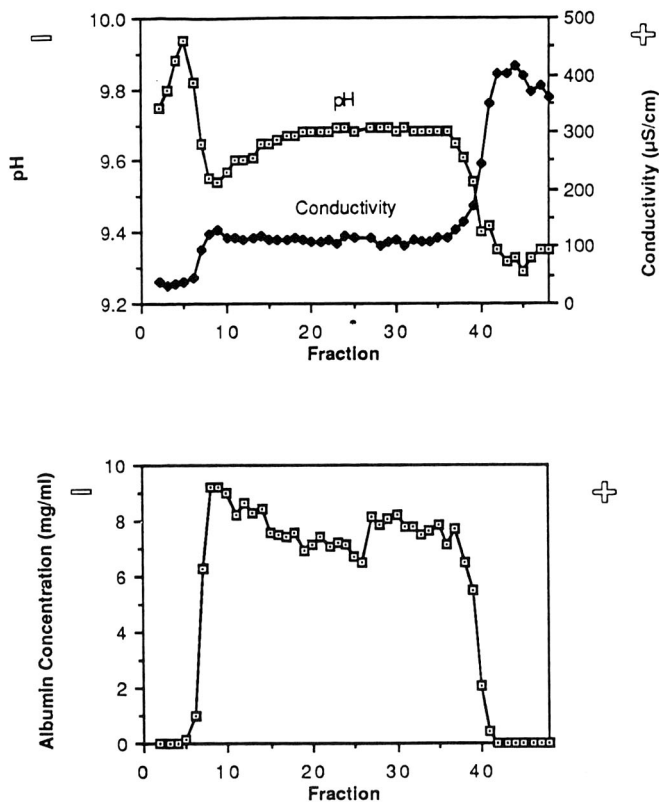
Fig. 6. Anionic RITP of 2880 mg bovine albumin with 5 mM hydrochloric acid adjusted with ammediol to pH 9.17 as the leading electrolyte. A 60 mM solution of EACA with ammediol at pH 10.44 was used as the catholyte and 15 mM hydrochloric acid with ammediol was employed as the anolyte. A constant current of 100 mA was applied. The total voltage at collection time was 1975 V.

move the boundary to any position in the cell which is desired. This capacity is very important for large scale processing of proteins. Careful control of the counterflow applied (or applying constant counterflow and varying the voltage applied) with the computer and an interfaced sensor makes it possible to immobilize the front. This process may extend the effective separation distance to any desired length (essentially infinite) without changing the physical dimensions of the separation chamber. When the migrating steady state has been attained and immobilized at the desired position, any further addition of sample will cause an increased amount of protein in each zone.

RITP offers several advantages to the current modes of preparative electrophoresis, the primary advantage being scale. In our preliminary experiments the loading factor was on the gram scale per processing hour which is a tremendous increase compared to the scale of separations currently obtained in gels. This scale is similar to that reported with CFITP methods[29]. Further research will reveal both the maximum processing rate and the resolution improvement due to recirculation. Many proteins suffer a decrease in activity as well as precipitation after long periods of exposure to

a

(b)
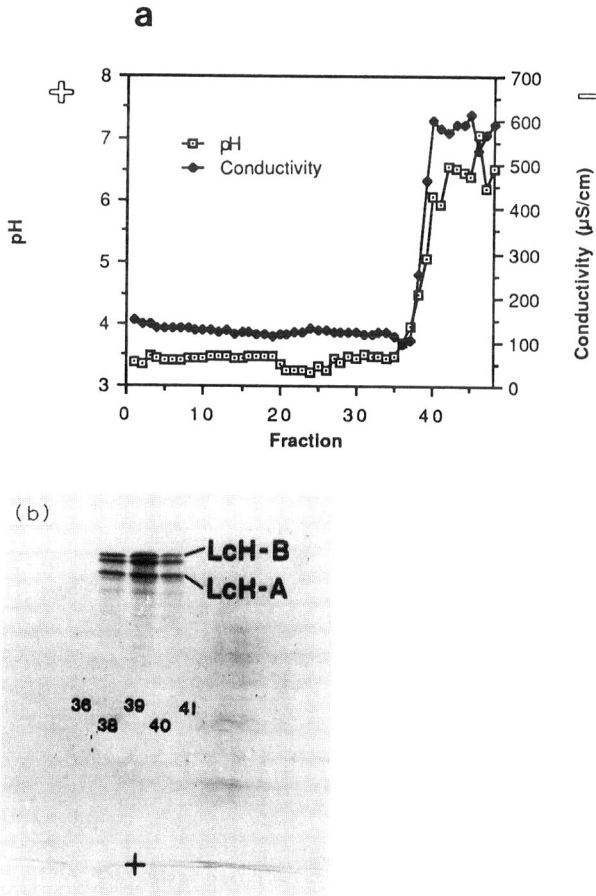
Fig. 7. Cationic RITP of 88 mg lentil lectins prepurified by electrophoresis in the Biostream separator[42]. The leading electrolyte was 10 mM potassium acetate, 50 mM acetic acid was the anolyte. A constant current of 100 mA was applied. The pH and conductivity profiles after collection (80 min of current flow with 13 min of counterflow) are depicted (a) as well as PAG IEF gel analyses of selected fractions in a pH 3.5–10 ampholine gradient (b).

their isoelectric point which makes preparative IEF a less attractive methodology when considering these proteins. Also, ITP usually does not dilute the sample as is the case with zone electrophoresis.

For complete automation of RITP the computer would have to follow (i) the attainment of the steady state by having arrays of universal and specific sensors, (ii) the monitoring of the position of the front edge of the zone structure and (iii) the activation of counterflow if the leading boundary passes a specified position along the separation axis or of changes of the applied current. Having a sensor specific to the product to be purified would further permit the on-line control of its condensation and recovery. The potential for full computer control of this electrophoretic method may represent a new acceptability of this method as a unit operation for the emerging biotechnology industry. Two different RITP processing procedures, batch and con-

tinuous, are possible. (1) Batch-wise processing: sample injection occurs into the leading electrolyte near the membrane towards the terminator electrode compartment seconds before power application. When the leading boundary passes a specified position bulk counterflow is activated which retards or even stops the further advancement of the front and processing is continued until full separation is achieved. Collection of the separated proteins may proceed in two ways; first bulk collection of the entire separation chamber into several discrete fractions by the use of a multichannel valve to switch all of the recycling channels to a collection apparatus. The second method of collection is by electrophoretic elution; the counterflow is turned off and the entire stack will migrate isotachophoretically to a specific channel which is connected to a computer controlled fraction collector. (2) Continuous operation: a continuous mode of operation can be achieved in which sample is continuously infused, the individual components come to rest at their appropriate position in an ITP stack held stationary by counterflow and a particular product of interest is steadily withdrawn from the appropriate channels.

REFERENCES

1 E. Schumacher and T. Studer, *Helv. Chim. Acta*, 47 (1964) 957.
2 F. M. Everaerts, J. L. Beckers and Th. P. E. M. Verheggen, *Isotachophoresis*, Elsevier, Amsterdam, 1976.
3 S. Hjalmarsson and A. Baldesten, *CRC Crit. Rev. Anal. Chem.*, 11 (1981) 261.
4 P. Boček, P. Gebauer, V. Dolník and F. Foret, *J. Chromatogr.*, 334 (1985) 157.
5 W. Thormann, *Sep. Sci. Technol.*, 19 (1984) 455.
6 W. Thormann, *J. Chromatogr.*, 334 (1985) 83.
7 A. Kopwillem, W. G. Merriman, R. M. Cuddeback, A. J. K. Smolka and M. Bier, *J. Chromatogr.*, 118 (1976) 35.
8 L. Arlinger, in P. G. Righetti (Editor), *Progress in Isoelectric Focusing and Isotachophoresis*, North-Holland, Amsterdam, 1975, pp. 331–340.
9 M. Bier, N. B. Egen, G. E. Twitty, R. A. Mosher and W. Thormann, in C. J. King and J. D. Navratil (Editors), *Chemical Separations, Vol. 1, Principles*, Litarvan Literature, Denver, CO, 1986, pp. 133–151.
10 M. Bier, R. M. Cuddeback and A. Kopwillem, *J. Chromatogr.*, 132 (1977) 437.
11 C. J. Holloway and R. V. Battersby, *Methods Enzymol.*, 104 (1984) 281 and references cited therein.
12 M. Bier, in H. E. Sandberg (Editor), *Proceedings of the International Workshop on Technology for Protein Separation and Improvement of Blood Plasma Fractionation*, DEW Publication No. NIH-78-1422, 1977, pp. 514–520.
13 C. F. Simpson and M. Whittaker, in C. F. Simpson and M. Whittaker (Editors), *Electrophoretic Techniques*, Academic Press, London, 1983, pp. 197–213.
14 F. Hampson, in C. F. Simpson and M. Whittaker (Editors), *Electrophoretic Techniques*, Academic Press, London, 1983, pp. 215–230.
15 J. E. Sloan, R. A. Mosher, W. Thormann, M. A. Firestone and M. Bier, in R. Burgess (Editor), *Protein Purification: Micro to Macro*, A. R. Liss, New York, 1987, pp. 329–335.
16 K. Hannig, *Electrophoresis*, 3 (1982) 235 and references cited therein.
17 P. Mattock, G. F. Aitchison and A. R. Thomson, *Sep. Purif. Methods*, 9 (1980) 1–68.
18 H. Wagner and R. Kessler, *GIT Labor.-Med.*, 7 (1984) 30.
19 E. Schumacher and R. Fluehler, *Helv. Chim. Acta*, 41 (1958) 1572.

20 I. Huszár, *Ph. D. Dissertation*, University of Zürich, 1965.
21 W. Preetz and H. L. Pfeifer, *Anal. Chim. Acta*, 38 (1967) 255.
22 W. Preetz, U. Wannemacher and S. Datta, *Z. Physiol. Chem.*, 353 (1971) 93.
23 J. S. Fawcett, *Ann. NY Acad. Sci.*, 200 (1972) 112.
24 Z. Prusík, *J. Chromatogr.*, 91 (1974) 867.
25 Z. Prusík, J. Stepanek and V. Kašička, in B. J. Radola (Editor), *Electrophoresis '79*, Walter de Gruyter, Berlin, 1980, pp. 287–294.
26 V. Kašička and Z. Prusík, *J. Chromatogr.*, 390 (1987) 27.
27 H. Wagner and V. Mang, in F. M. Everaerts (Editor), *Analytical Isotachophoresis*, Elsevier, Amsterdam, 1981, pp. 41–46.
28 H. Wagner and V. Mang, in C. J. Holloway (Editor), *Analytical and Preparative Isotachophoresis*, Walter de Gruyter, Berlin, 1984, pp. 357–363.
29 H. Wagner and V. Mang, *Voruntersuchungen und Empfehlungen zum Einsatz und zur wirtschaftlichen Nutzung der Elektrophorese unter Weltraumbedingungen*, Universitaet des Saarlandes, Saarbruecken, 1985.
30 E. Blasius, K. Mueller, W. Neumann and H. Wagner, *Fresenius' Z. Anal. Chem.*, 315 (1983) 448.
31 M. Bier, N. B. Egen, T. T. Allgyer, G. E. Twitty and R. A. Mosher, in E. Gross and J. Meienhofer (Editors), *Peptides: Structure and Biological Function*, Pierce Chemical, Rockford, IL, 1979, pp. 35–48.
32 M. Bier, *ACS Symp. Ser.*, 314 (1986) 185–192.
33 R. A. Mosher, N. B. Egen and M. Bier, in R. Burgess (Editor), *Protein Purification: Micro to Macro*, A. R. Liss, New York, 1987, pp. 315–328.
34 J. E. Sloan, W. Thormann, M. Bier, G. E. Twitty and R. A. Mosher, in M. Dunn (Editor) *Electrophoresis '86*, Verlag Chemie, Weinheim, 1986, pp. 696–698.
35 J. E. Sloan, *Thesis*, University of Arizona, 1987.
36 W. A. Gobie, J. R. Beckwith and C. F. Ivory, *Biotech. Progress*, 1 (1985) 60.
37 C. F. Ivory, W. Gobie and R. Turk, in H. Hirai (Editor), *Electrophoresis '83*, Walter de Gruyter, Berlin, 1984, pp. 293–300.
38 W. A. Gobie and C. F. Ivory, *ACS Symp. Ser.*, 314 (1986) 169–184.
39 M. Bier and G. E. Twitty, patent pending.
40 W. Thormann and R. A. Mosher, in A. Chrambach, M. J. Dunn and B. J. Radola (Editors), *Advances in Electrophoresis*, Vol. 2, VCH, Weinheim, in press.
41 W. Thormann, J. E. Sloan, T. D. Long, M. A. Firestone and R. A. Mosher, in preparation.
42 P. Wenger, A. Heydt, N. B. Egen, T. D. Long and M. Bier, *J. Chromatogr.*, 455 (1988) 225.

CHROM. 20 915

PHOTOMETRIC AND ELECTRON-CAPTURE MODES IN A DUAL-CHANNEL SENSOR*

YOU-ZHI TANG** and WALTER A. AUE*

Department of Chemistry, Dalhousie University, Halifax, Nova Scotia B3H 4J1 (Canada)

(Received August 18th, 1988)

SUMMARY

A simple, radioactive sensor was developed for potential use with gas chromatographic effluents and/or process streams. The sensor relies on earlier developed response modes of photometric detectors, particularly to (a) nitrogen in high-purity argon and (b) aroyl compounds in nitrogen. Its sole energy source is the weak β radiation from a ^{63}Ni foil. The radiation creates not only luminescence but also ion pairs, and some of the latter can provide a second response channel for electron-capturing substances.

Typical minimum detectable concentrations/amounts are 2 ppm of nitrogen in argon and 1 pg/s of benzaldehyde in nitrogen by photometry, as well as 0.1 pg/s of hexachloroethane in nitrogen by electron capture; with linear ranges of about two orders of magnitude in each case. Some analytes, *e.g.* fluorinated aroyl compounds in nitrogen, respond simultaneously on both channels. The sensor can also be run as a general detector (minimum detectable amount *ca.* 50 pg/s) by monitoring the quenching of background luminescence (the latter having been established by, for instance, a constant level of benzaldehyde in nitrogen).

INTRODUCTION

The flame photometric detector is widely used for the selective detection of gas chromatographic (GC) analytes containing sulfur, phosphorus or other hetero-elements[1]. The energy for producing the monitored luminescence is provided by a hydrogen-rich flame. Recently, such a flame was replaced in its role as the provider of energy by a steady stream of atoms or molecules in excited, metastable states. These energy carriers were produced in a strong electrical field, with a constant input of electrons being generated by the β radiation from a small ^{63}Ni foil. Metastable energy transfer then leads to a variety of response modes different from those of the typical

---

flame photometric detector. For instance, molecular nitrogen was detected in high-purity argon[2]; and a variety of simple aroyl compounds (benzaldehyde[3], benzophenone, anthraquinone[4] and the like) were determined with high sensitivity and selectivity in nitrogen.

Although the strong electrical field was necessary for producing a large number of metastable energy carriers and hence a strong detector response, it turned out that, in the absence of the strong electrical field, the radiation alone could provide enough energy for a luminescence level commensurate with the detection of GC analytes[5]. This effect seemed interesting and potentially useful in a variety of analytical contexts; however, its sensitivity needed improvement. One of the simplest and most obvious avenues for improving the performance of such a β-driven device would be to increase the light level reaching the photomultiplier tube.

The original study of a GC detector driven solely by β radiation[5] made use of a (slightly modified and obviously flameless) Shimadzu flame photometric detection (FPD) unit. The noise in a real detector originates usually in the flame (flicker noise); hence there had obviously been no advantage in maximizing light throughput from the flame to the photomultiplier tube of the Shimadzu detector *vis-a-vis* other design considerations, and a considerable distance had been put between light generation and light measurement by a connecting cylinder equipped with cooling coils, an interference filter, etc. When the detector is run without a flame, however, and the light level itself turns out to be the sensitivity-limiting parameter, the photosensitive cathode needs to be brought as close to the luminescence region as possible.

When, with this in mind, we drew up a blueprint that had a capillary carry the analyte close to a window adjoining the photomultiplier tube, it became immediately apparent that a sensor of this type could provide an additional response mode: the capillary could easily double as an electrode, and the weak β emitter was already in place. In short, the layout resembled that of an electron-capture detector. All that needed to be done was to add a source of polarization and a second electrometer, as well as to pay some attention to geometry and to which parts of the detector ought to be conducting, which insulating. Thus the constructing and testing of an exploratory dual-channel sensor became the objective of this study.

EXPERIMENTAL

The very simple prototype sensor consists of a photomultiplier tube (Hamamatsu R 374) and its housing (from the Shimadzu flame photometric detector), into which is fitted the luminescence-cum-ionization chamber with its various gas lines and electrical connections. The principal aim in designing this prototype was not to come up with the best and most conveniently operated device —that may be safely left to a second or third generation effort should the need for its exist or arise— but to demonstrate feasibility of concept in the most easily accomplished manner.

Fig. 1 shows the basic construction of the dual-channel sensor. The analyte flows from a gas chromatograph or other sample source via a heatable 1/16 in. stainless-steel tube, which connects to a similar introduction tube, 2, through an electrically insulating connector (a drilled-out 1/8 in. Swagelock union around a PTFE tube holding the two 1/16 in. tubes via suitable ferrules; not shown). The sample streams to the ionized and luminescent zone of gas surrounded by the cylindrical ^{63}Ni/Au foil, 4.
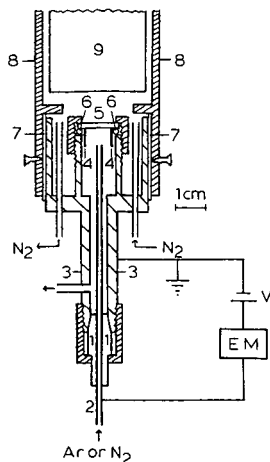
Fig. 1. Schematic of multifunctional sensor. 1 = PTFE ferrule; 2 = sample inlet tube; 3 = sensor base, fits into photomultiplier tube housing; 4 = cylindrical ^{63}Ni foil; 5 = quartz window; 6 = silicone O-ring; 7 = PTFE insulator sleeve; 8 = photomultiplier tube housing; 9 = photomultiplier tube; V = low-voltage supply; EM = electrometer.

The analyte input line and the lower part of the detector can be heated by externally applied resistance tape (the upper part of the photomultiplier tube housing could be kept at lower temperature, *e.g.* by cooling coils wrapped around it, but this was not done here). To avoid possible condensation and provide additional cooling, a flow of nitrogen passes between the quartz window, 5, of the luminescence chamber, and the quartz window of the photomultiplier tube, 9. Most of the experiments were carried out with the luminescence region at *ca.* 80°C. In its present configuration, the analyte path can not be heated much above 100°C.

The lower part of the sensor, which inserts into the photomultiplier tube housing, is separated from it by an insulating PTFE sleeve, 7, which serves as heat, light and electrical insulation (the latter to protect the electron-capture measurement from photomultiplier tube stray currents). The low-voltage power supply, V, polarizes only the sample inlet tube as the anode (as well as the floating electrometer, EM). Simple RC damping (R = 10 kΩ, C = 200 μF) is used for high-frequency noise reduction.

The main sample input is provided by a Shimadzu GC-4BMPF gas chromatograph, housing a 50 × 0.25 cm I.D. borosilicate column packed with 15% Carbowax 20M on Chromosorb W-AW, 45–60 mesh. Other inputs rely on an exponential dilution flask, or simply on mixing two gas streams (nitrogen analyte and various quenchers). The GC carrier gases, nitrogen of "high purity" and argon of "prepurified" grade, are further cleaned (or so one hopes) by sequential passage through molecular sieve 5A and a heated oxygen-scavenger cartridge (Supelco).

RESULTS AND DISCUSSION

In its photometric mode of operation, the sensor should be capable of two basic types of responses: to nitrogen in argon; and to aroyl compounds in nitrogen.

The first of these modes was thought to hold some potential interest for the

determination of nitrogen in high-purity argon streams. However, first there existed the need to establish that the system would respond at all. In the high-field photometric detector[2], the luminescence of molecular nitrogen comes from its second positive system ($C^3\Pi_u \rightarrow B^3\Pi_g$), which is excited by energy transfer from argon metastables, $^3P_2$ and $^3P_0$. In the high field (*ca.* 5000 V) set-up[2], the current can rise up to almost 100 nA. It has been estimated for a comparable system that the population of argon metastables is many times that of its ions[6]. Thus there should be available a large population of metastables.

In contrast, the maximum possible current under weak-field conditions simply represents the ion pairs created by β radiation, *i.e.* less than 2 nA for the particular foil used in the sensor. It is obvious that there exists the chance of metastables being created —from direct β impact, for instance, or from the excess energy of secondary electrons (the average energy expended by the β ray per ionization event is considerably larger than the ionization potential of argon— but their number must be orders of magnitude less than under strong-field conditions. It should be mentioned in this context that the reaction of nitrogen molecules with argon metastables is obviously not the only conceivable reaction channel for producing luminescence; for instance, direct β impact and/or ion pair recombination (*cf.* ref. 7) may directly transfer the necessary energy to molecular nitrogen. Furthermore, luminescence other than that from the second positive system of nitrogen can not be ruled out. Under high-field conditions, the latter band system was the only one found. However, under low- or no-field conditions, spectra were not determined because of the very low light levels involved. Hence it was unclear how much nitrogen response to expect, and an experiment was definitely called for.

Fig. 2 shows the calibration curve for nitrogen in a stream of prepurified-grade argon, obtained by exponential dilution flask (which had earlier been calibrated in its upper concentration ranges by direct injections of nitrogen into the argon supply line). The minimum detectable concentration (S/N = 2) is about 2 ppm; the linear range about two orders of magnitude.

This is quite remarkable considering the very small energy input, but it is admittedly worse than the minimum detectable concentration in the high-field photometric detector (0.3 ppm)[2]. Although the sensor's lower limit is significantly
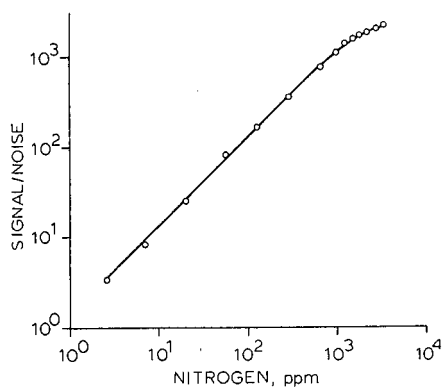
Fig. 2. Calibration curve of nitrogen in a stream of argon.
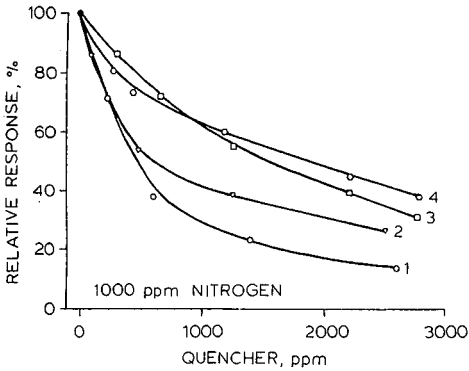
Fig. 3. Relative response of 1000 ppm (v/v) nitrogen in argon, as influenced by various background levels of (1) *n*-butane; (2) oxygen; (3) hydrogen; (4) nitrogen.

better than that of the no-field (*i.e.* solely β-driven) FPD-type detector (25 ppm)[5], it remains, at best, of marginal value for most practical applications. The only real interest it holds is (a) that it works at all and (b) that, if such is needed for a specialized purpose, detection limits could undoubtedly be improved.

For mechanistic as well as practical reasons, and in view of the very low level of energy available, the quenching of nitrogen luminescence by other gases needed to be looked at. Fig. 3 shows the correlation of a (directly injected) nitrogen peak of *ca.* 1000 ppm (v/v) peak concentration on a background of various additives established by exponential dilution flask. The efficiency of quenchers varies (on a volume, *i.e.* molar basis) in the order *n*-butane > oxygen > hydrogen. That is the sequence one would expect on general considerations of quenching cross-sections.

Nitrogen, as the injected analyte, is of course also quenched by a competing, (pseudo) constant level of nitrogen in the carrier. This does not really prevent analytical use, as long as the concentration of background nitrogen does not become exorbitant. The calibration curve for nitrogen analyte simply shifts slightly to the right. In fact, the very calibration curve shown in Fig. 2 represents such a case. It is extremely difficult to remove the last traces of nitrogen from argon streams, and it is not easy to keep traces of the atmosphere from diffusing into analytical instrumentation: hence, injected (analyte) nitrogen had really been determined not in a pure but in a nitrogen-contaminated stream of argon to start with.
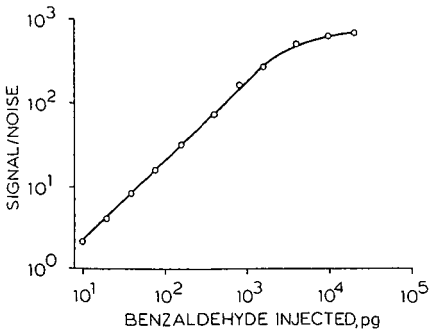
Fig. 4. Calibration curve of benzaldehyde in nitrogen.

The second of the photometric response modes, *i.e.* to aroyl compounds in nitrogen, was explored with the simplest structured analyte capable of producing strong luminescence, namely benzaldehyde (benzaldehyde also happens to be a product of the oxidative pyrolysis of various materials, and is therefore, among other possible applications, of potential interest as an indicator of low-level combustion processes).

As shown in Fig. 4, benzaldehyde has a minimum detectable limit (S/N = 2) of about 10 pg (*ca.* 1 pg/s). This is approximately ten times worse than with a high (*ca.* 5000 V) electrical field[3], but five times better than without such a field in the typical FPD configuration[5]. The sensor construction thus did have the desired effect of significantly improving sensitivity for both types of response modes —benzaldehyde in nitrogen, and nitrogen in argon— and further improvements could no doubt be made with a stronger (larger) radioactive foil, a more sensitive light detection system, etc. The linear range is two orders of magnitude shorter than under high-field conditions but still adequate for analytical purposes and, indeed, quite remarkable if one considers that the only energy input comes from a *ca.* 5 mCi [63]Ni foil.

Following the same logic as used above for nitrogen in argon, the quenching of luminescence by contaminants or co-elutants needed to be looked at. This is shown in Fig. 5, with 1 ng of benzaldehyde being injected into the gas chromatograph, and quenchers being added to a separate gas input via the exponential dilution flask. It should be realized that 0% quencher means 0% deliberately added quencher. There is always *some* quenching going on: from impurities in the detector, from contaminants in the gas supply, from column or septum bleed, from atmospheric diffusion into the analytical system, etc.

The additives were chosen for a variety of reasons: oxygen, because its diradical structure makes it a very efficient quencher under a variety of circumstances, and also because it happens to be a major constituent of the atmosphere; *n*-butane, because it can represent hydrocarbon contamination in a continuous stream, or a co-eluting compound in a GC effluent; and hydrogen, because it is the lightest and simplest non-noble gas (and, as well, because it is generally more difficult to determine than various other gases and the hope existed that any quenching effect, if strong enough, could be developed into an analytical method).
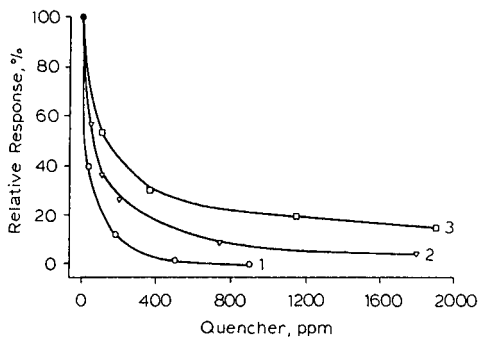
Fig. 5. Relative response of 1 ng benzaldehyde in nitrogen, as influenced by various background levels of (1) oxygen; (2) *n*-butane; (3) hydrogen.

The results of the quenching experiments show oxygen to be the strongest of the three quenchers on a molar basis, followed by butane and hydrogen (note, however, that —as earlier— hydrogen is a fairly strong quencher on a weight basis). This order is different from the one reported above for nitrogen–argon, but that is not surprising since the two systems differ in the carrier/reagent gas and the emitter (in other words, the quencher does not work on the same excited nitrogen species). The mechanism for benzaldehyde (or other aroyl) luminescence is not known at present; possibly, a metastable nitrogen intermediate is involved. It should be noted again that, although benzaldehyde luminescence is likely based on the same spectrum as had been obtained under high-field conditions[3], the low- or no-field emissions were not scanned because of the extremely low level and the spatially diffuse nature of the luminescence.

The fact that oxygen is a strong quencher rules out the direct trace analysis of an atmospheric sample (as, perhaps, in a sensor expected to signal the heat-up of polystyrene insulation); although trace benzaldehyde could, of course, be determined in air by using a preseparating technique such as GC.

It does not seem impossible to develop a GC detector for hydrogen on the basis of its quenching effect, but such an approach would have to be able to compete with other established and simpler methods. At the moment, its analytical utility remains questionable.

The same could be said for using the quenching effect to determine other analytes; yet, such an experiment still holds a certain interest because it can provide some insight into the magnitude of the process. A luminescence background was therefore established by doping a nitrogen carrier stream with benzaldehyde, then a variety of analytes were piped in from the gas chromatograph. The minimum detectable amounts of these analytes (a series of alkanes and carbon disulfide) were about 0.05 ng/s. Fig. 6 shows a calibration curve for the latter compound (which, incidentally, does not respond to any significant extent in a flame ionization detector —but does respond, and with much higher sensitivity than here, in a regular flame photometric detector).

Clearly the most attractive feature of the sensor is its ability to detect and determine a variety of aroyl compounds, of which benzaldehyde is the simplest
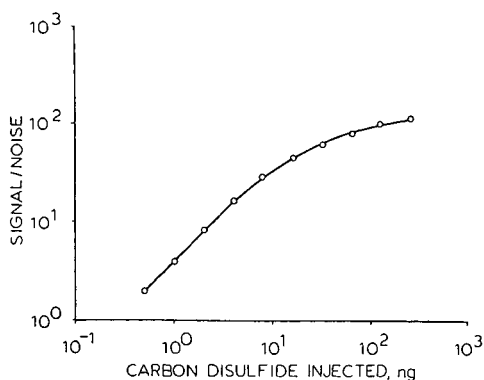
Fig. 6. Calibration curve for carbon disulfide, as determined by quenching a constant background of benzaldehyde luminescence in nitrogen.

example. In the high-field detector, some 18 compounds have so far shown luminescence at an intensity comparable to that of benzaldehyde (comparable meaning within one order of magnitude). These are simple aromatic aldehydes and ketones, including quinones. As a rule-of-thumb (cleanly obeyed up to now), substituents like Br, I, NO_2, OH, and *ortho*-alkyl obliterate response (such peaks are, in fact, weakly negative, *i.e.* one observes a quenching of the background luminescence). Not all simple structures respond; for instance, *p*-benzoquinone or the naphthaldehydes do not[8].

For this study, a number of the structures that had responded well in the high-field detector were tested in the sensor and yielded the expected results. These were mainly substituted benzaldehydes —some of the less volatile compounds, particularly the anthraquinones, were beyond the thermal limits of the sensor. However, there is no reason to believe that these would behave any different than their faster-eluting counterparts, as experiments with the thermally better equipped, β-driven FPD-type detector[5] have demonstrated.

If the sensor is to be used as a GC detector for substances of high elution temperature, the thermal barrier between the photomultiplier tube and the quartz window bordering the luminescence region ought to be improved. This could, for instance, be done by replacing the quartz window (see Fig. 1) by one end of a large-diameter light guide, whose other end would terminate at the face plate of a cool (or even cooled) high-quality photomultiplier tube. In essence, this construction would be analogous to replacing one end piece of a cylindrical electron-capture or argon ionization detector by a light conduit.

This suggests a discussion of the sensor's second channel, the electron-capture response mode. It is made possible by two features: First, the carrier gas nitrogen, indispensable for obtaining the aroyl luminescence, is also an excellent choice as an ECD carrier gas; second, the luminescence does not need a strong electrical field (which the electron-capture detector could not tolerate).

The cylindrical construction of the detector —forced here, really, by the need for concentrating radiation, hence luminescence, inside a relatively small volume— is conventional. The reversal of flow is not conventional, but should make little difference. This is borne out by the sensor's performance under one of the simplest ECD regimes possible, *i.e.* the d.c. mode of operation. Fig. 7 shows the response profile
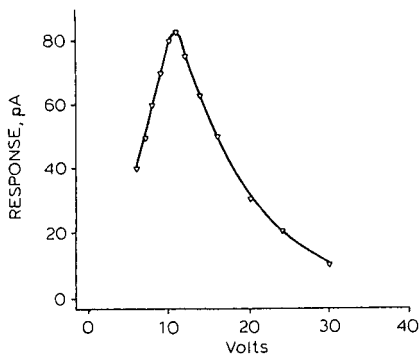
Fig. 7. Response *vs.* d.c. voltage for 15.5 pg hexachloroethane.
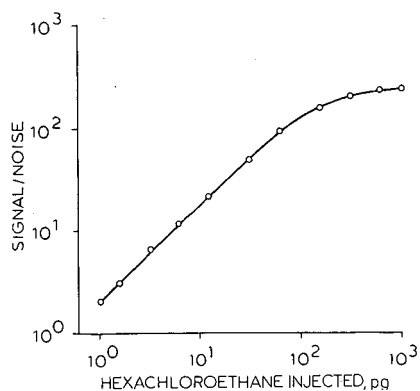
Fig. 8. Calibration curve for hexachloroethane in ECD mode at 11 V d.c. polarization.

over a range of voltages for a typical electron-capturing compound, hexachloroethane; which conforms to expectation.

Fig. 8 adds the calibration curve of hexachloroethane and, again, the minimum detectable limit of 1 pg (0.1 pg/s) is what one would expect. Thus, conventional ECD behaviour can be safely assumed for other compounds (and other polarization modes) as well.

It remains to be demonstrated that the two channels can operate simultaneously. This is done in Fig. 9 with a mixture of benzaldehydes, one of which carries a fluorine substituent (peak No. 1). Again, the responses are as hoped for in the two modes of detection. The luminescence is undisturbed by the simultaneous collection of electrons. (If, for instance, the luminescence had relied on the transfer of energy from the recombination of ion pairs, this would not have been the case.)
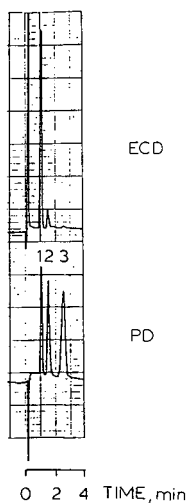
Fig. 9. Simultaneous chart recordings of electron-capture and photometric detector modes of 4 ng each of (1) 4-fluorobenzaldehyde; (2) 3-methylbenzaldehyde; (3) 4-ethylbenzaldehyde.

It is not immediately obvious in which areas of analysis the sensor will find application. Samples that come to mind are primarily those where interest centers on (luminescing) aromatic oxygenates, *e.g.* products of weathering or incomplete combustion, or certain types of flavors and essences (*cf.* 3). The simultaneous ECD trace could provide confirmation in this case (if it happens to be in the correct concentration range), or it could alert the analyst to the presence of compounds with high electron affinity (*e.g.* polychlorinated contaminants) somewhere else in the chromatogram. However, new types of detection devices rarely obey such predictions —more often they find or forge their own niche in the analytical arsenal.

ACKNOWLEDGEMENT

REFERENCES

1 M. Dressler, *Selective Gas Chromatographic Detectors* (*J. Chromatogr. Library*, Vol. 36), Elsevier, Amsterdam, 1986.
2 Y. Z. Tang and W. A. Aue, *Anal. Chem.*, 60 (1988) 1481.
3 Y. Z. Tang and W. A. Aue, *J. Chromatogr.*, 409 (1987) 243.
4 Y. Z. Tang and W. A. Aue, *Mikrochim. Acta*, 1987-II (1987) 21.
5 Y. Z. Tang and W. A. Aue, *Mikrochim. Acta*, 1987-II (1987) 29.
6 A. J. L. Collinson, J. R. Bennett and D. W. Hill, *Br. J. Appl. Phys.*, 16 (1965) 631.
7 M. C. Sauer and W. A. Mulac, *J. Chem. Phys.*, 56 (1972) 4995.
8 Y. Z. Tang, *Ph.D. Thesis*, Dalhousie University, Halifax, 1987.

CHROM. 20 903

CHROMATOGRAPHIC METHOD FOR STUDYING THE HYGROSCOPIC QUALITIES OF SOLIDS*

L. G. BEREZKINA* and V. I. SOUHODOLOVA

Research Institute for Fertilizers, Insecticides and Fungicides, Leninsky Prospect 55, Moscow 117333 (U.S.S.R.)

(First received October 12th, 1987; revised manuscript received July 13th, 1988)

SUMMARY

The features and advantages of chromatographic methods for investigating the complex water vapour sorption and desorption processes of soluble salts and mineral fertilizers were examined. Adsorption and absorption stages of the process were found, the sorption isotherms and chemisorption contributions were defined, the formation of a saturated solution film on the salt surface was demonstrated and the water desorption kinetics were studied. A chromatographic method for determining fertilizer moisture and hygroscopicity as quality characteristics was developed.

INTRODUCTION

Gas chromatography can be used for the investigation of the thermodynamics and kinetics of processes in gas–condensed phase systems and for the determination of practical indicators of product quality[1–7].

Hygroscopicity, defined by the characteristics of water vapour sorption and desorption processes, is one of the most important properties of soluble salts and salt-based fertilizers. The conventional methods (gravimetric and chemical determinations) are time consuming and labour intensive and characterize only the overall process[8,9].

It is more appropriate to apply chromatographic methods, being highly informative, sensitive and rapid, to physico-chemical investigations of the soluble salt–water vapour system and for the rapid evaluation of the moisture content and hygroscopicity of salts and fertilizers as indicators of their quality. The application of chromatography to the above-mentioned systems requires the development of special modifications.

EXPERIMENTAL

One of the methods for studying the sorption process is the impulse method, in

---

which a water vapour zone of initially rectangular shape is introduced into a column packed with the salt being examined and the peculiarities of its broadening as a result of sorption interactions are observed. The thermal desorption process was studied by observing the transfer of water from the specimen directly into a thermal conductivity detector and registering it as an elution curve.

The hygroscopic qualities of potassium chloride and nitrate, ammonium nitrate and dihydrogenphosphate, potassium dihydrogenphosphate and nitrogen–phosphorus–potassium (NPK) fertilizers were investigated, and it was found that the specific salt surface areas, measured by low-temperature nitrogen adsorption from a mixture with helium, are in the range 0.1–0.2 m^2/g. The apparatus used was essentially as described earlier[5,6].

For studying water vapour sorption, a specimen of salt of given dispersity was packed into the thermostated column of 3 mm I.D., directly ahead of the detector cell; the salt was heated before the experiment in a flow of carrier gas (at 60–80°C, depending on the thermal stability of the salt), until water ceased to be evolved. To create a water vapour zone of given constant concentration, sufficient water was introduced on to an inert layer of particles in the range 0.1–0.5 mm (melted quartz). The quartz layer, in which a primary rectangular impulse is formed, was placed on the net partition of the column directly above the specimen under examination. The stepwise elution curve obtained is presented in Fig. 1, curve 1. As can be seen, the broadening of the rear edge of the zone on the quartz and on the salt (CD) under investigation (curve 2) coincide. The broadening of the front edge AB (curves 2 and 3) differs from that for curve 1. The deviation of the front edge on curve 1 from the rectangular shape at a dead volume of the system $\leqslant$ 5 ml and a carrier gas velocity $\leqslant$ 50 ml/min does not exceed 7% [being evaluated as the area ratio AFB:ABCD (curve 1)]. The height of the step is directly proportional to the saturated water vapour pressure at the given temperature; the reproducibility of this calibration method is $\pm 5\%$.

Fig. 1 shows a typical chromatogram for water on the soluble salt (curve 2). By varying the conditions of solid and gaseous phase contact in a number of special experiments, it was found that it is possible to obtain a chromatogram for the salts
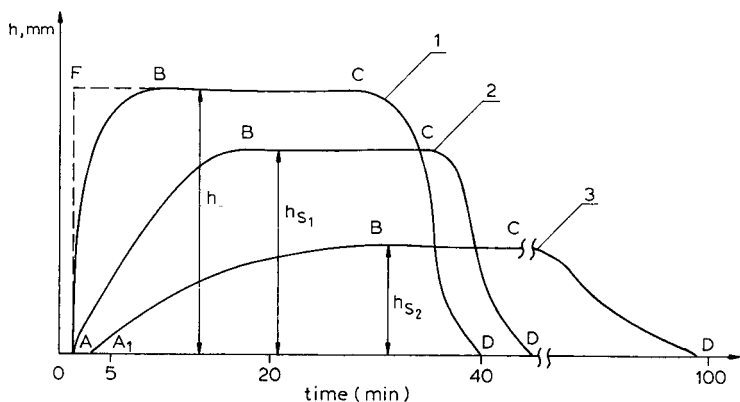
Fig. 1. Water chromatograms at 20°C: 1, Quartz particles; 2, potassium chloride; 3, NPK fertilizer. Step heights: h, for quartz; h_{s_1}, for potassium chloride; h_{s_2}, for NPK fertilizer.

studied, the shape of which, being mostly a result of equilibrium factors, characterizes the process of reversible sorption and does not depend on the experimental conditions (carrier gas velocity 30–80 ml/min, weight of salt 1–10 g, salt dispersity 0.05–0.1 mm, water introduced 1–20 mg).

In a series of experiments carried out to study the desorption kinetics, conditions were chosen such that the height of the detector signal was proportional to the rate of evolution of the volatile component (water)[6]. It was shown that with a weight of salt or fertilizer not exceeding 10 mg and a carrier gas velocity less than 60 ml/min, the time delay was 15 s and the effects of external diffusion and the distortion of the shape of the kinetic curve due to broadening in the dead volume were negligibly small.

RESULTS AND DISCUSSION

One can single out three parts of the equilibrium chromatogram (Fig. 1, curve 2). AB, corresponding to the broadening of the front edge of zone AB, characterizes the initial stage of the sorption process, then the horizontal section BC is registered, corresponding to a constant vapour pressure above the salt; the broadening of the rear edge of zone CD coincides with that obtained in the control experiment. The independence of the results obtained of the contact conditions of water vapour with the salt under investigation permits the conclusion that the contribution of kinetic factors to the broadening of the zone is insignificant.
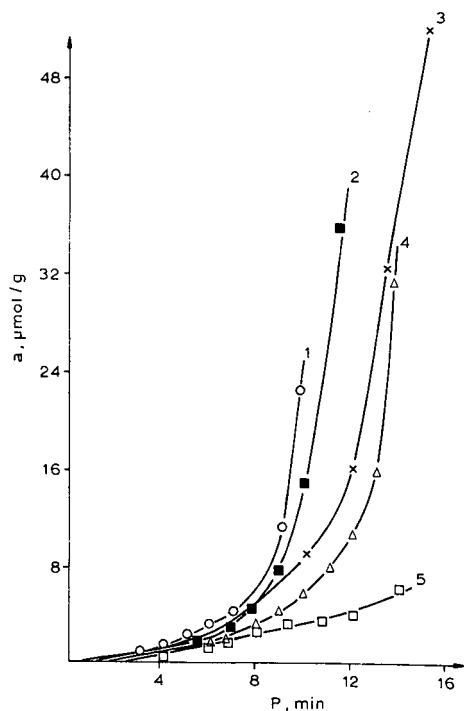
Fig. 2. Water vapour sorption isotherms for salts at 20°C: 1, NH_4NO_3; 2, KNO_3; 3, KH_2PO_4; 4, KCl; 5, $NH_4H_2PO_4$.

Having assumed that this is an adsorption process, the isotherm calculation method for the broadened boundary of the elution curve was applied to define the nature of the initial stage of the sorption process[4]; the isotherm, with its convex part facing the vapour pressure axis, corresponds to the broadening of the front edge of the chromatogram. In Fig. 2, the isotherms of water vapour adsorption on the salts studied at 20°C are shown.

From the equilibrium pressure dependence on temperature in the range 10–30°C for section AB the isotherms and differential heats of adsorption were calculated; they were in the range 17–42 kJ/mol for the salts studied.

The results for the initial process stage can be interpreted as follows. On contact of water vapour with the preliminarily dehydrated salt a certain amount of water is chemisorbed on the especially active areas of the surface. This is accompanied by modifications of the surface, which increases its homogeneity. This can be seen from the shape of the isotherms obtained, which is typical of adsorption on a non-specific homogeneous surface with a relatively high interaction between the adsorbate's molecules[10].

The first stage is completed with the formation of a sorption film (80–100 molecular layers), where a constant concentration of water vapour is established above the salt surface (section BC of the chromatogram, Fig. 1). Special experiments showed that this constant concentration corresponds to the equilibrium vapour pressure above the saturated solution film on the salt surface. Comparison of the data obtained with those in the literature confirmed the formation of a surface saturation solution film and equilibrium between the condensed and gaseous phases on section BC of the chromatogram. The heat of evaporation of water for a potassium chloride saturated solution, calculated from the dependence of the heights (h) of the horizontal parts of stepwise elution curves on temperature (Fig. 3), agrees satisfactorily with that calculated from results[11] obtained by the static method (44 ± 2 and 42 ± 2 kJ/mol, respectively). Therefore, the nature of the second stage is defined by the properties of the surface saturated salt solution.

When a salt is stored under conditions such that $P_{H_2O} \gg P_s$ (where P_{H_2O} and P_s are the pressures of water vapour in the gaseous phase and above the saturated salt
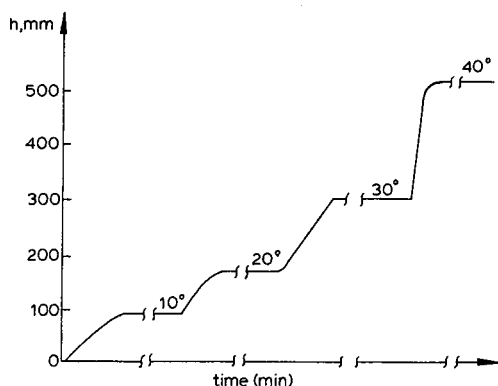
Fig. 3. Dependence of water step height on temperature in potassium chloride.

solution, respectively), the sorption process proceeds accompanied by a decreasing concentration in solution at the gas–liquid boundary.

Curve 3 in Fig. 1 depicts a typical water vapour sorption chromatogram for NPK fertilizers. In contrast to pure salts, a significant broadening of the front and rear edges of the chromatographic zone is observed. Special experiments showed that sections A B and CD present the sorption process under non-equilibrium conditions; however, the step height h_{s_2} (section BC) is directly proportional to the vapour pressure above the saturated solution on the surface of the fertilizer particles. ·

The stepwise chromatograms obtained, characterizing the features of the surface saturated solutions permitted a chromatographic method to be developed for the definition of the hygroscopic points (G) of salts and fertilizers, which are the basis for their hygroscopicity evaluation[8]:

$$G = \frac{P_s}{P_{H_2O}} = \frac{h_s}{h_{H_2O}} \cdot 100$$

where P_s, h_s and P_{H_2O}, h_{H_2O} are the water vapour pressures above the saturated surface solution and the step heights for the sample examined and calibration graph 1, respectively. The G values of salts and fertilizers allow absorption capacities under storage conditions to be correlated and predicted. Studies of the kinetics of water desorption from the salt or fertilizer showed that both the rate and amount of water desorbed (Fig. 4) are a function of temperature, which indicates non-homogeneity of the salt surface. Complete evolution of hygroscopic water is achieved at 65–80°C. The amount of water chemisorbed from the water impulse constitutes 20–40% of the total sorption. The apparent activation energy of the desorption of chemisorbed water is determined as 70 kJ/mol. The investigation of water desorption kinetics led to the conditions for the determination of salt and fertilizer moisture content from the area under the elution kinetic curve obtained by the chromatographic method.

Determinations of moisture content and hygroscopic point by the chromato-
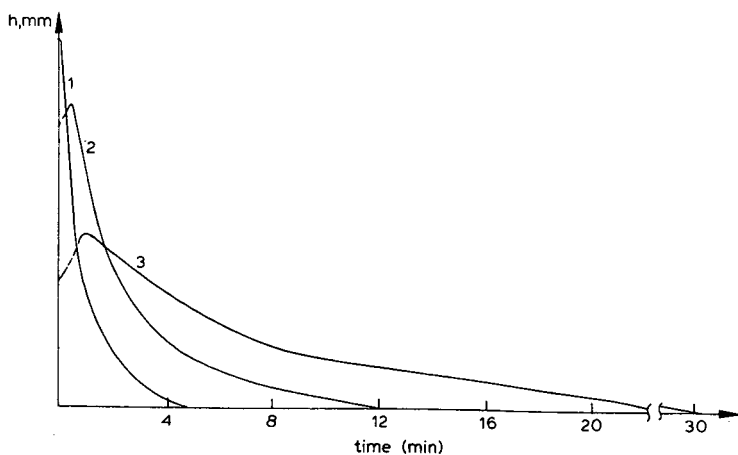
Fig. 4. Kinetic curves of thermal desorption of water from NPK fertilizer at (1) 30°C, (2) 50°C and (3) 70°C.

graphic method can be carried out on a single specimen in one experiment. The determination time is 30–40 min, including a time for moisture determination of 15 min, with a root mean square variation of $\pm 3\%$.

Chromatographic methods for determining the hygroscopic features of salts and fertilizers have found application in both laboratory and industry practice. Such chromatographic methods have allowed the specific features of water vapour sorption and desorption processes in complicated gas–liquid–solid systems formed by the interaction of water vapour with soluble salts and fertilizers to be examined, and also a rapid instrumental method for hygroscopic determination of substances of this type to be developed.

The results of this work indicate more extensive practical applications of gas chromatography.

REFERENCES

1 K. L. Mallik, *An Introduction to Nonanalytical Applications of Gas Chromatography*, Peacock Press, New Delhi, 1976.
2 R. J. Laub and R. L. Pecsok, *Physicochemical Applications of Gas Chromatography*, Wiley, New York, 1978, p. 237.
3 J. R. Conder and C. L. Young, *Physicochemical Measurements by Gas Chromatography*, Wiley, London, 1979, p. 551.
4 A. V. Kiselev and Ya. I. Yesin, *Gas- und Flüssigkeits Adsorptionchromatographie*, Hüthig, Heidelberg, 1985, p. 104.
5 L. G. Berezkina, S. I. Borisova and S. V. Melnikova, *J. Chromatogr.*, 365 (1986) 423.
6 L. G. Berezkina, S. I. Borisova and N. Tamm, *J. Chromatogr.*, 69 (1972) 31.
7 B. V. Stolyarov and L. A. Kravtzova, *Usp. Khim.*, 61 (1987) 1024.
8 N. E. Pestov, *Physical and Chemical Characteristics of Chemical Products in Grain and Powder*, U.S.S.R. Academy of Sciences, Moscow, 1947, p. 8.
9 Y. M. Kouvshinnikov, Z. A. Tichonovich and B. A. Frolkina, *Chemical Industry*, No. 7 (1970) 507.
10 S. Brunauer, *The Adsorption of Gases and Vapours, Vol. 1, Physical Adsorption*, Oxford University Press, London, 1943, p. 511.
11 *Chemist Book*, Vol. III, Khimiya, Moscow, 1965, p. 347.

CHROM. 20 881

HIGH-PERFORMANCE LIQUID CHROMATOGRAPHY OF PROTEINS ON COMPRESSED, NON-POROUS AGAROSE BEADS

I. HYDROPHOBIC-INTERACTION CHROMATOGRAPHY

STELLAN HJERTÉN* and JIA-LI LIAO

Institute of Biochemistry, University of Uppsala, Biomedical Centre, P.O. Box 576, S-751 23 Uppsala (Sweden)

(First received March 11th, 1988; revised manuscript received July 21st, 1988)

SUMMARY

Macroporous agarose beads were converted into non-porous beads by shrinkage and cross-linking in organic solvents. These beads could be used for high-performance hydrophobic-interaction chromatography without derivatization with non-polar ligands, because the 1,4-butanediol diglycidyl ether, used as cross-linker, gives relatively hydrophobic bridges. The resolution for compressed columns packed with these beads was determined as a function of gradient time at constant flow-rate, flow-rate at constant gradient volume and flow-rate at constant gradient time and as a function of loading capacity. Interestingly, the resolution is virtually independent of flow-rate at constant gradient volume even when the column is packed with relatively large beads (diameter 30 μm). The beads have the advantage of being stable up to pH 14.

INTRODUCTION

In a previous paper[1] we showed that peak widths for proteins, in terms of plate numbers, were constant or decreased very little with increasing flow-rate for a column packed with compressed, macroporous, cross-linked 12% agarose beads. Unfortunately, compression of these beads (diameter 3–10 μm) increased the flow resistance considerably, preventing the use of linear flow velocities higher than 3 cm/min for a 30-cm molecular-sieve chromatographic column. However, we have recently shown that columns of compressed, cross-linked, non-porous agarose beads for ion-exchange and hydrophobic-interaction chromatography (HIC) permit higher flow-rates and that the peak widths (and resolution) have the same attractive flow-velocity dependence (at constant gradient volume), even at extremely high flow-rates and for five-fold larger bead diameters; sometimes the resolution even increased with increasing flow-rate[2,3]. In this paper we give a more extensive description of the chromatographic properties of these non-porous, deformed agarose beads when used for the high-performance HIC of proteins. Ion-exchange chromatography on non-porous, deformed beads is treated in Part II[4].

Janzen *et al.*[5] have recently described the high-resolution HIC of proteins on non-porous and non-compressible 1.5-μm silica beads. For reversed-phase chromatography and ion-exchange chromatography of proteins on non-porous, non-compressed packing materials, see refs. 6–10 and 11–15, respectively.

EXPERIMENTAL AND RESULTS

Equipment
The chromatographic system consisted of the following units: a Model 2150 high-performance liquid chromatographic (HPLC) pump, a Model 5152 LC controller and a Model 2151 variable-wavelength monitor from LKB (Bromma, Sweden), a Model C-RIA integrator from Shimadzu (Kyoto, Japan) and a Model 7125 injection valve from Rheodyne (Cotati, CA, U.S.A.). The column tubes were made of Plexiglas (their design is described in ref. 3).

Materials
Phycoerythrin was prepared as described in ref. 16. Blue Dextran, bovine serum albumin, bovine pancreas ribonuclease A, hen egg ovalbumin, bovine liver catalase and horse spleen ferritin were purchased from Pharmacia (Uppsala, Sweden) and bovine α-chymotrypsinogen A and horse heart cytochrome c from Sigma (St. Louis, MO, U.S.A.). Human transferrin was a gift from Dr. L.-O. Andersson (KabiVitrum, Stockholm, Sweden).

Macroporous 11% agarose beads were prepared essentially as described in ref. 17. By wet sieving, beads of a diameter *ca.* 30 μm were collected. The diameter was reduced to about 20 μm by shrinkage and cross-linking (described below). These beads were used in all the experiments. In most runs, the column bed was equilibrated with 0.01 M sodium phosphate (pH 6.8) containing 2.1 M ammonium sulphate and eluted with a linear, negative salt gradient generated from this buffer and 0.01 M sodium phosphate (pH 6.8) containing 0.25 M ammonium sulphate.

Reagents were obtained as listed in Part II[4].

Shrinkage of agarose beads
A 5-g amount (about 5 ml) of sedimented 11% agarose beads was washed by centrifugation at 1500 g for 1–2 min successively with 5 ml of deionized water, 5 ml of dioxane–water (1:1) and two 5-ml portions of dioxane.

The sedimented agarose beads were suspended in 2.5 ml of dioxane–chloroform (1:1). Dioxane was added dropwise with stirring until the opalescent suspension became transparent (if the opalescence did not disappear after addition of 1 ml of dioxane, chloroform was added until the suspension became transparent). An additional 2.5 ml of dioxane were then added. Following stirring for 1 min and centrifugation, the supernatant was removed and the beads were washed with five 5-ml portions of dioxane–chloroform (1:1). The shrunken beads were then washed with three 5-ml portions of chloroform and suspended in 20 ml of chloroform. By these washing procedures the volume of the sedimented agarose beads was reduced five-fold.
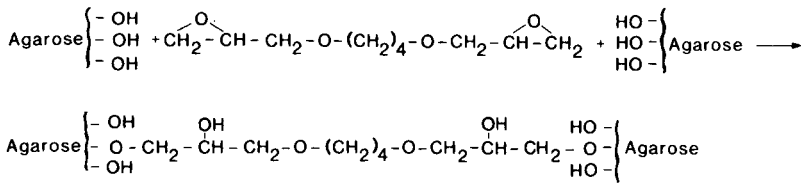
Fig. 1. Simplified reaction scheme for cross-linking of agarose with 1,4-butanediol diglycidyl ether.

Cross-linking of shrunken agarose beads with 1,4-butanediol diglycidyl ether

A simplified reaction scheme is shown in Fig. 1[18]. A 3.2-ml portion of 1,4-butanediol diglycidyl ether was added with stirring to the above suspension of shrunken agarose beads in chloroform, followed by dropwise addition during 10 min of 0.3 ml of boron trifluoride diethyl etherate diluted in 12 ml of chloroform. After stirring for 30 min in a covered beaker the beads were washed several times, first with dioxane and then with water. To increase their rigidity further the agarose beads were cross-linked again after transfer into chloroform using five 5-ml portions of dioxane, 5 ml of dioxane–chloroform (1:1), two 5-ml portions of carbon tetrachloride (this solvent has a high density and therefore facilitates flotation of the beads) and 5 ml of chloroform. The beads were suspended in 20 ml of chloroform and then cross-linked as described above.

When these beads were transferred into water and packed into a column for HIC, they shrank on exposure to high salt concentrations, resulting in a void at the top of the bed. To avoid this shrinkage the beads were treated with glycidol in a solution of dioxane, essentially as described in ref. 19. For this treatment the cross-linked shrunken agarose beads (which had a volume of about 1.5 ml) were washed several times with dioxane by centrifugation at 1500 g and then suspended in 10 ml of dioxane.

Glycidol (1.5 ml) was added with stirring followed by 200 μl of boron trifluoride diethyl etherate. After stirring for 1 h the gel was washed by centrifugation at 1500 g for 2 min with six 5-ml portions of water. The volume of the sedimented beads was still about 1.5 ml.

As 1,4-butanediol diglycidyl ether is relatively hydrophobic, no time-consuming derivatization with non-polar ligands is required in order to obtain amphiphilic beads suitable for HIC. (In a control expriment where the latter cross-linker was replaced with the more hydrophilic γ-glycidoxypropyltrimethoxysilane[2], the hydrophobic interaction with proteins was greatly reduced.) Two additional treatments of the agarose beads with glycidol makes them so hydrophilic that they cannot be used for HIC without derivatization with non-polar ligands.

Porosity of the shrunken, cross-linked beads

The porosity was studied by molecular-sieve chromatography on a 7.2 cm × 0.6 cm I.D. column of the shrunken, cross-linked 20-μm beads. After packing in water the column was equilibrated with 0.01 M sodium phosphate (pH 6.8). The sample consisted of Blue Dextran (mol.wt. 2 000 000), phycoerythrin (290 000), human transferrin (80 000), bovine serum albumin (67 000), hen egg ovalbumin (43 000),

horse heart cytochrome c (12 000) and potassium chromate (194). The retention times were plotted against the molecular weights (Fig. 2).

Pressure–flow-rate dependence

The experiment was conducted in 0.01 M sodium phosphate (pH 6.8) containing 2.1 M ammonium sulphate at flow-rates of 0.25, 0.50, 1.0, 2.0, 3.0 and 4.0 ml/min. The pressures were read and plotted against flow-rate. The linear form of the curve (Fig. 3) indicates that the column can be operated at flow-rates above 4 ml/min.

Recovery

The column was equilibrated with 0.01 M sodium phosphate (pH 6.8) containing 2.1 M ammonium sulphate. Ribonuclease (100 μg) dissolved in 50 μl of the equilibration buffer was applied. Desorption was achieved with 0.01 M sodium phosphate (pH 6.8).

Measurements of the absorption at 280 nm of the applied sample and the collected fractions indicated a recovery of 100%. For ovalbumin and catalase the recoveries were 99 and 98%, respectively.

Resolution on columns of compressed, non-porous agarose beads as a function of gradient time at constant flow-rate

A Plexiglas tube with a diameter of 0.6 cm was packed at a flow-rate of 2 ml/min with the cross-linked, shrunken beads with diameters of *ca.* 20 μm. The bed was then compressed to a height of 5.5 cm by increasing the flow-rate to 5 ml/min.

The sample consisted of ovalbumin (9 μg) and bovine α-chymotrypsinogen A (3 μg), dissolved in 20 μl of the equilibration buffer (0.01 M sodium phosphate, pH 6.8, containing 2.1 M ammonium sulphate). The elution was performed at a flow-rate of 1 ml/min with a linear, negative salt gradient formed from the buffer used for equilibration and 0.01 M sodium phosphate (pH 6.8) containing 0.25 M ammonium
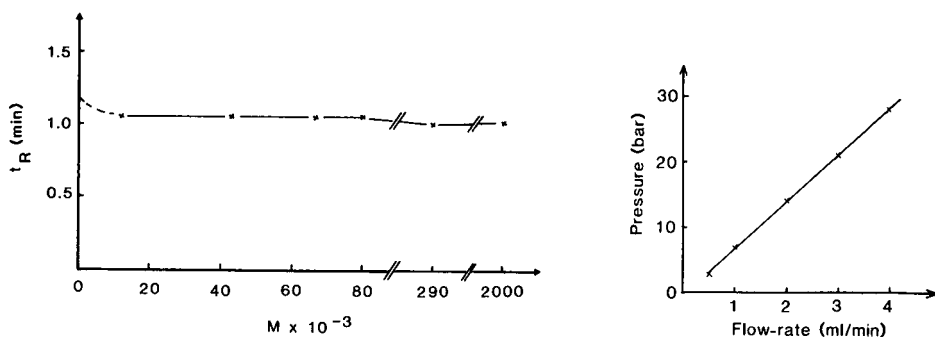
Fig. 2. Porosity of shrunken, cross-linked agarose beads. A column was packed with such beads (diameters *ca.* 20 μm) and the retention times (t_R) for proteins of different molecular weights (M) were determined in a molecular-sieve chromatography experiment. From the plot one can conclude that proteins (at least those with molecular weights above 12 000) cannot penetrate the beads.

Fig. 3. Pressure–flow-rate dependence. Bed dimensions: 5.5 cm × 0.6 cm I.D. Bead diameter: *ca.* 20 μm. Buffer: 0.01 M sodium phosphate (pH 6.8) containing 2.1 M ammonium sulphate.

sulphate. Gradient times of 1.0, 3.0, 6.5, 13, 25 and 50 min were used. The recorder chart speed was inversely proportional to the gradient time to give all the chromatograms the same width, thereby facilitating direct visual comparison. The resolution, R_s, between ovalbumin and α-chymotrypsinogen A was calculated from the following equation for each run:

$$R_s = \frac{t_2 - t_1}{0.5(t_{w2} + t_{w1})} \tag{1}$$

where t_1 and t_2 are the retention times for ovalbumin and α-chymotrypsinogen A, respectively, and t_{w1} and t_{w2} are their peak widths at half-height. Fig. 4 shows a plot of resolution against gradient time.

Fig. 5a and b give a visual impression of the variation in resolution with gradient time. The experimental conditions were the same as those described above.

Influence of flow-rate at constant gradient volume on the appearance of the chromatograms

The bed was equilibrated with 0.01 M sodium phosphate (pH 6.8) containing 2.1 M ammonium sulphate. The sample (3–6 μg of each of the proteins ribonuclease, ovalbumin, α-chymotrypsinogen A, catalase and ferritin) dissolved in 40 μl of the equilibration buffer was applied. At a flow-rate of 0.06 ml/min elution was achieved with a linear negative salt gradient formed from the equilibration buffer and 0.01 M sodium phosphate (pH 6.8) containing 0.25 M ammonium sulphate (pH 6.8). The experiment was repeated at the flow-rates of 0.13, 0.25, 0.5, 1, 2 and 4 ml/min (Fig. 6). The gradient volume was 3.2 ml in all expriments. The recorder chart speed was increased parallel to the increase in flow-rate for the reasons mentioned above under *Resolution on columns of compressed, non-porous agarose beads as a function of gradient time at constant flow-rate.*
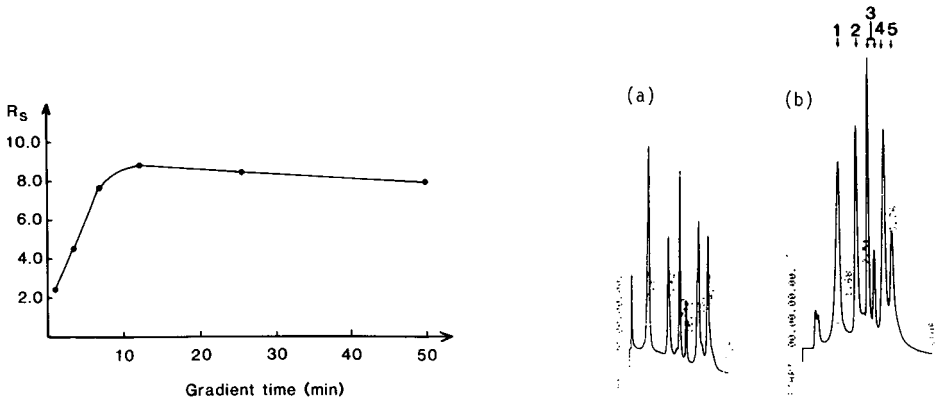
Fig. 4. Resolution (R_s) of ovalbumin and α-chymotrypsinogen A as a function of gradient time. Bed dimensions: 5.5 cm × 0.6 cm I.D. Bead diameter: 20 μm. Flow-rate: 1 ml/min. No gain in resolution is obtained for gradient times exceeding 12 min.

Fig. 5. Influence of gradient time at constant flow-rate on the appearance of the chromatograms. Bed dimensions: 5.5 cm × 0.6 cm I.D. Flow-rate: 1 ml/min. Bead diameter: 20 μm. Gradient time: (a) 15; (b) 3.2 min. For proteins 1–5 see legend to Fig. 6.
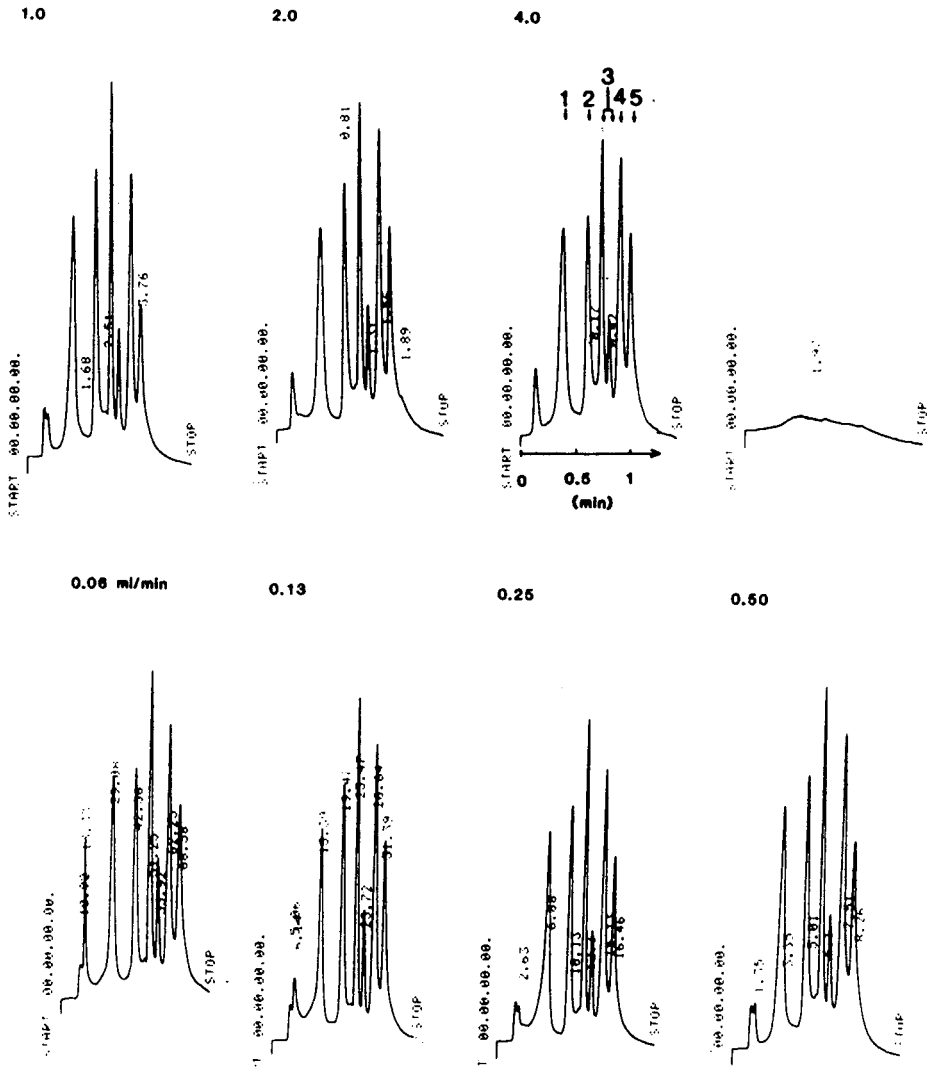
Fig. 6. Influence of flow-rate at constant gradient volume on the appearance of the chromatograms. Bed dimensions: 5.5 cm × 0.6 cm I.D. Bead diameter: 20 μm. Sample: 1 = ribonuclease; 2 = ovalbumin; 3 = α-chymotrypsinogen A; 4 = catalase; 5 = ferritin. The flow-rates are given at the top of each chromatogram. It is evident that the protein patterns are virtually identical, *i.e.*, independent of the flow-rate. The gradient volume was 3.2 ml in all experiments. The recorder chart speed was proportional to the flow-rate.

Influence of flow-rate at constant gradient time on the appearance of the chromatograms

The column was equilibrated with 0.01 M sodium phosphate (pH 6.8) containing 2.0 M ammonium sulphate. The sample consisted of about 7 μg of each of the proteins ribonuclease, ovalbumin, α-chymotrypsinogen A, catalase and ferritin and was dissolved in 20 μl of the equilibration buffer. The proteins were eluted with a negative
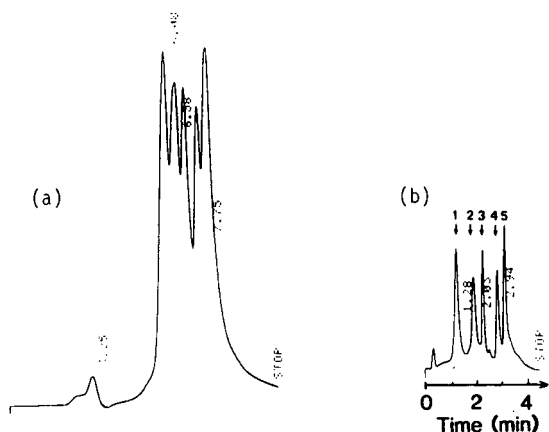
Fig. 7. Influence of flow-rate at constant gradient time on the appearance of the chromatograms. Bed dimensions, bead diameter and sample as in Fig. 6. Flow-rate: (a) 0.25; (b) 2.0 ml/min. The gradient time was 3.2 min in both experiments, whereas the recorder chart speed was constant. Linear gradient from 0.01 M sodium phosphate (pH 6.8) + 2.0 M ammonium sulphate to 0.01 M sodium phosphate (pH 6.8).

3.2-min linear salt gradient from the equilibration buffer to 0.01 M sodium phosphate (pH 6.8). The experiments were performed at flow-rates of 0.25 and 2.0 ml/min. The recorder chart speed was constant at 0.8 cm/min. At the higher flow-rate the gradient volume was larger and therefore the concentration gradient with respect to volume (dc/dV) is shallower which causes the peak heights to be lower in Fig. 7b than in Fig. 7a.

Resolution on columns of compressed, non-porous agarose beads as a function of flow-rate at constant gradient volume

The experimental conditions were similar to those described above under *Influence of flow-rate at constant gradient volume on the appearance of the chromatograms*, except for the bed height, which was 2.5 cm. The sample consisted of ovalbumin and α-chymotrypsinogen A. The resolution between these two proteins was calculated for different flow-rates from eqn. 1. Fig. 8 shows a plot of resolution against flow-rate.

Resolution and peak width on columns of compressed, non-porous agarose beads as a function of sample load at constant flow-rate and gradient time

The column and the experimental conditions were the same as those mentioned
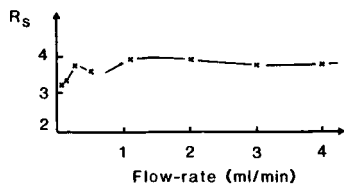
Fig. 8. Resolution (R_s) of ovalbumin and α-chymotrypsinogen A as a function of flow-rate at constant gradient volume. Bed dimensions: 2.5 cm × 0.6 cm I.D. Bead diameter: 20 μm. Gradient volume: 15 ml.
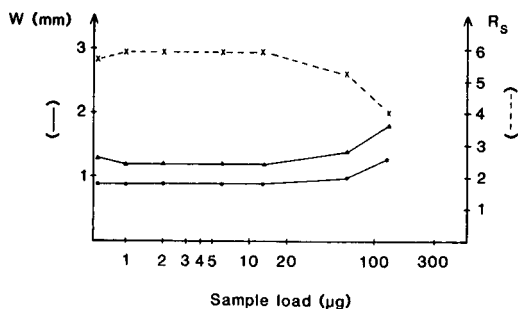
Fig. 9. Peak width (*W*) and resolution (*R$_s$*) as a function of sample load. Bed dimensions: 5.5 cm × 0.6 cm I.D. Bead diameter: 20 μm. Gradient time: 3.2 min. Sample: (▲) ovalbumin and (○) α-chymotrypsinogen A, each applied in the amounts given on the abscissa.

above under *Resolution on columns of compressed, non-porous agarose beads as a function of gradient time at constant flow-rate*, with the exceptions that the gradient time was fixed at 3.2 min and the amounts of each of the two proteins were varied from 0.5 to 120 μg (flow-rate 1 ml/min). Both the peak width and the resolution were determined in each run and were plotted against the amount of each protein applied (Fig. 9).

DISCUSSION

Shrinkage and cross-linking of agarose

Agarose is a polysaccharide built up of alternate residues of 3,6-anhydro-L-galactose and D-galactose[20]. In gels of agarose these polysaccharide chains form double helices collected in bundles, which confers a very porous structure on the gel[21]. When the water in the gel beads is replaced with a non-polar solvent, such as chloroform or carbon tetrachloride, one expects most of the hydrogen bonds to be broken, leading to collapse of the porous gel structure into non-porous beads. If these beads are cross-linked in the organic solvent the agarose retains its collapsed structure when the organic solvent is replaced with water. The shrunken, cross-linked beads will therefore swell only slightly when transferred to an aqueous medium, *i.e.*, their non-porous structure is preserved.

The preparation of amphiphilic beads for HIC often involves a derivatization with non-polar ligands. However, derivatization and cross-linking can be performed in one step if a cross-linker of an appropriate hydrophobicity is selected, as shown in this paper. The cross-linker chosen (1,4-butanediol diglycidyl ether) reacts with the OH groups in the agarose and gives ether bonds, which have the advantage of being stable up to pH 14.

That the agarose beads after shrinkage and cross-linking have lost their macroporous structure is evident from Fig. 2, which clearly shows that proteins do not penetrate the beads.

Resolution as a function of gradient time, flow-rate and sample load

Fig. 4 shows that the resolution (at constant flow-rate) first increases as the

gradient time increases (*i.e.*, when the slope of the salt gradient decreases) and then becomes constant. For each experiment (at constant flow-rate) there is accordingly an optimal run time. Shallower gradients will increase the duration of the experiment without any gain in resolution. Fig. 4 shows that maximal resolution of proteins on the column used in the experiment described herein was obtained at a gradient time of 12 min, *i.e.*, at a gradient volume of 12 ml, as the flow-rate was 1 ml/min. It is also evident that the resolution decreases rapidly with a decrease in gradient time (gradient volume), which is in agreement with the fact that the resolution is higher in the chromatogram in Fig. 5a (gradient volume 15 ml) than in Fig. 5b (gradient volume 3.2 ml).

   Flow-rate and gradient time strongly affect the resolution in any chromatographic experiment on macroporous gels. Columns packed with compressed, non-porous agarose beads have the advantage that only one of these parameters needs to be considered, namely gradient time, as the resolution on these columns is virtually independent of the flow-rate as shown in Figs. 6 and 8. In some instances we have even observed an increase in resolution with an increase in flow-rate[2,3]. We have no satisfactory explanation for this phenomenon, although some hypotheses have been put forward[2].

   When studying the resolution as a function of flow-rate, it is important to choose the experimental conditions such that it is meaningful to compare the chromatograms obtained. From the relationship

$$\frac{dc}{dV} \cdot \frac{dV}{dt} = \frac{dc}{dt} \tag{2}$$

where dV/dt is the flow-rate, one can see that one has to maintain either dc/dV (the concentration gradient with respect to the gradient volume) or dc/dt (the concentration gradient with respect to the gradient time) constant when the flow-rate is varied in a set of experiments. It is obvious that one should maintain dc/dV constant, because this is the gradient the proteins primarily "sense". If dc/dt is kept constant and the flow-rate is increased , then the steepness of the gradient dc/dV decreases according to eqn. 2, which contributes to changes (often increases) in the resolution. Accordingly, by keeping dc/dt constant one can get a false impression that the resolution increases with increasing flow-rate, when, in fact, it may increase instead as a consequence of the shallower dc/dV gradient, as is exemplified in Fig. 7.

   There seem to be no other reports on the separation of macromolecules in which it is stated that the resolution is independent of, or increases with, the flow-rate, except for a study by Blanquet *et al.*[22]. However, they used a constant gradient time, which is equivalent to constant dc/dt for a linear gradient. The chromatograms therefore do not permit a correct comparison as mentioned above.

   From diagrams in a paper by Duncan *et al.*[13] one can see that the plate height for proteins that are not adsorbed on a non-porous ion exchanger can be independent of or decrease or increase with the flow-rate. They did not comment on this and did not show any separations of proteins in which one could see the influence of flow-rate.

   Fig. 9 shows that the resolution is independent of the amount of protein applied up to about 50 μg of each of the model proteins. For macroporous agarose beads the capacity is, of course, larger.

Recovery and time for regeneration

One of the advantages of the non-porous beads is that they give a high recovery[13]. In our experiments the recoveries were calculated to be 100, 99 and 98%. Another important advantage is that only a few bed volumes are required for regeneration which, together with the high flow-rates, contributes to a shorter total time for an experiment on a non-porous bed in comparison with the same experiment performed on a macroporous bed.

ACKNOWLEDGEMENTS

REFERENCES

1 S. Hjertén and D. Yang, *J. Chromatogr.*, 316 (1984) 301.
2 S. Hjertén, K. Yao and J.-L. Liao, *Makromol. Chem., Macromol. Symp.*, 17 (1988) 349.
3 S. Hjertén, in M. T. W. Hearn (Editor), *HPLC of Proteins, Peptides and Polynucleotides*, VCH, Weinheim, in press.
4 J.-L. Liao and S. Hjertén, *J. Chromatogr.*, 457 (1988) 175.
5 R. Janzen, K. K. Unger, H. Giesche, J. N. Kinkel and M. T. W. Hearn, *J. Chromatogr.*, 397 (1987) 91.
6 K. K. Unger, G. Jilge, J. N. Kinkel and M. T. W. Hearn, *J. Chromatogr.*, 359 (1986) 61.
7 G. Jilge, R. Janzen, H. Giesche, K. K. Unger, J. N. Kinkel and M. T. W. Hearn, *J. Chromatogr.*, 397 (1987) 71.
8 R. Janzen, K. K. Unger, H. Giesche, J. N. Kinkel and M. T. W. Hearn, *J. Chromatogr.*, 397 (1987) 81.
9 K. Kalghatgi and Cs. Horváth, *J. Chromatogr.*, 398 (1987) 335.
10 Y.-F. Maa and Cs. Horváth, *J. Chromatogr.*, 445 (1988) 71.
11 D. J. Burke, J. K. Duncan, L. C. Dunn, L. Cummings, C. J. Siebert and G. S. Ott, *J. Chromatogr.*, 353 (1986) 425.
12 D. J. Burke, J. K. Duncan, C. Siebert and G. S. Ott, *J. Chromatogr.*, 359 (1986) 533.
13 J. K. Duncan, A. J. C. Chen and C. J. Siebert, *J. Chromatogr.*, 397 (1987) 3.
14 Y. Kato, T. Kitamura and T. Hashimoto, *J. Chromatogr.*, 398 (1987) 327.
15 I. Mazsaroff, M. A. Rounds and F. E. Regnier, *J. Chromatogr.*, 411 (1987) 452.
16 A. Tiselius, S. Hjertén and Ö. Levin, *Arch. Biochem. Biophys.*, 65 (1956) 132.
17 S. Hjertén, *Biochim. Biophys. Acta*, 79 (1964) 393.
18 J. Porath, J.-C. Janson and T. Låås, *J. Chromatogr.*, 60 (1971) 167.
19 K.-O. Eriksson, *J. Biochem. Biophys. Methods*, 15 (1987) 105.
20 C. Araki, *Bull. Chem. Soc. Jpn.*, 29 (1956) 543.
21 S. Arnott, A. Fulmer, W. E. Scott, I. C. M. Dea, R. Maorhouse and D. A. Rees, *J. Mol. Biol.*, 90 (1974) 269.
22 R. S. Blanquet, K. H. Bui and D. W. Armstrong, *J. Liq. Chromatogr.*, 9 (1986) 1933.

CHROM. 20 882

HIGH-PERFORMANCE LIQUID CHROMATOGRAPHY OF PROTEINS ON COMPRESSED, NON-POROUS AGAROSE BEADS

II. ANION-EXCHANGE CHROMATOGRAPHY

JIA-LI LIAO and STELLAN HJERTÉN*

Institute of Biochemistry, University of Uppsala, Biomedical Centre, P.O. Box 576, S-751 23 Uppsala (Sweden)

(First received March 11th, 1988; revised manuscript received July 21st, 1988)

SUMMARY

Macroporous agarose beads were rendered impermeable to proteins by shrinkage and cross-linking in organic solvents. The chromatographic properties of compressed beds of these non-porous beads derivatized for high-performance ion-exchange chromatography were studied, *e.g.*, the resolution as a function of gradient time, flow-rate (at constant gradient volume) and loading capacity. The columns permit high flow-rates and the resolution is about the same at low and high flow-rates. The beads are stable up to pH 14.

INTRODUCTION

In a recent paper[1] we briefly described the preparation of non-porous agarose beads and their application in the high-performance ion-exchange and hydrophobic-interaction chromatography of proteins. Axially compressed columns packed with these beads have the very attractive feature of giving a resolution that is almost constant with increase in flow-rate (at constant gradient volume), even when the beads are large (*e.g.*, a mixture of beads with diameters from 10 to 50 μm). On compression of the column the beads become deformed, resulting in a decrease in the average distance between them which, in combination with the lack of permeability for proteins, has a favourable effect on the partition rate of solutes between the beads. These circumstances partly explain the unique flow-rate-independent resolution, but in some experiments we have even observed an enhancement of resolution with an increase in flow-rate[1–3] (see ref. 1 for possible but uncertain explanations).

In Part I[4] we described in some detail the high-performance hydrophobic-interaction chromatography of proteins on compressed, non-porous agarose beads. This paper deals with analogous experiments on an anion exchanger.

For ion-exchange, reversed-phase and hydrophobic-interaction chromatography on non-compressible, non-porous packing materials, see refs. 5–9, 10–14 and 15, respectively.

EXPERIMENTAL AND RESULTS

Equipment

The chromatographic equipment was as described in Part I[4].

All experiments were performed on a 6.2 cm × 0.6 cm I.D. column of 3-dimethylamino-2-hydroxypropyl (DMAHP)-agarose beads (diameter *ca.* 15 μm), prepared as described below. If not stated otherwise, the column was equilibrated with 0.01 *M* Tris–HCl (pH 8.5) and eluted with a linear 10-ml gradient generated from this buffer and 0.01 *M* Tris–HCl (pH 8.5) containing 0.18 *M* sodium acetate.

The design of the Plexiglas columns was described in detail in ref. 2.

Materials

Horse skeletal muscle myoglobin, chicken egg albumin (ovalbumin) and bovine serum albumin were bought from Sigma (St. Louis, MO, U.S.A.). Human transferrin was a gift from Dr. L.-O. Andersson (KabiVitrum, Stockholm, Sweden). Human haemoglobin was prepared by haemolysis of outdated blood and phycoerythrin from *Ceramium rubrum* as described in ref. 16.

1,4-Butanediol diglycidyl ether and glycidol (2,3-epoxy-1-propanol) were obtained from Aldrich (Milwaukee, WI, U.S.A.), dimethylamine from EGA Chemie (Steinheim/Albuch, F.R.G.) and boron trifluoride diethyl etherate from Serva (Heidelberg, F.R.G.).

Preparation of non-porous beads

Macroporous 11% agarose beads were prepared essentially as described previously[17]. A fraction of the beads with diameters in the range 15–20 μm were collected by wet sieving and 5 ml of these beads (sedimented) were shrunk and cross-linked in organic solvents using 1,4-butanediol diglycidyl ether as cross-linker[1,4].

Glycidol was employed as an agent to enhance the hydrophilic character of the matrix, as described by Eriksson[18]. The detailed procedure, as adapted to the preparation of amphiphilic, non-porous agarose beads for high-performance hydrophobic-interaction chromatography, was given in Part I[4]. This procedure was also employed for glycidol treatment of the agarose beads used as a matrix for the ion-exchange chromatographic experiments described here. The only differences were (1) that (after the cross-linking with 1,4-butanediol diglycidyl ether) three treatments with glycidol instead of one was used to obtain the desired degree of hydrophilicity and (2) that 150 μl of the boron trifluoride diethyl etherate were diluted in 2 ml of dioxane before it was added slowly during 5 min, with stirring, to the suspension of the agarose beads. The latter modification slows down the reaction rate and thereby eliminates the risk of aggregation of the beads. The former modification increases the number of OH groups in the beads, which makes them more hydrophilic and also increases the chance of achieving a high ligand density of the ion-exchanging groups (which are coupled to the beads via OH groups).

Synthesis of the anion exchanger and packing of the column

Following the third treatment with glycidol, the agarose beads were washed by centrifugation at 1500 *g* with three 5-ml portions of dioxane and then suspended in 15

ml of dioxane. A 1-ml volume of 1,4-butanediol diglycidyl ether was added slowly, with stirring, followed by 0.1 ml of boron trifluoride dietyl etherate. After activation of the beads for 30 min, 1 ml of dimethylamine was added and the stirring was continued for 20 h at room temperature. The DMAHP-agarose beads thus synthesized were washed with six 5-ml portions of water. The reaction scheme is outlined in Fig. 1.

The beads were packed in deionized water into a Plexiglas column (0.6 mm I.D.) at a flow-rate of 2 ml/min. The bed was then compressed by about 3 mm to a height of 6.2 cm by increasing the flow-rate to 5 ml/min.

Porosity of the DMAHP-agarose beads

On replacing the water in the agarose beads with chloroform and subsequent cross-linking (see above), the volume of the sedimented macroporous beads was reduced from 5 to 1.5 ml. One treatment with glycidol gave no significant change in the volume of the sedimented beads. These moderately hydrophobic beads, which were used for high-performance hydrophobic-interaction chromatography, are impermeable to proteins, as shown in Part I[4]. To suppress strongly the hydrophobicity of the beads and make them more suitable for ion-exchange chromatography, two additional treatments with glycidol were required, as mentioned above.

After three derivatizations with glycidol the volume of the sedimented beads had increased to 3.5 ml. If this increase from 1.5 to 3.5 ml represented swelling of the beads, they could have partially reassumed the macroporous structure. To investigate this possibility, the ion-exchange chromatographic column used in the experiments shown in Figs. 2–7 was equilibrated with 0.01 M Tris–HCl (pH 8.5) containing 0.2 M sodium acetate. A sample consisting of the proteins ribonuclease (mol.wt. 13 600), ovalbumin (43 000) and albumin (67 000) was applied. The elution was performed with the same buffer (the proteins are not adsorbed in this buffer). The retention times of the proteins were plotted against their molecular weights (see Fig. 2) and it is evident that the beads are impermeable (non-porous) to proteins, at least to those with molecular weights above 12 000.

Pressure–flow-rate dependence

The experiment was conducted in 0.01 M Tris–HCl (pH 8.5) at flow-rates in the
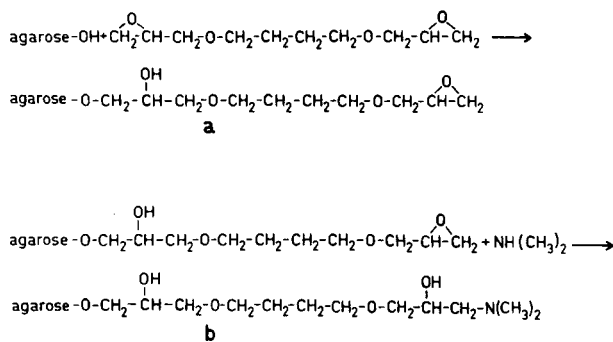
Fig. 1. Reaction scheme for the synthesis of 3-dimethylamino-2-hydroxypropyl (DMAHP)-agarose. (a) Activation of agarose with 1,4-butanediol diglycidyl ether. (b) Coupling of dimethylamine to activated agarose; a tertiary amino group, dimethylamino-2-hydroxypropyl (DMAHP), is formed.
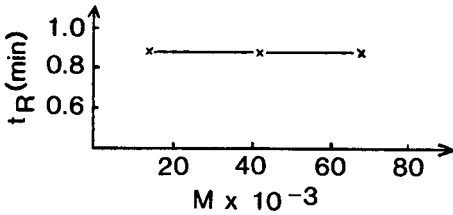
Fig. 2. Porosity of DMAHP-agarose beads. The column was equilibrated with 0.01 M Tris–HCl (pH 8.5) containing 0.2 M sodium chloride. The retention time (t_R) for three proteins of different molecular weights (M) was determined (these proteins were not adsorbed in this buffer). From the plot of retention time against molecular weight one can see that the beads are impermeable to proteins, as the retention time is independent of the molecular weight.

range 1–5 ml/min at increments of 0.5 ml/min and pressure was plotted against flow-rate (Fig. 3). The linear form of the curve indicates that the column can be operated at flow-rates above 5 ml/min.

Recovery

For determination of mass recovery we used ovalbumin, haemoglobin and transferrin. The proteins were adsorbed in the equilibration buffer [0.01 M Tris–HCl (pH 8.5)] and eluted with this buffer containing 0.2 M sodium acetate. Measurements of absorption at 280 nm of both the applied sample and the eluted fractions indicated recoveries of 96, 96 and 105%, respectively.

Resolution on columns of compressed, non-porous agarose beads as a function of gradient time at constant flow-rate

The sample [transferrin (20 μg) and ovalbumin (40 μg)] was dissolved in the equilibration buffer and elution was accomplished with a 2.5-min linear salt gradient (the composition of the equilibration buffer and the gradient is given under *Equipment*). The resolution (R_s) between the two proteins was determined using the equation

$$R_s = \frac{t_2 - t_1}{0.5(t_{w2} + t_{w1})} \tag{1}$$
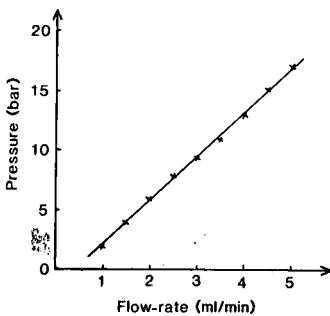
Fig 3. Pressure–flow-rate dependence. Bed dimensions: 6.2 cm × 0.6 cm I.D. Bead diameter: *ca.* 15 μm. Buffer; 0.01 M Tris–HCl (pH 8.5).
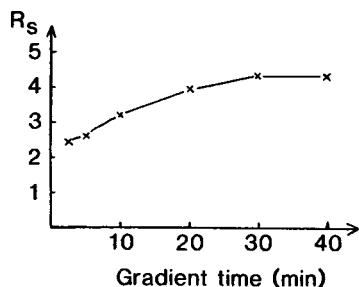
Fig. 4. Resolution (R_s) as a function of gradient time. Bed dimensions: 6.2 cm × 0.6 cm I.D. Bead diameter: 15 μm. Flow-rate: 1 ml/min. The diagram shows that there is no gain in resolution for gradient times exceeding 25–30 min.

where t_1 and t_2 are the retention times of transferrin and ovalbumin, respectively, and t_{w1} and t_{w2} are their peak widths at half-height. In an analogous way the resolution was calculated for gradient times of 5, 10, 20, 30 and 40 min. In Fig. 4 the resolution is plotted against gradient time. As this figure indicates, the highest resolution is obtained at gradient times of *ca.* 25–30 min.

Influence of flow-rate at constant gradient volume on the appearance of the chromatograms

For the composition of the equilibration buffer and the salt gradient, see *Equipment*. The sample [20–40 μg of each of the proteins myoglobin (1), haemoglobin (2), transferrin (3), ovalbumin (4), albumin (5) and phycoerythrin (6)] was dissolved in 20 μl of the equilibration buffer. A series of experiments were performed at flow-rates from 0.25 to 4.0 ml/min. The gradient volume was constant (10 ml). In each experiment the chart speed was proportional to the flow-rate to give chromatograms of the same width, which makes it easier to compare visually the protein patterns and the resolution at different flow-rates (Fig. 5). Fig. 5 shows that the protein pattern and the resolution are about the same at low and high flow-rates.

Resolution on columns of compressed, non-porous agarose beads as a function of flow-rate at constant gradient volume

Peaks 2 and 3 in Fig. 5, corresponding to haemoglobin and transferrin, exhibit a relatively high degree of symmetry (and homogeneity). These peaks were therefore selected for determination of resolution as a function of flow-rate. Eqn. 1 was used for calculation of the resolution at different flow-rates (Fig. 6). Fig. 6 shows that the resolution varies only slightly with flow-rate.

Resolution and peak width on columns óf compressed, non-porous agarose beads as a function of sample load

Most of the experimental conditions were similar to those described above under *Resolution on columns of compressed, non-porous agarose beads as a function of gradient time at constant flow-rate*. The flow-rate was 1 ml/min and the gradient time 10 min. Equal amounts of the model proteins transferrin and ovalbumin were dissolved in the equilibration buffer. The resolution between these two proteins was determined
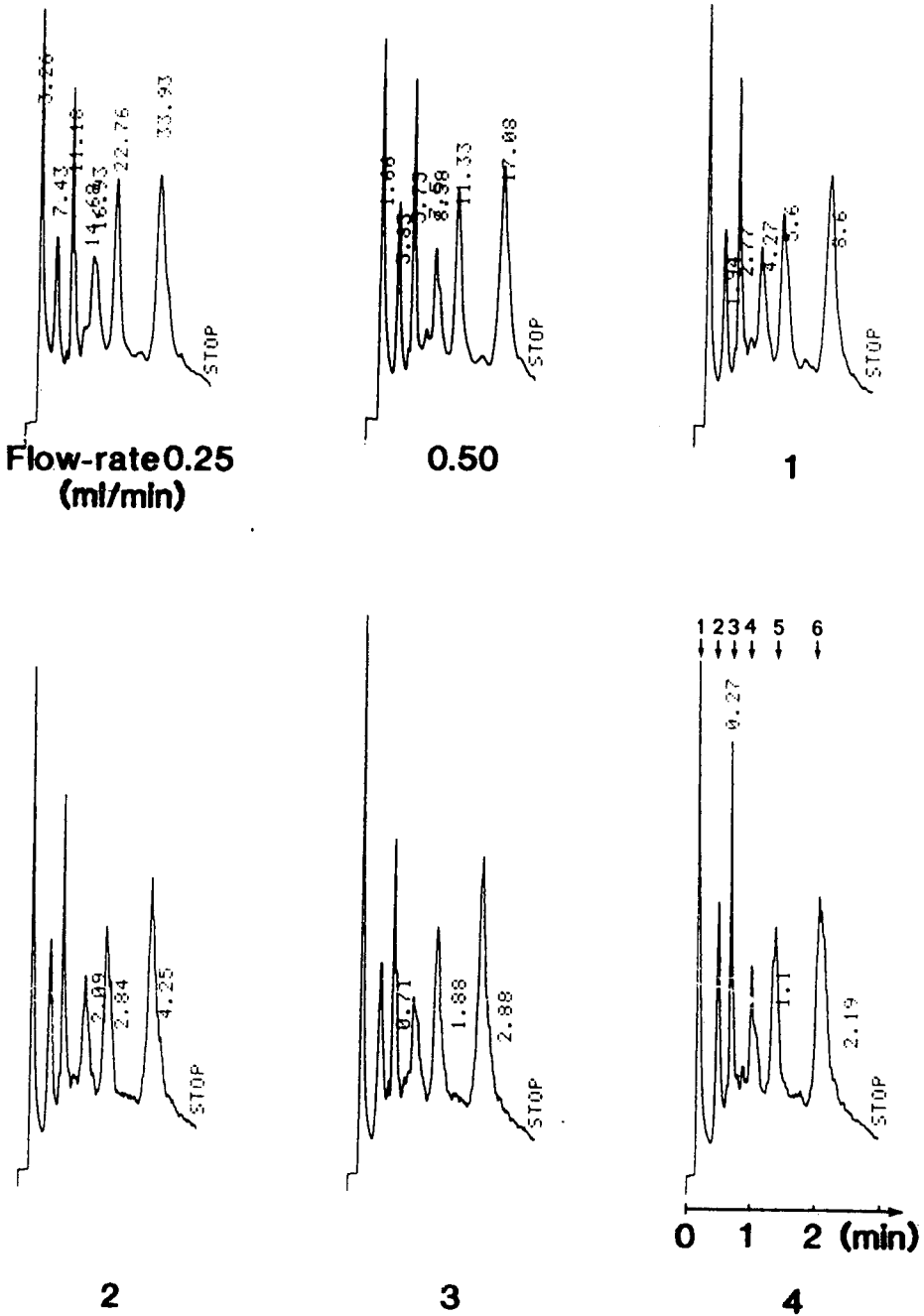
Fig. 5. Influence of flow-rate at constant gradient volume on the appearance of the chromatograms. Bed dimensions: 6.2 cm × 0.6 cm I.D. Bead diameter: 15 μm. Sample: 1 = myoglobin; 2 = haemoglobin; 3 = transferrin; 4 = ovalbumin; 5 = serum albumin; 6 = phycoerythrin. It is evident that the protein patterns and the resolution are virtually the same, *i.e.*, independent of the flow-rate. The gradient volume was 10 ml in all experiments. The recorder chart speed was proportional to the flow-rate.
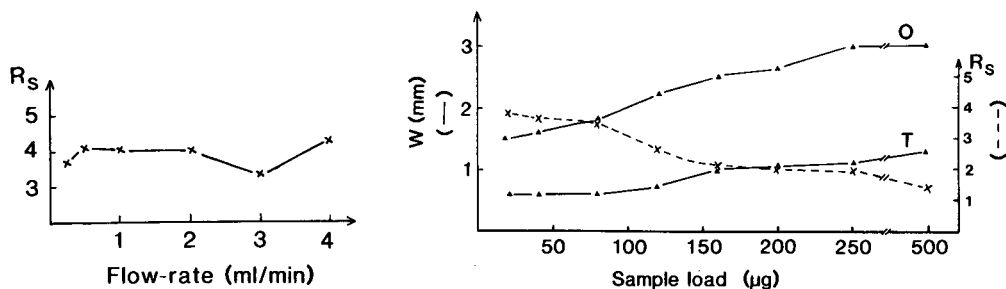
Fig. 6. Resolution (R_s) of haemoglobin and transferrin as a function of flow-rate at constant gradient volume. Bed dimensions: 6.2 cm × 0.6 cm I.D. Bead diameter: 15 μm. Gradient volume: 10 ml. The recorder chart speed was proportional to the flow-rate.

Fig. 7. Peak width (w) and resolution (R_s) as a function of sample load. Bed dimensions: 6.2 cm × 0.6 cm I.D. Bead diameter: 15 μm. Gradient time: 10 min. Sample: T = transferrin; O = ovalbumin, each applied in the amount given on the abscissa. The peak widths and the resolution were affected only slightly by sample size at loads below 100 μg and unexpectedly little at even higher loads.

according to eqn. 1 for different amounts of protein applied and was plotted against amount (Fig. 7). The peak widths at half-height are also plotted in Fig. 7. It is evident that the resolution declines relatively slowly with increasing load, particularly when less than 100 μg of each protein are applied.

DISCUSSION

Shrinkage and cross-linking of the agarose

The strategy behind the shrinkage and cross-linking was discussed in Part I[4], where we employed in a one-step procedure 1,4-butanediol diglycidyl ether both as a cross-linker and as an agent to create non-polar groups in the agarose beads. The same cross-linker, which has the advantage of giving pH-stable ether bonds, was used for the preparation of the beads employed in this study. To suppress the hydrophobic nature of the beads, three treatments with glycidol were required. With glycidol one can therefore modify the degree of hydrophobicity of the non-porous beads in a simple way[18]. The reason for wishing to minimize hydrophobic interactions in ion-exchange chromatography is that these, in combination with electrostatic interactions, can cause irreversible adsorption of proteins, as it may be impossible to find a salt concentration at which both types of interactions are very small[19], which is a prerequisite for desorption (an increase in salt concentration to decrease the electrostatic interactions increases the hydrophobic interactions). To minimize hydrophobic side-reactions, the ion exchanger used is based on derivatization with dimethylamine (see Fig. 1) instead of the more commonly used diethylamine.

Resolution as a function of gradient time, flow-rate and sample load

Fig. 2 shows that the ion-exchange beads are impermeable to proteins, which is one of the reasons why a high resolution is obtained also at very high flow-rates. Another reason is that the beads are deformed following the compression of the column bed, which means that the transport distances between the beads are smaller

than in a non-compressed bed, resulting in more rapid partition of the solutes. There are certainly also other reasons for the high resolution at high flow-rates (Fig. 5 and 6), although it is difficult to arrive at satisfactory explanations, particularly in a few instances where the resolution actually increased with an increase in flow-rate[1-3].

From Fig. 4 one can conclude that the resolution increases gradually with the gradient time (i.e., as the gradient becomes shallower) and finally becomes constant. Resolution is accordingly not impaired by the use of long gradient times. However, excessively shallow gradients give broad, diluted zones and increase the run time.

The resolution is affected relatively little by the sample load, as shown in Fig. 7: at a total load of 500 μg of protein the resolution is still about half of that at 80 μg. The recoveries were high for the three proteins tested (96, 96 and 105%).

This paper has been written with most section headings analogous to those used in Part I[4] to facilitate a general comparison between the two methods. Roughly one can state that the methods have similar features, taking into consideration that they are based on different separation parameters. For general information on agarose-based high-performance liquid chromatography, see ref. 2.

ACKNOWLEDGEMENTS

REFERENCES

1 S. Hjertén, K. Yao and J.-L. Liao, Makromol. Chem. Macromol. Symp., 17 (1988) 349
2 S. Hjertén, in M. T. W. Hearn (Editor), HPLC of Proteins, Peptides and Polynucleotides, VCH, Weinheim, in press.
3 S. Hjertén, K.-O. Eriksson, J.-L. Liao and J. Mohammad, in preparation.
4 S. Hjertén and J.-L. Liao, J. Chromatogr., 457 (1988) 165.
5 D. J. Burke, J. K. Duncan, L. C. Dunn, L. Cummings, C. J. Siebert and G. S. Ott, J. Chromatogr., 353 (1986) 425.
6 D. J. Burke, J. K. Duncan, C. Siebert and G. S. Ott, J. Chromatogr., 359 (1986) 533.
7 J. K. Duncan, A. J. C. Chen and C. J. Siebert, J. Chromatogr., 397 (1987) 3.
8 Y. Kato, T. Kitamura, A. Mitsui and T. Hashimoto, J. Chromatogr., 398 (1987) 327.
9 I. Mazsaroff, M. A. Rounds and F. E. Regnier, J. Chromatogr., 411 (1987) 452.
10 K. K. Unger, G. Jilge, J. N. Kinkel and M. T. W. Hearn, J. Chromatogr., 359 (1986) 61.
11 G. Jilge, R. Janzen, H. Giesche, K. K. Unger, J. N. Kinkel and M. T. W. Hearn, J. Chromatogr., 397 (1987) 71.
12 R. Janzen, K. K. Unger, H. Giesche, J. N. Kinkel and M. T. W. Hearn, J. Chromatogr., 397 (1987) 81.
13 K. Kalghatgi and Cs. Horváth, J. Chromatogr., 398 (1987) 335.
14 Y.-F. Maa and Cs. Horváth, J. Chromatogr., 445 (1988) 71.
15 R. Janzen, K. K. Unger, H. Giesche, J. N. Kinkel and M. T. W. Hearn, J. Chromatogr., 397 (1987) 91.
16 A. Tiselius, S. Hjertén and Ö. Levin, Arch. Biochem. Biophys., 65 (1956) 132.
17 S. Hjertén, Biochim. Biophys. Acta, 79 (1964) 393.
18 K.-O. Eriksson, Biochem. Biophys. Methods, 15 (1987) 105.
19 L. Hammar, S. Påhlman and S. Hjertén, Biochim. Biophys. Acta, 403 (1975) 554.

CHROM. 20 956

SYNTHESIS OF ATP–POLYETHYLENE GLYCOL AND ATP–DEXTRAN AND THEIR USE IN THE PURIFICATION OF PHOSPHOGLYCERATE KINASE FROM SPINACH CHLOROPLASTS USING AFFINITY PARTITIONING

LARS-OLOF PERSSON* and BJÖRN OLDE

Department of Biochemistry, University of Lund, Box 124, S 221 00 Lund (Sweden)

(First received June 6th, 1988; revised manuscript received August 24th, 1988)

SUMMARY

ATP was covalently bound to the polymers dextran of molecular weight 500 000 and polyethylene glycol (PEG) of molecular weight 7000–9000. The degree of substitution (the ATP:polymer molar ratio) was varied by using different concentrations of ATP in the synthesis of ATP–dextran. The partitioning of the ATP–dextran derivative in an aqueous two-phase system containing dextran and PEG was found to depend on the degree of substitution. The potential of the ATP–polymer derivatives obtained for the extraction of phosphoglycerate kinase (E.C. 2.7.2.3) from crude spinach leaf and chloroplast extract using affinity partitioning was studied and compared with the corresponding polymer derivatives of the reactive dye Procion Turquoise MX-G. Both ligands, whether bound to dextran or PEG, affected the target enzyme, phosphoglycerate kinase, but ATP showed a higher specificity. ATP bound to dextran was found to be the most powerful derivative and a rapid extraction procedure involving three main steps, precipitation with PEG, affinity partitioning with ATP bound to dextran as ligand and ion-exchange treatment, was designed. This procedure is rapid, easy to scale up and yields an enzyme preparation that is 80% pure.

INTRODUCTION

When two suitable polymeric substances (differing in molecular structure) are mixed in water at sufficiently high concentrations (3–8%), two phases are formed where the polymers are enriched in opposite phases. Because of the high water content of both phases, proteins can be included in the two-phase systems. The partitioning of proteins between the phases depends on a number of variables that can be adjusted to make these two-phase systems useful for protein purification[1]. One way of significantly and selectively influencing the partitioning is to introduce biospecific ligands that are covalently bound to one of the phase-forming polymers. This technique has been named affinity partitioning[1,2].

ATP has been used as a biospecific ligand in affinity chromatography but so far, to our knowledge, not in affinity partitioning. Chloroplast phosphoglycerate kinase,

an enzyme in the Calvin cycle (reductive pentose phosphate pathway), has been purified from spinach by affinity chromatography using ATP as ligand[3,4].

In this work, ATP was covalently bound to the two phase-forming polymers dextran and polyethylene glycol (PEG). As an illustation of the usefulness of ATP–polymer derivatives in affinity partitioning, the extraction of phosphoglycerate kinase from crude spinach leaf and chloroplast extract was compared with the corresponding derivatives of a reactive dye, Procion Turquoise MX-G. These dyes are widely used as ligands for nucleotide-binding enzymes[5]. ATP bound to dextran was found to be the most powerful derivative and was used for the batch extraction of phosphoglycerate kinase.

EXPERIMENTAL

All manipulations were carried out at $4 \pm 1°C$ unless indicated otherwise.

Materials

Dextran T500 ($\bar{M}_r$ = 500 000), Sephadex G-25 (fine) and DEAE-Sephadex A-50 were purchased from Pharmacia (Uppsala, Sweden) and polyethylene glycol (PEG) with M_r = 7000–9000 (Carbowax 8000) was obtained from Union Carbide (New York, NY, U.S.A.). Celite was a product of Johns-Manville (Denver, CO, U.S.A.) and glass-fibre filters of Whatman (Maidstone, U.K.). Tetrabutylammonium hydroxide, 2,2,2-trifluoroethanesulphonyl chloride (tresyl chloride) and adipic acid dihydrazide were obtained from Fluka (Buchs, Switzerland). Na_2ATP was supplied by BDH (Poole, U.K.) and other biochemicals by Sigma (St. Louis, MO, U.S.A.). The water was singly distilled and then passed through a mixed ion exchanger. All other chemicals were of analytical-reagent grade.

Spinach (*Spinacia oleracia* L., cv. Medania; Weibulls, Sweden) was grown hydroponically as described previously[6]. A 0.5 M stock solution of tetrabutyl-ammonium phosphate was prepared by adjusting the pH of 0.5 M phosphoric acid to 7.7 with 40% tetrabutylammonium hydroxide. When such a solution is used to prepare the two-phase systems in this work the pH on dilution will be 7.5.

Synthesis of ATP–polymer derivatives

Periodate-oxidized ATP was bound to dihydrazide-substituted PEG and dextran by condensation with the hydrazo group. The final products were analysed by gel filtration on a Sephadex G-25 column (20 × 1.5 cm I.D.) using 50 mM Tris–HCl (pH 7.5) as eluent. The effluent was monitored with an Optilab flow-through refractometer and a LKB Uvicord-S (280 nm filter) ultraviolet monitor in order to detect the polymers and the ligand separately. The amount of ATP bound to dextran was determined enzymatically by using the ATP–dextran derivative instead of free ATP in a phosphoglycerate kinase assay system[7]. The amount of bound nucleotide (ATP + ADP + AMP) was determined photometrically at 259 nm using a molar absorption coefficient of 15 400 l mol^{-1} cm^{-1}[8]. The amount of bound ATP was found to be 90% of the amount of bound nucleotide. The amount of ATP bound to PEG was obtained by correcting the measured absorbance value according to the above.

Tresyl-PEG. Tresyl activation was performed essentially as described else-where[9]. A 10-g amount of PEG was dissolved in 25 ml of dichloromethane containing

0.34 ml of triethylamine. The reaction mixture was cooled on ice and 0.300 g of 2,2,2-trifluoroethanesulphonyl chloride was added slowly. The mixture was stirred for 30 min on ice, 1 h at 4 ± 1°C and 24 h at room temperature. The solvent was removed by flushing with nitrogen and the residue was recrystallized three times from 100 ml of ice-cold ethanol.

Tresyl-dextran. Dextran (5 g) was dissolved in 25 ml of dimethyl sulphoxide, then 1 ml of triethylamine and 5 ml of dichloromethane were added slowly. The mixture was cooled on ice and 0.35 g of 2,2,2-trifluoroethanesulphonyl chloride was added slowly while stirring the mixture. The reaction mixture was stirred for 30 min on ice, 1 h at 4 ± 1°C and 24 h at room temperature. The reaction was terminated by precipitating the dextran with 50 ml of dichloromethane. The precipitate was washed and kneaded with several portions of dichloromethane.

Adipoyldihydrazo-PEG. Tresyl-PEG (10 g) was dissolved in 75 ml of 0.2 *M* carbonate buffer (pH 9.9) containing 0.5 *M* adipic acid dihydrazide. The reaction was conducted by stirring the mixture for 24 h at room temperature and was terminated by freeze-drying. The lyophilizate was extracted with chloroform and filtered through glass-fibre filters, first Whatman GF/C and then GF/F. The filtrate was clarified by passing it through a Celite column (20 × 2.5 cm I.D.) and the solvent was removed by evaporation. The yield was 2.3 g.

Adipoyldihydrazo-dextran. Tresyl-dextran (5 g) was dissolved in 50 ml of 0.2 *M* carbonate buffer (pH 9.9) containing 0.5 *M* adipic acid dihydrazide. The reaction mixture was stirred for 24 h at room temperature. After completion of the reaction, free adipic acid dihydrazide was removed by dialysing the reaction mixture against distilled water for 24 h. The dialysate was finally freeze-dried. The yield was 2.5 g.

Activation of ATP. ATP was activated by oxidation with sodium metaperiodate, essentially as described by Kuntz and Krietsch[4]. Briefly, 300 m*M* ATP (pH 8) and 300 m*M* sodium metaperiodate (pH 6) were mixed in equal volumes and the resulting mixture was stirred, while protecting it against light, for 2 h on ice. The reaction mixture was used directly in the coupling procedure.

ATP–adipoyldihydrazo-PEG. Adipoyldihydrazo-PEG (2.0 g) was dissolved in 10 ml of acetate buffer (pH 5.0) and activated ATP was added to give a final concentration of 50 m*M*. The coupling reaction was conducted by stirring the mixture for 24 h at room temperature. The reaction was terminated by freeze-drying, and the product formed was extracted with dichloromethane. The solid particles in the slurry were allowed to sediment, then the supernatant was collected and filtered. The solvent was finally removed by evaporation. The yield was 1.0 g and the degree of substitution was 0.06 mol of ATP per mole of PEG.

ATP–dipoyldihydrazo-dextran. Two couplings of ATP were conducted in order to give one low-substituted and one high-substituted end-product. In each coupling 2.0 g of adipoyldihydrazo-dextran were dissolved in 10 ml of 100 m*M* acetate buffer (pH 5.0). Activated ATP was then added to give final concentrations of 10 and 50 m*M*, respectively. The reaction mixtures were stirred for 24 h at room temperature and subsequently dialysed against distilled water for a further 24 h at 4 ± 1°C. After completing the dialysis, the solutions were freeze-dried. The yield was about 2 g in each instance and the degrees of substitutions were 4 and 40 mol of ATP per mole of dextran, respectively.

Synthesis of dye–polymer derivatives

Procion Turquoise MX-G was coupled to PEG as described by Johansson[2] and to dextran as described by Johansson and Andersson[10]. The amount of bound dye was determined photometrically at 620 nm using a molar absorption coefficient of 51 200 $l\,mol^{-1}\,cm^{-1}$. The degree of substitution was 1 mol of dye per mole of PEG and 6 mol of dye per mole of dextran, respectively.

Preparation of leaf extracts

Whole, freshly harvested leaves were homogenized in a household centrifugal juicer (Multipress MP50, type 4154; Braun, Frankfurt, F.R.G.) supplemented with filter-paper and the resulting solution was centrifuged (Sorvall SE-12) at 20 000 rpm (41 545 g at r_{max}) for 10 min. The pH of the clear, green supernatant was adjusted to 7.5 with sodium hydroxide and used without further manipulations.

Preparation of chloroplast extracts

Intact chloroplasts, prepared as described previously[6], were suspended in 25 mM tetrabutylammonium phosphate–1 mM 2-mercaptoethanol (pH 7.5) and treated in a Potter–Elvehjem glass–PTFE homogenizer on ice (20 strokes by hand) followed by centrifugation as above. The resulting clear supernatant showed a slight yellowish green colour and was used without further manipulations.

Aqueous two-phase systems

The two-phase systems were prepared from aqueous stock solutions of dextran (23.3%, w/w), PEG (40.0%, w/w), buffer, salts, sample solution and, when applicable, ligand–dextran derivative (2.75%, w/w) or ligand–PEG derivative (4.00%, w/w). The systems were equilibrated by mixing and samples from the upper and lower phases were withdrawn and analysed for phosphoglycerate kinase activity and protein content[2]. The partition coefficients, K, of the enzyme activity and protein is defined as the ratio between the concentrations of the component in the upper and lower phases, respectively. The separation factor, β, is defined as the ratio between the partition coefficients of phosphoglycerate kinase and total protein.

Precipitation with PEG

Chloroplast extracts were prepared as described above except that the isolated chloroplasts were suspended in 25 mM sodium phosphate–0.1 mM magnesium chloride–0.1 mM Na_2EDTA–1 mM 2-mercaptoethanol (pH 7.5) (NaPB) before treatment in a Potter–Elvehjem homogenizer. Appropriate weights of 50% (w/w) PEG in NaPB were added to chloroplast extracts in plastic micro-centrifuge tubes and the total weight of each sample was adjusted to 1.00 g with NaPB. The solutions were mixed with a vortex mixer, incubated for 1 h and centrifuged (Sorvall SS-34 with adapters) at 20 000 rpm (15 000 g) for 1 h. The supernatants were poured off, the tubes were flicked in order to remove as much liquid as possible and the pellets were dissolved in 1.0 ml of NaPB. The supernatants and the dissolved pellets were analyzed for enzyme activity and total protein content.

Purification of phosphoglycerate kinase from chloroplasts

A crude chloroplast extract was prepared by a simplified procedure involving

homogenization and a rapid centrifugation as described previously[6] except that the pelleted chloroplasts were suspended in 25 mM tetrabutylammonium phosphate–1 mM 2-mercaptoethanol (pH 7.5) and treated with a tight-fitting Dounce homogenizer. The extract was mixed with solid, ground PEG with gentle stirring until the concentration of the polymer was 30% (w/w) and centrifuged (Sorvall SS-34) at 20 000 rpm (48 200 g at r_{max}) for 1 h. The pellet was discarded and the supernatant, containing the main part of the phosphoglycerate kinase activity, was used as a 30% (w/w) PEG stock solution in the preparation of a two-phase system with the following final concentrations: 10.4% (w/w) dextran, 5.0% (w/w) PEG, 50 mM tetrabutylammonium phosphate (pH 7.5), 0.1 mM magnesium chloride, 0.1 mM Na$_2$EDTA and 1 mM 2-mercaptoethanol; 4% of the total dextran was low substituted ATP–dextran (4 mol of ATP per mole of dextran). The system was mixed and the phases were separated. The upper phase, enriched in the bulk proteins, was discarded and the lower phase, enriched in phosphoglycerate kinase activity, was washed with pure upper phase. The new lower phase was diluted with 40 mM Tris–HCl–5 mM magnesium chloride–1 mM 2-mercaptoethanol (pH 7.5) (Tris buffer) containing 4 mM Na$_2$ATP and 4 mM sodium hydrogensulphite in such a manner that the final concentrations of Na$_2$ATP and sodium hydrogensulphite were 3 mM each. After incubation for 5 min more Tris buffer was added to give a total dilution of 14-fold, which means that the dextran concentration had decreased to 1.6%. The resulting solution was passed through a bed of DEAE-Sephadex A-50 (18 × 2.5 cm I.D.). The bed was washed with Tris buffer until all of the dextran had eluted, as determined with a polarimeter, and then the adsorbed protein was eluted with Tris buffer containing 0.4 M sodium chloride.

Assays

Phosphoglycerate kinase activity was measured according to Kuntz and Krietsch[4] except that bovine serum albumin and dithioerythritol in the dilution buffer were omitted and the reaction was monitored at 340 nm using a molar absorption coefficient for NADH of $6.22 \cdot 10^3$ l mol^{-1} cm^{-1}. The initial velocity was determined and the concentration of 3-phosphoglycerate was 3 mM. The measured activities were corrected for the inhibitory effect caused by the polymer ligands. Protein was analysed according to Bradford[11] using calibration graphs obtained with bovine serum albumin. Sodium dodecylsulphate (SDS) polyacrylamide gel electrophoresis was run and analysed as described by Johansson and Joelsson[12].

RESULTS AND DISCUSSION

Properties of ATP–polymer derivatives

The final synthesis products consisted of one fraction and contained no free nucleotide as judged by gel filtration (data not shown). The moles of ATP bound per mole of polymer (the degree of substitution) was determined photometrically and enzymatically. The ATP–PEG derivative was found to contain 0.06 mol of bound ATP per mole of PEG. For the ATP–dextran derivative the degree of substitution was varied by using different concentrations of periodate-oxidized ATP in the coupling to adipoyldihydrazo-dextran. The ATP–dextran derivatives obtained were included (2% of the total dextran) in phase systems of the same composition as in the extraction experiments below (see Figs. 3 and 4) containing 50 mM tetrabutylammonium

phosphate as buffer. The partition coefficients of the derivatives were calculated from meaurements of the absorption at 259 nm in the upper and lower phases, respectively. The log K of the low-substituted derivative (4 mol of ATP per mole of dextran) was -0.45 and that of the high-substituted derivative (40 mol of ATP per mole of dextran) was -0.30.

This increase in the partition coefficient, due to an increase in the degree of substitution, has also been found for the reactive dye Procion Yellow HE-3G bound to dextran and was explained by the presence of aromatic elements in the dye (which are known to be better solvated in PEG solutions than in pure water) and the effect of phosphate buffer on negatively charged polymers[13]. When the ATP–dextran derivative is used for affinity partitioning (in a dextran–PEG two-phase system), the capacity to enrich the target enzyme in the lower phase will increase with a decreasing partition coefficient of the derivative. Hence, in order to optimize (the effectiveness of) the extraction, a derivative with a low degree of substitution should be used.

The ATP–polymer derivatives were capable of replacing ATP in the phosphoglycerate kinase assay, which shows that they are enzymatically active. Both derivatives partly inhibited the activity of phosphoglycerate kinase (from spinach leaf extract) at concentrations corresponding to those used in the extraction experiments below. Both derivatives reduced the enzyme activity by around 10% (Fig. 1).
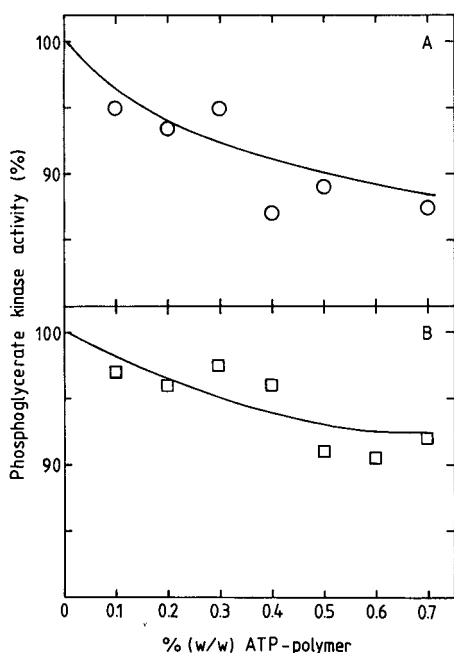
Fig. 1. Influence of ATP–polymer derivatives on the activity of phosphoglycerate kinase from spinach leaf extract. The extract was incubated at the indicated concentrations of derivative for at least 40 min at $4 \pm 1^{\circ}C$, diluted 10-fold whereupon the enzyme activity was measured as described under Experimental. Derivatives: (A) ATP–PEG; (B) ATP–dextran. The data points represent averages of duplicate determinations. No statistical calculations were made to determine the best fit.

Extraction of phosphoglycerate kinase

The usefulness of affinity partitioning for enzyme purification can be evaluated by comparing the partitioning of the target enzyme with that of total protein. When the affinity ligand is bound to PEG, PEG–dextran two-phase systems containing sodium phosphate buffer has been used to achieve an enrichment of the target enzyme in the upper phase and total protein in the lower phase[10]. For PEG–dextran systems containing ligand bound to dextran, tetrabutylammonium phosphate was tested as a replacement for sodium phosphate in order to enrich the total protein in the upper phase. A maximal partition coefficient of total protein was achieved by using tetrabutylammonium phosphate concentrations above 25 mM (Fig. 2).

Fig. 3A and C show the affinity partitioning of spinach leaf extract using increasing concentrations of ATP–polymer derivatives. For comparison, the same experiment was performed with the reactive dye Procion Turquoise MX-G as ligand instead of ATP (Fig. 3B and D). This, together with Procion Orange H-ER, was the most effective of the reactive dyes tested when the nucleotide-binding enzymes of glycolysis was extracted from yeast[14]. Both ligands, wether bound to PEG or dextran, affected the target enzyme, phosphoglycerate kinase. However, ATP showed a higher specificity, that is, it did not change the partitioning of total protein to the same extent as the dye did. The best separation between the target enzyme and total protein was achieved using ATP bound to dextran (Fig. 3C). When chloroplast extract was used instead of leaf extract as the starting material, the separation was further enhanced (Fig. 4).

Precipitation with PEG

The precipitation of phosphoglycerate kinase and total protein, when chloroplast extract was treated with increasing concentrations of PEG, is shown in Fig. 5. At PEG concentrations above 30% (w/w) the percentage of precipitated total protein reaches a plateau value of 60. The percentage of precipitated phosphoglycerate kinase
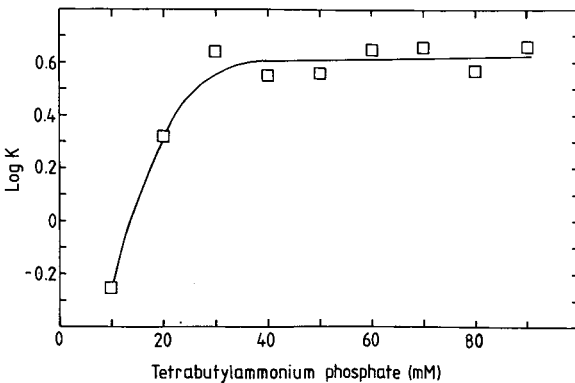
Fig. 2. Partitioning of total protein from spinach leaf extract as a function of the concentration of tetrabutylammonium phosphate. System: 8% (w/w) dextran–6% (w/w) PEG–tetrabutylammonium phosphate as indicated (pH 7.5)–0.1 mM magnesium chloride–0.1 mM Na$_2$EDTA–1 mM 2-mercaptoethanol–leaf extract. Temperature: 4 $\pm$ 1°C.
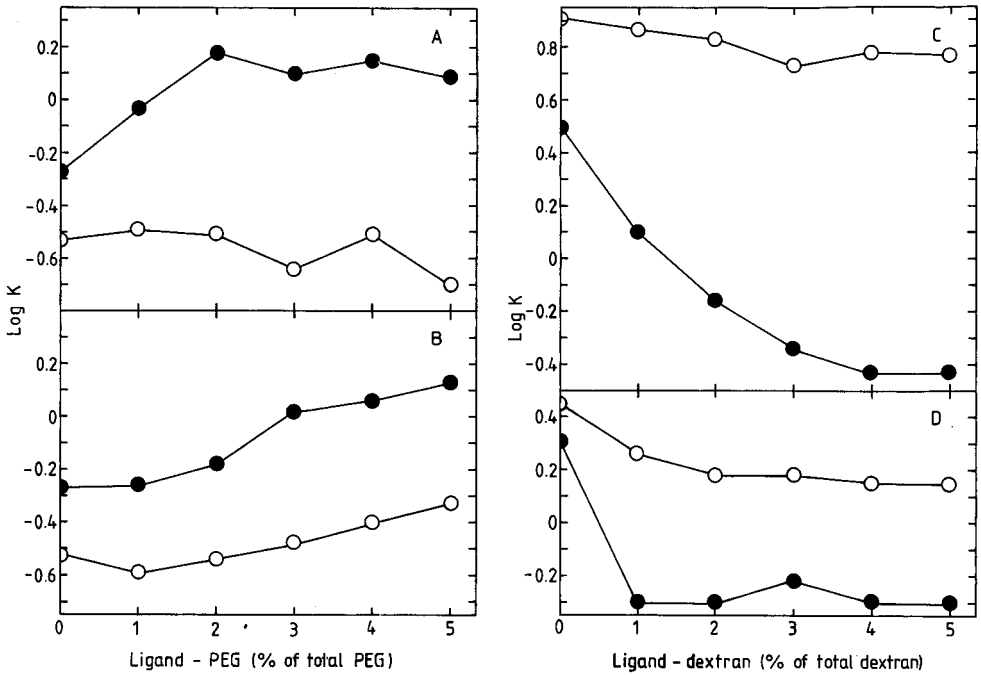
Fig. 3. Partitioning of phosphoglycerate kinase and total protein from spinach leaf extract as a function of the concentration of ligand–polymer derivative. System: 8% (w/w) dextran–6% (w/w) PEG–buffer as indicated (pH 7.5)–0.1 mM magnesium chloride–0.1 mM Na$_2$EDTA–1 mM 2-mercaptoethanol–leaf extract. The measured activities were corrected for the inhibitory effect caused by the polymer ligands. Temperature: 4 $\pm$ 1°C. Buffer: (A and B) 25 mM sodium phosphate; (C) 50 mM tetrabutylammonium phosphate; (D) 25 mM tetrabutylammonium phosphate. Derivatives: (A) ATP–PEG; (B) Procion Turquoise–PEG; (C) ATP–dextran; (D) Procion Turquoise–dextran. Curves: ●, phosphoglycerate kinase; ○, total protein.

increases linearly between 25 and 40% (w/w) PEG. At a PEG concentration of 30% (w/w), 55% of the total protein and less than 15% of phosphoglycerate kinase are precipitated.

Purification of phosphoglycerate kinase from chloroplasts

Using the data presented in Figs. 2–5, a procedure for the extraction of phosphoglycerate kinase from crude chloroplast extract was designed. The procedure, summarized in Table I and Fig. 6, involves three main steps: precipitation with PEG, affinity partitioning with dextran-bound ATP and ion-exchange chromatography. The main function of the last step is to remove the polymers (mainly dextran) from the extracted protein. The final preparation is 80% pure as judged by scanning of a SDS-polyacrylamide gel (Fig. 6B) and its specific activity. The molecular weight was determined to be 46 000 $\pm$ 1000, which is identical with the value reported by Kuntz and Krietsch[4]. The decrease in yield after the final ion-exchange treatment may be explained by the removal of the polymers, which are known to increase enzyme activity[15]. A final recovery of more than 100% has been explained by the presence of tannin-like substances that act as phosphoglycerate kinase inhibitors when the starting
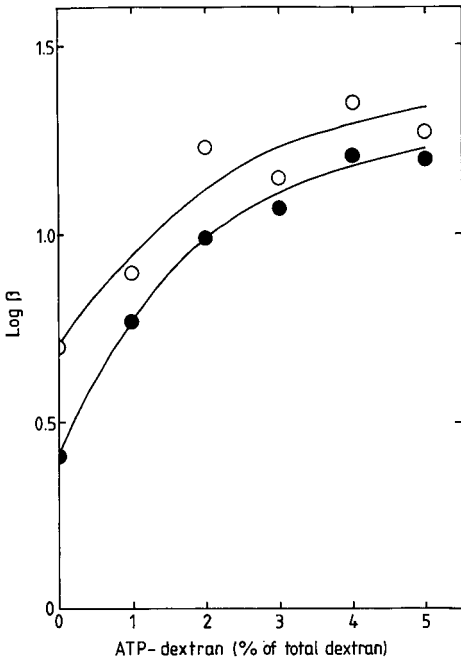
Fig. 4. Partitioning of extracts from spinach leaf and chloroplasts as a function of the concentration of ATP–dextran derivative. Experimental conditions as in Fig. 3. β = Separation factor = ratio between the partition coefficients of phosphoglycerate kinase and total protein. Curves: ●, leaf extract; ○, chloroplast extract. No statistical calculations were made to determine the best fit.
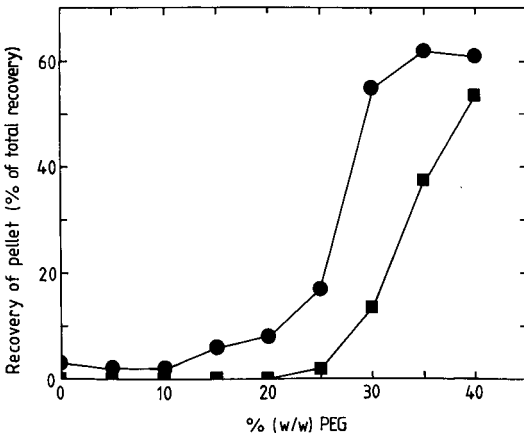
Fig. 5. Precipitation of phosphoglycerate kinase and total protein in spinach chloroplast extract by PEG. Temperature: 4 ± 1°C. Curves: ■, phosphoglycerate kinase; ●, total protein.

TABLE I

PURIFICATION OF CHLOROPLAST PHOSPHOGLYCERATE KINASE FROM 300 g OF DERIBBED SPINACH LEAVES

Experimental conditions as described under Experimental. U = units of phosphoglycerate kinase activity defined as the amount of enzyme phosphorylating 1 μmol/min of 3-phosphoglycerate at 25°C.

Fraction	Volume (ml)	Total protein (mg)	Total apparent activity (U)
Chloroplast (stroma) extract	13.5	198	123
30% (w/w) PEG supernatant	14.7	15	589*
Affinity partitioning:			
First lower phase	46	3.2	540*
Second, washed lower phase	38	0.8	467*
DEAE-Sephadex A-50 eluate	6	0.4	136**

  * Greater than the initial value because of enhancing effect of polymers on enzyme activity.
  ** Increase over the initial value because of removal of inhibitory (tannin-like) substances.
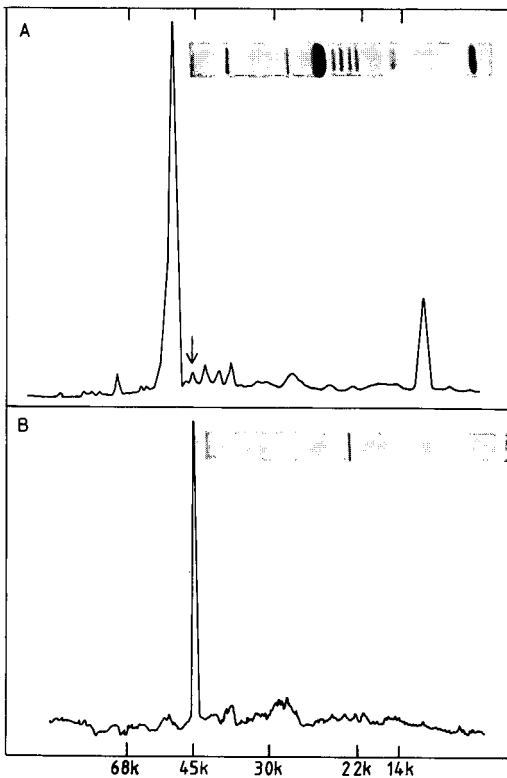
Fig. 6. Polypeptide pattern obtained by SDS-polyacrylamide gel electrophoresis, stained with Coomassie Brilliant Blue R and analysed by photometric scanning. Molecular weights ($\times$ 1000) are indicated. (A) Chloroplast (stroma) extract, band corresponding to phosphoglycerate kinase indicated by arrow; (B) DEAE-Sephadex A-50 eluate.

material was spinach leaf extract[4]. If these substances were present in the spinach chloroplast extract, they were then removed during the affinity partitioning and the final ion-exchange treatment.

The results obtained in this work demonstrate that ATP bound to dextran and PEG can be used for enzyme purification from crude extracts using affinity partitioning. They also show that suitable two-phase systems for preparative extraction can be designed. Determination of extraction curves, such as those in Figs. 3 and 4, in combination with analysis of the influence of the ligand–polymer derivative on the activity of the target enzyme (Fig. 1), is a fruitful strategy in formulating a two-phase system for the extraction. The last, and most time-consuming, step in the extraction procedure is the ion-exchange step, which can also be carried out as a batch procedure. The time for this three-step procedure can be considerably reduced by using centrifugal techniques for the separation of the phases and removal of the ion exchanger. The capacity can be increased many times by using suitable centrifugal separators. It is likely that the described procedure for coupling of ATP to the polymers could be adapted for other nucleotides[16], which will further increase the range of suitable target enzymes for purification.

ACKNOWLEDGEMENTS

REFERENCES

1 G. Johansson, in H. Walter, D. E. Brooks and D. Fischer (Editors), *Partitioning in Aqueous Two-Phase Systems*, Academic Press, New York, 1985, Ch. 6.
2 G. Johansson, *Methods Enzymol.*, 104 (1984) 356.
3 G. W. K. Kuntz, S. Eber, W. Kessler, H. Krietsch and W. K. G. Krietsch, *Eur. J. Biochem.*, 85 (1978) 493.
4 G. W. K. Kuntz and W. K. G. Krietsch, *Methods Enzymol.*, 90 (1982) 103.
5 P. D. G. Dean and D. H. Watson, *J. Chromatogr.*, 165 (1979) 301.
6 L.-O. Persson, *Photosynth. Res.*, 15 (1988) 57.
7 H. U. Bergmeyer, *Methoden der Enzymatischen Analyse*, Vol. II, Verlag Chemie, Weinheim/Bergstrasse, 2nd ed., 1970, p. 2021.
8 H. U. Bergmeyer, *Methoden der Enzymatischen Analyse*, Vol. I, Verlag Chemie, Weinheim/Bergstrasse, 2nd ed., 1970, p. 489.
9 K. Nilsson and K. Mosbach, *Biochem. Biophys. Res. Commun.*, 102 (1981) 449.
10 G. Johansson and M. Andersson, *J. Chromatogr.*, 303 (1984) 39.
11 M. M. Bradford, *Anal. Biochem.*, 72 (1976) 248.
12 G. Johansson and M. Joelsson, *Enzyme Microb. Technol.*, 7 (1985) 629.
13 G. Johansson and M. Joelsson, *J. Chromatogr.*, 393 (1987) 195.
14 G. Johansson and M. Andersson, *J. Chromatogr.*, 291 (1984) 175.
15 V. Jancsik, T. Keleti, G. Y. Biczok, M. Nagy, Z. Szabo and E. Wolfram, *J. Mol. Catal.*, 1 (1975/76) 137.
16 M. Wilchek and R. Lamed, *Methods Enzymol.*, 34 (1974) 475.

CHROM. 20 889

AFFINITY CHROMATOGRAPHY WITH TRIAZINE DYES IMMOBILIZED ONTO ACTIVATED NON-POROUS MONODISPERSE SILICAS

B. ANSPACH and K. K. UNGER

Institut für Anorganische Chemie und Analytische Chemie, Johannes Gutenberg-Universität, D-6500 Mainz (F.R.G.)

and

J. DAVIES and M. T. W. HEARN*

Department of Biochemistry, Monash University, Clayton, Victoria 3168 (Australia)

(Received August 8th, 1988)

SUMMARY

Non-porous monodisperse silicas with a particle diameter of 2.1 μm were modified with different silanes for immobilization of various triazine dyes including Procion Red HE3B, Procion Red MX5B, and Cibacron Blue F3GA. Lactate dehydrogenase and malate dehydrogenase from different species and aldehyde reductase from rat brain were purified by affinity elution using the substrate of the enzyme and NADH. With Cibacron Blue F3GA the selectivity for NADH-dependent enzymes was higher than with the two Procion dyes. The utility of these immobilized triazine dye systems on non-porous silica supports for the rapid separation of Cohn Fraction III plasma proteins, including plasminogen, is also described.

INTRODUCTION

Biospecific and biomimetic affinity chromatography are well known techniques for the purification of biopolymes. The high selectivity of the stationary phase for a single component, or a class of related components with similar ligand binding properties, is one of the characteristics of this method. In recent years there has been a pronounced trend to utilize mechanical stable matrices such as chemically modified silicas in place of the conventional soft polymer gel systems in most areas of affinity chromatography. For example, affinity adsorbents based on porous microparticulate silica have been successfully applied in the high-performance liquid affinity chromatographic purification and analysis of a variety of biologically active substances including serine proteases[1], oxidoreductases[2], lectins[3] and immunoglobulins[4]. Improvement in separation speed has been achieved with these silica based affinity media over conventional soft gel affinity media. However, the enhancement in separation performance is typically not as high as with chemically modified porous silicas in the bioaffinity mode as seen with, for example, the corresponding reversed-phase mode[5]. Several factors underlie this observation. First, chemical modification of silicas

used as affinity media in isolation of biomolecules can represent a level of technical difficulty not experienced with soft gel matrices[6]. Porous silica matrices, in common with their soft gel counterparts are often very heterogeneous with poorly defined surface compositional characteristics, and exhibit polydispersity in terms of particle size and pore size distribution. These effects can cause low mass recoveries in the separation process with concomitant effects on the bioactivity. Furthermore, the kinetics of the adsorption and desorption of the affinity complex can be a very slow process with all porous media due to resistance to mass transfer effects in the intraparticulate boundary and pore. These effects are manifested as a dependency of peak dispersion and peak capacity of the analytes on the pore size of the base materials[7]. These effects are most noticeable when using silicas with pore diameters from 6 to 50 nm as the parent matrices for the biospecific affinity separation of large proteins and can result in significantly tailed peaks[4]. This problem is still apparent with porous particles of less than 10 μm and has been attributed to kinetic effects associated with diffusion of solute molecules into the pores of the silica.

Phillips *et al.*[8] have described the use of non-porous glass beads with particle diameter > 10 μm to eliminate the diffusional effects due to the pore structure. In 1984 we have described[9] a new support material based on 1.5 μm non-porous monodisperse silica beads which exhibited many characteristics of a very efficient stationary phase for use in high-performance liquid chromatography (HPLC). Decreasing particle diameters from 10 μm to 1.5 μm or to smaller values increases the geometrical surface area within a unit column. From both theoretical and practical considerations non-porous particles of small particle diameter should thus have advantages especially for very rapid analytical and micropreparative affinity chromatography[9,10]. In this paper we describe the use of 2.1 μm non-porous silica using immobilized triazine dyes as affinity adsorbents in the fractionation of several enzymes present in biological extracts.

EXPERIMENTAL

Materials

The chromatographic matrix was a non-porous, monodisperse silica with 2.1 μm particle size previously developed in our laboratories. These silica particles are commercially available from E. Merck (Darmstadt, F.R.G.) under the tradename Monospher. The surface area of this silica matrix is 2.5 m^2 g^{-1} calculated with the BET III equation using nitrogen as adsorbate[11]. This value is higher than the theoretically calculated geometrical surface area (1.38 m^2 g^{-1}) assuming a true solid density of 2.2 g ml^{-1}. The concentration of silanol groups on the surface is *ca.* 8 μmol m^{-2} evaluated by the method from Holík and Matéjková[12] using ^{1}H NMR spectroscopy.

Chemicals

3-Aminopropyltriethoxysilane (APS) and 3-mercaptopropyltrimethoxysilane (MPS) were obtained from ECA (Steinheim, F.R.G.). Glycidoxypropyltrimethoxy-silane (Glymo) was obtained from Ventron. Procion Red MX5B and Procion Red HE3B were a gift from ICI (Melbourne, Australia). Cibacron Blue F3GA was obtained from Serva (Heidelberg, F.R.G.). Rabbit muscle dehydrogenase, strepto-kinase and pig heart malate dehydrogenase, lithium lactate, oxalacetate, sodium

malate, sodium pyruvate, NAD, NADH, and NADPH were obtained from Sigma (Sydney, Australia). Cohn Fraction III from human blood was a gift from the Commonwealth Serum Laboratories (Melbourne, Australia).

Preparation of activated silicas

All silicas were dehydrated and activated under reduced pressure at 10 Pa and 433 K for 12 h. The reaction procedure was carried out after cooling the silica to room temperature. In case of derivatisation of the silica in toluene, dry (sodium wire) and freshly distilled solvent was added to the silica under vacuum, in order to allow the solvent to wet completely the surface structure of the non-porous particles. In the case of chemical derivatisation of the silica in water, the suspension was held under vacuum (10 Pa) and sonicated in order to achieve solvent penetation of the surface. The silane was added to the suspension and the reaction carried out as described below.

Aminopropyl-silica. 0.19 g 3-aminopropyltriethoxysilane was added to 20 g silica suspended in 80 ml toluene. The reaction mixture was heated under reflux for 24 h under anhydrous conditions. The modified silica was suspended and centrifuged (8000 *g*) several times in toluene and then in chloroform in order to remove reaction components. The derivatised silica was stored under anhydrous conditions until used.

Diol-silica. An amount of 0.42 g glycidoxypropyltrimethoxysilane was added to 20 g silica suspended in 80 ml water pH 3.5 (adjusted with 0.1 *M* nitric acid). The reaction vessel was evacuated to 10 Pa, sonicated in an ultrasonic bath for 10 min and then heated to 363 K for 3 h with stirring essentially as described by Regnier and Noel[13]. After cooling, the derivatised silica suspension was neutralized by suspension in water and centrifuged (8000 *g*) several times. Subsequently the diol-silica was suspended and centrifuged 3 times in toluene and chloroform, in that order.

Mercaptopropyl-silica. An amount of 0.34 g 3-mercaptopropyltrimethoxysilane was added to 20 g silica suspended in 80 ml water pH 3.5 (adjusted with 0.1 *M* nitric acid). The reaction conditions and washing procedure were the same as described above.

Immobilization of triazine dyes

The modified silicas with immobilized diol-, mercapto-, or amino-group functionalities were suspended in 100 m*M* sodium carbonate, pH 8, containing the triazine dye according to a procedure described by Small *et al.*[14] for agarose based gels. The reaction was carried out at both 295 K and 333 K. The immobilized dye matrices were washed by centrifugation in an Eppendorf centrifuge and suspended in 50 m*M* sodium phosphate pH 7.0 several times until the washing supernatants were colorless.

Preparation of cell-free rat brain extracts

This extract was prepared by homogenization of rat brain, followed by centrifugation of the homogenate at 100 000 *g* for 1 h. The supernatant was then subjected to fractionation with solid ammonium sulphate to a final concentration of 4.5 *M* at 277 K. Resolved fractions were dialysed overnight against 10 m*M* sodium phosphate pH 8.0 at 277 K. Insoluble proteins were removed prior to injection by filtration through 0.22 μm sterile filters. The protein concentration in the soluble fractions was ca. 2 mg ml^{-1} as determined by UV adsorption at 280 nm. The solution was injected on the column without further preparation.

Preparation of Cohn III solution

An amount of 100 mg freeze dried Cohn Fraction III was dissolved in 2 ml 0.1 *M* sodium phosphate pH 7.0, centrifuged at 10 000 *g* and filtered through a 0.22-μm filter. This solution was diluted 10 times to a final concentration of about 2 mg ml^{-1} protein with 10 m*M* sodium phosphate (5 ml), in order to decrease the salt concentration prior to loading directly onto the dye affinity columns.

Lactate dehydrogenase (LDH) assay[15]

The reacion mixture contained the following reagents in a total volume of 3 ml: 2.83 ml 0.1 *M* sodium phosphate pH 7.0, 0.1 ml sodium pyruvate (2.5 mg ml^{-1}), 0.05 ml sodium NADH (10 mg ml^{-1}), 0.02 ml of the enzyme diluted in the buffer. The reaction was initiated by the addition of the enzyme solution to the cuvette and monitored continuously at 340 nm at room temperature using a Varian UV spectrophotometer.

Malate dehydrogenase (MDH) assay[15]

The reaction mixture contained the reagents following in a total volume of 3 ml: 2.83 ml 0.1 *M* sodium phosphate pH 7.5, 0.1 ml oxalacetate (2 mg ml^{-1}), 0.05 ml sodium NADH (10 mg ml^{-1}), 0.02 ml of the enzyme diluted in the buffer. The reaction was initiated as described above for the LDH assay and monitored at the same conditions.

Aldehyde reductase assay

The assay for aldehyde reductase was based on the method described by Turner and Hryszko[16]. In brief, 2.5 mg NADPH and 3.85 mg pyridine-3-aldehyde were dissolved in 20 ml 0.1 *M* sodium phosphate, pH 7.2. The reaction was initiated by adding 0.03 ml of control or test samples to 2.97 ml of the mixture described above and monitored at room temperature at 340 nm using a Varian UV spectrophotometer.

Thrombin, kallikrein and plasminogen microassay

Assays for these enzyme activities were performed at 310 K in 50 m*M* Tris–HCl, 50 m*M* sodium chloride, pH 7.5. The chromogenic substrates S 2238, S 2302, and S 2251 (Kabi Vitrum, Stockholm, Sweden) were used to measure thrombin, kallikrein and plasminogen activities respectively[17]. Assays were carried out as a microassay technique, using procedures developed in these laboratories[18], in microtitre plates with 25 μl sample, 25 μl of 1 m*M* substrate solution and 50 μl of buffer. In the case of the plasminogen assay 5 μl of Streptokinase (10 000 units ml^{-1}) and 45 μl of buffer were added to 25 μl of sample and incubated for 10 min in order to activate the plasminogen. Substrate was added to initiate the reaction. The rate of *p*-nitroaniline release was determined by measuring the change in optical absorbance at 405 nm (A_{405}) using a Titretech Multiscan reader.

Chromatographic procedures

Chromatographic and column packing was carried out using a Beckman 344 HPLC system. All triazine immobilized silicas were packed into stainless-steel columns (40 mm × 6 mm I.D.) containing sintered metal frits with 0.5 μm pore sizes. The columns were filled using the downward slurry technique in 2-propanol–toluene (2:3,

v/v) at constant flow-rate. During column packing the maximum pressure reached was 40 MPa. All columns were equilibrated in 10 mM sodium phosphate, pH 7.0, containing 0.5 M sodium chloride. To avoid the possibility of protein adsorption on the stainless-steel frits, the column surface and the affinity silica matrix, a solution of bovine serum albumin (BSA) (1 mg ml^{-1}) in buffer, pH 7.0, was continuously pumped through the column overnight in order to saturate these binding sites.

On-line monitoring of enzyme activities

When specific elution was carried out with substrate and cofactor, enzyme elution was monitored at 340 nm. An increase in absorbance at 340 nm indicated the presence of the eluted enzyme due to the conversion of NADH to NAD.

RESULTS

Three different reactive dyes (Procion Red HE3B, Procion Red MX5B and Cibacron Blue F3GA) were immobilized onto 2.1 μm non-porous silica chemically modified with either APS, MPS or diol ligands. To examine the influence of temperature on dye immobilization, parallel coupling reactions were carried out at 296 K and 333 K. A porous silica phase, the Merck Si 60 diol with a particle size of 20–30 μm, was used to compare the immobilization yields and binding capacities of porous and non-porous supports. The amount of silica-based immobilized dye of stationary phases with nominally equivalent surface area per ml gel (2.5 m^2 g^{-1}) was estimated by measuring the UV absorption at 615 nm for Cibacron Blue F3GA and 546 nm for the Procion Red dyes before and after coupling to the activated silica supports. Measured ligand densities were higher when the reaction was carried out at 333 K rather than 295 K. All subsequent immobilization procedures for the chromatographic matrices were carried out at the higher temperature. Ligand content was highest with the APS-modified silica (Table I). However, the dye–silica linkage was not stable and continuous leaching of dyes from the column occurred when using the APS-modified silica support. Low ligand densities were observed when dyes were immobilized to the diol-modified silica (Table I). Similar results were obtained when using commercially available Merck diol-silica Si 60 and dye immobilization procedures described in the

TABLE I

AMOUNT OF DYES BOUND AT 333 K TO NON-POROUS SILICAS WITH DIFFERENT FUNCTIONALITIES

Functionality	Procion Red MX5B ($\mu g\ ml^{-1}$)	Procion Red HE3B ($\mu g\ ml^{-1}$)
Aminopropyl –(CH$_2$)$_3$–NH$_2$	1200	920
Mercaptopropyl –(CH$_2$)$_3$–SH	630	300
Diol –(CH$_2$)$_3$–CH$_2$–CH–CH$_2$		OH OH	< 100	< 100

experimental section of this paper or the immobilization procedure of Small *et al.*[14]. This finding was surprising since it is not concordant with the reported observations of the Lund workers. Immobilization of dye to MPS-modified silicas resulted in a stable dye–silica linkage with no leaching of dye evident after washing with 2500 column volumes of buffer (10 mM sodium phosphate, 500 mM sodium chloride, pH 7.2). All studies described below were consequently done using dye immobilized to MPS-modified silicas.

From preliminary experiments it was apparent that careful selection of the equilibration buffer (10 mM sodium phosphate pH 8.0) was necessary for the retention of the dehydrogenases LDH and MDH to the dye affinity supports. With buffers at or below pH 7.0, non-specific interaction between most proteins from the tissue extract and the immobilized dyes was evident. In these lower pH cases these proteins were indiscriminately bound in the adsorption step. Furthermore the amount of adsorbed enzyme was very sensitive to changes in salt concentration of the loading buffer. Salt concentration, larger than 20 mM at pH 8.0 decreased the amount of bound enzyme. Sensitivity of sample loadability to changing salt concentration has previously been shown to be much less responsive with porous particles of surface areas $> 50 \text{ m}^2 \text{ g}^{-1}$ and lower pore diameter. The sensitivity of loadability to varying salt concentrations reflects the relatively low association constants of the solute–dye affinity complexes compared to other protein ligand affinity complexes[19].

Using partial purified enzyme fractions, rabbit muscle LDH and pig heart MDH
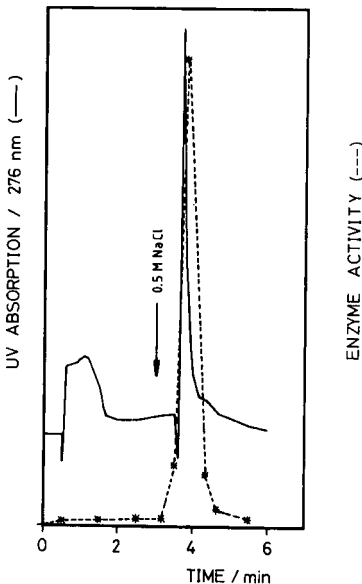
Fig. 1. Elution of rabbit muscle lactate dehydrogenase (LDH) on Procion Red MX5B immobilized on non-porous silica. Injection volume, 1 ml; sample concentration, 40 μg ml^{-1} in 10 mM sodium phosphate pH 8.0 + 8 mM ammonium sulphate (from storage solution); temperature, ambient, flow-rate, 1 ml min^{-1}; column back pressure, 7.8 MPa; detector, 276 nm; 0.05 a.u.f.s.; eluent (a) 10 mM sodium phosphate pH 8.0 (b) 0.5 M sodium chloride in (a), step gradient as indicated in chromatogram.

both adsorbed to and could be eluted from all three dye columns (Cibacron Blue F3GA, Procion Red HE3B and Procion Red MX5B) using 500 mM sodium chloride (Fig. 1). Specific elution of a mixture of the two enzymes from Cibacron Blue was achieved using 2 mM NADH and 2 mM lactate (LDH) or malate (MDH) in 10 mM phosphate buffer pH 8.0 (Fig. 2) but could not be achieved with NADH alone. This suggests LDH and MDH were bound to Cibacron Blue F3GA at both the substrate and cofactor binding sites[20]. Elution from both the Red dye columns was achieved in the same buffer with 2 mM NADH alone.

Aldehyde reductase, LDH and MDH from rat brain mitochondria all bound strongly to Cibacron Blue F3GA column. Rat brain mitochondrial LDH and MDH could be specifically eluted with 2 mM NADH and 2 mM lactate (LDH) or 2 mM malate (MDH). In particular, aldehyde reductase could be specifically eluted with 2 mM NADPH and 2-pyridine-aldehyde (Fig. 3). Other unrelated proteins adsorbed to the dye columns were eluted using a salt gradient from 0–500 mM sodium chloride. Specific elution of all enzymes could not be achieved from the Procion Red columns under the conditions described above.

Using Procion Red HE3B non-porous silica partial purification of plasminogen was also achieved directly from human Cohn Fraction III (Fig. 4). Most Cohn fraction III proteins did not bind to this matrix and eluted in the breakthrough peak. Plasminogen was bound and eluted with a step gradient of 500 mM sodium chloride. Since Cohn Fraction III contains a number of other protease activities, the binding behaviour of these enzyme activities was monitored using the chromogenic substrates
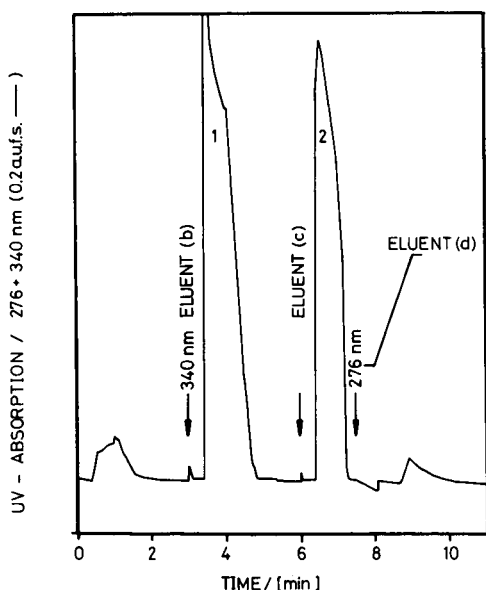
Fig. 2. Affinity elution with substrate and cofactor on Cibacron Blue F3GA immobilized non-porous silica. Injection volume, 1 ml; sample concentration, LDH (40 μg ml^{-1}) MDH (40 μg ml^{-1}) in (a); eluent (a) 10 mM sodium phosphate pH 8.0 (b), 2 mM NADH-Na + 2 mM lactate, (c) 2 mM NADH + 2 mM malate, (d) 0.5 M sodium chloride in (a); temperature, ambient: flow-rate, 1 ml min^{-1}; column back pressure, 8.5 MPa; detector, 276 nm and 340 nm; 0.2 a.u.f.s. as indicated with arrows. (1) LDH activity, (2) MDH activity.
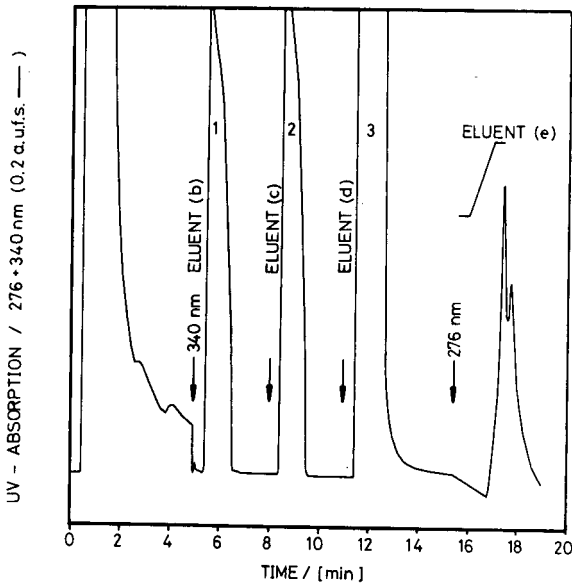
Fig. 3. Affinity elution of LDH, MDH and aldehyde reductase from rat brain mitochondria with substrate and cofactor on Cibacron Blue F3GA immobilized non-porous silica. Injection volume, 1 ml; sample concentration (>2 mg ml^{-1}) in (a); eluent (a) 10 mM sodium phosphate pH 8.0, (b) 2 mM NADH-Na + 2 mM lactate, (c) 2 mM NADH-Na + 2 mM malate, (d) 2 mM NADPH + 2 mM pyridine-3-aldehyde, (e) 0.5 M sodium chloride, eluent b, c, d, e in (a); temperature, ambient; flow-rate, 1 ml min^{-1}; pressure, 8.5 MPa; detector, 276 nm and 340 nm; 0.2 a.u f.s. as indicated with arrows. (1) LDH activity, (2) MDH activity, (3) aldehyde reductase activity.
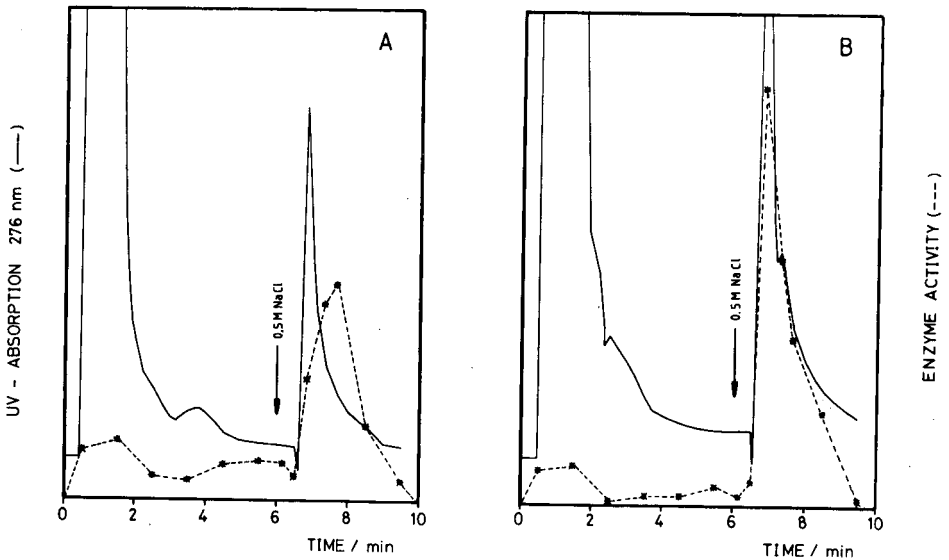
Fig. 4. Elution of plasminogen with a salt gradient on Procion Red HE3B (A) and Cibacron Blue F3GA (B) immobilized on non-porous silica. Injection volume, 1 ml; sample concentration, >2 mg ml^{-1} in 27 mM sodium phosphate pH 7.5; eluents (a) 10 mM sodium phosphate pH 7.5 (b) 0.5 M sodium chloride in (a); temperature, ambient; flow-rate, 1 ml min^{-1}; detector, 276 nm; 0.05 a.u.f.s.

S 2302 (kallikrein like activity) and S 2238 (thrombin like activity). Both these activities were resolved from plasminogen using this system. Higher selectivity of Procion Red HE3B for plasminogen as the silica based matrix was demonstrated and in agreement of previous findings using immobilized Procion Red HE3B-agarose[21]. Resolution of these components using Procion Red MX5B and Cibacron Blue F3GA column was also examined and similar results were obtained.

DISCUSSION

This study documents the use of non-porous monodisperse silica beads in biomimetic affinity chromatography with immobilized reactive dyes. Previously Janzen et al.[22] and Jilge et al.[23] have demonstrated the use of these particles in reversed-phase chromatography and in hydrophobic interaction chromatography. As evident from the present study the low surface area of the 2.1-μm non-porous silica particle is not a critical parameter in micropreparative separation of proteins by biomimetic affinity chromatography. High loadings in the range $>$ 0.6 nmol protein per ml immobilized dye support can in fact be achieved at low salt concentrations (10 mM) in the loading buffer. The necessity for high accessibility of the immobilized ligand is important in case of expensive ligands like monoclonal antibodies and other biospecific or biomimetic ligands. The capacity and stability of these new silica based materials is sufficiently higher to permit very rapid analytical and micropreparative HPLC applications. Despite the small particle size the back pressure of laboratory scale columns is in the normal operational range (8–10 MPa) with the consequence that the current generation of HPLC equipment can handle both the flow-rate and back pressure requirements.

Using the MPS immobilization chemistry introduced in this paper, immobilization of reactive dyes to silica supports can be achieved in a two step procedure. Thus microparticulate non-porous MPS silica can be used to exploit a wide variety of dye selectivities. Such support matrices may find wide applications in the rapid laboratory scale preparation of enzymes from crude extracts or in the monitoring and control of large scale bioprocess purifications involving dye affinity systems.

ACKNOWLEDGEMENTS

REFERENCES

1 H. W. Jarret, J. Chromatogr., 363 (1986) 456–461.
2 E. Cabrera and M. Wilchek, Anal. Biochem., 159 (1986) 267–272.
3 D. Renauer, F. Oesch, J. Kinkel, K. K. Unger and R. J. Wieser, Anal. Biochem., 151(1985) 424–427.
4 S. Ohlson, L. Hansson, P.-O. Larsson and K. Mosbach, FEBS Lett., 93 (1978) 5–9.
5 M. T. W. Hearn and M.-I. Aguilar, in A. Neurberger (Editor), Modern Separation Methods, Elsevier, Amsterdam, 1988, pp. 65–90.

6 R. R. Walters, *Anal. Chem.*, 57 (1985) 1099–1114.

7 R. R. Walters, *J. Chromatogr.*, 249 (1982) 19–28.

8 T. M. Phillips, W. D. Queen, N. S. More and A. M. Thompson, *J. Chromatogr.*, 327 (1985) 213–219.

9 B. Anspach, K. K. Unger, H. Giesche and M. T. W. Hearn, *Paper presented at the 4th International Symposium on HPLC of Proteins, Peptides, and Polynucleotides, Baltimore, MD, December 10–12, 1984*, paper No. 103.

10 K. K. Unger, G. Jilge, J. N. Kinkel and M. T. W. Hearn, *J. Chromatogr.*, 359 (1986) 61.

11 L. G. Joyner, E. B. Weinberger and C. W. Montgomery, *J. Am. Chem. Soc.*, 67 (1945) 2182–2188.

12 M. Holík and B. Matéjková, *J. Chromatogr.*, 213 (1981) 33–39.

13 F. E. Regnier and R. Noel, *J. Chromatogr. Sci.*, 14 (1976) 316.

14 D. A. P. Small, A. Atkinson and C. R. Lowe, *J. Chromatogr.*, 266 (1983) 151–156.

15 H. U. Bergmeyer, M. Grassl and H. E. Walter, in H. U. Bergmeyer (Editor), in *Methods of Enzymatic Analysis, Vol. 2*, Verlag Chemie, Weinheim, 3rd ed., 1983, p. 232 and 246.

16 A. J. Turner and J. Hryszko, *Biochim. Biophys. Acta*, 613 (1980) 256–265.

17 V. V. Kakker (Editor), in *Chromogenic Substrates*, Churchill Livingston, Edinburgh, 1978.

18 J. Davies and M. T. W. Hearn, *Anal. Biochem.*, submitted for publication.

19 R. K. Scopes, *J. Chromatogr.*, 376 (1986) 131–140.

20 J. C. Pearson, S. J. Burton and C. R. Lowe, *Anal. Biochem.*, 158 (1986) 382–389.

21 N. D. Harris and P. G. H. Byfield, *FEBS Lett.*, 103 (1979) 162.

22 R. Janzen, K. K. Unger, H. Giesche and M. T. W. Hearn, *J. Chromatogr.*, 397 (1987) 91–97.

23 G. Jilge, R. Janzen, H. Giesche, K. K. Unger, J. N. Kinkel and M. T. W. Hearn, *J. Chromatogr.*, 397 (1987) 71–80.

CHROM. 20 921

ELUTION BEHAVIOUR OF SOME PROTEINS ON FRESH, ACID- OR BASE-TREATED SEPHACRYL S-200 HR

BO-LENNART JOHANSSON* and JAN GUSTAVSSON

Department of Quality Control, Pharmacia LKB Biotechnology AB, S-751 82 Uppsala (Sweden)

(First received May 5th, 1988; revised manuscript received August 22nd, 1988)

SUMMARY

The influence of sodium chloride concentration and the pH of the mobile phase on the distribution coefficient of proteins with different pI values was studied on Sephacryl® S-200 HR. The non-size-related behaviour of this gel filtration packing is mainly attributed to small amounts of groups that are negatively charged within the pH range investigated (4.2–10.0). These anionic groups on the packing gave rise to ion-exchange or ion-exclusion interactions depending on the charge characteristics of the protein. Hydrophobic interactions at high ionic strength and intramolecular electrostatic repulsive interactions at low ionic strength were also observed for some proteins.

The chemical stability of Sephacryl S-200 HR was studied by comparing the chromatographic results with Sephacryl S-200 HR that had been treated in acidic or basic solutions with those with fresh Sephacryl. After Sephacryl S-200 HR had been stored for 2 weeks in 0.10 M sodium hydroxide the chromatographic results at low ionic strengths clearly showed that groups that are positively charged at pH 4.2 had been formed. However, storage for 2 weeks in 0.01 M hydrochloric acid did not change the chromatographic behaviour of the proteins from that observed when injected on fresh Sephacryl S-200 HR.

INTRODUCTION

Gel filtration chromatography (GFC) has been used for a long time for the characterization and separation of water-soluble biopolymers[1–3]. In an ideal GFC system molecules are separated on the basis of molecular size[4]. However, other retention mechanisms are also associated with GFC, resulting in non-size-related separation effects[5]. Therefore, to develop reliable GFC methods it is important to understand and document these effects.

Recently, an improved cross-linked copolymer of allyldextran and N,N′-methylenediacrylamide for GFC has become commercially available under the trade-name Sephacryl® S-200 HR. The purpose of this study was to interpret the chromatographic results obtained with this gel under different elution conditions for a number of proteins. Also, the separation characteristics of Sephacryl S-200 HR were studied

after it has been treated for 2 weeks with 0.10 M sodium hydroxide or 0.010 M hydrochloric acid.

EXPERIMENTAL

Equipment

Chromatographic measurements were carried out with a Pharmacia FPLC system consisting of an LCC-500 control unit, two P-500 high-precision pumps, a UV-1 UV monitor (280 nm, HR 10 cell), an MV-7 sample injector with a 500-μl loop, an MV-8 sample holder, a P-1 peristaltic pump and an REC-481 recorder. Sephacryl S-200 HR was packed in Pharmacia K 26/40 columns (40 cm × 2.6 cm I.D.) according to the packing instructions for the gel.

Reagents

The mobile phase buffers were prepared from sodium acetate and acetic acid (pH 4.2), sodium dihydrogenphosphate and disodium hydrogenphosphate (pH 7.0) or sodium hydrogencarbonate and disodium carbonate (pH 10.0). The buffers were prepared from 0.020 M stock solutions of these acid and base components. Variation of the ionic strength was obtained by addition of sodium chloride to the stock solutions. The aqueous ethylene glycol buffer solutions contained 20% (v/v) ethylene glycol. The pH readings for these buffers were taken in the aqueous ethylene glycol buffer solution with a pH meter standardized against aqueous buffer solutions. The proteins used are listed in Table I. These proteins were dissolved in the mobile phase at a concentration of *ca.* 2 mg/ml.

Treatment of Sephacryl S-200 HR

To study the chemical stability of Sephacryl S-200 HR, the gel (about 300 ml) was stored for 15 days in 0.010 M hydrochloric acid or in 0.10 M sodium hydroxide. The temperature at these tests was controlled by the ambient temperature (*ca.* 20°C). Before the gel was incubated it was washed with 3 l of the storage solution. The two treated gel samples were packed in K 26/40 columns and the chromatographic behaviour of the acid- and base-treated gel was compared with that of a column packed with fresh Sephacryl S-200 HR.

TABLE I

PHYSICAL PROPERTIES OF THE PROTEINS USED IN THE RETENTION MAPPING STUDY

Protein	Source	Molecular weight	Isoelectric point (pI)
Pepsin	Porcine stomach	33 000	2.9
Bovine serum albumin	Bovine	69 000	4.98, 5.07, 5.18
Transferrin	Human	76 500	5.5
Myoglobin	Horse heart	17 500	6.9, 7.3
α-Chymotrypsinogen A	Bovine pancrease	25 000	8.7, 8.8
Lysozyme	Egg white	13 930	11

Chromatographic procedure

The columns were conditioned by the passage of at least five bed volumes of mobile phase before being used for experimental observations. The chromatographic runs were performed by individual injections of the proteins on the column to avoid interactions between proteins. The flow-rate was 1.5 ml/min and 500 μl of the protein samples were injected. The resulting retention volumes were then used to calculate the distribution coefficient (K_{av}) from the equation

$$K_{av} = (V_e - V_o) / (V_c - V_o)$$

where V_e, V_o and V_c are the solute elution volume, void volume and the total bed volume of fluid and gel combined, respectively. Blue Dextran 2000 was employed as a marker of the void volume. V_o was determined for all ionic strengths investigated at pH 7.0 and 10.0.

RESULTS AND DISCUSSION

It is well known that under certain conditions proteins may deviate from the ideal gel filtration retention mechanism[6-11]. Some of the most important causes of non-size-related separations are (A) hydrophobic, (B) ion-exchange and (C) ion-exclusion interactions between the stationary phase and the sample molecules and (D) intramolecular electrostatic repulsive interactions[12]. Hydrophobic interactions will be favoured if the ionic strength of the mobile phase is increased, whereas at low ionic strength electrostatic interactions (B, C and D) dominate. Ion-exchange or ion-exclusion interactions will be manifested depending on the sign of the net charge on Sephacryl S-200 HR and the proteins. Because proteins are amphoteric, these two interactions can be manipulated by changing the pH of the mobile phase below or above the isoelectric point (pI) of the proteins. To test the extent of interactions A, B and C on Sephacryl S-200 HR, the influence of ionic strength on the K_{av} values of various proteins (Table I) was studied at different pH.

Influence of ionic strength and pH on the chromatographic results with Sephacryl S-200 HR

To stress the non-size-related separation mechanisms caused by electrostatic interactions, the protein probes chosen covered a broad pI range (Table I).

Pepsin. As the pI value of pepsin is 2.9 it will have a net negative charge for all mobile phase buffers investigated. Therefore, the increasing K_{av} value of pepsin with increasing ionic strength (Fig. 1) is interpreted as a decreasing ion-exclusion effect. Accordingly, this interpretation also means that Sephacryl S-200 HR consists of groups that are negatively charged in the pH range 4.2–10.0. As the amount of negative charge on pepsin is reduced as the pH decreases it can be expected that the ion-exclusion effect will also be reduced. Consequently, a higher K_{av} value of pepsin should be obtained with decreasing pH. This trend was also observed (Fig. 1). In addition, the K_{av} value of pepsin is not influenced by the concentration of sodium chloride in the range 0.3–0.5 M at pH 4.2 This plateau probably is an effect of charge shielding and indicates that a pure size separation dominates under these conditions. Any hydrophobic interactions that may contribute to the separation mechanism at pH 4.2 were also investigated but are discussed later.
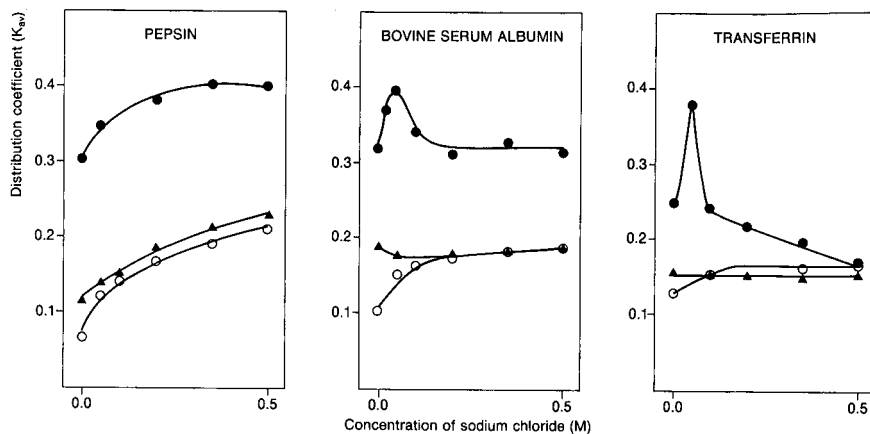
Fig. 1. Influence of sodium chloride concentration on K_{av} of pepsin, bovine serum albumin and transferrin on fresh Sephacryl S-200 HR with various mobile phase buffers. Mobile phase: (●) 0.020 M acetate, pH 4.2; (▲) 0.020 M phosphate, pH 7.0; (○) 0.020 M carbonate, pH 10.0

Bovine serum albumin (BSA). Owing to the higher pI value of BSA (Table I), the ion-exclusion interaction should not influence the retention of BSA to such a great extent as for pepsin. Fig. 1 shows that this interaction is only observed at low ionic strength at pH 10.0. At high ionic strength ([NaCl] > 0.2 M) at pH 10.0 the K_{av} values of BSA merge with the results at pH 7.0 (Fig. 1). Therefore, it can be concluded that this K_{av} plateau (*ca.* 0.18) represents an ideal size separation behaviour. On the other hand, at pH 4.2, where BSA has a positive net charge, the results in Fig. 1 suggest that several separation mechanisms are involved. Ion-exchange between positively charged BSA molecules and anionic groups on Sephacryl S-200 HR explains why K_{av} increases when the sodium chloride concentration decreases from 0.2 to 0.05 M. In addition, an increasing hydrophobic interaction superimposed on a decreasing ion-exchange interaction probably explains the constant K_{av} value of BSA at high ionic strength ([NaCl] > 0.2 M) at pH 4.2 (Fig. 1). Further, it is known that BSA molecules expand in acidic solutions because of intramolecular repulsive interactions[13,14]. As these interactions are most pronounced at low ionic strength, this expansion of BSA can explain the decrease in K_{av} at low concentrations of sodium chloride (0.05–0 M).

Transferrin. Ion exclusion influences the chromatographic behaviour of this protein at pH 10.0 only when the sodium chloride concentration is low ([NaCl] < 0.1 M). At higher ionic strengths the K_{av} value for transferrin coincides with the result at pH 7.0 (Fig. 1). This indicates that the ideal K_{av} value of this protein is about 0.16 on Sephacryl S-200 HR. At pH 4.2 transferrin is positively charged and the gel is negatively charged. Therefore, ion-exchange interactions probably cause the variation in K_{av} with ionic strength (between 0.05 and 0.5 M NaCl) at this pH. The sharp decrease in K_{av} of transferrin at 0 M sodium chloride (Fig. 1) is explained by intramolecular repulsive interactions, in accordance with the interpretation of the results for BSA at low ionic strengths. However, in contrast to BSA, no hydrophobic interactions were observed for transferrin at high ionic strengths.

Myoglobin. The effect of ionic strength on K_{av} of myoglobin at pH 10.0 is
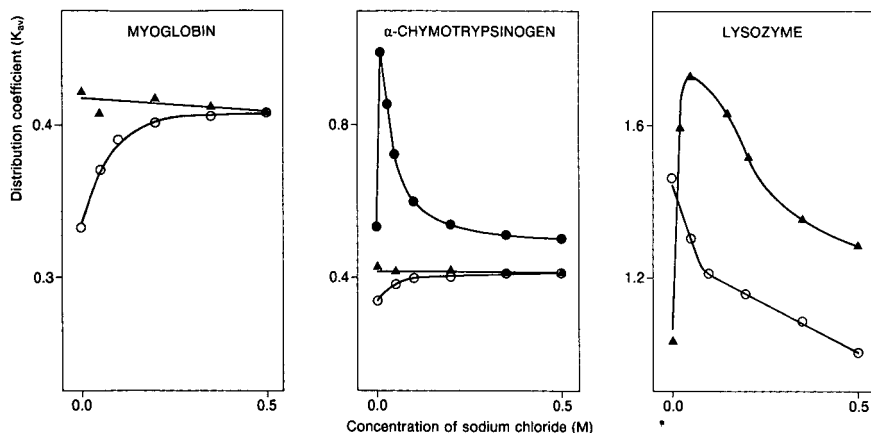
Fig. 2. Influence of sodium chloride concentration on K_{av} of myoglobin, α-chymotrypsinogen and lysozyme on fresh Sephacryl S-200 HR with various mobile phase buffers. Mobile phase: (●) 0.020 M acetate, pH 4.2; (▲) 0.020 M phosphate, pH 7.0; (○) 0.020 M carbonate, pH 10.0

caused by ion-exclusion interactions as for the previously discussed proteins (Figs. 1 and 2). At pH 7.0 no significant trend of the K_{av} of myoglobin was observed (Fig. 2), indicating that only an ideal size separation mechanism determines the retention time. In the acidic mobile phase buffer myoglobin was denatured and precipitated in the column top filter.

Chymotrypsinogen. Chymotrypsinogen shows a general K_{av} trend with all the mobile phase buffers investigated, which is in agreement with the results for serum albumin (Fig. 2). Consequently, as for BSA, four non-size-related separation mechanisms are involved, namely, ion-exclusion, ion-exchange, hydrophobic and intramolecular repulsive electrostatic interactions. The higher amount of positive charge on chymotrypsinogen at pH 4.2 compared with BSA is probably the cause of the greater influence of ion-exchange and intramolecular interactions on K_{av} of chymotrypsinogen at this pH (Fig. 2).

Lysozyme. The high pI value of lysozyme means that this protein has a net positive charge in all the mobile phase buffers used. As Sephacryl S-200 HR contains anionic groups, it can be expected that ion-exchange interactions will influence K_{av} of lysozyme to a great extent. As shown in Fig. 2, the expected increase in K_{av} of lysozyme with decreasing ionic strength was also observed. However, K_{av} was greater than 1 even at 0.5 M sodium chloride at pH 7.0 and 10.0, which suggests that at least one more non-size-related mechanism influenced the retardation of lysozyme. It has been shown[9] that lysozyme has a strong hydrophobic nature. Therefore, we postulate that hydrophobic interactions also contribute to the retardation. This interpretation will be discussed in more detail later. The dominating non-size-related interaction at acidic pH (4.2) is probably an ion-exchange mechanism, which is illustrated by the very high K_{av} values of 2.5, 4.1 and 6.6 at 0.5, 0.2 and 0.1 M sodium chloride, respectively. At low ionic strengths at pH 7.0 K_{av} decreases with decreasing ionic strength. This is probably an effect of intramolecular electrostatic repulsion[6]. Fur-

TABLE II

INFLUENCE OF ETHYLENE GLYCOL ON THE RETARDATION OF PROTEINS ON SEPHA-
CRYL S-200 HR

Protein	Distribution coefficient K_{av}*			
	A_1	A_2	B_1	B_2
Pepsin	0.399	0.361	0.299	n.d.**
Bovine serum albumin	0.326	0.263	0.187	0.203
Transferrin	0.193	n.d.	0.155	0.176
Myoglobin	n.d.	n.d.	0.406	0.483
α-Chymotrypsinogen A	0.509	0.477	0.409	0.452
Lysozyme	3	n.d.	1.29	0.929

   * A_1 = 0.020 M acetate (pH 4.2) and 0.35 M sodium chloride; A_2 = A_1 in 20% (v/v) ethylene
glycol; B_1 = 0.020 M phosphate (pH 7.0) and 0.35 M sodium chloride; B_2 = B_1 in 20% (v/v) ethylene
glycol.
   ** n.d. = not determined.

ther, at pH 4.2 K_{av} of lysozyme decreased from 6.6 to 1.7 when the concentration of
sodium chloride was changed from 0.1 to 0 M. This phenomenon cannot be explained
only by the expansion of the lysozyme molecules. However, if the ion-exchange inter-
action also decreases because of restricted accessibility to the anionic groups on Se-
phacryl S-200 HR when the lysozyme molecules are expanded, the result may be
rationalized.

Influence of ethylene glycol on K_{av} for some proteins
        At high ionic strengths relatively high K_{av} values were observed for BSA and
chymotrypsinogen at pH 4.2 and for lysozyme at pH 10.0 and 7.0 (Figs. 1 and 2). In
order to verify that these high K_{av} values were caused by hydrophobic interactions,
20% (v/v) ethylene glycol was added to the mobile phase. Table II shows that K_{av} of
BSA and chymotrypsinogen at pH 4.2 decreased when ethylene glycol was added.
This behaviour was also observed for lysozyme at pH 7.0 (Table II). These results
support the suggestion that hydrophobic interactions contribute to the retardation of
these proteins. In addition, it was also noted that K_{av} of pepsin at pH 4.2 decreased
after the addition of ethylene glycol. Consequently, the influence of ionic strength on
the retardation of pepsin at pH 4.2 (Fig. 1) can be partly explained by hydrophobic
interactions and not only by ion exclusion (see above).
        Under certain mobile phase conditions it was also observed that K_{av} of some
proteins increased after addition of ethylene glycol. For example, at high ionic
strengths at pH 7.0 BSA, transferrin, myoglobin and chymotrypsinogen behave in
this way (Table II). Therefore, the effect of ethylene glycol on hydrophobic interac-
tions can be confusing. However, more experiments need to be performed in order to
elucidate the mechanism that increases the retardation of some proteins after addition
of an organic modifier.

Chemical stability of Sephacryl S-200 HR at pH 2 and 13
        Chemical structure of Sephacryl. Sephacryl is produced via a polymerization

process between N,N'-methylenediacrylamide and allyldextran[15]. The production procedure means that N,N'-methylenediacrylamide polymerizes to seven-membered ring units or reacts with allyldextran[15-17]. The chromatographic behaviour of the six proteins investigated (Figs. 1 and 2) clearly proves that Sephacryl S-200 HR contains anionic groups. As these groups are charged even at pH 4.2 they must have a pK_a value that is lower than *ca.* 4. It is known that dextran gels (Sephadex) contain small amounts of carboxyl groups[15]. Therefore, it is reasonable to assume that the observed ion-exchange and ion-exclusion interactions are caused by carboxyl groups in the dextran structures of Sephacryl S-200 HR. However, it is also possible that both carboxyl groups and amino groups can be formed because of the cleavage of amide bonds in polymerized N,N'-methylenediacrylamide units in Sephacryl S-200 HR after acid or base treatment.

*Chromatographic behaviour of Sephacryl S-200 HR after treatment at high or low pH.*The chemical stability of Sephacryl S-200 HR was studied by suspending the gel in 0.010 *M* hydrochloric acid or 0.10 *M* sodium hydroxide for 15 days. The stability of the gel was then evaluated by comparing the chromatographic results obtained after the treatment with the chromatographic behaviour of fresh Sephacryl S-200 HR (Figs. 1 and 2). Fig. 3 shows that the chromatographic results (at pH 4.2) from three representative proteins were different, depending on whether the gel had been treated at pH 2 or 13. It can also be noted that the chromatographic results with fresh gel (Figs. 1 and 2) are in agreement with those obtained from the gel that had been treated at pH 2. This indicates that Sephacryl S-200 HR is chemically stable at pH 2.0. However, the increasing K_{av} value of pepsin with decreasing ionic strength (Fig. 3 B) indicates that groups that are positively charged at pH 4.2 are formed on the base-promoted hydrolysis of Sephacryl S-200 HR. These cationic groups that are formed retard pepsin via an ion-exchange mechanism. Conversely, it can be expected that transferrin and chymotrypsinogen, which are positively charged at pH 4.2, should be eluted earlier on base-treated Sephacryl S-200 HR because of ion-exclusion interactions. Accordingly, Fig. 3 shows that the ion-exchange effect observed for
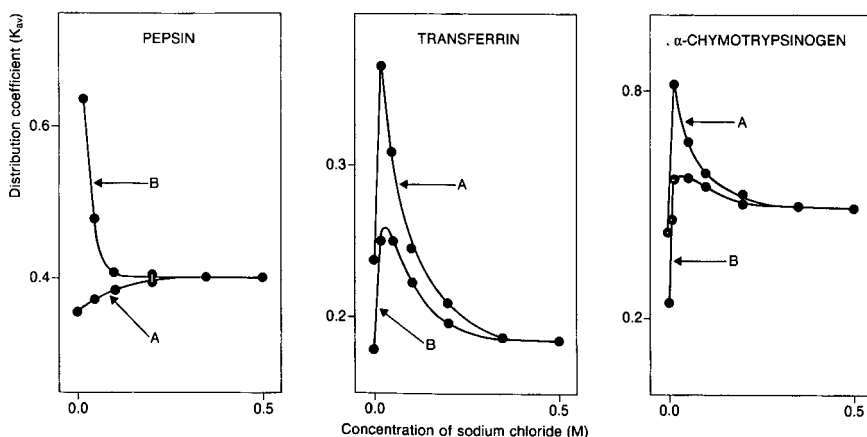
Fig. 3. Influence of sodium chloride concentration on K_{av} of pepsin, transferrin and α-chymotrypsinogen on (A) acid- and (B) base-treated Sephacryl S-200 HR. The mobile phase buffer was 0.020 *M* acetate (pH 4.2).
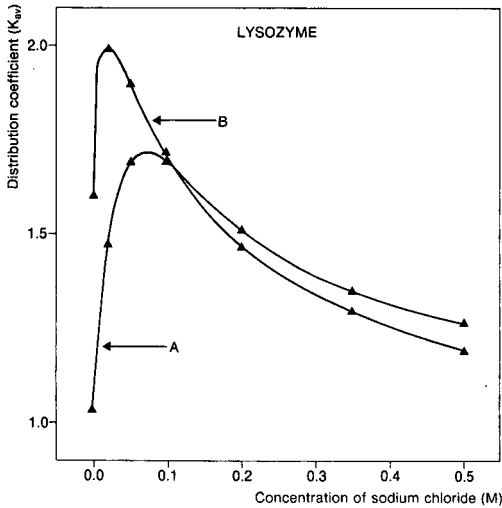
Fig. 4. Influence of sodium chloride concentration on K_{av} of lysozyme on (A) acid- and (B) base-treated Sephacryl S-200 HR. The mobile phase buffer was 0.020 phosphate (pH 7.0).

these proteins on fresh gel at pH 4.2 has decreased considerably on a sodium hydroxide-treated gel because of the counteracting ion-exclusion interactions.

The cationic groups formed on base treatment of Sephacryl S-200 HR only influenced the chromatographic results when an acidic mobile phase was used. This behaviour can probably be related to decreasing ionization of these cationic groups with increasing pH. However, with basic mobile phases one of the proteins investigated, lysozyme, was retarded to a greater extent at low ionic strength when a base-treated gel was used (Fig. 4). This could indicate that also a small amount of anionic groups had been formed during the treatment with 0.10 M sodium hydroxide. As fresh Sephacryl S-200 HR contains anionic groups, a small increase in this amount, as a result of base treatment, may significantly influence the K_{av} of lysozyme, probably because it has the highest net positive charge of the proteins investigated.

CONCLUSIONS

The objective of this work was to examine the interactions of various proteins with the gel filtration packing Sephacryl S-200 HR. From the results obtained it may be concluded that both pH and ionic strength must be carefully optimized in order to eliminate or reduce the non-size-related exclusion separation behaviour. Proteins with intermediate pI values (5–9) seem not to give rise to any interactions with Sephacryl S-200 HR when the pH of the mobile phase is 7.0 or 10 and the sodium chloride concentration is higher than 0.2 M. However, lysozyme (pI = 11) and pepsin (pI = 2.9) interact with the support under all the conditions investigated. Further, as a general rule, protein–support interactions are most dominant at acidic pH (4.2).

REFERENCES

1 J.-C. Jansson, *Chromatographia*, 23 (1987) 361.
2 T. Kremer and L. Boross, *Gel Chromatography, Theory, Methodology, Applications*, Wiley, New York, 1979.
3 L. Fisher, in T. S. Work and R. H. Burdon (Editors), *Laboratory Techniques in Biochemistry and Molecular Biology, Gel Filtration Chromatography*, Elsevier, Amsterdam, 1980, pp. 137–190.
4 L. R. Snyder and J. J. Kirkland, *Introduction to Modern Liquid Chromatography*, Wiley-Interscience, New York, 1979.
5 K. W. Williams, *Lab. Pract.*, 21 (1972) 667.
6 W. Kopaciewicz and F. E. Regnier, *Anal. Biochem.*, 126 (1982) 8.
7 H. Engelhardt and D. Mathes, *Chromatographia*, 14 (1981) 325.
8 H. Engelhardt, G. Ahr and M. T. W. Hearn, *J. Liq. Chromatogr.*, 4 (1981) 1361.
9 D. E. Schmidt, R. W. Giese, D. Conron and B. L. Karger, *Anal. Chem.*, 52 (1980) 177.
10 E. Pfannkoch, K. C. Lu and F. E. Regnier, *J. Chromatogr. Sci.*, 18 (1980) 430.
11 C. L. de Ligny, W. J. Gelsema and A. M. P. Roozen, *J. Chromatogr. Sci.*, 21 (1983) 174.
12 H. G. Barth, *LC Liq. Chromatogr. HPLC Mag.*, 2 (1984) 24.
13 K. Aoki and J. F. Forster, *J. Am. Chem. Soc.*, 79 (1957) 3385.
14 C. Tanford, J. G. Buzzel, D. G. Rands and S. A. Swanson, *J. Am. Chem. Soc.*, 77 (1955) 6421.
15 L. Fisher, in T. S. Work and R. H. Burdon (Editors), *Laboratory Techniques in Biochemistry and Molecular Biology, Gel Filtration Chromatography*, Elsevier, Amsterdam, 1980, pp. 37–38.
16 A. Gopalan, S. Paulrajan and N. R. Subbaratnam, *J. Polym. Sci.*, 23 (1985) 1861.
17 A. Gopalan, S. Paulrajan, K. Venkatarao and N. R. Subbaratnam, *Eur. Polym. J.*, 19 (1983) 817.

PHOSPHORIC ACID-MODIFIED AMINO BONDED STATIONARY PHASE FOR HIGH-PERFORMANCE LIQUID CHROMATOGRAPHIC CHEMICAL CLASS SEPARATION

JOHN W. HAAS, III*, WILLIAM F. JOYCE**, YU-JIING SHYU and PETER C. UDEN*

Department of Chemistry, Lederle GRC, Tower A, University of Massachusetts, Amherst, MA 01003-0035 (U.S.A.)

(Received August 18th, 1988)

SUMMARY

A new stationary phase for high-performance liquid chromatography was produced by reacting a conventional amino bonded phase with phosphoric acid. Characterization of the modified amino phase indicated that ammonium phosphate salt groups and "free" phosphoric acid were present on the stationary phase surface. The column's capability for separating complex sample mixtures into chemical classes was tested using model compounds representing those typically found in fossil fuels. A solvent gradient program was developed which effectively separated hydrocarbon standards into aliphatic, non-polar aromatic, neutral/acidic polar aromatic, and basic polar aromatic classes.

INTRODUCTION

The direct characterization of complex mixtures, such as fossil fuels or other environmental samples, is often difficult even when high-resolution chromatography is combined with universal and selective detection. However, preliminary fractionation of complex mixtures simplifies their analysis and provides partial characterization of the samples. The most effective prefractionation methods are those which separate sample components rapidly and reproducibly into well-defined chemical classes. In the case of fossil fuels, solvent extraction and liquid column chromatography are the prefractionation methods used most often. Extraction procedures have major drawbacks, however; solvent–solvent partition is poorly class selective while acid–base extraction often forms emulsions, polymerizes components, or produces artifacts in samples.

Numerous liquid chromatographic (LC) stationary phases have been used to fractionate fossil fuels and many have been discussed in recent papers[1–6]. Although new bonded phases have often displaced stationary phases such as liquid–solid

---

* Present address: Oak Ridge National Laboratory, Oak Ridge, TN, U.S.A.
** Present address: Stauffer Chemical Corporation, Dobbs Ferry, NY, U.S.A.

chromatography (LSC) adsorbents, coordination chromatography adsorbents, and gel permeation chromatography (GPC) gels, for this application, silica[1,7] and alumina[2,3,8] LSC adsorbents are still widely used. Because of the excellent class selectivity of these materials for compounds of widely ranging polarity, quite extensive fractionation can be achieved in a single chromatographic run. However, primary disadvantages of silica and alumina include poor recovery of some polar species[8] and bioactivity[9], and sensitivity to water in the mobile phase[8]. Varying moisture content impairs reproducibility and increased water levels reduce adsorbent activity such that overlap of chemical classes occurs. An elaborate system for maintaining constant moisture levels in solvents has been constructed[3], but is not generally available. GPC gels are also still used[10,11]; although these materials efficiently separate aliphatic hydrocarbons from aromatics with high sample recovery, they demonstrate little selectivity for polar-substituted aromatic hydrocarbon classes.

Bonded stationary phases are popular for fossil fuel fractionations because they offer improved efficiency, reproducibility, insensitivity to mobile phase moisture content (normal-phase packings), and better recovery of polar compounds and biological activity than LSC adsorbents. Four studies comparing various stationary phases for chemical class separation have been conducted[4,5,12,13]. In the first investigation[12], dimethylamino and tetranitrofluorenone packings used under normal-phase conditions, and octadecylsilane (ODS) and inorganic anion-exchange packings used under reversed-phase conditions, provided the most effective chemical class separations. Nitroaromatic, diol, polyamide, amino, cyano, alumina, silica, octyl, and other ion-exchange columns fractionated the coal liquid sample less efficiently. However, none successfully separated all classes under consideration (saturates, aromatics, neutral heterocycles, acids, and bases). The use of reversed-phase conditions is limited further by solubility problems encountered when aqueous eluents are employed with hydrocarbon based fossil fuel samples.

In the second comparison study[4], a mixed amino/cyano packing resolved saturated, olefinic, aromatic, and polar classes more efficiently than amino, cyano, diol, or phenyl bonded phases. Although this bonded phase has not been fully characterized, other work[14] suggests that resolution between polar compound classes would probably be incomplete.

Nitrophenyl, amino, cyano, and sulfonic acid bonded phases, silica and alumina adsorbents, and a porous styrene–divinylbenzene copolymer phase have been compared[13]. None of the columns could efficiently separate all the chemical classes represented by over 40 model compounds. An interesting observation was the effective separation of polar acidic, polar basic, and non-polar aromatic classes by a sulfonic acid column under normal-phase conditions. However, non-polar aromatic and polar fractions overlapped when shale oil and petroleum samples were chromatographed. Ion-exchange materials must also be prepared and used carefully to avoid artifacts[15]. Despite these limitations, their use for class separations of fossil fuels is increasing[6,15–17].

The fourth study[5], comparing silica, alumina, nitrophenyl, amino, cyano, and ODS columns emphasizing the separation of nitrogen heterocycles and non-polar aromatics, showed silica to be superior. Other studies using tetranitrofluorenone[12] and tetrachlorophthalimide[18] charge-transfer phases also gave incomplete resolution of chemical classes.

The limitations of existing stationary phases encourage the development of new materials, especially normal bonded phases, for class separation of fossil fuels. Recently, we developed a phosphoric acid-modified amino bonded phase for this application[19]. The acidic nature of this packing is promising because acidic silica and cation-exchange columns have provided some of the best class separations. The modified amino bonded phase was used successfully with rapid solvent switching to fractionate shale oils[19]. In the present study, model organic compounds encompassing a wide range of functionalities and polarities have been separated using a continuous solvent gradient, providing a basis for comparison with other prefractionation schemes. The substrate (and a compound modelling it) was characterized by elemental analysis, IR spectrometry, inductively coupled plasma (ICP) spectrometry, and acid–base titration.

EXPERIMENTAL

Reagents

Chemical standards were obtained from Aldrich (Milwaukee, WI, U.S.A.) and Eastman Kodak (Rochester, NY, U.S.A.) and were purified by distillation or recrystallization. HPLC-grade hexane and dichloromethane, 85% phosphoric acid, and silver nitrate (Fisher Scientific, Fair Lawn, NJ, U.S.A.), HPLC-grade isopropanol (J. T. Baker, Phillipsburg, NJ, U.S.A.), n-butylamine (Aldrich), and glacial acetic acid and sodium hydroxide (MCB Manufacturing Chemists, Cincinnati, OH, U.S.A.) were used.

Column preparation

The 10-μm aminopropyl bonded stationary phase (Chromosorb LC-9, Johns Manville, Denver, CO, U.S.A.) was packed into two 25 cm × 4.0 mm stainless-steel columns equipped with zero dead volume fittings. Column packing was in a downward configuration using a constant pressure Haskel Engineering and Supply (Burbank, CA, U.S.A.) Model DST-122 pump operated at 6000 p.s.i.g. Isopropanol was slurry and packing solvent. One of the packed columns was connected to an HPLC pump and 25–30 ml of 1% phosphoric acid in isopropanol were pumped through, followed by 50 ml each of isopropanol and dichloromethane prior to equilibration with hexane. The unmodified amino bonded phase column was washed with 50 ml dichloromethane prior to equilibration with hexane.

HPLC methods

Gradient HPLC was performed with a modular Laboratory Data Control/Milton Roy (Riviera Beach, FL, U.S.A.) liquid chromatograph consisting of Constametric I and II pumps, a Spectromonitor II variable-wavelength UV detector, and a Rheodyne (Cotati, CA, U.S.A.) Model 7125 injector equipped with a 20-μl loop. Various binary solvent gradients employing hexane, or acetic acid in hexane, and isopropanol were evaluated. An IBM Instruments (Wallingford, CT, U.S.A.) Model 9533 instrument (254 nm detection) was used for the ternary solvent studies using hexane, 3.5% acetic acid in hexane, and isopropanol. Standard compounds used to evaluate the various solvent programs were prepared in hexane at concentrations ranging from 1 to 50 μg/ml. Solvent flow-rate was maintained at 2.0 ml/min.

Characterization of the modified amino bonded phase

The product of *n*-butylamine reacted with phosphoric acid was examined as a model system for the modified amino bonded phase. Approximately 5 ml *n*-butylamine was added dropwise to 50 ml of 5% phosphoric acid in isopropanol. A white precipitate formed immediately, was filtered, washed with isopropanol, and dried at 100°C for 48 h. It was insoluble in ethanol, isopropanol, dichloromethane, and hexane but was soluble in methanol and water. The product was also soluble in basic solution (with release of the free amine) and formed yellow silver phosphate on addition of silver nitrate. The original reaction product was further characterized by elemental and IR spectrometric (potassium bromide pellet) analyses.

The modified amino bonded phase was characterized by titration with sodium hydroxide. The sample for titration was produced by stirring a mixture of 1.5 g Chromosorb LC-9 amino-propyl bonded phase in 35 ml of 0.5% phosphoric acid in isopropanol solution for 15 min. The phase was filtered, washed with 2 × 20 ml isopropanol, and dried overnight at 100°C. After drying, 1.0753 g was added to 20 ml distilled, deionized water stirred with a magnetic stirrer in a 100-ml beaker. The solution was titrated with standard 0.03732 M sodium hydroxide solution; pH was measured with a Fisher combination electrode connected to a Corning Glass Works (Corning, NJ, U.S.A.) Model 7 pH meter.

Phosphorus analysis was conducted by ICP spectrometry for comparison with the titration results. A weighed modified amino bonded phase sample (58.4 mg) was placed in a 50-ml volumetric flask. To the sample was added 2 ml concentrated sulfuric acid and 20 drops concentrated nitric acid. The mixture was first warmed gently on a hot plate for 1 h and then heated at maximum hot plate temperature for 2 h. Finally, the digested sample was cooled to room temperature and diluted to 50.00 ml with distilled, deionized water prior to ICP analysis.

RESULTS AND DISCUSSION

Characterization of the modified amino bonded phase

Studies were undertaken to characterize three aspects of the amino bonded phase modification: (1) the nature of the bonding of phosphoric acid to the amino bonded phase; (2) the stoichiometry of the bonding; (3) the quantity of bonded phosphoric acid. It was considered that phosphoric acid reacted with the amino groups of the bonded stationary phase to form either a phosphoramide (eqn. 1) or an amine phosphate salt (eqn. 2).

$$R-NH_2 + H_3PO_4 \rightarrow R-NH-PO(OH)_2 + H_2O \qquad (1)$$

$$R-NH_2 + H_3PO_4 \rightarrow R-NH_3^+ {}^-OPO(OH)_2 \qquad (2)$$
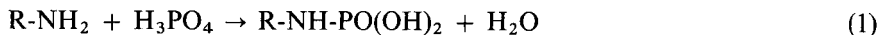
The experiments using *n*-butylamine as a model for the amino bonded phase indicated that the amine phosphate salt was the predominant reaction product. First, phosphoramides are most readily formed from chloro-acids[20] which are more reactive than free phosphoric acid; they decompose readily to amine-phosphate salts in the presence of trace amounts of water[20]. The facile reaction of free phosphoric acid with *n*-butylamine to form a stable product in the presence of water (85% phosphoric acid

was used) therefore suggested formation of a phosphate salt. In addition, the product decomposed in basic solution, producing free n-butylamine and PO_4^{3-}. The amine was confirmed by its odor and gas chromatographic analysis of an diethyl ether extract of the basic solution. The PO_4^{3-} was confirmed by the formation of the silver phosphate salt on addition of a few drops 10% silver nitrate solution. This decomposition is characteristic of amine phosphate salts; phosphoramides, on the other hand, are stable at high pH[20].

Elemental carbon, hydrogen, and nitrogen analyses of the n-butylamine–phosphoric acid reaction product are given in Table I. Comparison with theoretical percentages calculated for phosphoramide and amine phosphate salt products support amine–phosphate salt formation. The IR spectrum was dominated by broad, intense peaks corresponding to strongly hydrogen bonded –OH groups, a feature consistent with either product. However, the conspicuous lack of a P–N stretching band at 850 cm^{-1} and an N–H bending band at 1400 cm^{-1} contraindicated phosphoramide formation. Furthermore, weak bands observed at about 1500 cm^{-1} and 1600 cm^{-1} were within the ranges of N–H bending vibrations of amine phosphate salts.

An amine phosphate salt similar to that obtained with n-butylamine should have been formed when phosphoric acid in isopropanol solution was pumped through the amino bonded phase column. Elemental analysis results for the n-butylamine–phosphoric acid reaction product also demonstrated that each molecule of phosphoric acid reacted with one amino group. However, the possibility that phosphoric acid molecules reacted with two amino groups on the bonded phase was considered. The two reaction products are shown in Fig. 1. In the one-to-one bonding scheme (Fig. 1a), two protons of the triprotic ($pK_1 = 2.12$, $pK_2 = 7.21$, $pK_3 = 12.67$) phosphoric acid remain unbound on the product, whereas in the two-to-one bonding scheme (Fig. 1b) only one proton remains free. The relative contributions of the two reaction products could be determined by base titration of the unbound protons, the predicted titration curves being shown in Fig. 1. In the two-to-one scheme, no equivalence point is expected for the single weakly acidic proton. A single equivalence point is expected for the one-to-one scheme. The weak acidity of the ammonium ion precludes interference from protonated amino bonded phase during the titration.

The experimental titration curve is shown in Fig. 2. Surprisingly, two equivalence points were observed during the titration, one at pH 4.7 and the other at pH 9.7. This indicated that free phosphoric acid (no proton loss) was bound to the stationary phase surface, probably by hydrogen bonding with amino groups, silanol groups, ionically bonded phosphate groups, or combinations of these. However, based upon the volume of titrant used to reach the two equivalence points, it could be concluded

TABLE I

ELEMENTAL ANALYSES (%) OF THE PHOSPHORIC ACID–n-BUTYLAMINE REACTION PRODUCT

Product	C	H	N
Phosphoramide	31.4	7.90	9.15
Amine phosphate salt	28.1	8.25	8.18
Experimental	27.8	8.34	7.96
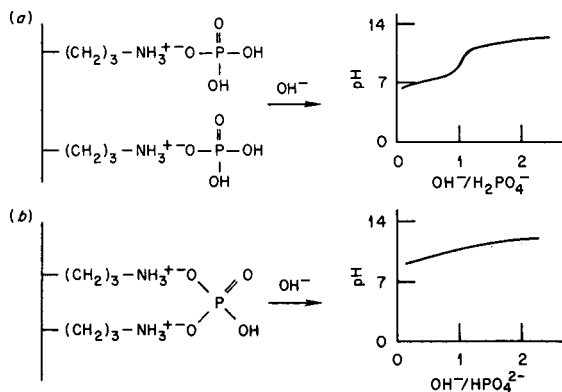
Fig. 1. Possible products of the reaction between phosphoric acid and amino stationary phase groups, and predicted titration curves for the products. (a) One-to-one reaction product, (b) two-to-one reaction product.

that most of the phosphoric acid was bonded to the stationary phase as amine dihydrogenphosphate salt groups (Fig. 1a). The $[H_2PO_4^-]/[H_3PO_4]$ ratio was 2.3:1. Furthermore, the total hydrogen bonded phosphoric acid plus dihydrogenphosphate salt on the stationary phase surface comprised 0.97 mmol phosphorus groups/g bonded phase. Nitrogen content of the original amino bonded phase was 1.38% which corresponded to a loading of 0.99 mmol amino groups/g bonded phase. Assuming that the free phosphoric acid was preferentially hydrogen bonded to amino groups (this assumption is reasonable, considering that the strength of a hydrogen bond is enhanced by acid–base interaction), the coverage of amino groups by phosphoric acid or dihydrogenphosphate was nearly complete (98% maximum coverage) and no appreciable amount of hydrogen phosphate was bonded to amino groups as suggested in Fig. 1b.

ICP spectrometry was used to quantitate directly the amount of phosphoric acid reacted with amino bonded phase groups. The result for a single phosphorus determination was 0.74 mmol phosphorus groups/g bonded phase, which agrees reasonably with the titration result. The lower value obtained by ICP may have been due in part to incomplete digestion of the bonded phase sample.
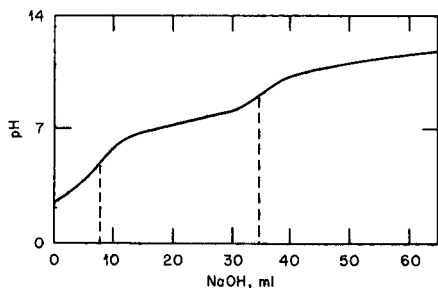
Fig. 2. Experimental titration curve for the product of the reaction between phosphoric acid and amino bonded stationary phase.

HPLC separations

Binary solvent gradients. Initial chromatographic study was directed toward developing effective separation of aromatic hydrocarbon (AH) classes in fossil fuels. These classes included unsubstituted AH, neutral nitrogen-containing AH (neutral NAH), hydroxy-AH (HAH), and basic nitrogen-containing AH (basic NAH) compounds. Overlap between polar compound classes was frequently observed when conventional HPLC stationary phases were employed in prefractionation schemes. A second goal of the preliminary studies was to determine if the extent of phosphoric acid modification was enough to produce separations significantly different from the unmodified amino bonded phase. This was accomplished by direct comparison of modified and unmodified columns.

Using simple hexane–isopropanol gradients, separations using both the modified and unmodified amino bonded phase columns were achieved on the basis of polarity. Polar compound classes were poorly resolved with both columns, as shown in Fig. 3a for the phosphoric acid-modified amino bonded phase. However, the selectivities of the columns for polar compounds were markedly different, confirming
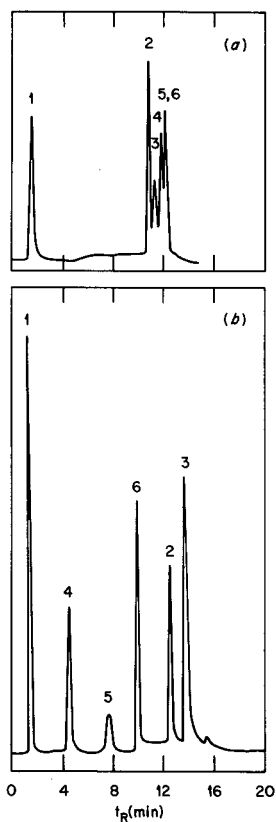
Fig. 3. Separation of model fossil fuel compounds on the phosphoric acid-modified amino bonded phase column. (a) Exponential gradient of 15 min from hexane to isopropanol, (b) 6 min isocratic elution with 5% acetic acid in hexane followed by a 15-min linear gradient to isopropanol. Peak identities: 1 = phenanthrene, 2 = pyridine, 3 = acridine, 4 = carbazole, 5 = phenol, and 6 = 1-naphthol.

that phosphoric acid had modified the amino bonded phase surface considerably. Using the same solvent conditions, acidic compounds such as phenol eluted last from the amino column whereas basic species (*e.g.* pyridine) were preferentially retained on the modified amino column. More subtle selectivity differences were noted for compounds of the same chemical class and will be reported in detail later.

In order to improve separation of the polar classes with the modified amino bonded phase column, glacial acetic acid was added at 5% (v/v) to the hexane mobile phase. The acetic acid displaced neutral NAH and HAH compounds from the column earlier in the gradient while only minimally reducing the retention of basic NAH species (Fig. 3b). Under these conditions, non-polar AH compounds such as phenanthrene eluted first from the column, followed by the displaced neutral NAH and HAH compounds. Basic NAH species eluted last from the modified amino column because of their strong hydrogen bonding interactions with the acidic dihydrogenphosphate and phosphoric acid hydroxyl groups. The separation of neutral and basic NAH classes was better than with an unmodified amino column[21]. The basic amino groups interacted preferentially with phenolic species (as noted above) and the neutral and basic NAH compounds were relatively weakly retained and overlapped.

The amount of acetic acid added to the hexane mobile phase had a pronounced effect on the separation with the modified amino bonded phase. From Table II it is apparent that added acetic acid increased mobile phase strength, capacity factors for all species being reduced. The desired elution sequence was maintained with high acetic acid content (10%), but resolution between classes was lowered significantly. For some samples this could lead to overlap of chemical classes, particularly those eluting early in the gradient. Very low acetic acid content (1.5%) gave inadequately resolved basic NAH (phenanthridine) and HAH (phenol) species, this behavior being similar to that found in the absence of acetic acid. A level of 3.5% acetic acid was chosen for subsequent work because it eluted HAH species before the basic NAH class while maintaining adequate resolution of early eluting compounds.

Ternary solvent gradients. As many complex samples such as synthetic fuels contain high levels of non-polar and moderately polar compounds, it was necessary to weaken the solvent strength at the beginning of the binary solvent gradient in order to separate these species more effectively into chemical classes with the modified amino bonded phase. The results using a ternary solvent program (hexane added to the

TABLE II

EFFECT OF ACETIC ACID CONCENTRATION IN THE HEXANE MOBILE PHASE ON THE RETENTION (k') OF MODEL FOSSIL FUEL COMPOUNDS

Compound	Chemical class	Acetic acid concentration (%)		
		1.5	*5*	*10*
Pentacene	ALH	2.43	1.01	0.58
Carbazole	Neutral NAH	5.04	2.29	0.87
Phenol	HAH	16.4	4.45	1.53
Phenanthridine	Basic NAH	15.5	9.04	3.96

beginning of the binary gradient) and an extensive series of standard compounds covering a wide range of functionalities are shown in Fig. 4 and Table III. Inspection of the early portion of the "elution sequence profile" (Fig. 4) showed that after aliphatic hydrocarbon (ALH) species, which were not retained by the modified amino bonded phase, non-polar AH compounds eluted well before the polar compounds. Included in the non-polar AH fraction were unsubstituted AH, alkylated AH, heterocyclic sulfur AH (SAH), and heterocyclic oxygen AH (OAH) compounds. Within each of these classes, elution was according to the number of fused aromatic rings. This allows for subfractionation of the non-polar aromatic compounds according to ring number, an objective of some previous studies[1,18].

As actic acid in hexane was added to the mobile phase, the moderately polar (very weak hydrogen bonding) AH compounds, including cyano- and nitro-substituted AH species as well as quinones, eluted quickly from the column. They were followed, in turn, by neutral NAH compounds such as carbazoles, indoles, and phenazines. Although the fraction eluting between 25 and 75% of 3.5% acetic acid in hexane was enriched in neutral NAH species, *ortho*-substituted alkyl-HAH compounds also eluted in this fraction because hydrogen bonding with their hydroxyl groups was sterically hindered. Unhindered HAH compounds eluted only after the addition of acetic acid was complete.

The basic NAH class was well-separated from the HAH class, eluting only when a significant proportion of isopropanol was present in the mobile phase. Amino-substituted AH (AAH) compounds eluted close together allowing an enriched "subfraction" of these species to be isolated. This is significant since AAH compounds have been implicated as the principal mutagenic components in synthetic fuels. It is interesting that the basic NAH compounds considered here eluted approximately according to their base strengths (Table III), indicating further that the basicity of these species was primarily responsible for their selective retention on the modified amino column. However, the elution order of basic NAH compounds is also strongly dependent on structural features. It has been reported that basic NAH compounds with sterically hindered nitrogens elute from polar bonded phase columns before their unhindered isomers[22]. In the present study, 7,8-benzoquinoline, containing a nitrogen
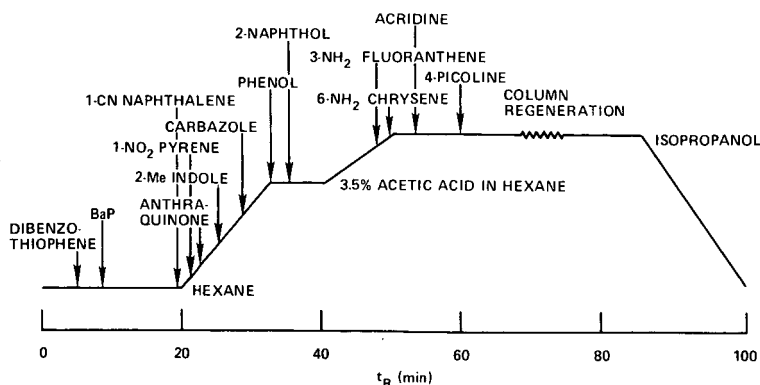
Fig. 4. Elution sequence profile of model fossil fuel compounds on the phosphoric acid-modified amino bonded phase column.

TABLE III

RETENTIONS OF MODEL FOSSIL FUEL COMPOUNDS

Compound	Chemical class	k'	Compound	Chemical class	k'
1-Octadecane	ALH	0.00			
1-Octadecene	ALH	0.00	2-Methylindole	Neutral NAH	10.4
Toluene	Non-polar AH	0.36	5-Methylindole	Neutral NAH	10.7
Thionaphthene	SAH	0.68	Indole	Neutral NAH	11.0
Naphthalene	Non-polar AH	0.72	Carbazole	Neutral NAH	11.1
Dibenzofuran	OAH	0.96	2,4-Dimethylphenol	HAH	11.4
Dibenzothiophene	SAH	1.24	2-Methylphenol	HAH	11.6
Fluorene	Non-polar AH	1.32	3,4-Dimethylphenol	HAH	13.1
Anthracene	Non-polar AH	1.72	3-Methylphenol	HAH	13.7
Pyrene	Non-polar AH	2.24	Phenol	HAH	14.0
Chrysene	Non-polar AH	4.40	1-Naphthol	HAH	14.1
Benzo[a]pyrene	Non-polar AH	5.76	2-Naphthol	HAH	15.3
Perylene	Non-polar AH	7.57	9-Phenanthrol	HAH	15.3
1-Nitronaphthalene	Nitro-AH	9.64	7,8-Benzoquinoline	Basic NAH (9.8)[*]	19.4
9-Nitroanthracene	Nitro-AH	9.68	3-Aminofluoranthene	Basic NAH	19.8
1-Cyanonaphthalene	Cyano-AH	9.72	6-Aminochrysene	Basic NAH	19.8
9-Cyanoanthracene	Cyano-AH	9.76	9-Aminophenanthrene	Basic NAH	20.3
9-Fluorenone	Quinone	9.76	1-Aminonaphthalene	Basic NAH (10.1)	20.3
1-Nitropyrene	Nitro-AH	9.84	Phenanthridine	Basic NAH (9.5)	20.6
Anthraquinone	Quinone	9.84	Quinoline	Basic NAH (9.1)	21.7
2,4,6-Trimethylphenol	HAH	9.92	5,6-Benzoquinoline	Basic NAH (8.9)	22.0
2,3,5-Trimethylindole	Neutral NAH	9.92	7-Azaindole	Basic NAH	22.6
Benzanthrone	Quinone	10.0	Acridine	Basic NAH (8.4)	22.7
1,4-Chrysenequinone	Quinone	10.0	Quinaldine	Basic NAH (8.2)	23.3
2,3-Dimethylindole	Neutral NAH	10.0	8-Hydroxyquinoline	Basic NAH; HAH	23.9
7-Methylindole	Neutral NAH	10.4	4-Picoline	Basic NAH	24.6

[*] pK_b values in parentheses.

shielded in a bay region, eluted from the modified amino column before phenanthridine and 5,6-benzoquinoline, containing unhindered nitrogens. Alkylated NAH species with sterically hindered nitrogens would also be expected to elute early in the basic NAH class fraction.

Finally, polyfunctional basic compounds were most strongly retained on the modified amino column. The second polar functional group enhanced retention; thus, 8-hydroxyquinoline eluted after quinoline. Other polyfunctional compounds, especially those of high molecular weight and possibly including species without basic functional groups, would be expected to elute in the final HPLC fraction.

Column regeneration

It was observed that column activity decreased after several (3–5) repetitions of the ternary solvent gradient. In particular, the basic NAH class eluted earlier and began to overlap the HAH compounds. However, column performance never reverted to that of an unmodified amino bonded phase column. This behavior was probably due to removal of some hydrogen bonded phosphoric acid (and acetic acid, some of which may have replaced or associated with the phosphoric acid during the elution sequence), but not the ionically bonded dihydrogenphosphate, from the stationary

phase surface when isopropanol, a strong protic solvent, was passed through the column. The modified amino bonded phase was easily regenerated by pumping 15–20 ml of 0.5% phosphoric acid in isopropanol through the column. In order to maintain retention reproducibility, the reactivation procedure was repeated between chromatographic runs, thus adding about 10 min to the ternary solvent program (Fig. 4). Continuous column regeneration using a low concentration of phosphoric acid in the isopropanol mobile phase could not be used because insoluble salts are formed with strongly basic solutes such as acridine.

Practical considerations

The facile preparation procedure is an attractive feature of the phosphoric acid-modified amino bonded phase. Many other stationary phases for HPLC might be produced as easily provided that a suitably acidic functionality is present on the organic or inorganic modifier. It has been demonstrated that the efficacy of synthesis and characterization of new bonded phases can be quickly evaluated using *n*-butylamine as a model for amino bonded phase material.

The phosphoric acid-modified amino bonded phase column effectively fractionated model fossil fuel compounds into the following chemical classes: (a) aliphatic hydrocarbons, (b) non-polar aromatic hydrocarbons, (c) neutral/acidic polar aromatic hydrocarbons (including quinone, cyano-, and nitro-aromatic hydrocarbon enriched, neutral nitrogen-containing aromatic hydrocarbon enriched, and hydroxy aromatic hydrocarbon enriched subclasses), and (d) basic polar aromatic hydrocarbons (including an aminoaromatic hydrocarbon enriched subclass). The elution sequence of polar compounds is complementary to that obtained with an amino bonded phase; the columns could be used for two-dimensional fractionation of polar mixtures.

The ternary gradient method developed for the phosphoric acid-modified amino bonded phase separates complex mixtures in about 1 h, followed by a short step to reactivate the stationary phase. The method can be scaled up to semi-preparative size and used to prefractionate synthetic fuel samples as will be reported in detail elsewhere[23].

ACKNOWLEDGEMENTS

REFERENCES

1 H. S. Karam, H. M. McNair and F. M. Lancas, *Mag. Liq. Gas Chromatogr.*, 5 (1987) 41.
2 R. B. Lucke, D. W. Later, C. W. Wright, E. K. Chess and W. C. Weimer, *Anal. Chem.*, 57 (1985) 633.
3 M. Radke, H. Willsch and D. H. Welte, *Anal. Chem.*, 56 (1984) 2538.
4 R. Miller, *Anal. Chem.*, 54 (1982) 1742.
5 S. C. Ruckmick and R. J. Hurtubise, *J. Chromatogr.*, 321 (1985) 343.
6 M. G. Strachan and R. B. Johns, *Anal. Chem.*, 58 (1986) 312.
7 J. Chmielowiec, *Anal. Chem.*, 55 (1983) 2367.

8 D. W. Later and M. L. Lee, in C. W. Wright, W. C. Weimer and W. D. Felix (Editors), *Advanced Techniques in Synthetic Fuels Analysis*, NTIS, Springfield, VA, 1983, p. 44.
9 A. L. Lafleur, A. G. Braun, P. A. Monchamp and E. F. Plummer, *Anal. Chem.*, 58 (1986) 568.
10 M. R. Guerin, I. B. Rubin, T. K. Rao, B. R. Clark and J. L. Epler, *Fuel*, 60 (1981) 282.
11 Y.-H. E. Sheu, C. V. Philip, R. G. Anthony and E. J. Soltes, *J. Chromatogr. Sci.*, 22 (1984) 497.
12 W. Holstein and D. Severin, *Anal. Chem.*, 53 (1981) 2356.
13 A. Matsunaga, *Anal. Chem.*, 55 (1983) 1375.
14 R. S. Brown and L. T. Taylor, *Anal. Chem.*, 55 (1983) 723.
15 M. G. Strachan and R. B. Johns, *Anal. Chem.*, 59 (1987) 636.
16 P.-L. Desbene, D. C. Lambert, P. Richardin, J.-J. Basselier, A. Y. Huc and R. Boulet, *Anal. Chem.*, 56 (1984) 313.
17 J. B. Green, R. J. Hoff, P. W. Woodward and L. L. Stevens, *Fuel*, 63 (1984) 1290.
18 W. Holstein, *Chromatographia*, 14 (1981) 468.
19 P. C. Uden and W. F. Joyce, in C. W. Wright, W. C. Weimer and W. D. Felix (Editors), *Advanced Techniques in Synthetic Fuels Analysis*, NTIS, Springfield, VA, 1983, p. 353.
20 N. H. Stokes, *Am. Chem. J.*, 15 (1893) 198.
21 A. P. Toste, D. S. Sklarew and R. A. Pelroy, in C. W. Wright, W. C. Weimer and W. D. Felix, *Advanced Techniques in Synthetic Fuels Analysis*, NTIS, Springfield, VA, 1983, p. 74.
22 H. Colin, J.-M. Schmitter and G. Guiochon, *Anal. Chem.*, 53 (1981) 625.
23 J. W. Haas, III and P. C. Uden, *Energy Fuels*, submitted for publication.

CHROM. 20 924

CHARACTERISTICS OF AN AVIDIN-CONJUGATED COLUMN IN DIRECT LIQUID CHROMATOGRAPHIC RESOLUTION OF RACEMIC COM-, POUNDS

TOSHINOBU MIWA* and TAKESHI MIYAKAWA

Eisai Co. Ltd., Pharmaceutical Research Laboratory, 1 Takehaya-machi, Kawashima-cho, Hashima-gun, Gifu 483 (Japan)

and

YASUO MIYAKE

Eisai Co. Ltd., Tsukuba Laboratory, 5-1-3 Tokodai, Toyosato-cho, Tsukuba-shi, Ibaragi 300-26 (Japan)

(First received May 20th, 1988; revised manuscript received July 28th, 1988)

SUMMARY

An avidin-conjugated column exhibited chiral recognition of acidic compounds such as profen derivatives. Amine enantiomers were not resolved by this column, of which biotin acted as a potent modifier. Avidin showed hydrophobic interaction with the solutes. A differential scanning calorimetry study showed that thermodynamically stable avidin is inapplicable as a chiral recognition ligand.

INTRODUCTION

Avidin, present in small amounts in egg protein, has a number of interesting characteristics. It is a rare basic protein having a pI of between 9.5 and 10.0. Avidin is composed of four identical subunits, the sequence of which has been determined, and each of which has a molecular weight of 16 400 daltons[1,2]. Each subunit bears a glycosidic chain linked to asparagine 17, and binds one molecule of biotin[3]. The avidin–biotin interaction, having an association constant of 10^{15} M^{-1}, is utilized in many fields of molecular biology including immunochemistry[4].

Proteins utilized as column ligands for direct optical resolution are almost all acidic. We have reported that chicken egg-white ovomucoid is a useful column ligand for the resolution of racemic amines[5]. This column also separated racemic profen derivatives, but the chromatograms obtained were not satisfactory[6]. It may be concluded empirically that a column ligand effectively retains and resolves oppositely charged solutes. We therefore selected avidin as a column ligand and employed it in the resolution of racemic acids. We used the succinimide activation method for the conjugation of avidin to the stationary phase, as reported previously. We also investigated the chiral recognition principle of avidin by measuring the thermodynamic stability of this protein.

EXPERIMENTAL

Apparatus
        A Shimadzu LC-6A pump equipped with an SPD-6A variable-wavelength UV monitor and with an SCL-6A automatic sample injector was used. Circular dichroism (CD) spectra were measured with a Jasco J-20 spectropolarimeter. A Seiko instrument DSC-100 calorimetric apparatus was used for the differential thermal analysis of protein solutes.

Chemicals
        Ibuprofen, ketoprofen, and atropine from Nihon Balk Yakuhin, flurbiprofen from Kaken, chlorprenaline from Eisai, chlorpheniramine from Kowa, and pindolol from Shiratori Seiyaku, all of pharmaceutical grade, were used. Oxprenolol was extracted from a pharmaceutical (Trasacor® from Ciba-Geigy) with ethanol. CM-Sephadex C-25 was obtained from Pharmacia Fine Chemicals and Duolite C-464 from Diamond Shamrock. 4-Hydroxyazobenzene 2'-carboxylic acid (HABA) was obtained from Tokyo-Kasei. All other chemicals were of reagent grade or higher quality.

Assay and preparation of chicken avidin
        Avidin was assayed according to the spectrophotometric titration with HABA described by Green[7]. All steps of the preparation process were performed at 4°C. The buffer used in all cases in the assay and preparation was 0.1 M phosphate buffer pH 6.8 which is referred to as "the buffer" in this section.
        Powdered egg white (20 kg) was dissolved in 80 l of the buffer and passed through a Duolite C-464 column (volume 30 l) equilibrated with the buffer. The column was washed with the buffer and subsequently eluted with 0.1 M phosphate buffer containing 1 M sodium chloride. The active fractions were dialyzed against the buffer, then applied to a CM-Sephadex C-25 column equilibrated and washed with the same buffer. Avidin was eluted with a linear gradient of 0–1 M sodium chloride and active fractions were collected. The pH of these fractions was adjusted to 3.5 with hydrochloric acid, and they were centrifuged at 8000 g for 20 min. Sodium ammonium sulphate was added to the supernatant to 50% saturation, and the resulting liquid was allowed to stand for 1 h and centrifuged at 8000 g for 20 min. The supernatant was 80% saturated with ammonium sulphate, and the resulting precipitate was collected by centrifugation. The precipitate was dissolved in a small volume of water and dialyzed against water.
        The avidin obtained was electrophoretically homogeneous and lyophilized.

Column preparation
        LiChrosorb NH_2 (2 g) and N,N-disuccinimidyl carbonate (3 g) were allowed to react overnight in 60 ml of coupling buffer (0.1 M sodium bicarbonate, pH 6.8) at room temperature, using a rotary evaporator without aspiration. After the activated silica gel had been washed with 50 ml of coupling buffer and then suspended in 30 ml of the same buffer, 30 ml of avidin solution (2 g in 30 ml of coupling buffer) were added gradually over a period of 30 min with shaking. This mixture was stirred for 2 h and the avidin-conjugated silica gel obtained was washed with coupling buffer. Stainless-steel columns (15 cm × 4.6 mm I.D.) were slurry-packed with avidin-conjugated silica gel

by using coupling buffer. The amount of avidin conjugated was determined by subtracting the amount recovered by washing from the amount used for conjugation.

Differential scanning calorimetry (DSC) of avidin, and of avidin–biotin and avidin–ketoprofen complexes

A 3-ml sample of 5% avidin solution was mixed with 220 mg of biotin or 230 mg of ketoprofen and left to stand for 2 h at 4°C. Each solution was dialyzed against water for 48 h at 4°C. Free ketoprofen was absent from the dialyzed solution, as was confirmed by high-performance liquid chromatography (HPLC). A 70-μl volume of dialyzed solution was sealed in a silver beaker and its thermal absorption was measured using the same amount of water as a control.

RESULTS AND DISCUSSION

A 1-g amount of LiChrosorb NH_2 adsorbed 120–163 mg of avidin, according to our method. Fig. 1 shows the resolution of profen-derivatized racemates using a column of silica gel conjugated with 163 mg of avidin per g. The effect of adding ethanol to the mobile phase when the same column is used is shown in Table I. Ethanol concentrations of 6% and below decreased the retention and resolution of profen derivatives, though the separation factors of ketoprofen and flurbiprofen were not changed. The separation factor of ibuprofen decreased between 0 and 3% ethanol, which resulted in a substantial decrease in resolution (R_s). The decrease in retention between 0 and 3% ethanol was very marked for ketoprofen (more than seven-fold), whereas a decrease in retention of only 20% was observed between 3 and 6% ethanol. The behaviour of ketoprofen may be attributed to the fact that it has the lowest solubility in water of the three profen derivatives, and also to the existence of a second hydrogen bonding group (carbonyl).

Table II shows the effect of mobile phase pH on the retention and resolution of solutes. In this experiment, a column of silica gel conjugated with 120 mg/g of avidin
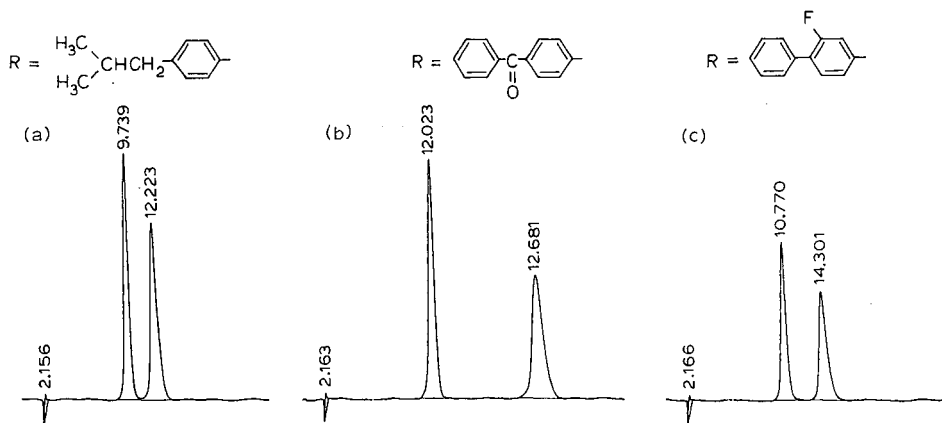
Fig. 1. Separation of the enantiomers of profens, RCH(CH₃)COOH, on an avidin-conjugated column. (a) Ibuprofen; (b) ketoprofen; (c) flurbiprofen (compound structures shown above figures). Mobile phase: 20 mM potassium phosphate (pH 6.5) containing 6% ethanol. UV detection at 220 nm. Column temperature: 20°C. Flow-rate: 1.2 ml/min. Numbers at peaks indicate retention times in min.

TABLE I

EFFECTS OF ETHANOL ON THE RETENTION AND RESOLUTION OF PROFEN DERIV-ATIVES

Mobile phase: 20 mM potassium phosphate (pH 6.5). Column: avidin bound to LiChrosorb NH$_2$ (163 mg/g), 150 mm × 4.6 mm I.D.

Ethanol (%)	Derivative	k'_1	k'_2	α	R_s
0	Ibuprofen	14.92	27.5	1.84	2.39
	Ketoprofen	> 50			
	Flurbiprofen	23.55	37.79	1.61	1.89
3	Ibuprofen	7.42	9.59	1.29	0.82
	Ketoprofen	7.29	14.34	1.97	2.67
	Flurbiprofen	7.79	10.94	1.41	1.17
6	Ibuprofen	4.41	5.79	1.31	0.64
	Ketoprofen	5.68	11.04	1.95	1.93
	Flurbiprofen	4.98	6.94	1.39	0.84

was used. Amine racemates were not resolved by this column. Acidic compounds were strongly retained by the column at a low pH, and higher capacity factors (k') for amines were obtained at higher pH values. This behaviour is the same as that with an acidic protein-immobilized column such as an orosomucoid-conjugated Enantiopak® (ref. 8) or an ovomucoid column[6], though avidin has the opposite charge. As for chiral selectivity, the mobile phase pH did not alter the separation factor, α, of acidic solutes, and this phenomenon also accords with the result obtained with Enantiopak, but it must be emphasized that profen enantiomers were better resolved by an avidin-conjugated column than by an acidic protein column.

The amount of avidin immobilized on the supports affected the retention and separation of solutes (Tables I and II). The decreased amount of avidin (the column

TABLE II

EFFECTS OF MOBILE PHASE pH ON THE RETENTION AND SEPARATION OF RACEMIC COMPOUNDS

Mobile phase: 20 mM potassium phosphate. Column: avidin bound to LiChrosorb NH$_2$ (120 mg/g), 150 mm × 4.6 mm I.D.

Compound	pH 5.5		pH 6.0		pH 6.5		pH 7.0	
	k'_1	α	k'_1	α	k'_1	α	k'_1	α
Ibuprofen	14.1	1.28	7.64	1.38	4.46	1.53	2.7	1.53
Flurbiprofen	21.2	1.32	12.5	1.29	6.96	1.39	4.78	1.37
Ketoprofen							4.74	2.34
Chlorprenaline	0	1	0	1	0.34	1	0.38	1
Chlorpheniramine					2.30	1	3.49	1
Oxprenolol	0	1	0.37	1	0.45	1	0.69	1
Pindolol	0	1	0.23	1	0.36	1	0.49	1
Atropine	0	1	0.19	1	0.61	1	0.95	1
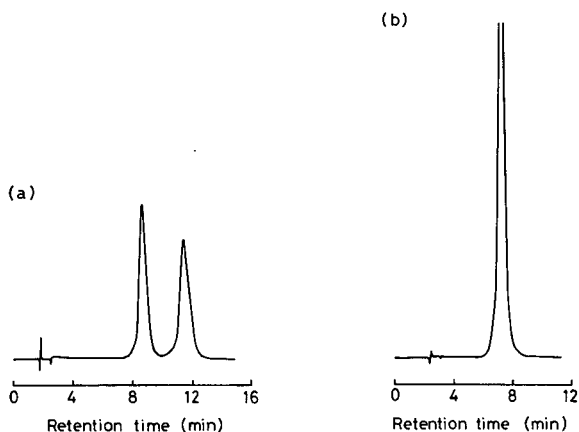
Fig. 2. Chromatogram of ketoprofen on an avidin-conjugated column. (a) Free avidin-conjugated column: mobile phase, 20 mM potassium phosphate buffer (pH 6.0); UV detection at 220 nm; column temperature, 20°C; amount of sample, 5 μg. (b) After 20 mg biotin had been passed through the column: the same amount of ketoprofen as for (a) was injected.

used in Table II bound 74% of the avidin that bound to the column used in Table I) caused 17% and 14% decreases in α, for ibuprofen and flurbiprofen, respectively. On the other hand, the capacity factors of these solutes obtained from a column conjugated with 120 mg/g avidin were 30% of that from the column conjugated with 163 mg/g of avidin, which may indicate that avidin has more than two sites in one molecule for interaction with solutes. Though Schill et al.[8] reported a plate height, H,
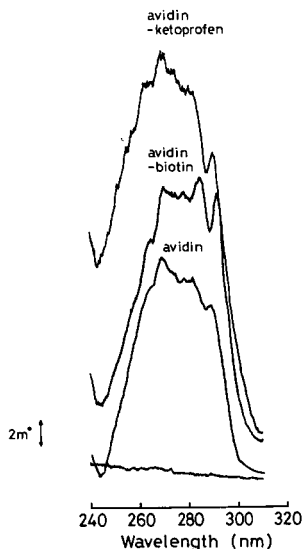
Fig. 3. Circular dichroism of avidin, avidin–biotin complex and avidin–ketoprofen complex. The dialyzed solutions obtained in experiments for DSC analysis were diluted in water to 1 mg/ml. Cell length: 0.5 cm. 2m° = 2° · 10⁻³.

of 0.1 mm for carboxylic acids using Enantiopak, an avidin-conjugated column showed $H = 0.3$ mm for profens. The best way to improve the resolution is to increase the α value of protein-immobilized columns, because these columns are limited in relation to increasing the theoretical number of plates. Though α increases in proportion to the amount of protein immobilized, this operation causes increased retention. It is important to determine the appropriate amount of protein which results in high efficiency.

The effect of biotion on this column is shown in Fig. 2. A biotin-bound avidin-conjugated column did not exhibit chiral recognition of profens. This was also confirmed by conjugating a biotin–avidin complex with silica gel. A column packed with this silica gel showed a chromatogram of ketoprofen similar to that seen in Fig. 2b, and the chiral recognition effect of these columns could not be restored by washing with 50% 2-propanol or 0.5 M sodium chloride. The biotin–avidin binding could be separated at 132°C[9], but this temperature is not practical for protein-conjugated silica gel.

We attempted spectroscopic and thermodynamic studies to elucidate the effect of biotin on the chiral recognition ability of avidin. The molecule of avidin contains no α-helix[2], as we have confirmed by examination of its CD spectrum. The effects of biotin and ketoprofen are recognized around 280 nm (Fig. 3), which reflects a $\pi-\pi$ transition of aromatic amino acid residues in proteins. Biotin altered the shape of the spectrum, while ketoprofen affected its magnitude. We consider that biotin modifies the structure of avidin, whereas ketoprofen does not, forming a $\pi-\pi$ bond with avidin.

The DSC study yielded similar results. Fig. 4 shows the changes in the thermal absorption temperature of avidin caused by biotin and ketoprofen. Biotin-bound avidin has no transition temperature under 100°C, while biotin-free avidin is
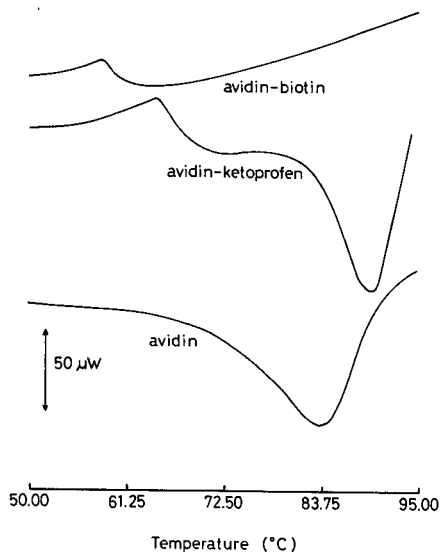
Fig. 4. Differential thermal analysis of avidin, avidin–biotin complex and avidin–ketoprofen complex. Details as in the Experimental section.

denaturated at 85°C. The ketoprofen–avidin complex showed a higher absorption temperature than did free avidin, but this temperature change may not reflect a structural change in the protein, such as is seen in the biotin–avidin complex. The result of integration of the DSC curve for the ketoprofen–avidin complex between 70 and 95°C is half of that for free avidin. This thermal stability may be related to the absence of chiral selectivity, and also to the decrease in capacity factor for ketoprofen-complexed avidin.

REFERENCES

1 N. M. Green and E. J. Toms, *Biochem. J.*, 133 (1973) 687.
2 N. M. Green, L. Konieczny, E. J. Toms and R. C. Valentine, *Biochem. J.*, 125 (1971) 781.
3 R. J. De Lange and T. S. Huang, *J. Biol. Chem.*, 246 (1971) 698.
4 J. L. Guesdon, T. Ternynck and S. Avrameas, *J. Histochem. Cytochem.*, 27 (1979) 1131.
5 T. Miwa, M. Ichikawa, M. Tsuno, T. Hattori, T. Miyakawa, M. Kayano and Y. Miyake, *Chem. Pharm. Bull.*, 35 (1987) 682.
6 T. Miwa, T. Miyakawa, M. Kayano and Y. Miyake, *J. Chromatogr.*, 408 (1987) 316.
7 N. M. Green, *Biochem. J.*, 94 (1965) 230.
8 G. Schill, I. W. Wainer and S. A. Barkan, *J. Chromatogr.*, 365 (1986) 73.
9 J. W. Donovan and K. D. Ross, *Biochemistry*, 12 (1973) 512.

CHROM. 20 886

HIGH-PERFORMANCE LIQUID CHROMATOGRAPHY ON CHIRAL PACKED MICROBORE COLUMNS WITH THE 3,5-DINITROBENZOYL DERIVATIVE OF *TRANS*-1,2-DIAMINOCYCLOHEXANE AS SELECTOR[*]

F. GASPARRINI*, D. MISITI and C. VILLANI

Dipartimento di Studi di Chimica e Tecnologia delle Sostanze Biologicamente Attive, Università "La Sapienza", P. le A. Moro 5, 00185 Rome (Italy)

F. LA TORRE

Istituto Superiore di Sanità, Laboratorio Chimica del Farmaco, Viale Regina Elena 299, 00185 Rome (Italy)

and

M. SINIBALDI

Istituto di Cromatografia, Consiglio Nazionale delle Ricerche, Area della Ricerca di Roma, C.P. 10, 00016 Monterotondo Stazione (Italy)

(Received July 29th, 1988)

SUMMARY

Columns of small inner diameter have clear advantages over conventional columns, *e.g.*, reduced consumption of mobile phase and of expensive stationary phases, high column efficiency, enhanced mass sensitivity on concentration-sensitive detectors and easy interfacing with mass spectrometers. Columns with inner diameters of 4.0, 2.0 and 1.2 mm were prepared using a chiral stationary phase containing the 3,5-dinitrobenzoyl derivative of $(S,S)(+)$- or $(R,R)(-)$-1,2-diaminocyclohexane covalently bonded to the siliceous matrix. Two classes of racemic compounds of pharmaceutical interest were chosen to investigate the performance of chiral microcolumns: α-methylarylacetic acid anti-inflammatory agents (as 1-naphthalene-methylamides) and amino alcohol β-blocking agents (as oxazolidin-2-ones). These compounds were easily resolved ($\alpha = 1.21$, 1.41 and 1.49 for ibuprofen, flurbiprofen and naproxen, respectively, and 1.40 for propanolol and pindolol) with very short analysis times. Hydrogen bonding, π–π interactions and steric hindrance are involved in the chromatographic resolution process.

INTRODUCTION

The technology of high-performance liquid chromatographic (HPLC) columns has recently been improved with respect both to the setting up of new chiral and achiral

stationary phases and to the development of columns with different geometries. During our research on the direct resolution of enantiomeric mixtures by means of chiral stationary phases (CSPs), we obtained better results on packed microbore columns (I.D. 2.0 or 1.2 mm) than on traditional columns (I.D. 4.6–4.0 mm).

The development of micro-HPLC is mainly due to Scott and co-workers[1–4], Novotny and co-workers[5–9] and Ishii and co-workers[10–13]; most technological problems involved with this new technique pertaining to column packing, pumping and injecting systems and detection have been solved, at least for microbore columns (I.D. 0.5–2.0 mm), which can now be used in routine practice.

The main advantages achieved with the use of the above columns can be considered from two points of view, general and more specific. The general advantages are a considerable saving of mobile phase, an improved resolution of complex mixtures, easy interfacing with mass spectrometers, their compatibility with the small-scale manipulation required in modern biology and medicine and a higher sensitivity when the same amount of sample has to be injected when using concentration-sensitive detectors in sample-limited situations. Other advantages derive directly from the specificity of the selected columns, for instance, the possibility of using expensive and sophisticated mobile and/or stationary phases; in such instances, small volumes of mobile phase and small amounts of chiral stationary phases are necessary for good resolution.

In previous work on chiral stationary phases[14–16], we reported the design and preliminary evaluation of some that are particularly effective in the enantiomeric separation of many compounds of different classes. In this paper, a microbore column with a chiral stationary phase containing as selector the 3,5-dinitrobenzoyl derivative of (S,S)(+)- or (R,R)(−)-1,2-diaminocyclohexane (DACH-DNB), covalently bonded to the siliceous matrix, is described.

Two classes of products of interest from the pharmaceutical point of view were considered: racemic anti-inflammatory α-methylarylacetic acids and β-blocking amino alcohols. Recently the resolution of several derivatives of racemic α-methylarylacetic acids has been achieved using different systems and covalently bonded (R)-N-(3,5-dinitrobenzoyl)phenylglycine[17], cellulose tribenzoate[18] and triphenylcarbamate[19] chiral stationary phases have been described.

Racemic β-blocking amino alcohols have generally been resolved as oxazolidin-2-one derivatives on several chiral stationary phases[20–22]. This paper reports the resolution of racemic ibuprofen, flurbiprofen and naproxen as 1-naphthalenemethylamides and of propranolol and pindolol as oxazolidin-2-ones on microbore chiral columns containing an (S,S)- or (R,R)-DACH-DNB as selector, and a critical comparison between the microbore and traditional columns.

The resolution of enantiomers of such compounds is of interest from the pharmaceutical point of view; it has been found that R isomers of ibuprofen[23] and naproxen[24] are converted *in vivo* into the corresponding S isomers; moreover, differences[25] in the disposition of the active S enantiomers of propranolol and its R enantiomer have been reported. Therefore, it is important to have a method of analysis that is rapid, sensitive and precise and that can be used for *in vitro* and *in vivo* studies of enantioselectivity in the biological activity of a racemic drug and to verify its enantiomeric composition; it is also important to be able to handle very small amounts of biological materials in sample-limited situations.

The most convenient approach to such a problem is direct resolution using chiral stationary phases (CSP); the indirect approach (derivatization with a chiral reagent) has some limitations owing to the possibility of partial racemization of the chiral derivative agent and of different reaction rates.

EXPERIMENTAL

Apparatus

HPLC was performed with a Carlo Erba Phoenix 20 syringe pump, a Knauer variable-wavelength UV detector (3-mm optical path length, 0.8-μl cell volume, time constant τ = 150 ms) and a Rheodyne Model 8125 5-μl loop injector. Chromatographic data were collected and processed on a Waters TM 840 data and chromatography control station.

Materials

LiChosorb Si 100 (5-μm particle size) and HPLC-grade solvents were purchased from Merck (Darmstadt, F.R.G.), 3-glycidoxypropyltrimethoxysylane (GOPTMS) from Janssen (Belgium); (S,S)(+)-DACH, (R,R)(−)-DACH, 1,1'-carbonyldiimidazole (CDI) and a 20% solution of phosgene in toluene from Fluka (Buchs, Switzerland), 1-naphthalenemethylamine from Aldrich-Chemie (Steinheim, F.R.G.). Racemic and enantiomerically pure drugs were obtained from the respective manufacturers and the remaining chemicals were of analytical-reagent grade and used as purchased.

The amides of α-methylarylacetic acids were synthesized by standard methods[17]. β-Blocking agents were converted into their oxazolidin-2-ones as described in the literature[21] or by reaction with CDI by the following precolumn derivatization micro-scale method. A 10-mg amount of propranolol hydrochloride (0.034 mmol) and 300 μl of triethylamine were dissolved in 2 ml of anhydrous tetrahydrofuran (solution A), and 10 mg of CDI (0.062 mmol) were dissolved in 2 ml of anhydrous tetrahydrofuran (solution B). Then 100 μl of solution A and 100 μl of solution B were mixed in a microvial and heated at 40°C and, after 5 min, the solution was injected into the HPLC system.
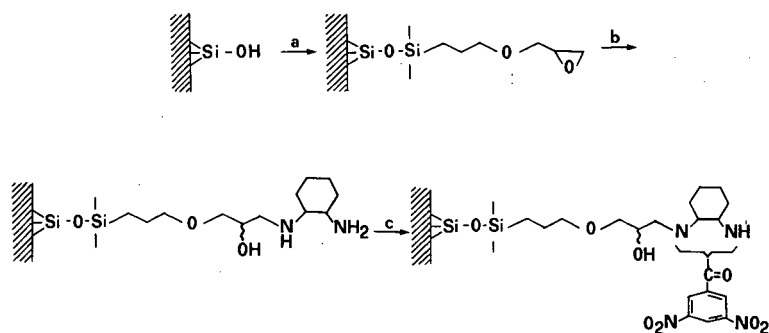
Fig. 1. Preparation of DACH-DNB chiral stationary phases. (a) Glycidoxypropyltrimethoxysilane, toluene, 4 h reflux; (b) (S,S)(+)- or (R,R)(−)-diaminocyclohexane, dimethylformamide, 96 h, room temperature; (c) dinitrobenzoyl chloride, tetrahydrofuran, triethylamine, 2 h reflux.

Chiral stationary phase
        CSP was prepared as shown in Fig. 1.

Column packing
        The column was made of stainless steel (150 mm × 4.0, 2.0 and 1.2 mm I.D.), packed with LiChrosorb Si 100 DACH-DNB (5 μm) using the slurry packing procedure.
        Grafted silica (1.500, 0.700 or 0.200 g) was dispersed in chloroform (50, 10 or 5 ml, respectively) and then treated ultrasonically for 5 min. The slurry thus obtained was packed with a Haskel Model pump DSTV-122 using *n*-hexane as pressurizing agent.

Column evaluation
        The eluent used in the evaluation of the kinetic performance of chiral columns of different inner diameter was *n*-hexane–isopropanol (99:1, v/v) and the solvent for the test mixture (benzene, naphthalene and anthracene) was *n*-hexane. The column dead volume (V_0) was determined from the retention of an unretained peak (benzene, using dichloromethane as eluent).
        Dimensionless parameters such as reduced plate height (h), flow resistance parameter (ϕ), separation impedance (E) and reduced velocity (v) were calculated according to Bristow and Knox[26]; diffusion coefficients of solutes in the mobile phase were determined using the empirical Wilke–Chang equation[27].

RESULTS AND DISCUSSION

        The direct resolution of racemates by HPLC needs the presence of an external chiral environment, which can be the stationary phase (CSP), the mobile phase or both. In these instances, the use of microbore columns permits a large reduction in the amount of chiral stationary and/or mobile phase, allowing the use of very sophisticated chiral sorbents and of "exotic" mobile phase; further, the amount of mobile phase necessary to optimize the separation conditions is dramatically reduced. Table I lists the amounts of CSP (DACH-DNB) used in the preparation of columns of different I.D.
        The kinetic performance of the columns was evaluated especially on the basis of the results obtained using an achiral test (see Experimental); comparison of the Van Deemter curves obtained with the different columns is shown in Fig. 2. The flow-rates for optimum chromatographic efficiency of each column were determined and are

TABLE I

AMOUNTS OF CSP AND VOID VOLUMES FOR 150-mm LONG COLUMNS

I.D. (mm)	Amount of chiral packing (mg)	Void volume (ml)
4.0	900	1.60
2.0	225	0.40
1.2	80	0.14
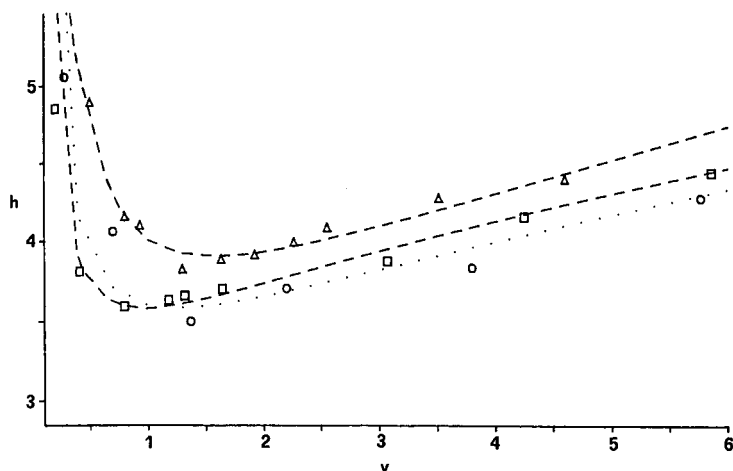
Fig. 2. Van Deemter plots (reduced plate height *vs.* reduced velocity of eluent) for different I.D. columns. (△) 4.0 mm I.D.; (○) 2.0 mm I.D.; (□) 1.2 mm I.D. See Table II for experimental conditions.

given in Table II. The results obtained show that, at mobile phase velocities close to optimum (v = 1.59, 1.37 and 0.80, respectively) the lowest h_{min} values, in the range 3.5–3.8, were obtained.

Although the lowest h_{min} value was obtained with the 2.0-mm I.D. column, the best performances (E value) were recorded with the 1.2-mm I.D. column. For this particular type of 5-μm irregular chiral stationary phase, the h_{min} value is higher than those previously reported in the literature for microcolumns containing 5-μm polar spherical stationary phases, but not very different from that reported for an NH_2 type of microcolumn which are the most difficult to optimize as far as the packing procedure is concerned[28].

The value of the reduced velocity (v) at which the best efficiency is registered decreases with decrease in the column I.D., in agreement with literature data[28].

An additional interesting result is the increase in the permeability of the columns as the I.D. decreases; it is therefore possible to connect several microbore columns in series, making feasible the resolution of mixtures of enantiomers with very low α values. Such resolution cannot be achieved with columns of standard dimensions.

TABLE II

COLUMN PERFORMANCES

Solute, benzene, k' = 0.15; eluent, *n*-hexane–2-propanol (99:1, v/v); CSP, (*S,S*)-DACH-DNB–LiChrosorb Si 100, 5 μm; column length, 150 mm.

I.D. (mm)	h_{min}	v_{opt}	Φ	E
4.0	3.8	1.59	760	10.900
2.0	3.5	1.37	622	7.620
1.2	3.6	0.80	538	6.970
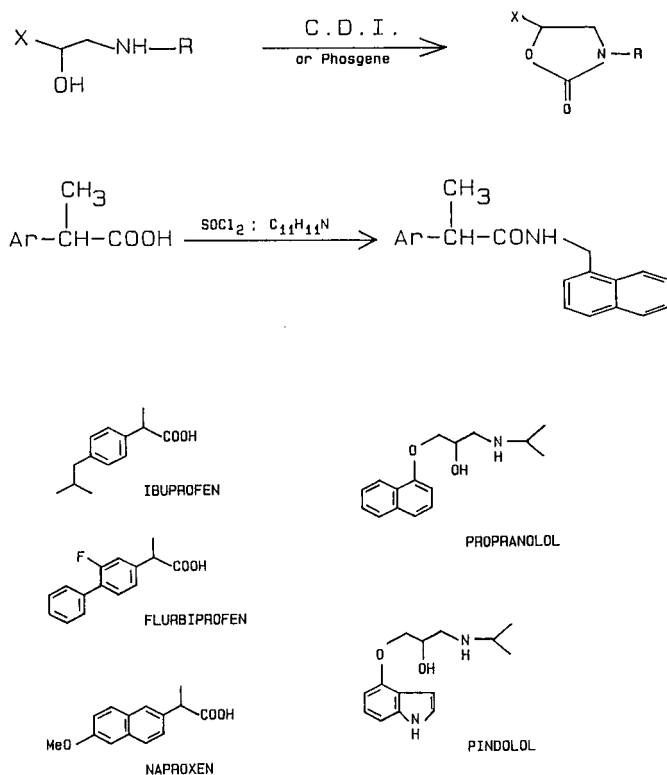
Fig. 3. Structures of racemic pharmaceuticals and derivatization procedures.

Chromatographic separation of chiral species

The above columns were successfully utilized in the direct resolution of racemates of substances of pharmaceutical interest, belonging to classes of racemic β-blocking amino alcohols and α-methylarylacetic acid anti-inflammatory agents. These substances were previously derivatized as shown in Fig. 3.

The derivatization reaction was carried out following previously described procedures[17,21] or, for β-blockers, using a micromethod of precolumn derivatization with CDI (see Experimental). The results reported in Table III show high values of α and relatively low capacity factors (k'), providing evidence for easy and rapid resolutions.

Fig. 4 compares the performances of analytical columns of different I.D. The signal-to-noise ratio (S/N) increases as the I.D. of the column decreases; in fact, when the same amount of substance is injected, S/N varies from 4.3 (B:C ratio) to 12.1 (A:C ratio) for the naproxen derivative, on passing from the 4.0-mm through the 2.0-mm to the 1.2-mm I.D. column, respectively.

The results indicate that microbore columns will be particularly useful in the biochemical field, when only small amounts of sample are available. Fig. 5 shows the analysis of a very small sample of the propranolol derivative at 230 nm using the 1.2-mm I.D. column.

TABLE III

CHROMATOGRAPHIC RESULTS

CSP: (S,S)-DACH DNB-LiChrosorb Si 100, 5 μm. All compounds were eluted at a linear velocity of 110 mm/s at 22°C. UV, detection 230 nm.

Compound	k'_1	α	R^*	Eluent
Ibuprofen	1.76 (R)	1.21	1.3	n-Hexane–2-propanol–dichloromethane (60:20:20, v/v)
Flurbiprofen	2.54 (R)	1.41	2.2	n-Hexane–2-propanol–dichloromethane (60:20:20, v/v)
Naproxen	4.11 (R)	1.49	3.4	n-Hexane–2-propanol–dichloromethane (50:25:25, v/v)
Propranolol	2.22 (S)	1.40	2.8	Dichloromethane–methanol (99:1, v/v)
Pindolol	1.36	1.40	2.7	Dichloromethane–methanol (90:10, v/v)

* Resolution factors obtained on a 150 × 1.2 mm I.D. column.

In addition, the utilization of microbore columns allows the determination of enantiomeric excess (e.e.) with an high degree of precision. In Fig. 6, as an example, the determination of the enantiomeric excess (99.94%) of (S)-propranolol, utilizing
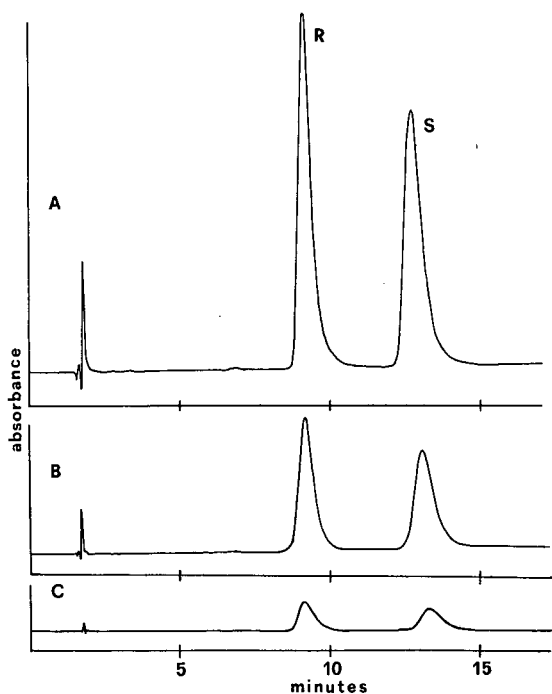
Fig. 4. Resolution of enantiomeric mixture of naproxen 1-naphthalenemethylamide. Injections of identical samples (0.2 μg) on to standard and microbore columns at similar linear velocities. See Table III for experimental conditions. (A) Column, 150 × 1.2 mm I.D.; flow-rate, 0.080 ml/min. (B) Column, 150 × 2.0 mm I.D.; flow-rate, 0.200 ml/min. (C) Column, 150 × 4.0 mm I.D.; flow-rate, 0.800 ml/min.
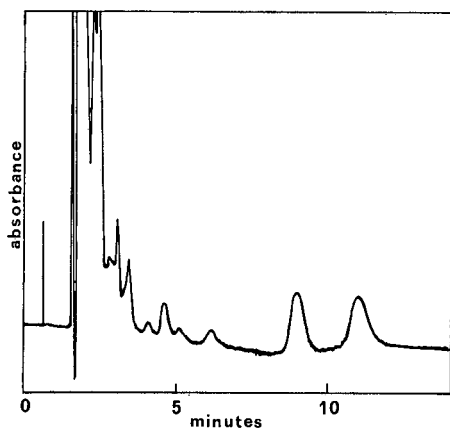
Fig. 5. Resolution of enantiomeric mixture of propranolol oxazolidin-2-one (1 ng). Column, 150 × 1.2 mm I.D.; eluent, *n*-hexane–2-propanol–methanol (40:30:30, v/v); flow-rate, 0.140 ml/min; UV detection, 230 nm; 0.01 a.u.f.s. $k'_1 = 7.30$; $\alpha = 1.30$.

a 1.2-mm I.D. column, is reported. Fig. 7a–c, showing some separation of enantiomers on 1.2-mm I.D. microbore columns, illustrates the potential of these columns.

In order to demonstrate the practical application of these columns to the control of the enantiomeric excess of chiral active principles in pharmaceutical specialities, a study of the precision and linearity of the detector response was carried out; the results are shown in Table IV and Fig. 8. The values of both the linear regression coefficients and the coefficients of variation indicate that the methodology is suitable for everyday routine use.
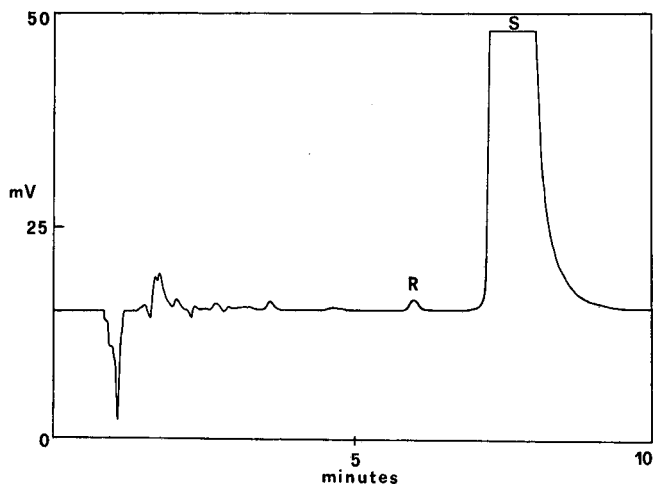
Fig. 6. Optical purity determination of (*S*)-propranolol (e.e. 99.94%). Column, 150 × 1.2 mm I.D., packed with (*R,R*)-DACH-DNB CSP–LiChrosorb Si 100, 5 μm; eluent, dichloromethane–methanol (99:1, v/v); flow-rate, 0.080 ml/min; UV detection, 230 nm; 0.04 a.u.f.s. $k' = 2.22$; $\alpha = 1.40$.
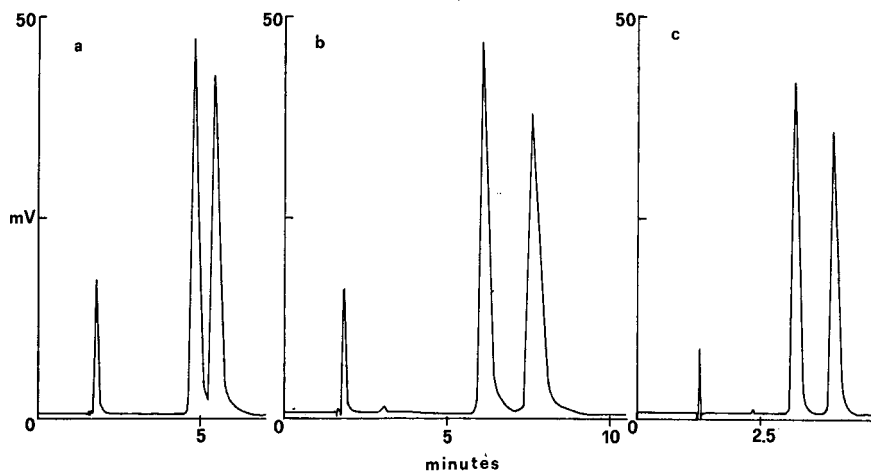
Fig. 7. Resolution of enantiomeric mixtures on a 150 × 1.2 mm I.D. column. See Table III for experimental conditions. (a) Ibuprofen 1-naphthalenemethylamide; (b) flurbiprofen 1-naphthalenmethylamide; (c) pindolol oxazolidin-2-one.

The mechanism of recognition assumes stereospecific attractive interactions between the racemic solutes and the selector through amide groups (hydrogen bonds) and 3,5-dinitrophenyl groups (π–π bonds) of the latter; further, the strong selector rigidity is partly responsible for the high values of α observed.

With derivatives of α-methylarylacetic acids, increases in the values of k' and α with increasing π-donor capacity of the aryl moiety have been observed, showing that it is directly involved in the mechanism of resolution through a π-base–π-acid interaction with the 3,5-dinitrophenyl groups present in the CSP.

TABLE IV

REPRODUCIBILITY STUDY

Sample: racemic propranolol oxazolidin-2-one. See Table III for experimental conditions.

Injection	Area of 1st peak*	Area of 2nd peak*
1	958 919	960 336
2	973 016	966 993
3	965 430	960 195
4	963 286	964 009
5	956 930	941 711
6	966 636	967 231
7	984 893	985 192
8	974 009	974 502
9	961 511	961 278
10	962 248	962 451

* 1st peak: mean value 966 688; standard deviation σ = 8001; coefficient of variation = 0.83%. 2nd peak: mean value 964 389; standard deviation σ = 10 544; coefficient of variation = 1.09%.
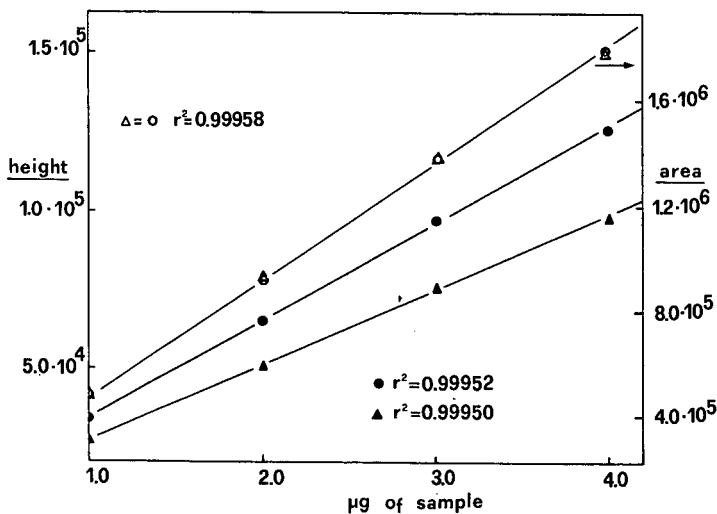
Fig. 8. Linear relationship between the amount of sample injected and the detector response. Solute: racemic propranolol oxazolidin-2-one. Column, 150 × 1.2 mm I.D. packed with (R,R)-DACH-DNB CSP–LiChrosorb Si 100, 5 μm; eluent, dichloromethane–methanol (99:1, v/v); flow-rate, 0.080 ml/min; UV detection, 230 nm; 0.16 a.u.f.s. (○) R isomer and (△) S isomer areas; (●) R isomer and (▲) S isomer heights.

The general mechanism of chromatographic resolution involves the temporary formation of CSP–solute complexes; the different stabilities of the complexes formed by the R and S isomers with the selector are determined by enthalpic and entropic factors. Under our experimental conditions, at room temperature, the chromatographic resolution is essentially an enthalpy-controlled process, whereas the entropic factor adversely affects the resolution. In fact, the more retained enantiomer is the one which simultaneously creates the greatest number of attractive interactions and therefore it is the one that loses the most degrees of freedom during the interaction with the CSP.

The reaction of propranolol and pindolol with phosgene or CDI produces cyclic derivatives with structural rigidity; this permits the disadvantageous effect of the entropic contribution on the enantioselectivity to be minimized and high values of α to be obtained, even in the presence of very polar mobile phases.

CONCLUSIONS

Recent progress in microcolumn instrumentation has made microbore packed chiral columns extremely useful for difficult separations of enantiomers. The possibility of working with very small amounts of substances permits studies of pharmacodynamics and pharmacokinetics on very small samples of precious biological fluids; further, the reduced amounts of chiral phases required in columns of small I.D. permit the utilization of extremely sophisticated and/or expensive chiral matrices.

REFERENCES

1 R. P. W. Scott and P. Kucera, *J. Chromatogr.*, 125 (1976) 251.
2 R. P. W. Scott and P. Kucera, *J. Chromatogr.*, 169 (1979) 51.
3 R. P. W. Scott, P. Kucera and M. Munroe, *J. Chromatogr.*, 186 (1979) 475.
4 R. P. W. Scott and P. Kucera, *Adv. Chromatogr.*, 22 (1984) 247.
5 T. Tsuda and M. Novotny, *Anal. Chem.*, 50 (1978) 271.
6 T. Tsuda and M. Novotny, *Anal. Chem.*, 50 (1978) 632.
7 Y. Hirata, M. Novotny, T. Tsuda and D. Ishii, *Anal. Chem.*, 51 (1979)1807.
8 Y. Hirata and M. Novotný, *J. Chromatogr.*, 186 (1979) 521.
9 M. Novotny, *Anal. Chem.*, 53 (1981) 1294A.
10 D. Ishii, K. Asai, K. Hibi, T. Jonokuchi and M. Nagaya, *J. Chromatogr.*, 144 (1977) 157.
11 T. Tsuda, K. Hibi, T. Nakanishi, T. Takeuchi and D. Ishii, *J. Chromatogr.*, 158 (1978) 227.
12 D. Ishii, T. Tsuda and T. Takeuchi, *J. Chromatogr.*, 185 (1979)73.
13 D. Ishii, K. Hibi, K. Asai and M. Nagaya, *J. Chromatogr.*, 152 (1978) 341.
14 G. Gargaro, F. Gasparrini, D. Misiti and C. Villani, paper presented at the *Italian–Israeli Symposium on Modern Trends in Organic Chemistry, Rehovot, Israel, 1985*.
15 G. Gargaro, F. Gasparrini, D. Misiti, G. Palmieri, M. Pierini and C. Villani, *Chromatogaphia*, 24 (1987) 505.
16 F. Gasparrini, D. Misiti and C. Villani, paper presented at the *1st International Symposium on Separation of Chiral Molecules, Paris, May 31–June 2, 1988*.
17 I. W. Wainer and T. D. Doyle, *J. Chromatogr.*, 284 (1984) 117.
18 I. W. Wainer and M. C. Alemblik, *J. Chromatogr.*, 358 (1986) 85.
19 D. M. McDaniel and B. G. Snider, *J. Chromatogr.*, 404 (1987) 123.
20 I. W. Wainer, T. D. Doyle, K. H. Donn and J. R. Powell, *J. Chromatogr.*, 306 (1984) 405.
21 J. Hermansson, *J. Chromatogr.*, 325 (1985) 379.
22 W. A. König, O. Weller and J. Shulze, *J. Chromatogr.*, 403 (1987) 263.
23 D. Kaiser, G. Vangiessen, R. Reischer and W. Wechter, *J. Pharm. Sci.*, 65 (1976) 269.
24 J. Goto, N. Goto and T. Nambara, *J. Chromatogr.*, 239 (1982) 559.
25 L. Low and N. Castagnoli, *Ann. Rep. Med. Chem.*, 13 (1978) 304.
26 P. Bristow and J. Knox, *Chromatographia*, 10 (1977) 279.
27 C. Wilke and P. Chang, *AIChE J.*, 1 (1955) 264.
28 M. Novotny, F. Andreolini and C. Borra, *Anal. Chem.*, 59 (1987) 2428.

CHROM. 20 931

INDIRECT METHOD FOR THE DETERMINATION OF WATER USING HEADSPACE GAS CHROMATOGRAPHY

JOSEPH M. LOEPER* and ROBERT L. GROB*

Chemistry Department, Villanova University, Villanova, PA 19085 (U.S.A.)

(First received May 16th, 1988; revised manuscript received August 30th, 1988)

SUMMARY

This research investigated an analytical method for the quantitative determination of water using headspace gas chromatography (HSGC) and the reaction of calcium carbide and water to produce acetylene. Samples containing water were transferred to a dry vial containing calcium carbide, after which the vial was sealed. The acetylene which formed inside of the vial was then measured by HSGC and used to calculate the original concentration of water in the sample.

The investigation indicates that the method is a viable alternative for the determination of water in various organic solvents, for concentration ranging from 60 to 400 ppm (μl l^{-1}).

INTRODUCTION

The reliable determination of water in solid, liquid and gaseous materials is an important part of many chemical operations. Both large- and small-scale processes might be adversely affected by small amounts of water. Its presence in a reaction medium might significantly alter the speed or course of a reaction, or contribute to the degradation of a product. Consequently, a significant amount of research has been devoted to the development of new and better methods for determining water.

The Karl Fischer titration is one of the most popular techniques for water determinations. This widespread recognition is as good a testimony as any to the great utility of this technique. But there are certain chemical interferences which make the Karl Fischer titration unsatisfactory for certain applications[1,2].

Gas chromatography (GC) has been investigated as an alternative technique for water determinations. Direct measurement of trace concentrations of water by GC has been complicated by two factors, however. The extremely polar nature of the water molecule made it difficult to chromatograph prior to the introduction of porous polymers as packing materials for GC[3,4]. The lack of a sensitive detector for water also posed a problem, but advances with the helium ionization detector have made direct gas chromatographic determinations a more viable alternative[5,6].

---

* Present address: Weston Analytics, Lionville, PA, U.S.A.

Chemical conversion of water to acetylene followed by gas chromatographic determination of the acetylene is a technique that has been used for indirect measurements of water. Samples containing water are brought into contact with calcium carbide. The water and calcium carbide react to form acetylene, a compound

$$2H_2O + CaC_2 \rightarrow C_2H_2 + Ca(OH)_2$$
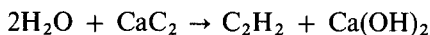
with a very favorable response using a flame ionization detector. The acetylene is measured, and the amount of water originally present in the sample can then be calculated.

This technique has been employed in different ways, but the most prevalent is the use of a pre-column of calcium carbide in the gas chromatograph itself[7,8]. The use of the pre-column has enabled some researchers to determine water down to the 5–10 ppm (μl l^{-1}) range, but long turnaround times for sample analysis and the need for frequent replacement of the pre-column make this an unattractive alternative for routine applications.

This research has investigated the possibility of using the calcium carbide–water reaction in a different fashion. The sample containing water is transferred to a dry vial containing calcium carbide. The acetylene is formed inside the sealed vial and determined using headspace gas chromatography (HSGC). This variation offers the advantages of a faster turnaround time for sample analysis and the potential for completely automated analysis, using one of the commercially available Automatic Head Space Samplers.

EXPERIMENTAL

Apparatus

A Hewlett-Packard Model 5880A gas chromatograph and terminal, equipped with a flame ionization detector was used for the analysis. The separation was accomplished with a 6 ft. × 0.25 in. (4 mm I.D.) glass column with a packing of 5% SE-30 on Porapak Q (80–100 mesh) (Waters Chromatography Division, Millipore, Milford, MA, U.S.A.). The headspace samples were injected manually with a gas-tight precision sampling syringe (Series A-2, 2.0 ml) available from Precision Sampling Corp. (Baton Rouge, LA, U.S.A.). The sample reaction and subsequent headspace equilibration was completed in 50-ml glass reaction vials available from Supelco (Bellefonte, PA, U.S.A.). The vials were sealed with septa of brominated butyl rubber, obtained from The West Co. (Phoenixville, PA, U.S.A.), and aluminum seals, Wheaton Scientific (Millville, NJ, U.S.A.).

Reagents

Methanol, ethanol, 2-propanol, toluene, hexane, methylene chloride and acetonitrile, all reagent grade, were purchased from J. T. Baker (Phillipsburg, NJ, U.S.A.). Calcium carbide (10–40 mesh) was obtained through Fisher Scientific (Fair Lawn, NJ, U.S.A.).

RESULTS

Sample preparation

With the practice of headspace analysis (HSA) one usually conducts some preliminary tests with samples prepared in the laboratory to optimize or troubleshoot some of the experimental variables. The nature of this project (indirect determination of water) was different than most other HSA application. It involved chemical conversion of the analyte into another form within the head space vial. This meant that sufficient time had to be allowed for the conversion reaction to occur, as well as the equilibration of the product between the vapor and liquid phases. Consequently, many of the HSA variables could not be evaluated until some other aspects of the sample preparation procedure were understood.

Potential sources of contamination were also an important aspect to consider. All glassware, solvents or other equipment must be made as anhydrous as possible. It is not always practical to eliminate all of the water from these sources. Many solvents, for instance, are particularly difficult to completely dry (*i.e.*, the lower chain alcohols). Once they are anhydrous, one must be concerned with further contamination from atmospheric moisture. A practice which is frequently used with water determination methods is to measure the amount of water in a blank solution which has been handled in a manner similar to samples or standards. The amount of water found in the blank solution is then subtracted from the total amount of water found in the samples or standards. So the emphasis is not on completely eliminating the water in the solvents, but rather on attaining as low and reproducible a level of water as possible.

In a similar vein, we found that it would be difficult, time consuming and impractical to add a constant amount of calcium carbide to several headspace vials and eliminate all of the acetylene which forms before analyte is added. Thus, an excess but not necessarily a constant amount of calcium carbide was always added. The goal then changed to decreasing the amount of background acetylene to as low a reproducible level as possible.

Headspace vials and septa. Some preliminary experiments on headspace vial preparations were done by adding only calcium carbide to the vials, sealing them, and measuring the amount of acetylene produced. Before using the vials they were dried in a vacuum oven overnight at a temperature of 250°C, and then cooled in a desiccator over indicating Drierite. The calcium carbide was taken from its storage container and measured into a small plastic cup which held 1 g of the material. The calcium carbide was then transferred to the vial, and the vial was purged with a stream of dry nitrogen. It was hoped that this nitrogen purge would eliminate any acetylene formed on transfer of the calcium carbide from the storage container to the headspace vial. Following the purge, the vials were sealed with the septa and equilibrated in a water bath at 32°C. Initially, the septa used in the experiments were stored in a desiccator overnight. It was then discovered that these septa could be dried in an oven at temperatures of 120°C for short periods of time with no deleterious effects. Some simple drying experiments were performed on the septa. The results of these experiments, listed in Table I, indicate a significant decrease in the concentration of acetylene in the vial as the drying conditions become more rigorous (*i.e.*, oven drying). This would seem to indicate that the septa adsorb and/or absorb a certain amount of moisture, which can then migrate into the dry headspace vial and form acetylene. Drying the septa at 120°C improves the

TABLE I

SEPTA PREPARATIONS

$n = 9$ measurements.

Preparation technique	Average acetylene peak area
(1) Overnight desiccation	$100 \cdot 10^3 \pm 17 \cdot 10^3$
(2) 30 min at 120°C	$64 \cdot 10^3 \pm 18 \cdot 10^3$
(3) 60 min at 120°C	$60 \cdot 10^3 \pm 20 \cdot 10^3$

situation significantly. Drying times over 1 h were not attempted since the septa began to melt and deform after a period of 1 h.

Calcium carbide transfers. To evaluate potential interferences introduced in the handling of the calcium carbide, some additional tests were conducted. Calcium carbide was added to each of 20 vials after which they were purged with dry nitrogen for a period of 5 min, sealed and equilibrated overnight. A second set of 20 vials were prepared. These headspace vials, septa and calcium carbide were placed in a glovebag which was purged with dry nitrogen. The calcium carbide was transferred to all of the vials and the septa put in place. The vials were then removed from the glovebag and the septa sealed with the aluminum caps. These vials were also equilibrated overnight. The acetylene was then determined in all of the vials.

The average acetylene peak area in the vials obtained by the two transfer techniques are listed in Table II. Comparison of the results indicate that the use of the glovebag would be more desirable in two respects: (i) the amount of acetylene produced is significantly reduced when the transfers are carried out in a glovebag, and (ii) the standard deviation of the results for the glovebag is lower, indicating that these vials can be prepared in a more reproducible manner.

A plot of the peak areas obtained from the analysis of the individual vials *versus* the vial number is shown in Fig. 1, with the vial number referring to the order which the calcium carbide was added to the vials. From this graph, one can see that the peak areas for both techniques begin at approximately the same values for the first few vials. As the vial number increases, the magnitude and scatter of the data for the vials prepared using the nitrogen purge increases significantly in comparison with the results with the glovebag. Consequently, all transfers of calcium carbide for subsequent studies were done using the glovebag technique.

TABLE II

COMPARISON OF TRANSFER TECHNIQUES

$n = 20$ measurements.

Transfer technique	Average acetylene peak area (counts)	Standard deviation (counts)
Glovebag	$33 \cdot 10^3$	$4 \cdot 10^3$
Nitrogen purge	$45 \cdot 10^3$	$9 \cdot 10^3$
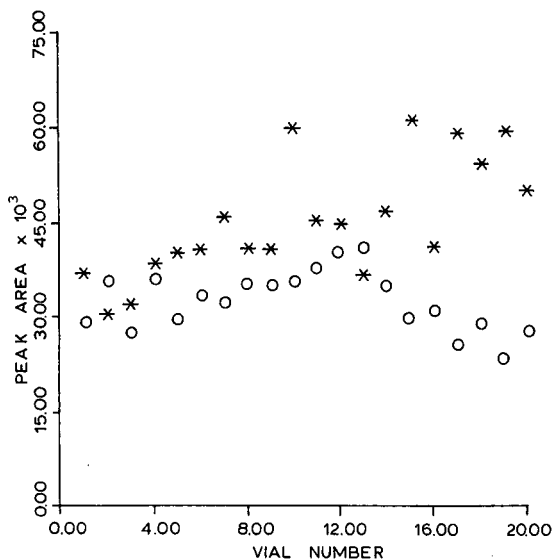
Fig. 1. Graphical comparison of calcium carbide transfer techniques. (○) Glovebag; (*) nitrogen purge.

Determination of water in solvents

Different aspects of the calcium carbide–water reaction, such as reaction times and interfering or non-specific reactions, had to be understood before the technique could be successfully applied to the determination of water. Control of the parameters which affected the HSA was important as well (*i.e.*, equilibration time, equilibration temperature and sample matrices). The successful evaluation of any one of these variables could be very dependent on the control of many others.

Adequate preparation of the solvents used in the proposed technique can have a significant effect on the reliability of the results obtained. Using reagent grade solvents with no preparations could mean working with blank solutions which might contain 300 ppm (μl l^{-1}) of water or more. To do a water determination at or below the 100 ppm (μl l^{-1}) level, the error introduced by a blank which is at least three times larger than the sample could be significant; especially when considering all of the other variables which need to be controlled. Consequently, all solvents were dried with either molecular sieves or a combination of anhydrous calcium sulfate for a preliminary treatment followed by molecular sieves. Measures were also taken to ensure that all glassware was as dry as possible and that all solutions were handled in a consistent manner. This was to prevent any contaminations from atmospheric moisture.

Reaction times and temperatures. To study the reaction times, headspace vials were prepared as described in the previous sections. Several blank solutions of 2-propanol and solutions spiked with water to a concentration of 100 ppm (v/v) (μl l^{-1}) were prepared. Aliquots of 10 ml of either a blank or spiked solution were added to a series of prepared headspace vials. Some of the vials were shaken by hand (both spiked and blank solution) and others were shaken mechanically. All of the vials were equilibrated in a water bath at 32°C for a measured period of time. After the equilibration, the headspace of a vial containing a blank solution was analyzed

TABLE III

RESPONSE FACTOR FOR 2-PROPANOL SOLUTIONS SPIKED WITH WATER

$$\text{Response factor} = \frac{\text{area counts (spike)} - \text{area counts (blank)}}{\text{spike concentration (ppm water)}}$$

Conditions	Reaction time	Response factor (counts/ppm)
Hand shaking (1 min)	100 min	311
Mechanical shaking (1 min)	30 min	154
Mechanical shaking (1 min)	75 min	1384
Mechanical shaking (1 min)	100 min	1226
Hand shaking (1 min)	18 h	2785

followed by that of a spiked solution. Results were erratic and it appeared that complete conversion of all water in a vial would take several hours. Ten blank and ten spiked vials were prepared in the same manner and allowed to equilibrate for a period of 18 h (overnight). The headspace analysis of these vials resulted in a significant increase in the peak area of acetylene for spiked solutions compared to the blank solutions. Table III lists the response factors found for different reaction times as well as different shaking methods.

The results in Table III show a response factor which almost doubles with an 18-h reaction period. Fig. 2 shows a plot of the acetylene peak areas versus time (following overnight reaction) for vials containing either the 60-ppm spiked solution or the blank solution. The x-axis on the graph refers to the time following the analysis of the first vial. The fact that the acetylene peak areas for both the blank and spiked
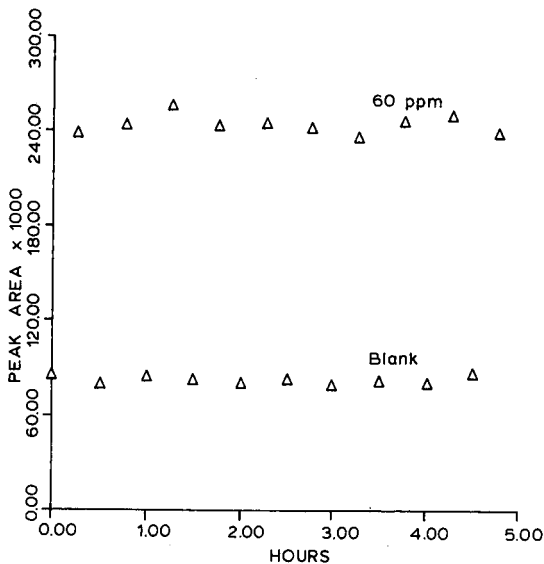
Fig. 2. Plot of acetylene peak areas for spiked and blank solutions of 2-propanol versus time (after 18-h reaction time).

solutions remain farily constant over a 5-h period indicates that reaction of all of the water is complete. Shaking times had an effect with shorter reaction periods but were not studied for the overnight reaction, as it appeared the conversion was complete.

It is very possible that the reaction would be complete in less than 18 h, but this aspect was not investigated. Overnight reaction proved satisfactory and was used in the remainder of the research. In terms of completing an experiment, it was more practical to prepare a large number of samples one day and complete the headspace analysis the following day. With an automated headspace analyzer, ith might be more practical to implement a shorter reaction time.

The temperature of the water bath in which the vials were equilibrated was varied to determine if there was any effect on the response factors. The study was conducted at two other temperatures; *i.e.* 26°C and 41°C. There was no change in the response factor which was obtained at 32°C, and all subsequent work was done with an equilibration temperature of 32°C.

Determinations of water in 2-propanol. Solutions of 2-propanol spiked with known amounts of water were used for the investigations for the quantitative measurements. Calibration curves were prepared and reproducibility studies performed using different volumes (*i.e.* 5, 10 and 15 ml) of solvent added to the 60-ml headspace vial. These experiments helped in determining the limitations of the technique in terms of accuracy and precision, as well as evaluating the effects of increasing solvent volumes added to the headspace vials. Fig. 3 illustrates the calibration curves.

The increase in slope of the calibration curve accompanying the increase in solvent volume is to be expected. Adding 5.0 ml of a given concentration to one vial and 10.0 ml of that same concentration to another vial would mean that twice the amount of water is added to the second vial. Looking at the change in slope of the lines
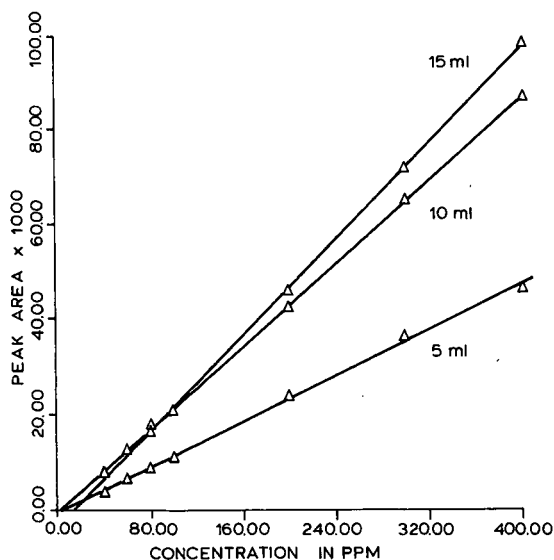
Fig. 3. Calibration curves of water in 2-propanol for increasing liquid phase volumes.

as related to the change in solvent volume, one can see that doubling the volume does not double the slope of the line. This would be due to a certain portion of the acetylene remaining as a solute in the liquid phase. Even though more acetylene is produced and a smaller headspace volume is present, the increased amount of liquid phase will retain more of the acetylene.

To assess the accuracy and precision which could be expected with the actual measurement of water in a sample, some additional experimentation was done with 2-propanol. A solution spiked with water was prepared and treated as a sample whose water content was to be determined. Two different calibration standards, whose water concentrations bracketed that of the sample solution, were also prepared. All three of the solutions were then analyzed by the calcium carbide technique. The peak areas of the standards were used to calculate a response factor, which was then used to experimentally determine the water concentration of the sample solution. The concentration of water in the sample solution was then determined from the average of ten measurements, and compared to the "true" concentration of the solution. The uncertainty of these measurements was also computed.

The sample solution concentrations were studied in the range of 80 to 400 ppm (v/v) (μl l^{-1}). The volume of solvent added to the vial was also varied (5.0, 10.0 and 15.0 ml) in an attempt to find the optimum solvent volume for practical applications. The results of these experiments are listed in Table IV.

The accuracy of all of the experimental results is high. The percent error of all but four of the results was 1% or lower. But there are some discrepancies in the precision of the results obtained for a given concentration determined with different liquid phase volumes. Looking at the values listed in Table IV, one can see that only those

TABLE IV

DETERMINATIONS OF WATER IN 2-PROPANOL

True conc. ppm (v/v)	Exptl. conc.* ppm (v/v)	% Error	R.S.D. (%)
5.0 ml liquid phase volume			
80	82	2.50	13.13
200	197	1.50	9.58
300	308	2.67	4.51
400	400	0	4.51
10.0 ml liquid phase volume			
80	80	0	2.59
100	102	2.00	4.89
200	201	0.50	3.98
300	303	1.00	3.19
400	396	1.00	1.77
15.0 ml liquid phase volume			
80	80	0	7.13
100	100	0	4.65
200	199	0.50	3.42
300	300	0	3.58
400	396	1.00	5.38

* Average of 10 determinations.

determinations done using a 10.0-ml solvent volume furnish relative standard deviation (R.S.D.) values which are all below 5%. For the 15.0-ml volume, one of the R.S.D. values is above 5%. With the 5.0-ml volume, two of the values are above 5%.

Some of these trends in the precision are actually as expected. Referring back to Fig. 3 the plots indicate that the response factor increases as the solvent volume in the headspace vial increases. If one assumes then, that the errors introduced in the procedure remain constant (*i.e.*, sample preparations, the headspace analysis and the conversion of water to acetylene), one should expect that as the solvent volume is increased, lower concentrations could be determined with better precision. The results are as expected when the solvent volume is increased from 5.0 to 10.0 ml, but not for the increase of 10.0 to 15.0 ml. It is quite likely that the overnight reaction is insufficient for the 15.0-ml solvent volume, but longer reaction time were never investigated. The change in the response factor going from the 10.0- to the 15.0-ml volume is not that large, and the possible benefit of a marginal improvement in the precision is not worth a longer turn around time for sample analysis.

From a practical standpoint, the actual level at which a determination is being done and the precision needed in the analysis should dictate the volume of solvent to be used. For the remainder of this research, 10.0-ml liquid phase volumes were added to the headspace vials. But for other applications, the 5.0-ml solvent volume might be appropriate. Using one half the amount of a sample which is limited in supply can be a definite advantage. There appears to be no advantage at all to using a 15.0-ml solvent volume with the conditions used in these experiments.

Determinations of water below 80 ppm ($\mu l \ l^{-1}$). To get a feel for the level of precision which could be expected at lower concentration levels, additional measurements were performed using 2-propanol, methylene chloride, acetonitrile, hexane and toluene. Calibration curves for acetonitrile and methylene chloride were prepared as a check with solvents other than 2-propanol. The results of these studies, listed in Table V, indicate a linear response for the concentration ranges [0–80 ppm ($\mu l \ l^{-1}$)] studied.

Spiked [60 ppm ($\mu l \ l^{-1}$) or lower] and blank solutions were then prepared using all of the solvents. There were four vials prepared containing the solvent blank and seven containing the spiked solutions. The analyses were then completed on all of the vials and the net peak areas determined for each concentration. The relative standard deviation of the measurements at each concentration were calculated and can be found in Table VI along with the response factors obtained for each solvent.

Poor precision was obtained for all determinations at the 20-ppm ($\mu l \ l^{-1}$) level, with the R.S.D. values being well over 10% for all of the solvents. All determinations at the 40-ppm level have an R.S.D. below 7% except toluene. The results obtained at the 40-ppm level might be acceptable under some circumstances, but it would have to be considered the limit for the practical application of the technique.

TABLE V

LINEARITY STUDIES

Solvent	Slope	Intercept	Correlation coeff.
Acetonitrile	1716	2685	0.998
Methylene chloride	1619	−7	1.000

TABLE VI

DETERMINATIONS OF WATER BELOW 60 ppm

Solvent	Conc. (ppm)	R.S.D. (%)	Response factor (counts/ppm)
2-Propanol	60	3.55	2871
	40	6.51	
	20	14.63	
Acetonitrile	60	4.76	1862
	40	5.29	
	20	13.80	
Hexane	41	6.82	1525
	22	18.18	
Methylene chloride	57	6.26	1317
	23	18.51	
Toluene	40	8.64	1720
	20	30.79	

The change in the response factors for the different solvents is interesting in that it probably reflects a change in the distribution coefficient of acetylene in the different solvents. The increased response factor for 2-propanol does not result in any profound benefits in terms of the precision which is achievable at lower concentration levels.

CONCLUSION

The primary objective of the research was the development of an analytical method which could be used for the quantitative determination of water. Initial investigations were undertaken with 2-propanol to optimize the calcium carbide technique and gain some insight into its limitations. Concentrations ranging from 60 to 400 ppm (μl l^{-1}) of water in 2-propanol were measured accurately, with an R.S.D. below 5% for ten individual determinations. The technique was also useful for the determination of water in toluene, methylene chloride, hexane and acetonitrile. Measurements at 60 ppm (μl l^{-1}) typically had a relative standard deviation ranging from 5 to 7%. Determinations below 60 ppm (μl l^{-1}) for all of the solvents had poor precision.

REFERENCES

1 J. Mitchell, Jr. and D. M. Smith, *Aquametry, Part III*, Vol. 5, Wiley, New York, 2nd ed., 1980.
2 J. Mitchell, Jr., D. M. Smith, E. C. Ashby and W. M. D. Bryant, *J. Am. Chem. Soc.*, 63 (1941) 2927.
3 O. L. Hollis, *Anal. Chem.*, 38 (1966) 309.
4 O. L. Hollis and W. V. Hayes, *J. Gas Chromatogr.*, 4 (1966) 235.
5 F. F. Andrawes, *Anal. Chem.*, 55 (1983) 1869.
6 F. F. Andrawes, *J. Chromatogr.*, 290 (1984) 65.
7 A. Goldup and M. T. Westaway, *Anal. Chem.*, 38 (1966) 1657.
8 S. Latif, J. K. Haken and M. S. Wainwright, *J. Chromatogr.*, 258 (1983) 233.

CHROM. 20 939

DETERMINATION OF N-*n*-PROPYLNORAPOMORPHINE IN SERUM AND BRAIN TISSUE BY GAS CHROMATOGRAPHY–NEGATIVE ION CHEMICAL IONIZATION MASS SPECTROMETRY

T. M. TRAINOR and PAUL VOUROS*

Barnett Institute and Department of Chemistry, Northeastern University, 360 Huntington Avenue, Boston, MA 02115 (U.S.A.)

P. LAMPEN and J. L. NEUMEYER

Section of Medicinal Chemistry, College of Pharmacy and Allied Health Professions, Northeastern University, 360 Huntington Avenue, Boston, MA 02115 (U.S.A.)

and

R. J. BALDESSARINI and N. S. KULA

Mailman Research Center McLean Hospital and Departments of Psychiatry, Harvard Medical School, Belmont, MA 02178 (U.S.A.)

(Received August 31st, 1988)

SUMMARY

A method for the determination of the neuroactive compound N-*n*-propylnorapomorphine (NPA) in biological tissues is described. Isolation of NPA from serum or brain tissue was achieved via liquid–liquid extraction from phosphate-buffered tissue extract (0.25 *M*, pH 7.2) into ethyl acetate. The NPA, along with a [^{2}H$_7$]NPA analogue serving as internal standard, was converted to the corresponding bis(trifluoroacetyl) ester by treatment with excess trifluoroacetic anhydride at 75°C. The electrophoric derivatives were analyzed by fused-silica capillary gas chromatography–mass spectrometry in the negative ion chemical ionization mode. Selected ion monitoring of the [M − CF$_3$CO]$^-$ ions of derivatized NPA (*m/z* 390) and internal standard [^{2}H$_7$]NPA (*m/z* 397) permitted the quantitation of NPA in serum and brain samples obtained from rats treated with either free NPA or the prodrug methylenedioxy-NPA (MDO-NPA). Calibration was conducted down to a practical limit of assay sensitivity, at 0.50 ng NPA per ml of serum and 0.50 ng NPA per g of brain. The relative standard deviation for replicate serum samples spiked at 20 ng/ml was 4.2% (*n* = 5) and for brain samples at 10 ng/g, it was 3.6%. This method revealed differences in the free NPA brain/serum ratios in rats treated separately with the stereoisomers *R*-(−)-MDO-NPA and *S*-(+)-MDO-NPA.

INTRODUCTION

N-*n*-Propylnorapomorphine (NPA, 1, Table I) and apomorphine (APO, 2) are members of the aporphine class of isoquinoline-based alkaloids[1–3]. They have been

TABLE I

STRUCTURES OF APORPHINE DERIVATIVES
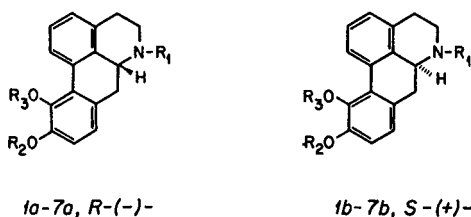
Compound	R_1	R_2	R_3
NPA (1a and 1b)	n-C_3H_7	H	H
APO (2a and 2b)	CH_3	H	H
MDO-NPA (3a and 3b)	n-C_3H_7	$R_2, R_3 = CH_2$	
(TFA)$_2$-NPA (4a and 4b)	n-C_3H_7	CF_3CO	CF_3CO
[$^2H_7$]NPA (5a)	n-$C_3{}^2H_7$	H	H
[$^2H_7$](TFA)$_2$-NPA (6a)	n-$C_3{}^2H_7$	CF_3CO	CF_3CO
10,11-DME-NPA (7a and 7b)	n-C_3H_7	CH_3	CH_3

tested clinically for the treatment of Parkinson's disease and other neuropsychiatric disorders[4–6]. Potent and selective activity of these compounds has been attributed to their agonist interactions with dopamine receptors in the mammalian central nervous system[2,7,8]. The clinical use of these compounds has been hampered by side effects (such as nausea), low oral absorption, chemical instability, and rather short duration of action. Effects to alleviate some of these problems has led to the development of several aporphine prodrugs in which the free catechol oxygens are bound to short-chain ether or ester groups. In particular, the compound methylenedioxy-N-*n*-propylnoraporphine (MDO-NPA, 3) provides for oral activity and somewhat extended duration of action, presumably via the slow metabolic conversion to the active free catechol, NPA, after prevention of its "first-pass" metabolism[6].

Numerous analytical approaches for the determination of either NPA or APO in biological samples include: gas chromatography (GC) with flame ionization detection (FID)[9–11], electron-capture detection (ECD)[12,13], or electron impact ionization mass spectrometry (MS)[14,15]; liquid chromatography (LC) with UV[16–20], fluorescent[21], or electrochemical detection (ED)[22–27]; and also thin-layer chromatography (TLC)[28–31], spectrophotometry[32], spectrofluorometry[33], radioenzymatic assay[34], and radioreceptor assay[6]. Each method possesses particular advantages and disadvantages, the choice of which depends largely on the required applications and detection limits and the instrumentation available. However, for the analysis of NPA at low concentration (ng/ml or ng/g) levels, which are pharmacologically significant, only the high-performance liquid chromatography (HPLC)–ED work of Sperk *et al.*[23] provides for linear detection at limits of less than 10 ppb*. For APO, detection limits below 10 ppb in biological matrices have been achieved using both HPLC–ED[22] and a non-linear radioreceptor assay[6].

The quantitation of drugs and metabolites at the trace level by GC–MS is an

---

* Throughout the article the American billion (10⁹) is meant.

important analytical technique[35]. The studies of Watanabe *et al.* detailed the determination of APO in plasma[14] and brain[15] by conversion of APO to the bis(trimethylsilyl) derivative and subsequent analysis by packed column GC–electron impact ionization MS. Low detection limits for APO in plasma (30 ng/ml) and brain (50 ng/g) were achieved when NPA was used as an internal standard.

We now report a GC–MS method for the determination of NPA in rat serum and brain that employs fused-silica column gas chromatography–negative ion chemical ionization mass spectrometry (GC–NICI-MS), an approach that provides the requisite sensitivity and selectivity for pharmacological studies. The precision and accuracy of quantitative GC–MS can be improved significantly through the use of stable isotope analogues as internal standards, for isotope dilution MS[36]. With the recent availability of multideuteriated aporphines of high isotopic purity[37], we have been able to develop an isotope dilution GC–MS assay of NPA in serum and brain tissue. Due to the trace levels of free NPA expected in animal tissues following treatment with typical mg/kg pharmacologic doses of NPA or its prodrug MDO–NPA, the demonstrated sensitivity of NICI-MS[38] was exploited. The conversion of NPA to the bis(trifuoroacetyl) derivative (4) was accomplished so as to provide an electrophoretic derivative necessary for this analysis.

EXPERIMENTAL

Reagents

Solvents used included methanol, toluene, and ethyl acetate of residue grade (J. T. Baker, Phillipsburg, NJ, U.S.A.). The following reagents were also obtained from Baker at the highest quality available: ascorbic acid, EDTA, phosphoric acid, sodium dihydrogenphosphate, disodium hydrogenphosphate, trisodium phosphate, and sodium hydroxide. The derivatization reagents trifluoroacetic anhydride (TFAA) and hexamethyldisilazane were obtained from Aldrich (Milwaukee, WI, U.S.A.). All of the aporphine compounds studied, including *R*-(−)-N-*n*-propylnorapomorphine hydrochloride (1a), *R*-(−)-10,11-methylenedioxy-N-*n*-propylnoraporphine hydrochloride (3a), *S*(+)-10,11-methylenedioxy-N-*n*-propylnoraporphine hydrochloride (3b), and ^{2}H$_7$-*R*-(−)-N-*n*-propylnorapomorphine hydrobromide (5a), were synthesized and characterized in these laboratories. Rat serum and brain from untreated animals was obtained from Charles River Laboratories (Wilmington, MA, U.S.A.).

Glassware

Serum and brain extractions were conducted in glass culture tubes (100 × 15 mm) containing PTFE-lined screw caps. Brain homogenates were centrifuged in Corex (VWR Scientific, Boston, MA, U.S.A.) 15-ml centrifuge tubes. Derivatizations were carried out in conical glass Reacti-vials (Pierce, Rockville, IL, U.S.A.) (1.0 ml) equipped with screw caps containing PTFE septa. All glassware employed was initially cleaned by soaking in a detergent solution (RBS-35, Pierce) for 24 h, rinsed with deionized water and then methanol, and dried overnight at 110°C. The glassware was then subjected to a vapor phase silanization with hexamethyldisilazane[39] so as to minimize analyte losses due to surface adsorption.

Solutions

Stock solutions of NPA and [^{2}H$_7$]NPA were prepared, on a daily basis, by

weighing out 1.000–2.000 mg of material into a 0.5-dram glass vial. The solid was transferred to a 10-ml volumetric flask by adding to the vial aliquots of methanol (3 × 0.5 ml) and quantitatively transferring the methanol solution via glass pipette to the volumetric flask, and filling to the mark with an aqueous ascorbic acid solution (2 g/l). Working solutions of 1.00 ng/μl NPA and 1.00 ng/μl [^{2}H$_7$]NPA were prepared by making appropriate dilutions of the stock solutions using the ascorbic acid solution as diluent. All NPA solutions were kept chilled (5°C) and in the dark prior to use to minimize degradation.

Treatment of animals

Male Sprague–Dawley rats, 190–210 g body weight (Charles River, Wilmington, MA, U.S.A.), were used for the experiments. Rats were given various doses of R-(–)-MDO-NPA and S-(+)-MDO-NPA in isotonic saline solution (1:4, v/v) by intraperitoneal (i.p.) injection. The animals were killed by decapitation 30 min later and the tissues were rapidly removed, frozen on dry ice, and kept frozen at -70°C until analysis after initial separation of serum from clotted rich-wound blood by centrifugation at 1000 g at 4°C for 15 min.

Extraction of rat serum samples

An aliquot of thawed rat serum, 1.0 ml, was transferred to a silanized glass culture tube containing 100 μl of the ascorbic acid solution and 100 μl of a 10 g/l EDTA solution in 0.25 M sodium hydroxide. The tubes, kept chilled throughout sample preparation by immersion in an ice–water bath, were spiked with 50 μl of the [^{2}H$_7$]NPA internal standard solution. At this level of spiking, the internal standard [^{2}H$_7$]NPA was introduced at a concentration of 50 ng per ml of serum. Each tube was then vortexed for 30 s and allowed to equilibrate in the ice bath for 30 min.

Following equilibration, ethyl acetate (2.0 ml) and the phosphate buffer (2.0 ml) were added to each tube and the tubes were shaken on a rotary shaker for 5 min. The tubes were then centrifuged for 5 min to effect phase definition. The organic layer (upper) was transferred via a silanized glass pipette to a clean culture tube containing chilled 0.1 M hydrochloric acid (0.5 ml). The tubes were placed on a rotary shaker for 5 min, centrifuged, and the organic layer (upper) was discarded. To the aqueous layer was then added phosphate buffer (2.0 ml) and the pH of the resulting solution checked with indicator paper to be between 7.0 and 7.4. A pH adjustment, if required, was then made by dropwise addition of a 0.5 N trisodium phosphate solution. Next, ethyl acetate (1.0 ml) was added, the mixture placed on a rotary shaker for 5 min, and centrifuged. The organic layer (upper) then was transferred via silanized pipette to a silanized 1.0-ml Reacti-vial. All of the solvent was removed via a stream of nitrogen and to the dried residue was added the derivatization reagent TFAA (100 μl).

Derivatization was accomplished by placing the glass Reacti-vial in an aluminum block held at a temperature of 75°C for 60 min. Just prior to GC–MS analysis, the excess TFAA was removed via a nitrogen stream and toluene (25 μl) was added to dissolve the derivatized sample.

Extraction of rat brain samples

Individual rat brains, previously frozen, were transferred in dry ice, weighed on a balance to a precision of 0.01 g. The brain was then minced into ten or more pieces

and added to a chilled 15-ml Corex centrifuge tube containing 5.0 ml 0.1 *M* hydrochloric acid, 100 μl of the ascorbic acid solution, and 100 μl of the EDTA–sodium hydroxide solution. The tubes were spiked with 50 μl of the [^{2}H$_7$]NPA internal standard solution. At this level of spiking, the internal standard [^{2}H$_7$]NPA was introduced at an absolute amount of 50 ng or at a concentration of 25–35 ng per g of brain, depending on the net weight.

The contents of the centrifuge tubes were homogenized using a high-speed spinning PTFE-tipped rod for 60 s. The brain homogenates were then centrifuged at 12 000 *g* for 15 min. The clear supernatant from each tube was transferred to a clean culture tube and 3.0 ml ethyl acetate were added. The mixture was shaken for 10 min on the rotary shaker, centriguged for 10 min at 1200 *g*, and the upper organic layer was discarded. The pH of the aqueous solution was adjusted by dropwise addition of a 0.5 *M* trisodium phosphate solution to give a pH of 7.0–7.4, checked with pH paper. For a majority of samples this pH adjustment required 0.70 ml of base. Ethyl acetate (2.0 ml) was then added to the tube, which was then shaken for 10 min, and then centrifuged for 10 min at 1200 *g*.

The upper organic layer was again transferred to a 1.0-ml Reacti-vial, the ethyl acetate removed via a nitrogen stream, and 100 μl of TFAA were added to the residue. The derivatization was carried out at 75°C for 1 h. After allowing the vials to cool, the excess TFA was removed via a nitrogen stream, and 25 μl of toluene were added.

Gas chromatography–mass spectrometry

All GC–MS analyses were carried out on a Finnigan 4021 GC–MS system equipped with the pulsed positive ion negative ion chemical ionization (PPINICI) option. Control of the mass spectrometer and acquisition of data were carried out with the Finnigan-Incos data system and software. The Finnigan Model 9600 gas chromatograph was modified to accept a capillary on-column injector obtained from J&W Scientific (Rancho Cordova, CA, U.S.A.). A DB-5 fused-silica capillary column (15 m × 0.25 mm I.D.) (J&W Scientific) with a film thickness of 0.25 μm was employed for all analyses and was inserted directly into the ion source of the mass spectrometer. Helium (Matheson, UHP) was used as carrier gas, while methane (Matheson, UHP) serving as the CI reagent gas was admitted into the source to provide a pressure of 0.30 Torr. Mass spectrometer operating parameters included: 70 eV ionizing potential, 0.50 mA filament current, 250°C source temperature, and 1000 V electron multiplier voltage. Optimal mass spectrometer ion source tuning was conducted by admitting perfluorotri-*n*-butylamine (FC-43) into the source and monitoring the intensity and peak shape of an ion at *m/z* 395, a minor fragment ion of this calibrant compound. The GC oven initially was set at 95°C and , upon injection, ramped linearly to 250°C at a rate of 15°C/min. Under these conditions, the bis(trifluoroacetyl) derivative of NPA eluted at a temperature of 220°C with a retention time of 7.5 min. For the trace level analyses, selected ion monitoring data acquisition was accomplished by scanning on an equal basis for a total of 0.45 s over the two ions of interest, *m/z* 390 and *m/z* 397.

Calculation

Individual calibration curves were constructed for rat serum and brain by preparing drug-free serum and brain samples using the identical procedures as described for the treated samples, with the exception that known amounts of unlabeled

R-($-$)-NPA were spiked into the samples prior to extraction. For serum, levels of 0, 1.0, 2.0, 5.0, 10, 20, 50, and 100 ng NPA per ml of serum were prepared. For brain, total fortifications of 0, 1.0, 2.0, 5.0, 10, 20, 50 and 100 ng NPA were added to individual brains (1.0–2.0 g wet weight).

Peak areas in the ion current profiles for NPA (m/z 390) and [^{2}H$_7$]NPA (m/z 397) were integrated using the Finnigan-Incos software. Calibration curves for both serum and brain were constructed by plotting the ion current ratios I_{390}/I_{397} *versus* the corresponding concentration ratios NPA/[^{2}H$_7$]NPA. Linear regression analysis on the resulting plots was performed to provide the constants for the equation $y = mx + b$ where m represents the slope and b the intercept of the curve. Concentrations of NPA in the treated samples were obtained by introducing the observed ion current ratio into the equation $C_{NPA} = (I_{390}/I_{397} - b)/m$ and solving for C_{NPA}.

As a check of the method's precision and accuracy, replicate blank rat serum samples were spiked at a level of 20 ng NPA per ml and replicate blank rat brain samples spiked at a total amount of 10 ng NPA per brain sample (1–2 g). Extraction and analysis were performed on these samples concurrently with samples from treated animals. To assess contributions of interferences from tissue matrix or reagents, blank samples were prepared and analyzed alongside samples from treated animals.

RESULTS AND DISCUSSION

The NICI mass spectrum of the bis(trifluoroacetyl) ester derivative of NPA (4) consists primarily of the fragment ions [M$-$CF$_3$CO]$^-$ at m/z 390 and [CF$_3$CO]$^-$ at m/z 113 (Fig. 1). The [M$-$CF$_3$CO]$^-$ ion from this electrophoretic derivative was
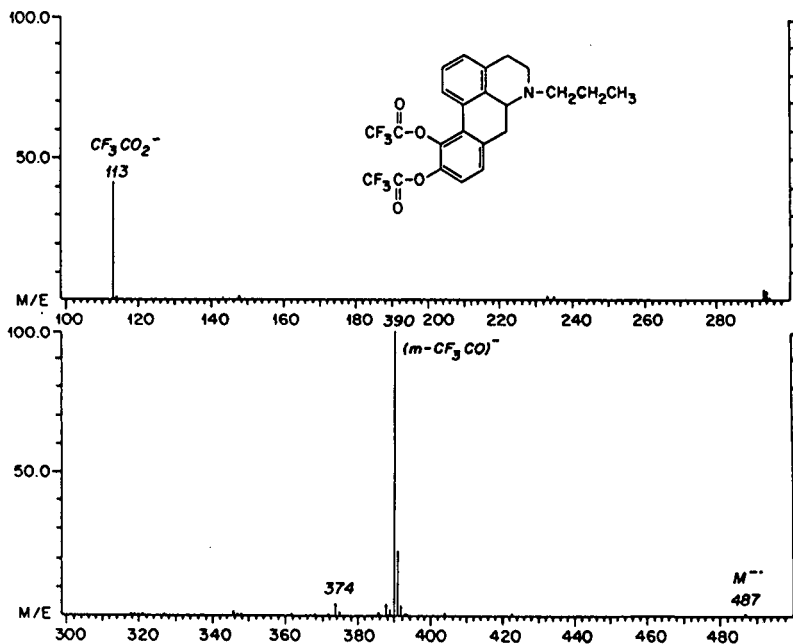

Fig. 1. Electron-capture negative ion CI mass spectrum of bis(TFA)-NPA.

found to provide both adequate sensitivity and specificity for the cetermination of NPA at the required ppb levels in serum and brain. Picogram quantities of derivative 4 injected into the GC–MS system can be observed readily by operating under methane conditions with selected ion monitoring data acquisition. Stable isotope dilution with the internal standard [^{2}H$_7$]NPA (5) provided a reliable means of quantitation for NPA, as the NICI-MS spectrum of derivatized [^{2}H$_7$]NPA (6) gave the expected [M − CF$_3$CO]$^-$ ion at m/z 397.

The isolation and derivatization procedures for NPA were adapted largely from a GC–ECD method developed previously in these laboratories[12]. Extraction with ethyl acetate provided for high recoveries of NPA or APO from biological tissues when sample pH is within the optimum range of 6–8[10,17]. Furthermore, back-extraction into dilute hydrochloric acid has been employed to facilitate the removal of neutral and acidic components known to have detrimental effects on GC-based assays of NPA or APO in serum[9,12]. As degradation of the catechol NPA by oxidation to the corresponding quinone[40] has been a concern in these and related catecholamine[41] assays, precautions taken to reduce this occurrence included the use of ascorbic acid as an antioxidant and the use of EDTA[18,22].

Typical selected ion monitoring mass chromatograms are shown for a calibration sample of rat serum spiked at 1.0 ng/ml (Fig. 2), where the ion current traces at m/z 390 and m/z 397 are from the derivatives 4 and 6, respectively. With the fused-silica capillary column employed, the labeled analogue (6) eluted approximately 3 s before the unlabeled derivative (4) with a retention time of 7.5 min. Inspection of the ion current profiles obtained for all blank tissue samples revealed no interference at m/z 390 near the retention time of 4.

The linear regression analyses performed on the calibration curves generated using drug-free rat serum and brain extract revealed excellent linearity and are summarized in Table II. Method precision and accuracy were assessed by spiking
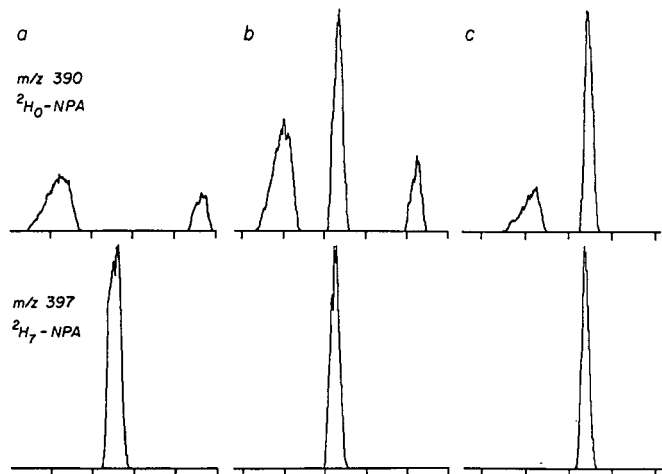
Fig. 2. Determination of NPA in rat serum. Mass chromatograms obtained from rat serum extracts at m/z 390 [M − CF$_3$CO]$^-$ for NPA and m/z 397 [M − CF$_3$CO]$^-$ for [^{2}H$_7$]NPA. (a) Blank serum sample. (b) Blank serum spiked at 20 ng/ml NPA. (c) Serum extract from a 3.0-mg/kg *R*-(−)-MDO-NPA treatment (4.2 ng/ml NPA observed in this sample). Note: 50 ng [^{2}H$_7$]NPA spiked in all serum samples; all mass chromatograms normalized to [^{2}H$_7$]NPA peaks.

TABLE II

LINEAR REGRESSION ANALYSIS OF NPA CALIBRATION CURVES

Matrix	Linear regression constants*		
	m	b	r^2
Serum	1.30	−0.059	0.998
Brain	1.42	−0.056	0.996

* $y = mx + b$; $y = I_{390}/I_{397}$; $x = $ NPA/$[^2H_7]$NPA.

replicate rat serum and brain samples with known levels of NPA and analyzing. The results (Table III) indicate a relative standard deviation of 4.2% at the 20 ng/ml level for rat serum ($n = 5$) and 3.6% at the 10 ng level in rat brain ($n = 3$). It should be noted that these spiking studies were not carried out alongside the calibration study, but were conducted on separate days with fresh solutions.

TABLE III

METHOD PRECISION AND ACCURACY

Matrix	NPA spike	NPA calc.	S.D.	Rel. S.D.	n
Serum	20 ng/ml	19.5 ng/ml	0.81	4.2%	5
Brain	10 ng/g	10.0 ng/g	0.36	3.6%	3

This method was utilized for pharmacological studies concerning the metabolic production of NPA *in vivo* following the administration of the prodrug MDO-NPA (6). Earlier work by Sperk *et al.*[23] and Maksoud *et al*[12] detected free catechol NPA in the tissue of animals treated with the prodrug MDO-NPA. The present study served to confirm these identifications, as the GC–MS data provide a more definite identification than either the HPLC–ED[23] or GC–ECD[12] methods.

TABLE IV

DETERMINATION OF NPA IN SERUM AND BRAIN AFTER TREATMENT WITH MDO-NPA

Treatment (mg/kg)	NPA concentration*,**		Brain/serum concentration ratio
	Serum (ng/ml)	Brain (ng/g)	
R-(−)-MDO-NPA(1.0)	2.77 ± 0.10	19.6 ± 10.4	7.1
R-(−)-MDO-NPA(3.0)	7.64 ± 3.55	46.0 ± 25.1	6.0
R-(−)-MDO-NPA(10)	19.6 ± 2.30	114 ± 32.4	5.8
S-(+)-MDO-NPA(1.0)	14.1 ± 11.3	7.87 ± 4.59	0.56
S-(+)-MDO-NPA(3.0)	118 ± 15.3	38.1 ± 6.23	0.32
S-(+)-MDO-NPA(10)	118 ± 31.6	35.2 ± 8.70	0.30

* Animals sacrificed 30 min after i.p. injection of test agents.
** Concentrations represent the mean ± standard deviation from the separate analysis of three identically dosed animals.
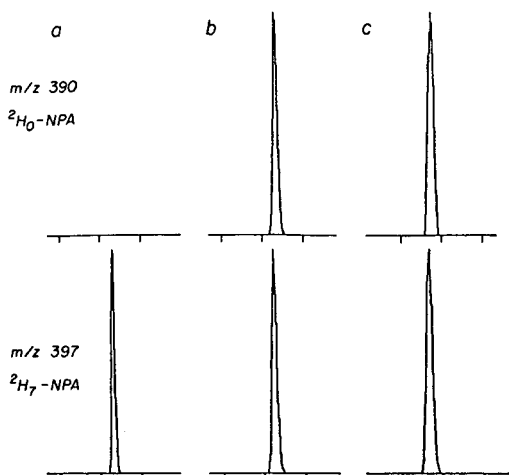
Fig. 3. Determination of NPA in rat brain. Mass chromatograms from rat brain extracts at m/z 390 [M − CF$_3$CO]$^-$ for NPA and m/z 397 [M − CF$_3$CO]$^-$ for [^{2}H$_7$]NPA. (a) Blank brain sample. (b) Blank brain spiked at 14 ng/g NPA. (c) Brain extract from a 3.0-mg/kg *R*-(−)-MDO-NPA treatment (21 ng/g NPA observed in this sample). Note: 50 ng [^{2}H$_7$]NPA spiked in all brain samples (1–2 g), and mass chromatograms normalized to [^{2}H$_7$]NPA peaks.

Another biological question we wished to explore in utilizing the GC–NICI-MS method was a comparison of resultant NPA levels in the rat after treatment with either stereoisomer *R*-(−)-MDO–NPA (3a) or *S*-(+)-MDO–NPA (3b). Previous pharmacological studies have shown marked differences in the behavior of rats treated with *R*-(−)-NPA (1a) *versus* *S*-(+)-NPA (1b), their MDO prodrugs, or with *R*-(−)-APO (2a) *versus* *S*-(+)-APO (2b)[42]. In this study, the stereoisomers *R*-(−)-MDO–NPA and *S*-(+)-MDO–NPA were administered to rats at three dose levels, 1.0, 3.0, and 10 mg/kg (i.p.). The animals were sacrificed 30 min later and the serum and brain analyzed for the presence of free NPA, the presumed bioactive form of MDO-NPA. In Table IV are presented the results of this experiment, and representative selected ion monitoring mass chromatograms for both serum and brain extracts from animals treated in this study are shown in Figs. 2 and 3, respectively.

Distinct differences in the tissue concentrations and distribution between serum and brain tissue of free *R*-(−)-NPA and *S*-(+)-NPA were observed. At all three dose levels, a concentration of *R*-(−)-NPA predominated in the brain (brain/serum) ratios between 5.8 and 7.1) while concentration of *S*-(+)-NPA favored serum (brain/serum ratios between 0.30 and 0.56). These differences may arise from isomeric selectivity in the distribution of NPA between serum and brain or to isomeric differences in the metabolism of MDO-NPA by enzymatic O-dealkylation conversion of MDO-NPA to free NPA. An analogous situation was observed for the regiospecific and stereoselective microbial O-dealkylation of 10,11-dimethoxy-NPA (7) reported by Neumeyer *et al.*[43]. Work is currently in progress to clarify this phenomenon.

ACKNOWLEDGEMENTS

REFERENCES

1 J. L. Neumeyer, S. Lal and R. J. Baldessarini, in G. L. Gessa and G. U. Corsini (Editors), *Apomorphine and Other Dopaminonimetics, Vol. 1, Basic Pharmacology*, Raven Press, New York, 1981, pp. 209–218.
2 J. L. Neumeyer in D. Phillipson (Editor), *The Chemistry and Biology of Isoquinoline Alkaloids*; Springer-Verlag, Berlin, 1985, pp. 146–170.
3 M. Shamma, *The Isoquinoline Alkaloids-Chemistry and Pharmacology*, Academic Press, New York, 1972.
4 R. S. Schwab and A. C. England, *Trans. Am. Neurol. Assoc.*, 81 (1956) 51–57.
5 C. Tamminga, M. D. Gotts and M. R. Miller, *Acta Pharm. Suec.*, 2 (1983) 153–158.
6 R. J. Baldessarini, G. W. Arana, N. S. Kula, A. Campbell and M. Harding in G. L. Gessa and G. U. Corsini (Editors), *Apomorphine and Other Dopaminomimetics, Vol. 1, Basic Pharmacology*, Raven Press, New York, 1981, pp. 219–228.
7 J. L. Neumeyer, R. J. Baldessarini, G. W. Arana, S. A. Cohen and A. Campbell, in C. Melchiorre and G. M. Gianella (Editors), *Highlights in Receptor Chemistry*, Elsevier, Amsterdam, 1984, pp. 49–74.
8 J. L. Neumeyer, S. J. Law and J. S. Lamont in G. L. Gessa and G. U. Corsini (Editors), *Apomorphine and Other Dopaminomimetics, Vol. 1, Basic Pharmacology*, Raven Press, New York, 1981, pp. 209–218.
9 D. M. Baaske, J. E. Keiser and R. V. Smith, *J. Chromatogr.*, 140 (1977) 57–64.
10 R. V. Smith and A. W. Stocklinski, *Anal. Chem.*, 47 (1975) 1321–1325.
11 R. V. Smith and A. W. Stocklinsky, *J. Chromatogr.*, 77 (1972) 419–421.
12 H. M. Maksoud, S. H. Kuttab, J. L. Neumeyer and P. Vouros, *J. Chromatogr.*, 274 (1983) 149–159.
13 J. R. Miller, J. W. Blake and T. Tobin, *Res. Commun. Chem. Pathol. Pharmacol.*, 15 (1976) 447–455.
14 H. Watanabe, S. Nakano and N. Ogawa, *J. Chromatogr.*, 229 (1982) 95–102.
15 H. Watanabe, S. Nakano, N. Ogawa and T. Suzuki, *Biomed. Mass Spectrom.*, 7 (1980) 160–163.
16 R. V. Smith, A. E. Klein and D. O. Thompson, *Mikrochim. Acta*, Part I (1980) 151–187.
17 B.-M. Eriksson, B.-A. Persson and M. Lindberg, *J. Chromatogr.*, 185 (1980) 575–581.
18 R. V. Smith, A. E. Klein, A. M. Clark and D. W. Humphrey, *J. Chromatogr.*, 179 (1979) 195–198.
19 R. V. Smith, A. E. Klein, R. E. Wilcox and W. H. Riffee, *J. Pharm. Sci.*, 70 (1981) 1144–1147.
20 R. V. Smith, D. W. Humphrey, S. Szeinbach and J. C. Glade, *Anal. Lett.*, 12 (1979) 371–379.
21 R. V. Smith and M. R. De Moreno, *J. Chromatogr.*, 274 (1983) 376–380.
22 G. Bianchi and M. Kandi, *J. Chromatogr.*, 338 (1985) 230–235.
23 G. Sperk, A. Campbell, R. J. Baldessarini, A. Stoll and J. L. Neumeyer, *Neuropharmacology*, 21 (1982) 1311–1316.
24 R. Yang, J. Y. Hsieh, K. S. Kendler and K. L. Davis, *J. Liq. Chromatogr.*, 7 (1984) 191–200.
25 R. V. Smith and D. W. Humphrey, *Anal. Lett.*, 14 (1981) 601–613.
26 D. W. Humphrey, M. E. Goldman, R. E. Wilcox, C. K. Erickson and R. V. Smith, *Microchem. J.*, 25 (1980) 186–195.
27 B. H. Westerink and A. S. Horn, *Eur. J. Pharmacol.*, 58 (1979) 39–48.
28 J. Combie, J. W. Blake, T. E. Nugent and T. Tobin, *Res. Commun. Chem. Pathol. Pharmacol.*, 35 (1982) 27–41.
29 P. W. Erhardt, R. V. Smith, T. T. Sayther and J. E. Keiser, *J. Chromatogr.*, 116 (1976) 218–224.
30 R. V. Smith and M. R. Cook, *J. Pharm. Sci.*, 63 (1974) 161–162.
31 R. V. Smith, M. R. Cook and A. W. Stocklinski, *J. Chromatogr.*, 87 (1973) 294–297.
32 P. N. Kaul, E. Brochmann-Hansen and E. L. Way, *J. Pharm. Sci.*, 50 (1961) 244–247.
33 A. M. Burkman and W. K. Van Tyle, *J. Pharm. Sci.*, 60 (1971) 1736–1738.
34 J. W. Kebabian, *J. Neurochem.*, 30 (1978) 1143–1148.
35 W. A. Garland and M. L. Powell, *J. Chromatogr. Sci.*, 19 (1981) 392–434.
36 S. P. Markey, *Biomed. Mass Spectrom.*, 8 (1981) 426–430.
37 J. L. Neumeyer, Y. Gao, T. M. Trainor and P. Vouros, *J. Labelled Comp. Radiopharm.*, 25 (1987) 293–299.
38 K. F. Faull and J. D. Barchas, in D. Glick (Editor), *Methods of Biochemical Analysis*, Vol. 29, Wiley, New York, 1983, pp. 325–383.
39 D. C. Fenimore, C. M. Davis, J. H. Whitford and C. A. Harrington, *Anal. Chem.*, 48 (1976) 2289–2290.
40 H. Y. Cheng, E. Strope and R. N. Adams, *Anal. Chem.*, 51 (1979) 2243–2246.
41 K. F. Faull and J. D. Barchas, in S. Parvez, T. Nagatsu and H. Parvez (Editors), *Methods in Biogenic Amine Research*, Elsevier, Amsterdam, 1983, pp. 189–236.
42 A. Campbell, R. J. Baldessarini, N. S. Kula, V. J. Ram and J. L. Neumeyer, *Brain Res.*, 403 (1986) 393–397.
43 J. L. Neumeyer, H. M. Abdel-Maksoud, T. M. Trainor, P. Vouros and P. J. Davis, *Biomed. Mass Spectrom.*, 13 (1986) 223–229.

CHROM. 20 906

PERFLUORO AND CHLORO AMIDE DERIVATIVES OF ANILINE AND CHLOROANILINES

A COMPARISON OF THEIR FORMATION AND GAS CHROMATOGRAPHIC DETERMINATION BY MASS SELECTIVE AND ELECTRON-CAPTURE DETECTORS

HING-BIU LEE

Research and Applications Branch, National Water Research Institute, Environment Canada, 867 Lakeshore Road, P.O. Box 5050, Burlington, Ontario L7R 4A6 (Canada)

(First received April 22nd, 1988; revised manuscript received August 19th, 1988)

SUMMARY

The preparation of the amide derivatives of aniline and 16 chloroanilines by reaction with trifluoroacetic, pentafluoropropionic, heptafluorobutyric, chloroacetic, and dichloroacetic anhydrides is described. Separation of these derivatives by capillary columns was investigated and mass spectral data of 85 derivatives obtained by a mass selective detector were summarized. Electron-capture relative response factors of the amides were also obtained. A comparison of the five derivatization reactions indicated that the heptafluorobutyryl derivatives were most suitable for the analysis of the present group of anilines.

INTRODUCTION

Aniline is an industrial chemical of many applications. It is used to produce numerous azo dyes or dye intermediates and aniline-based pharmaceuticals. Aniline and its chlorinated analogues are also used in the manufacture of many carbamate and urea pesticides. The production of aniline in the United States totalled 823 million lbs. in 1986[1]. Since the toxicity of aniline and other aromatic amines to mammals and fish is well established[2,3], there is a need to develop analytical procedures for the determination of such compounds in toxic wastes or as contaminants in the environment.

Although the analyses of underivatized aniline and halogenated anilines have been performed by some workers using high-performance liquid chromatography (HPLC)[4,5] with suitable detectors, others preferred to analyze aniline derivatives by gas chromatography (GC) using electron-capture and other detectors[6,7] to enhance sensitivity and/or selectivity. Among the derivatization procedures, acylation of the amino group in aromatic amines by carboxylic acid anhydrides is one of the most popular reactions, although other acylation reactions with benzyl halide reagents and

alkylation reactions with substituted phenyl and benzyl halides have also been performed[6,8].

Recently, the analysis of aniline and a few other halogenated anilines using several acylation and alkylation procedures was reported by Bradway and Shafik[8]. The determination of aniline and aminophenols in aqueous solutions by a combined acetylation and trifluoroacetylation procedure has also been demonstrated by Coutts *et al.*[9]. Other acylation methods for the analysis of aromatic amines using electron-capture[10] and nitrogen-selective[11] detectors were also reported. Before an analytical method for chlorinated anilines is developed for environmental samples, it is necessary to select the most desirable derivative by comparing their chromatographic and synthetic properties. In this work, we shall describe the preparation of amide derivatives resulting from the reactions of three perfluoro anhydrides: trifluoroacetic anhydride (TFAA), pentafluoropropionic anhydride (PFPA), and heptafluorobutyric anhydride (HFBA) and two chloroacetic anhydrides: monochloroacetic anhydride (CAA) and dichloroacetic anhydride (DCAA) with aniline and 16 chloroanilines. The chloroanilines studied in this work included three monochloro-, six dichloro-, four trichloro-, and two tetrachloroanilines as well as pentachloroaniline. See Table I for the complete list. A comparison of the above five types of amide derivatives in terms of their ease of formation, completeness of reaction, and interference by reaction side-products will be presented. Their mass spectral data (MSD) and chromatographic properties will also be discussed.

EXPERIMENTAL

Apparatus

For GC–MS work, a Hewlett-Packard Model 5880A gas chromatograph equipped with a Level 2 terminal, split/splitless injection port, a Model 5970B mass selective detector and data system was used. For GC–electron-capture detection (ECD) work, a Hewlett-Packard Model 5880A gas chromatograph equipped with a Level 4 terminal, spit/splitless injection port and an electron-capture detector was used.

Chromatographic conditions

MSD analysis. A 30 m × 0.25 mm I.D. SPB-5 (Supelco) fused-silica capillary column was directly interfaced to the electron-impact ion source for maximum sensitivity. The operating temperatures were: injection port, 250°C; interface, 280°C column initial temperature, 70°C (held for 0.5 min); programming rates, 30°/min (from 70°C to 90°C) and 5°/min (from 90°C to 240°C). Carrier gas was helium and column head pressure was 4 p.s.i. Septum purge flow was 1.5 ml/min. Splitless valve was on for 0.5 min after a 1-μl sample was injected in the splitless mode using the hot needle technique[12].

ECD analysis. A 30 m × 0.25 mm I.D. DB-5 (J. and W. Scientific) fused-silica capillary column was used. The operating temperatures were: injection port 250°C; detector, 300°C; column initial temperature, 70°C (held for 0.5 min); programming rates, 30°/min (from 70°C to 140°C), 1°/min (from 140°C to 160°C) and 10°/min (from 160°C to 240°C). Carrier gas was helium with a column head pressure of 10 p.s.i. and linear velocity of 27 cm/s at 240°C. Make-up gas for ECD was argon–methane (95 : 5)

TABLE I

MASS NUMBER (m/z) AND RELATIVE ABUNDANCE (%) OF SOME CHARACTERISTIC IONS OBSERVED FOR THE TFAA DERIVATIVES OF ANILINES UNDER EI CONDITIONS

Parent aniline	$M^{+\cdot}$	$(M-Cl)^+$	$(M-CF_3)^+$	$(M-COCF_3)^+$	Others
Aniline	189 (100)	–	120 (85)	92 (58)	77 (64), 65 (39)
2-Chloro	223 (37)	188 (100)	154 (13)	126 (42)	99 (25)
3-Chloro	223 (100)	–	154 (77)	126 (64)	99 (24)
2,4,-Dichloro	257 (34)	222 (110)	188 (8)	160 (50)	133 (35)
4-Chloro	223 (100)	–	154 (35)	126 (74)	99 (26)
2,5-Dichloro	257 (17)	222 (100)	188 (5)	160 (13)	133 (19)
2,3-Dichloro	257 (33)	222 (100)	188 (11)	160 (29)	133 (24)
2,6-Dichloro	256 (9)	222 (100)	188 (6)	160 (28)	133 (23)
3,5-Dichloro	257 (94)	–	188 (100)	160 (62)	133 (27)
2,4,5-Trichloro	293 (38)	256 (100)	222 (6)	196 (34)	167 (33)
2,4,6-Trichloro	291 (19)	256 (100)	222 (7)	196 (35)	169 (24)
2,3,4-Trichloro	291 (35)	256 (100)	222 (6)	196 (34)	167 (22)
3,4-Dichloro	257 (100)	–	188 (67)	160 (87)	133 (85)
2,3,4,5-Tetrachloro	327 (39)	292 (100)	258 (5)	230 (27)	203 (33)
2,3,5,6-Tetrachloro	327 (8)	292 (100)	258 (6)	230 (13)	203 (26)
3,4,5-Trichloro	293 (100)	–	222 (61)	196 (88)	167 (22)
Pentachloro	361 (12)	326 (100)	292 (4)	264 (16)	237 (29)

with a flow-rate of 25 ml/min. Septum purge flow was 1.5 ml/min. Splitless time was 0.5 min and 2-μl injections were made manually as per MSD analysis.

Mass spectral data acquisition

Full scan GC–electron impact (EI)-MS data were obtained by scanning the MSD from m/z 50 to 500 at a rate of 0.95 scans per s and a scan threshold of 1000. The electron energy and electron multiplier voltage were 70 eV and 2000 V, respectively.

Materials

Chloroanilines. Aniline and all chloroanilines except pentachloroaniline were obtained from Aldrich (Milwaukee, WI, U.S.A.). Pentachloroaniline was obtained from Riedel-de Haen through Caledon (Georgetown, Canada). Stock solutions of individual chloroaniline at 1000 μg/ml were prepared in methanol. A mixture of all 17 anilines each at 20 μg/ml was also prepared in methanol and used for the synthesis of amide derivatives.

Anhydrides. TFAA, PFPA, and HFBA were purchased from Pierce (Rockford, IL, U.S.A.). CAA and DCAA were obtained from Aldrich.

Solvents. All solvents were distilled-in-glass grade available from Burdick and Jackson.

Phosphate buffer. A 0.05 M solution was prepared by dissolving potassium dihydrogenphosphate (0.025 mol) and sodium dihydrogenphosphate (0.025 mol) in 1 l of organics-free water.

Derivatization of anilines

A 0.5-ml aliquot of the 17 aniline mixture was transferred to a 15-ml centrifuge tube. After the solvent (methanol) was evaporated and replaced by 100 μl of benzene, 100 μl of the anhydride (except CAA) was added. For the CAA reactions, 500 μl of a saturated solution of chloroacetic anhydride in benzene was used. The contents were mixed well by a vortex mixer and were allowed to stand at 22°C (room temperature) or 60°C. The optimal reaction conditions were: (a) 15 min at 22°C for TFAA, (b) 2 h at 22°C for PFPA, (c) 30 min at 60°C for HFBA, (d) 60 min at 60°C for CAA, and (e) 16 h at 22°C for DCAA. In all cases, the reaction mixture was sealed with a tightly-capped ground glass stopper to prevent losses. After the reaction time had elapsed, 4 ml of the above phosphate buffer was added to the reaction mixture. Since TFAA reacts violently with water, addition of the aqueous buffer must be very slow. The amide derivatives of chloroanilines were isolated by extracting the mixture twice with 4 ml of benzene. The combined organic extract was passed through a 5-cm anhydrous sodium sulfate column prepared in a Pasteur pipette. After water removal, the solvent was evaporated and replaced by 1 ml of isooctane using a gentle stream of nitrogen and a water bath of 60°C. This solution was ready for MSD analysis or for further column cleanup, if required (see later discussion). For ECD analysis, a 1:100 dilution of the above solution with isooctane was made before injection into the gas chromatograph.

Column cleanup

Cleanup of amide derivatives of chloroanilines was achieved with a 1 g 5% deactivated silica gel column prepared in a disposable Pasteur pipette. After the column was washed with 5 ml of hexane, a 500-μl aliquot of the concentrated sample in isooctane was applied to the column. After a pre-elution of the column with 5 ml of hexane, quantitative recovery of the amides was obtained by eluting with 10 ml of benzene.

RESULTS AND DISCUSSION

Derivatization of anilines

Although the derivatization of anilines requires extra manipulation in the analytical procedure, the resulting amide derivatives have the benefits of being more stable and amenable to column cleanup than the parent compounds. The formation of derivatives with perfluoro and chloro substitution can further enhance the detection limits of the non-chlorinated as well as the mono- and dichloroanilines when an electron-capture detector is used. In order to compare the chromatographic properties and to select the most desirable amide derivatives of the present group of anilines, their reactions with three commonly used perfluorocarboxylic acid anhydrides as well as chloro- and dichloro-acetic anhydrides were evaluated.

Among all the anhydrides tested, TFAA was the most reactive. In fact, the TFAA reaction was complete in 5 min at room temperature with all anilines except for pentachloroaniline (*ca.* 70% reacted) and for 2,3,5,6-tetrachloroaniline (*ca.* 85% reacted). Quantitative formation of the trifluoro derivatives of all anilines was achieved in 15 min. Acylation of anilines with PFPA was also fast. Maximum yields of the PFPA derivative were obtained in 15 min for all anilines but pentachloroaniline and 2,3,5,6-tetrachloroaniline, although complete reaction for the above two anilines

would require 2 h at room temperature. Among the three perfluoro anhydrides, HFBA was the slowest to react with anilines. Nevertheless, quantitative yields of all heptafluoro derivatives was achieved in 18 h. However, the same reaction was complete in 30 min if the reaction temperature was raised to 60°C.

Although chloroacetic anhydride reacted readily with most anilines, its reactions with 2,3,5,6-tetrachloroaniline and pentachloroaniline were far from complete even after an 18-h reaction period at room temperature or a 60-min reaction at 60°C. The reaction of dichloroacetic anhydride with all anilines proceeded to completeness in 18 h at room temperature.

The working range of the HFBA derivatization procedure was further tested by reacting mixtures of anilines at 100, 10, 1, and 0.1 μg levels with 100 μl of the anhydride. In all cases, no unreacted aniline was observed at the end of the reactions, indicating that the derivatization was quantitative over a 1000-fold range.

Cleanup

The reaction products of chloroanilines and the three perfluoro anhydrides were sufficiently free of interference for subsequent analysis and, unless a determination of anilines at low levels by ECD was performed, no further cleanup was required. However, more side-products were experienced with the CAA and especially the DCAA reactions so that the silica gel column cleanup described above was necessary to improve the quality of the chromatograms.

GC separation of aniline derivatives

As shown in Figs. 1–5, separation of the perfluoro and chloro amide derivatives of the 17 anilines on a 30-m SPB-5 column was satisfactory. For the heptafluoro-butyryl (Fig. 3) and the dichloroacetyl (Fig. 5) derivatives, complete resolution of all aniline derivatives was achieved. However, the pentafluoropropionyl derivatives of
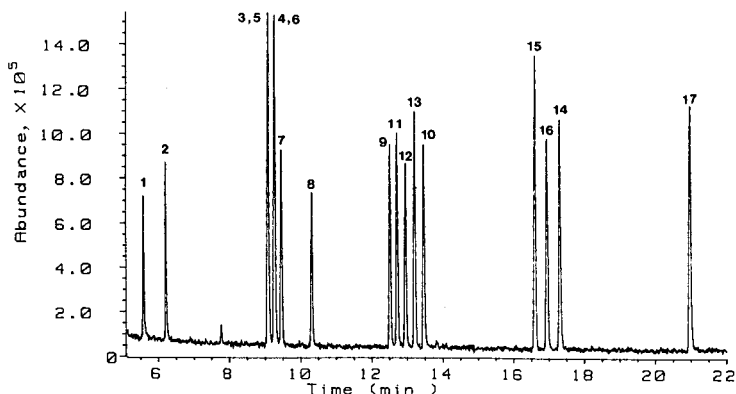

Fig. 1. Total ion chromatogram of the TFAA derivatives of anilines. See Experimental for GC–MS conditions. Peaks: 1 = aniline, 2 = 2-chloroaniline, 3 = 3-chloroaniline, 4 = 4-chloroaniline, 5 = 2,4-dichloroaniline, 6 = 2,5-dichloroaniline, 7 = 2,3-dichloroaniline, 8 = 2,6-dichloroaniline, 9 = 3,5-di-chloroaniline, 10 = 3,4-dichloroaniline, 11 = 2,4,5-trichloroaniline, 12 = 2,4,6-trichloroaniline, 13 = 2,3,4-trichloroaniline, 14 = 3,4,5-trichloroaniline, 15 = 2,3,4,5-tetrachloroaniline, 16 = 2,3,5,6-tetra-chloroaniline, and 17 = pentachloroaniline.
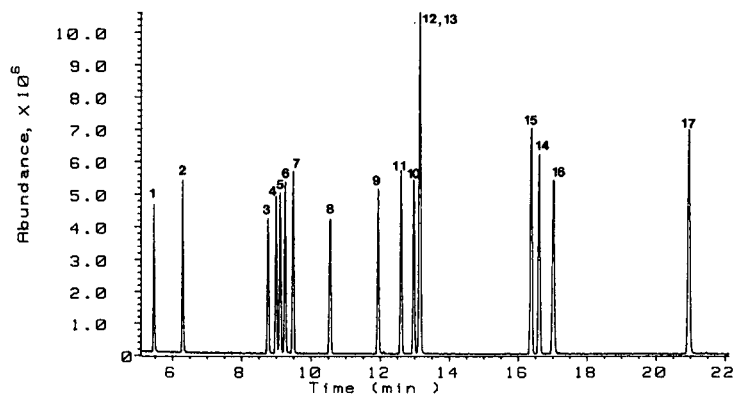
Fig. 2. Total ion chromatogram of PFPA derivatives of anilines. See Fig. 1 for peak identification.

2,3,4- and 2,4,6-trichloroanilines (Fig. 2) as well as the monochloroacetyl derivatives of 2,4- and 2,6-dichloroanilines (Fig. 4) were unresolved. Similarly, two pairs of the trifluoroacetyl derivatives, namely 3-chloroaniline and 2,4-dichloroaniline together with 4-chloroaniline and 2,5-dichloroaniline, were also unresolved (Fig. 1). The same order of elution and similar resolution of the amide derivatives were obtained when a 30-m DB-5 column was used. Attempts on other fused-silica capillary columns such as a 25-m OV-1 and a 15-m OV-17 column were also made, however, a less number of resolvable peaks was observed with these columns than the SPB-5 or DB-5 column. Thus the OV-1 and OV-17 columns were not further evaluated.

Other than a few exceptions noted below, the order of elution on the SPB-5 or DB-5 column for all amide derivatives with the same level of chlorination on the ring was very similar. For instance, the first and the last derivatives eluted were always those of aniline and pentachloroaniline, respectively. For the monochloroanilines, the order of elution was invariably in the sequence of 2-, 3-, and 4-. For the dichloroanilines, the elution order was always 2,4-, 2,5-, 2,3-, 2,6-, 3,5-, and 3,4- except that the chloroacetyl derivatives of 2,4- and 2,6- dichloroanilines coeluted. All
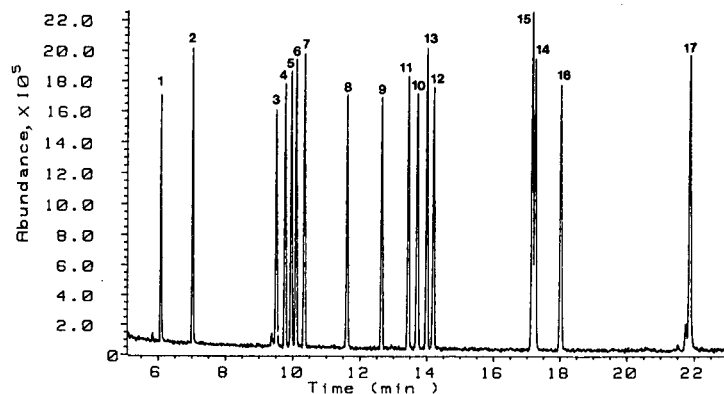

Fig. 3. Total ion chromatogram of HFBA derivatives of anilines. See Fig. 1 for peak identification.
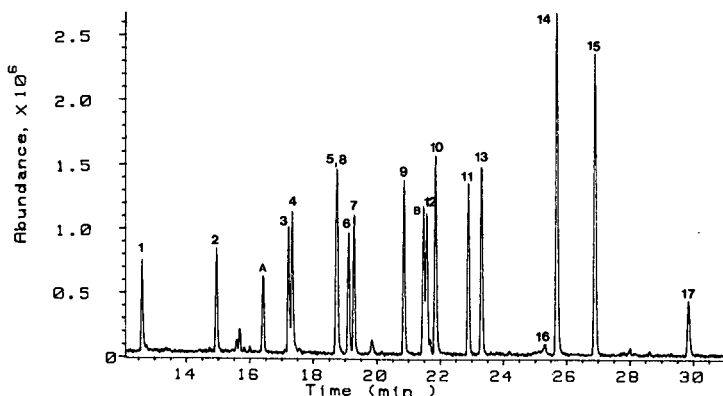
Fig. 4. Total ion chromatogram of CAA derivatives of anilines. Peak A is the underivatized 2,3,5,6-tetra-chloroaniline and peak B is the underivatized pentachloroaniline. See Fig. 1 for the identification of other peaks.

derivatives of the trichloroanilines chromatographed in the order of 2,4,5-, 2,3,4- and 3,4,5-, although the amides of 2,4,6-trichloroaniline emerged at different places for different derivatives. The order of elution for the tetrachloroanilines was 2,3,4,5-followed by 2,3,5,6- for the three perfluoro derivatives, however, the order of elution was reversed in the cases of the monochloroacetyl and dichloroacetyl derivatives.

GC–EI-MS data

Although diacylated derivatives have been reported for aniline and benzyl-amine[9], mass spectral data of all derivatives prepared in this work were consistent with a monoacylated structure. Under EI conditions, perfluoro amide derivatives of the 17 anilines exhibited most or all of the following characteristic fragmentation ions: the molecular ion $(M^{+ \cdot})$, $(M-Cl)^+$, $(M-C_nF_{2n+1})^+$ and $(M-COC_nF_{2n+1})^+$ where $n = 1–3$. In addition, m/z 69 (CF_3^+) was observed for all three perfluoro derivatives of anilines while m/z 119 $(C_2F_5^+)$ and m/z 169 $(C_3F_7^+)$ were present for all PFPA and
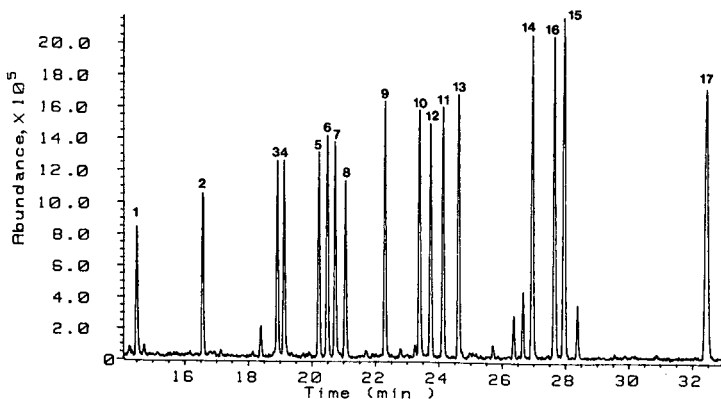

Fig. 5. Total ion chromatogram of DCAA derivatives of anilines. See Fig. 1 for peak identification.

TABLE II

MASS NUMBER (*m/z*) AND RELATIVE ABUNDANCE (%) OF SOME CHARACTERISTIC IONS
OBSERVED FOR THE PFPA DERIVATIVES OF ANILINES UNDER EI CONDITIONS

Parent aniline	$M^{+\cdot}$	$(M-Cl)^+$	$(M-C_2F_5)^+$	$(M-COC_2F_5)^+$	Others
Aniline	239 (100)	—	120 (93)	92 (46)	77 (71), 65 (22)
2-Chloro	273 (26)	238 (100)	154 (8)	126 (26)	99 (10)
3-Chloro	273 (100)	—	154 (91)	126 (44)	99 (14)
4-Chloro	273 (100)	—	154 (52)	126 (84)	99 (18)
2,4-Dichloro	307 (27)	272 (100)	188 (8)	160 (34)	133 (15)
2,5-Dichloro	307 (15)	272 (100)	188 (6)	160 (12)	133 (12)
2,3-Dichloro	307 (17)	272 (100)	188 (7)	160 (15)	133 (10)
2,6-Dichloro	307 (5)	272 (100)	188 (5)	160 (13)	133 (10)
3,5-Dichloro	307 (100)	272 (1)	188 (95)	160 (42)	133 (17)
2,4,5-Trichloro	341 (16)	306 (100)	222 (7)	194 (18)	169 (14)
3,4-Dichloro	307 (100)	272 (1)	188 (59)	160 (67)	133 (17)
2,3,4-Trichloro	341 (17)	306 (100)	222 (8)	196 (22)	169 (13)
2,4,6-Trichloro	341 (9)	306 (100)	222 (6)	194 (19)	169 (13)
2,3,4,5-Tetrachloro	375 (13)	340 (100)	256 (6)	230 (18)	203 (15)
3,4,5-Trichloro	341 (100)	306 (1)	222 (58)	196 (62)	169 (14)
2,3,5,6-Tetrachloro	375 (3)	340 (100)	256 (4)	230 (8)	203 (10)
Pentachloro	411 (6)	376 (100)	292 (5)	264 (13)	237 (17)

HFBA derivatives, respectively. The observation of the above ions was consistent with
the EI mass spectra reported by other workers on the amide derivatives of aromatic
amines[8–10].

It was noted that for the perfluoro derivatives of anilines without a chlorine
substitution at the ortho- positions (*e.g.*, aniline, 3- and 4-chloroaniline, 3,4- and

TABLE III

MASS NUMBER (*m/z*) AND RELATIVE ABUNDANCE (%) OF SOME CHARACTERISTIC IONS
OBSERVED FOR THE HFBA DERIVATIVES OF ANILINES UNDER EI CONDITIONS

Parent aniline	$M^{+\cdot}$	$(M-Cl)^+$	$(M-C_3F_7)^+$	$(M-COC_3F_7)^+$	Others
Aniline	289 (100)	—	120 (88)	92 (53)	77 (69), 65 (27)
2-Chloro	323 (16)	288 (100)	154 (12)	126 (31)	99 (16)
3-Chloro	323 (77)	288 (1)	154 (100)	126 (66)	99 (27)
4-Chloro	323 (91)	288 (1)	154 (59)	126 (100)	99 (33)
2,4-Dichloro	357 (23)	322 (100)	188 (10)	160 (42)	133 (23)
2,5-Dichloro	357 (14)	322 (100)	188 (7)	160 (22)	133 (18)
2,3-Dichloro	357 (16)	322 (100)	188 (9)	160 (28)	133 (14)
2,6-Dichloro	357 (3)	322 (100)	188 (5)	160 (25)	133 (13)
3,5-Dichloro	357 (76)	322 (2)	188 (100)	160 (73)	133 (22)
2,4,5-Trichloro	391 (22)	356 (100)	222 (8)	196 (40)	169 (29)
3,4-Dichloro	357 (90)	322 (2)	188 (85)	160 (100)	133 (33)
2,3,4-Trichloro	391 (21)	356 (100)	222 (9)	196 (42)	169 (22)
2,4,6-Trichloro	391 (10)	356 (100)	222 (4)	196 (31)	169 (19)
2,3,4,5-Tetrachloro	427 (19)	392 (100)	258 (8)	230 (33)	203 (23)
3,4,5-Trichloro	391 (87)	356 (2)	222 (94)	196 (100)	169 (43)
2,3,5,6-Tetrachloro	427 (2)	392 (100)	258 (6)	230 (20)	203 (26)
Pentachloro	461 (6)	426 (100)	292 (5)	264 (26)	237 (28)

3,5-dichloroaniline, 3,4,5-trichloroaniline, etc.), the M^+ was either the base peak or the second most intense peak in their mass spectra. The corresponding $(M-C_nF_{2n+1})^+$ and $(M-COC_nF_{2n+1})^+$ fragments, resulted from simple cleavages at both sides of the carbonyl group, were also intense. However, for those anilines with a 2-chloro substitution, the base peaks were always the $(M-Cl)^+$ fragments resulted from elimination of an *ortho* chlorine atom from the molecular ion. Meanwhile, the. intensity for M^+ was relatively weak for chloroanilines with a chlorine substitution at one of the *ortho* positions and very weak for those bearing chlorine atoms at both *ortho* positions. See Tables I–III for a listing of the mass number and relative abundance of the characteristic ions for the trifluoroacetyl, pentafluoropropionyl, and heptafluoro-butyryl derivatives, respectively.

While the molecular ion and the characteristic ions $(M-Cl)^+$, $(M-COCH_2Cl)^+$ and $(M-COCHCl)^+$ were observed for most chloroacetyl derivatives of anilines, the $(M-COCH_2Cl)^+$ fragment was absent. For these derivatives, the base peak was either the $(M-Cl)^+$ or the $(M-COCHCl)^+$ ion and the $M^{+\cdot}$ was either very weak or absent for those chloroanilines with chlorine with chlorine substitution at both *ortho* positions. Again, the intensity for the $(M-Cl)^+$ ion was very weak for those derivatives without a chlorine substitution at the *ortho* positions. In addition to the $CHCl_2^+$ species (m/z 83 and 85), the molecular ion and characteristic ions such as $(M-Cl)^+$, $(M-CHCl_2)^+$, and $(M-COCHCl_2)^+$ resulted from similar fragmentation pattern as the perfluoro derivatives, were observed for all dichloroacetyl derivates of anilines. With only a minor exception in 2,4-dichloro-aniline, the base peak of these dichloroacetyl derivatives was either the $(M-Cl)^+$ or the $(M-CHCl_2)^+$ fragment. Similar to the other derivatives, the $M^{+\cdot}$ is usually weak for those aniline derivatives with chlorine substitution at both *ortho* positions. The

TABLE IV

MASS NUMBER (m/z) AND RELATIVE ABUNDANCE (%) OF SOME CHARACTERISTIC IONS OBSERVED FOR THE CAA DERIVATIVES OF ANILINES UNDER EI CONDITIONS

Parent aniline	$M^{+\cdot}$	$(M-Cl)^+$	$(M-CH_2Cl)^+$	$(M-COCHCl)^+$	Others
Aniline	169 (71)	134 (3)	120 (55)	93 (100)	77 (43), 65 (35)
2-Chloro	203 (21)	168 (100)	154 (9)	127 (99)	99 (24)
3-Chloro	203 (43)	168 (2)	154 (28)	127 (100)	99 (13)
4-Chloro	203 (37)	168 (1)	154 (15)	127 (100)	99 (17)
2,6-Dichloro	237 (2)	202 (100)	188 (5)	161 (92)	133 (20)
2,4-Dichloro	237 (20)	202 (62)	188 (4)	161 (100)	133 (27)
2,5-Dichloro	237 (15)	202 (100)	188 (6)	161 (88)	133 (32)
2,3-Dichloro	237 (22)	202 (100)	188 (8)	161 (93)	133 (32)
3,5-Dichloro	237 (37)	202 (3)	188 (25)	161 (100)	133 (18)
2,4,6-Trichloro	273 (6)	236 (72)	224 (2)	195 (100)	169 (23)
3,4-Dichloro	237 (27)	202 (1)	188 (11)	161 (100)	133 (13)
2,4,5-Trichloro	273 (29)	236 (90)	224 (4)	195 (100)	169 (30)
2,3,4-Trichloro	273 (32)	236 (81)	224 (5)	197 (100)	167 (25)
2,3,5,6-Tetrachloro	–	272 (100)	258 (2)	231 (68)	203 (21)
3,4,5-Trichloro	273 (36)	236 (2)	224 (9)	197 (100)	167 (12)
2,3,4,5-Tetrachloro	307 (27)	272 (100)	258 (4)	231 (80)	203 (27)
Pentachloro	–	306 (100)	–	265 (88)	237 (21)

mass number and relative abundance of the characteristic ions for chloroacetyl and dichloroacetyl derivatives of anilines are listed in Table IV and V, respectively.

Other fragmentation masses common to all types of derivatives with the same number of ring-substituted chlorine atoms were: m/z 65 ($C_5H_5^+$) for all aniline derivatives, m/z 99 ($C_5H_4Cl^+$) for all 2-, 3-, and 4-chloroaniline derivatives, m/z 133 ($C_5H_3Cl_2^+$) for all dichloroaniline derivatives, m/z 167 ($C_5H_2Cl_3^+$) for all trichloroaniline derivatives, m/z 203 ($C_5HCl_4^+$) for all tetrachloroaniline derivatives and m/z 237 ($C_5Cl_5^+$) for all pentachloroaniline derivatives. It should be noted that, for the sake of simplicity, only the mass of the highest abundance in each chlorine cluster of the polychloro species was used in the discussion and tables. The fragment $C_6H_{5-n}Cl_n^+$ ($n = 0$–5) resulting from the cleavage between the nitrogen and aromatic ring was also detected in many derivatives. In this respect, the ion $C_6H_5^+$ (m/z 77) was very prominent for all derivatives of aniline. The abundance of the ions $C_6H_4Cl^+$ (m/z 111, monochloroanilines), $C_6H_3Cl_2^+$ (m/z 145, dichloroanilines) and $C_6H_2Cl_3^+$ (m/z 179, trichloroanilines) was mostly less than 20% of their corresponding base peaks. As a general rule, these ions were more prominent for those anilines without a chlorine substitution at the ortho position. The ions $C_6HCl_4^+$ (m/z 215, tetrachloroanilines) and $C_6Cl_5^+$ (m/z 249, pentachloroaniline) were either very weak or absent.

ECD response factors of derivatives

One of the reasons why these fluoro and chloro derivatives were prepared for the analysis of anilines was their ECD sensitivities. For a comparison of ECD response, response factors of all aniline derivatives, relative to that of 2,3,4,5-tetrachloroaniline, the most responsive member of the group, were calculated for each type of derivative and shown in Table VI. Variation in the relative response factors within the same type

TABLE V

MASS NUMBER (m/z) AND RELATIVE ABUNDANCE (%) OF SOME CHARACTERISTIC IONS OBSERVED FOR THE DCAA DERIVATIVES OF ANILINES UNDER EI CONDITIONS

Parent aniline	$M^{+\cdot}$	$(M-Cl)^+$	$(M-CHCl_2)^+$	$(M-COCHCl_2)^+$	Others
Aniline	203 (31)	168 (1)	120 (100)	92 (36)	77 (41), 65 (27)
2-Chloro	237 (23)	202 (79)	154 (100)	126 (82)	99 (44)
3-Chloro	237 (27)	202 (1)	154 (100)	126 (40)	99 (17)
4-Chloro	237 (33)	202 (2)	154 (100)	126 (68)	99 (27)
2,4-Dichloro	273 (38)	236 (76)	188 (97)	160 (100)	133 (58)
2,5-Dichloro	273 (29)	236 (100)	188 (96)	160 (74)	133 (70)
2,3-Dichloro	273 (33)	236 (78)	188 (100)	160 (78)	133 (51)
2,6-Dichloro	273 (7)	236 (100)	188 (84)	160 (85)	133 (50)
3,5-Dichloro	273 (28)	236 (1)	188 (100)	160 (39)	133 (19)
3,4-Dichloro	273 (35)	236 (2)	188 (100)	160 (56)	133 (22)
2,4,6-Trichloro	307 (14)	272 (100)	222 (73)	194 (99)	167 (53)
2,4,5-Trichloro	307 (46)	272 (100)	222 (99)	194 (90)	167 (60)
2,3,4-Trichloro	307 (45)	272 (90)	222 (100)	194 (96)	167 (45)
3,4,5-Trichloro	307 (36)	272 (2)	222 (100)	194 (51)	167 (16)
2,3,5,6-Tetrachloro	341 (1)	306 (100)	258 (27)	230 (28)	203 (28)
2,3,4,5-Tetrachloro	341 (31)	306 (100)	258 (63)	230 (64)	203 (49)
Pentachloro	375 (5)	340 (100)	292 (33)	264 (44)	237 (42)

TABLE VI

RELATIVE RESPONSE FACTORS OF VARIOUS AMIDE DERIVATIVES OF ANILINES BY ELECTRON-CAPTURE DETECTION

Response factors relative to the derivative of 2,3,4,5-tetrachloroaniline.

Parent aniline	TFAA	PFPA	HFBA	CAA	DCAA
Aniline	⟨0.1	3.9	3.3	⟨0.1	3.3
2-Chloro	1.1	3.9	3.6	1.3	3.7
3-Chloro	1.4	5.4	5.1	1.4	4.5
4-Chloro	1.7	6.5	6.4	1.7	5.1
2,4-Dichloro	2.3	5.3	5.5	5.6	6.1
2,5-Dichloro	1.8	6.2	6.1	4.7	5.9
2,3-Dichloro	2.1	6.1	6.6	5.2	6.2
2,6-Dichloro	1.3	2.9	3.6	2.6	4.9
3,5-Dichloro	6.2	6.0	5.9	4.4	5.4
2,4,5-Trichloro	4.0	5.4	5.5	5.5	6.1
3,4-Dichloro	6.7	7.4	7.5	3.8	5.6
2,3,4-Trichloro	4.2	7.5	9.0	6.6	8.3
2,4,6-Trichloro	4.0	6.2	5.2	5.2	6.0
2,3,4,5-Tetrachloro	10.0	10.0	10.0	10.0	10.0
3,4,5-Trichloro	7.7	8.1	8.6	7.2	6.1
2,3,5,6-Tetrachloro	7.3	7.4	7.6	*	7.8
Pentachloro	9.1	8.7	8.4	*	9.2
Hexachlorobenzene	10.1	9.3	10.8	7.8	9.8

* Relative response factors not calculated because of incomplete reaction.

of derivative was less than a factor of 4 for the PFPA, HFBA, and DCAA derivatives. Formation of such derivatives thereby enhanced the detection of anilines with no or only one chlorine substitution to a sensitivity level similar to those of polychlorinated anilines. However, the same did not apply to the TFAA and CAA derivatives of aniline, as these compounds were over 100 times less sensitive to ECD than the corresponding 2,3,4,5-tetrachloroaniline derivatives. Also included in Table VI were the relative response factors of hexachlorobenzene so that comparison of the response factors between different types of derivatives could also be made.

Detection limits and linear range

For GC–MSD full scan analysis, the detection limit of all aniline derivatives was approximately 1 ng for a signal-to-noise (S/N) ratio of 5:1. The detection limits for the HFBA derivatives by GC–ECD were in the range of 0.1 to 0.3 pg for a S/N ratio of 10. Detection limits for the other derivatives can be estimated by using the relative response factors listed in Table VI. The ECD calibration curve for the HFBA derivatives was linear over the concentration range from 10 to 250 pg/μl.

CONCLUSIONS

Considering all aspects such as the ease and completeness of reaction, GC resolution, ECD sensitivity, and freedom of side-products and interference, the HFBA reaction is the derivatization technique of choice for the present group of anilines. These derivatives also produced intense molecular ions and or characteristic ions

suitable for confirmation and quantitation by GC–MSD. If a column can be found to resolve the PFPA derivatives of 2,3,4- and 2,4,6-trichloroanilines or the simultaneous analysis of these two anilines is not required, the faster PFPA reaction would have been a better choice than the HFBA reaction. Although the TFAA derivatives of aniline are too insensitive for its ECD determination, this reaction may still be useful for the analysis of other chloroanilines provided that the GC resolution of the derivatives does not present a problem as mentioned before. Although they are all sensitive, the DCAA derivatives of anilines are generally less suitable for ECD analysis than the perfluoro derivatives because of the amount of interferring side-products present in the reaction mixture. Among all the anhydrides tested in this work, CAA is considered as the least satisfactory reagent for the 17 anilines since it suffers from the disadvantages such as incomplete reaction for some chloroanilines, presence of interferring side-products, and low ECD sensitivity for the derivatives of aniline and monochloroanilines.

REFERENCES

 1 *Chem. Eng. News*, June 8 (1987) 24.
 2 J.M. Sontag (Editor), *Carcinogens in Industry and the Environment*, Marcel Dekker, New York, 1981, Ch. 9.
 3 F.S. H. Abram and I. R. Sims, *Water Res.*, 16 (1982) 1309.
 4 E. M. Lores, F. C. Meekins and R. F. Moseman, *J. Chromatogr.*, 188 (1980) 412.
 5 K. Thyssen, *J. Chromatogr.*, 319 (1985) 99.
 6 K. Blau and G. King (Editors), *Handbook of Derivatives for Chromatography*, Heyden, 1978.
 7 C. F. Poole and S. K. Poole, *J. Chromatogr. Sci.*, 25 (1987) 434.
 8 D. E. Bradway and T. Shafik, *J. Chromatogr. Sci.*, 15 (1977) 322.
 9 R. T. Coutts, E. E. Hargesheimer, F. M. Pasutto and B. G. Baker, *J. Chromatogr. Sci.*, 19 (1981) 151.
10 G. Skarping, L. Renman and B. E. F. Smith, *J. Chromatogr.*, 267 (1983) 315.
11 G. Skarping, L. Renman and M. Dalene, *J. Chromatogr.*, 270 (1983) 207.
12 K. Grob, Jr. and S. Rennhard, *J. High Resolut. Chromatogr. Chromatogr. Commun.*, 3 (1980) 627.

CHROM. 20 959

PENTAFLUOROBENZYLATION OF CAPSAICINOIDS FOR GAS CHROMATOGRAPHY WITH ELECTRON-CAPTURE DETECTION

ANNA M. KRAJEWSKA* and JOHN J. POWERS

Department of Food Science and Technology, University of Georgia, Athens, GA 30602 (U.S.A.)
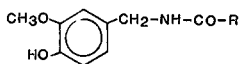(First received June 9th, 1988; revised manuscript received August 17th, 1988)

SUMMARY

The alkylation of capsaicinoids with pentafluorobenzyl (PFB) bromide for gas chromatography with electron-capture detection was studied. The PFB derivatives were formed within 30 min at 60°C and did not show any signs of decomposition. The alkylated capsaicinoids had a hydrophobic character making them suitable for gas chromatography on a non-polar column. The electron-capture response for the PFB derivatives of capsaicinoids was very sensitive and amounts of capsaicin down to 10 pg were easily detected. The method was succesfully applied to measurement of capsaicinoids in *Capsicum* products using vanillylamide of octanoic acid as an internal standard.
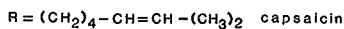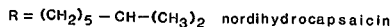
INTRODUCTION

Due to growing interest in the pharmacological actions of capsaicin and its analogues called capsaicinoids[1–3], there is a need for sensitive and accurate analytical methods for their detection. Colorimetric[4], direct and differential spectrophotometric[5,6], thin-layer and paper chromatographic[7,8] methods can be used only for the analysis of total capsaicinoids. Gas chromatography (GC)[9,10], high-performance liquid chromatography (HPLC)[11–13] as well as high-performance thin-layer chromatography (HPTLC)[4] have been succesfully used for identification and quantitation of individual capsaicinoids with varying degrees of sensitivity. Recently Kawada *et al.*[13] reported an HPLC method with electrochemical detection (ED) capable of detecting capsaicin down to the picogram level. However, this highly sensitive method does not appear to be very practical because it requires an expensive detector that is not commonly found in research laboratories.

GC with electron-capture detection (GC–ECD) has been demonstrated to be a very sensitive tool for quantitative determinations of low concentrations of a variety of compounds. Compounds with low or no electron-capture response can usually be made electron-capture sensitive by means of derivatization. Capsaicinoids, due to the presence of a polar hydroxyl group in the molecules (see Fig. 1) require derivatization to improve their chromatographic performance. Silylation[9] and methylation[10] of a hydroxyl group have been used to modify the chromatographic properties of capsai-

CH3O $\diagdown$ CH2-NH-CO-R
HO $\diagup$

naturally occurring:

R = (CH$_2$)$_5$ — CH—(CH$_3$)$_2$ nordihydrocapsaicin

R = (CH$_2$)$_4$—CH=CH —(CH$_3$)$_2$ capsaicin

R = (CH$_2$)$_6$ —CH—(CH$_3$)$_2$ dihydrocapsaicin

synthetic analogues:

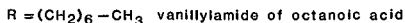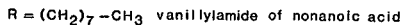R = (CH$_2$)$_7$ —CH$_3$ vanillylamide of nonanoic acid

R =(CH$_2$)$_6$ —CH$_3$ vanillylamide of octanoic acid
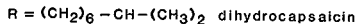
Fig. 1. Structures of capsaicinoids.

cinoids by rendering them less polar and thus reducing undesirable column interactions. Derivatives containing a pentafluorobenzyl (PFB) group have been reported to have a high electron-capture response[15,16]. Pentafluorobenzylation has been applied to a broad spectrum of organic compounds containing an active hydrogen by reacting the compounds with PFB bromide in acetone in the presence of potassium carbonate[17–20].

The goal of this work was to study conditions for the pentafluorobenzylation of capsaicinoids and to evaluate the GC and ECD properties of the PFB derivatives.

EXPERIMENTAL

Gas chromatography

Electron-capture detection. The GC analysis of PFB derivatives of capsaicinoids was performed on a Varian 3400 gas chromatograph (Varian, Palo Alto, CA, U.S.A.) fitted with a ^{63}Ni-electron-capture detector. The column was a 30 m × 0.326 mm I.D. fused-silica capillary column with a chemically bonded DB-5 stationary phase at a film thickness of 0.25 μm (J&W Scientific, Rancho Cordova, CA, U.S.A.). Nitrogen was used as a carrier gas at a flow-rate of 1.5 ml/min as well as a make-up gas at a flow-rate of 20 ml/min. The oven temperature program for optimal peak separation was as follows: initial temperature = 200°C, initial time = 0 min, program rate = 8°C/min, final temperature = 265°C. The injector and detector temperatures were 250 and 350°C, respectively. A 1-μl volume of a sample was injected at an attenuation of 32 in a splitless mode with an open insert fitted in a 1075 split/splitless capillary injector. Peaks were recorded and integrated by a 3390A Hewlett-Packard integrator.

Flame ionization detection (FID). A Varian Model 3700 gas chromatograph equipped with a FID system was used for a model study of the pentafluorobenzylation reaction of capsaicinoids. A glass column (2.1 m × 2 mm I.D.) packed with 5% SE-52 on Chromosorb W AW DMCS 100–120 mesh (Supelco, Bellefonte, PA, U.S.A.) was prepared. The injector and detector temperatures were 250 and 270°C, respectively. The temperature program was the same as in GC–ECD. A 2-μl volume of a sample was injected into the gas chromatograph at a sensitivity setting of $8 \cdot 10^{-10}$ A f.s. Peaks were recorded using a Varian Model 9176 recorder and areas integrated by Varian CDS 111 data system.

Materials

PFB bromide was obtained from Pierce (Rockford, IL, U.S.A.). Vanillylamide of nonanoic acid, a commercially available synthetic capsaicin analogue, used in the study of the derivatization reaction, was from Pfaltz and Bauer (Waterbury, CT, U.S.A.). Pure nordihydrocapsaicin, capsaicin and dihydrocapsaicin used for GC standards were isolated from natural capsaicin (Pfaltz and Bauer), by liquid chromatographic (LC) methods[10,21].

Vanillylamide of octanoic acid used as an internal standard (I.S.) for determination of capsaicinoids in *Capsicum* products was prepared from vanillylamine and octanoyl chloride[22]. The concentration of vanillylamide of octanoic acid was adjusted to yield a GC peak area comparable to the areas of the capsaicinoid peaks. Solution of I.S. was added to the samples before the extraction.

Tetracosane and 1,2-dibromododecane used as I.S. for GC–FID and GC–ECD injections, respectively, were obtained from Fisher Scientific (Pittsburgh, PA, U.S.A.) and from Fluka Chemical (Ronkonkoma, NY, U.S.A.).

All solvents used for the extraction, purification and derivatization of samples for GC analysis were "Baker Analyzed" reagents (J. T. Baker, Phillipsburg, NJ, U.S.A.).

Synthesis and characterization of PFB capsaicinoids

The PFB derivatives of two representative capsaicinoids, namely vanillylamide of nonanoic acid and capsaicin, were synthesized as follows: 40 mg capsaicinoid (about 0.13 mmol) were dissolved in 2 ml acetone in a micro round-bottom flask; 100 μl PFB bromide (0.71 mmol) and 300 mg of anhydrous potassium carbonate were added. The mixture was heated under reflux for 5 h. The acetone was evaporated under a gentle stream of nitrogen, the residue dissolved in 10 ml distilled water and the derivative was extracted into diethyl ether. After washing with 0.1 *M* sodium hydroxide, 0.1 *M* hydrochloric acid and water, the ether was evaporated and the derivative crystallized from the acetone–water mixture.

The purity and identity of the synthesized derivatives was established by IR spectrometry, mass spectrometry (MS) and melting point determination. IR and MS demonstrated that only the phenolic hydroxyl group underwent pentafluorobenzylation. No alkylation occurred on an amide group although pentafluorobenzylation[23,24] as well as other derivatizations[25–28] involving an active hydrogen of an –NH group have been reported. Characteristic bands of a hydroxyl group, i.e. at 3400–3200 cm^{-1} and at 1200 cm^{-1} were absent in the IR spectra of both derivatized compounds. This allowed the detection of a characteristic band of an "associated" –NH group of a secondary amide at 3300 cm^{-1}, indicating no change in the amide structure and alkylation of only a hydroxyl group. The mass spectra confirmed the introduction of one PFB group into the molecule. Both derivatives showed molecular ion peaks increased by 180 a.m.u. (*m/e* 473 and *m/e* 485 for PFB derivative of vanillylamide of nonanoic acid and capsaicin, respectively). Fragment ions, also increased by 180 a.m.u., showed patterns similar to the parent compounds with additional peaks present in the spectra corresponding to cleavage of the PFB group from the derivatized molecule. PFB capsaicin melted at 87–88.5°C while PFB vanillylamide of nonanoic acid softened at 104.5°C and melted at 106.5–108°C.

These synthesized analogues were used for verification of the identity of the

products of the derivatization reaction by co-chromatography and MS. Injection of a reaction mixture containing either derivatized vanillylamide of nonanoic acid or capsaicin yielded single peaks with identical retention times as those of synthesized analogues using both FID and ECD. Also, mass spectra of both derivatized capsaicinoids were identical with their respective synthesized analogues.

Model study of capsaicinoid pentafluorobenzylation

The optimal conditions for the pentafluorobenzylation of capsaicinoids were determined using vanillylamide of nonanoic acid and tetracosane as an I.S. Tetracosane did not undergo derivatization and therefore served as a constant reference. A 7.126 mM solution of vanillylamide of nonanoic acid was prepared in acetone containing tetracosane (0.25 g/1000 ml); 1 ml of the above solution was transferred to the screw-cap vial. The reaction was carried out varying the following conditions: the reaction time at different temperatures, the amount of anhydrous potassium carbonate, the volume of acetone in the reaction mixture at different temperatures, and the amount of PFB bromide.

After stopping the reaction, samples were evaporated to dryness under a stream of nitrogen at 40°C; 1 ml benzene and 2 ml water were added and the vials shaken vigorously. After the layers separated, 2 μl of the benzene layer were injected into the GC–FID system. Changes of both the PFB derivative as well as underivatized vanillylamide of nonanoic acid were plotted against the I.S. peak.

Sample preparation

Samples were prepared by a procedure described elsewhere[10] involving extraction of capsaicinoids with acetone in a Soxhlet apparatus, purification with petroleum ether and reextraction of capsaicinoids from the aqueous phase with diethyl ether. The diethyl ether was evaporated, the residue dissolved in 5 ml acetone and 1 ml of this solution transferred into a screw-cap vial. The volume was reduced to 0.3 ml with a gentle stream of nitrogen at 40°C. Next, 500 mg anhydrous potassium carbonate and 20 μl PFB bromide were added, the vial was tightly capped and the reaction mixture heated for 0.5 h in a water bath maintained at 60°C. The vials were carefully agitated every 10 min. After completion of the reaction, the acetone and the derivatizing agent were evaporated under a stream of nitrogen at 40°C and 1 ml benzene and 2 ml distilled water were added. The mixture was vigorously shaken, the layers were allowed to separate and 15 μl of the organic layer diluted further with 1 ml acetone. A 1-μl volume of this solution was injected into the GC–ECD system. The concentration of the alkylated capsaicinoids was determined from the ratio of the peak areas to that of the I.S. by reference to calibration curves for nordihydrocapsaicin, capsaicin and dihydrocapsaicin.

RESULTS AND DISCUSSION

Optimal conditions for capsaicinoid pentafluorobenzylation

The pentafluorobenzylation was considered complete when no underivatized vanillylamide of nonanoic acid was detected by GC–FID, and the amount of derivative formed was constant. As can be seen in Fig. 2, large differences were found in the extent of pentafluorobenzylation of vanillylamide of nonanoic acid with varying
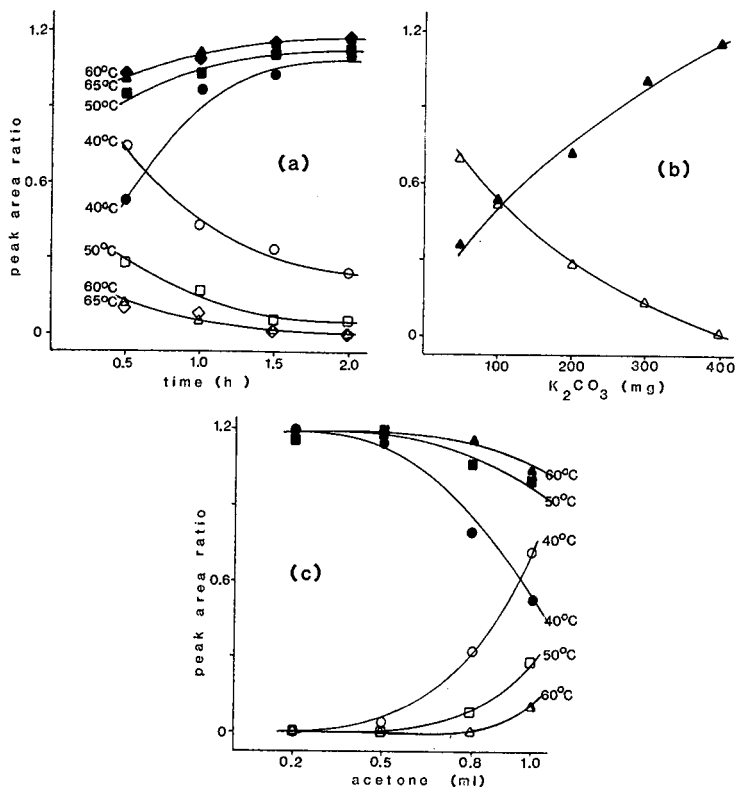
Fig. 2. Yield of pentafluorobenzylated vanillylamide of nonanoic acid as determined by GC–FID; 7.126 μmol vanillylamide of nonanoic acid reacted with 4 μl PFB bromide; underivatized vanillylamide of nonanoic acid at 40°C (O), 50°C (□), 60°C (△), 65°C (◇); PFB derivative at 40°C (●), 50°C (■), 60 °C (▲), 65°C (◆). (a) Effect of reaction time at different temperatures with 400 mg K_2CO_3 used in 1 ml acetone; (b) effect of amount of K_2CO_3 in the reaction mixture; reaction carried out for 1.5 h at 60°C in 1 ml acetone; (c) effect of volume of acetone at different temperatures; reaction carried out for 0.5 h in the presence of 400 mg K_2CO_3.

time, temperature, the amount of anhydrous potassium carbonate and the volume of acetone in the reaction mixture. The reaction was practically complete after heating for 1.5 h at 60°C (see Fig. 2a). As shown in Fig. 2b, 400 mg potassium carbonate were adequate, but any smaller amount resulted in incomplete derivatization. As seen in Fig. 2c, when the volume of acetone was reduced to 0.2 ml, 0.5 h at 40°C was sufficient to complete pentafluorobenzylation. The reaction was found to be equimolar and 1 μl PFB bromide (7.126 μmol) was enough for the complete derivatization of 1 ml of the vanillylamide of nonanoic acid solution.

Thus, it was concluded that the pentafluorobenzylation reaction of vanillyl-amide of nonanoic acid was complete and reproducible when the reaction mixture was heated for 0.5 h in the presence of 400 mg anhydrous potassium carbonate in 0.3 ml acetone and when an adequate volume of PFB bromide was added.
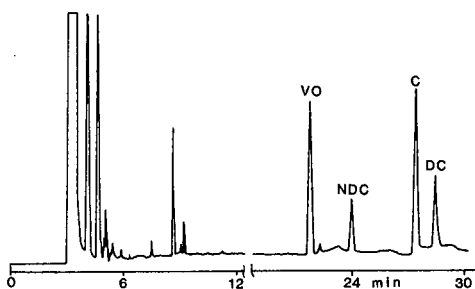
Fig. 3. GC–ECD of pentafluorobenzylated standard mixture of capsaicinoids; VO = vanillylamide of octanoic acid (I.S.), NDC = nordihydrocapsaicin, C = capsaicin, DC = dihydrocapsaicin; 1 μl injected at attenuation × 32 representing 3.0, 10.5 and 6.0 ng of NDC, C and DC, respectively; GC conditions: capillary column (30 m × 0.326 mm I.D.) with chemically bonded DB-5 stationary phase; nitrogen flow-rate = 1.5 ml/min, initial temperature = 200 °C, initial time = 0 min, program rate = 8 °C/min, final temperature = 265 °C.

Electron-capture detection of PFB derivatives of capsaicinoids

Using the conditions determined for pentafluorobenzylation of vanillylamide of nonanoic acid, a series of capsaicin solutions in the range of 4.3–192.4 μM was derivatized and injected with 1,12-dibromododecane (0.14 g/1000 ml) as an I.S., into the GC–ECD system. A linear relationship (r^2 = 0.99) was obtained within the range tested. The PFB capsaicin was stable in solution for several weeks at room temperature. A series of dilutions of PFB capsaicin was injected to determine the electron-capture detection limit. As little as 10 pg of capsaicin was easily detected. This value is comparable to the sensitivity of HPLC–electrochemical detection (ED), *i.e.*, 12 pg reported by Kawada *et al.*[13]. Sensitivities of other chromatographic systems for capsaicin are much lower: 100 ng by HPLC with UV (279 nm) detection[11], 3 ng by HPLC with fluorescence (270/330 nm) detection[12] and 12.5 ng by GC–FID of methyl derivatives[29].

The applicability of the method was examined using the extracts of two kinds of peppers and one oleoresin. To assure completeness of the pentafluorobenzylation of the extracts, more PFB bromide and anhydrous potassium carbonate than needed for a pure capsaicinoid was used in case other substances present in the extracts underwent derivatization. Vanillylamide of octanoic acid was used as an I.S. in the extracts and standard solutions. Standard solutions for the determination of the three major
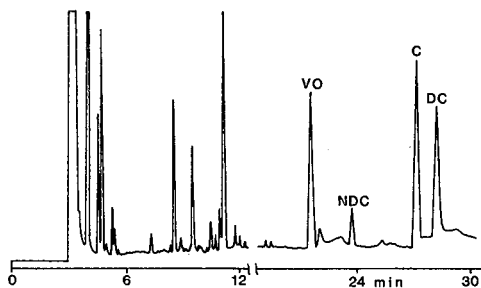

Fig. 4. GC–ECD of pentafluorobenzylated extract of jalapeno peppers; codes and GC conditions as in Fig. 3.

TABLE I

CAPSAICINOID CONTENT IN SELECTED *CAPSICUM* PRODUCTS AS DETERMINED BY GC–ECD OF PFB DERIVATIVES

Product	Capsaicinoid content* (mg/100 g original wt.)					
	NDC**	C.V. (%)	C**	C.V. (%)	DC**	C.V. (%)
Jalapeno peppers	3.36	2.7	20.81	2.3	17.06	3.5
Red finger hot peppers	4.41	4.0	28.08	2.7	10.04	3.9
Oleoresin (African chillies)	763.90	3.0	1154.62	1.3	1182.21	3.7

* Average of three determinations.
** NDC = Nordihydrocapsaicin, C = capsaicin, DC = dihydrocapsaicin.

capsaicinoids were in the ranges 1.5–6.0, 5.25–21.0, and 3.0–12.0 µg/ml I.S. solution for nordihydrocapsaicin, capsaicin and dihydrocapsaicin, respectively. The relative concentrations of each capsaicinoid in the standard mixtures were such that they reflected the relative content of capsaicinoids in *Capsicum* extracts (see Figs. 3 and 4).

The results of the determination of capsaicinoid content in selected *Capsicum* products are presented in Table I. Coefficient of variation (C.V.) in the range of 1.3–4.0% based on three replications indicated excellent reproducibility of the method. This was mainly due to use of vanillylamide of octanoic acid, a synthetic analogue of capsaicinoids, as an I.S. Its addition before sample preparation decreased the error in the extraction and purification and its behaviour during pentafluorobenzylation identical with capsaicinoids reduced the error of derivatization. The extraction and purification procedure of capsaicinoids from *Capsium* products used in this study was examined earlier and the recovery established[10].

As seen in Fig. 3 and 4, excellent GC separation of PFB derivatives of capsaicinoids was obtained using the GC conditions described. Peaks were very well resolved and therefore easy to quantitate.

CONCLUSIONS

This study demonstrated that pentafluorobenzylation is a useful method of derivatization for capsaicinoids. This derivatization results in formation of stable analogues suitable for GC with increased sensitivity to ECD. Use of vanillylamide of octanoic acid or other closely related compound as an I.S. is strongly recommended for reproducible results.

REFERENCES

 1 J. Szolcsanyi, in A. S. Milton (Editor), *Handbook of Experimental Pharmacology*, Springer, Berlin, Heidelberg, New York, 1982, Ch. 14, p. 437.
 2 S. H. Buck and T. F. Burks, *Pharmacol. Rev.*, 38 (1986) 179.
 3 R. M. Virus and G. F. Gebhart, *Life Sci.*, 25 (1979) 1273.
 4 K. L. Bajaj, *J. Assoc. Off. Anal. Chem.*, 63 (1980) 1314.
 5 A. T. Gonzalez and C. W. Altamirano, *J. Food Sci.*, 38 (1973) 342.
 6 J. J. DiCecco, *J. Assoc. Off. Anal. Chem.*, 62 (1979) 998.
 7 M. S. Karawya, S. I. Balbaa, A. N. Girgis and N. Z. Yousseff, *Analyst (London)*, 92 (1967) 581.
 8 N. C. Rajpoot and V. S. Govindarajan, *J. Assoc. Off. Anal. Chem.*, 64 (1981) 311.
 9 J. Jurenitsch, *Sci. Pharm.*, 47 (1979) 31.
10 A. M. Krajewska and J. J. Powers, *J. Chromatogr.*, 409 (1987) 223.
11 O. Sticher, F. Soldati and R. K. Joshi, *J. Chromatogr.*, 166 (1978) 221.
12 A. Saria, F. Lembeck and G. Skofitsch, *J. Chromatogr.*, 208 (1981) 41.
13 T. Kawada, T. Watanabe, K. Katsura, H. Takami and K. Iwai, *J. Chromatogr.*, 329 (1985) 99.
14 T. Suzuki, T. Kawada and K. Iwai, *J. Chromatogr.*, 198 (1980) 217.
15 N. K. McCallum and R. J. Armstrong, *J. Chromatogr.*, 78 (1973) 303.
16 A. C. Moffat and E. C. Horning, *Anal. Lett.*, 3 (1970) 205.
17 F. K. Kawahara, *Anal. Chem.*, 40 (1968) 1009.
18 K. Chan and J. F. McCann, *J. Chromatogr.*, 164 (1979) 394.
19 D. G. Kaiser and R. S. Martin, *J. Pharm. Sci.*, 63 (1974) 1579.
20 A. Sioufi and F. Pommier, *J. Chromatogr.*, 181 (1980) 161.
21 A. M. Krajewska and J. J. Powers, *J. Chromatogr.*, 367 (1986) 267.
22 E. K. Nelson, *J. Am. Chem. Soc.*, 41 (1919) 2121.
23 O. Gyllenhaal and H. Ehrsson, *J. Chromatogr.*, 107 (1975) 327.
24 S. Sun and A. H. C. Chun, *J. Pharm. Sci.*, 66 (1977) 477.
25 H. Ehrsson and B. Mellstrom, *Acta Pharm. Suec.*, 9 (1972) 107.
26 F. S. Tanaka and R. G. Wien, *J. Chromatogr.*, 87 (1973) 85.
27 H. V. Street, *J. Chromatogr.*, 109 (1975) 29.
28 W. A. Dechtiaruk, G. F. Johnson and H. M. Solomon, *Clin. Chem.*, 22 (1976) 879.
29 A. M. Krajewska and J. J. Powers, *J. Assoc. Off. Anal. Chem.*, 70 (1987) 926.

IDENTIFICATION OF METHYL DIETHANOLAMINE DEGRADATION PRODUCTS BY GAS CHROMATOGRAPHY AND GAS CHROMATOGRAPHY–MASS SPECTROMETRY

AMITABHA CHAKMA and AXEL MEISEN*

Department of Chemical Engineering, The University of British Columbia, 2324 Main Mall, Vancouver, BC V6T 1W5 (Canada)

(First received April 5th, 1988; revised manuscript received July 27th, 1988)

SUMMARY

Partially degraded, aqueous methyl diethanolamine solutions were analyzed by a gas chromatograph equipped with a Tenax column and flame ionization detector; nitrogen was used as the carrier gas. To aid in product identification, the gas chromatograph was coupled to a mass spectrometer operating either in electron impact or chemical ionization mode. The most important degradation products were found to be: methanol, ethylene oxide, trimethylamine, ethylene glycol, 2-(dimethylamino)ethanol, 1,4-dimethylpiperazine, N-(hydroxyethyl)methylpiperazine, triethanolamine; and N,N-bis(hydroxyethyl)piperazine.

INTRODUCTION

Aqueous solutions of methyl diethanolamine (MDEA) are gaining industrial acceptance as solvents for the selective removal of hydrogen sulphide from light hydrocarbon gases containing carbon dioxide (Kohl and Riesenfeld[1]). MDEA's selectivity for hydrogen sulphide is attributed to its inability to form carbamates with carbon dioxide. In addition, the lack of carbamate formation also suggests that CO_2 is unlikely to degrade MDEA, *i.e.* convert it into compounds from which MDEA cannot be regenerated under normal processing conditions. Blanc and Elgue[2] have stated that "No one has been able to show any degradation products in (MDEA) solutions having been used for several years in industrial units". However, Yu *et al.*[3] have suggested that MDEA may also form carbamate ions with carbon dioxide and Chakma and Meisen[4] found in preliminary experiments that MDEA degrades at elevated temperatures and carbon dioxide partial pressures. The formation of degradation compounds is undesirable because they represent a loss of valuable MDEA, may interfere with acid gas aborption and may cause operating problems such as corrosion, fouling and foaming.

The basic objective of the present work was to identify the principal MDEA degradation compounds. Based on preliminary experiments and by using the gas chromatographic technique previously developed by Kennard and Meisen[5] for indus-

trial diethanolamine (DEA) solutions, it was found that partially degraded MDEA solutions contained several compounds with similar retention times in the gas chromatographic (GC) column. GC coupled with various forms of mass spectrometry (MS) were therefore used in product identification.

EXPERIMENTAL

Degradation of MDEA solutions

Partially degraded MDEA solutions were obtained in a manner similar to that utilized by Kennard and Meisen[6] for DEA. Aqueous solutions of known concentrations were prepared by mixing distilled water with 99 + % pure MDEA (supplied by Aldrich, Milwaukee, WI, U.S.A.). The purity of the MDEA was confirmed by GC. A 600-ml stainless-steel autoclave (Model 4560, Parr Instrument, Moline, IL, U.S.A.), was purged with carbon dioxide before heating it to the desired temperature. A known volume of MDEA solution (typically 250 ml) was then transferred into the autocalve and the solution placed under a blanket of carbon dioxide. The autoclave was constantly stirred and the solution temperature was kept at the desired value by means of a controller (Model 4831EB, Parr Instrument). Solution samples (typically 5 ml) were withdrawn from the autoclave at appropriate intervals and their contents analyzed as described below.

Gas chromatographic technique

The GC technique developed by Kennard and Meisen[5] for DEA was modified for the analysis of degraded MDEA solutions. The final, optimal operating conditions are summarized in Table I. The elution times of the important degradation compounds were generally less than about 30 min (see Table II). After each run

TABLE I

SPECIFICATION OF THE GAS CHROMATOGRAPHIC SYSTEM

Gas chromatograph	
Manufacturer	Hewlett-Packard
Model	5830A
Detector	H_2 flame ionization
Chromatographic column	
Material	Stainless steel
Dimensions	1/8 in. O.D., 9 ft. long
Packing	Tenax GC, 60–80 mesh
Operating conditions	
Carrier gas	Nitrogen at 25 ml/min
Injection port temperature	300°C
Detector port temperature	300°C
Column temperature	Isothermal at 100°C for 0.5 min, then raised at 8°C/min to 300°C.
Syringe	
Manufacturer	Hamilton, Reno, NV, U.S.A.
Model	701, 0.01 ml with fixed needle and Chaney adeptor
Injected sample size	0.001 ml

TABLE II

RETENTION TIMES OF VARIOUS COMPOUNDS IN GC COLUMN

Compound name	Abbreviation	Retention time (min)
Ethylene oxide	EO	1.3–1.4
Trimethylamine	TMA	1.9–2.0
Ethylene glycol	EG	7.2–7.3
N,N-Dimethylaminoethanol	DMAE	8.4–8.6
2-Methylaminoethanol	MAE	8.5–8.6
Dimethylpiperazine	DMP	11.5–11.6
Methyl diethanolamine	MDEA	14.7–14.8
Diethanolamine	DEA	14.8–14.9
Hydroxyethylmethylpiperazine	HMP	16.5–16.7
Triethanolamine	TEA	20.1–20.3
N,N-bis(hydroxyethyl)piperazine	BHEP	21.4–21.6
3-(Hydroxyethyl)-2-oxazolidone	HEOD	22.2–22.4
N,N,N-Tris(hydroxyethyl)ethylenediamine	THEED	25.5–25.7
N,N,N,N-Tetra-(hydroxyethyl)ethylenediamine	TEHEED	27.8–28.0

lasting approximately 40 min, the column was cooled from 300 to 100°C over a 10-min period.

GC–MS techniques

To facilitate the identification of degradation compounds, a microprocessor based gas chromatograph–mass spectrometer (Model 5985B, Hewlett-Packard, Palo Alto, CA, U.S.A.) was used. This instrument could be operated in electron impact (EI) and chemical ionization (CI) mode. In the latter case, methane was chosen as the reagent gas[7]. The computer was equipped with the EPA/NIH mass spectral data base[8] which enabled ready comparison of experimental and reference spectra.

Hydroxyl group number determination

Many of the compounds in degraded MDEA solutions contain hydroxyl groups. The silylation techniques described by Hsu and Kim[7] and Hsu[9] were used to determine the number of hydroxyl groups as further confirmation of a compound's identity.

Since water may interfere with the silylation technique, it was first removed by saturating the samples with potassium carbonate and extracting them with isopropyl alcohol. The alcohol was later eliminated again by vaporization.

Two silylation reagents were examined. The first consisted of hexamethyldisilazane (HMDS), trimethylchlorosilane (TMCS) and anhydrous pyridine as suggested by Hsu and Kim[7]. Mixtures of 1 ml HMDS, 0.5 ml TMCS and 2 ml pyridine were added to 5 ml of dehydrated samples in 10-ml screw-cap vials. The vials were shaken vigorously for about 5 min and then allowed to stand for at least 10 min to ensure complete silylation. It was observed that, in some cases, silylation of amino groups occurred as well.

The second reagent was N-trimethylsilyl imidazole (TSIM). A 5-ml volume of TSIM were added to 5-ml samples in 20-ml screw-cap vials and reacted following the

procedure described above. TSIM was found to silylate the hydroxyl groups only while leaving the amino groups unaffected. Consequently, TSIM was primarily used for selective hydroxyl silylation in this study.

Selective silylation results in the addition of silyl groups to hydroxyl groups in the sample. This increases the mass-to-charge ratio of the pseudomolecular ions in proportion to the number of hydroxyl groups present. Thus by comparing the mass-to-charge ratios of the pseudomolecular ions of CI spectra before and after silylation, the number of hydroxyl groups in a compound can be calculated. For example, when MDEA is silylated with TSIM, the active hydrogens are replaced by the trimethyl silyl group $-Si(CH_3)$ or TMS:
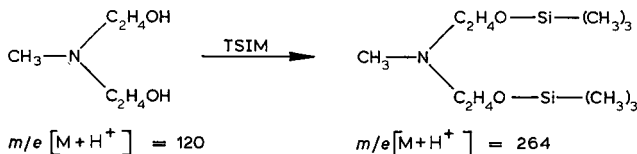
The formula mass of the TSIM group is 73 a.m.u. and it replaces one active hydrogen atom. Therefore, the addition of each TSIM group increases the mass-to-charge ratio of the pseudomolecular ion by 72. In general, the number of hydroxyl groups can simply be calculated from the difference in the mass-to-charge ratios of the pseudomolecular ions before and after silylation, *i.e.*

Number of OH groups = $\{m/e[M + H^+]_{silylated} - m/e[M + H^+]_{unsilylated}\}/72$.

Synthesis of select MDEA degradation compounds

In order to identify the MDEA degradation compounds conclusively and to determine their concentrations, the suspected compounds were purchased, whenever possible, in pure form. However, HMP, HEOD and THEED were unavailable in sufficiently pure form and had to be synthesized.

HMP synthesis

HMP was formed by placing approximately 20 ml of 1-methylpiperazine (MP) into a glass beaker and bubbling ethylene oxide (EO) through the mixture at ambient conditions. The following reaction occurred:
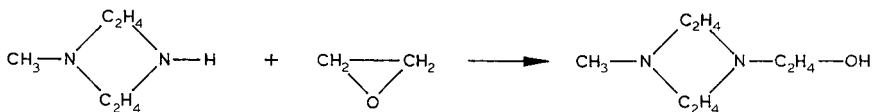

Bubbling was continued until MP was no longer detectable. A product purity of over 97% HMP was obtained.

HEOD synthesis

Kennard[10] attempted various method of HEOD synthesis, but was unsuccesful in obtaining sufficient purity for GC calibration. A procedure similar to that of Kim and Sartori[11] and Drechsel[12] was therefore adopted for this study.

A 210-g amount of DEA, 260 g of diethylcarbonate and 2 g of sodium methoxide were placed into the autoclave described before. The temperature was gradually raised to 130°C while continuously stirring the solution and keeping the pressure at 1 atm. The following reaction occurred:
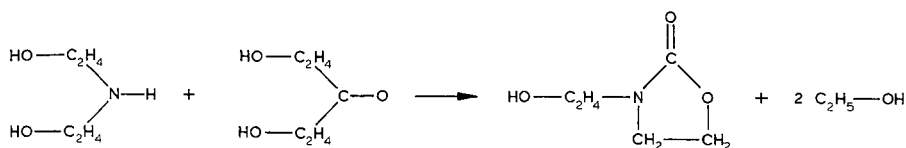
After approximately 2 h, the ethanol formation ceased. The autoclave was then cooled to room temperature by passing water through its internal cooling coil. The reaction product was found to be a mixture of ethanol and HEOD with a purity (as determined by GC analysis) in excess of 90%. The HEOD was further purified to over 95% by adding SGL activated carbon (Calgon, Pittsburg, PA, U.S.A.) to the sample.

THEED synthesis

THEED was synthesized according to Kennard's unpublished procedure[10]:
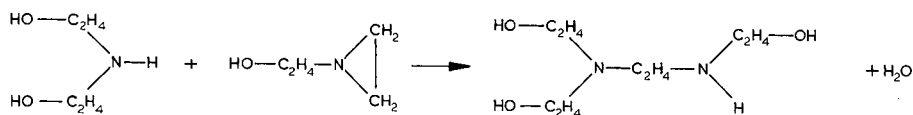
A 105-g amount of DEA, 87 g of N-(2-hydroxyethyl)ethylimine (HEM) and 5 g of aluminum chloride were placed inside the previously described autoclave fitted with a pyrex liner. The autoclave was then sealed and pressurized to 0.7 MPa with nitrogen. The contents were constantly stirred and maintained at 120°C for 24 h. Upon rapid cooling, THEED of 80+% purity was obtained. This product was further refined by diluting it with water and then passing it at a flow-rate of 0.5 ml/min through a 0.40m x 20 mm I.D. long glass column filled with 60–200 mesh silica gel and trace amounts of aluminum hydroxide. The product was concentrated by boiling to drive off the water. THEED of 98+% purity was thus obtained.

RESULTS AND DISCUSSION

Fig. 1 shows a typical chromatogram of a 4.28 M MDEA solution after it was degraded for 144 h at 180°C under a CO_2 partial pressure of 2.59 MPa. Apart from the MDEA peak (peak 9), various other peaks representing degradation compounds are evident.

Peaks 1–7 were found to be methanol, ethylene oxide (EO), trimethylamine (TMA), N,N-dimethylethanamine, ethylene glycol (EG), 2-(dimethylamino)ethanol (DMAE) and 4-methylmorpholine, respectively, by matching their EI mass spectra with library spectra[8] stored in the GC–MS.
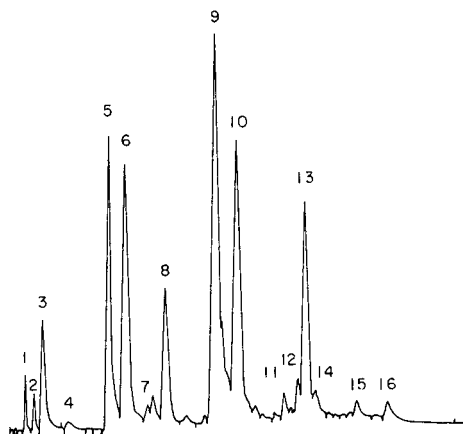
Fig. 1. Chromatogram of a partially degraded MDEA solution of 4.28 M initial concentration, degraded at 180°C under a carbon dioxide partial pressure of 2.59 MPa for 144 h.
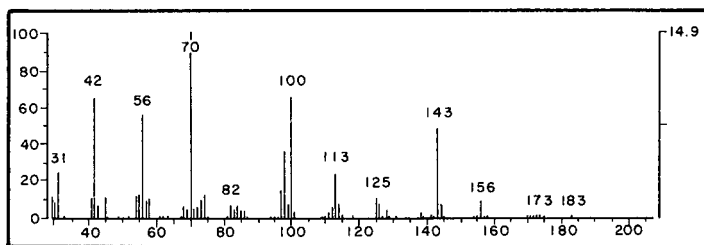

Fig. 2. EI mass spectrum of peak 13 identified as BHEP.

Peak 8 was identified to be 1,4-dimethylpiperazine (DMP) by matching its EI mass spectrum with that given in the *Eight Peak Index of Mass Spectra*[13].

The EI mass spectra of peaks 13, 14 and 15, which are shown in Figs. 2–4, were attributed to N,N-bis-(2-hydroxyethyl)piperazine (BHEP), 3-(hydroxyethyl)-2-oxazolidone (HEOD), and N,N,N-tris-(hydroxyethyl)ethylenediamine (THEED), respectively. The reason for this is that they matched the unpublished spectra obtained by Kennard[10].
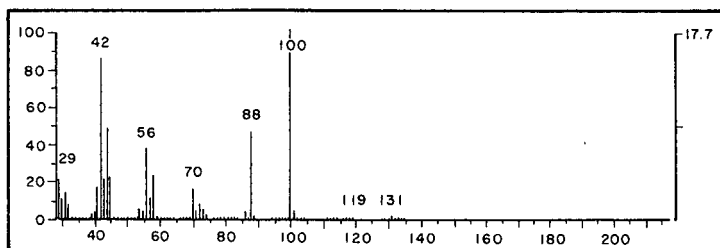
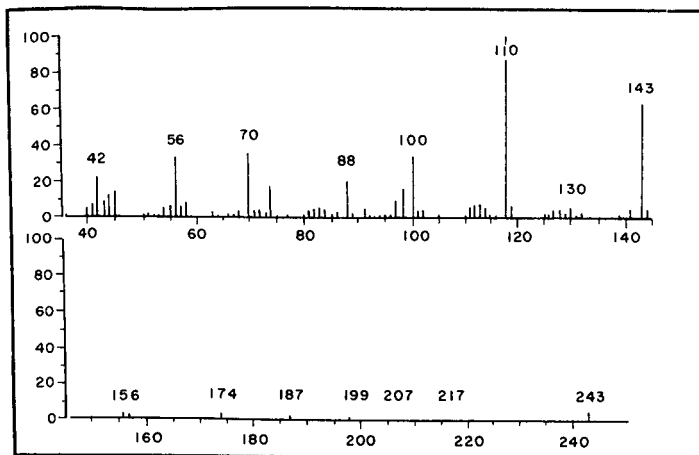Fig. 3. EI mass spectrum of peak 14 identified as HEOD.

Fig. 4. EI mass spectrum of peak 15 identified as THEED.

The EI mass spectrum of peak 12 is shown in Fig. 5 and, based on the charged ion distribution, was suspected to be either N,N-bis-(hydroxyethyl) glycine (BHG) or triethanolamine (TEA). These compounds were purchased in pure form and their standard EI mass spectra produced. The mass spectrum corresponding to peak 12 is quite similar to the BHG and TEA spectra (see Figs. 6 and 7). Therefore, definite identification was not possible based on the EI mass spectra. However, peak 12 had a retention time in the GC column of 20.1–20.3 min. which compares well with that of TEA. By contrast, BHG had a retention time of 22.1–22.2 min. To provide further evidence that peak 12 is due to TEA, known quantities of TEA were added to a partially degraded MDEA sample. The chromatograms of samples before and after TEA addition resulted in an area increase of peak 12. When a similar experiment was performed with an aqueous BHG solution, a new peak arose. Consequently, it was concluded that peak 12 is due to TEA.

Peak 10, whose EI mass spectrum is given in Fig. 8, corresponds to another major, unknown degradation compound. Although the fragmentation pattern suggested the compound to be some kind of piperazine, no satisfactory match with a library mass spectrum was found. Based on Fig. 8, the molecular peak was thought to contain 126 a.m.u. However, no plausible piperazine compound with a molecular mass of 126 could be formulated.
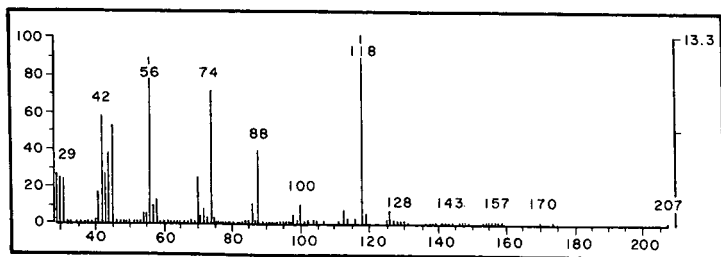
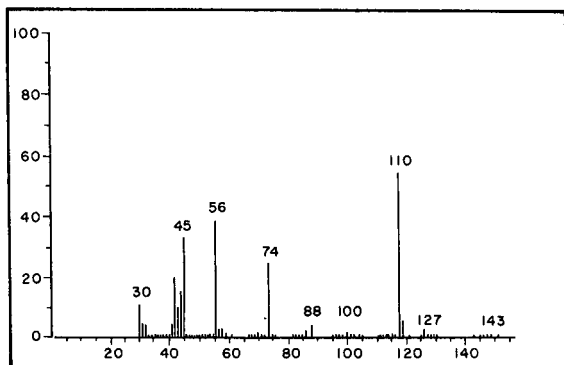

Fig. 5. EI mass spectrum of peak 12.
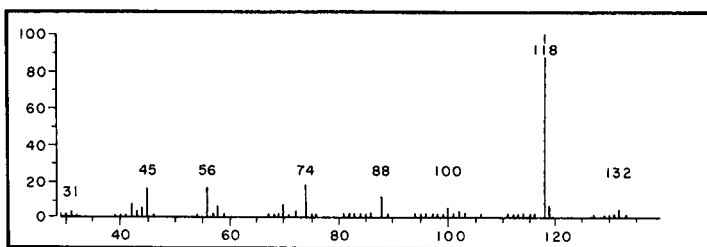
Fig. 6. EI mass spectrum of BHG.

Fig. 7. EI mass spectrum of TEA.

Molecular mass determination by CIMS

The methane CI mass spectra of MDEA, BHEP and HEOD are presented in Figs. 9–11, respectively. It is evident that the peaks of the protonated molecular ions, [M + H]+, are very distinctive in the methane CI spectra compared with the molecular ion peaks in the EI spectra. The methane CI mass spectrum of peak 10 is shown in Fig. 12. Although the molecular ion peak appears to be 126 a.m.u. in the EI spectrum, the methane CI spectrum shows a protonated molecular ion peak of 145 a.m.u. thus indicating a molecular mass of 144 a.m.u. Careful inspection of the EI spectrum also shows a very small peak at 144 a.m.u. which is easily overlooked in favour of the more distinct peak at 126 a.m.u. This clearly indicates that molecular mass determination from EI spectra may sometimes be misleading.
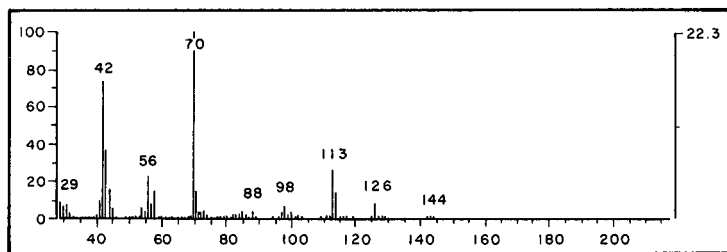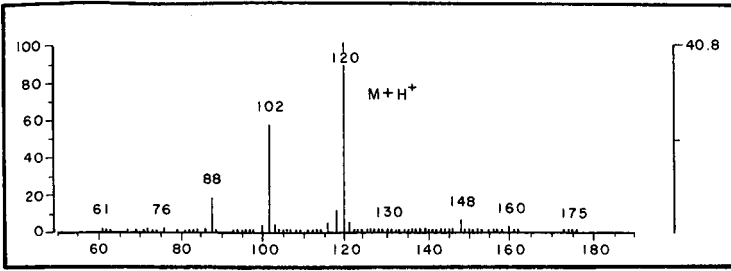

Fig. 8. EI mass spectrum of peak 10.

Fig. 9. Methane CI mass spectrum of MDEA.
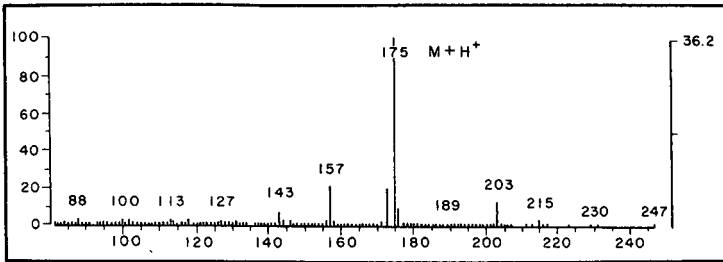

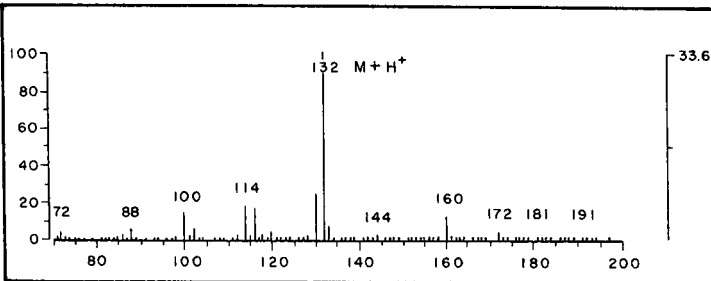Fig. 10. Methane CI mass spectrum of BHEP.
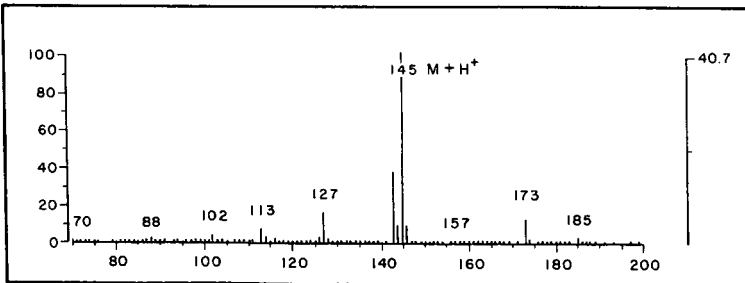

Fig. 11. Methane CI mass spectrum of HEOD.

Fig. 12. Methane CI mass spectrum of peak 10.

TABLE III

RESULTS OF HYDROXYL GROUP CALCULATIONS

Compound	$[M + H^+]$ unsilylated (a.m.u.)	$[M + H^+]$ silylated (a.m.u.)	Number of $-OH$ groups
MDEA	120	264	2
TEA	150	366	3
BHEP	175	319	2
Peak 10	145	217	1

Hydroxyl group determination

The methane CI spectra of MDEA, BHEP, TEA and peak 10 after silylation were obtained and the results of the hydroxyl group calculation are summarized in Table III. The validity of the silylation method is demonstrated by the accurate hydroxyl group determination for MDEA, TEA and BHEP. Peak 10 has a molecular mass of 144 and contains one–OH group. Based on this information and its fragmentation pattern, which suggested the presence of a piperazine ring, the compound was identified as 1-(2-hydroxyethyl)-4-methyl piperazine (HMP). As a further check, HMP was synthesized as described before. Its retention time in the GC column and its mass spectrum were compared with those of peak 10. A good match was found and HMP was thus confirmed as being responsible for peak 10. The mass spectrum of synthesized HMP is shown in Fig. 13.
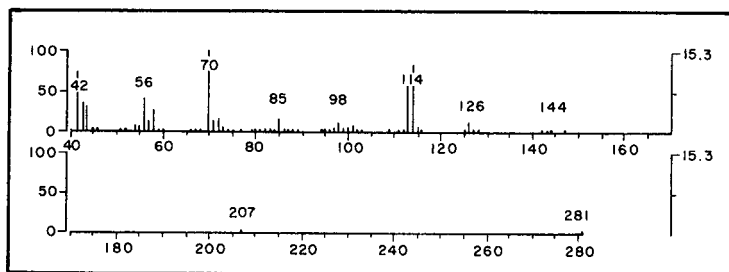

Fig. 13. EI mass spectrum of HMP synthesized in the laboratory.

CONCLUSIONS

The major MDEA degradation products, which result from its exposure to carbon dioxide at elevated temperatures and pressures, have been identified by GC coupled with EI- and CI-MS.

REFERENCES

1 A. L. Kohl and F. C. Riesenfeld, *Gas Purification*, Gulf Publishing Co., Houston, TX, 4th ed., 1985.
2 C. Blanc and J. Elgue, *Hydrocarbon Process*, 60 (1981) 111.
3 W. C. Yu, G. Astarita and D. W. Savage, *Chem. Eng. Sci.*, 40 (1985) 1585.
4 A. Chakma and A. Meisen, *Proc. 35th Can. Soc. Chem. Eng. Conf., Calgary*, Can. Soc. Chem. Eng., Ottawa, 1985, p. 37.
5 M. L. Kennard and A. Meisen, *J. Chromatogr.*, 267 (1983) 373.
6 M. L. Kennard and A. Meisen, *Ind. Eng. Chem. Fundam.*, 24 (1985) 129.
7 C. S. Hsu and C. J. Kim, *Ind. Eng. Chem. Prod. Res. Dev.*, 24 (1985) 630.
8 *EPA/NIH Mass Spectral Data Base; Natl. Stand. Ref. Data Service*, National Bureau of Standards, Washington, DC, 1983.
9 C. S. Hsu, *Proc. Ann. Conf. on Mass Spectrometry and Allied Topics*, San Diego, CA, 1985, p. 943.
10 M. L. Kennard, *Ph. D. Thesis*, University of, Vancouver, 1983.
11 C. J. Kim and G. Sartori, *Int. J. Chem. Kinet.*, 16 (1984) 1257.
12 E. K. Drechsel, *J. Org. Chem.*, 22 (1957) 849.
13 *Eight Peak Index of Mass Spectra*, Mass Spectrometry Data Centre, AWRE, Aldermaston, 2nd ed., 1974.

CHROM. 20 925

HIGH-PERFORMANCE LIQUID CHROMATOGRAPHY OF ALIPHATIC ALDEHYDES BY MEANS OF POST-COLUMN EXTRACTION WITH FLUOROMETRIC DETECTION

HITOSHI KOIZUMI* and YOSHIHITO SUZUKI

Department of Basic Engineering, Faculty of Engineering, Yamanashi University, Takeda 4, Kofu, Yamanashi 400 (Japan)

(First received April 29th, 1988; revised manuscript received August 3rd, 1988)

SUMMARY

7-Hydrazino-4-nitrobenzo-2,1,3-oxadiazole (NBD hydrazine) was synthesized from a reaction of NBD chloride with hydrazine. NBD hydrazones were formed from aldehydes and ketones but only the aldehyde derivatives were fluorescent in an antiprotonic solvent. An on-line post-column extraction system suitable for fluorometric detection of aldehyde-NBD hydrazones in reversed-phase high-performance liquid chromatography is presented. The system consists of a segmentor, a PTFE extraction coil and a PTFE membrane phase separator. The determination of aldehydes in whisky is described.

INTRODUCTION

In many foods, aliphatic aldehydes occur which smell of oxidative rancidity[1] over prolonged storage. Since long chain aldehydes are produced as degradation products of many kinds of polymers and the raw materials for polymer syntheses, it is required to determine trace amounts of aldehydes in order to evaluate the extent of deterioration. The presence of carbonyl compounds in the environment arises also from industrial pollution and from automobile exhausts. Carbonyl compounds, aldehydes in particular, are analyzed in order to estimate environmental pollutions in air and waste water. Since, in many cases, all kinds of carbonyl compounds exist in samples, it is necessary to separate a homologous series and determine them.

Several derivatization reactions have been described for liquid chromatographic (LC) determination of trace amounts of carbonyl compounds. Derivatization with 2,4-dinitrophenyl (DNP) hydrazine is usually employed for the determination of carbonyl compounds in automobile exhaust gases[2,3] and in rain-water[4] since increased sensitivity is achieved by the enhanced molar absorptivity of the derivatized compounds with respect to the starting carbonyl compounds. Recently, dabsylhydrazine was synthesized from the reaction of dabsyl chloride with hydrazine. This newly developed chromophoric reagent has been demonstrated to be very promising for the determination of aliphatic aldehydes with resonance Raman detection[5] and for that

of monosaccharides[6]. For highly sensitive detection, dansylhydrazine[7] as a fluorescent reagent has been employed. Hydrazine type reagents react readily with carbonyl compounds. Derivatizations by the Hatzsch reaction for fluorometric detection have been reported: reaction with ethyl acetoacetate[8], acetylacetone[9] and cyclohexane-1,3-dione[10,11]. These derivatization reactions are specific with respect to aldehyde. In particular, the reaction product of methanal with ethyl acetoacetate in the presence of ammonium acetate has a very intensive fluorescence.

    In this work, 7-hydrazino-4-nitrobenzo-2,1,3-oxadiazole (NBD hydrazine) was synthesized from the reaction of NBD-Cl with hydrazine. Both aldehydes and ketones were treated with NBD hydrazine[12] and converted into hydrazones, but only the aldehyde derivatives was fluorescent. The aldehyde derivatives give a light green fluorescense, only when present in an anti-protonic solvent such as carbon tetrachloride, chloroform and ethyl acetate, not in a protonic solvent. As described above, NBD hydrazones would promote a selective fluorometric detection in high-performance liquid chromatography (HPLC). However, when NBD hydrazones are separated in reversed-phase HPLC, fluorometric detection cannot be applied because of the lack of fluorescence in aqueous solvents.

    As in conventional HPLC, detection systems can be improved by making use of on-line post-column detection techniques. The use of on-line liquid–liquid extraction techniques for flow injection analysis[13,14] and in post-column systems for HPLC[15–18] has been reported. The extraction is performed by adding an immiscible organic solvent such as chloroform or benzene to the aqueous LC effluent, thereby producing a stream of extremely small aqueous and organic solvent segments. A approach to phase separation has been employed by exploiting semipermeable membranes. In general, the design of the phase separator consists of a manifold through which a segmented flow comes into contact with a hydrophobic membrane. The aqueous solvent cannot pass through the membrane, while the organic one can.

    In the present paper, we report the use of a membrane phase separator suitable for selective fluorometric detection of NBD hydrazones in a reversed-phase HPLC system with post-column extraction.

EXPERIMENTAL

Chemicals
    The aliphatic aldehydes methanal, ethanal, propanal, butanal, pentanal, 2-methylbutanal and aliphatic ketones acetone and 2-butanone were used as obtained without further purification. NBD-Cl and hydrazine monohydrate were obtained from Tokyo Kasei (Tokyo, Japan). Potassium dihydrogenphosphate and sodium dihydrogenphosphate were obtained from Kanto (Tokyo, Japan). All solvents were HPLC grade. Acetonitrile, chloroform and carbon tetrachloride were obtained from Nakarai (Kyoto, Japan). The distilled water was purified in-house using a Milli-Q II system (Nippon Millipore, Tokyo). Purified water was used in all experiments.

Apparatus
    Fig. 1 shows a schematic diagram of the post-column extraction chromatographic system. The mobile phase was delivered with a Tri Rotar V pump (JASCO, Tokyo, Japan) and samples were injected by a Rheodyne Model 7125 equipped with a
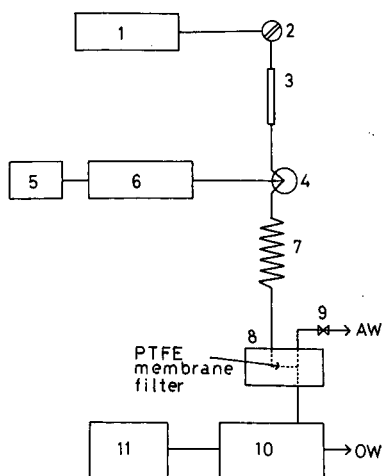
Fig. 1. Schematic diagram of the post-column extraction system: 1 = mobile phase pump; 2 = loop injector; 3 = analytical column (Develosil C$_8$, 5 μm, 150 mm × 4.6 mm I.D.); 4 = segmentor; 5 = degasser; 6 = segmenting liquid pump; 7 = extraction coil (1 m × 0.5 mm I.D. PTFE); 8 = membrane phase separator; 9 = needle valve; 10 = fluorescence detector; 11 = recorder; AW = aqueous waste; OW = organic waste.

50-μl loop. The column was packed with 5-μm Develosil C$_8$ (Nomura, Japan) using a slurry packing technique. A JASCO FP-110 spectrofluorometer equipped with a xenon lamp (output 75 W) was used. The detector, equipped a 17-μl flow cell, was operated with the excitation monochromator set at 470 nm and the emission monochromator set at 530 nm. The chromatograms were recorded with a SIC chromatocorder 11 (System Instrument, Tokyo, Japan). For the post-column extraction system, a JASCO Tri Rotar V pump which delivers flows in the range 0.3–1.0 ml/min, previously degassed on-line with a Shodex degas (Showa Denko, Tokyo). The column effluent and the segmenting liquid were mixed with a mixing joint (PTFE: Chromato Research, Sagamihara, Japan) in which three 1/16 in. O.D. PTFE tubings were jointed at angles of 60°. The extraction coil consisted of 100 cm × 0.5 mm I.D. PTFE tubing.

Several types of phase separator have ben reported[13,16–21]. The design of the phase separator used in this work[14] was a modification of that of Apffel et al.[16] who designed a miniaturized post-column extraction system. It consisted of two stainless-steel blocks, each of which has a semicylindrical groove of volume approximately 10 μl (2·mm width × 10 mm length × 0.5 mm depth) drilled into it. The membranes were Fluoropore type FG PTFE filters (Nippon Millipore) which have 0.2-μm pores and were bonded to a PTFE net facing the segmented liquid inlet. With a needle valve (Type BMCV; Gasukuro Kogyo, Tokyo) connected to the aqueous outlet, and applying back pressure, the amount of organic phase passing through the membrane filter can be regulated. In this work, the flow through the membrane filter was adjusted to 80% by a needle valve.

Synthesis of NBD hydrazine

Hydrazine monohydrate (0.3 ml) was dissolved in a mixture of 5 ml tetrahydrofuran and 5 ml of disodium hydrogenphosphate (1/15 *M*). NBD-Cl (400 mg, 2

mM) dissolved in 50 ml acetonitrile was added dropwise with stirring to the hydrazine solution at 40°C for 30 min, then for 60 min and finally cooled to room temperature. The reaction solution was filtered, and to the filtrate was added enough acetonitrile to give 100 ml. This reagent solution contains NBD hydrazine and has been stored for 2 weeks in the dark at -20°C without loss of potency.

Preparation of standard carbonyl-NBD hydrazone

A 1.0-ml volume of an aqueous solution containing 45 ppm of each carbonyl compound was mixed with 1.0 ml of NBD hydrazine solution and one drop of hydrochloric acid. The mixture was heated at 40°C for 20 min, and then cooled to room temperature. The carbonyl compounds were converted into NBD hydrazones. Aliquots (5μl) of the reaction mixture were injected directly for HPLC.

Determination procedure for HPLC

A 1-ml volume of an aqueous solution of aliphatic aldehyde containing 10 μg of 2-methylbutanal as an internal standard was placed in a 5-ml vial, followed by 1 ml NBD hydrazine solution and one drop of hydrochloric acid. The vial was sealed with a PTFE-lined screwcap and placed in a water-bath. The yields of the derivatization were examined at reaction temperatures of 40, 50 and 60 °C and reaction times of 10, 20 and 30 min. A 10-μl volume of reaction mixture was injected for HPLC. No difference in peak height or peak area obtained from chromatograms were detected under the above reaction conditions. The derivatization reaction at 40°C was complete after 10 min. Since a very small amount of NBD hydrazine was extracted into an organic solvent and fluoresced, fluorometric detection of NBD hydrazones was subject to interference by the excess of reagent. So the vial contents were mixed with 20 μl of 2-butanone in order to destroy the excess of NBD hydrazine. The vial was returned to the water-bath (40°C) for 10 min. According to this procedure, the excess of NBD hydrazine was converted into the hydrazone of the ketone which did not fluoresce. A 10-μl aliquot of the reaction mixture was injected for HPLC with post-column extraction.

Determination of aldehydes in whisky

To a 10-ml volume of a commercial whisky were added 1 ml of 2-methylbutanal (200 μg/ml) as an internal standard (IS) and enough water to give 20 ml. A 1.0-ml aliquot of the diluted solution was derivatized with NBD hydrazine as described above. A blank experiment was also performed with water–carbonyl free ethanol (70:30, v/v) containing an internal standard. A 10-μl aliquot of the reaction mixture was injected for HPLC.

RESULTS AND DISCUSSION

HPLC separation of NBD hydrazone

Isocratic elution conditions were investigated by using acetonitrile–water mixtures with the post-column extraction system (0.6 ml/min carbon tetrachloride as an organic solvent) as shown in Fig. 1. NBD hydrazones were not separated successfully because of weak interactions with the stationary phase. So we investigated the retention behaviour of NBD hydrazones using acetonitrile–phosphate buffers (Michaelis

buffer, potassium dihydrogenphosphate–disodium hydrogenphosphate, 1/30 M, pH 7.0) in volume ratios ranging between 20 and 50% acetonitrile, at a flow-rate of 1.0 ml/min.

Stable segments were not produced with mobile phases containing above 50% acetonitrile in water. As a result, the retention time of each NBD hydrazone increased with decreasing acetonitrile content. However, a complete separation of methanal and ethanal was not achieved at 20% acetonitrile. On the other hand, when the pH value of the phosphate buffer solution was varied in the range between 6.4 and 7.7, the retention time decreased with increasing pH, and was constant above pH 7.0. Good separation of NBD hydrazones was obtained by using acetonitrile–phosphate buffer pH 7.0 (22:5:77.5, v/v) on a Develosil C_8 column.

Effect of extraction coil

In order to examine the extraction efficiency, the length and inside diameter of the extraction coils were studied with the post-column extraction system. The helical coiling of the tubings (coiling diameter 20 mm) was used in order to reduce band broadening by introducing secondary flow phenomena. The measurements of the total band broadening of the HPLC system with post-column extraction were based on peak widths at half height and at 10% peak height.

At a mobile phase flow-rate of 1.0 ml/min a flow-rate of extraction solvent of 0.6 ml/min the maximum peak heights and minimum band broadenings were obtained when the tubing was 100 cm × 0.5 mm I.D. as shown in Table I. This tubing was therefore routinely used. It has a volume of approximately 196 μl and yields an extraction time of 7.4 s.

Effect of extraction solvent

For extractions in flowing systems[22], the detection sensitivity increases when the ratio of the flow-rate of the organic (extractant) phase to that of the aqueous phase decreases. Also band broadening increases with decreasing flow-rate of the organic solvent at a constant flow-rate of LC effluent.

In the present system, the flow-rate of carbon tetrachloride as the extraction solvent was varied from 0.3 to 1.0 ml/min, while the LC effluent flow-rate was kept constant at 1.0 ml/min. Eighty percent of the extraction solvent at each flow-rate was

TABLE I

EFFECT OF EXTRACTION COIL ON DETECTION

Develosil C_8 column: acetonitrile–phosphate buffer (22.5:77.5) mobile phase; flow-rate 1.0 ml/min; extraction solvent, carbon tetrachloride 0.6 ml/min; sample, propanal-NBD hydrazone. Number of experiments: 5.

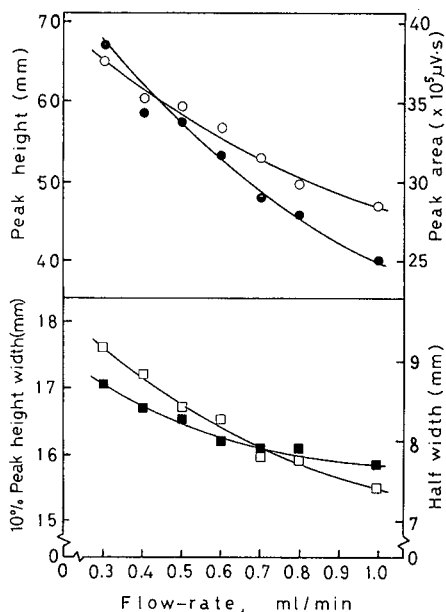| Coil dimension (cm × mm I.D.)	Peak height	Half width	Width at 10% peak height
50 × 0.8	79 ± 0.5	7.0 ± 0.0	14.9 ± 0.1
100 × 0.8	78 ± 0.8	7.0 ± 0.1	15.0 ± 0.1
50 × 0.5	77 ± 0.6	7.5 ± 0.0	14.5 ± 0.0
100 × 0.5	85 ± 0.8	6.6 ± 0.0	14.0 ± 0.0

Fig. 2. Effect of flow-rate on extraction efficiency. Extraction solvent; carbon tetrachloride. Sample: propanal-NBD hydrazone. ○ = Peak height; ● = peak area; □ = width at 10% peak height; ■ = half width. Number of experiments: 5. Average values plotted, R.S.D. within 3.2%.

led through the detector by adjustment of the back pressure regulator. The extraction efficiency was investigated by measuring not only the peak height and peak area for detection sensitivity but also the width at 10% peak height and the half width for band broadening as a function of the flow-rate of the extraction solvent. The results are shown in Fig. 2.

As shown in Fig. 2, band broadening at 10% peak height increases clearly with decreasing flow-rate of the organic solvent. On the other hand, both the peak height and peak area decrease because the concentration of NBD hydrazone in the extraction solvent will be lower. This indicates that the lower the flow-rate of extraction solvent, the higher is the detection sensitivity. In practice, however, unstable segments were frequently produced in the extraction coil at a flow-rate of 0.4 ml/min, often followed by a breakthrough of the aqueous phase to the fluorometric detector. In view of these results, the preferred flow-rate of the extraction solvent 0.5 ml/min, seems to be a good compromise.

One further contrast between the use of carbon tetrachloride and chloroform as extraction solvent, was examined. In the case of carbon tetrachloride, the extraction efficiency increased for NBD hydrazones of aliphatic aldehydes with longer alkyl chains. With chloroform, the extraction efficiency of aliphatic aldehydes having short alkyl chain were higher, and the detection sensitivity as a whole was about three times better than that with carbon tetrachloride. The extraction efficiency of NBD hydrazones was influenced by the extraction solvent, therefore we have examined the extraction efficiency by varying the contents of each extraction solvent (chloroform–carbon tetrachloride). Fig. 3 shows the percentage of the relative peak area of each
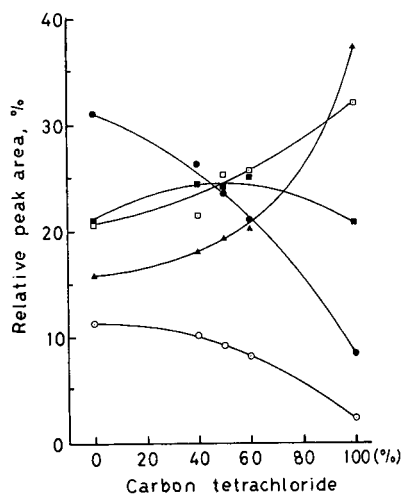
Fig. 3. Effect of the extraction solvent composition (carbon tetrachloride–chloroform) on the peak area. ○ = Methanal; ● = ethanal; ■ = propanal; □ = butanal; ▲ = pentanal.

NBD hydrazone as a function of the carbon tetrachloride contents in chloroform.

The results show that the extraction efficiency of propanal-NBD hydrazone was little affected by the composition of the extraction solvent, but those of methanal and ethanal decreased with increasing carbon tetrachloride content and those of butanal and pentanal increased. Consequently, chloroform–carbon tetrachloride (50:50, v/v) was used as the extraction solvent in order to reduce the differencies between the extraction efficiency of each NBD hydrazone. A typical chromatogram obtained under the optimum conditions is shown in Fig. 4.
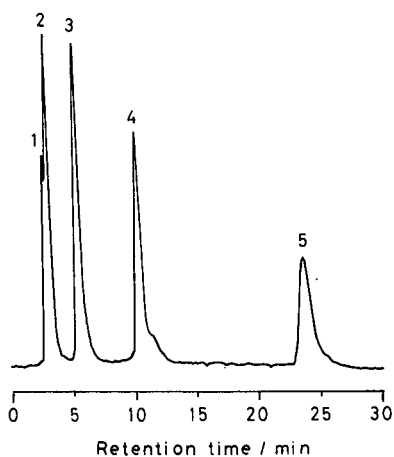

Fig. 4. Typical chromatogram of NBD hydrazones obtained under optimum conditions. Column: Develosil C$_8$ (5 μm, 150 mm × 4.6 mm I.D.). Mobile phase: acetonitrile–phosphate buffer pH 7.0 (22.5:77.5, v/v). Flow-rate: 1.0 ml/min. Extraction solvent: carbon tetrachloride–chloroform (50:50, v/v), 0.5 ml/min. Fluorescence detector; excitation 470 nm; emission 530 nm. Peaks: 1 = methanal; 2 = ethanal; 3 = propanal; 4 = butanal; 5 = pentanal.

TABLE II

CALIBRATION GRAPHS AND RELATIVE SENSITIVITY OF ALIPHATIC ALDEHYDES WITH POST-COLUMN EXTRACTION DETECTION

Develosil C_8 column; acetonitrile–phosphate buffer (22.5:77.5); flow-rate 1.0 ml/min; extraction solvent, carbon tetrachloride–chloroform (50:50), flow-rate 0.5 ml/min; extraction coil, 100 cm × 0.5 mm I.D. a = Slope, b = intercept, r^2 = regression coefficient.

Aldehyde	Area				Height			
	Calibration graph			Relative sensitivity	Calibration graph			Relative sensitivity
	a	b	r^2		a	b	r^2	
Ethanal	2.18	0.11	0.997	1.00	4.64	0.08	0.998	1.00
Propanal	3.02	0.05	0.999	1.38	7.88	0.07	0.999	1.70
Butanal	4.03	0.20	0.998	1.85	7.41	0.06	0.999	1.60
Pentanal	3.73	0.14	0.999	1.71	3.38	0.05	0.999	0.73

Calibration graph and reproducibility for aldehydes

Mixtures containing various amounts of four aliphatic aldehydes except methanal were determined with the procedure described for HPLC. Table II shows the calibration graphs obtained by plotting the ratios of the peak areas of NBD hydrazones to that of the internal standard against the known concentration of aldehydes. Linear relationships were found with the peak area and/or peak height ratio in the concentration ranges of 1.7–55 ppm (0.038–1.25 μmol/ml) for ethanal, 2.5–82 ppm (0.044–1.41 μmol/ml) for propanal, 2.8–90 ppm (0.039–1.25 μmol/ml) for butanal and 3.0–97 ppm (0.035–1.13 μmol/ml) for pentanal. The varying relative sensitivity shown in Table II evidenced by the different slopes of the regression lines reflects the varying extraction efficiency of NBD hydrazones with the post-column extraction HPLC system. However, the variation of responce was less than 1.85-fold by the peak area method, 1.70-fold by the peak height method.

The within-run precision of the method was measured by processing aliquots of reaction mixture through the procedure during a single day. The relative standard
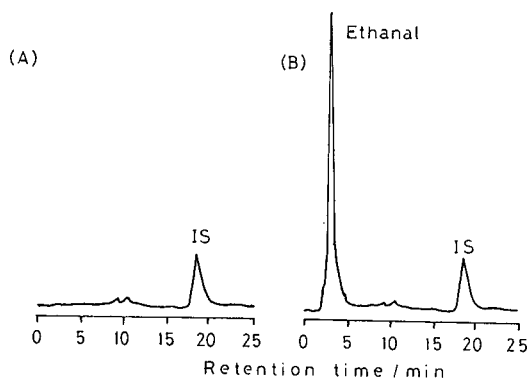

Fig. 5. Chromatagram of NBD hydrazones obtained from (A) a blank experiment and (B) a whisky. Chromatographic conditions as in Fig. 4.

deviation (R.S.D.) of the peak area ratio obtained by means of the internal standard procedure for five analyses of ethanal was 2.3% at 20 ppm (0.45 μmol/ml) and 5.4% at 4.5 ppm (0.10 μmol/ml).

Application

The present method was applied to the determination of aliphatic aldehydes in a commercial whisky. Chromatograms obtained from a blank experiment and a whisky are shown in Fig. 5. Ethanal was determined to be 90.6 ppm (2.06 μmol/ml) from the calibration graph using the peak area method. Other aldehydes were not detected in whisky.

In the present study NBD hydrazones were formed from carbonyl compounds but only the aldehyde derivatives were fluorescent in the anti-protonic solvent. A selective fluorometric detection of only aldehyde derivatives was achieved by means of a post-column extraction system which consists of a segmentor, an extraction coil and a membrane phase separator.

ACKNOWLEDGEMENT

REFERENCES

1 E. Puputti and P. Lehtonen, *J. Chromatogr.*, 353 (1986) 163.
2 J. B. DeAndrade and A. H. Mignel, *Int. J. Environ. Anal. Chem.*, 21 (1985) 229.
3 M. Possanzini, P. Ciccioli, V. DiPalo and R. Draisci, *Chromatographia*, 23 (1987) 829.
4 M. Matsumoto, Y. Nishikawa, K. Murano and T. Fukuyama, *Bunseki Kagaku*, 36 (1987) 179.
5 H. Koizumi, H. Koshiyama and Y. Suzuki, *Bunseki Kagaku*, 34 (1985) 376.
6 Jen-Kun Lin and Shan-Shou Wu, *Anal. Chem.*, 59 (1987) 1320.
7 R. W. Frei, J. F. Flawrence, J. Hope and R. M. Cassidy, *J. Chromatogr. Sci.*, 12 (1974) 40.
8 Y. Suzuki and K. Tani, *Bunseki Kagaku*, 29 (1980) 849.
9 Y. Suzuki and K. Tani, *Bunseki Kagaku*, 34 (1985) 55.
10 Y. Suzuki, *Bunseki Kagaku*, 34 (1985) 314.
11 K. Yoshino, T. Mastuura, M. Sano, S. Saito and I. Tomita, *Chem. Pharm. Bull.*, 34 (1986) 1694.
12 D. R. Knapp, *Handbook of Analytical Derivatization Reactions*, Wiley, New York, 1979.
13 S. Motomizu, Y. Hazaki, M. Oshima and K. Toei, *Anal. Sci.*, 3 (1987) 265.
14 H. Koizumi and Y. Suzuki, *Anal. Sci.*, 4 (1988) 537.
15 J. F. Lawrence, U. A. Th. Brinkman and R. W. Frei, *J. Chromatogr.*, 171 (1979) 73.
16 J. A. Apffel, U. A. Th. Brinkman and R. W. Frei, *Chromatographia*, 18 (1984) 5.
17 F. A. Maris, M. Nijenhuis, R. W. Frei, G. J. de Jong and U. A. Th. Brinkman, *Chromatographia*, 22 (1986) 235.
18 J. W. Hellgeth and L. T. Taylor, *Anal. Chem.*, 59 (1987) 295.
19 J. Kawase, *Anal. Chem.*, 52 (1980) 2124.
20 T. Imasaka, T. Harada and N. Ishibashi, *Anal. Chim. Acta*, 129 (1981) 195.
21 K. Ogata, K. Taguchi and T. Imanari, *Anal. Chem.*, 54 (1982) 2127.
22 A. H. M. T. Scholten, U. A. Th. Brinkman and R. W. Frei, *Anal. Chem.*, 54 (1982) 1932.

CHROM. 20 960

CHROMATOGRAPHIC SEPARATION OF THE DIASTEREOMERS OF A DI-HYDROPYRIDINE-TYPE CALCIUM CHANNEL ANTAGONIST AS THE BIS-3,5-DINITROBENZOATES

JOHN R. KERN*, DAVID M. LOKENSGARD and TAIYIN YANG

Analytical and Environmental Research, Syntex Research, Palo Alto, CA 94304 (U.S.A.)

(First received May 10th, 1988; revised manuscript received August 22nd, 1988)

SUMMARY

The diastereomeric components of the calcium channel antagonist RS-93522-004 are separated as the bis-3,5-dinitrobenzoate ester by reversed-phase high-performance liquid chromatography. The diastereomer ratio determination is shown to be precise, accurate and sensitive, and is not affected by the reaction yield of the derivatization with 3,5-dinitrobenzoyl chloride. The four individual stereoisomers of RS-93522-004 were independently shown to have equal reactivity toward 3,5-dinitro-benzoyl chloride.

INTRODUCTION

2-[4-(2,3-Dihydroxypropoxy)phenyl]ethyl methyl 1,4-dihydro-2,6-dimeth-yl-4-(3-nitrophenyl)-3,5-pyridinedicarboxylate (1), is a dihydropyridine-type calcium channel antagonist. It is being developed by Syntex Research under the code number RS-93522-004 for treating congestive heart failure and possibly hypertension. RS-93522-004 is unique among known dihydropyridine calcium entry blockers in-sofar as it features two asymmetric carbons and therefore exists as a mixture of four stereoisomers. More precisely, they consist of two enantiomeric pairs of diastereom-ers. The two asymmetric carbons, one at the junction of the dihydropyridine and phenyl rings and the other at the secondary hydroxyl group, are separated by 11 atoms. Animal studies on each individual isomer have shown that the most active isomers are those which have the (*S*) configuration at the C-4 (dihydropyridine ring junction) carbon. These would be the (*S,R*) and (*S,S*) isomers. Since the drug is currently being studied as the racemic mixture, quantitation of the amount of each isomer would be informative from a clinical as well as a regulatory standpoint. As an alternative, one may choose to monitor the ratio of the diastereomer pairs.
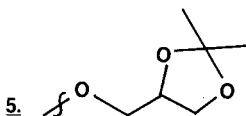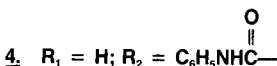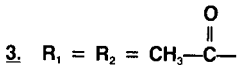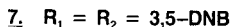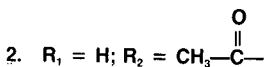
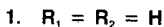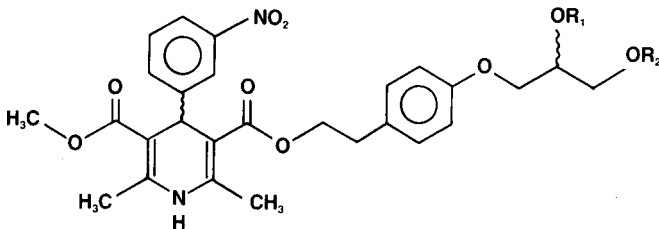The application of chiral high-performance liquid chromatography (HPLC) columns for diastereomer separation has been proposed[1] and several applications have appeared in the literature. Pirkle *et al.* have reported the diastereomeric sep-arations of the α-naphthamide of a quinoline[2], 3,5-dinitrobenzoyl α-amino acids[3], bis-3,5-dinitrophenyl carbamates of alicyclic diols[4], as well as di-and tri-peptides[5].

Extreme selectivity (resolution greater than 80) has also been observed for the diaste-reomers of 1,10-bis-(3,5-dinitrobenzoylleucine)decane by Pirkle and Pochapsky[6]. It is of interest to note, however, that recent reviews on this subject[7-20] do not mention the use of chiral HPLC columns for the resolution of diastereomers.

In a continuing program of analyzing the enantiomeric and diastereomeric purity of all new research compounds, we have successfully separated the diastereom-ers of an angiotensin-converting enzyme inhibitor using either a Pirkle-type column or an α_1-acid glycoprotein chiral column. In the present work, a number of commer-cially available chiral HPLC columns were investigated for their ability to separate the individual optical isomers or diastereomers of RS-93522-004. The columns in-vestigated include: (1) Pirkle covalent phenyglycine; (2) Pirkle covalent naphthylala-nine; (3) Cyclobond β-cyclodextrin; (4) Resolvosil bovine serum albumin; and (5) Enantiopak α_1-acid glycoprotein columns. The mobile phases employed were the ones typically suggested for chiral separation by either the column manufacturers or presented in the literature. In no case did the individual optical isomers or diastere-omers of RS-93522-004 resolve on the columns tested.

The remainder of this work focused on the separation of the diastereomer pairs of RS-93522-004. Preliminary analysis of RS-93522-004 using conventional reversed-phase and normal-phase HPLC with a variety of mobile phases gave no separation of the diastereomers, although in many attemps the compound eluted as a very broad peak, suggesting partial resolution of the diastereomers.

Since RS-93522-004 contains a diol functionality which could be easily deriv-atized, several different derivatives were prepared in an effort to achieve either indi-

1. $R_1 = R_2 = H$

2. $R_1 = H; R_2 = CH_3{-}\overset{\overset{\displaystyle O}{\|}}{C}{-}$

3. $R_1 = R_2 = CH_3{-}\overset{\overset{\displaystyle O}{\|}}{C}{-}$

4. $R_1 = H; R_2 = C_6H_5NH\overset{\overset{\displaystyle O}{\|}}{C}{-}$

5.

6. $R_1 = H; R_2 = 3,5{-}DNB$

7. $R_1 = R_2 = 3,5{-}DNB$

vidual optical isomer or diastereomer separation. RS-93522-004 was derivatized with: (i) acetic anhydride, producing both the monoacetate (2) and the diacetate (3); (ii) phenylisocyanate[21], producing only the monoderivative (4); (iii) 2,2-dimethoxy-propane[22], producing the acetonide (5); and (iv) 3,5-dinitrobenzoyl chloride[23], producing both the mono- (6) and bis- (7) derivatives.

Each derivative was analyzed by conventional reversed-phase and normal-phase HPLC, as well as by using the above mentioned chiral HPLC columns. Only compound 7, the bis-3,5-dinitrobenzoate (bis-3,5-DNB) derivative, afforded separation of the diastereomer pairs. This was accomplished on a reversed-phase system using methanol–water as the mobile phase (Fig. 1). Again, the bis-3,5-DNB derivative did not separate into diastereomers on any of the chiral columns tested.

EXPERIMENTAL

Apparatus

The HPLC equipment consisted of a Spectra-Physics Model 8100 liquid chromatograph equipped with a Valco fixed-loop injector and a Hewlett-Packard 1040A photodiode array UV–VIS detector set at 254 nm. The detector output was monitored using a Spectra-Physics SP4000 recording integrator.

Materials

RS-93522-004 and its optically pure stereoisomers were synthesized by the Institute of Organic Chemistry, Syntex Research, Palo Alto, CA, U.S.A. 3,5-Dinitrobenzoyl chloride (98% +) and triethylamine (99% +) were obtained from Aldrich (Milwaukee, WI, U.S.A.). HPLC-grade methanol and dichloromethane were obtained from Burdick and Jackson (Muskegon, MI, U.S.A.). Double distilled deionized water was used throughout the experiments.

Chiral HPLC columns

The chiral HPLC columns used were: (1) Pirkle Covalent D-Phenylglycine (Regis, Morton Grove, IL, U.S.A.); (2) Pirkle Covalent D-Naphthylalanine (Regis); (3) Cyclobond β-cyclodextrin (Astec, Whippany, NJ, U.S.A.); (4) Resolvosil bovine serum albumin (Machery Nagle, Düren, F.R.G.); and (5) Enantiopak α_1-acid glycoprotein (LKB, Bromma, Sweden).

Derivatization procedures

In a dry 75 × 12 mm I.D. test tube 44 mg (approximately 10-fold excess) of 3,5-dinitrobenzoyl chloride and 10 mg of RS-93522-004, or the individual stereoisomer, are dissolved in 3.0 ml of dichloromethane. A 26-μl volume of triethylamine (in 1.0 ml dichloromethane) is slowly added to the reaction mixture. The test tube is gently shaken intermittently over a 10–15-min period. A white precipitate appears after about 5 min. The reaction mixture is then evaporated to dryness and the product is dissolved in 5.0 ml of acetonitrile and slowly filtered through a C_{18} Sep-Pak (Waters, Milford, MA, U.S.A.). The reaction mixture is diluted to 25 ml with acetonitrile and further diluted to 100 ml with the HPLC mobile phase prior to HPLC analysis.

Chromatographic conditions

Determination of the diastereomer ratio was performed on an Alltech Spheri-sorb C$_8$, 5 μm, 250 × 4.6 mm I.D. HPLC column (Alltech Deerfield, IL, U.S.A.) using methanol–water (63:37, v/v) as the mobile phase. The column was maintained at 40°C. The mobile phase was delivered at 2.0 ml/min and the column eluent was monitored at 254 nm. The sample loading was typically 4 μg of the derivatization product with a 25-μl sample loop.

For the preparative HPLC isolation of the resolved diastereomers, an Alltech Ultrasphere C$_8$, 5 μm, 250 × 10 mm I.D. column maintained at 40°C was used. The mobile phase was methanol–water (65:35, v/v) and the flow-rate was 6.0 ml/min. The column eluent was monitored at 254 nm and the sample loading was 1.0 mg.

RESULTS AND DISCUSSION

Identification of diastereomers

Reversed-phase HPLC of the bis-3,5-DNB derivative (7) afforded the chroma-togram shown in Fig. 1. The diastereomers of 7 separate into two peaks which elute at about 41 and 44 min. These will be referred to as peaks A and B, respectively. Peaks A and B were identified as diastereomers by isolation of the individual peaks using preparative HPLC, and characterization of each by spectroscopic analyses. Proton
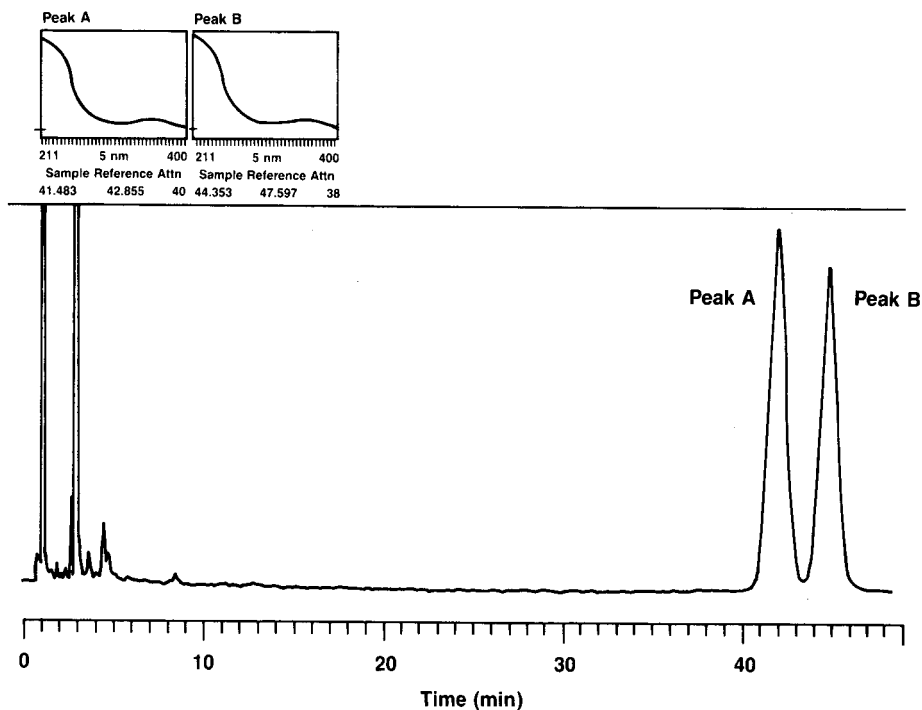

Fig. 1. Chromatographic resolution of the diastereomers of the bis-3,5-DNB derivative (7) on a 250 × 4.6 mm I.D. Spherisorb C$_8$, 5 μm column. Mobile phase: methanol–water (63:37, v/v). Flow-rate: 2.0 ml/min. UV spectra of peak A at 41 min and peak B at 44 min were obtained with an HP 1040A photodiode array detector at 254 nm.

TABLE I

RELATIVE RETENTION TIMES OF THE BIS-3,5-DNB DERIVATIVES OF THE OPTICAL ISO-
MERS OF RS-93522-004

Compounds	RRT*	
	Peak A	Peak B
RS-93522-004	0.39	0.37
(R,R) isomer	0.40	
(S,S) isomer	0.40	
(R,S) isomer		0.38
(S,R) isomer		0.38

$$* \text{ Relative retention time} = \frac{\text{Retention time of compound 6}}{\text{Retention time of peak A or B}}$$

NMR and UV spectra (Fig. 1) confirmed the isolated compounds to be the diastereo-
mers of the bis-3,5-DNB derivative of RS-93522-004. Negative-ion chemical ion-
ization mass spectrometry using methane as the reagent gas gave a quasi-molecular
ion $[M - 2H]^-$ at m/z 912. The above spectral analyses of the two resolved peaks
confirmed that the two are of the same chemical structure, suggesting the two peaks
to be stereoisomers, namely diastereomers.

The elution order of the diastereomers of the bis-3,5-DNB derivative (7) was
established by comparing the retention times with those of the bis-3,5-DNB deriv-
atives of the individual optically active stereoisomers. Each individual isomer was
derivatized and chromatographed using the described method. Since the mono-3,5-
DNB derivative (6) was usually present in the derivatization mixture, it could be used
as an internal reference peak for retention time comparison of the diastereomeric
bis-3,5-DNB derivatives from different sample preparations. The relative retention
time obtained for the bis-3,5-DNB derivatives of each optical isomer are in good
agreement with the values obtained for RS-93522-004 (Table I). These data indicate
that the order of elution is first the (R,R) (S,S) enantiomer pair and secondly the (R,S)
(S,R) enantiomer pair.

Effect of yield on diastereomer ratio determination

Throughout the course of developing optimal reaction conditions, variable
yields of the bis-3,5-DNB derivative were obtained. These yields ranged from approx-
imately 28% to essentially quantitative. However, the diastereomer ratio of each
RS-93522-004 sample determined by this method remained constant irrespective of
reaction yield (Table II). These data indicate that the individual isomers react at the
same rate during derivatization and that the diastereomer ratio determination is not
affected by the reaction yield of the bis-3,5-DNB derivative and does not require
quantitative derivatization.

Precision and accuracy

The precision of the chromatographic method was determined by performing
six replicate injections of a reaction product from the 3,5-dinitrobenzoyl chloride

TABLE II

EFFECT OF YIELD ON DIASTEREOMER RATIO DETERMINATION

Yield (%)	Peak A (%)	Peak B (%)
28	52.82	47.18
40	52.92	47.08
54	52.45	47.55
100	53.25	46.75
100	53.06	46.94
100	52.38	47.62
Mean ± S.D.	52.81 ± 0.34	47.29 ± 0.34

derivatization of RS-93522-004. The ratios of the areas of the two diastereomer peaks (A:B) from the six injections gave a relative standard deviation of 0.06%, demonstrating the chromatographic method to be precise and repeatable.

The diastereomer ratio determination involves several steps, including derivatization and chromatography. In order to properly evaluate the accuracy of the method the products of six separate derivatization reactions of a single sample of RS-93522-004 were analyzed by HPLC. The diastereomer ratios from the six reactions resulted in a relative standard deviation of 0.68%, indicating that the analytical error associated with derivatization, reaction work-up, sample preparation and chromatography is not excessive.

Sensitivity

Under the given HPLC conditions, the diastereomers of the bis-3,5-DNB derivative separate with nearly baseline resolution, with a resolution factor ranging typically from 1.1 to 1.4. The varying degree of resolution reflects column to column variation. The sensitivity of the method was evaluated at a minimum resolution of 1.1 in two respects; first, the effect of injected sample amount on diastereomer ratio determination, and secondly, the detection limit of the (R,R) (S,S) diastereomer in the presence of the (R,S) (S,R) diastereomer and the converse. Solutions of the bis-3,5-DNB derivative, each containing 3.7, 4.4, 5.0 and 8.7 μg of 7 in a 25-μl injection volume were injected and gave the diastereomer ratios listed in Table III. The results indicate that within the concentration range examined the diastereomer ratio remains constant and is independent of sample amount injected.

TABLE III

EFFECT OF INJECTED SAMPLE AMOUNT ON DIASTEREOMER RATIO DETERMINATION

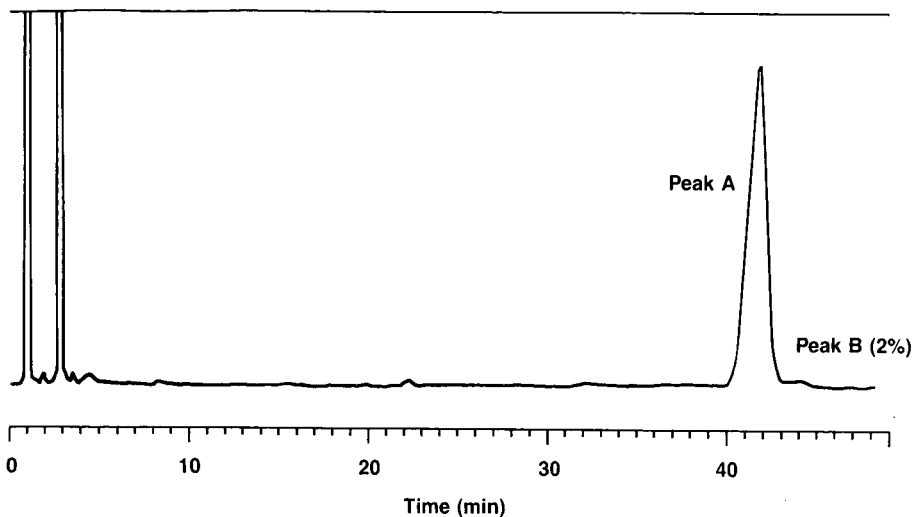| Sample amount (µg)	Diastereomer ratio
3.7	50.91 : 49.09
4.4	50.90 : 49.10
5.0	50.93 : 49.07
8.7	51.25 : 48.75

Fig. 2. Quantitation and chromatographic resolution of 2.0% (R,S) isomer in (R,R) isomer. Chromatographic conditions are the same as for Fig. 1.

The limit of detection was established for each diastereomer in a diastereomer mixture. Individual isomers, each containing a known small amount of the corresponding diastereomer, were derivatized and the detection limit for the minor diastereomer in the mixture was found to be about 0.3% for a typical 4-μg injection. Fig. 2 illustrates the quantitation of 2.0% of the (R,S) isomer in a sample of the (R,R) isomer. The method offers good sensitivity for the diastereomeric purity determination of RS-93522-004 and its stereoisomers.

CONCLUSION

We have described a simple procedure for the diastereomer ratio determination of a dihydropyridine-type calcium entry blocker, RS-93522-004, which contains a diol moiety. The procedure involves derivatization with 3,5-dinitrobenzoyl chloride followed by HPLC analysis of the resulting bis-3,5-dinitrobenzoate ester. The derivatization may be conveniently performed at a small (20 μmol) scale in a test tube with minimal sample work-up. The chromatography employs conventional reversed-phase HPLC on a C_8 column. The described procedure does not require quantitative derivatization. The reaction is very fast, being completed in 15 min and the analysis has been shown to be precise, accuate and sensitive.

REFERENCES

1 T. J. Sowin and A. Tsipouras, *Regis Lab Notes*, 1(2) (1985) 4.
2 W. H. Pirkle, C. J. Welch, G. S. Mahler, A. I. Meyers, L. M. Fuentes and M. Boes, *J. Org. Chem.*, 49 (1984) 2504.
3 W. H. Pirkle, T. C. Pochapsky, G. S. Mahler, D. E. Corey, D. S. Reno and D. M. Alessi, *J. Org. Chem.*, 51 (1986) 4991.
4 W. H. Pirkle, G. S. Mahler, T. C. Pochapsky and M. H. Hyun, *J. Chromatogr.*, 388 (1987) 307.
5 W. H. Pirkle, D. M. Alessi, M. H. Hyun and T. C. Pochapsky, *J. Chromatogr.*, 398 (1987) 203.
6 W. H. Pirkle and T. C. Pochapsky, *J. Chromatogr.*, 369 (1986) 175.
7 S. G. Allenmark, *J. Biomed. Biophys, Methods*, 9 (1984) 106.
8 S. G. Allenmark, *Trends Anal. Chem.*, 4 (1985) 106.
9 D. W. Armstrong, *J. Liq. Chromatogr.*, 7 (1984) 353.
10 R. Audebert, *J. Liq. Chromatogr.*, 2 (1979) 1063.
11 G. Blatschke, *Angew. Chem. Int. Ed. Engl.*, 19 (1980) 13.
12 W. H. Pirkle and J. M. Finn, in J. Morris (Editor), *Asymmetric Synthesis*, Vol. 1, Academic Press, New York, 1983, p. 87.
13 W. H. Pirkle, J. M. Finn, B. C. Hamper, J. Schreiner and J. R. Pribish, *ACS Symp. Ser.*, 185 (1982) 245.
14 W. H. Pirkle, *ACS Symp. Ser.*, 297 (1986) 101.
15 C. H. Lochmüller and R. Souter, *J. Chromatogr.*, 113 (1975) 283.
16 I. W. Wainer, in E. Reid (Editor), *Bioactive Analytes*, Plenum Press, New York, 1985, p. 243.
17 T. D. Doyle and I. W. Wainer, *Pharm. Technol.*, 2 (1985) 28.
18 I. W. Wainer, *Chromatogr. Forum*, 1 (1986) 55.
19 T. A. G. Noctor, B. J. Clark and A. F. Fell, *Anal. Proc.*, 23 (1986) 441.
20 H. T. Karnes and M. A. Sarkar, *Pharmaceutical Research*, Vol. 4, Plenum, New York, 1987, p. 285.
21 W. Periera, V. A. Bacon, W. Patton, B. Halpern and G. E. Pollock, *Anal. Lett.*, 3 (1970) 23.
22 T. G. Bonner, *Methods in Carbohydrate Analysis*, Academic Press, New York, 1963, p. 309.
23 N. D. Cheronis, J. B. Entirkin and E. M. Hodnett, *Semimicro Qualitative Organic Analysis*, Interscience, New York, 1965, p. 467.

CHROM. 20 941

LARGE-SCALE PURIFICATION OF THE CHROMOSOMAL β-LACTAMASE FROM *ENTEROBACTER CLOACAE* P99

CHRISTOPHER R. GOWARD*, GARRY B. STEVENS, PETER M. HAMMOND and MICHAEL D. SCAWEN

Division of Biotechnology, PHLS, Centre for Applied Microbiology and Research, Porton Down, Salisbury, Wiltshire SP4 0JG (U.K.)

(First received April 21st, 1988; revised manuscript received August 1st, 1988)

SUMMARY

Homogeneous β-lactamase (β-lactam hydrolase, E.C. 3.5.2.6) from *Enterobacter cloacae* P99, an enzyme that has an important function in antibiotic resistance, was prepared using a single cation-exchange chromatographic step with CM-Sepharose fast-flow. A 6-g amount of the enzyme was isolated from 5 kg of cell paste, with 84% of the enzyme activity in the cell homogenate being recovered by the single cation-exchange step. The specific activity of the β-lactamase was 587 U/mg protein. The relative molecular mass of the enzyme was determined to be 45 kDa by polyacrylamide gel electrophoresis in the presence of sodium dodecyl sulphate and the isoelectric point was 8.95.

INTRODUCTION

The β-lactamases (β-lactam hydrolase, E.C. 3.5.2.6) are a class of enzymes that are of increasing clinical significance because of their role in mediating resistance to β-lactam antibiotics. They are also of biochemical interest because they form a diverse group of enzymes, all of which catalyse the hydrolysis of the β-lactam ring in penicillins and cephalosporins. The enzymes have been classified into three classes, A, B and C, on the basis of their amino acid sequences[1,2].

Many Gram-negative bacteria produce chromosomally encoded β-lactamases; the Class C enzyme from *Enterobacter cloacae* is of particular interest as it is most active against cephalosporins and has a different evolutionary origin from the Class A penicillinases, although sharing a similar active site[3]. In addition, this enzyme has recently been crystallized[4]. The enzyme has been purified by a variety of methods, including chromatography on Sephadex G-50 followed by QAE-Sephadex[5] and chromatography on phenylboronic acid–agarose[6]. We describe here a simple method for the large-scale purification of this enzyme, based on a single chromatographic step using CM-Sepharose fast-flow. The facile and inexpensive nature of this purification makes it suitable for almost any scale of operation, from a laboratory scale to the pilot scale operation described in this paper, to produce several grams of homogeneous enzyme in a few days.

EXPERIMENTAL

Antibiotics and chemicals

Cephalosporin C, cephaloridine, cephalothin, cefazolin, cephalexin, cefamandole, cefuroxime and [2-hydroxy-1,1-bis(hydroxymethyl)ethyl]amino-1-propanesulphonic acid (TAPS) were obtained from Sigma (Poole, U.K.). Nitrocefin was obtained from Glaxo (Greenford, U.K.). All other chemicals were AnalaR grade from BDH (Poole, U.K.).

Culture methods

Enterobacter cloacae P99 was grown in a medium containing yeast extract (10 g/l), casamino acids (10 g/l), glucose (4 g/l), sodium β-glycerophosphate (2.27 g/l), and magnesium sulphate (0.25 g/l) (pH 7.2)[7] in a 400-l fermenter operated as described previously[8]. When the β-lactamase activity in the culture reached a maximum, after 4–6 h of growth, the temperature in the vessel was rapidly reduced to below 10°C and the bacteria were harvested by centrifugation in a Westfalia KA25 centrifuge at a flow-rate of 250 l/h. The cells were washed by suspension in 100 mM sodium phosphate buffer (pH 7.0) and harvested by centrifugation as above. The washed cell paste was quick-frozen and stored at −20°C.

Enzyme assay

The β-lactamase activity was determined by a spectrophotometric assay using cephalosporin C as substrate[9]. Cephalosporin C (0.2 mM) was dissolved in 50 mM TAPS–sodium hydroxide solution (pH 8.5). The reaction was started by the addition of 0.005–0.05 ml of enzyme solution and the decrease in absorbance at 260 nm was followed. The molar absorptivity for the complete hydrolysis of the substrate was determined as 6000 l mol^{-1} cm^{-1} from UV spectra recorded before and after complete hydrolysis. One unit of enzyme is defined as that amount which catalyses the hydrolysis of 1 μmol of cephalosporin C per minute at 30°C and pH 8.5. The activity of the enzyme against other substrates was determined in a similar manner, using 0.1–0.2 mM solutions of the reagents.

Determination of protein

Protein was determined by using the Coomassie Blue binding method[10], using bovine γ-globulin as standard. Column eluates were monitored at 280 nm.

Cation-exchange chromatography

CM-Sepharose fast-flow was obtained from Pharmacia (Milton Keynes, U.K.). It was suspended in 10 mM potassium phosphate buffer (pH 6.0) and packed into a column (16 × 1.6 cm I.D.). It was also slurry-packed into a Whatman Prep 25 column (16 × 45 cm I.D.) at a linear flow-rate of 750 cm/h, as described by the manufacturer (Whatman, Maidstone, U.K.). The column was equilibrated in 10 mM potassium phosphate buffer (pH 6.0) at a linear flow-rate of 550 cm/h.

Electrophoresis

Polyacrylamide gel electrophoresis in the presence of sodium dodecyl sulphate (SDS-PAGE) was performed in a Pharmacia Phast Gel apparatus with gradient gels of
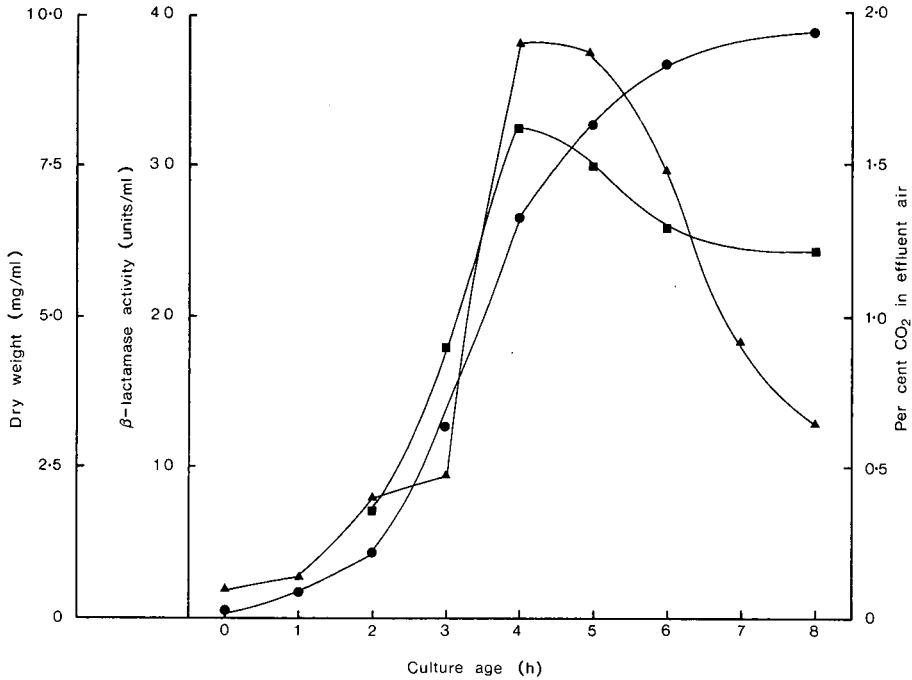
Fig. 1. Growth and β-lactamase production of *Enterobacter cloacae* P99 in 400-l culture. Culture conditions were as described in the text. ($\bullet$) Dry weight; ($\blacksquare$) β-lactamase activity; ($\blacktriangle$) CO_2 (%) in the effluent air.

10–15% acrylamide and using low relative molecular mass (M_r) marker proteins from Pharmacia (Milton Keynes, U.K.). The proteins were stained with Coomassie Blue R350 and densitometer scans were used to estimate the M_r.

The isoelectric point (pI) was determined by isoelectric focusing on Servalyt precoated polyacrylamide IEF gels (pH 3–10.5) with pH 5–10.5 standards from Pharmacia. Prefocusing was performed for 500 V h and electrofocusing was continued for a further 2000 V h after application of the samples. Proteins were detected with Coomassie Blue R350 and densitometer scans were used to estimate the pI.

RESULTS AND DISCUSSION

Growth of the organism

Fig. 1 shows the growth of *Enterobacter cloacae* P99 in a 400-l culture. A typical culture was harvested after 6 h of growth and yielded about 12 kg wet weight of cell paste, containing about 800 U β-lactamase/g of cells (equivalent to 2.9 kg dry cell mass, containing 3310 U β-lactamase/g of dry cells).

Small-scale purification of the enzyme

Frozen cell paste (6 g) was thawed in 33 ml of 100 mM potassium phosphate buffer (pH 6.0) at 4°C. About 1.5 mg of deoxyribonuclease was added to the suspension and the bacteria were disrupted by sonication at 20 kHz for six 30-s
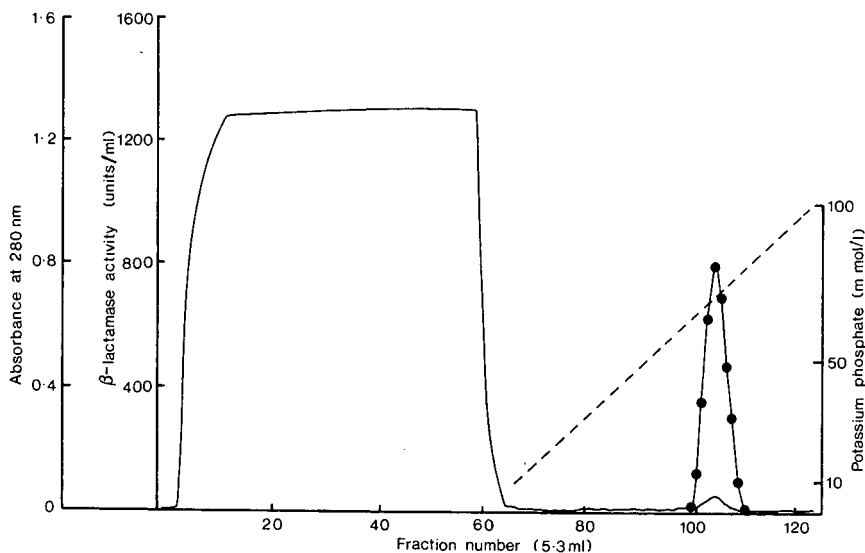
Fig. 2. Small-scale cation-exchange chromatography. The column of CM-Sepharose was 16 × 1.6 cm I.D. and was eluted with a 320-ml linear gradient of 10–100 mM potassium phosphate buffer (pH 6.0). Fractions 99–107 were combined. (–––) Potassium phosphate; (——) protein absorbance at 280 nm; (●) β-lactamase activity (units/ml).

intervals with cooling between each exposure. Cell debris was removed from the homogenate by centrifugation at 21 000 *g* at 8°C for 30 min. The supernatant was diluted to the same conductivity as 10 mM potassium phosphate buffer (pH 6.0). The diluted supernatant was applied to the 32-ml column of CM-Sepharose fast-flow (16 × 1.6 cm I.D.), equilibrated in 10 mM potassium phosphate buffer (pH 6.0) at a linear flow-rate of 190 cm/h. The column was washed with 55 ml of equilibrating buffer at a linear flow-rate of 190 cm/h and eluted with a 320-ml linear gradient from 10 to 100 mM potassium phosphate buffer (pH 6.0) at a linear flow-rate of 100 cm/h. The breakthrough and eluate were collected in fractions of 5.3 ml, as shown in Fig. 2. Fractions containing the enzyme activity were combined and concentrated to 5 ml by ultrafiltration using an Amicon PM 10 membrane. The concentrated enzyme was dialysed against 5 mM potassium phosphate buffer (pH 6.0). A summary of this purification is shown in Table I. Similar results were obtained when the enzyme from

TABLE I

PURIFICATION OF *ENTEROBACTER CLOACAE* β-LACTAMASE FROM 6 g OF CELL PASTE

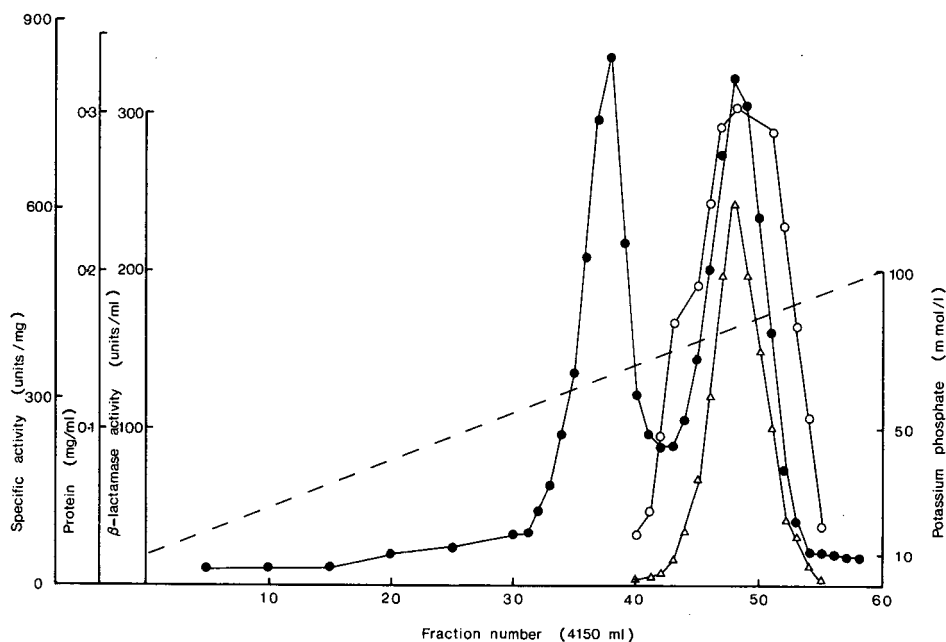| Step	Volume (ml)	Total enzyme (U)	Total protein (mg)	Specific activity (U/mg)	Recovery (%)
Homogenate	37	4452	374.0	11.9	100
Supernatant	90	4098	136.0	30.2	92
CM-Sepharose fast-flow	48	3786	5.6	676.0	85
Concentrate	5	3590	5.3	677.0	80

Fig. 3. Large-scale cation-exchange chromatography. The column of CM-Sepharose fast-flow was 16 × 45 cm I.D. and was eluted with a 240-l linear gradient of 10–100 mM potassium phosphate buffer (pH 6.0). Fractions 44–52 were combined. (—–) Potassium phosphate; (●) protein (mg/ml); (△) β-lactamase activity (units/ml); (○) specific activity (units/mg).

100 g of cell paste was prepared using a 500-ml column of CM-Sepharose fast-flow, so the process was scaled-up to prepare the enzyme from kilogram amounts of cell paste.

Large-scale purification of the enzyme

A 5-kg amount of frozen cell paste was suspended in 20 l of 100 mM potassium phosphate buffer (pH 6.0) and allowed to thaw overnight at 4°C. About 100 mg of deoxyribonuclease were added to the suspension and the bacteria were disrupted by a single passage through a Manton–Gaulin homogenizer at 55 MPa. The homogenate was centrifuged at 17 000 g at 8°C and a flow-rate of 50 l/h in a Sharples AS-26

TABLE II

PURIFICATION OF *ENTEROBACTER CLOACAE* β-LACTAMASE FROM 5 kg OF CELL PASTE

Step	Volume (l)	Total enzyme (MU)	Total protein (g)	Specific activity (U/mg)	Recovery (%)
Homogenate	23.50	4.13	226.0	18.3	100
Supernatant	250.00	3.84	138.0	27.8	93
CM-Sepharose fast-flow	38.60	3.46	6.0	577.0	84
Concentrate	1.52	3.11	5.3	587.0	75

continuous-flow centrifuge. The supernatant was diluted to the same conductivity as 10 mM potassium phosphate buffer (pH 6.0). The diluted supernatant was applied to the 25-l column of CM-Sepharose fast-flow (16 × 45 cm I.D.), equilibrated in 10 mM potassium phosphate buffer (pH 6.0) at a linear flow-rate of 190 cm/h. The column was washed with 40 l of equilibrating buffer at a linear flow-rate of 190 cm/h and eluted with a 250-l linear gradient from 10 to 100 mM potassium phosphate (pH 6.0) at a linear flow-rate of 100 cm/h. The eluate was collected in fractions of 4.15 l, as shown in Fig. 3. The fractions containing the enzyme activity were combined and concentrated to 1520 ml by ultrafiltration using Amicon PM 10 membranes. The concentrated enzyme was dialysed against 5 mM potassium phosphate buffer (pH 6.0) before being freeze-dried for storage. A summary of this purification is shown in Table II.

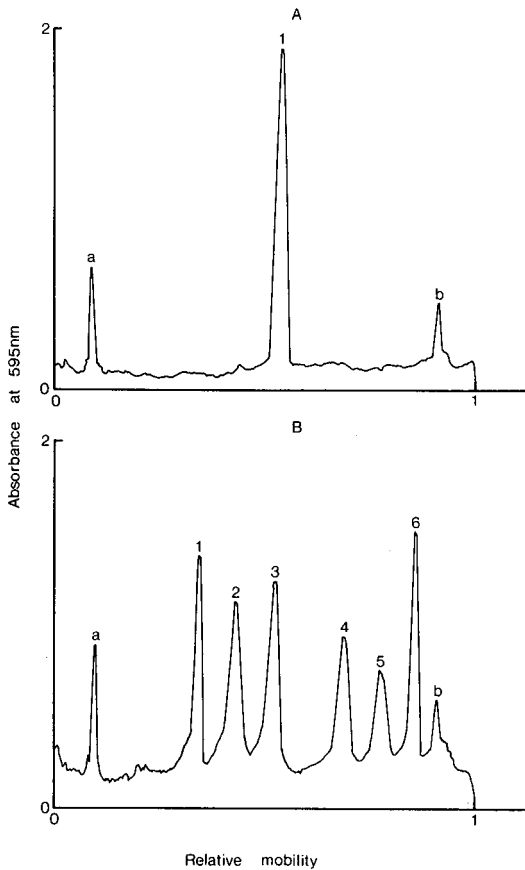A purification process has been described that uses phenylboronic acid–

Fig. 4. Densitometer scans following SDS-PAGE. The gel was scanned with a Joyce-Loebl Chromoscan 3. (A) 1 = β-lactamase (M_r 45 kDa). (B) Calibration proteins: 1 = phosphorylase b (M_r 94 kDa), 2 = bovine serum albumin (67 kDa), 3 = ovalbumin (43 kDa), 4 = carbonic anhydrase (30 kDa), 5 = soybean trypsin inhibitor (20.1 kDa) and 6 = α-lactalbumin (14.4 kDa). The gel boundary is designated peak a and the dye marker peak b.

agarose[6], which is a good method for use on the small scale (20-ml matrix), but it is impractical for large-scale applications. A procedure with two chromatographic steps has been described that uses gel filtration followed by application to a 500-ml column of an anion-exchange matrix, QAE-Sephadex, which binds contaminating protein but does not adsorb the enzyme[5]. The specific activity of the purified enzyme (134 U/mg) was considerably lower than that obtained using phenylboronic acid–agarose (750 U/mg). We have developed a procedure for the large-scale purification of the enzyme that is both rapid and economical. The high degree of purification achieved with CM-Sepharose fast-flow takes advantage of the high p*I* of the enzyme; at pH 6.0 most of the proteins in the cell free extract do not bind to the cation-exchange matrix (Fig. 2). CM-Sepharose fast-flow is used instead of the phenylboronic acid–agarose, which would have been prohibitively expensive for the preparation of the enzyme on the large scale. The procedure described allows the economical purification of β-lactamase from kilogram amounts of *Enterobacter cloacae* P99 cells. The specific activities of the
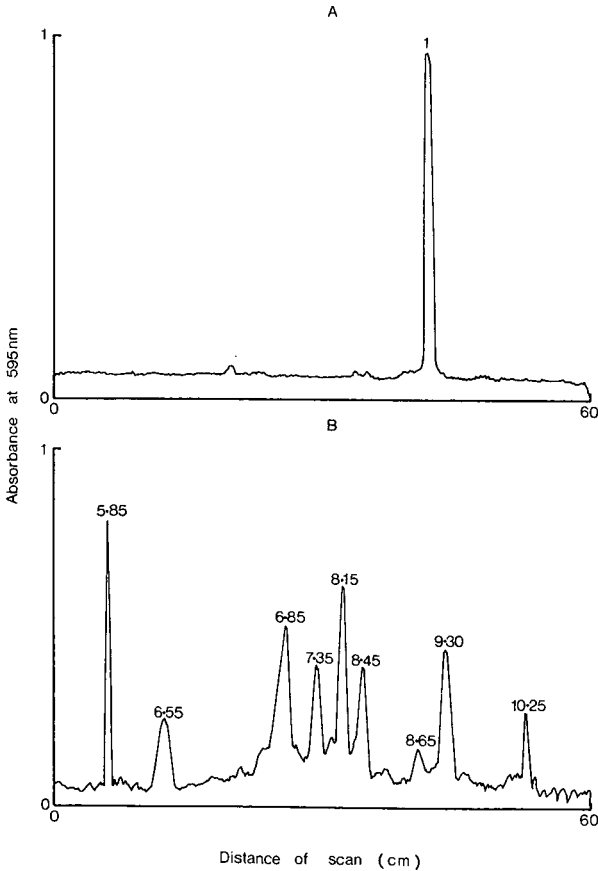

Fig. 5. Densitometer scans following isoelectric focusing. The gel was scanned with a Joyce-Loebl Chromoscan 3. (A) 1 = β-Lactamase (p*I* 8.95). (B) Calibration proteins: bovine carbonic anhydrase b (p*I* 5.85), human carbonic anhydrase b (6.55), horse myoglobin (6.85), horse myoglobin (7.35), lentil lectin (8.15), lentil lectin (8.45), lentil lectin (8.65), trypsinogen (9.30) and cytochrome c (10.25).

TABLE III

RELATIVE $V_{max.}$ OF THE β-LACTAMASE WITH DIFFERENT SUBSTRATES

Rates relative to cephalosporin C = 100%.

Substrate	Relative $V_{max.}$ (%)	Substrate	Relative $V_{max.}$ (%)
Nitrocefin	170.0	Cefazolin	24.7
Cephalothin	105.7	Cephalexin	13.1
Cephalosporin C	100.0	Cefamandole	1.8
Cephaloridine	54.7	Cefuroxime	0.12

β-lactamase, 677 and 587 U/mg, were lower than the 750 U/mg protein reported by Cartwright and Waley[6], but are considerably higher than the 134 U/mg protein described by Ross and Boulton[5].

The β-lactamase was shown to be homogeneous, giving a single protein band of M_r 45 000 on SDS-PAGE (Fig. 4). The M_r for *E. cloacae* P99 β-lactamase has previously been reported as 49 000 $\pm$ 3000[5]. Further evidence of purity is shown by the densitometer scan of an isoelectric focusing gel and the pI of the β-lactamase was determined to be 8.95 (Fig. 5). The enzyme from *E. cloacae* P99 has previously been reported to have a pI of 7.9[5], 8.0[11] and 8.25[6]. The enzyme was shown to be active against a series of antibiotics, particularly against the antibiotic-like substrate nitrocefin, as shown in Table III.

REFERENCES

1 R. P. Ambler, *Philos. Trans. R. Soc. London, Ser. B*, 289 (1980) 321–331.
2 B. Jaurin and T. Grundström, *Proc. Natl. Acad. Sci. U.S.A.*, 78 (1981) 4897–4901.
3 B. Joris, J. Dusart, J.-M. Frère, J. Van Beeuman, E. L. Emanuel, S. Petursson, J. Gagnon and S. G. Waley, *Biochem. J.*, 223 (1984) 271–274.
4 P. Charlier, O. Dideberg, J.-M. Frère, P. C. Moews and J. R. Knox, *J. Mol. Biol.*, 171 (1983) 237–238.
5 G. W. Ross and M. G. Boulton, *Biochim. Biophys. Acta*, 309 (1973) 430–439.
6 S. J. Cartwright and S. G. Waley, *Biochem. J.*, 221 (1984) 505–512.
7 R. P. Novick, *Biochem. J.*, 83 (1962) 229–235.
8 J. Melling and G. K. Scott, *Biochem. J.*, 130 (1972) 55–62.
9 C. H. O'Callaghan, P. W. Muggleton and G. W. Ross, *Antimicrob. Agents Chemother.*, 1 (1969) 57–63.
10 M. M. Bradford, *Anal. Biochem.*, 72 (1976) 248–254.
11 M. Matthew, A. M. Harris, M. J. Marshall and G. W. Ross, *J. Gen. Microbiol.*, 88 (1975) 169–178.

CHROM. 20 884

DETERMINATION OF MOLLUSCICIDAL SESQUITERPENE LACTONES FROM *AMBROSIA MARITIMA* (COMPOSITAE)

I. SLACANIN, D. VARGAS, A. MARSTON and K. HOSTETTMANN*

Institut de Pharmacognosie et Phytochimie, École de Pharmacie de l'Université de Lausanne, Rue Vuillermet 2, CH-1005 Lausanne (Switzerland)

(Received August 5th, 1988)

SUMMARY

A high-performance liquid chromatographic method is described for the determination of sesquiterpene lactones in the molluscicidal plant *Ambrosia maritima* (Compositae). The four major constituent lactones were measured at 220 nm, using naphthalene as internal standard, and a comparison of different extraction procedures was carried out, with a view to investigating variations in sesquiterpene lactone content.

INTRODUCTION

A number of plants are currently being investigated as potential sources of molluscicides for the treatment of sites infested with aquatic snails, the intermediate hosts of schistosomiasis[1,2]. The aim is thereby to reduce the incidence of this widespread tropical disease by removing the intermediate host of the parasitic schistosomes. One plant that enters into the category of promising plant molluscicides is *Ambrosia maritima* L. (Compositae), an annual herbaceous plant widely distributed throughout the Mediterranean region. The effects of *A. maritima* extracts on schistosomiasis-transmitting snails have been studied in the laboratory by Sherif and El-Sawy[3], who suggested growing the plant along the banks of water courses in order to introduce them directly into the water for the control of snails[4]. *A. maritima* has now reached the stage of large-scale field trials[5,6] and the numbers of live snails can be reduced by more than 90% when canals are treated with 70 mg/l of fresh or dry whole plant material[5].

The sesquiterpene lactones ambrosin (2) and damsin (3) have been isolated from the crude herb[7–9] and found to have molluscicidal activity. Further phytochemical investigations have revealed the presence of additional constituents, including the sesquiterpene lactones parthenin[10], neombrosin (4)[10], hymenin (1)[11], fifteen further pseudoguaianolides[10,12], two nor-sesquiterpene lactones[12] and two dimeric lactones[12]. Some of these constituents are only present in trace amounts[12].

The analytical high-performance liquid chromatography (HPLC) of sesquiterpene lactones has not been extensively investigated but separations of *Parthenium*
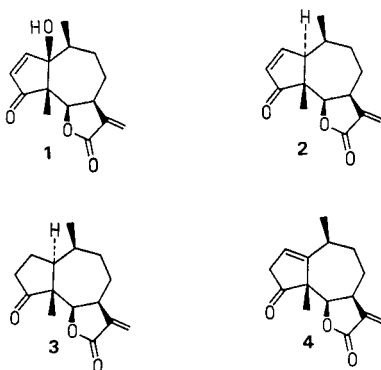
(Compositae) constituents on RP-8 columns included ambrosin, damsin, hymenin and parthenin among the substances investigated[13]. Here we report an HPLC method for the determination of sesquiterpene lactones in *A. maritima*. This has proved necessary for several reasons: (1) the content of molluscicidal sesquiterpenes in plant material from different strains and geographical locations needs to be known; (2) it is essential to investigate the efficiency of different extraction methods so that an optimized procedure can be introduced; this requires varying certain parameters, such as solvent, extraction time and temperature; and (3) the determination of amounts of sesquiterpene lactones is required for biodegradation and toxicological studies.

EXPERIMENTAL

Isolation of pure sesquiterpene lactones

In order to have standards available for qualitative and quantitative determinations, it was necessary to isolate the major sesquiterpene lactones 1–4 from *A. maritima*. A chloroform extract of the ground aerial parts of Egyptian *A. maritima* was flash chromatographed on silica gel, eluting first with chloroform, then ethyl acetate and finally methanol. Six fractions (I–VI) were obtained. The reference sesquiterpene lactones were all purified by low-pressure liquid chromatography on Lobar Li-Chroprep RP-8 (40–63 μm) columns (27 cm × 2.5 cm I.D.; Merck, Darmstadt, F.R.G.), using the following solvent systems: damsin and neoambrosin from flash fraction II, methanol–water (35:65); ambrosin from fraction III, methanol–water (50:50); and hymenin from fraction V, methanol–water (20:80). The sesquiterpene lactones were identified by comparison of their ^{1}H NMR and IR data with literature values[9,10].

Apparatus

HPLC analyses with UV detection were carried out on a system consisting of a Spectra-Physics (San Jose, CA, U.S.A.) 8700 pump, a Rheodyne injector, a Hewlett-Packard (Palo Alto, CA, U.S.A.) 1040A photodiode array detector, an HP-85 computer and an HP 7470A plotter. Quantitative analyses were performed with a Spectra-Physics 8700 pump, an LKB 2151 variable-wavelength monitor and an LKB 2221 integrator. For separations, a 5-μm Nucleosil 120-5 C$_8$ (12.5 cm × 4 mm I.D.) (Macherey-Nagel, Düren, F.R.G.) column was used.

Chromatographic conditions

For all analyses, an acetonitrile–water gradient was employed, starting with 35% of acetonitrile in water for 10 min and then increasing to 40% of acetonitrile in water over a further 10 min. The elution rate was 1 ml/min, with detection at 220 nm.

Sesquiterpene lactones were dissolved in methanol at a concentration of 0.25 mg/ml and samples of 10 μl were injected for analytical runs. For aqueous extracts, 10 μl of a 20 mg/ml solution in methanol were injected and for chloroform extracts 10 μl of a 2 mg/ml solution.

A 0.02 mg/ml solution of naphthalene in methanol was used as internal standard for quantitative measurements. A 1-ml volume of this solution was added to 1 ml of a solution containing 0.25 mg/ml of each of the four reference sesquiterpene lactones and 10 μl of the resulting solution were injected. For quantitative analyses of extracts, 1 ml of internal standard solution was added to either 2 ml of a 20 mg/ml solution of aqueous extract in methanol or 2 ml of a 2 mg/ml solution of chloroform extract. In each instance, 10 μl of the mixture were injected.

Determination

Quantitative analysis was carried out with naphthalene as internal standard. In order to obtain a standard correction factor (*SCF*) for the four sesquiterpene lactones, the solution of naphthalene with the lactones was injected three times and the correction factor calculated as follows.

$$SCF = \frac{A(\text{L}) \cdot W(\text{St})}{A(\text{St}) \cdot W(\text{L})}$$

where $A(\text{L})$ = peak area of sesquiterpene lactone, $A(\text{St})$ = peak area of naphthalene standard, $W(\text{L})$ = weight of sesquiterpene lactone and $W(\text{St})$ = weight of naphthalene standard. The correction factors calculated were ambrosin = 27.12, damsin = 43.03, neoambrosin = 35.26 and hymenin = 78.95.

The linearity of the relationship between peak area and amount injected (over the range used for the determinations) was checked by constructing calibration graphs for each of the sesquiterpene lactones.

The four sesquiterpene lactones in *A. maritima* extracts were determined by injecting samples with naphthalene (prepared as above) and calculating their content from the standard correction factors. HPLC runs were carried out in triplicate to obtain average results.

Extractions

Ground aerial parts (1 g) of *A. maritima* were stirred with either 100 ml of water or 100 ml of chloroform at room temperature. A portion (50 ml) of the extract was filtered, lyophilized and weighed. This procedure was repeated for different time intervals.

RESULTS AND DISCUSSION

An artificial mixture of the four major sesquiterpene lactones from *A. maritima* was efficiently separated on an RP-8 column with an acetonitrile–water gradient with detection at 220 nm (Fig. 1).
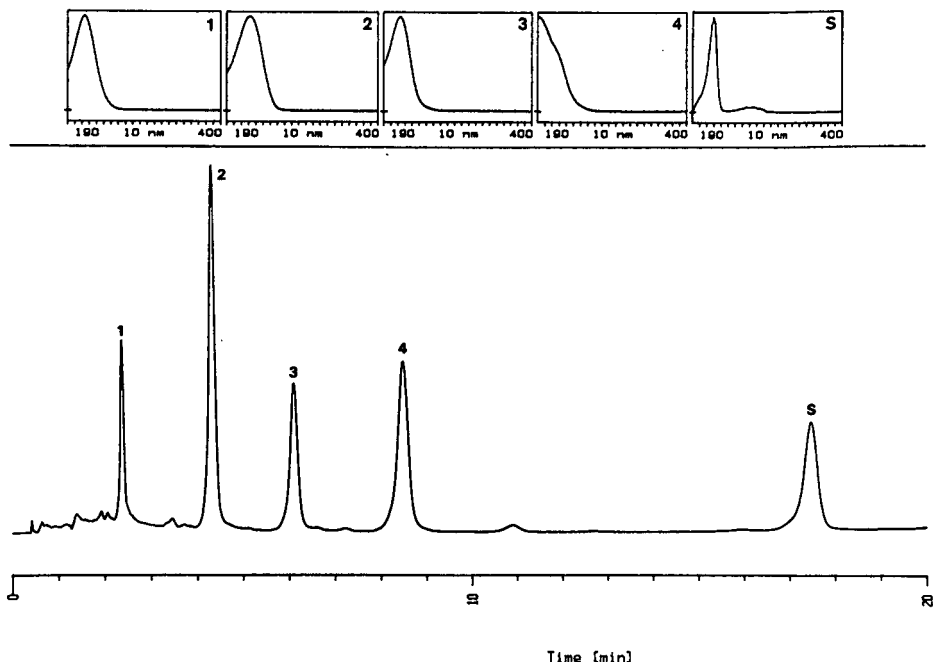
Fig. 1. HPLC separation of the pure sesquiterpene lactones hymenin (1), ambrosin (2), damsin (3) and neoambrosin (4). Column, Nucleosil 120-5 C_8 (12.5 cm × 4 mm I.D.); eluent, 35% acetonitrile for 10 min, increasing to 40% acetonitrile over 10 min; flow-rate, 1 ml/min; detection, 220 nm; internal standard (S), naphthalene.

Determinations of sesquiterpene lactones were carried out using naphthalene as internal standard because the UV maximum at 220 nm of naphthalene corresponds well with the UV maxima of the sesquiterpenes. Further, naphthalene elutes after the sesquiterpene lactones and does not interfere with peaks involved in the determinations.

An HPLC analysis of a water extract of *A. maritima* obtained after stirring for 12 h at room temperature is shown in Fig. 2. The most abundant sesquiterpene lactones are ambrosin (2), damsin (3) and hymenin (1), while neoambrosin (4) occurs in only very small amounts.

The HPLC trace of a chloroform extract of *A. maritima* after stirring for 24 h is shown in Fig. 3. Again, ambrosin (2), damsin (3) and hymenin (1) are the most important constituents. Between 0 and 3 min fewer polar constituents are eluted than with the aqueous extract.

The weights of extract obtained after extraction with water and chloroform for different time intervals are given in Table I. It is obvious that much more material is extracted with water than with chloroform. What is more surprising is that after a maximum at 12 h, the amount of aqueous extract subsequently diminishes at 24 h, 48 h and 7 days. Table I also gives the results obtained from the determination of sesquiterpene lactones 1–4 after extraction for different time intervals. These values are expressed as percentages of the total extracts and vary from a maximum of about 1.8%
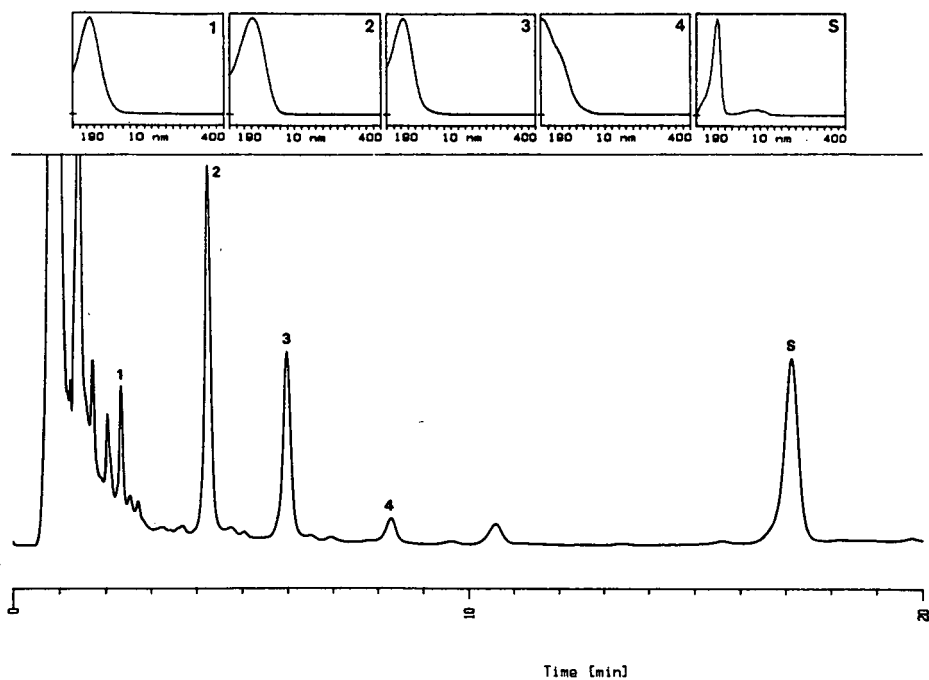
Fig. 2. HPLC analysis of a water extract (12 h) of *A. maritima*. Conditions and peaks as in Fig. 1.
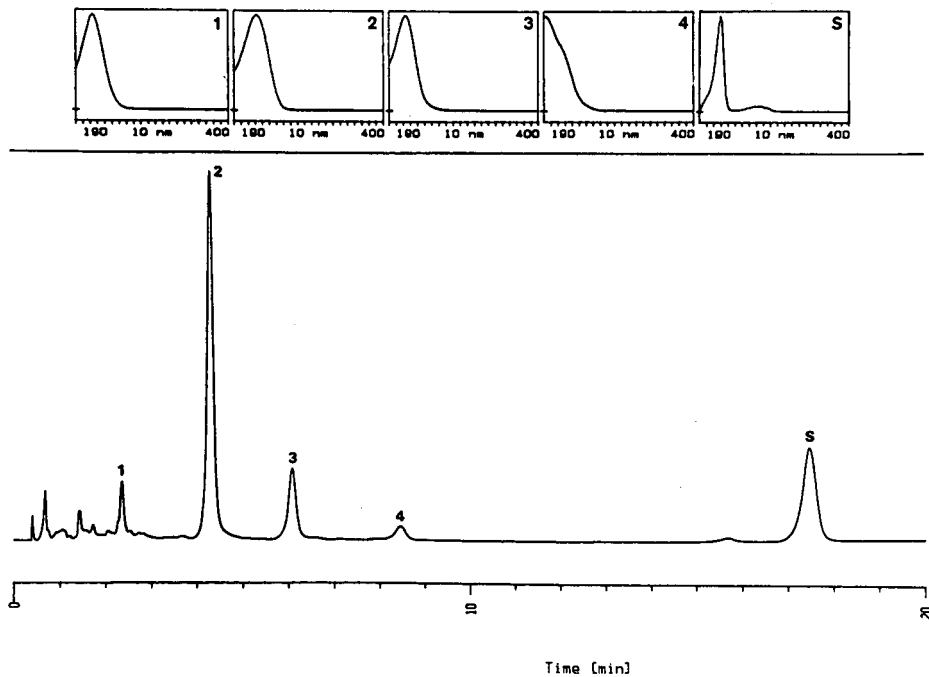

Fig. 3. HPLC analysis of a chloroform extract (24 h) of *A. maritima*. Conditions and peaks as in Fig. 1.

TABLE I

SESQUITERPENE LACTONE CONTENT OF *AMBROSIA MARITIMA* EXTRACTS

Extract	Extraction time (h)	Total weight of extract (g)	Sesquiterpene lactones (%, w/w)			
			1	*2*	*3*	*4*
Aqueous	6	0.3066	1.15	1.18	1.13	0.20
	12	0.3185	1.28	1.38	1.29	0.22
	24	0.2730	1.54	1.04	1.45	0.22
	48	0.2592	1.76	0.76	1.52	0.21
	7 days	0.2204	0	0	0	0
Chloroform	24	0.0503	7.98	21.49	9.80	2.17

for hymenin (1) after 48 h to 0.2% for neoambrosin (4). Whereas the percentages of damsin and hymenin increase with increasing time of extraction, the percentage of ambrosin actually decreases from 1.4% to a 0.8% over a period of 48 h. After 7 days, none of the four sesquiterpene lactones is detectable by the HPLC method. Instead, a peak with a retention time of *ca.* 11 min is detected (Fig. 4). Although this peak is already present after extraction for 12 h (Fig. 2), it is only in the HPLC trace of the 7-day extract (Fig. 4) that it represents the major product. The determination of the structure of substance 5 corresponding to this peak is in progress.
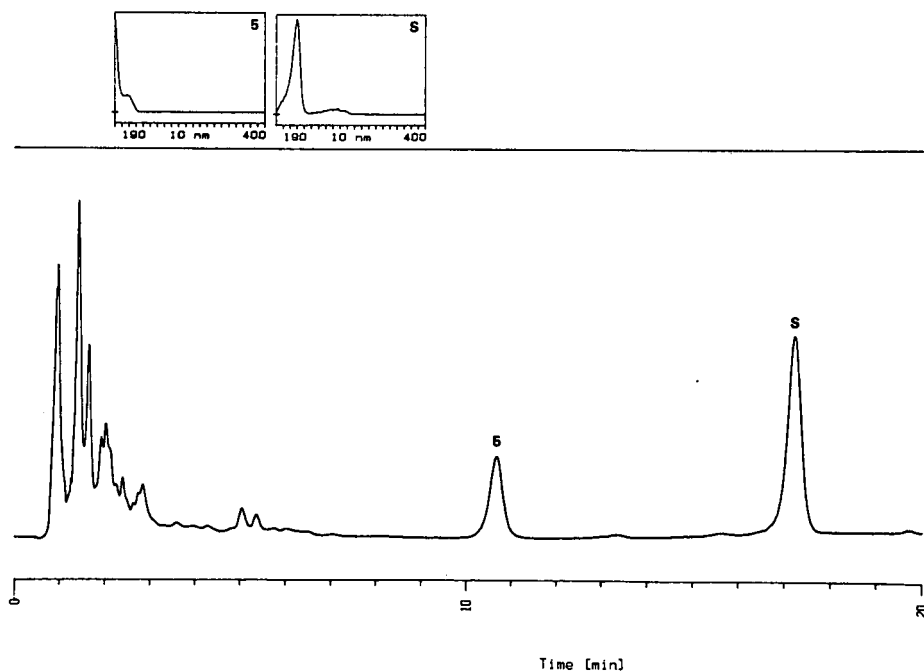

Fig. 4. HPLC analysis of a water extract (7 days) of *A. maritima*. Conditions as in Fig. 1. Compound 5 is a degradation product produced during extraction (see text).

CONCLUSION

An HPLC method on a reversed-phase support has been developed for the determination of sesquiterpene lactones from the molluscicidal plant *A. maritima* (Compositae). Ambrosin and damsin are known to be molluscicidal but insufficient amounts of the other lactones were isolated to test their molluscicidal activities. However, these two sesquiterpene lactones, together with hymenin, represented the largest proportion of the sesquiterpene lactones in the extracts. The aqueous extracts obtained after 24 h, 48 h and 7 days were inactive at 400 mg/l against snails of the species *Biomphalaria glabrata*, but the chloroform extract obtained after 24 h was active at 200 mg/l. This is presumably the result of the higher relative content of sesquiterpene lactones in this extract (21.5% ambrosin, for example).

There is obviously a slow degradation of the sesquiterpene lactones in the aqueous extracts, so much so that after 7 days none of the four lactones remains. A possible explanation is the weak alkalinity of the aqueous extract, which may cause the degradation. In fact, a solution of ambrosin in water at pH 9 is completely degraded after 48 h.

The information obtained from these studies should help in devising protocols for standardizing extracts of *A. maritima*. This aspect is especially important during the stage of field trials, in order to ascertain the amounts of sesquiterpene lactones present in different batches of material, from different countries, from different sub-species and from collection at different periods. Toxicological investigations also require an accurate indication of sesquiterpene lactone content.

REFERENCES

1 K. E. Mott, *Plant Molluscicides*, Wiley, Chichester, 1987.
2 K. Hostettmann, in H. Wagner, H. Hikino and N. R. Farnsworth (Editors), *Economic and Medicinal Plant Research*, Vol. 3, Academic Press, London, in press.
3 A. F. Sherif and M. F. El-Sawy, *Alexandria Med. J.*, 8 (1962) 139.
4 A. F. Sherif and M. F. El-Sawy, *Bull. High Inst. Public Health Alexandria*, 7 (1977) 1.
5 M. F. El-Sawy, J. Duncan, T. F. de C. Marshall, M. A. R. Shehata and N. Brown, *Tropenmed. Parasitol.*, 35 (1984) 71.
6 M. F. El-Sawy, H. K. Bassiouny and N. M. Badr, *Bull. High Inst. Public Health Alexandria*, 16 (1986) 107.
7 H. Abu-Shady and T. O. Soine, *J. Am. Pharm. Assoc.*, 42 (1953) 387.
8 L. Bernardi and G. Büchi, *Experientia*, 13 (1957) 467.
9 W. Herz, M. Watanabe, M. Miyazaki and Y. Kishida, *J. Am. Chem. Soc.*, 84 (1962) 2601.
10 N. A. Abdel Salam, Z. F. Mahmoud, J. Ziesche and J. Jakupovic, *Phytochemistry*, 23 (1984) 2851.
11 A. K. Picman, J. T. Arnason and J. D. H. Lambert, *J. Nat. Prod.*, 49 (1986) 556.
12 J. Jakupovic, H. Sun, S. Geerts and F. Bohlmann, *Planta Med.*, 53 (1987) 49.
13 B. Marchand, H. M. Behl and E. Rodriguez, *J. Chromatogr.*, 265 (1983) 97.

CHROM. 20 946

SIMULTANEOUS DETERMINATION OF NINE FOOD ADDITIVES USING HIGH-PERFORMANCE LIQUID CHROMATOGRAPHY

YOSHITOMO IKAI*, HISAO OKA, NORIHISA KAWAMURA and MASUO YAMADA

Aichi Prefectural Institute of Public Health, Tsuji-machi, Kita-ku, Nagoya 462 (Japan)

(First received April 12th, 1988; revised manuscript received August 29th, 1988)

SUMMARY

A technique for the simultaneous determination of sorbic acid, benzoic acid, dehydroacetic acid, p-hydroxybenzoic acid esters (ethyl, isopropyl, n-propyl, isobutyl and n-butyl p-hydroxybenzoate) and saccharin sodium using ion-pair reversed-phase high-performance liquid chromatography is described. The nine food additives were separated on a Nucleosil $3C_{18}$ (3 μm) column (75 × 4.6 mm I.D.) using methanol–acetonitrile–0.05 M aqueous acetonic acid solution (pH 4.5) (1.5:1:3.1) containing 2.5 mM cetyltrimethylammonium chloride as the mobile phase at a flow-rate of 1.0 ml/min, and detected at 233 nm. The food additives were separated within 18 min and their calibration graphs were linear between 2 and 200 ng.

INTRODUCTION

Sorbic acid (SOA), benzoic acid (BA), dehydroacetic acid [DHA, 3-acetyl-6-methyl-2H-pyran-2,4(3H)-dione] and p-hydroxybenzoic acid esters (ethyl-, isopropyl-, n-propyl-, isobutyl- and n-butyl-PHBA) as preservatives and saccharin sodium (SA) as a sweetener are food additives commonly used in Japan. One of the most important duties of a public health agency is to check quantitatively these food additives in foods. They are usually analysed according to individual methods, which is very inefficient from the point of view of analytical processing time and materials, so a simple and simultaneous analytical method for additives in various foods is required.

As the food additives differ considerably in polarity, their simultaneous determination by gas or thin-layer chromatography is difficult. However, we considered that high-performance liquid chromatography (HPLC) using solvent gradient and ion-pair techniques might be a more promising approach. Although some HPLC systems for the simultaneous determination of food additives except DHA have already been reported using these HPLC techniques[1–6], no system for all of the above food additives has been established. We attempted to modify the reported HPLC systems[3,4] so as to make them applicable to the determination of the nine food additives including DHA, but satisfactory results could not be obtained because DHA appeared as an extremely tailing peak on the chromatogram. Therefore, we investigated the control of the tailing of DHA and established a simultaneous method

for the nine food additives using an HPLC system. This paper describes techniques for the simultaneous determination of the nine food additives including DHA using ion-pair reversed-phase (RP) HPLC.

EXPERIMENTAL

Materials

Acetic acid, acetonic acid (2-hydroxyisobutyric acid), acetonitrile, acetylacetone, adipic acid, anhydrous sodium sulphate, citric acid, diethyl ether, malonic acid, methanol, oxalic acid, phosphoric acid, propionic acid, sodium chloride, sodium hydroxide, sulphuric acid and tartaric acid were of analytical-reagent grade.

p-Hydroxybenzoic acid and its esters (methyl, ethyl, isopropyl, *n*-propyl, *sec.*-butyl, isobutyl and *n*-butyl *p*-hydroxybenzoate), DHA, salicylic acid, thiabendazole (TBZ), *o*-phenylphenol (OPP), diphenyl (DP), butylhydroxyanisole (BHA), dibutylhydroxytoluene (BHT), cetyltrimethylammonium chloride (CTA), *n*-tetradecyltrimethylammonium bromide (TTA) and tetrabutylammonium bromide (TBA) were purchased from Tokyo Chemical Industry (Tokyo, Japan) and SOA, BA, SA, ascorbic acid, erithorbic acid, nicotinic acid and nicotinamide from Wako (Osaka, Japan).

Apparatus

A chromatograph equipped with a constant-flow pump (LC-5A, Shimadzu, Kyoto, Japan) was used together with a variable-wavelength detector (Shimadzu SPD-2AM).

Separations were performed on Nucleosil $3C_{18}$ (3 μm) (Macherey-Nagel, Düren, F.R.G.) packed in a stainless-steel column (75 $\times$ 4.6 mm I.D.).

Preparation of mobile phase

The appropriate amounts of methanol, acetonitrile and aqueous solutions were mixed, then the ion-pair reagents were dissolved in the mixture to give the calculated concentrations. The pH values of aqueous solutions were adjusted with sodium hydroxide.

RESULTS AND DISCUSSION

As described in the Introduction, SOA, BA, DHA and SA have very different polarities to PHBAs. In order to separate such analytes by RP-HPLC, solvent gradient and ion-pair techniques are generally used. However, the solvent gradient method is unsuitable for routine analysis, because it is time consuming and requires expensive apparatus. Therefore, we tried to separate the nine food additives using an ion-pair technique. After various studies of the retention behaviour of the additives, we achieved their baseline separation. A typical HPLC trace under the optimal conditions is shown in Fig. 1. Methanol–acetonitrile–0.05 M aqueous acetonic acid solution (pH 4.5) (1.5:1:3.1) containing 2.5 mM CTA was used as the mobile phase and Nucleosil $3C_{18}$ (3 μm) packed in short column (75 $\times$ 4.6 mm I.D.) was used as the stationary phase. The flow-rate and measurement wavelength were adjusted at 1.0 ml/min and 233 nm, respectively.

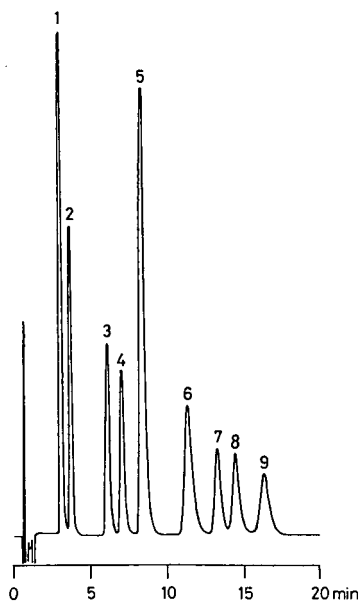In order to optimize the HPLC conditions described above, the following pa-

Fig. 1. Typical high-performance liquid chromatogram of food additives under the optimal conditions. 1 = DHA; 2 = ethyl-PHBA; 3 = isopropyl-PHBA; 4 = n-propyl-PHBA; 5 = SOA; 6 = BA; 7 = isobutyl-PHBA; 8 = n-butyl-PHBA; 9 = SA (100 ng each). HPLC conditions: column, Nucleosil 3C$_{18}$ (3 μm) (75 × 4.6 mm I.D.); mobile phase, methanol–acetonitrile–0.05 M aqueous acetonic acid solution (pH 4.5) (1.5:1:3.1) containing 2.5 mM CTA; flow-rate, 1.0 ml/min; detection, 233 nm.

rameters were examined: (1) effect of acetonic acid, (2) effect of ion-pair reagent, (3) proportion of methanol and acetonitrile and (4) proportions of organic solvents and aqueous solution. The results of these examinations are described below. In interpreting the chromatograms, the parameters used are (a) the asymmetry factor (A_s), which is the ratio of the length of the rear (tailing edge) to that of the front (leading edge) of the peak along a line parallel to 10% of its height above the baseline, and (b) the capacity factor, $k' = (t_R - t_0)/t_0$, where t_R is the retention time of the sample peak and t_0 that of a non-retained peak.

Effect of acetonic acid
      When SOA, BA, DHA and SA are determined by RP-HPLC, the pH of the mobile phase is one of the most important factors for the separation. In order to stabilize the pH of the mobile phase, phosphate and acetate buffer solutions are generally used. However, we could not obtain satisfactory results in attempts to separate the nine food additives using these buffer solutions. Between pH 3.0 and 5.0, the determination of DHA was prevented by its extreme peak tailing. On the other hand, outside that pH range, satisfactory separation of the additives could not be achieved under any HPLC conditions, although DHA did not appear as a tailing peak. We therefore considered that these pH buffer solutions are unsuitable for the determination of the nine food additives including DHA.
      In a previous study[7], we were able to determine successfully some tetracycline antibiotics that are similar to DHA in their HPLC behaviour, using a mobile phase

containing 0.01 M aqueous oxalic acid solution. We tested the effect of oxalic acid for DHA using methanol–0.01 M aqueous oxalic acid solution (1:2) as the mobile phase, and good chromatograms of DHA were obtained even when aqueous oxalic acid solutions adjusted to pH 3.0–5.0 were used. We assume that the tailing is due to the interaction between DHA and residual silanol groups of the stationary phase and that oxalic acid has the ability to block such silanol groups. It seemed likely that the tailing of DHA could be controlled by other compounds that have similar structures to oxalic acid, and several compounds were tested. The A_s values of DHA were investigated using aqueous solutions of these compounds at concentrations in the mobile phase of 0.005–0.05 M and typical values for DHA are given in Table I. Although the A_s values of DHA improved with increasing concentration of the test compounds, satisfactory results were not obtained at any concentrations except with acetylacetone, oxalic acid and acetonic acid. Acetylacetone was most effective in controlling the tailing of DHA in spite of the low concentration; however, it was not suitable for practical analysis, because it did not give a stable baseline. Oxalic acid was also unsuitable for high-sensitivity determinations, because it shows a strong absorption band at wavelengths shorter than 250 nm. Therefore, we used acetonic acid solution as the aqueous component in the mobile phase in subsequent work.

The influence of the concentration of acetonic acid was examined. As shown in Fig. 2, the A_s values of DHA were almost constant above a concentration of 0.05 M. Fig. 3 shows that the k' values of SOA, BA, DHA and SA decreased with increase in concentration of acetonic acid, whereas those of PHBAs were independent of concentration. When 0.05 M aqueous acetonic acid solution was used, a satisfactory separation was obtained.

Next, the influence of the pH of the aqueous acetonic acid solution was examined. As shown in Fig. 4, the k' values of PHBAs were not influenced very much, but those of SOA, BA, DHA and SA were influenced significantly by pH. A satisfactory

TABLE I

COMPARISON OF ASYMMETRY FACTORS OF DHA USING VARIOUS AQUEOUS SOLUTIONS IN THE MOBILE PHASE

Column, Nucleosil 3C$_{18}$ (3 μm) (75 × 4.6 mm I.D.); mobile phase, methanol–aqueous solution (1:2); flow-rate, 1.0 ml/min; detection, 225 nm.

Aqueous solution*	Asymmetry factor of DHA
0.01 M phosphoric acid	7.0
0.01 M acetic acid	6.0
0.01 M tartaric acid	4.6
0.01 M citric acid	4.3
0.01 M malonic acid	3.4
0.01 M lactic acid	3.2
0.01 M oxalic acid	2.5
0.01 M acetonic acid	2.0
0.001 M acetylacetone**	1.8

* adjusted to pH 4.5 with sodium hydroxide.
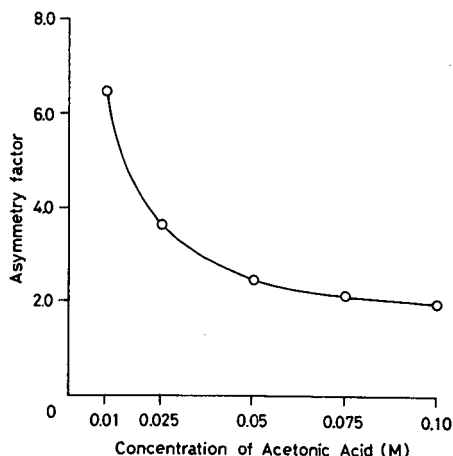** 0.01 M acetic acid solution.

Fig. 2. Influence of concentration of acetonic acid on asymmetry factor of DHA. Mobile phase, methanol–acetonitrile–aqueous acetonic acid solution (pH 4.5) (1.5:1:3.1) containing 2.5 mM CTA.

separation was obtained when the aqueous acetonic acid solution was adjusted to pH 4.5, and in subsequent work we used 0.05 M aqueous acetonic acid solution adjusted to pH 4.5.

Effect of ion-pair

As mentioned above, the polarities of SOA, BA, DHA and SA are much higher than those of PHBAs. Accordingly, the retention times of SOA, BA, DHA and SA are so short that they cannot be determined together with PHBAs on the same chro-
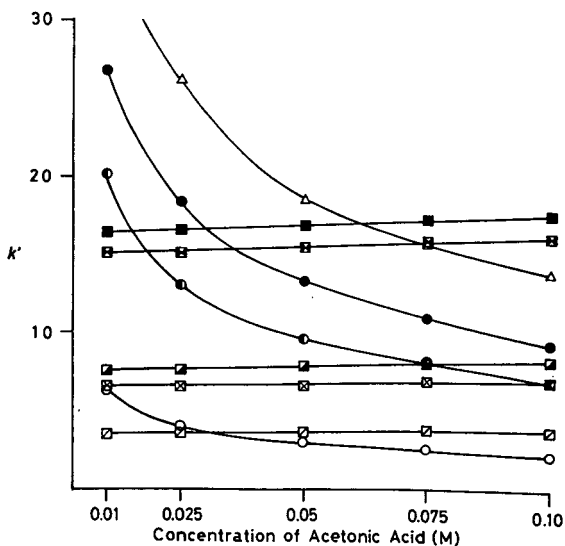
Fig. 3. Influence of concentration of acetonic acid on k' values of food additives. ○, DHA; ◐, SOA; ●, BA; △, SA; ▨, ethyl-PHBA; ⊠, isopropyl-PHBA; ◪, n-propyl-PHBA; ◨, isobutyl-PHBA; ■, n-butyl-PHBA. Mobile phase as in Fig. 2.
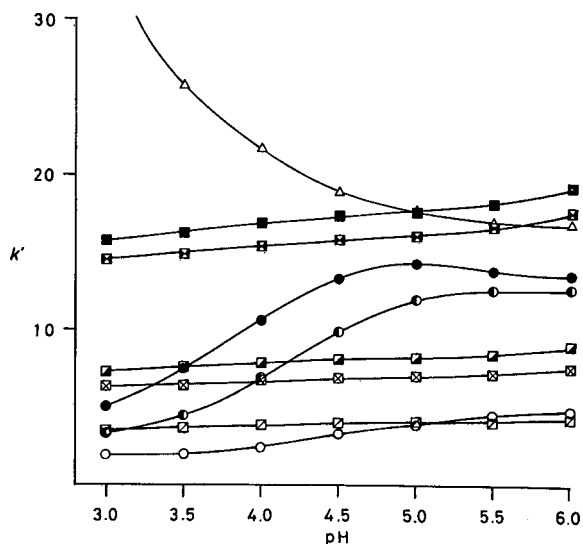
Fig. 4. Influence of pH of aqueous acetonic acid solution on k' values of food additives. Symbols as in Fig. 3. Mobile phase, methanol–acetonitrile–0.05 M aqueous acetonic acid solution (1.5:1:3.1) containing 2.5 mM CTA.

matogram using RP-HPLC. Therefore, we attempted to increase the retention of SOA, BA, DHA and SA to the level of those of PHBAs by adding an ion-pair reagent to the mobile phase. In order to select a suitable ion-pair reagent, the retention times of SOA, BA, DHA and SA were compared with those of PHBAs using TBA, TTA
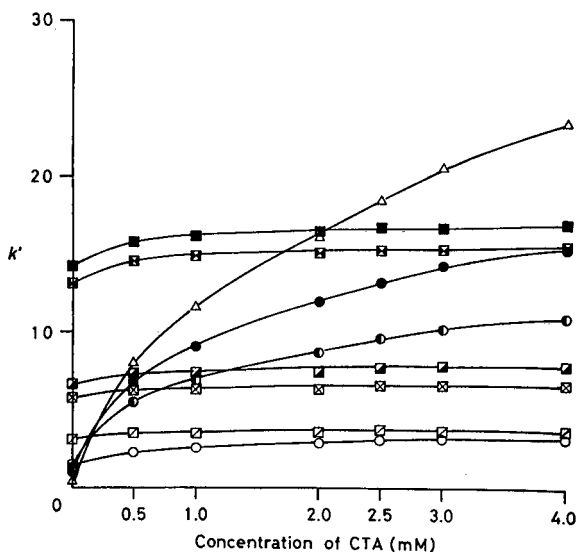
Fig. 5. Influence of concentration of CTA on k' values of food additives. Symbols as in Fig. 3. Mobile phase, methanol–acetonitrile–0.05 M aqueous acetonic acid solution (pH 4.5) (1.5:1:3.1) containing CTA.

and CTA as ion-pair reagents. Although CTA was effective enough to increase the retention of SOA, BA, DHA and SA, TBA and TTA were ineffective at any concentration in the mobile phase. Therefore, CTA was used as the ion-pair reagent in subsequent work.

The influence of the concentration of CTA was examined. As shown in Fig. 5, a satisfactory separation was obtained when the concentration of CTA was 2.5 mM, and this concentration was therefore used in the mobile phase.

Proportion of methanol and acetonitrile

Because a satisfactory separation could not be obtained when we used methanol or acetonitrile alone as an organic solvent in the mobile phase, we tried mixtures of them and the effect of the proportions of the components was investigated. As shown in Fig. 6, the relative k' values of SOA, BA, DHA and SA with respect to that of PHBAs decreased with increasing proportion of acetonitrile. Because the efficiency of the ion-pair reagent decreased with increasing proportion of acetonitrile, we concluded that acetonitrile acts as a kind of inhibitor for the ion-pair reagent in this instance. As SA showed the greatest effect with acetonitrile, a ratio of methanol to acetonitrile of 1.5:1 was adopted based mainly on the separation of SA.
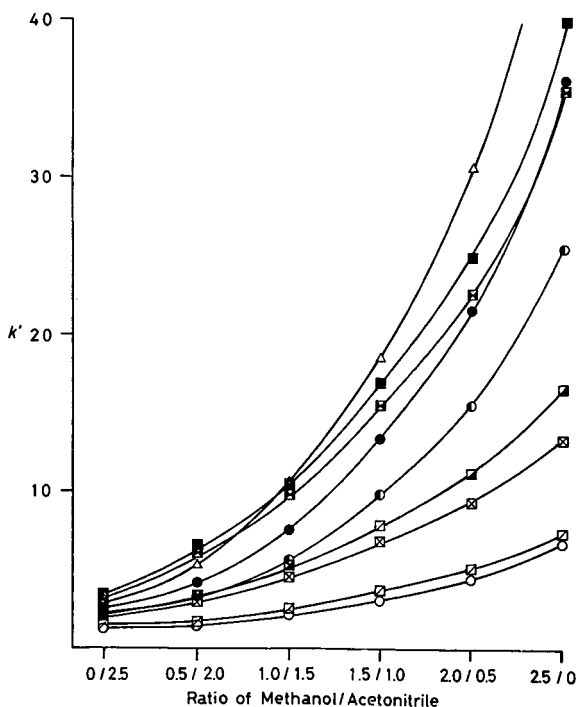

Fig. 6. Influence of ratio of methanol to acetonitrile on k' values of food additives. Symbols as in Fig. 3. Mobile phase, (methanol–acetonitrile)–0.05 M aqueous acetic acid solution (pH 4.5) (2.5:3.1) containing 2.5 mM CTA.

Proportions of organic solvents and aqueous solution

The effect of the proportions of organic solvents and aqueous solution was investigated (Fig. 7). We chose a 3.1 ratio of aqueous solution in the mobile phase, because a baseline separation of the nine food additives was achieved.

Application to practical analysis

Using the above HPLC system, the time required for the analysis of the nine food additives was only 18 min. The linearity of the calibration grpahs was tested by peak-height and -area methods, and both calibration graphs were linear between 2 and 200 ng of each food additive. The retention times of other food additives were investigated under the optimal HPLC conditions. As shown in Table II, *p*-hydroxybenzoic acid, methyl-PHBA and *sec.*-butyl-PHBA could also be determined. Some compounds appeared as interfering peaks on the chromatogram, but their influence on the analysis of the food additives was considered to be very slight because they are used in only a limited range of foods at very low concentrations.

In order to clean up food additives present in various foods, steam distillation[8], dialysis[9] and solvent extraction[10] methods are frequently used. We considered applying these clean-up methods to the present HPLC system. The steam distillation and dialysis methods were applied very easily without complicated additional treatments such as extraction, concentration and derivatization, but the steam distillation meth-
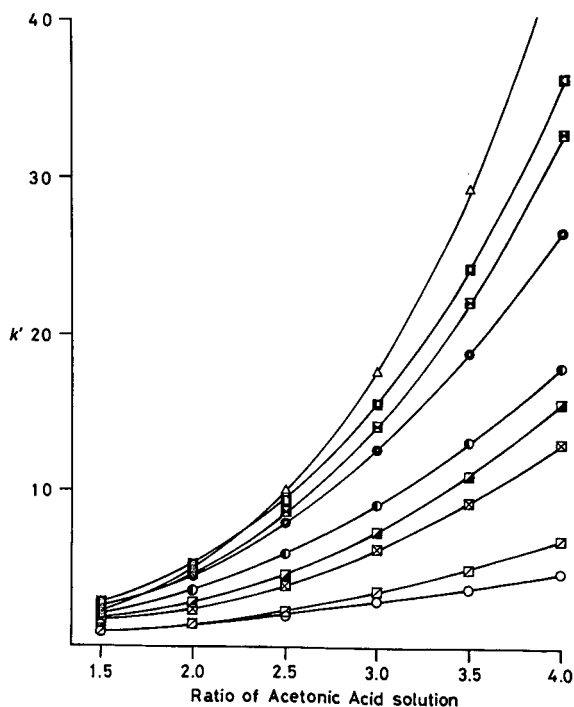

Fig. 7. Influence of ratio of organic solvent to aqueous solution on k' values of food additives. Symbols as in Fig. 3. Mobile phase, methanol–acetonitrile–0.05 M aqueous acetonic acid solution (pH 4.5) (1.5:1:x) containing 2.5 mM CTA.

TABLE II

RETENTION TIMES OF VARIOUS FOOD ADDITIVES

For HPLC conditions, see Fig. 1.

Compound	Retention time (min)	Compound	Retention time (min)
Nicotinamide	0.8	Isopropyl-PHBA	6.3
Acetic acid	1.3	n-Propyl-PHBA	7.3
Propionic acid	1.3	SOA	8.8
Citric acid	1.3	sec.-Butyl-PHBA	11.5
Tartaric acid	1.3	BA	12.0
Adipic acid	1.3	Isobutyl-PHBA	13.5
Ascorbic acid	2.1	OPP	14.6
TBZ	2.1	BHA	14.6
Erithorbic acid	2.2	n-Butyl-PHBA	14.7
Methyl-PHBA	2.3	SA	16.5
p-Hydroxybenzoic acid	2.8	Salicylic acid	35.3
DHA	3.2	DP	38.2
Ethyl-PHBA	3.8	BHT	> 60.0
Nicotinic acid	3.8		

od was inapplicable to SA and the dialysis method to PHBAs. Using the following solvent extraction method, the recoveries of nine food additives from some foods (soy sauce, orange juice and yoghurt) were investigated at the level of 100 ppm. After addition of 10 ml of saturated sodium chloride solution and 2 ml of 10% sulphuric acid to 2 g of sample, the food additives were extracted twice with 100 and 50 ml of diethyl ether. The extracts were combined, washed twice with 10 and 10 ml of saturated sodium chloride solution, dried with anhydrous sodium sulphate, evaporated to 1–2 ml and dried by blowing with air. The food additives in the residue were dissolved in 10 ml of the mobile phase and determined by the above HPLC system.

TABLE III

RECOVERIES OF NINE FOOD ADDITIVES FROM SOME FOODS BY THE SOLVENT EXTRACTION METHOD

Results are averages of three replicate determination at the revel of 100 ppm.

Food additive	Recovery (%)*					
	Soy sauce		Orange juice		Yoghurt	
DHA	91.0	(0.4)	94.5	(0.2)	92.2	(0.2)
Ethyl-PHBA	91.1	(0.9)	96.5	(3.1)	91.4	(0.8)
Isopropyl-PHBA	93.1	(1.3)	93.7	(4.4)	89.6	(1.3)
n-Propyl-PHBA	91.8	(1.6)	91.4	(3.9)	88.1	(1.6)
SOA	91.7	(0.4)	93.2	(2.2)	90.5	(1.0)
BA	89.8	(2.1)	95.1	(2.6)	90.8	(1.0)
Isobutyl-PHBA	85.7	(3.6)	88.5	(3.9)	88.0	(1.4)
n-Butyl-PHBA	90.1	(1.8)	87.1	(3.7)	88.5	(2.6)
SA	92.6	(1.7)	91.4	(3.9)	92.5	(2.4)

* Coefficients of variation in parentheses.

(A)
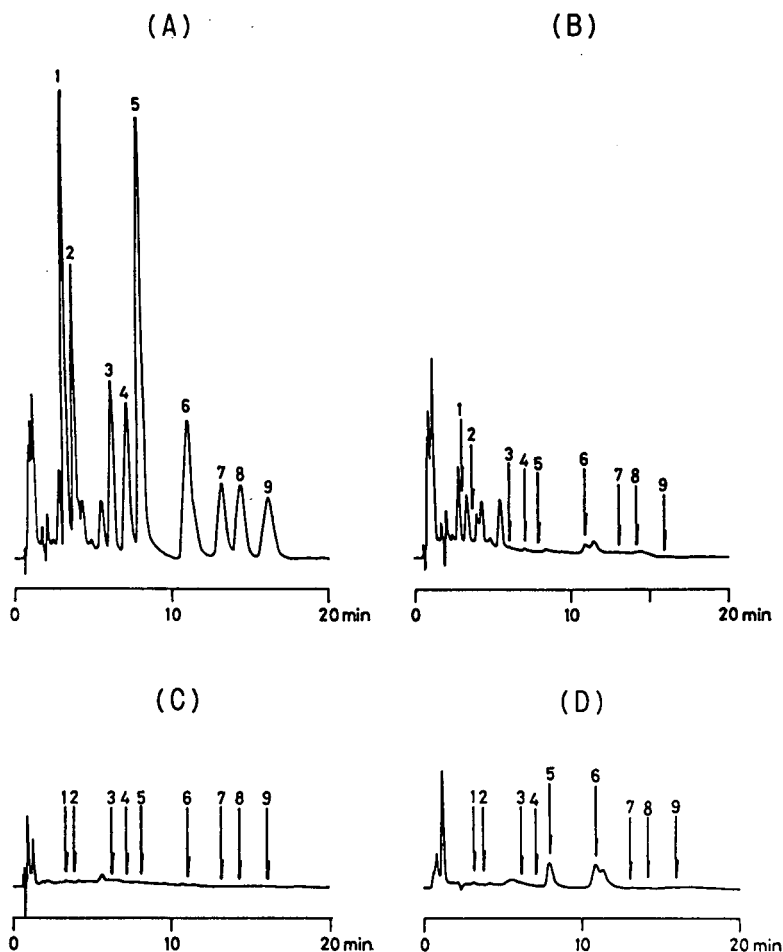
(B)

(C)

(D)

Fig. 8. Typical chromatograms for some foods. HPLC conditions and peak numbers as in Fig. 1. (A) Fortified soy sauce (100 ppm); (B) soy sauce; (C) orange juice; (D) yoghurt.

As shown in Table III, the nine food additives could be simultaneously determined with good recoveries and coefficients of variation (C.V.). However, some interfering peaks appeared on the chromatograms, as shown in Fig. 8, and this method is not applicable to fatty foods such as butter and margarine. We consider that it is the best to consider the use of all three clean-up methods, depending on the particular samples involved. We are currently planning to establish a universal clean-up method and this study will be reported elsewhere in the near future.

CONCLUSION

An ion-pair RP-HPLC system for the simultaneous determination of SAO, BA, DHA, ethyl-, isopropyl-, propyl-, isobutyl- and butyl-PHBA and SA was established. The separation of the nine food additives was performed on a Nucleosil $3C_{18}$ (3 μm)

column (75 × 4.6 mm I.D.) using methanol–acetonitrile–0.05 M aqueous acetonic acid solution (pH 4.5) (1.5:1:3.1) containing 2.5 mM CTA as the mobile phase, with detection at 233 nm. In this system, acetonic acid was effective in controlling the tailing of DHA and CTA was successfully utilized as an ion-pair reagent for baseline separation. Using this system, the nine food additives were successfully separated within 18 min, and their calibration graphs were linear between 2 and 200 ng. Therefore, we recommend this HPLC system for the routine analysis of food additives.

ACKNOWLEDGEMENTS

REFERENCES

1 Y. Kitada, K. Tamase, M. Sasaki, Y. Nishikawa and K. Tanigawa, *J. Food Hyg. Soc. Jpn.*, 21 (1980) 480.
2 H. Terada, K. Hisada, Y. Maruyama and Y. Sakabe, *Eisei Kagaku*, 29 (1983) 297.
3 A. Matsunaga, A. Yamamoto and M. Makino, *Eisei Kagaku*, 31 (1985) 269.
4 H. Terada and Y. Sakabe, *J. Chromatogr.*, 346 (1985) 333.
5 M. Sher Ali, *J. Assoc. Off. Anal. Chem.*, 68 (1985) 488.
6 J. T. Hann and I. S. Gilkison, *J. Chromatogr.*, 395 (1987) 317.
7 H. Oka, H. Uno, K.-I. Harada, K. Yasaka and M. Suzuki, *J. Chromatogr.*, 298 (1984) 435.
8 *Standard Methods of Analysis for Hygienic Chemists – with Commentary*, Pharmaceutical Society of Japan, Kinbara, Tokyo, 1980, p. 300.
9 *Standard Methods of Analysis for Hygienic Chemists – with Commentary*, Pharmaceutical Society of Japan, Kinbara, Tokyo, 1980, p. 338.
10 *Standard Methods of Analysis for Hygienic Chemists – with Commentary*, Pharmaceutical Society of Japan, Kinbara, Tokyo, 1980, p. 305.

LIQUID CHROMATOGRAPHIC DETERMINATION OF BROMIDE AFTER PRE-COLUMN DERIVATIZATION TO 4-BROMOACETANILIDE

KRISHNA K. VERMA*, SUNIL K. SANGHI, ARCHANA JAIN and DAYASHANKER GUPTA

Department of Chemistry, Rani Durgavati University, Madhya Pradesh, Jabalpur 482001 (India)

(First received February 8th, 1988; revised manuscript received July 20th, 1988)

SUMMARY

A pre-column reaction of bromide with 2-iodosobenzoic acid and acetanilide and reversed-phase high-performance liquid chromatography of the 4-bromo-acetanilide formed has permitted sensitive, selective and accurate determination of bromide with the use of an UV detector. Employing 4-N-acetylaminotoluene as an internal standard, the method has been applied to determine bromide in natural and seawater, pharmaceutical formulations and blood. As low as 6 μg l^{-1} of bromide were assayed. Large amounts of ions such as chloride, nitrate, phosphate, ammonium sulphide, thiocyanate, sulphate, iodide, thiosulphate, cyanide and nitrite can be tolerated. The method is rapid, simple and precise, and has a limit of detection of 0.2 ng of bromide.

INTRODUCTION

Bromide may occur in varying amounts in some fresh water streams due to industrial discharges or in well water and ground water supplies in coastal areas as a result of seawater intrusion. To determine possible contamination or the treatment level of bromide-containing biocides, there is a need for a simple and rapid procedure for the assay of trace amounts of bromide. Bromide determination in blood may also be required in the instances of intoxication from overdoses of bromide-containing sedatives.

Many different methods are available for determining bromide. Titrimetric procedures are based on oxidation[1–5] or silver(I) salt formation[6,7] and are subject to interference by the procedure of several other anions. Spectrophotometric procedures involve oxidation to bromine which is converted for its measurement either into triiodide ion by reaction with iodide[8], or to eosin[9] and bromophenol blue[10–12] by reaction with fluorescein and phenol red respectively. The oxidants used for this purpose include permanganate[8], peroxymonosulphate[10] and chloramine T[11,12]. The chloramine T concentration severely affects the absorbance of bromophenol blue and a secondary reaction with phenol red requires destruction of the excess of reagent or a very short reaction time. Though the peroxymonosulphate method is free from these shortcomings, a positive interference is caused by chloride and a negative interference

by ammonium ion. Anion-exchange minicolumns included a flow injection manifold have been applied to the spectrophotometric determination of anions (including bromide) based on displacement of an equivalent amount of thiocyanate and its evaluation as the iron(III) complex[13]. In another procedure, bromide was enriched on an ion exchanger, eluted with perchlorate, oxidized by peroxydisulphate to bromate, which was subsequently treated with iodide and the absorbance of the triiodide ion formed was measured[14,15]. This method has been adapted to flow injection analysis[16]. Ion chromatography with the use of a concentrator column is sometimes preferred over spectrophotometry[17–19]. Other methods are based on anion exchange[20–23], ion-pair formation[24,25] and liquid chromatography with UV detection at 190–200 nm[26,27].

The application of high-performance liquid chromatography (HPLC) to the analysis of inorganic anions with pre-column derivatization reaction and their sensitive UV detection is a new and as yet relatively unexplored field. The only report available is ostensibly that of Moss and Stephen[28] which concerned conversion of halide into phenylmercury(II) halide with the use of benzeneboronic acid and mercury(II) nitrate. After extraction into chloroform, the phenylmercury halides were determined by reversed-phase HPLC and detection at 220 nm. Improved separations and quantitative recoveries were obtained with the use of 4-bromobenzeneboronic acid (detection at 230 nm). However, the method may not be suitably disposed to analyse samples, e.g., of seawater, which have one halide in very large excess over others. The following method is proposed.

EXPERIMENTAL

Apparatus

The liquid chromatographic system consisted of a Shimadzu LC-5A constant flow solvent delivery pump, a manual loop injector, a Zorbax C_{18} reversed-phase column (particle diameter 5 μm; 25 cm × 4.6 mm I.D.) and a Shimadzu C-R2AX integrator fitted with a printer-plotter. The peak area was used for quantitation.

Materials

2-Iodosobenzoic acid was synthesized by a modification of the method of Chinard and Hellerman[25].

In a 5-l Pyrex round-bottomed flask, equipped with a mechanical stirrer, 25 g of potassium permanganate were dissolved in 1 l of water. To this was added a solution of 45 ml of concentrated sulphuric acid in about 100 ml of water, followed by a slurry of 50 g of 2-iodobenzoic acid in 100 ml of water. The mixture was stirred, 500 ml of warm water were added and the solution was boiled for 15 min. About 500 ml more of boiling water were added and boiling was continued for 10 min. The hot solution was filtered. On cooling the filtrate afforded 42 g (80% yield) of 2-iodosobenzoic acid which was collected and recrystallized from hot water. The product was 99.8% pure as found by iodometric determination[29].

Acetanilide, 4-N-acetylaminotoluene and 4-bromoacetanilide were synthesized and purified by repeated recrystallization by using the reported methods[30].

A mixture of acetanilide and 2-iodosobenzoic acid was prepared by dissolving 150 mg of 2-iodosobenzoic acid and 100 mg of acetanilide in 100 ml of methanol in

a standard flask. It was filtered through a 0.45-μm membrane filter. A sulphuric acid solution was prepared by diluting 1.2 ml of analytical reagent grade concentrated sulphuric acid to 100 ml in methanol.

The mobile phase was prepared by mixing methanol and water, 65:35 (v/v).

Standards

Potassium bromide solution was prepared by dissolving 223.1 mg of AnalaR-grade potassium bromide (BDH) in 100 ml of water in a standard flask, and diluting 2 ml of this solution to 100 ml in a standard flask. This solution contained 30 μg ml^{-1} of bromide.

4-N-Acetylaminotoluene (N-acetyl-4-toluidine) as internal standard contained 25 mg of purified substance in 250 ml of methanol in a standard flask.

Procedures

Determination of bromide in standard solutions. A 200–1000-μl aliquot of a standard solution containing 6–30 μg of bromide was mixed with 200 μl of the internal standard solution of 4-N-acetylaminotoluene, 500 μl of the mixed reagent and 200 μl of sulphuric acid. The solution was diluted to 10 ml in mobile phase in a standard flask, shaken well for 1 min and a 10-μl aliquot was injected on the HPLC column. The solvent flow-rate was 1 ml min^{-1} and the column back pressure was approximated 50 kg cm^{-2}. The eluate was monitored by an UV detector set at 240 nm with a sensitivity of 0.04 a.u.f.s.

Determination of bromide in natural water. A 5-ml volume of filtered (0.45-μm membrane filter) natural water, containing 6–60 μg l^{-1} of bromide, was mixed with 20 μl of internal standard solution, 500 μl of the mixed reagent and 200 μl of sulphuric acid, and diluted to 10 ml in methanol in a standard flask. The solution was shaken well and an 100-μl aliquot was injected into the liquid chromatograph. The detector sensitivity was 0.005 a.u.f.s. and the other chromatographic conditions were as above.

Determination of bromide in seawater. A 50-ml volume of filtered (Whatman No. 42 paper) seawater was diluted to 100 ml in distilled water in a standard flask, and a 200–1000-μl portion of this solution was mixed with 200 μl of internal standard solution, 500 μl of mixed reagent and 200 μl of sulphuric acid, and made up to volume with mobile phase in a 10-ml standard flask. This solution was filtered through a 0.45-μm membrane filter and 10 μl of filtrate were injected in the HPLC column; the chromatographic conditions were as described before.

Determination of bromide in pharmaceutical injections. The contents of a known number of injection ampoules were mixed and diluted to known volume. A suitable portion was subjected to pre-column derivatization reaction and HPLC analysis as described for standard bromide solutions.

Determination of bromide in blood. A 2-ml volume of blood was mixed with 2 ml of water and 4 ml of acetonitrile in a 15-ml centrifuge tube and stirred for 10 min. The precipitated material was separated by centrifugation (*ca.* 5000 *g*) and the clear supernatant was transferred to another centrifuge tube. The solvent was evaporated to dryness at 50°C under a stream of nitrogen and the residue was reconstituted in mobile phase. The volume of mobile phase used depended on the anticipated concentration of bromide in the sample. A known aliquot of the reconstituted residue was subjected to pre-column derivatization and HPLC analysis as described for standard bromide solution.

RESULTS AND DISCUSSION

In the present work the determination of bromide is based on a sequence of pre-column reactions involving oxidation with 2-iodosobenzoic acid in an acidic medium to give bromine and the substitution reaction of bromine with acetanilide to form 4-bromoacetanilide.
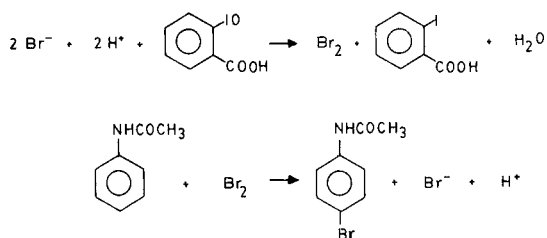
The bromide liberated from the substitution is again oxidized by 2-iodosobenzoic acid and this sequence of reactions continues until all the bromine is covalently bonded. Many compounds undergo substitution reaction with bromine but acetanilide was selected as a bromine scavenger because of its rapid reaction and the formation of a monobromo derivative as the sole product. The two positions *ortho* to the acetylamino group in acetanilide are sterically hindered and do not undergo electrophilic substitution. The 4-N-acetylaminotoluene internal standard does not react with bromine because the *para* position is already occupied by a methyl group. 2-Iodosobenzoic acid was chosen because it rapidly oxidizes bromide to bromine without any deleterious side reaction either with other reagents used or any organic matter present in the sample. The selectivity of 2-iodosobenzoic acid has already been demonstrated[5,31-34]. Its redox potential at 25°C was found to be 1.21 V at pH 1, 1.08 V at pH 2, 0.53 V at pH 4 and 0.48 V at pH 7[33].

Preliminary studies showed that the best separation of 4-bromoacetanilide from acetanilide, 2-iodo- and 2-iodosobenzoic acid was achieved on a C_{18} reversed-phase column by a mixture of methanol and distilled water (70:30, v/v). The internal standard was eluted near to the acetanilide peak but use of methanol–distilled water (65:35, v/v) avoided overlapping, and the analysis was complete in about 8 min (Fig. 1).

A response factor of 0.5930 for bromide (as 4-bromoacetanilide) *versus* 4-N-acetylaminotoluene was calculated by injecting pre-column reacted mixed standards in various concentration ratios. The bromide concentrations, C, were thus calculated from

$$C = 0.5930 \frac{A}{A_{IS}} \cdot C_{IS}$$

where A/A_{IS} is the ratio between the peak areas of 4-bromoacetanilide and the internal standard, and C_{IS} is the concentration of the internal standard.

The peaks in the HPLC chromatogram were identified by comparison of their HPLC retention times with those of the authentic substances under the same chromatographic conditions. These compounds of corresponding retention times had
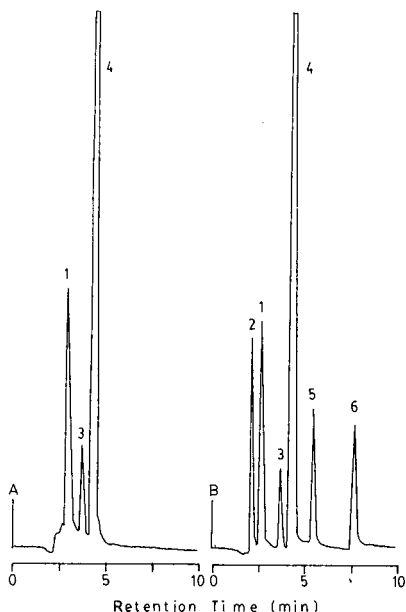
Fig. 1. Chromatograms of (A) reagents blank and (B) pre-column reacted bromide (31.07 ng) with the same reagents and 4-N-acetylaminotoluene (51.40 ng) used as the internal standard. Peaks: 1 = 2-iodosobenzoic acid; 2 = 2-iodobenzoic acid; 3 = impurity; 4 = acetanilide; 5 = 4-N-acetylaminotoluene and 6 = 4-bromoacetanilide. Mobile phase: methanol–water (65:35, v/v). Detection at 240 nm a.u.f.s. 0.04.

identical UV and IR spectra. Also, the agreement (within ± 1.5%) between the peak areas of equivalent molar masses of authentic 4-bromoacetanilide and of bromide (after derivatization to 4-bromoacetanilide) confirmed the quantitative nature of the pre-column reaction. The reaction mixture maintained the peak area for its 4-bromoacetanilide content for several days.

Calibration standard solutions of bromide were subjected to pre-column derivatization and the following quantities of bromide were injected: 6.4, 12.9, 19.4, 25.9, 32.4 and 38.9 ng; an UV detector (240 nm), sensitivity 0.04 a.u.f.s. A plot of peak

TABLE I

HPLC DETERMINATION OF BROMIDE IN PURE SOLUTIONS (n = 6)

R.S.D. = Relative standard deviation.

Solution No.	μg of bromide per 100 ml		
	Taken	Found	% R.S.D.
1	60.76	61.21	0.36
2	91.38	91.03	0.25
3	132.7	133.4	0.18
4	183.0	181.7	0.27
5	251.1	252.9	0.32
6	302.6	301.4	0.41

TABLE II

HPLC DETERMINATION OF TRACE LEVELS CONCENTRATION OF BROMIDE IN NATURAL WATER ($n = 5$)

The "standard composition, 0.005 N" contains (mequiv./l): Ca^{2+}, 3.175; Mg^{2+}, 0.870; Na^+, 0.785; K^+, 0.170; Cl^-, 0.5; SO_4^{2-}, 0.785 and HCO_3^-, 3.715[15].

Solution No.	Bromide added ($\mu g/1000$ ml)	% Recovery	% R.S.D.
1	6.1	95.4	3
2	9.9	96.3	2
3	20.4	96.8	2
4	31.7	97.7	1.5
5	42.0	98.9	0.7
6	50.1	99.7	0.3
7	62.3	100.8	0.4

area *versus* the amount (ng) injected was linear and gave a slope, intercept and correlation coefficient of 298, 12 and 0.9999 respectively.

Six solutions of bromide were prepared as the standards and analysed by the present method (Table I). The interference from a number of diverse ions was studied. Ions which do not vitiate the results when present up to 1000-fold w/w excess over bromide include chloride, nitrate, phosphate, calcium, barium, manganese, chromium(III), copper(II), zinc, cadmium, iron(III), cobalt(II), perchlorate, iodate and sulphate. Up to an 100-fold excess of ammonium ion can be tolerated. Reducing ions such as sulphide, thiocyanate, manganese(II), sulphite, thiosulphate, iron(II), thalium(I), iodide, cyanide and nitrite can be tolerated up to a 50-fold excess. Lead(II) and mercury(II) do not interfere when present up to a 20-fold excess over bromide. Sufficient excess of 2-iodosobenzoic acid should be added to compensate its consumption by any reducing agent or to speed up the oxidation of non-ionic bromide.

TABLE III

HPLC DETERMINATION OF BROMIDE IN SEAWATER ($n = 6$)

Sample*	mg of bromide/1000 ml				
	Taken	Present method	% R.S.D.	Comparison method	Ref.
Laboratory-made seawater:					
Sample No. 1[a]	25	25.83	0.3	24.36	10
Sample No. 2[b]	75	78.31	0.4	78.91	8
Sample No. 3[c]	150	152.5	0.2	153.7	14
Arabian Sea water	—	179.1	0.3	181.6	8

    * The other substances present (mg/1000 ml) in the sample were (a) medium chloride (4000) and magnesium sulphate (200); (b) sodium chloride (2000), sodium hydrogencarbonate (500) and potassium chloride (200) and (c) sodium chloride (5000).

TABLE IV

HPLC ASSAY OF BROMIDE IN PHARMACEUTICAL INJECTIONS ($n = 6$)

Drug*	mg of total bromide/10 ml of injection					
	Label claim	Present method	% R.S.D.	Comparison method	% R.S.D.	Ref.
Calcibronat[a]	186.6	182.6	0.3	181.3	0.5	10
Calcibion[a]	186.6	195.0	0.3	195.7	0.4	14
Sedival[b]	310.8	301.4	0.4	302.8	0.5	8
Laboratory made						
Injection No. 1[c]	887.9	888.6	0.4	884.9	0.6	10
Injection No. 2[d]	788.7	790.2	0.4	790.7	0.5	6

    * Each 10 ml of injection included (a) calcium bromide/lactobionate (1240 mg); (b) sodium bromide (400 mg), chloral hydrate (200 mg) and phenobarbitone sodium (26.66 mg); (c) potassium bromide (500 mg), sodium bromide (500 mg) and ammonium bromide (200 mg) and (d) sodium bromide (600 mg), potassium bromide (200 mg), calcium bromide (7 mg), strontium bromide (3 mg), ammonium bromide (220 mg) and chloral hydrate (0.71 mg).

Any organic matter that also undergoes bromination, e.g., phenol and aniline, interferes severely and should be removed, e.g., by passing the test solution through a column packed with non-polar porous polystyrene–divinylbenzene resin (Amberlite XAD-2)[12].

    The present method has been applied to the determination of bromide in fresh water (at levels as low as $6 \mu g \, l^{-1}$) and seawater. Seven laboratory-made synthetic fresh water samples of the relative ionic composition used previously[15] were analysed (Table II). Some laboratory made seawater samples and that collected from the Arabian Sea, Bombay, produced the results given in Table III. Due to a lower bromide content, a larger sample volume of river-water was taken for derivatization and diluted in methanol (instead of mobile phase as done in other analyses) to match the solvent composition approximately to that of the mobile phase. Results for the assay of bromide in pharmaceutical injections are given in Table IV, and those for blood samples doped with known amounts of bromide are given in Table V. In precision studies, the R.S.D. was determined by single injections of five or six samples

TABLE V

HPLC ASSAY OF BROMIDE IN BLOOD ($n = 5$)

Sample No.	μg of bromide per ml of blood		
	Added	Found by present method	% R.S.D.
1	3.18	3.12	0.5
2	10.81	10.89	0.3
3	16.36	16.20	0.3
4	21.74	21.82	0.3

TABLE VI

COMPARISON OF SENSITIVITY OF BROMIDE DETERMINATION BY DIVERSE METHODS

Serial No.	Method	Detector	LD*	Ref.
1	Ion chromatography; post-column reaction with chloramine T and 4,4'-bis(dimethylamino)-diphenylmethane	600 nm	15 ng	35
2	Liquid chromatography on Zipax SAX column	200 nm	10 ng	26
3	Reversed-phase ion-interaction chromatography	205–220 nm	24 ng	36
4	Liquid chromatography on aminopropyl bonded silica	214 nm	1 ng	37
5	Liquid chromatography on μBondapak NH$_2$	210 nm	10 ng	38
6	Ion-pair chromatography	205 nm	6 ppb	39
7	Ion-interaction liquid chromatography	205–220 nm	40 ng	40
8	Anion-exchange chromatography	Conductivity	1 ppm	41
9	Anion-exchange chromatography	Conductivity	20 ng	42
10	Ion-exchange chromatography	190 nm	1 ppb	27
11	Precolumn derivatization to 4-bromoacetanilide	240 nm	0.2 ng	Present work

* LD = Limit of detection; in ppb, the American billion (10^9) is meant.

derivatized separately. None of the samples of seawater, pharmaceutical injections and blood produced peaks closely eluted to those of the internal standard and 4-bromoacetanilide. The limit of detection is 0.2 ng of bromide (signal-to-noise ratio = 2).

It is clear that the proposed HPLC method for bromide involving precolumn derivatization to 4-bromoacetanilide is simple, rapid and precise, and free from interferences due to high level concentrations of diverse ions that adversely affect other methods. For the determination of bromide concentrations lower than 10 μg l^{-1} the present method should be a valuable asset. Table VI demonstrates the advantages of derivatization.

REFERENCES

1 J. H. Vander Meulen, *Chem. Weekbl.*, 28 (1931) 82.
2 J. H. Vander Meulen, *Chem. Weekbl.*, 28 (1931) 238.
3 I. M. Kolthoff and H. Yutzy, *Ind. Eng. Chem., Anal. Ed.*, 9 (1937) 75.
4 A. Berka, J. Vulterin and J. Zyka, *Newer Redox Titrants*, Pergamon, Oxford, 1965, p. 32.
5 K. K. Verma and A. K. Gulati, *Talanta*, 30 (1983) 279.
6 J. Bassett, R. C. Denney, G. H. Jeffery and J. Mendham, *Vogel's Textbook of Quantitative Inorganic Analysis*, Longman, London, 1978, p. 339.
7 S. Pinzauti, G. Papeschi and E. La Porta, *J. Pharm. Biomed. Anal.*, 1 (1983) 47.
8 S. Utsumi, M. Kotaka and A. Isozaki, *Bunseki Kagaku*, 34 (1985) 81.
9 M. Oosting and H. F. R. Reijnders, *Fresenius' Z. Anal. Chem.*, 301 (1980) 28.
10 H. F. Dobolyi, *Anal. Chem.*, 56 (1984) 2961.

11 C. L. Basel, J. D. Defreese and D. O. Whittemore, *Anal. Chem.*, 54 (1982) 2090.

12 P. I. Anagnostopoulou and M. A. Koupparis, *Anal. Chem.*, 58 (1986) 322.

13 A. T. Faizullah and A. Townshend, *Anal. Chim. Acta*, 179 (1986) 233.

14 U. Lundstrom, *Talanta*, 29 (1982) 291.

15 U. Lundstrom, A. Olin and F. Nydahl, *Talanta*, 31 (1984) 45.

16 A. Carlsson, U. Lundstrom and A. Olin, *Talanta*, 34 (1987) 615.

17 C. M. Morrow and R. A. Minear, *Water Res.*, 18 (1984) 1165.

18 P. R. Haddad and A. L. Heckenberg, *J. Chromatogr.*, 318 (1985) 279.

19 K. Katoh, *Bunseki Kagaku*, 32 (1983) 567.

20 K. J. Stetzenbach and G. M. Thompson, *Ground Water*, 21 (1983) 36.

21 R. S. Bowman, *J. Chromatogr.*, 285 (1984) 467.

22 H. J. Cortes and T. S. Stevens, *J. Chromatogr.*, 295 (1984) 269.

23 D. R. Jenke and G. K. Pagenkopf, *Anal. Chem.*, 56 (1984) 85.

24 F. G. P. Mullis and G. F. Kirkbright, *Analyst (London)*, 109 (1984) 1217.

25 A. Mangi and M. T. Lugari, *Anal. Chim. Acta*, 159 (1984) 349.

26 T. Kamiura, Y. Mori and M. Tanaka, *Anal. Chim. Acta*, 154 (1983) 319.

27 N. Ferrer and J. J. Perez, *J. Chromatogr.*, 356 (1986) 464.

28 P. E. Moss and W. I. Stephen, *Anal. Proc. (London)*, 22 (1985) 5.

29 F. P. Chinard and L. Hellerman, *Methods Biochem. Anal.*, 1 (1961) 9.

30 A. I. Vogel, *A Textbook of Practical Organic Chemistry*, Longman, London, 1956, pp. 576–584.

31 K. K. Verma and S. Bose, *Anal. Chim. Acta*, 70 (1974) 227.

32 K. K. Verma and S. Bose, *Analyst (London)*, 100 (1975) 366.

33 K. K. Verma, *Talanta*, 29 (1982) 41.

34 K. K. Verma and A. K. Gupta, *Talanta*, 29 (1982) 779.

35 W. Buchberger, *J. Chromatogr.*, 439 (1988) 129.

36 W. E. Barber and P. W. Carr, *J. Chromatogr.*, 316 (1984) 211.

37 C. E. Goewie and E. A. Hogendoorn, *J. Chromatogr.*, 344 (1985) 157.

38 U. Leuenberger, R. Gauch, K. Rieder and E. Baumgartner, *J. Chromatogr.*, 202 (1980) 461.

39 J. P. de Kleijn, *Analyst (London)*, 107 (1982) 223.

40 W. E. Barber and P. W. Carr, *J. Chromatogr.*, 260 (1983) 89.

41 D. T. Gjerde, J. S. Fritz and G. Schmuckler, *J. Chromatogr.*, 186 (1979) 509.

42 M. J. van Os, J. Slanina, C. L. de Ligny, W. E. Hammers and J. Agterdenbos, *Anal. Chim. Acta*, 144 (1982) 73.

CHROM. 20 919

Note

Application of inverse gas chromatography to solid propellants

YULI REN* and PEIFEN ZHU

Department of Chemical Engineering, Beijing Institute of Technology, P.O. Box 327, Beijing (China)

(First received April 1st, 1988; revised manuscript received July 21st, 1988)

Inverse gas chromatography (IGC) has been widely used to study the physico-chemical properties and related thermodynamic parameters of polymers since it was first reported in 1966[1]. In this work, nitrocellulose (NC) or/and polyether (PE) gel, which are main components of solid propellants, and some small molecules including acetone, ethanol, diethyl ether and ethyl acetate were chosen as samples and their solubilities were characterized by IGC. This provides a method and measuring conditions for the study of system solubility. At the same time, it provides a basis for the formulation of recipes and the choice of processing conditions for the practical production of solid propellants.

NC is the main energetic ingredient of single-base, double-base and other complex gunpowders[2]. As its viscous fluid flow temperature (T_f) is higher than its decomposition temperature (T_d), it cannot be processed at increased temperatures. Therefore, with the help of small molecules, NC can be prepared as concentrated solutions so that it can be easily processed[3]. The solubility of NC–small molecules has a great influence on the physico-chemical properties, trajectory performance and processing behaviour of gunpowder and the quality of the final products. This has been studied previously[4–7], but the methods used were indirect, *i.e.*, the solubility of the system was studied by rheological analysis, which does not allow determination of the solubility of the NC system.

PE is a sticking agent in NEPE gunpowder and its solubility with other components of the system influences the properties of the gunpowder, such as mechanical properties, combustion performance and stability. The synthesis and study of the properties of PE have not previously been reported, and there are no conclusions on characterizing the solubility of PE.

THEORY

The Flory–Huggins interaction parameter for an infinitely dilute solution of a volatile component 1 in a polymer 2 is expressed by[8]

$$\chi_{12}^{\infty} = \ln\left(\frac{273.2RV_2}{P_1^0 V_g^0 V_1}\right) - 1 \tag{1}$$

where

$$V_g^0 = \frac{273.2}{W} \cdot \frac{t_R - t_M}{T_c} \cdot F_{corr} \cdot j$$

$$j = \frac{3}{2} \cdot \frac{(P_i/P_0)^2 - 1}{(P_i/P_0)^3 - 1}$$

$$F_{corr} = F_{obs} \cdot \left(\frac{P_0 - P_{0,flo}}{P_0}\right)$$

W (g) is the amount of stationary phase, t_R is the retention time of the sample on the stationary phase, t_M is the dead time, T_c i s the column temperature (80°C in this work), F_{obs} is the volume flow-rate of the carrier gas when it is out of the column at atmospheric temperature (measured with a soap bubble flow meter and requiring a correction for saturation of the carrier gas with water vapour from the soap solution), P_0 is the outlet pressure, P_i is the inlet pressure, $P_{0,flo}$ is the saturated vapour pressure of water at the temperature of the flow meter, V_g (ml g^{-1}) is the elution volume corrected to 0°C per gram of stationary phase in the column and V_2 and V_1 are the specific volume of the polymer and sample, respectively.

The excess enthalpy of mixing is related to the temperature dependence of χ by[8]

$$\Delta H_M^\infty = \frac{\partial\chi/\partial(1/T)}{T} \tag{2}$$

The solubility parameter of the polymer (δ_2) can be calculated by eqn. 3 and substituted in eqn. 4:

$$\delta_2 = \frac{\Sigma F}{V} = \frac{\Sigma F}{M} \cdot d_2 \tag{3}$$

$$\Delta H_M = V\varphi_1\varphi_2(\delta_1 - \delta_2)^2 \bar{M}_n \tag{4}$$

where $V = V_1 + V_2$, $\varphi_1 = V_1/V$, $\varphi_2 = V_2/V$, ΣF is the sum of the attraction constant per mole in each repeat unit, M is the molecular weight of the repeat unit, δ_1 is the solubility of the sample and $\bar{M}_n$ is the number-average molecular weight of the polymer. If the φ_1, φ_2, δ_1 and $\bar{M}_n$ are known, we can obtain δ_2 from eqn. 4 approximately after measuring ΔH_M.

EXPERIMENTAL

Instruments

A Model SP-2305 gas chromatograph (Beijing Analytical Instrument Factory, China) with a thermal conductivity detector and a U-shaped stainless-steel column (0.5 × 4 mm I.D.) was employed with hydrogen as the carrier gas. A standard Calvet microcalorimeter (Setaram, France) was used.

TABLE I

CHARACTERISTIC PARAMETERS OF NC SAMPLES

No. of NC	Nitrogen content (%)	Degree of nitration, v	Density, d_2^{25} (g cm^{-3})	Solubility parameter, δ_2 (cal$^{1/2}$ cm$^{-3/2}$)
1	13.47	2.75	1.66	9.12
2	12.11	2.29	1.64	9.60
3	11.90	2.25	1.64	10.02

Samples

NC samples 1–3 were provided by Xinan Chemical Factory (China) and their characteristics are listed in Table I. PE was provided by the Institute of Chemistry, Academic Sinica (Beijing, China) and its properties are as follows: $\bar{M}_n$ = 1620, OH value = 0.6046 mequiv./g (mequiv. = milligram equivalents), degree of polymerization DP = 1.62, density = 1.0267 g cm^{-3}. The small molecules used were dimethyl sulphoxide (DMSO), diethyl ether, ethanol, ethyl acetate and acetone. The support was white support 101 produced by the Shanghai Reagent Factory (Shanghai, China), containing SiO_2 (89.9%), Al_2O_3 (3.6%), Fe_2O_3 (1.65%), TiO_2 (0.30%) and CaO + MgO (2.45%).

Processing

The required amount of sample, according to the loading, was dissolved in acetone to form a solution, then a suitable amount of support was slowly added with stirring. After evaporation of the solvent, the NC or PE sample was loaded on the column as the stationary phase. Finally, the column was conditioned at 60°C for 6–8 h.

RESULTS AND DISCUSSION

Measurement of reliability of the instruments

There are many factors that influence the heat of mixing, *e.g.*, error of weighing PE (0.05%), instrumental error of the Calvet microcalorimeter (0.2%), error of measuring column loading (0.5%), error of measuring carrier gas flow-rate (1–2%), calculation error (0.5%) and the error involved in IGC itself (1%). The errors in the data from two different methods were within the range of the experimental error, as indicated in Table II. Hence the instruments used were suitable for studying the solubility of the components in solid propellants.

TABLE II

HEATS OF MIXING OF PE–ETHANOL SYSTEM

Parameter	Calvet method	IGC method
Heat of mixing, ΔH_M (kJ mol^{-1})	22.75	20.89
Relative standard deviation (%)	<5	<5
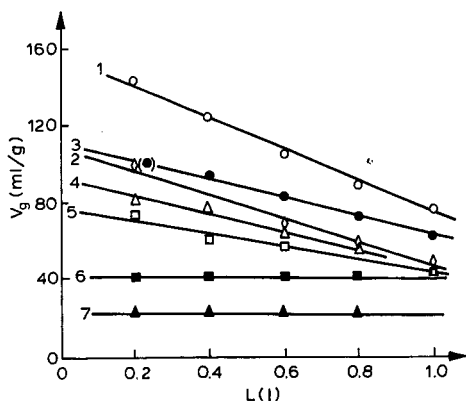
Fig. 1. V_g–L graphs for samples on NC 3 column. 1 = Ethyl acetate, F_{corr} = 13.7 ml min^{-1}, W = 6.4%; 2 = ethyl acetate, F_{corr} = 7.2 ml min^{-1}, W = 7.2%; 3 = ethyl acetate, F_{corr} = 13.7 ml min^{-1}, W = 8.2%; 4 = ethanol, F_{corr} = 20.3 ml min^{-1}, W = 6.4%; 5 = ethanol, F_{corr} = 26.8 ml min^{-1}, W = 7.2%; 6 = diethyl ether, F_{corr} = 39.9 ml min^{-1}, W = 2.7%; 7 = diethyl ether, F_{corr} = 33.4 ml min^{-1}, W = 6.4%.

Factors influencing V_g

Sample size, L. Fig. 1 illustrates V_g–L graphs for different sample probes on an NC 3 column. These graphs are linear and the slopes (k) decrease in the order ethyl acetate, ethanol, diethyl ether. The order of symmetry of the peak shapes is diethyl ether, ethanol, ethyl acetate. The solubility order of NC 3–small molecule systems is[9]
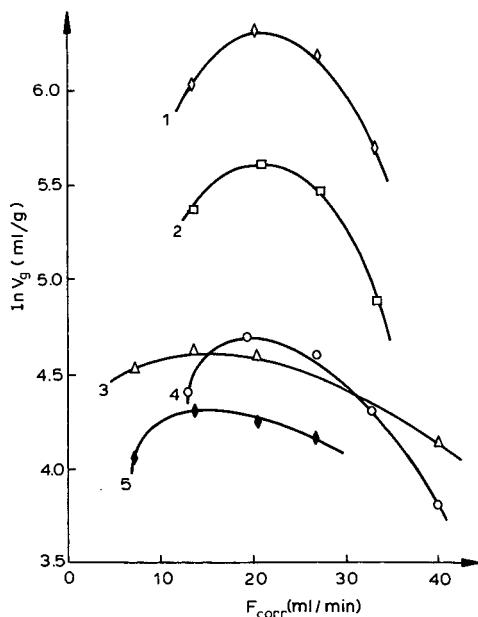
Fig. 2. Ln V_g–F_{corr} graphs for samples on NC 3 column. Column temperature, 80°C. 1 = Ethyl acetate, W = 2.7%; 2 = ethanol, W = 2.7%; 3 = ethyl acetate, W = 8.2%; 4 = diethyl ether, W = 2.7%; 5 = ethanol, W = 8.2%.

NC–ethyl acetate, NC–ethanol, NC–diethyl ether. From these results, it can be concluded that the better the solubility of the system, the stronger is the dependence of V_g on L and the more asymmetric is the peak shape. V_g can be obtained correctly when L is extrapolated to zero.

Carrier gas flow-rate, F_{corr}. Ln V_g–F_{corr} graphs for different samples on the NC 3 column are shown in Fig. 2. If F_{corr} is within a certain range (20 $\pm$ 5 ml min^{-1}), V_g is independent of F_{corr}. This provides a basis for the choice of a suitable F_{corr} in NC systems with different percentages of nitrogen.

Column loading, W. Fig. 3 illustrates ln V_g–W graphs for different samples on different NC columns. It can be concluded that, for different NC columns, there exist critical values (W_c) that are related to the percentage of nitrogen in the NC. The higher is the percentage of nitrogen, the smaller is W_c. When W is lower than W_c, both an interaction between sample and the active group of the stationary phase surface and an interaction between the sample and the bulk polymer exist simultaneously, and are independent of each other. In contrast, when W is higher than W_c, surface action can be omitted and only the contribution of bulk action need be considered. V_g is independent of W. Therefore, the retention behaviour of a sample on an NC column is in accordance with the parallel retention model[10].

Study of solubility of NC–small molecule systems

Thermodynamics of NC–small molecule solution systems. Table III lists the characteristic parameters of NC–small molecule systems. It can be seen that the greater the $\Delta\delta$ of the system, the smaller is V_g of the sample on NC column, the greater are ΔH_M and χ_{12} and the worse is the solubility of the systems. These parameters are of identical use in judging the solubility of the system.

Solubility dynamics of NC–small molecule systems. When dissolved in good solvents, NC first swells. As it swells continuously, the orientational domain of the NC chain disappears gradually, and NC can be dissolved to give a homogeneous system. The phenomena in Fig. 4 can be explained easily according to the model mentioned above: if the sample is not a good solvent for NC it can only be absorbed by solid NC
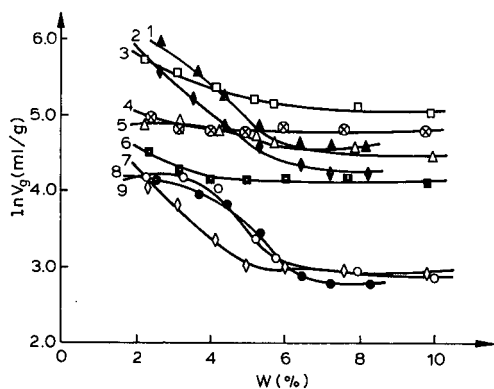

Fig. 3. Ln V_g–W graphs for samples on NC columns. Column temperature, 80°C; F_{corr} = 20.3 ml min^{-1}. 1 = Ethyl acetate (NC 3); 2 = ethanol (NC 3); 3 = ethyl acetate (NC 2); 4 = ethyl acetate (NC 1); 5 = ethanol (NC 2); 6 = ethanol (NC 1); 7 = diethyl ether (NC 1); 8 = diethyl ether (NC 3); 9 = diethyl ether (NC 2).

TABLE III

CHARACTERISTIC PARAMETERS OF NC–SMALL MOLECULE SYSTEMS

No. of NC	Sample	$\Delta\delta$ $(cal^{1/2} \, cm^{-3/2})$	V_g $(ml \, g^{-1})$	χ_{12}	ΔH_M $(kJ \, mol^{-1})$
1	Diethyl ether	1.72	18.39	−0.31	2.51
	Ethanol	3.58	66.07	0.44	3.20
	Ethyl acetate	0.02	117.16	−0.68	−6.13
2	Diethyl ether	2.20	17.40	−0.23	3.17
	Ethanol	3.10	67.57	0.44	2.37
	Ethyl acetate	0.50	104.41	−0.55	−4.78
3	Diethyl ether	2.62	16.46	−0.18	3.50
	Ethanol	2.68	71.26	−0.38	1.54
	Ethyl acetate	0.92	95.44	−0.46	−0.63

and does not destroy the ordered sequence portion of NC. As the carrier gas flows continuously, it is desorbed from NC and flows out of column to form a chromatographic peak. On the other hand, if the sample is a good solvent for NC, some of it can be absorbed by NC, then desorbed from NC, and flows out of the column to form the first peak (this mechanism is similar to that with poor solvents). The rest of the sample penetrates the bulk of NC, dissolves slowly in NC, and flows out of the column with the carrier gas to form the second peak. The severe tailing of the second peak indicates that the dissolution process is very slow. Fig. 5 shows that the solution involves two steps, the first being endothermic and the second exothermic.

Study of solubility of PE–small molecule systems

Solubility thermodynamics of PE–small molecule systems. ΔH_M of PE was measured with a Calvet microcalorimeter and calculated from theory. The results are listed in Table IV.
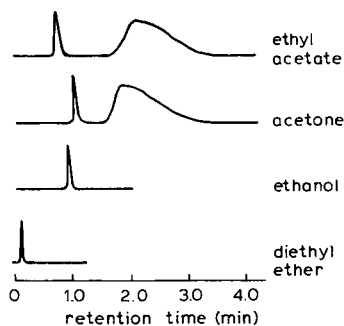
Fig. 4. Schematic chromatograms of samples on NC 3 column. Column temperatures, 80°C; F_{corr} = 20.3 ml min^{-1}; W = 5.3%.
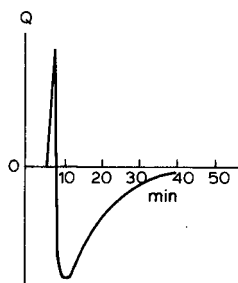
Fig. 5. Heat of solution of NC 3–acetone system determined with a Calvet microcalorimeter.

Table V illustrates that the greater is $\Delta\delta$ between PE and a small molecule, the greater is ΔH_M and the worse is the solubility of the system. This demonstrates further that the results from the IGC method and the Calvet microcalorimeter method are identical. For some explosive solvents which are often used during the practical production, if ΔH_M cannot easily be measured by other methods, good solvents can be selected according to $\Delta\delta$ of the PE–solvent system. Therefore, the results provide an important basis for the choice of suitable solvents.

Solubility dynamics of PE–small molecule systems. In view of the dynamic factors, PE reacts faster with polar protonated solvents (*e.g.*, ethanol) than with polar non-protonated solvents (*e.g.*, DMSO). However, the solubility of PE–solvent systems is dependent not only on dynamic factors but also on their thermodynamic properties

TABLE IV

ESTIMATED δ_2 OF PE

System	Weight (PE), W_2 (g)	Volume (PE), V_2 (cm³)	V (cm³)	φ_2 (V_2/V)	ΔH_M (kJ mol⁻¹)	δ_2^* ($cal^{1/2}$ $cm^{-3/2}$)
PE–ethanol	0.2270	0.2209	2.7209	0.08	22.57	8.6
PE–ethanol	0.2040	0.1985	2.6985	0.07	23.00	8.3
PE–DMSO	0.1270	0.1236	2.6236	0.05	16.61	8.9
PE–DMSO	0.2302	0.2250	2.7250	0.08	16.76	9.8

* Calculated δ_2 of PE = 9.0.

TABLE V

CHARACTERISTIC PARAMETERS OF PE–SMALL MOLECULE SYSTEMS

Sample	δ_1 ($cal^{1/2}$ $cm^{-3/2}$)	$\Delta\delta$ ($cal^{1/2}$ $cm^{-3/2}$)	ΔH_M (kJ mol⁻¹)
Ethanol	12.7	2.9–4.4	20.87
Diethyl ether	7.4	0.9–2.4	13.77
Acetone	9.9	0.1–1.6	10.85
Ethyl acetate	9.1	0.7–0.8	7.24

and on other factors that affect the solubility. The explosive solvents used in production are generally nitro compounds, which are non-protonated solvents, and which react with PE very slowly. This factor should be considered when selecting processing conditions.

CONCLUSION

Characteristic parameters, including V_g, χ_{12} and ΔH_M, of different NCs with various small molecules were systematically measured and used to establish the solubility of different systems. This provides the characteristic parameters for concentrated solutions of NC with different percentages of nitrogen.

Various factors that affect V_g were investigated. The results indicate that the better the solubility of NC–small molecule systems, the more sensitive is V_g to L and F_{corr}; when L is extrapolated to zero, V_g can be obtained correctly. When F_{corr} is within a certain range (20 $\pm$ 5 ml min^{-1}), V_g remains constant. As a result, measuring conditions can be determined for the study of different systems.

There exist different critical values, W_c, for different NC columns. W_c is related directly to the percentage of nitrogen in the NC; the higher is the percentage of nitrogen, the smaller is W_c. Experiments demonstrated the retention mechanism of samples on NC columns.

The basic model of the dissolution of NC in good solvents was demonstrated by IGC and Calvet microcalorimeter experiments. This provides theoretical and experimental bases for the study of the solubility dynamics of concentrated NC systems.

The solubility parameter, δ_2, of PE was calculated from theory and measured with a Calvet microcalorimeter, and was used to judge the solubility of PE–small molecule systems. The results are in accordance with the results of IGC experiments. This provides data for judging the solubility between PE and explosive solvents and for selecting suitable energetic solvents.

The solubility dynamics of the system composed of PE and two typical solvents (protonated solvent, ethanol; polar non-protonated solvent, DMSO) were studied, and it was shown that the interaction between PE and the protonated solvent is faster than that between PE and the non-protonated solvent. This indicated that the interaction of the PE–energetic system is very slow. These results provide a basis for selecting suitable processing conditions.

REFERENCES

1 T. C. Davis, J. C. Peterson and W. E. Haines, *Anal. Chem.*, 38 (1966) 241.
2 Y. Ren *et al.*, *Chemistry and Technology of Gunpowder* (in Chinese), Defence Industry Publishing House, Beijing, 1981.
3 B. Li *et al.*, *Chemical Technology of Nitrocellulose* (in Chinese), Defence Industry Publishing House, Beijing, 1982.
4 Y. Ren, *et al.*, *Study on Solubility of NC in Double-Base Gunpowder with Some Explosive and Non-Explosive Substances*, paper presented at the Gunpowder Society Symposium, Beijing, 1979.
5 Y. Ren, *et al.*, *Chemical Communication* (Chinese), No. 1 (1981) 23.
6 J. Dai, *et al.*, *Chemical Communication* (Chinese), No. 1 (1980) 18.
7 Y. Ren, *et al.*, *Scientific Material* (Chinese), (1983).
8 J. S. Aspler, in S. A. Liebman and E. J. Levy (Editors), *Pyrolysis and GC in Polymer Analysis*, Marcel Dekker, New York, Basle, 1985, pp. 399–523.
9 J. H. Hildebrand and R. L. Scott, *The Solubility of Nonelectrolytes*, Reinhold, New York, 3rd ed., 1950.
10 Al-Saigh and P. Munk, *Macromolecules*, 18 (1985) 5.
11 J. S. Aspler and D. G. J. Gray, *Polym. Sci., Polym. Phys. Ed.*, 21 (1983) 1675.

CHROM. 20 961

Note

Electromigration of carrier-free radionuclides

IX. Protolysis of [^{131}I]iodate in aqueous solutions

F. RÖSCH*,*, TRAN KIM HUNG, M. MILANOV and V. A. KHALKIN

Joint Institute for Nuclear Research, Dubna, P.O. Box 79, 10100 Moscow (U.S.S.R.)

(First received July 15th, 1988; revised manuscript received September 8th, 1988)

In addition to the hydrolysis and complex formation equilibria of metal cations, protolysis reactions of oxoanions can also be investigated by means of electrophoretic methods. In particular, for amino acids, carboxylic acids and dipeptides isotachophoretic methods have yielded pK_a data[1–3]. Electrochromatography on paper[4] and quartz powder[5] has also been used to study the dissociation equilibria of phenols, aromatic amines, amino acids and carboxylic acids.

It was the aim of this work to demonstrate the possibilities of a modified version of the electromigration method in electrolyte solutions free from any supporting materials. A chemical system was chosen for which the application of other analytical methods had yielded many representative data on the protolysis constant, but for which no data had been obtained by means of the electromigration technique. The protolysis of the iodate anion satisfies both criteria. Table I summarizes the pK_a values of iodate published up to 1976[6,7].

EXPERIMENTAL

[^{131}I]IO$_3^-$

The isotope ^{131}I was obtained from Contor Isotope (Moscow, U.S.S.R.) in an isotonic solution of sodium chloride. After evaporation iodate was synthesized by adding 10^{-3} *M* sodium peroxodisulphate (Na$_2$S$_2$O$_8$) in a weakly acidic solution and heating for 10 min in a water-bath. Syntheses with chloramine-T in perchloric acid (pH 2–4) at room temperature were also successful.

The reaction yields were controlled by elecromigration of [^{131}I]IO$_3^-$ in an aqueous perchlorate solution. Separation from [^{131}I]I$^-$ proceeds because the iodate ion moves significantly more slowly than the iodide ion.

The tests showed that the syntheses were complete. Amounts of ≤5% of iodide were neglected in the iodate electromigration measurements.

---

* Present address: Academy of Sciences of the G.D.R., Central Institute for Nuclear Research, Rossendorf, PF 19, 8051 Dresden, G.D.R.

TABLE I

PROTOLYSIS CONSTANTS OF IODATE ION PUBLISHED UP TO 1976[6,7]

Con = conductivity; sol = solubility; sp = spectroscopy; nmr = nuclear magnetic resonance; ram = Raman spectroscopy; var = other methods.

Method	T (K)	μ	pK_a	Year
con	298.1	Variable	0.73	1903
con	298.1	0	1.14	1923
con	298.1	0	0.77	1927
con	298.1	0	0.77	1933
sol	298.1	0	0.74	1934
sol	298.1	0	0.79	1939
sol	298.1	0	0.79	1941
sol	301.1	0	0.82	1941
sol	308.1	0	0.84	1941
sp	298.1	0	0.78	1944
nmr	301.1	0	0.74	1959
sol	Room temp.	1 (Li)ClO$_4$	0.33	1959
con	298.1	0	0.85	1962
ram	303.1	0	0.74	1965
var	298.1	0	0.80	1967
sol	274.1	1 (Li)ClO$_4$	0.22	1973
sol	288.1	1 (Li)ClO$_4$	0.30	1973
sol	298.1	1 (Li)ClO$_4$	0.31	1973
sol	274.1	1 (Li)ClO$_4$	0.57 (^{2}H$_2$O)	1973
sol	288.1	1 (Li)ClO$_4$	0.60 (^{2}H$_2$O)	1973
sol	298.1	1 (Li)ClO$_4$	0.63 (^{2}H$_2$O)	1973

Electrolytes

For investigations of the protolysis equilibrium, inert salt solutions of the type H(K)NO$_3$ and H(Na)ClO$_4$ were used. The overall ionic strength (μ) and temperature (*T*) of the solutions were constant (μ = 0.25 and *T* = 298.1(2) K). For measurements of the pH of the electrolytes glass and potassium chloride electrodes, calibrated with standard buffer solutions, were used. The experimental error in the pH measurements was *ca.* 0.03. Doubly distilled water and chemically pure reagents were used to prepare the electrolyte solutions.

Not more than 5 μl of the [^{131}I]IO$_3^-$ stock solution with pH and ionic strength close to those of the background electrolyte solution were injected into the start position of the electromigration tube.

Electromigration method

Details of the construction and measurement principles of the electromigration apparatus developed in our laboratory have been published elsewhere[8,9]. Migration velocities were measured in a glass tube (40 mm × 3 mm I.D.) by means of an NaI(Tl) scintillation detector. The detector continuously scanned the tube during the experiment. At the same time a multi-channel analyser, operating in the multi-scale mode, recorded time and distance covered by the radioelement zone from the beginning of the experiment.

Continuous electrolyte exchange in vessels containing platinum electrodes guaranteed constancy of the pH in the electromigration tube. Connection of this tube with electrodes through Nuclepore filters prevented generation of liquid flows and distortion of the shape of the radioelement zone. For details and a schematic view of the electromigration cell, see ref. 10.

Ion mobilities were determined at constant voltage gradients of $\Delta E = 10.00(1)$ and $5.00(1)$ V cm^{-1} in solutions of pH $\geqslant 1$ and pH < 1, respectively.

RESULTS AND DISCUSSION

To study the protolysis reaction

$$HIO_3 \overset{K_a}{\rightleftharpoons} IO_3^- + H^+$$

(1)

the dependence of the overall ion mobility, $\bar{u}_{IO_3^-}$, on the proton concentration must be measured. Fig. 1 illustrates the experimental results as the function $\bar{u}_{IO_3^-} = f(pH)$.

No significant differences or trends in the $\bar{u}_{IO_3^-}$ data between the nitrate and perchlorate electrolyte systems were observed. This is clear because replacement of the anionic component of the inert electrolytes does not affect the protolysis equilibrium. This was also the case with background cations K^+ and Na^+, at least at the overall ionic strength applied.

Calculations of the stoichiometric protolysis constant start from the experimental pairs ($[H^+]$; $\bar{u}_{IO_3^-}$) and the general electromigration equation for reaction 1:

$$\bar{u}_{IO_3^-} = u^0_{IO_3^-} \alpha_{IO_3^-} = \frac{u^0_{IO_3^-} K_a}{K_a + [H^+]}$$

(2)
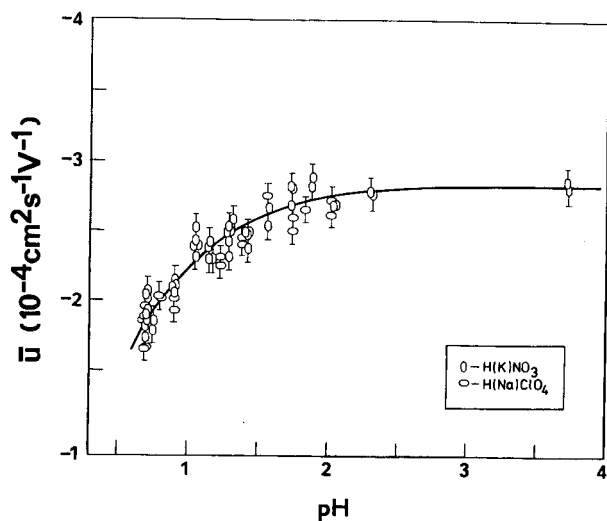
Fig. 1. Overall ion mobilities of $[^{131}I]IO_3^-$ *versus* pH of background electrolytes H(K)NO$_3$ and H(Na)ClO$_3$. $\mu = 0.25$; $T = 298.1(2)$ K.

where $\bar{u}_{IO_3^-}$ is the overall ion mobility of IO_3^- in the equilibrium reaction of interest, $\alpha_{IO_3^-}$ is the molar fraction of IO_3^-, $u_{IO_3^-}^0$ is the individual ion mobility of IO_3^-, valid at $\alpha_{IO_3^-} = 1$. and K_a is the stoichiometric protolysis constant.

Both the variables K_a and $u_{IO_3^-}^0$ in eqn. 2 were calculated by the least-squares fit of the experimental function $\bar{u}_{IO_3^-} = f([H^+])$ using the MINUIT program[11]. The results are $u_{IO_3^-}^0 = -2.82 \pm 0.05 \cdot 10^{-4}$ cm^2 s^{-1} V^{-1} and $K_a = 0.37 \pm 0.01$ mol l^{-1} (pK_a = 0.44 $\pm$ 0.01). The value of K_a calculated for $\mu = 0.25$ corresponds to the literature data for $\mu = 0$ and $\mu = 1$ and the weak dependence of the iodate protolysis constant on the overall ionic strength.

The results demonstrate the analytical capacity of the modified electromigration method for the investigation of protolysis equilibria of γ-radioactively labelled oxoanions. Similar demonstrations of the hydrolysis and complex formation of γ-radioactively labelled metal cations are summarized in refs. 12 and 13. It should be emphasized that by variation of the experimental electrolyte parameters (μ, T), thermodynamic protolysis data and information on the individual ion mobility behaviour can be obtained.

REFERENCES

1 T. Hirokawa, T. Gojo and Y. Kiso, *J. Chromatogr.*, 390 (1987) 59 and 201.
2 V. Kašička, J. Vacík and J. Prusík, *J. Chromatogr.*, 320 (1985) 33.
3 J. L. Beckers, *J. Chromatogr.*, 320 (1985) 147.
4 D. Waldron-Edward, *J. Chromatogr.*, 20 (1965) 556.
5 A. V. Stepanov and E. M. Pazuchin, *Zh. Neorg. Khim.*, 15 (1970) 1483.
6 L. G. Sillen and A. E. Martell, *Stability Constants of Metal–Ion Complexes, Special Publications Nos. 17 and 25 (Supplement to No. 17)*, Chemical Society, London, 1964 and 1971.
7 E. Högfeldt, *Stability Constants of Metal-Ion Complexes. Part A: Inorganic Ligands*, IUPAC Chemical Data Series No. 21, Pergamon Press, Oxford, 1982.
8 M. Milanov, W. Doberenz, A. Marinov and V. A. Khalkin, *J. Radioanal. Nucl. Chem.*, 82 (1981) 101.
9 M. Milanov, Tran Kim Hung, D. Shoninski, F. Rösch and V. A. Khalkin, *Radiokhimiya*, 29 (1987) 650.
10 F. Rösch, Tran Kim Hung, M. Milanov, N. A. Lebedev and V. A. Khalkin, *J. Chromatogr.*, 396 (1987) 43.
11 F. James and M. Roos, *MINUIT program*, CERN Computer Centre, Program Library, Long-Write-Up D 506, D 59C, Genève, 1971.
12 F. Rösch, Tran Kim Hung, V. A. Khalkin, M. Milanov and R. Dreyer, in S. Niese (Editor), *Proceedings of the 4th Meeting on Nuclear Analytical Methods, Dresden, May 4–8, 1987*, Vol. 2, CINR Rossendorf of the Acad. Sci. G.D.R. and the Chemical Society of the G.D.R., Dresden, 1987, pp. 566–573.
13 F. Rösch, V. A. Khalkin, M. Milanov, Tran Kim Hung and R. Dreyer, *Z. Chem.*, 27 (1987) 358.

Note

Retention behaviour of diastereomeric truxillic and truxinic diamides and separation of an enantiomeric pair in high-performance liquid chromatography

SALVATORE CACCAMESE

Dipartimento di Scienze Chimiche, Università di Catania, Viale A. Doria 6, 95127 Catania (Italy)
(First received March 21st, 1988; revised manuscript received August 18th, 1988)

The retention behaviour of a solute reflects all interactions that occur between the solute and the solvent and between the solute and the bonded phase in reversed-phase liquid chromatography (RPLC). These factors include the polarity of the solutes, the polarity and the dielectric constant of the mobile phase, the length of the hydrocarbonaceous bonded chain in the stationary phase and the stereochemistry and size of the solute molecules.

We are interested in the contribution to the retention caused by the interaction of the area of the non-polar segment of the diastereomeric α- and ε-truxillic (1 and 2, respectively) and β- and δ-truxinic (3 and 4, respectively) derivatives, where X = N(CH$_3$)$_2$, with the alkyl chains of the bonded phase (C$_{18}$ and C$_8$).
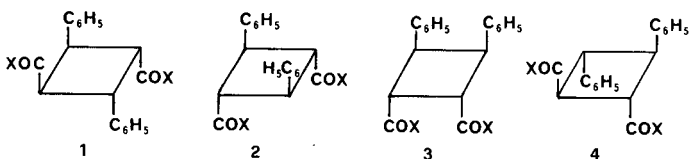
Also we describe the use of a chiral stationary phase (CSP Pirkle 1A) for the separation of these diastereomers. The enantiomers of δ-truxinic N,N-dimethylamide (4) were separated using a more efficient and recently reported chiral stationary phase.

The superiority of octadecyl-bonded RPLC over the use of the normal silica gel phase for separating diastereomers is also shown.

EXPERIMENTAL

Chemicals and solvents

N,N-Dimethylamides 1–4 were prepared by interfacial condensation of the corresponding acid chloride dissolved in dry diethyl ether with dimethylamine hydrochloride dissolved in water in the presence of dilute sodium hydroxide with stirring. Preparative details for the diamides[1] and for the corresponding acid precursors obtained by photodimerization of cinnamic acid[2] have been reported previously. We should point out that the reported[1] m.p. of compound 2 was erroneous,

being actually the m.p. of the corresponding acid chloride. The m.p. of compound 2 is in fact 187–188°C. High-performance liquid chromatographic (HPLC)-grade water, acetonitrile, 2-propanol and hexane were obtained from Fluka (Buchs, Switzerland).

HPLC apparatus and conditions

The HPLC apparatus consisted of the following components: a Varian Model 5060 liquid chromatograph with a 10-μl Valco sample loop, a Jasco Model Uvidec-100 III UV spectrophotometric detector and a Varian CDS 401 Data System. The chromatographic columns were MOS-Hypersil C_8 and C_{18} Hypersil silica (all 5 μm) (150 mm $\times$ 3.9 mm I.D.) from Shandon (Runcorn, U.K.) and LiChrosorb RP-18 (10 μm) (250 mm $\times$ 4 mm I.D.) from Merck (Darmstadt, F.R.G.), a Pirkle Type 1A chiral column, packed with (R)-N-3,5-dinitrobenzoylphenylglycine ionically bonded to γ-aminopropylsilanized silica from Regis Chemical (Morton Grove, IL, U.S.A.) and a Pirkle chiral column packed with cis-3-(1,1-dimethylethyl)-4-phenyl-2-azetidinone bonded silica gel[3].

Capacity factors (k') were calculated according to the equation $k' = (t - t_0)/t_0$, where t_0 is the retention time of an unretained solute. The void volume of the column was determined by injecting water (for the reversed phase) or hexane (for normal and chiral phases) when pumping a mixed mobile phase. Retention times were mean values of two replicate determinations.

RESULTS AND DISCUSSION

Reversed-phase HPLC

The solvophobic theory assumes that the solute interactions with bonded phases are weak, whereas the contribution of the solute–solvent interaction is fairly large. An increase in the concentration of the organic modifier in the eluent leads to a decrease in retention. According to this model, the variation of the logarithm of the capacity factors of the four diamides with the water–acetonitrile mixture is as shown in Fig. 1, the slope being very sensitive to minor changes in the composition of the mobile phase.

The retention mechanism of RPLC is very complex. However, considering that in compounds 1–4 the large molecular size and the functional groups are identical, the intermolecular solute–solvent interaction can be related mainly to the single parameter of the polarity of the solutes. The polarity sequence of these compounds is $\alpha \ll \delta \ll \varepsilon < \beta$, as from their measured solution dipole moments[4] ($\alpha = 1.90$ D, $\delta = 3.04$ D, $\varepsilon = 5.95$ D and $\beta = 6.22$ D). Hence in the reversed-phase mode we expect the elution order to be $\beta < \varepsilon \ll \delta < \alpha$. However, as shown in Fig. 1, this is not so.

Remarkably, minor stereochemical effects due to the relative configuration of the ring substituents strongly affect the retention behaviour. The layered alkyl "skin" of the bonded phase interacts with the non-polar region of the solutes and according to this partition mechanism[5] the bonded phase interacts better with large solute molecules, such as compounds 1–4, if its solvophobic surface area relative to the alkyl chain length is large enough to overlap with the hydrocarbonaceous segment area of the molecules.

These interactions are depicted in Fig. 2, constructed using Dreiding models for compounds 1–4. The plane shows the surface of the alkyl-bonded phase as normal to
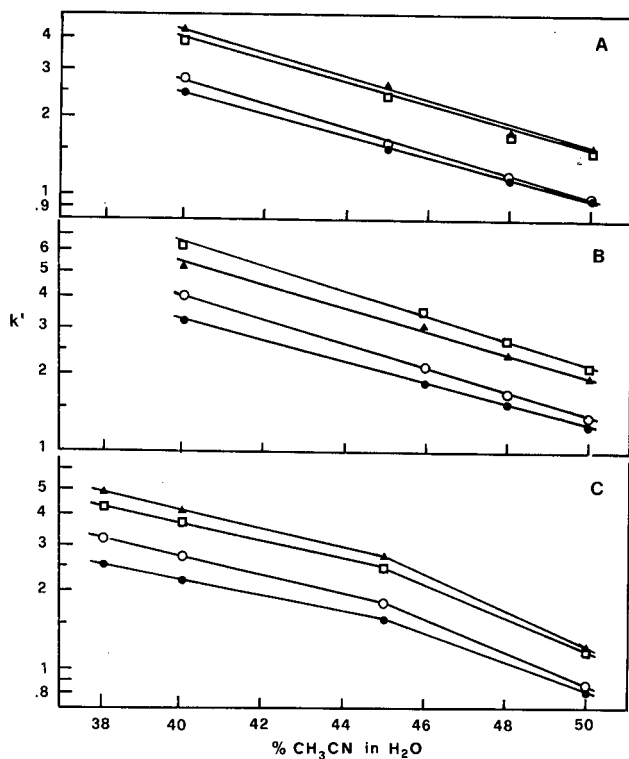
Fig. 1. Effect of acetonitrile concentration in water on the capacity factors (k') of (●) compound 1; (▲) compound 2; (○) compound 3; (□) compound 4. (A) On Shandon C_{18} phase; (B) on Merck C_{18} phase; (C) on C_8 phase.
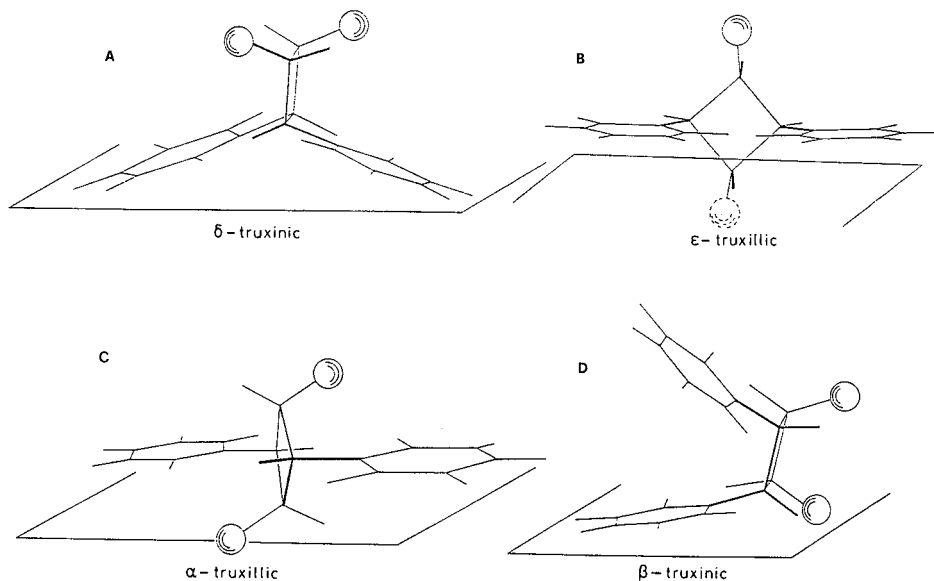

Fig. 2. Interaction of compounds 1–4 with the bonded alkyl chain of the reversed-phase: (A) compound 4; (B) compound 2; (C) compound 1; (D) compound 3. Spheres illustrate the bulky amide groups.

the cyclobutane ring and the spheres illustrate the bulky amide groups. In particular, the hydrocarbonaceous surface in Fig. 2B intersects the ring (which lies on the page) and both amide groups are disected behind the page.

In these compounds the preferred conformations of the phenyl rings and of the amide groups shown, arising from the rotation around the single bond connecting the cyclobutane carbon to the aromatic or carbonyl carbon, respectively, were previously found by contour energy maps[2] and can be easily obtained by a careful examination of their Dreiding models. Moreover, the interatomic distances between the *para* position of the phenyl groups in the four diastereomers are very different and only in the ε-truxillic (2) and δ-truxinic (4) configurations can the phenyl rings remain, in the preferred conformation, almost coplanar *without* hindrance resulting from the bulky polar amide groups both pointing in opposite directions from the phenyl rings plane. This non-polar region of the molecules can therefore perfectly overlap with the alkyl surface of the bonded phase, thus explaining their higher chromatographic retention. In contrast, in the α-truxillic configuration 1 a polar amide group is intercalated in the plane containing the phenyl rings, thus strongly disturbing the overlap of the non-polar region of the solute with the hydrocarbonaceous sheath of the stationary phase. In the β-truxinic configuration 3, the dihedral angle between the phenyl rings in the preferred conformation is very small (about 60°) and therefore again large area interactions of the non-polar region of the molecule with the bonded phase are not possible. Hence the retentions of the α and β compounds are lower than those of the ε and δ compounds. This behaviour was not expected from the strong polarity difference between α and β compounds. A typical separation of the four diastereomers is shown in Fig. 3.

The marked difference between the retention times of the α and β and those of the ε and δ compounds is therefore related to the interaction mechanism depicted above and it is confirmed when using C_{18} phases from different manufacturers, as shown in Fig. 1A and B. Fig. 1A and B also show that the resolution between the ε and δ isomers
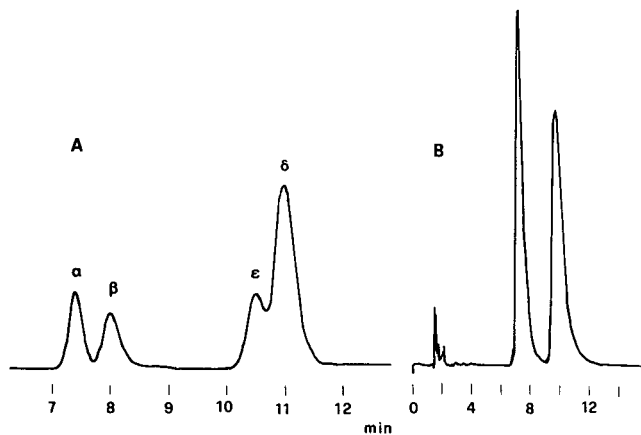
Fig. 3. Typical chromatograms showing (A) separation of the four diastereomers on a C_{18} reversed-phase column, mobile phase acetonitrile–water (46:54), flow-rate 1 ml/min, detection at 225 nm; (B) separation of the enantiomers of compound 4 on a CSP 2 column, mobile phase 2-propanol–hexane (10:90), flow-rate 2 ml/min, detection at 254 nm.

and between the α and β isomers is poor on the Shandon C_{18} column whereas it is much better on the Merck C_{18} column. This result is probably due to a different carbon content bonded to the silica or to a different history. In fact, the k' values of all compounds are larger on the Merck than on the Shandon phase, evidently owing to a larger solute–stationary phase interaction, which leads to a higher selectivity in the isomeric pair.

Remarkably, a change in the retention order of the ε/δ pair occurs between the C_{18} columns from the two manufacturers.

Shortening of the alkyl chain length of the bonded reversed-phase leads, as expected, to a decreased retention of a given solute, as shown by comparing the k' values obtained with C_{18} phases with those obtained with C_8 phase (Fig. 1). In addition, the decrease in log k' in Fig. 1C with a 50% acetonitrile mobile phase, resulting in incomplete separation of the compounds, is related to the weaker interaction of these large solute molecules with the shorter alkyl C_8 chains compared with the stronger solute–solvent interaction. Similar deviations from the theoretical linear relationship of log k' vs. phase composition have been reported for compounds exhibiting hydrogen bonding with the aqueous phase.

Chiral stationary phase

As δ-truxinic diamide (4) possesses only a simple two-fold axis of symmetry, the racemic compound synthesized by us is in principle resolvable into an enantiomeric pair.

In view of the considerable success demonstrated by the Pirkle amino acid-derived stationary phase CSP 1A in the enantiomeric resolution of compounds of forty structural types[6,7], we tried this phase. However, no enantiomeric resolution of the δ-truxinic compound 4 was obtained. Using 2–20% of 2-propanol in hexane as the mobile phase at a flow-rate of 1 ml/min and detection at 254 nm, only a single peak appeared. The configuration of the four large substituent groups inhibits the separability of enantiomers, presumably owing to steric congestion in a region important to chiral recognition. The CSP 1A was instead extremely selective in the separation of diastereomeric α-truxillic and δ-truxinic diamides. The k' values were 2.86 and 2.28, respectively, in 2-propanol–hexane (10:90). Remarkably, the ε and β isomers (both possessing the strongly polar amide groups *cis* oriented and not disturbed by the phenyl groups extending in the opposite direction) were retained in the column. In this instance, the retention behaviour is presumably controlled by dipole interactions of the amide groups with the acyl group of the CSP.

A new Pirkle chiral stationary phase (CSP 2) derived from *cis*-3-(1,1-dimethylethyl)-4-phenyl-2-azetidinone[3] was effective for the separation of the δ-isomer into its enantiomers. Fig. 3 illustrates the facility with which the enantiomers of compound 4 were resolved on this new phase, with a separation factor $\alpha = 1.30$ and $k' = 3.44$.

The improved chiral recognition of CSP 2 with respect to that of CSP 1A may be due to the presence in the former of an additional stereogenic centre and to the better ability of the enantiomers to "conform" to the shape of CSP 2[3].

Normal-phase HPLC

With the exception of inverted k' values for the δ and ε isomers, the

chromatographic behaviour of compounds 1–4 is related to their dipole moments, as expected. At a flow-rate of 1.5 ml/min and using 2-propanol–hexane (10:90) as the mobile phase, the capacity factors k' were 14.5 for the δ, 9.6 for the ε and 1.35 for the α isomers. The extremely polar β isomer ($\mu = 6.22$ D) is irreversibly retained in the column. This behaviour, in addition to the broadening of the peaks for the δ and ε isomers, is due to the strong interaction of the *cis* amide dipoles with the silanol groups of the adsorbent. Hence the general performance of this phase for the separation of this class of diastereomers is not as high as that of the reversed-phase.

ACKNOWLEDGEMENTS

REFERENCES

1 G. Montaudo, P. Maravigna, S. Caccamese and V. Librando, *J. Org. Chem.*, 39 (1974) 2806.
2 G. Montaudo and S. Caccamese, *J. Org. Chem.*, 38 (1973) 710.
3 W. H. Pirkle and J. E. McCune, *J. Chromatogr.*, 441 (1988) 311.
4 G. Pugliares, *Thesis*, University of Catania, 1973.
5 C. H. Löchmuller and D. R. Wilder, *J. Chromatogr. Sci.*, 17 (1979) 574.
6 W. H. Pirkle and T. C. Pochapsky, *Adv. Chromatogr.*, 27 (1987) 73.
7 W. H. Pirkle, M. H. Hyun and B. Bank, *J. Chromatogr.*, 316 (1984) 585.

CHROM. 20 923

Note

Industrial applications of chromatography

I. Determination of methanol, *n*-butanol and toluene by direct aqueous injection gas chromatography

ALEŠ HORNA

Research Institute of Industrial Chemistry, East Bohemia Chemical Works Synthesia, 532 17 Pardubice-Semtín (Czechoslovakia)

The processing of industrial waste waters is a very important operation in which chromatography is one of the most frequently used analytical methods.

Gas chromatographic (GC) methods for the determination of volatile compounds in aqueous liquids, reviewed in many recent papers[1,2], usually utilize headspace analysis[3] or organic solvent extraction[4]. On the other hand, only a small number of methods for the determination of organic compounds by direct injection GC have been reported[5–8], although this very simple method seems to be very advantageous. Moreover, because of possible errors associated with purging efficiency or the efficiency of extraction of volatile polar organic compounds, the direct aqueous injection of an aliquot of the effluent on to a GC column is considered to be the only realistic approach to the determination of polar organics[5]. In addition, using existing modern column and detector technology, this rapid and not labour-intensive technique can be used for the analysis of water-based samples for parts per 10^9 to low percentage levels of many organic compounds[5].

In this paper, direct aqueous injection GC employing a flame ionization detector and an Apiezon L packed column for the simultaneous determination of methanol, *n*-butanol and toluene in industrial waste waters is described, together with the effects of water on both the retention behaviour and detection.

EXPERIMENTAL

A Fractovap GV gas chromatograph (Carlo Erba, Milan, Italy) equipped with a flame ionization detector was used. The injector and detector temperatures were both 250°C; the nitrogen carrier gas flow-rate was, *ca.* 30 ml/min and the chart speed 0.05 mm/s.

A glass column (2.5 m × 4 mm I.D.) containing 17.5% Apiezon L on acid-washed Chromosorb W (60–80 mesh) was operated at an oven temperature of 97°C. A glass column (2.5 m × 4 mm I.D.) packed with 120–150-mesh Porapak Q (Waters Assoc., Milford, MA, U.S.A.) was operated at 180°C. A 1-μl sample volume was injected into the instrument, and the methanol, *n*-butanol and toluene were eluted

with attenuation producing peaks of reasonable size. The retention times and peak areas were measured with an Autolab System IV computing integrator (Spectra-Physics, Mountain View, CA, U.S.A.).

The amounts of the organic solvents were calculated from calibration graphs of the ratio of the amounts of the organic solvent and internal standard *versus* their peak-area ratio. The calibration was performed on Apiezon L using standard solution of methanol, *n*-butanol, toluene and *n*-propanol (internal standard) in distilled water at various mass ratios. A least-squares determination of the line of best fit of the points was performed with a TI 58 C calculator. With the exception of methanol (correlation coefficient 0.989), correlation coefficients of better than 0.999 were obtained, indicating good linearity of the calculated straight lines. Hence with toluene, *n*-butanol or isobutanol daily calibration was performed using only one standard concentration for each solvent.

For the determination of trace amounts of methanol in water, an absolute calibration graph on Porapak Q for methanol concentration in the range 0.005–0.250% in distilled water was established.

RESULTS AND DISCUSSION

For the analysis of water-based samples, the choice of the GC column is limited because water can cause chemical changes to the GC packing or interfere in the analysis. On the other hand, it is generally known that the flame ionization detector selectively detects low-molecular-organic compounds but hardly responds to water. Hence a glass column packed with Chromosorb W AW coated with Apiezon L and a flame ionization detector were selected for the simultaneous determination of methanol, *n*-butanol and toluene for monitoring industrial waste water processing.

On non-polar Apiezon L stationary phase water elutes at about the same time as methanol. Hence it can be expected that with a high flame ionization detector
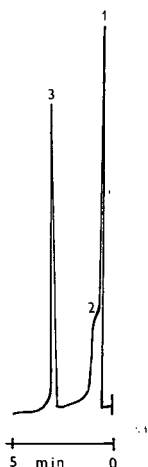
Fig. 1. Chromatography of distilled water containing 0.01% of each alcohol on an Apiezon L glass column (2.5 m × 4 mm I.D.) at 97°C. Peaks: 1 = methanol; 2 = water; 3 = and *n*-butanol.
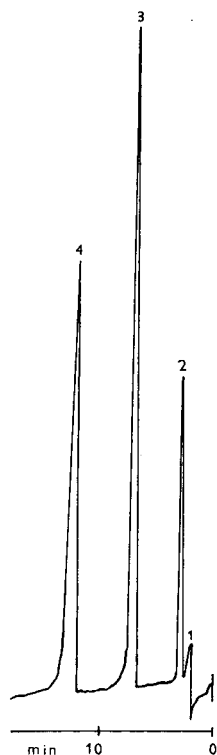
Fig. 2. Chromatography of distilled water containing 0.01% of each alcohol on a Porapak Q glass column (2.5 m × 4 mm I.D.) at 180°C. Peaks: 1 = "water"; 2 = methanol; 3 = n-propanol; 4 = n-butanol.

sensitivity, which is needed for trace analysis, the water response will be large enough to affect the methanol peak. According to our experiments, when the methanol concentration in water approached 0.01% the water response was large enough to distort the methanol peak (Fig. 1). For this reason, a Porapak Q packed column was employed for trace methanol determination to separate water effectively from the methanol peak (Fig. 2). For the routine analysis of industrial waste waters and with extraction- and/or distillation-isolated organics, an Apiezon L packed column was preferred owing to the short analysis time.

When methanol, n-butanol and toluene were determined in both water- and organic-based samples on an Apiezon L column a shift in the retentions of the organic solvents relative to one another was observed. To illustrate how the concentration of organic compounds affects the retention of methanol and n-butanol on Apiezon L, the relative retention times (internal standard n-propanol) were calculated and plotted against the total concentration of volatile organics in the injected sample. From Fig. 3, it can be seen that the relative retention time of methanol tends to increase with increasing proportion of volatile organic compounds in the sample. On the other hand (Fig. 4), the relative retention time of n-butanol tends to decrease with increasing proportion of organics in the sample.
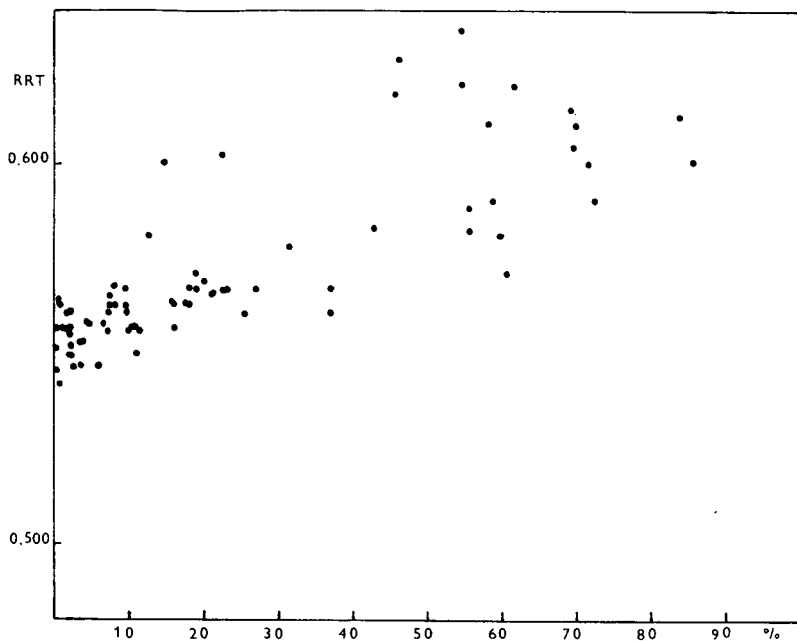
Fig. 3. Relationship between the relative retention time (RRT) of methanol and the total concentration of the determined solvents in water on Apiezon L Chromosorb W AW packed column. For *n*-propanol employed as the internal standard, RRT = 1.000.
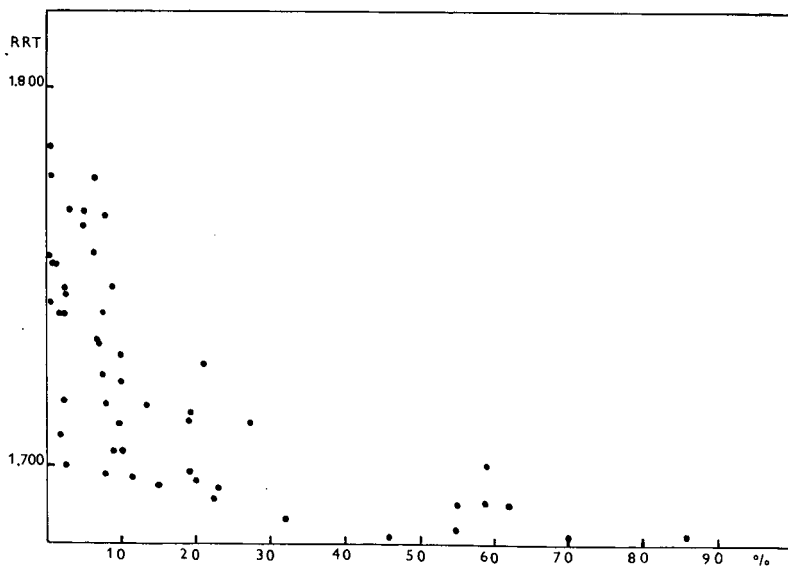
Fig. 4. Relationship between the relative retention time (RRT) of *n*-butanol and the total concentration of the determined solvents in water on Apiezon L Chromosorb W AW packed column. For *n*-propanol employed as the internal standard, RRT = 1.000.

TABLE I

RETENTION TIMES OF METHANOL, n-PROPANOL, n-BUTANOL AND TOLUENE ON APIE-ZON L AT THE DIFFERENT TOTAL CONCENTRATIONS OF THE ORGANIC SOLVENTS IN DISTILLED WATER

Five injections were performed for each concentration.

Total concentration (%, w/w)	Retention time ± S.D.			
	Methanol	n-Propanol	n-Butanol	Toluene
6.1	53.3 ± 0.6	94.8 ± 1.0	161.5 ± 0.6	407.5 ± 0.7
9.5	53.3 ± 0.6	94.7 ± 0.6	161.7 ± 0.6	406.3 ± 0.6
16.7	53.0 ± 0.1	94.0 ± 0.1	161.8 ± 0.5	407.8 ± 0.5
52.5	54.3 ± 1.0	95.0 ± 0.8	161.5 ± 0.6	408.0 ± 1.2
100	56.6 ± 0.6	95.4 ± 0.6	162.2 ± 0.5	408.8 ± 1.6

To confirm the above-mentioned observations in the analysis of real samples, model mixtures containing methanol, n-propanol, n-butanol and toluene (2:2:2:1, w/w) in distilled water with a total concentration from 6.1 to 52.5% (w/w) were prepared and 1-μl samples were injected. With decreasing content of water in the injected samples the retention times of the solvents began to shift slightly (Table I). However, when a dry organic solvent mixture was injected, maximum retention times for all solvents were obtained. Especially with methanol more a 3 s increase in the retention time was observed.

The reduction in the retention times of organic compounds injected together with a large volume of water is in agreement with earlier work[9,10] and can be explained by the carrier gas being temporarily saturated with water.

No significant changes in the efficiency or polarity of the Apiezon L column were observed after many hundred injections.

ACKNOWLEDGEMENT

REFERENCES

1 J. R. Garbarino, T. R. Steinheimer and H. E. Taylor, Anal. Chem., 57 (1985) 46R.
2 A. Cailleux, A. Turcant, P. Allain, D. Toussaint, J. Gaste and A. Roux, J. Chromatogr., 391 (1987) 280; and references cited therein.
3 B. V. Ioffe and A. G. Vitenberg, Headspace Analysis and Related Methods in Gas Chromatography, Wiley, New York, 1984.
4 J. Curvers, T. Noij, C. Cramers and J. Rijks, Chromatographia, 19 (1984) 225.
5 B. S. Middleditch, N.-J. Sung, A. Zlatkis and G. Settembre, Chromatographia, 23 (1987) 273.
6 S.-T. Cheung and W.-N. Lin, J. Chromatogr., 414 (1987) 248.
7 GC Bull., No. 816, Supelco, Bellefonte, PA, 1984.
8 Supelco Reporter, Vol. 4, No. 2, Supelco, Bellefonte, PA, 1985, p. 4.
9 G. Urbach, J. Chromatogr., 404 (1987) 163.
10 J. Janák, J. Růžičková and J. Novák, J. Chromatogr., 99 (1974) 689.

CHROM. 20 958

Note

Study of the adsorption of methyl red on thermally treated gas–liquid chromatographic packings

GEOMIL PEKOV*, NIKOLAY PETSEV and ROSINA OBRETENOVA

Faculty of Chemistry, University of Sofia, Sofia (Bulgaria)

(First received May 11th, 1988; revised manuscript received August 17th, 1988)

A major requirement of supports for gas–liquid chromatography (GLC) is they should have low adsorption activity. Different methods for deactivation of support surfaces are used for this purpose[1]. Aue *et al.*[2] and Winterlin and Moseman[3] obtained strongly deactivated materials by heating GLC packings in an inert atmosphere at temperatures little above the maximum allowed temperature, followed by exhaustive extraction. The materials obtained are the original support coated with a chemically bound unextractable monolayer of a stationary phase, and are highly effective chromatographic supports.

Following Aue *et al.*'s idea, packings for GLC consisting of a diatomite support and various liquid stationary phases were heated at temperatures higher than the critical level for their use, and subsequently were Soxhlet extracted with the solvent used for stationary phase coating. The chromatographic retention of test solutes on the treated materials showed that they differ in the degree of deactivation from the untreated packings and the original support[4]. The deactivation depends on the initially coated liquid stationary phase. The adsorption activity of these materials, determined as described previously[5], decreases according to the chromatographic retention of different test solutes (benzene, methanol, diethyl ether, dioxane, acetone, methyl ethyl ketone, pyridine) on them, which indicates that it is possible to measure the extent of modification of GLC packings by this method easily and rapidly[6].

In this work the changes in the adsorption activity of some of these packings when heated in an oxidizing atmosphere at temperatures much above the allowed level were studied. The purpose was to establish the role of temperature and extraction in the modification process[4].

EXPERIMENTAL

Sterchamol (Schuhardt, Munich, F.R.G.), screen fraction 0.200–0.315 mm, was used as the support. The liquid stationary phases were SE-30 (BDH, Poole, U.K.) and squalane (Fluka, Buchs, Switzerland) with a 10% (w/w) coating on the packing; these two packings showed the most and the least modification effect, respectively[4]. They were heated stepwise from 100 to 1000°C for 1–4 h in air. Samples were taken after every 100°C increase and were Soxhlet extracted for 10–30 h with the solvent used for the stationary phase coating (chloroform for SE-30 and *n*-hexane for squalane). The

TABLE I

DEPENDENCE OF METHYL RED ADSORPTION (μmol/g) ON TEMPERATURE AND TIME OF TREATMENT (HEATING AND SOXHLET EXTRACTION) OF THE SE-30–STERCHAMOL PACKING

Temperature (°C)	Heating (h)	Extraction (h)			
		0	10	20	30
100	1	2.13	1.03	1.01	1.14
100	2	1.11	1.09	0.95	0.94
100	4	1.11	1.01	0.94	0.95
200	2	0.98	0.82	0.74	0.76
300	2	0.61	0.51	0.47	0.47
400	2	1.42	1.41	1.40	1.42
500	2	7.40	7.42	7.42	7.41

purpose of this treatment was to follow the alterations in the stationary phases with respect to the adsorption activity of the packings until the support surface was regenerated.

The adsorption capacity of the materials studied was determined at each level of treatment by measuring the adsorption of methyl red. A sample of the adsorbent (0.2 g) was shaken with 5 ml of a 0.6 mM solution of methyl red in benzene; after equilibrium had been established, the solution was removed and the dye retained on the adsorbent was eluted with ethanol and measured photometrically in the suitably acidified eluate. The analytical procedure was described in detail previously[5].

RESULTS

Thermal treatment of original Sterchamol slightly influences its adsorption activity. There is only a small increase of 1.8% in methyl red adsorption up to 300°C, which is in the range of the standard error (3.5%). At higher temperatures a decrease is observed and at 1000°C the amount of dye adsorbed is 12% less than that on an
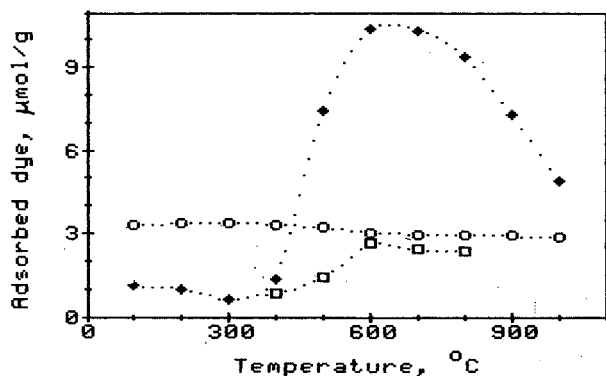
Fig. 1. Adsorption of methyl red on thermally treated (○) Sterchamol, (◆) SE-30–Sterchamol packing and (□) SE-30–Sterchamol packing Soxhlet extracted after heating at 300°C.

air-dried sample. Thermal analysis showed that Sterchamol does not undergo any definite energy transition in the studied temperature range (Fig. 3a), but from 300 to 560°C an oxidation process occurs on its surface (Fig. 3b).

SE-30–Sterchamol packing (SE-P)

The time of treatment (heating and extraction) influences the adsorption activity only at the lowest temperature. The results in Table I show that (i) heating at 100°C for more than 2 h does not change the adsorption capacity of the packing; (ii) Soxhlet extraction for more than 20 h has no influence when the sample is heated for 2 h or more; and (iii) Soxhlet extraction is not necessary for samples heated at temperatures higher than 300°C (the values in the last two columns and two lines are statistically indistinguishable).

The dependence of the SE-P adsorption activity on temperature (curve ◆) compared with that for Sterchamol (curve ○) is shown in Fig. 1. Coating the support with the stationary phase reduces its activity 3-fold. Heating this packing to 300°C leads to maximum thermal deactivation; it adsorbes 5.5 times less methyl red than Sterchamol. Extraction decreases the adsorption activity of SE-P when it is heated to this temperature but not as much as the heat treatment (Table I). Samples heated at higher temperatures show virtually no change in activity after Soxhlet extraction.

A large increase in the adsorption of methyl red occurs on further heating at higher temperature. Maximum dye adsorption is reached at *ca.* 600°C, *i.e.*, 3.5 times more than that of the support itself. The term "packing" is used conventionally because at this high temperature the material surface differs in composition and properties from those of the initial packing. This is confirmed by the fact that heat treatment up to 1000°C does not restore the adsorption capacity of the support; SE-P adsorbes 1.7 times the amount adsorbed by similarly heated Sterchamol. The adsorption surface of the support is regenerated when the initial SE-P is heated directly to 1000°C. In this instance a white amorphous substance (silica) forms on the packing surface and the solid under this white coating adsorbs to the same extent as Sterchamol heated at 1000°C (2.88 μmol/g of methyl red).

The behaviour of SE-P is different if the most deactivated sample (300°C plus extraction) is exposed to higher temperatures. The adsorption activity increases and reaches a maximum at *ca.* 600°C, but at any temperature the amount of dye adsorbed is lower than that of the support (Fig. 1. curve □).

A burn exotherm in the differential thermal analysis (DTA) curve of SE-P (Fig. 3a) begins at 380°C and ends at *ca.* 630°C, where the maximum adsorption activity of the packing occurs. The weight loss of SE-P at 630°C is 3.8% higher than that of Sterchamol at this temperature. This difference corresponds to the mass of carbon and hydrogen in the SE-30 molecule and remain unchanged up to 1000°C. The oxidation mass peak of the Sterchamol thermogravimetric analysis (TGA) curve is absent from the TGA curve of SE-P (Fig. 3b), which shows that up to 560°C the support surface is screened by the stationary phase or its decomposition products.

Squalane–Sterchamol packing (SQU-P)

The temperature dependence of the adsorption activity of SQU-P without (curve ◆) and with (curve □) extraction compared with that of Sterchamol (curve ○) is shown in Fig. 2. The heating leads to substantial modification of the packing whereas
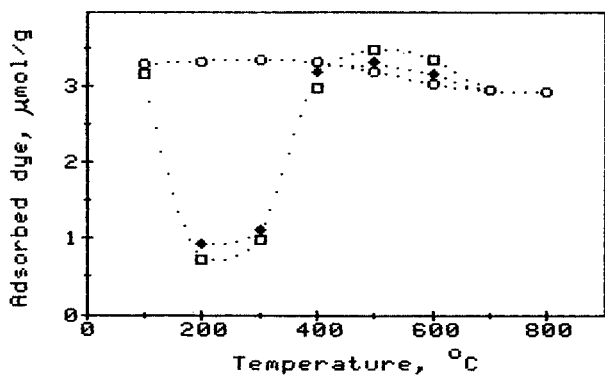
Fig. 2. Adsorption of methyl red on thermally treated (○) Sterchamol and squalane–Sterchamol packing before (◆) and after (□) Soxhlet extraction. Adsorption of methyl red on a sample heated only at 100°C cannot be measured as the squalane dissolves in benzene.
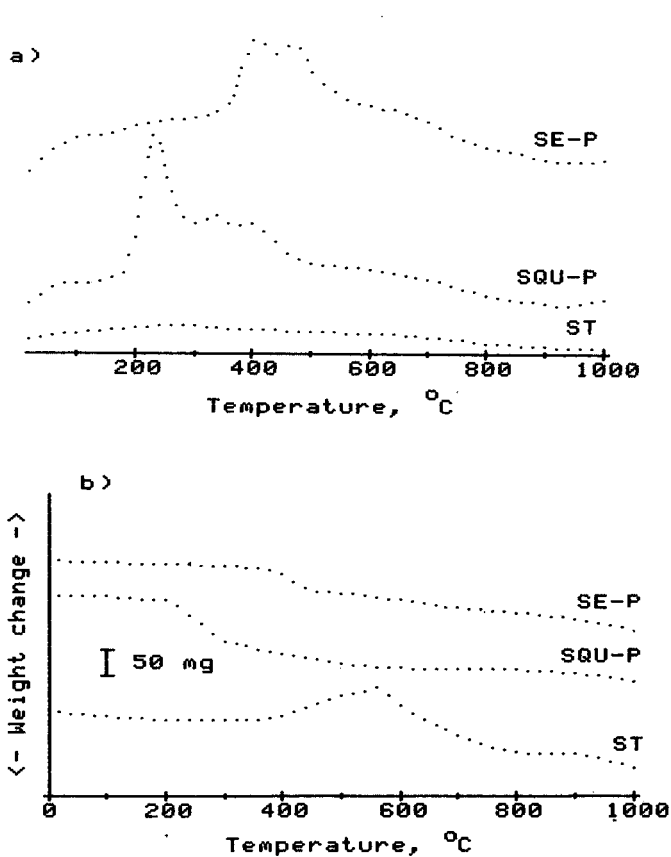

Fig. 3. (a) DTA and (b) TGA curves for Sterchamol (ST) and packings of Sterchamol with SE-30 (SE-P) and squalane (SQU-P) as stationary phases.

the extraction influences it only slightly. A SQU-P sample heated at 200°C has a 3.5-fold lower adsorption activity before extraction and a 4.7-fold lower activity after extraction than Sterchamol. This treated sample is the most deactivated of the SQU-P type; it adsorbs 0.71 μmol/g of methyl red. There is an exothermic peak in the SQU-P DTA curve at this temperature (Fig. 3a). Heating up to 500°C increases the adsorption activity of the packing, which is 2.8% higher without extraction and 8.8% higher with extraction than that of Sterchamol at this temperature. Complete regeneration of the support surface is achieved when the packing is heated up to 700°C. The weight loss of SQU-P at this temperature is 10.2% higher than that of Sterchamol and corresponds to total burning of the stationary phase. The absence of the Sterchamol oxidation mass peak from the TGA curve of SQU-P (Fig. 3b) shows that up to 560°C the support surface is blocked by some decomposition products of squalane.

DISCUSSION

The deactivation of Sterchamol by treatment at high temperatures is due to the reduction of its active surface[7]. Such treatment influences the adsorption activity of the packings studied by modifying the stationary phase. It is accepted that the liquid is retained on the support surface by adhesion forces. Depending on the subsequent heat treatment, the mode of binding of the liquid to the support and between the stationary phase can change.

Heating to 300°C deactivates the SE-P. Extraction with the stationary phase solvent does not regenerate the adsorption activity of the support but extends the deactivation process. This means that high temperatures lead to the formation of chemical bonds between the liquid and the support. At 380°C burning of SE-30 begins, which involves its organic part and linking between –Si–O–Si– chains of the SE-30 molecules becomes possible. After the organic part of the liquid has completely burnt (at ca. 630°C), a new surface of SE-P is formed. It is looser than that of Sterchamol and differs from it mainly in number of the active sites. Further heating of SE-P causes the same changes as for Sterchamol, i.e., reduction of the active sites. The number of active groups on the packing surface is greater and the effect of deactivation is stronger than those for bare Sterchamol. When SE-P is heated directly to very high temperatures there is not enough time for linking between the stationary phase and the support to occur, and SE-30 volatilizes prior to undergoing oxidation to silica.

The temperature of maximum deactivation of SQU-P (ca. 200°C) is too high for squalane to be used as the stationary phase. The surface of SQU-P when heated in the range 200–300°C is hydrophobic even after extraction, in contrast to all other SQU-P samples. This means that another (different from the squalane) unextractable compound is formed on the support surface. This compound binds with the support more weakly than for SE-P and the Sterchamol adsorption capacity regenerates at ca. 700°C.

The most deactivated samples of the packings studied adsorb 0.47 (SE-P) and 0.71 (SQU-P) μmol/g of methyl red. These values are comparable to the adsorption of methyl red (less than 1 μmol/g) on some firm silanized diatomite supports[6]. This indicates that the treatment of the GLC packings studied leads to blockage of the active sites of the support with the stationary phase or its decomposition products, which could be as effective as silanization.

CONCLUSIONS

Thermal treatment of GLC packings with SE-30 or squalane as the stationary phase decreases the adsorption activity if the heating is carried out near to (for SE-30) or higher than (for SQU-P) the corresponding maximum allowed operating temperature. To achieve this effect it is not necessary to carry out the heating in an inert atmosphere. The deactivation is due to chemical changes in the stationary phase which binds to the support surface. Packings deactivated in this manner could serve as effective chromatographic supports.

The usual conditioning of GLC columns improves their properties not only by removing the undesirable lower boiling compounds, but also by reducing the adsorption activity of the packing at the moderate temperatures applied.

By measuring the adsorption of methyl red, it is possible to control the modification process in order to find the optimal conditions for support/packing deactivation and for support regeneration by heat treatment. Not only the temperature but also the method of heating (stepwise or direct) have a considerable effect on the results, whether the support is regenerated from the GLC packing or not.

REFERENCES

1 D. M. Ottenstein, *Adv. Chromatogr.*, 3 (1966) 163.
2 W. A. Aue, C. R. Hastings and S. Kapila, *J. Chromatogr.*, 77 (1973) 299.
3 W. L. Winterlin and R. F. Moseman, *J. Chromatogr.*, 153 (1978) 409.
4 N. D. Petsev, G. I. Pekov, M. D. Alexandrova and Chr. Dimitrov, *Chromatographia*, 20 (1985) 228.
5 G. Pekov and N. Petsev, *God. Sofii. Univ. Khim. Fak.*, 80 (1986) in press.
6 G. Pekov and N. Petsev, *God. Sofii. Univ. Khim. Fak.*, 80 (1986) in press.
7 J. F. K. Huber and A. I. M. Keulemans, *Nature (London)*, 198 (1963) 742.

CHROM. 20 984

Note

Diazotized dapsone as a reagent for the detection of cannabinoids on thin-layer chromatographic plates

B. D. MALI* and P. P. PARULEKAR

Regional Forensic Science Laboratory, State of Maharashtra, Cantonment, Aurangabad-431 002 (India)

(First received May 31st, 1988; revised manuscript received September 9th, 1988)

Cannabis and other forms of cannabis plants (bhang, ganja, charas) are very frequently submitted to forensic laboratories. In routine cases the identification of cannabinoids in marihuana is achieved unequivocally by the 'three-parameter approach' [morphology, colour tests and thin-layer chromatography (TLC)] as suggested by Coutts and Jones[1]. Although the instrumental methods are sensitive they are expensive and there are limitations to their use in routine forensic work owing to the large number of samples to be handled.

A number of chromogenic reagents such as Duquenois reagent[2], Fast Blue Salt B[3], 1-nitroso-2-naphthol[4], Fast Blue Salt 2B[5] and 2-hydrazono-2,3-dihydro-3-methylbenzothiazole hydrochloride (HMBT)[6,7] have been reported for the detection of cannabinoids. Although Fast Blue Salt B as a chromogenic reagent seems to be the most commonly used reagent, its safety is questionable because of its potential carcinogenicity[7,8]. In a search for an alternative chromogenic reagent, diazotized dapsone was found to be suitable for the detection of cannabinoids in marihuana.

EXPERIMENTAL

All the solvents used were of analytical-reagent grade.

Solutions

Recrystallised dapsone tablets (Burroughs Wellcome) and sulphadiazine tablets (May and Baker) and other analytical-reagent grade chemicals such as aniline, *p*-chloroaniline, *p*-toluidine, α-naphthylamine, *o*-aminobenzoic acid and *p*-aminobenzoic acid were dissolved in ethanol to give 1 mg/ml solutions.

For the extraction of cannabis, the cannabis sample (bhang, ganja or charas) was extracted with chloroform, the extract was filtered and evaporated to dryness and the residue was dissolved in chloroform for spotting.

Cannabinol and cannabidiol pure reference standards were dissolved in ethanol.

A solution of α-naphthol in ethanol was prepared.

Spray reagent

A 10-ml volume of dapsone solution was pipetted into a 25-ml volumetric flask

TABLE I

R_F VALUES OF CANNABINOIDS·WITH RESPECT TO α-NAPHTHOL

Cannabinoid	R_F value ± S.D.**		Colour of spot
	I*	II*	
Cannabinol	1.29 ± 0.03	1.62 ± 0.03	Brownish yellow
Cannabidiol	1.45 ± 0.03	2.02 ± 0.02	Yellow
Δ^9Tetrahydrocannabinol	1.62 ± 0.03	1.78 ± 0.02	Yellow
α-Naphthol	1.00	1.00	Red

    * Solvent systems: I = n-hexane–acetone (85:15) (α-naphthol, R_F = 0.36); II = n-hexane–diethyl ether (80:20) (α-naphthol, R_F = 0.30).
    ** Standard deviations based on 10 measurements.

and 2 ml of 0.1 M hydrochloric acid followed by 6 ml of 0.1% sodium nitrite solution were added. The solution was allowed to stand for 10 min and then diluted to 25 ml with distilled water.

    Other spray reagents were prepared using the requisite amounts of acid and sodium nitrite.

Thin-layer chromatography

    Standard glass plates (10 × 20 cm) were coated with a 0.25-mm layer of silica gel G (ACME, Bombay, India) in water (1:2), allowed to dry at room temperature and then activated at 110°C for 1 h before use. Two solvent systems, n-hexane–acetone (85:15) and n-hexane–diethyl ether (80:20), were used for developing the plates. The cannabis extract together with α-naphthol and the standard reference solutions of cannabinol (CBN) and cannabidiol (CBD) were spotted on the plate, which was developed by the ascending technique in a presaturated chamber. After a run of about 10 cm the plate was removed and allowed to dry at room temperature. It was sprayed uniformly with freshly prepared diazotized dapsone reagent. The R_F values of cannabioids with respect to α-naphthol (red spot) are given in Table I.

UV spectra of THC

    The cannabis extract was spotted on a TLC plate, the plate was developed with either of the above solvent systems and one of the resolved spots was made visible by spraying the diazotized dapsone reagent. An equal area of silica gel layer was scraped off from a distance equal to the R_F value of $\triangle^9$-tetrahydrocannabinol ($\triangle^9$-THC), treated with 5 ml of ethanol and the solution mixed throughly. The solution was centrifuged and the UV spectrum of the supernatant liquid was recorded.

RESULTS AND DISCUSSION

    Most of the cannabinoids have a phenolic group with the *ortho* and *para* positions free. As phenols couple in the *para* position with diazonium salts[9] the cannabinoids also undergo similar reactions with diazotized dapsone to yield coloured products.

    The cannabis extract gave three spots, a brownish yellow spot corresponding to

TABLE II

MINIMUM DETECTABLE AMOUNTS OF CANNABINOIDS USING DIFFERENT SPRAY RE-
AGENTS

Diazotized reagent	Minimum amount detectable (µg)	
	Cannabinol	Cannabidiol
Dapsone	0.6	0.8
Aniline	1	1
p-Chloroaniline	2	2.5
p-Toluidine	2	2.5
Sulphadiazine	2	2
α-Naphthylamine	1	1
o-Aminobenzoic acid	1.5	1.5
p-Aminobenzoic acid	1	1
Fast Blue Salt B[3]	0.01	0.01
HMBT[7]	2.5	2.5

CBN, a yellow spot corresponding to CBD and another yellow spot of $\triangle^9$-THC, which was confirmed by recording its UV spectra. The UV absorpion maximum for $\triangle^9$-THC was in good agreement with reported values (277 and 282 nm)[10]. This also shows that cannabinoids are well separated using either of the solvent systems. The R_F values of $\triangle^9$-THC were confirmed by mixed spotting with control CBN and CBD samples. The colour of the spots was stable for several days. The reagent can be used in routine analysis owing to its high sensitivity (0.6 µg for CBN and 0.8 µg for CBD).

Other diazotized arylamines such as aniline, p-chloroaniline, p-toluidine, α-naphthylamine, amino-substituted benzoic acids and sulphadiazine were also tried as detection reagents. All diazotized arylamines except α-naphthylamine gave the coloured spots for cannabinoids as given with dapsone. Diazotized α-naphthylamine followed by a 0.1% aqueous sodium carbonate spray gave a reddish brown colour with CBN and a yellow colour with CBD and $\triangle^9$-THC. To reveal and intensify the coloured spots it is essential to spray the reagent followed by 0.1% aqueous sodium carbonate for completion of coupling, as described by Feigl[11]. However, with dapsone, p-aminobenzoic acid and sulphadiazine the 0.1% sodium carbonate spray does not increase the sensitivity of reagent.

Table II shows that the minimum detectable amounts of CBN and CBD for all the reagents used and that reported for HMBT[7] are higher than those obtained with dapsone. Some of the arylamines used are carcinogenic and/or expensive. Dapsone is a cheap, readily available pharmaceutical preparation used as an antibacterial agent (leprostatic)[12].

It was observed that the colour of the CBN and CBD spots after spraying diazotized reagents such as aniline, p-chloroaniline and α-naphthylamine faded rapidly. No fading of the colours was observed for the other reagents studied. Diazotized dapsone was stable for a sufficient time. Among the arylamines used in this study, diazotized aniline has been used for the detection of sulpha drugs and phenols by TLC[13]. For the colorimetric determination of aniline, p-chloroaniline and dapsone they are diazotized and coupled with tetrahydrobenzoquinolinol, β-naphthol and p-aminophenol, respectively[14–16]. However, none of the reagents studied has been reported previously for the detection of cannabinoids.

Diazotized dapsone was also used to detect the alkali hydrolysis products of carbamate insecticides, such as baygon, carbaryl and carbofuran, at a level of 0.1 μg of each as red, violet and red spots, respectively. These insecticides are of interest in forensic toxicology.

REFERENCES

1 R. T. Coutts and G. R. Jones, *J. Forensic. Sci.*, 24 (1979) 291.
2 P. Duquenois and H. N. Mustapha, *Bull. Sci. Pharm.*, 45 (1938) 203.
3 F. Korte and H. Sieper, *J. Chromatogr.*, 13 (1964) 90.
4 N. V. R. Rao, *Curr. Sci.*, 46 (1977) 140.
5 M. J. De Faubert Maunder, *J. Chromatogr.*, 100 (1974) 196.
6 S. Z. Mobarak, D. Bieniek and F. Korte, *Forensic Sci.*, 11 (1978) 189.
7 T. R. Baggi, *J. Forensic Sci.*, 25 (1980) 691.
8 T. A. Gough and P. B. Baker, *J. Chromatogr. Sci.*, 20 (1982) 289.
9 I. L. Finar, *Organic Chemistry*, Vol. I, Longmans, Green, London, 1964, p. 622.
10 R. Mechoulam, *Marijuana: Chemistry, Pharmacology, Metabolism and Clinical Effects*, Academic Press, New York, 1973, p. 149.
11 F. Feigl, *Spot Tests in Organic Analysis*, Elsevier, Amsterdam, Oxford, New York, 7th ed., 1983, p. 143.
12 L. S. Goodman and A. Gilman, *The Pharmacological Basis of Therapeutics*, MacMillan, New York, 7th ed., 1985, p. 1212.
13 H. N. Katkar and V. P. Barve, *Indian J. Pharm.*, 37 (1975) 116.
14 V. Kratochvil and J. Kroupa, *Chem. Prum.*, 36 (1986) 465.
15 A. P. Arzamastsev, L. I. Kovalenko, D. M. Popov and A. A. Skuratovich, *Khim. Farm. Zh.*, 17 (1983) 247.
16 R. T. Sane, V. K. Shastri, P. G. Anaokar and V. G. Nayak, *Indian Drugs*, 19 (1982) 198.

CHROM. 20 954

Note

Comparison of sulphuric acid treatment and column chromatographic clean-up procedures for the gas chromatographic determination of organochlorine compounds in some food commodities

PARM PAL SINGH* and RAM PARKASH CHAWLA

Department of Entomology, Punjab Agricultural University, Ludhiana-141 004 (India)

(First received March 15th, 1988; revised manuscript received August 5th, 1988)

There is a worldwide concern over the presence of residues of organochlorine compounds in various components of the environment[1–3]. As the diet is the major route of exposure of the general public to chemical contaminants[4,5], the determination of these residues in foodstuffs is of major importance. The determination of organochlorine compounds in food samples involves solvent extraction, clean-up to remove extraneous substances, determination of residues by gas chromatography (GC) and confirmation of the nature of the contaminants[6–9]. Adsorption column chromatography, used to clean-up the extracts before GC determination in standard methods of pesticide residue analysis[8,9], is a major factor affecting the reproducibility of the overall analytical procedure[10]. Moreover, this technique is time consuming and requires large amounts of highly purified solvents and costly adsorbents. Hence there is a need for rapid and inexpensive clean-up techniques[11,12].

The treatment of light petroleum extracts of both fatty[13–17] and non-fatty foods[18] with sulphuric acid to remove co-extractives from acid-stable compounds has been suggested as a convenient alternative to column chromatographic clean-up. This paper reports the relative efficacy of these two clean-up procedures for the determination of organochlorine residues in food commodities.

EXPERIMENTAL

Gas chromatograph

A Packard Model 7624 equipped with a tritium source electron-capture detector and a 1.84 m × 2 mm I.D. glass column packed with 1.5% OV-17 + 1.95% OV-210 on 110–120-mesh Gas Chrom Q was used. The injection port temperature was 210°C, the column oven temperature 190°C and the detector temperature 200°C and the carrier gas was nitrogen at a flow-rate of 70 ml min^{-1}.

Reference standards

The α, β, γ and δ isomers of HCH (1,2,3,4,5,6-hexachlorocyclohexane), *p,p'*-DDT [1,1,1-trichloro-2,2-bis(4-chlorophenyl)ethane], *p,p'*-DDD [1,1-dichloro-2,2-bis(4-chlorophenyl)ethane] and *p,p'*-DDE [1,1-dichloro-2,2-bis(4-chlorophenyl)-ethene] of greater than 95% purity were obtained from the U.S. Environmental Protection Agency, Research Triangle Park, NC, U.S.A.

Reagents

Acetone, acetonitrile, anhydrous sodium sulphate, benzene, concentated sulphuric acid (sp. gr. 1.84), hexane (boiling range 67–70°C), methanol, silica gel (60–100 mesh) and sodium chloride was used. The suitability of the reagents for residue analysis was ensured by running reagent blanks.

Sample preparation

The amounts of various food items constiuting food groups of the total diet were determined by conducting a dietary survey (Table I). Representative amounts of constituents of each food group were processed according to local practice and their edible parts homogenized to obtain composite material.

TABLE I

CONSTITUTION OF FOOD COMPOSITES USED FOR RECOVERY STUDIES

Food composite	Composition*
Cereals	Wheat flour (79), rice (16), bread (5)
Pulses and legumes	French beans (25), black gram (25), green gram (25), soya beans (25)
Root vegetables	Potato (69), onion (23), carrot (8)
Non-root vegetables	Tomato (60), cauliflower (24), coriander leaves (6), gourd (6), green chillies (4)
Fruits	Mango (66), sapota (34)
Meat and eggs	Chicken (45), eggs (55)

* Figures in parentheses are percentage contributions of different food items in a food composite on a raw weight basis.

Fortification studies

Composites equivalent to 50 g fresh weight were fortified with various organochlorine compounds at the concentrations given in Table II. For calculating recoveries, background levels of residues in unfortified samples were subtracted from the values obtained for fortified samples. All analyses were carried out in duplicate.

Extraction and partitioning

Cereals, pulses, legumes, root vegetables and non-root vegetables. Composites equivalent to 50 g fresh weight were extracted twice with 100- and 50-ml portions of acetonitrile by blending for 3 min each time. The combined extracts were transferred into a separating funnel, diluted with 600 ml of 5% aqueous sodium chloride and partitioned with two 100-ml portions of hexane. The aqueous phase was discarded and the hexane phases were pooled, dried over anhydrous sodium sulphate and concentrated to about 10 ml.

Fruits. Composites representing 50 g fresh weight were extracted twice with 100- and 50-ml portions of acetonitrile–water (2:1, v/v) by blending for 3 min each time and processed further as described for cereals, etc.

Meat and eggs. Composites equivalent to 50 g fresh weight were extracted twice with 100- and 50-ml portions of hexane–acetone (2:1, v/v) by blending for 3 min each time. The combined extracts were transferred into a separating funnel and washed twice with 300-ml portions of 5% aqueous sodium chloride. The aqueous phases were discarded and the hexane layer was dried and concentrated as described for cereals, etc.

Clean-up

Sulphuric acid clean-up. To a concentrated hexane extract in a 25-ml separating funnel, sulphuric acid was added dropwise until the hexane phase became clear. The lower layer of acid was discarded and the upper phase was washed with two 10-ml portions of distilled water.

Column chromatographic clean-up. Silica gel washed with acetone–methanol (1:1, v/v) was air dried, activated at 130°C for 1 h and a 20-g portion was packed in a glass column (40 cm × 2 cm I.D.) between 1-cm layers of anhydrous sodium sulphate. The column was pre-washed with 100 ml of hexane and extracts from the extraction and partitioning step were added to it after concentration to about 2 ml. The column was eluted with 100 ml of hexane–benzene (1:1, v/v) and the eluate was concentrated to about 10 ml[19].

Determination of residues

Suitable aliquots of the cleaned-up extracts were injected onto the GC column to obtain peak heights of compounds of interest within the scale. The residues were identified and quantified by comparison of the retention times and peak heights of the sample chromatograms with those of standards run under identical conditions.

RESULTS AND DISCUSSION

The average recoveries for DDT derivatives and HCH isomers following sulphuric acid clean-up of samples belonging to various food groups ranged from 80.6 to 107.0% (Table II) and were satisfactory. The corresponding mean recoveries from the column chromatographic clean-up of cereals, pulses, legumes, root vegetables, non-root vegetables and fruit composite ranged from 71.8 to 112.4%. Considering that a latitude of 20–50% is considered permissible in trace analysis[20], these recoveries values are similar to those observed for acid clean-up. For the column chromatographic clean-up of meat and eggs composite, adequate recoveries (85.0–89.7%) of DDT derivatives were observed. However, low recoveries (47.5–58.7%) for HCH isomers, which eluted late during column chromatography, were obtained. This may be due to a decrease in the resolving power of the adsorbent owing to the lipids present in the extract of this fatty substrate.

Gas chromatograms of samples and reagent blanks cleaned up with sulphuric acid were generally found to be free from extraneous peaks (Fig. 1). For pulse, legume and non-root vegetable composites, a light green colour persisted after acid treatment. It did not produce interfering peaks but, considering that the presence of co-extractives could reduce the lifetime of the GC column and result in a decrease in detector sensitivity, attempts were made to remove it. Centrifugation at 2000 rpm for 20 min or allowing the acid-treated extracts to stand for about 12 h was found to result in sedimentation of the colouring matter.

Reagent blanks and sample extracts cleaned-up by column chromatography frequently gave noisy baselines and early eluting peaks that could interfere in the determination of HCH residues (Fig. 1). This was probably due to the accumulation of impurities from adsorbents and concentration of large volumes of solvents used for column elution. Stringent quality control therefore had to be maintained for the samples being analysed by column chromatographic clean-up to ensure that the solvents and reagents did not produce interferences.

TABLE II

AVERAGE AND RANGE OF RECOVERIES OF VARIOUS ORGANOCHLORINE COMPOUNDS FROM FORTIFIED SAMPLES OF DIFFERENT FOOD COMPOSITES

Compound	Level of fortification ($\mu g\ g^{-1}$)	Recovery (%)					
		Cereals		Pulses		Root vegetables	
		S^*	C^{**}	S^*	C^{**}	S^*	C^{**}
α-HCH	0.016	93.1 ± 2.9	82.5 ± 4.1	96.8 ± 1.8	78.1 ± 1.8	98.7 ± 1.0	82.1 ± 0.8
β-HCH	0.064	92.5 ± 1.8	106.2 ± 8.2	97.5 ± 1.0	85.1 ± 1.6	100.0 ± 0.0	74.2 ± 1.1
γ-HCH	0.016	91.9 ± 0.0	80.6 ± 4.3	80.6 ± 0.0	79.6 ± 2.4	93.1 ± 1.7	71.8 ± 0.5
δ-HCH	0.032	92.0 ± 2.1	100.5 ± 6.2	96.5 ± 1.5	82.1 ± 4.1	98.7 ± 0.2	90.5 ± 0.5
p,p'-DDE	0.02	99.0 ± 2.9	82.4 ± 2.1	99.1 ± 1.0	84.5 ± 1.7	89.4 ± 1.9	89.8 ± 3.2
p,p'-DDD	0.04	94.4 ± 2.4	103.1 ± 3.6	93.2 ± 2.2	80.0 ± 1.9	87.2 ± 0.8	93.2 ± 0.0
p,p'-DDT	0.04	95.6 ± 1.5	112.4 ± 4.3	94.5 ± 1.5	89.6 ± 2.2	95.5 ± 1.5	91.2 ± 2.0

* Sulphuric acid clean-up.
** Column chromatographic clean-up using silica gel as adsorbent.
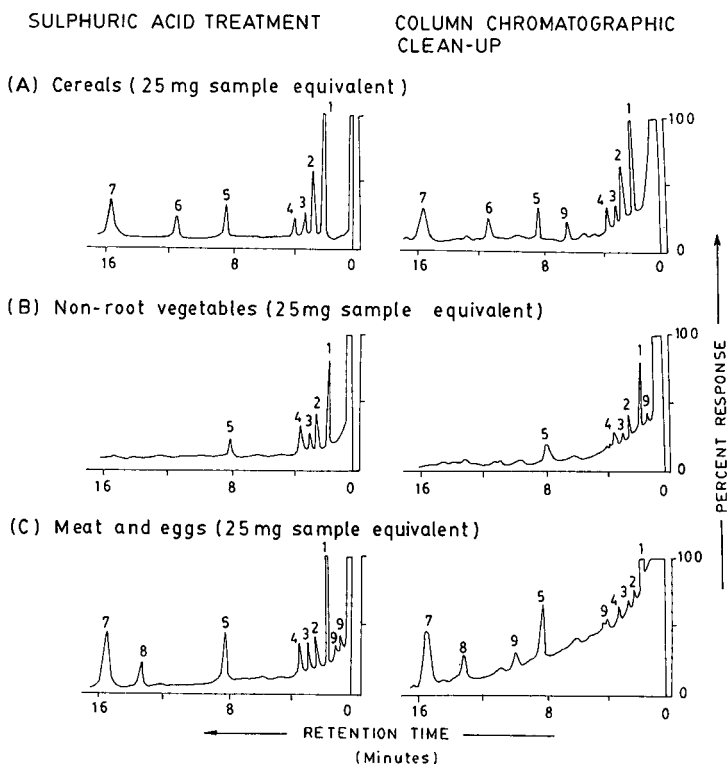
Fig. 1. Gas chromatograms of extracts of some unfortified food composites cleaned up by sulphuric acid treatment or the column chromatographic procedure. Peaks: 1 = α-HCH; 2 = γ-HCH; 3 = β-HCH; 4 = δ-HCH; 5 = p,p'-DDE; 6 = o,p'-DDT; 7 = p,p'-DDT; 8 = p,p'-DDD; 9 = unidentified.

Non-root vegetables		Fruits		Meat and eggs	
S^*	C^{**}	S^*	C^{**}	S^*	C^{**}
92.7 ± 0.1	80.7 ± 0.6	94.0 ± 2.5	83.6 ± 2.4	91.1 ± 5.2	49.7 ± 0.8
91.8 ± 2.8	84.4 ± 0.9	99.0 ± 1.1	82.1 ± 3.2	93.8 ± 4.2	56.7 ± 2.0
89.8 ± 2.1	81.2 ± 0.2	90.7 ± 2.1	87.4 ± 2.1	84.2 ± 0.9	47.5 ± 0.9
92.0 ± 3.5	86.3 ± 0.3	102.9 ± 1.1	81.0 ± 1.6	81.4 ± 2.3	52.6 ± 3.0
90.0 ± 3.2	81.8 ± 0.1	106.0 ± 1.0	82.4 ± 2.7	95.0 ± 3.0	86.4 ± 3.3
84.6 ± 1.6	85.0 ± 2.6	107.0 ± 1.0	84.6 ± 4.1	83.2 ± 3.0	85.7 ± 1.7
86.0 ± 2.8	84.4 ± 2.0	94.3 ± 3.3	88.4 ± 2.8	82.9 ± 1.5	85.0 ± 0.0

When residues are being determined by GC with electron-capture detection, confirmation of the identity of the peaks obtained is considered essential[6,8,9]. The extracts cleaned up with sulphuric acid were generally found suitable for micro-alkali derivatization[21] and thin-layer chromatographic (TLC)[22] confirmatory techniques. However, TLC of meat and eggs composites sometimes produced streaks, even though the GC analysis of such extracts did not show any co-extractives. Such behaviour of fatty foods has also been reported by McGill and Robinson[23], who attributed it to the probability that when an extract is injected into the GC system, less volatile co-extractives such as fats remain at the injection port and do not reach the detector to produce extraneous peaks. However, they interfere with the adsorption mechanism in TLC and cause streaking. Veierov and Aharonson[14] also observed that some lipid carryover or small amounts of undigested fats remain after acid treatment of extracts of fatty substrates.

In addition to the DDT derivatives and HCH isomers determined in this study, sulphuric acid clean-up has been reported to be applicable to other organochlorine residues such as aldrin, Aroclor 1254,α- and γ-chlordane, heptachlor, hexachlorobenzene (HCB) and o,p'-TDE[13]. However, sulphuric acid treatment allows the determination only of acid-stable compounds and column chromatographic clean-up has to be used if the determination of acid-labile compounds is required. For example, dieldrin, endosulfan A, B and sulphate, endrin and heptachlor epoxide are degraded by sulphuric acid and cannot be determined by this technique[13,24].

Recently Hernández et al.[25] evaluated the efficacy of sulphuric acid clean-up for the determination of 24 organochlorine compounds in wastewater samples. Four compounds (dichloran, dieldrin, endrin and trifluralin) were destroyed after treatment with this acid, whereas complete recoveries (90.3–118.6%) were obtained for sixteen organochlorine residues. Fenson and tetradifon were partially degraded by this treatment.

As sulphuric acid treatment clean-up is simple, rapid, efficient and requires less solvents and glassware, it is to be preferred to column chromatographic clean-up for the determination of acid-stable compounds in food products.

REFERENCES

1 H. Frehse and H. Geissbühler (Editors), *Pesticide Residues —A Contribution to Their Interpretation, Relevance and Legislation*, Pergamon Press, Oxford, 1979.
2 J. A. R. Bates, *J. Sci. Food Agric.*, 30 (1979) 401.
3 J. Miyamoto and P. C. Kearney (Editors), *Pesticide Chemistry: Human Welfare and the Environment*, Vol. 4, Pergamon Press, Oxford, 1983.
4 J. P. Frawley and R. E. Duggan, in H. Geissbühler, G. T. Brooks and P. C. Kearney (Editors), *Advances in Pesticide Science*, Vol. 3, Pergamon Press, Oxford, 1979, p. 82.
5 W. J. Hayes, Jr., *Toxicology of Pesticides*, Williams and Wilkins, Baltimore, 1975.
6 J. H. Ruzicka, in C. A. Edwards (Editor), *Environmental Pollution by Pesticides*, Plenum Press, London, 1973, p. 11.
7 H. Rohleder and S. Gorbach, in J. Miyamoto and P. C. Kearney (Editors), *Pesticide Chemistry: Human Welfare and the Environment*, Vol. 4, Pergamon Press, Oxford, 1983, p. 43.
8 Food and Drug Administration, *Pesticide Analytical Manual*, Vol. I, U.S. Department of Health, Education and Welfare, Washington, DC, 1977, Ch. 2.
9 W. Horwitz (Editor), *Official Methods of Analysis of the Association of Official Analytical Chemists*, Association of Official Analytical Chemists, Washington, DC, 1980, Section 20.015.
10 J. Lantos, A. Ambrus and E. Visi, in J. Miyamoto and P. C. Kearney (Editors), *Pesticide Chemistry: Human Welfare and the Environment*, Vol. 4, Pergamon Press, Oxford, 1983, p.129.
11 W. P. McKinley, *J. Assoc. Off. Anal. Chem.*, 63 (1980) 158.
12 H. P. Thier, in J. Miyamoto and P. C. Kearney (Editors), *Pesticide Chemistry: Human Welfare and the Environment*, Vol. 4, Pergamon Press, Oxford, 1983, p. 89.
13 D. Veierov and N. Aharonson, *J. Assoc. Off. Anal. Chem.*, 61 (1978) 253.
14 D. Veierov and N. Aharonson, *J. Assoc. Off. Anal. Chem.*, 63 (1980) 202.
15 D. Veierov and N. Aharonson, *J. Assoc. Off. Anal. Chem.*, 63 (1980) 532.
16 R. S. Battu, R. P. Chawla and R. L. Kalra, *Indian J. Ecol.*, 7 (1980) 1.
17 S. K. Kapoor, R. P. Chawla and R. L. Kalra, *J. Assoc. Off. Anal. Chem.*, 64 (1981) 14.
18 P. P. Singh and R. P. Chawla, *Talanta*, 29 (1982) 231.
19 R. L. Kalra and R. P. Chawla, *Studies on Pesticide Residues and Monitoring of Pesticidal Pollution*, Department of Entomology, Punjab Agricultural University, Ludhiana, 1983, p. 101.
20 F. A. Gunther, *Residue Rev.*, 76 (1980) 155.
21 R. R. Watts (Editor), *Analysis of Pesticide Residues in Human and Environmental Samples*, Environmental Protection Agency, Research Triangle Park, NC, 1980, Section 12 D(1).
22 D. C. Abbott, J. O'G. Tatton and N. F. Wood, *J. Chromatogr.*, 42 (1969) 83.
23 A. E. J. McGill and J. Robinson, *Food Cosmet. Toxicol.*, 6 (1968) 45.
24 R. P. Chawla and A. K. Kakkar, *J. Food Sci. Technol.*, 18 (1981) 152.
25 F. H. Hernández, F. J. López, J. M. Escriche and J. C. B. Ubeda, *J. Assoc. Off. Anal. Chem.*, 70 (1987) 727.

CHROM. 21 022

Note

Horizontal flow-through coil planet centrifuge equipped with a set of multilayer coils around the column holder

Counter-current chromatography of proteins with a polymer-phase system

YOICHIRO ITO* and HISAO OKA*

Laboratory of Technical Development, National Heart, Lung, and Blood Institute, National Institutes of Health, Building 10, Room 5D12, Bethesda, MD 20892 (U.S.A.)

(First received July 12th, 1988; revised manuscript received October 3rd, 1988)

During the preceding decade, the horizontal flow-through coil planet centrifuge has been introduced for performing preparative counter-current chromatography (CCC)[1,2]. The apparatus holds a coil assembly around the column holder which undergoes synchronous planetary motion to provide efficient mixing of the two solvent phases in the coil. Because the system permits stable retention of low-interfacial-tension two-phase solvent systems, the apparatus has been extensively used for separations of peptides and other polar compounds with hydrophilic butanol solvent systems[3]. The partition efficiency of the original apparatus, however, is largely limited by its long coil assembly (50 cm), which tends to be deformed under a strong centrifugal force field, thus the maximum revolutional speed which can be applied safely is 400 rpm. Recently, the design of the apparatus has been improved by shortening the column holder shaft to about one-third (18 cm) while the column capacity was almost recovered by doubling the layer of coil in each column unit. Using conventional butanol two-phase solvent systems, the capability of the apparatus has been demonstrated by efficient chromatographic separations of dipeptides and partition of bovine insulin at a high revolutional speed of 800 rpm[4].

The present paper describes a new design of the column assembly which consists of a set of multilayer coils symmetrically arranged around the holder shaft to double the column capacity. The capability of the present apparatus was demonstrated in protein separation with an aqueous–aqueous polymer two-phase system.

EXPERIMENTAL

Apparatus

Fig. 1 shows a photograph of the apparatus. The overall design of the apparatus was described previously[4,5]. The rotary frame of the apparatus holds a column holder and a counterweight holder diametrically at a distance of 10 cm from the

---

* Visiting scientist from the Aichi Prefectural Institute of Public Health, Nagoya, Japan.
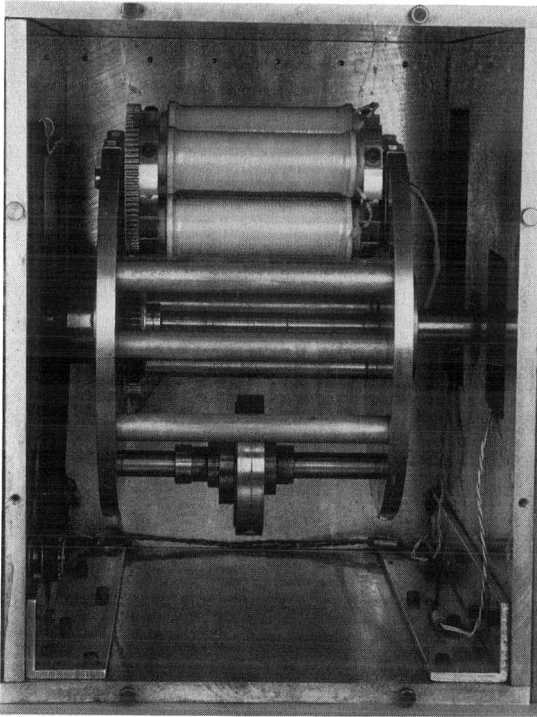
Fig. 1. Photograph of the present apparatus. The apparatus holds a set of multilayer coil separation columns connected in series while the mechanical balance of the centrifuge system is maintained with a counterweight placed in the opposite side of the rotary frame. The desired planetary motion of the holder is effected by coupling the planetary gear on the column holder shaft to an identical stationary sun gear mounted on the central stationary shaft. Temperature of the unit can be regulated up to 50°C with a set of electric heating pads and a temperature control unit.

central axis of the centrifuge. Engagement of the planetary gear, mounted on the holder shaft, to an identical stationary sun gear on the central axis of the apparatus produces a desired planetary motion of the holders, *i.e.*, revolution of the holder around the central axis of the apparatus and simultaneous rotation of the holder about its own axis at the same angular velocity in the same direction.

The column holder is removable from the rotary frame by loosening a pair of screws on each bearing block. The holder accommodates four identical multilayer coils symmetrically around the holder shaft. Each multilayer coil was prepared from an approximately 25 m length of 1.6 mm I.D. polytetrafluoroethylene (PTFE) tubing (Zeus Industrial Products, Raritan, NJ, U.S.A.) by winding it onto a spool-shaped holder hub, measuring 12.5 cm in length and 1.25 cm in diameter, making 6 layers of tightly wound coil. In order to secure the multilayer coil against the holder, the entire column and the flanges were covered with a heat-shrinkable poly(vinyl chloride) tube which was tempered by a heat gun. Four identical multilayer coils were symmetrically mounted around the holder shaft at a distance of 3.5 cm from the holder axis. Using short pieces of PTFE tubing (2 mm O.D.), these four columns were connected in series in such a way that the external terminal of the first column was connected to the

internal terminal of the second column, the external terminal of the second column to the internal terminal of the third, and so forth. The total capacity of the entire column measured about 200 ml. A pair of flow tubes from the column was first led through the center hole of the holder shaft and then passed through the side hole of the short coupling pipe to enter the opening of the central stationary pipe. At the exit of the centrifuge, they are securely clamped with the tube support. As described elsewhere, these flow tubes are free from twisting and serve for continuous elution through the rotating column without the use of the conventional rotary seal device[1].

The revolutional speed of the apparatus can be regulated up to 800 rpm with a speed control unit (Bodine Electric, Chicago, IL, U.S.A.). The present apparatus is also equipped with a column-temperature control system which regulates the ambient temperature from room temperature to 50°C with a set of electric heating pads and a temperature control unit (RFL, Boonton, NJ, U.S.A.).

Procedure

The aqueous–aqueous two-phase polymer system was prepared by dissolving 150 g of polyethylene glycol 1000 (Sigma, St. Louis, MO, U.S.A.) and 150 g of anhydrous dibasic potassium phosphate (J. T. Baker, Phillipsburg, NJ, U.S.A.) in 900 ml of distilled water. The solvent mixture was thoroughly equilibrated in a separatory funnel at room temperature and the two phases separated shortly before use. The sample solution consisted of 100 mg of each cytochrome *c* and lysozyme (both from Sigma) dissolved in 3 ml of the above solvent system.

The experiment was initiated by filling the entire column with the stationary upper phase. This was followed by sample injection through the sample port. Then, the apparatus was rotated at 800 rpm while the mobile lower phase was eluted through the column at a flow-rate of 0.5 ml/min or 1.0 ml/min. The effluent from the outlet of the column was continuously monitored with an LKB Uvicord S at 275 nm and then fractionated into test tubes at 3 ml/tube with an LKB fraction collector. After the two peaks were eluted, the apparatus was stopped and the column contents were collected into a graduated cylinder to measure the volume of the stationary phase retained in the column. An aliquot of each fraction was diluted with distilled water and the absorbance was determined with a Zeiss PM6 spectrophotometer at 280 nm and 550 nm (for cytochrome *c*) to draw a chromatogram.

RESULTS AND DISCUSSION

Fig. 2 shows a chromatogram of cytochrome *c* and lysozyme obtained with the aqueous–aqueous polymer-phase system composed of 12.5% (w/w) polyethylene glycol 1000 and 12.5% (w/w) anhydrous dibasic potassium phosphate in distilled water. The fractions containing cytochrome *c* peak were easily identified by their color and quantitated by its absorbance measured at 550 nm as indicated by the broken curve. At a flow-rate of 1.0 ml/min, the two peaks were completely resolved in 5 h. The partition efficiency may be calculated from the chromatogram according to the conventional gas chromatographic formula, *i.e.*, $N = (4t_R/W)^2$, where N denotes the partition efficiency expressed in terms of theoretical plate number; t_R, the retention time of the peak maximum; and W, the peak width expressed in the same unit as t_R. Using the above formula, the partition efficiency computed from the second peak was
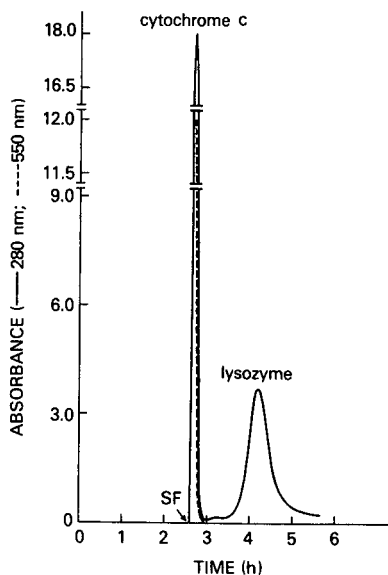
Fig. 2. Separation of cytochrome *c* and lysozyme with the aqueous–aqueous two-phase system composed of 12.5% (w/w) polyethylene glycol 1000 and 12.5% (w/w) anhydrous dibasic potassium phosphate in distilled water. Sample size: each component 100 mg; flow-rate: 1 ml/min; mobile phase: lower phase; revolution: 800 rpm. SF = Solvent front.

about 350 theoretical plates. The retention of the stationary phase was 26% of the total column capacity and the maximum column pressure measured at the outlet of the pump was 170 p.s.i. Application of a lower flow-rate of 0.5 ml/min substantially improved the peak resolution but with a longer elution time of 10 h.

Among various separation methods, the liquid–liquid two-phase partition method with polymer-phase systems is particularly suitable for separations of biopolymers and cell particles, because of its gentle separation procedure with a non-hostile environment provided by the media. However, high viscosity and low interfacial tension between the two phases tend to delay the phase settling, resulting in long separation times. Although various centrifuge devices[6–10] have been introduced to overcome this problem, high cost of these instruments generally prevents universal use of the method.

The present method yields a high partition efficiency in relatively short separation times (1 theoretical plate is produced in less than 30 s), while the apparatus is simple in design and relatively inexpensive. The method may be applied to various other biopolymers and cell particles by choosing the proper phase composition. We believe that the present method will be extremely useful for separation of various biological samples.

REFERENCES

1 Y. Ito and R. L. Bowman, *Anal. Biochem.*, 82 (1977) 63.
2 Y. Ito and R. L. Bowman, *J. Chromatogr.*, 147 (1978) 221.
3 M. Knight, in N. B. Mandava and Y. Ito (Editors), *Countercurrent Chromatography – Theory and Practice*, Marcel Dekker, New York, 1988, Ch. 10, p. 583.

4 J. L. Sandlin and Y. Ito, *J. Liq. Chromatogr.*, 11 (1988) 55.
5 Y. Ito, *J. Chromatogr.*, 207 (1981) 161.
6 Y. Ito, G. T. Bramblett, R. Bhatnagar, M. Huberman, L. Leive, L. M. Cullinane and W. Groves, *Sep. Sci. Technol.*, 18 (1983) 33.
7 I. A. Sutherland and Y. Ito, *Anal. Biochem.*, 108 (1980) 367.
8 H.-E. Akerlund, *J. Biochem. Biophys. Methods*, 9 (1984) 133.
9 W. Murayama, T. Kobayashi, Y. Kosuge, H. Yano, Y. Nunogaki and K. Nunogaki, *J. Chromatogr.*, 239 (1982) 643.
10 Y. Ito and T. Y. Zhang, *J. Chromatogr.*, 437 (1988) 121.

Note

Determination of ethylenethiourea in beverages without sample pretreatment using high-performance liquid chromatography and amperometric detection on a copper electrode

HEPING WANG*, VĚRA PACÁKOVÁ and KAREL ŠTULÍK*

Department of Analytical Chemistry, Charles University, Albertov 2030, 128 40 Prague 2 (Czechoslovakia)

(Received September 10th, 1988)

Ethylenethiourea (ETU) is important as a degradation product of the widely employed ethylenebis(dithiocarbamate) fungicides. Whereas the fungicides themselves are not highly toxic, ETU poses a substantially higher risk to human health and has been found to be mutagenic and teratogenic in rats[1–8]. The formation of ETU in foodstuffs is greatly enhanced by their thermal treatment[9,10]. Moreover, ETU is also produced in humans through metabolism of the fungicides inhaled or absorbed through the skin[11]. Therefore, there is considerable interest in the routine determination of low concentrations of ETU in a wide variety of samples that are mostly characterized by highly complex matrices.

Paper[12] and thin-layer[13–16] chromatographic methods are simple but necessarily insufficiently sensitive and only semiquantitative. Gas chromatography[6,9,10,15,17–20] is sufficiently sensitive and selective, but requires derivatization and positive errors are often caused by thermal degradation of the parent fungicides and some matrix components during analysis[21]. High-performance liquid chromatography (HPLC) is considered to be the most suitable method for these analyses[22].

When UV photometric detection is used in HPLC, at 240 nm[10,22,23], 233 nm[24], 254 or 264 nm[25,26], complicated sample pretreatment involving, *e.g.*, extraction and adsorption chromatography, is usually required for suppression of interferences and analyte preconcentration. The sample pretreatment is simplified and the limit of detection lowered when ETU is detected amperometrically, employing its oxidation at a glassy carbon electrode[11,25]. A further improvement in the selectivity is achieved when ETU is detected at a dropping mercury electrode using the complex formation between mercury(II) ions and ETU[25,26], but the limit of detection is higher than in detection on a glassy carbon electrode[25].

Amperometric detection on a passivated copper electrode combines the advantages of the high sensitivity of solid electrode measurement and the selectivity of the complexation reaction between the analyte and copper(II) ions[27,28]. Therefore, we utilized this approach for the HPLC determination of ETU in some beverages without any sample pretreatment.

---

* On leave from the Iron and Steel Institute, Beijing, China.

EXPERIMENTAL

Apparatus

A HPP 5001 high-pressure pump, an ADLC 1 electrochemical detector (Laboratorní Přístroje, Czechoslovakia) with a tubular copper working electrode[29], a silver–silver chloride reference electrode and a stainless-steel counter electrode and a Rheodyne 7125 injector with 20- and 200-μl loops were used. The copper electrode was activated in the mobile phase at -0.3 V for 15 min and then maintained at a working potential of $+0.15$ V (*vs.* Ag/AgCl).

Two column types were used: (a) a glass column (150 $\times$ 4 mm I.D.) packed with Separon SIG C_{18} reversed phase (7 μm) and (b) a stainless-steel column (80 $\times$ 8 mm I.D.) with Separon HEMA Bio-1000 DEAE weakly basic anion exchanger (7 μm) (both from Tessek, Czechoslovakia).

Chemicals

All chemicals used were of analytical-reagent grade, obtained from Lachema (Czechoslovakia), except for ethylenethiourea (ETU), which was obtained from Fluka (Switzerland).

The mobile phases were (A) 0.025 M aqueous phosphate buffer (pH 7.0), (B) 0.02 M aqueous acetate buffer (pH 7.3), (C) 0.04 M aqueous acetate buffer (pH 7.3) and (D) 0.02 M aqueous acetate buffer (pH 7.3)–methanol (85:15).

The flow-rate was 0.3 ml min^{-1}. The mobile phases were degassed in an ultrasonic bath and by passage of helium.

Stock solutions of ETU were prepared by dissolving an appropriate amount of ETU in a given mobile phase or in the sample matrix and were stored in a refrigerator. The stock solutions were diluted before measurement.

The test samples included Müller Thurgau white wine from Mikulov, Czechoslovakia, Pilsner Urquell lager beer and Florida peach and orange juice. The juice was filtered before injection. All the experiments were carried out at laboratory temperature (20 $\pm$ 2°C).

RESULTS AND DISCUSSION

In optimizing the experimental conditions for the separation of ETU from the other components of wine, beer and juice samples, the specific properties of amperometric detection on a copper electrode[27–29] must be considered. As the detection mechanism involves complex formation between the analyte and the copper (II) ions contained in the porous passive layer on the electrode, the pH of the mobile phase should not be lower than *ca.* 6; further, the composition of the buffer solution is important (phosphate or acetate buffers are preferable) and the content of any organic modifier should be low in order to attain a high detection sensitivity.

First, we tested the determination in a reversed-phase system that has been commonly employed for the purpose, using a C_{18} stationary phase. However, with the mobile phases A–D, which meet the requirements of amperometric detection on a copper electrode, the retention times of ETU are too short (2–3 min) and the separation from the matrix components is poor.

We therefore investigated the weakly basic anion exchanger Separon HEMA

Bio-1000 DEAE, based on a hydroxymethylmethacrylate matrix. The retention times of ETU were then around 14 min for mobile phases A–C. The detection was about twice as sensitive in the phosphate buffer than in the acetate buffer, but the determination of ETU in phosphate buffer was disturbed by substances present in the matrix that elute simultaneously with ETU. In subsequent work we therefore used the acetate buffer and studied the effect of an increased salt concentration (mobile phases B and C) and the presence of methanol (mobile phases B and D). An increase in the acetate concentration from 0.02 to 0.04 M caused no change in the retention time of ETU; addition of methanol led to a decrease in the retention time of ETU (7 min), but the separation efficiency simultaneously decreased. In agreement with our previous results[28], the detector response decreased with increasing flow-rate of the mobile phase (by *ca.* 20% for an increase from 0.3 to 0.5 ml min^{-1}). All the subsequent measurements were therefore carried out in the purely aqueous 0.02 M acetate mobile phase of pH 7.3 at a flow-rate of 0.3 ml min^{-1}. Under these conditions, ETU can be determined directly in wine, beer and soft drinks.

The UV absorption maximum of ETU lies at 224 nm. Most substances present in the test samples also absorb radiation around this wavelength, and hence the determination of ETU is impossible without prepurification of the sample. On the other hand, amperometric detection with a copper electrode is highly selective and permits the direct injection of the samples into the chromatographic system.

Determinations of ETU in wine and beer are illustrated in Fig. 1. A further advantage of this detection method is that the parent diethyldithiocarbamate fungicides (*e.g.*, Mancozeb) do not give detector response.

The parameters of the calibration dependence for ETU were obtained. The detection is very sensitive and the limit of detection, defined as the signal equal to twice the peak-to-peak noise value, is 0.4 ng of ETU in the injected volume of 20 μl. The linear dynamic range extends over three orders of magnitude of ETU concentration, from 0.4 to 1500 ng, with a correlation coefficient of 0.9996. The above limit of
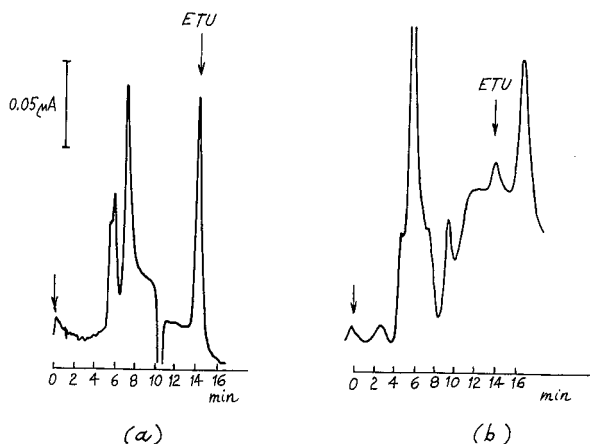
Fig. 1. Chromatograms of (a) wine and (b) beer spiked with ETU. Amount of ETU added: (a) 0.85 μg/ml; (b) 0.10 μg/ml. The Separon HEMA Bio-1000 DEAE column was used with mobile phase B at a flow-rate of 0.3 ml/min.

TABLE I

RESULTS OF THE DETERMINATION OF THE ETU IN WINE AND BEER

Results are means of seven replicate determinations.

Matrix	ETU concentration		Relative standard deviation (%)
	Added (µg/ml)	Found (µg/ml)	
Wine	0.10	0.09 ± 0.005	5.5
	0.70	0.69 ± 0.02	2.9
Beer	0.10	0.095 ± 0.005	5.2
	0.70	0.695 ± 0.002	2.9

detection corresponds to 20 ng/ml of the sample, and can be further decreased by injecting larger volumes. With injection of a 200-µl volume, the limit of detection decreases to *ca.* 3 ng/ml (of course, the injection of a ten times greater sample volume leads to a greater dispersion, so that the plate number of 47 800 per metre for a 20-µl sample decreases to 8640 per metre for a 200-µl sample).

The test samples of beer, wine and juice did not contain measurable amount of ETU, so we added measured amounts of ETU to them and determined the precision of the determination from repeated analyses of the spiked samples. The results are given in Table I. It can be seen that the method is applicable to the direct determination of low ETU concentrations in wine, beer and soft drinks without sample pretreatment.

REFERENCES

1 S. L. Graham, W. H. Hansen, K. J. Davis and C. H. Perry, *J. Agric. Food Chem.*, 21 (1973) 324.
2 S. L. Graham, K. L. Daves, W. H. Hansen and C. H. Graham, *Food Cosmet. Toxicol.*, 113 (1975) 493.
3 J. A. Ruddick and K. S. Khera, *Teratology*, 12 (1975) 277.
4 J. A. Ruddick, W. H. Newsome and L. Nash, *Teratology*, 13 (1976) 263.
5 J. H. Onley, L. Giuffrida, N. F. Ives, R. R. Watts and R. W. Storherr, *J. Assoc. Off. Anal. Chem.*, 60 (1977) 1105.
6 J. H. Onley, *J. Assoc. Off. Anal. Chem.*, 60 (1977) 1111.
7 K. S. Khera and F. Iverson, *Teratology*, 18 (1978) 311.
8 W. M. O'Neill and W. D. Marshall, *Pestic. Biochem. Physiol.*, 21 (1984) 92.
9 J. Hajšlová, V. Kocourek, Z. Jehličková and J. Davídek, *Z. Lebensm. Unters. Forsch.*, 183 (1986) 348.
10 V. Kocourek and I. Zemanová, *Potravin. Vědy*, (1987) 279.
11 J. L. Prince, *J. Agric. Food Chem.*, 33 (1985) 93.
12 E. I. Johnson and J. F. C. Tyler, *Chem. Ind. (London)*, (1962) 304.
13 L. Fishbein and J. Fawkes, *J. Chromatogr.*, 19 (1965) 364.
14 G. Czeglédi-Jankó and A. Hollo, *J. Chromatogr.*, 31 (1967) 89.
15 J. H. Onley and G. Yip, *J. Assoc. Off. Anal. Chem.*, 54 (1971) 165.

16 M. B. Devanii, C. J. Shishoo and B. K. Dadia, *J. Chromatogr.*, 105 (1975) 186.
17 W. H. Newsome, *J. Agric. Food Chem.*, 20 (1972) 967.
18 R. G. Nash, *J. Assoc. Off. Anal. Chem.*, 57 (1974) 1015.
19 R. R. King, *J. Agric. Food Chem.*, 25 (1977) 73.
20 W. P. Cochrane, *J. Chromatogr. Sci.*, 17 (1979) 124.
21 D. S. Farrington, *Meded. Fac. Landbouwwet. Rijksuniv. Gent*, 44 (1979) 901.
22 D. S. Farrington and R. G. Hopkins, *Analyst (London)*, 104 (1979) 111.
23 H. Kobayashi, O. Matano and S. Goto, *J. Chromatogr.*, 207 (1981) 281.
24 J.-C. Van Damme, M. Galoux and J. Verdier, *J. Chromatogr.*, 206 (1981) 125.
25 H. B. Hanekamp, P. Bos and R. W. Frei, *J. Chromatogr.*, 186 (1979) 489.
26 J. F. Lawrence, F. Iverson, H. B. Hanekamp, P. Bos and R. W. Frei, *J. Chromatogr.*, 212 (1981) 245.
27 W. Th. Kok, H. B. Hanekamp, P. Bos and R. W. Frei, *Anal. Chim. Acta*, 142 (1982) 31.
28 K. Štulík, V. Pacáková, Kang Le and B. Hennissen, *Talanta*, 35 (1988) 455.
29 K. Štulík, V. Pacáková, M. Weingart and M. Podolák, *J. Chromatogr.*, 367 (1986) 311.

Note

Simultaneous determination of niacin and niacinamide in meats by high-performance liquid chromatography

TAKASHI HAMANO*, YUKIMASA MITSUHASHI, NOBUMI AOKI and SUSUMU YAMAMOTO

Public Health Research Institute of Kobe City, Minatozimanaka-machi 4-6, Chuo-ku, Kobe 650 (Japan)

and

YOSHIKIYO OJI

Faculty of Agriculture, Kone University, Rokkodai-cho 1-1, Nada-ku, Kobe 657 (Japan)

(First received June 2nd, 1988; revised manuscript received September 5th, 1988)

Niacin and niacinamide belong to the vitamin B group. They are widely distributed in living cells and exist mainly in bound forms as part of nicotinamide adenine dinucleotide. They also occur in free form and are used as colour fixatives to develop and maintain a fresh colour in meats[1]. However, because high intakes of niacin from treated meats cause hyperaemia symptoms in humans, *i.e.*, red, flushed, itchy skin and headaches, such uses of niacin and niacinamide have been prohibited in Japan since 1982. Hence, the levels of niacin and niacinamide in meats are of concern to health authorities.

The conventional method for the assay of total niacin and niacinamide involves spectrophotometry after hydrolysis and derivatization (König reaction)[2]. However, this method suffers from several drawbacks: niacin and niacinamide are not distinguished, sample workup is tedious and the reagents used are noxious and unstable. Since the advent of high-performance liquid chromatography (HPLC) in the 1970s, in a number of studies this technique has been applied for the determination of niacin and/or niacinamide in pharmaceuticals[3], biological fluids[4] and foodstuffs[5-7]. Whereas the determination of niacin or niacinamide in food samples was achievable using different chromatographic conditions[6,7], their simultaneous determination by HPLC was difficult owing to the different polarities of the two vitamins and/or accompanying interfering substances in the sample extract.

The aim of this study was to introduce a convenient and reliable method for the determination of niacin and niacinamide. This paper deals with the simple extraction of meats and suitable chromatographic conditions for the simultaneous detection of niacin and niacinamide.

EXPERIMENTAL

Apparatus and conditions

The HPLC apparatus consisted of a Model 3A liquid chromatograph (Shimadzu, Japan) with a 20-μl loop injector (Rheodyne Model 7125), a Shimadzu UV detector set

at 260 nm and a data processor (Shimadzu Model C-R3A). The chromatographic separation was carried out using a 25 cm × 4.6 mm I.D. cation-exchange column (Partisil SCX, 10 μm) (Sumitomo, Japan). The flow-rate of the mobile phase (50 mM phosphate buffer, pH 3.0) was 1.0 ml/min. Separations were performed at ambient temperature (25°C).

Reagents

Niacin and niacinamide were obtained from Wako (Osaka, Japan). They were of the highest purity available and were not further purified. Ultrapure HPLC water was generated by a Milli-RO4 coupled to a Milli-Q water purification system (Millipore, Bedford, MA, U.S.A.). Stock solutions of niacin and niacinamide (1 mg/ml each) were prepared in ultrapure water. A mixed working standard solution was prepared by diluting the stock solution to give 5–50 μg/ml of each vitamin in ultrapure water. This solution was prepared freshly before use.

Procedure

A 5-g meat sample was weighed accurately into a 50-ml test-tube and about 30 ml of deionized water were added. The sample was homogenized using a Polytron blender (Model PT 20; Brinkmann, Westbury, NY, U.S.A.) for 1 min at maximum speed. The solution was boiled gently for 10 min, cooled, diluted to 50 ml with deionized water, allowed to stand briefly and the supernatant liquid filtered through 0.45-μm filter. The filtrate was subjected to HPLC analysis as described below.

HPLC analysis

A portion (10 μl) of the filtrate was injected into the HPLC system and the eluent was detected at 260 nm. The peak heights of niacin and niacinamide were measured and the concentration of each vitamin in the sample was determined from a calibration graph obtained with a working standard.

RESULTS AND DISCUSSION

Conditions for HPLC analysis

Takatsuki *et al.*[6] reported that reversed-phase chromatography is convenient for the routine determination of niacin and niacinamide in meats. However, different

TABLE I

EFFECT OF pH OF PHOSPHATE BUFFER ON THE RETENTION TIMES OF NIACIN, NIACINAMIDE, ASCORBIC ACID AND SORBIC ACID

pH^*	Retention time (min)			
	Niacin	Niacinamide	Sorbic acid	Ascorbic acid
6.0	3.66	7.02	3.80	2.92
5.0	4.26	7.22	4.77	3.05
4.0	4.69	8.26	5.70	3.09
3.0	5.49	10.3	7.30	3.22

* The pH of 50 mM phosphate buffer was adjusted with 0.1 M phosphoric acid.

chromatographic conditions are needed for the determination of each vitamin in the method reported. Hence the simultaneous detection of both vitamins was impossible by reversed-phase chromatography. We therefore attempted to make use of cation-exchange chromatography[8] for their simultaneous detection.

Table I shows the effect of the pH of the phosphate buffer on the retention times of niacin and niacinamide. Retention times of ascorbic acid and sorbic acid, which are commonly used additives in meat products, are also given in Table I.

Within the examined pH range (3–6), the lower the pH of the buffer the longer were the retention times of niacin and niacinamide, and also those of ascorbic acid and sorbic acid. In general, the best separation of the two vitamins from ascorbic acid and sorbic acid was achieved when 50 mM phosphate buffer (pH 3.0) was used.

Next, the effect of the concentration of the buffer (pH 3.0) on the retention times of the four compounds was evaluated in the range 10–100 mM. As was expected from the separation principle using ion-exchange column materials, the retention times of all four comoounds decreased with increasing concentration of the buffer. A concentration of 50 mM was a compromise between the speed of analysis and the best separation of the compounds.

Fig. 1 shows a typical chromatogram obtained for the four compounds under the
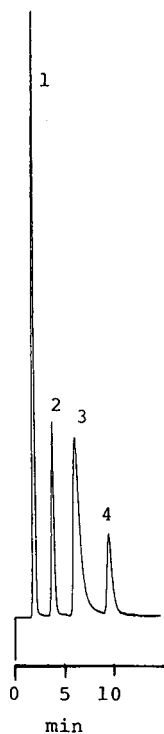
Fig. 1. Chromatogram of two vitamins and two additives. Conditions: Partisil SCX column (25 cm × 4.6 mm I.D.); mobile phase, phosphate buffer (50 mM, pH 3.0); flow-rate, 1 ml/min; detection, UV at 260 nm. Peaks: 1 = ascorbic acid; 2 = niacin; 3 = sorbic acid; 4 = niacinamide. Concentration of each compound, 2 μg/ml.

TABLE II

AMOUNTS OF NIACIN AND NIACINAMIDE PRESENT IN MEAT SAMPLES AND RECOVERIES

Recoveries were determined in triplicate. N.D. = Not detected.

Sample	Niacin				Niacinamide			
	Amount present (µg/g)	Amount added (µg/g)	Amount recovered (µg/g)	Recovery (%)	Amount present (µg/g)	Amount added (µg/g)	Amount recovered (µg/g)	Recovery (%)
Beef	N.D.	50	48.8	97.6	18.7	50	68.9	100.4
Pork ·	N.D.	50	48.2	96.4	32.1	50	81.5	98.8

conditions described under Experimental. Niacin and niacinamide were well separated from each other and from ascorbic acid and sorbic acid.

Linearity, repeatability and detection limit

Under the described chromatographic conditions, a rectilinear chromatographic response was demonstrated over at least a ten-fold range of concentration (5–50 µg/ml) for niacin and niacinamide. The relative standard deviations obtained for niacin and
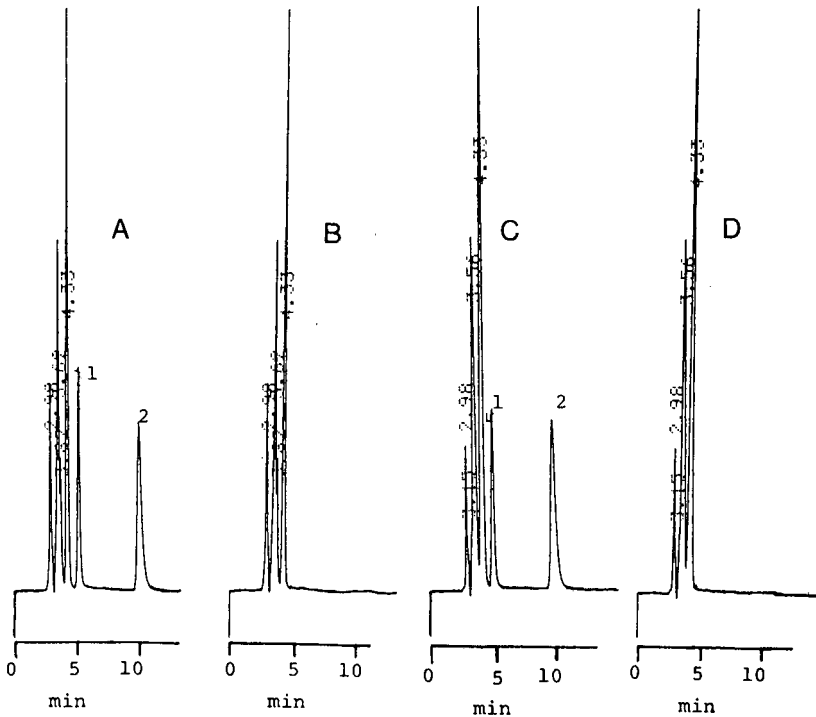
Fig. 2. Typical chromatograms obtained with samples of beef and pork using the proposed procedure. Conditions as in Fig. 1. (A) Extract from beef spiked with standards; (B) extract from blank beef; (C) extract from pork spiked with standards; (D) extract from blank pork. Peaks: 1 = niacin; 2 = niacinamide. Spiked levels of niacin and niacinamide, 50 µg/g each.

niacinamide based on four replicate analyses were 1.57 and 0.98%, respectively. The minimum detectable amounts of niacin and niacinamide determined at a signal-to-noise ratio of 3:1 were 2 and 4 ng per 10-μl injection, respectively.

Recovery studies and comparison with spectrophotometric analysis

Recovery studies were performed using beef and pork. To the weighed samples (5 g) in a 50-ml test-tube, 0.25 ml of each standard solution (1 mg/ml in water) of niacin and niacinamide was added and subjected to analysis as described under Experimental. In this way, potential losses occurring during the sample treatment procedure were assessed, together with interferences occurring during the chromatographic separation. The results are given in Table II and indicate that satisfactory recoveries were achieved for the samples tested.

Fig. 2A and C show typical chromatograms obtained with samples of beef and pork spiked with a standard mixture of niacin and niacinamide. Comparison of the chromatograms of blank samples (Fig. 2B and D) with those of the spiked samples clearly indicates that the system did not suffer from interferences from accompanying substances in the sample extracts.

Table III shows a comparison of the results for beef and pork using the proposed method and a standard spectrophotometric method[2]. The latter method gives the sum of the niacin and niacinamide contents. The agreement of the two methods was poor, and this situation persisted when the analysis was repeated several times. The recovery data given in Table II suggest that the lack of agreement between the two analytical procedures may be attributed to deficiencies in the spectrophotometric procedure. These deficiencies include such factors as a low specificity and the hydrolysis procedure for separating free niacin from complex molecules. In comparison, the proposed chromatographic method is rapid and precise.

Typical results obtained when using the proposed method for the routine examination of commercial beef and pork were as follows: none detected to 8.7 μg/g of niacin and none detected to 47.5 μg/g of niacinamide for twenty samples of beef; and none detected to 9.7 μg/g of niacin and none detected to 50.3 μg/g of niacinamide for

TABLE III

COMPARISON OF CHROMATOGRAPHIC AND SPECTROPHOTOMETRIC METHODS FOR THE DETERMINATION OF NIACIN AND NIACINAMIDE

N.D. = Not detected.

| Sample | Chromatographic method | | Spectrophotometric method: total niacin[*] (μg/g) |
	Niacin (μg/g)	Niacinamide (μg/g)	
Beef	N.D.	18.7	26.7
	N.D.	28.6	33.7
	8.3	40.6	52.3
Pork	N.D.	25.7	41.8
	N.D.	32.1	43.7
	7.9	38.3	63.9

[*] Sum of niacin and niacinamide.

ten samples of pork. These values were considered to be within the naturally occurring levels compared with the values reported in the literature[7].

In conclusion, the sumultaneous determination of free niacin and ciacinamide in meats can be reliably performed by HPLC using a cation-exchange column and successfully applied to the routine inspection of such samples.

REFERENCES

1 L. Bertling and J. Tietz, *Fleischwirtschaft*, 58 (1978) 621.
2 *Standard Methods for Hygienic Chemists*, Pharmaceutical Society of Japan, Tokyo, 3rd ed., 1980, p. 215.
3 F. Lam, I. J. Holcomb and S. A. Fusari, *J. Assoc. Off. Anal. Chem.*, 67 (1984) 1007.
4 Y. Tsuruta, K. Kohashi, S. Ishida and Y. Ohkura, *J. Chromatogr.*, 309 (1984) 309.
5 P. J. Niekerk, S. C. C. Smit, E. S. P. Strydom and G. Armbruster, *J. Agric. Food Chem.*, 32 (1984) 304.
6 K. Takatsuki, S. Suzuki, M. Sato, K. Sakai and I. Ushizawa, *J. Assoc. Off. Anal. Chem.*, 70 (1987) 698.
7 M. Oishi, E. Amakawa, T. Ogiwara, N. Taguchi, K. Onishi and M. Nishijima, *J. Food Hyg. Soc. Jpn.*, 29 (1988) 32.
8 R. C. Williams, D. R. Baker and J. A. Schmit, *J. Chromatogr. Sci.*, 11 (1973) 621.

CHROM. 20 973

Note

Determination of chlorine and chlorine dioxide in workplace air by impinger collection and ion-chromatographic analysis

EVA BJÖRKHOLM*, ANNIKA HULTMAN and JAN RUDLING

National Institute of Occupational Health, 171 84 Solna (Sweden)

(First received June 15th, 1988; revised manuscript received September 7th, 1988)

Chlorine and chlorine dioxide (ClO_2) can be encountered as individual compounds or as mixtures in many working environments such as pulp and textile bleaching and water disinfection. Both gases are known irritants to respiratory organs in very low concentrations. The standard for occupational exposure in Sweden is 0.5 ppm for Cl_2 and 0.1 ppm for ClO_2 as a time-weighted average (8 h). The short-term exposure limit (15 min) is 1.0 ppm for Cl_2 and 0.3 ppm for ClO_2. These values correspond well with standards used in European countries and in the U.S.A.

Most methods for determining Cl_2 and ClO_2 in workplace air are based on absorption in an impinger containing some form of redox indicator, followed by spectrophotometric analysis[1-3]. The estimation of low levels of both chlorine and chlorine dioxide requires two different absorption solutions[4], but since Cl_2 and ClO_2 contribute to the colour change in both of the reagent solutions, the absorption values must be corrected yielding lower accuracy. The chlorine that interferes with the analysis of ClO_2 can be removed by sulphaminic acid and sodium hydroxide[1].

One method employs the different reactions of chlorine and chlorine dioxide with potassium iodide in acidic and neutral media respectively[5]. The reactions are as follows:

Acidic medium:
$$Cl_2 + 2 I^- \rightleftarrows 2 Cl^- + I_2$$
$$2 ClO_2 + 10 I^- + 8 H^+ \rightleftarrows 2 Cl^- + 5 I_2 + 4 H_2O$$

Neutral medium:
$$Cl_2 + 2 I^- \rightleftarrows 2 Cl^- + I_2$$
$$2 ClO_2 + 2 I^- \rightleftarrows 2 ClO_2^- + I_2$$
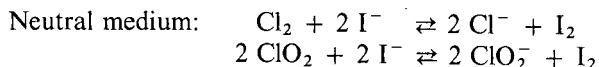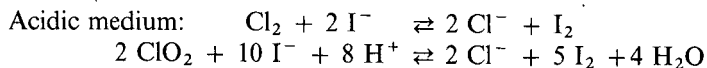
The absorption occurs in a neutrally buffered solution which is then acidified. The iodine liberated by the reaction reacts with N,N-dimethyl-*p*-phenylenediamine, and a coloured complex is formed which is then determined photometrically. This method is non-specific, being interfered with by other substances which oxidize iodide to iodine or reduce iodine to iodide. According to the reactions above, chlorine and chlorine dioxide are reduced in neutral potassium iodide solution to chloride and chlorite (ClO_2^-) ions respectively. This paper presents the possibility to separate and quantify the ions formed in one chromatographic experiment.

EXPERIMENTAL

Known levels of Cl_2 and ClO_2 were generated by diluting concentrated gas in air in a dynamic system. For Cl_2, a gas flask containing 1000 ppm of Cl_2 in nitrogen was used. The ClO_2 was generated by passing helium at 1 l/min over a solution of ClO_2 in water at 13°C (prepared according to ref. 6) in a dark glass bottle. Different concentrations of ClO_2 were obtained by varying the concentration of the solution (vapour pressure of ClO_2) and by changing the diffusion path of the gas by varying the volume of the solution in the bottle. The amount of ClO_2 emitted from the bottle was calculated from the difference shown by thiosulphate titrations immediately before and after the generation.

The chlorine and chlorine dioxide gas was passed into a 5-l round bottom flask, and mixed with air (20 l/min). All flows in the system were regulated with thermal mass-flow gauges which controlled magnetic needle valves. The flows were checked with a bubble gauge or rotometer. The gas mixture was passed forward to a glass container with an outlet for sampling. All connections in the gas-generating system were made of poly(tetrafluoroethylene).

Samples were taken with 30-ml midget impingers, whose 15.0-ml charge of absorption solution consisted of neutrally buffered 10 mM potassium iodide solution (Merck No. 5043). The buffer contained 10^{-3} M potassium dihydrogenphosphate and 10^{-3} M sodium hydrogenphosphate. For sampling, a vacuum pump was used with a flow-rate adjusted to 1 l/min.

To minimize the background from chloride, all glass equipment was soaked carefully with 1 M carbonate solution and rinsed with distilled water prior to sampling and analysis.

The analysis was performed by ion chromatography. Since the absorption solution contains high levels of potassium and sodium ions, these cause interference peaks at the beginning of the chromatogram. To separate ClO_2^- from these ions, and from formate which is a stabilizer added to potassium iodide* a very weak eluent must be used, yielding a long retention time for I^-.

In order to shorten the analysis time, a simple recoupling was made of the ion chromatograph's two systems (Fig. 1). By first passing the sample through a pre-column, I^- was separated from ClO_2^- and Cl^-. The last two ions were passed on to the separation column and after 1 min the valves were switched so that I^- and phosphate ions were diverted to waste with the aid of pump 2. After the completion of the experiment (elution of Cl^-), the precolumn was ready for another injection and the valves switched back to the original position.

The ion-chromatographic analysis apparatus and conditions were as follows: Dionex 14 ion chromatograph with conductivity detector; HP 3388 integrator; columns, 50 mm × 4 mm anion concentrator, HPIC-AG1 (Dionex), 250 mm × 4 mm anion separator, HPIC-AS3 (Dionex), 100 mm × 4 mm anion suppressor, ASC1 (Dionex); flow-rates, 138 ml/h (analytical column, pump 1), 300 ml/h (pump 2);

---

* Formate occurred in all the five lots investigated (Merck No. 5043), varying from 0.1 to 0.6%. No formate was seen in potassium iodide Suprapur (Merck No. 5044) and sodium iodide (Merck No. 6523).
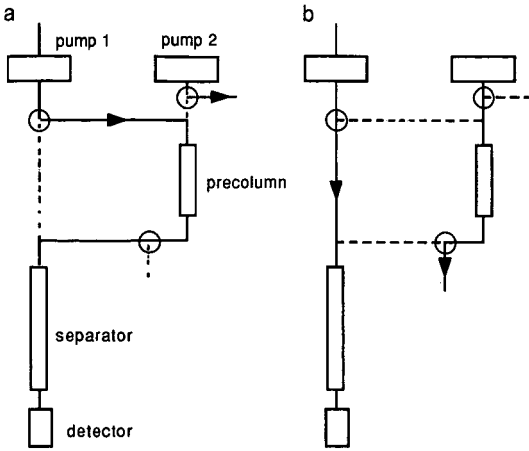
Fig. 1. The two flow systems of the ion chromatograph. (a) Sample passes through the precolumn. (b) Parts of the sample pass through the separation column while the precolumn is cleaned.
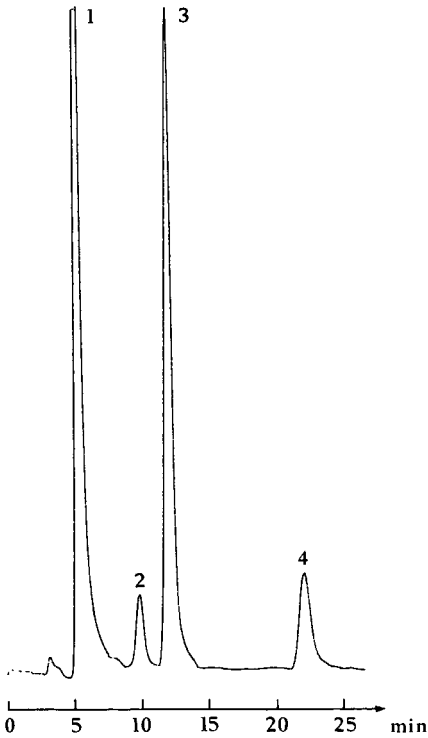
Fig. 2. Chromatogram from analysis of chloride and chlorite ions. Peaks: 1 = sodium and potassium ions; 2 = formate; 3 = 122 μM chlorite; 4 = 24 μM chloride.

injection volume, 100 μl; eluent, 0.75 mM sodium bicarbonate (both systems); retention times, ClO$_2^-$ $ca.$ 10 min, Cl$^-$ $ca.$ 20 min; measurement region, 3 or 10 μS.

A typical chromatogram is shown in Fig. 2.

RESULTS AND DISCUSSION

The uptake efficiency of the impinger was determined by sampling with two impingers connected in series. The sampling time varied from 30 to 70 min and the concentrations were 1 ppm of Cl$_2$ and 0.1–0.3 ppm of ClO$_2$. After sampling, the analysis result from the first impinger was compared with the sum from the two impingers. This indicated a collection efficiency of 96 $\pm$ 5% for ClO$_2$ and 100 $\pm$ 2% for Cl$_2$ ($n = 6$). Consequently, one impinger can be considered adequate for obtaining a quantitative yield in sampling.

The accuracy and precision were determined for different levels of Cl$_2$ and ClO$_2$ with sampling times varying from 30 to 60 min. The results of the chromatographic analyses were compared with the calculated content in the gas-generating system (Table I). The precision of the analysis step was investigated further for ClO$_2^-$. For a 5 μM chlorite solution (corresponding to 0.061 ppm at 20°C with a sampling time of 30 min), a coefficient of variation (C.V.) of 1.2% ($n = 5$) was obtained. A concentration of 1.8 μM ClO$_2^-$ (corresponding to 0.022 ppm under the same conditions) yielded a C.V. of 3.9% ($n = 7$). The calibration graph for ClO$_2^-$ is linear at least within two orders of magnitude. It is thus possible to analyze levels lower than 0.022 ppm, although the C.V. will exceed 3.9%.

The smallest analyzable concentration of Cl$^-$ (twice the chloride background) was about 10 μM (corresponding to 0.06 ppm Cl$_2$ at 20°C with a sampling time of 30 min; C.V. = 1.2%, $n = 8$). This rather high level was due to difficulties in fully eliminating the chloride background.

Interfering gases, which may occur in environments where Cl$_2$ and ClO$_2$ are encountered, are primarily sulphur dioxide and hydrogen sulphide. These reducing compounds may influence the result for ClO$_2$ by reacting with ClO$_2^-$ in the solution. Since the reaction between ClO$_2$ and I$^-$ is very rapid and I$^-$ is present in a vast excess,

TABLE I

ACCURACY AND PRECISION OF THE METHOD

C.V. denotes the coefficient of variation in percent, defined as 100 · standard deviation/mean value of the content obtained.

n	Generated (ppm)		Obtained (ppm)		Yield (%)		C.V. (%)	
	ClO$_2$	Cl$_2$	ClO$_2$	Cl$_2$	ClO$_2$	Cl$_2$	ClO$_2$	Cl$_2$
5	0.41	—	0.42	—	104	—	3.2	—
2	—	1.09	—	1.08	—	99	—	1.4
2	0.38	1.18	0.36	1.24	95	105	2.1	2.3
6	0.10	0.99	0.094	0.91	94	92	4.0	3.5
6		*	1.1	0.8	—	—	4.4	7.3

* Generated concentrations not calculable due to fault in one of the flow gauges.

there is no reason to believe that H_2S or SO_2 interferes with the adsorption process itself. Therefore a simplified test was made. Gases which are representative of current environments (0.14 ppm SO_2, 2 ppm H_2S) were passed through absorption solutions spiked with ClO_2^-. The sampling time was 30 min and the flow-rate 1 l/min. The concentrations of ClO_2^- in solution corresponded to 0.39 and 0.04 ppm ClO_2 for the SO_2 tests, and 0.20 and 0.02 ppm for the H_2S tests. The analyses were made directly after the sampling, and the stronger chlorite solutions were refrigerated for 2 days and analyzed thereafter. No significant decrease in chlorite contents was registered.

The stability of the solutions during storage was studied by preparing mixtures with known concentrations of Cl^- and ClO_2^- in absorption solution. Each solution was divided into four and placed in separate containers (dark polypropylene bottles) which were completely filled. The four samples were stored thus: (a) 2–5 h at room temperature, (b) 2 days at room temperature, (c) 3 days in a refrigerator and (d) 2 days at room temperature followed by 6 days in a refrigerator. Table II shows that the chlorite concentration decreases during storage at room temperature, but is stable during refrigeration, while the chloride concentration is not affected by storage.

To test the method under more realistic conditions, samples were taken at a pulp bleaching plant. The chlorine dioxide content in the workplace air varied drastically. Besides chlorine and chlorine dioxide, sulphur dioxide and chloroform occurred. The sampling was performed at four fixed sites. At each site, three to five samples were taken simultaneously. The sampling time varied from 110 to 200 min. Two samples were taken consecutively and mixed later. In order to compensate for evaporation, the impingers were weighed before and after sampling. Three of the measuring points were located next to washing filters. One sampling site was chosen near a chlorine dioxide tower on the mixer-level where the pulp is mixed with chemicals. In connection with this test, a serious disturbance of operation occurred, resulting in greatly increased levels of ClO_2. The precision of the sampling was rather good, the C.V. obtained being less than 6.8%. The results are shown in Table III.

In conclusion, the results reported show that both Cl_2 and ClO_2 in air can be determined simultaneously by ion-chromatographic analysis. As expected, the method is not sensitive to interference. However, the tests reveal that the chlorine dioxide

TABLE II

STORAGE STABILITY

Room denotes storage at 22°C and cold storage at 7°C.

Concentration (μM)		Yield (%) obtained after storage							
		2–5 h room		2 d room		3 d cold		2 d room + 6 d cold	
ClO_2^-	Cl^-	ClO_2^-	Cl^-	ClO_2^-	Cl^-	ClO_2^-	Cl^-	ClO_2^-	Cl^-
2	0	100	—*	104	—	—	—	—	—
2	100	100	100	100	—	—	100	96	100
2	200	100	—	100	—	—	100	100	—
10	100	100	—	88	101	99	100	86	—
10	200	100	—	85	—	96	—	84	—

* Not determined.

TABLE III

FIELD TEST AT A PULP BLEACHING PLANT

Total sampling time was 170–350 min. Coefficient of variation (C.V.) defined as 100 · standard deviation/mean value of content obtained.

Test site	n	Obtained (ppm)		C.V. (%)	
		ClO_2	Cl_2	ClO_2	Cl_2
At filter A	3	0.11	0.30	4.0	5.6
At filter B	4	0.053	0.090	6.0	6.8
Mixer-level	3	1.67	1.59	2.5	2.6
At filter C	5	0.22	0.12	5.7	3.8

content decreases with storage at room temperature. If analyses cannot be conducted along with the sampling, storage in a refrigerator is recommended. The method makes it possible with a 30-min sampling time to determine levels as low as 0.02 ppm ClO_2 and 0.06 ppm Cl_2 with acceptable precision.

REFERENCES

1 W. K. Fowler and H. K. Dillon, *Methods Development for Sampling and Analysis of Chlorine, Chlorine Dioxide, Bromine and Iodine: Research Report for Chlorine Dioxide*, Southern Research Institute, Birmingham, AL, 1982.
2 J. D. Johnson and R. Overby, *Anal. Chem.*, 41 (1969) 1744.
3 *NIOSH Manual of Analytical Methods; Vol. I, P/CAM 211*, U.S. Department of Health, Education and Welfare, Public Health Service, Center for Disease Control, National Institute for Occupational Safety and Health, Cincinnati, OH, 2nd ed., 1977.
4 Y. H. Lee, *Measurement of Chlorine and Chlorine Dioxide in the Working Environment*, Swedish Water and Air Pollution Research Institute, Gothenburg, 1982.
5 J. Howard and D. W. Duncan, *Conference of Tech. Sect. of Pacific and Western Branches, Canadian Pulp and Paper Association, Jasper*, 1980.
6 M. A. Post and W. A. Moore, *Anal. Chem.*, 31 (1959) 1872.

CHROM. 20 977

Note

Non-suppressed ion chromatography of arsenic anions using sodium nitrite solutions as eluents

NAOKI HIRAYAMA and TOORU KUWAMOTO*

Department of Chemistry, Faculty of Science, Kyoto University, Kitashirakawa-Oiwake-Cho, Sakyo-ku, Kyoto 606 (Japan)

(First received June 27th, 1988; revised manuscript received September 9th, 1988)

One analytical technique for the separation and the detection of inorganic and organic arsenic compounds is a reduction method, by which arsenic species are reduced to volatile arsine compounds[1–4] and separated by gas chromatography[1,3] or thermal volatilization[2,4] and determined spectroscopically. On the other hand, most direct methods involve liquid chromatography[5,6] equipped with voltammetric[5] or absorption spectrometric[6] detectors. Suppressed ion chromatography (IC)[7] has recently been used to separate and to determine some arsenic compounds[8–16] with conductivity detection[8,13,14,16], pulse polarography[9], atomic absorption[10–12], inductively coupled argon plasma–atomic emission spectrometry[15] or electrochemical detection[16].

Non-suppressed IC[17,18] is a very useful system with various kinds of eluents. We have previously reported on the analysis of inorganic or organic arsenic anions using potassium hydroxide eluents and potassium hydroxide–aromatic salts mixed eluents[19,20], but the effect of neutral eluent solutions on the chromatography has not been examined in spite of the fact that the charge of these arsenic anions decreases and that the burden of the IC system is relieved.

For these reasons, the efficiency of neutral eluents such as sodium chloride, sodium sulphate, sodium nitrite and sodium nitrate in the separation and determination of arsenic anions by non-suppressed IC has been studied. It was found that the most suitable eluent for the elution of the arsenic compounds is sodium nitrite solution.

EXPERIMENTAL

Standard solutions

The stock solutions of 1000 μg/ml (as As) potassium arsenate [As(V)], dimethylarsinic acid (DMA), *o*-aminophenylarsonic acid (*o*-APA), *p*-aminophenylarsonic acid (*p*-APA), phenylarsonic acid (PA) and *o*-nitrophenylarsonic acid (*o*-NPA) were prepared by dissolving analytical grade salts or acids in distilled water, respectively. The stock solution of 1000 μg/ml (as As) sodium methylarsonate (MMA) was prepared by dissolving the salt, synthesized according to method of Quick and Adams[21], in distilled water. Working standard solutions were obtained by diluting the stock solutions in

TABLE I

DISSOCIATION CONSTANTS OF ARSENIC COMPOUNDS AT 25°C[22]

Compound	pK_{a1}	pK_{a2}	pK_{a3}
1 Arsenic acid [As(V)]	2.22	6.98	11.50
2 Methylarsonic acid (MMA)	3.41	8.18	
3 Dimethylarsinic acid (DMA)	6.273		
4 o-Aminophenylarsonic acid (o-APA)*	≈ 2	3.77	8.66
5 p-Aminophenylarsonic acid (p-APA)*	≈ 2	4.02	8.92
6 Phenylarsonic acid (PA)	3.47**	8.48	
7 o-Nitrophenylarsonic acid (o-NPA)	3.37	8.54	

* Values are pK_a of $NH_3{}^+C_6H_4AsO_3H_2 \rightleftharpoons NH_3{}^+C_6H_4AsO_3H^- + H^+$, $NH_3{}^+C_6H_4AsO_3H^- \rightleftharpoons NH_2C_6H_4AsO_3H^- + H^+$ and $NH_2C_6H_4AsO_3H^- \rightleftharpoons NH_2C_6H_4AsO_3{}^{2-} + H^+$, respectively[23].
** From ref. 23.

distilled water. The dissociation constants of sample arsenic acids are shown in Table I[22,23].

River-water

As an example of an application, river-water collected at the Kamo river (Kyoto , Japan) was used after filtration through a 0.45-μm millipore filter.

Eluents

The eluents were prepared by dissolving analytical grade sodium chloride, sodium sulphate, sodium nitrate and sodium nitrite ($pK_a = 3.14$[22]), respectively, and then deaerated.

Apparatus

A Tosoh Model non-suppressed ion chromatograph HLC-601 equipped with an anion-exchange column (50 mm × 4.6 mm I.D.) packed with TSKgel IC-Anion-PW (particle size 10 ± 0.005 μm, capacity 0.03 ± 0.003 mequiv./g) was used. It consisted of a computer-controlled pump, a conductivity detector, a sample injector (100 μl) and an oven. The flow-rate was maintained at 1.0 ml/min under a pressure of 15–30 kg/cm². The separator column and the conductivity detector were placed in an oven regulated at 30°C. The data were recorded by a Shimadzu Model Chromatopack C-R1A.

RESULTS AND DISCUSSION

Sodium chloride, sulphate and nitrate eluents

The elution power of these eluents was observed to lie in the order sulphate > nitrate > chloride for the elution of the sample anions, but the differences were small.

In unbuffered solution, the pH of these solutions is theoretically 7.0, but it is difficult to maintain their pH constant. In this case, the elution behaviour of arsenic (V) anion was significantly affected by a small change in the eluent pH, since the charge of the anion is changed. At pH < 7, the peak of As(V) is slightly overlapped by that of o-APA anion and at pH > 7 the retention time of As(V) depends on the eluent

pH. As seen in Table I[22,23], the eluent pH has to be controlled to 7.0–8.1, at which the charge of As(V) is -2, for the effective separation and determination of arsenic anions.

Even when the buffer solution is used to control the pH, the eluent containing buffer is unsuitable for ion chromatography with conductivity detection due to acting as eluent of the buffer anion itself. For this reason, solutions of these salts cannot be used as eluents for the separation and the determination of arsenic anions.

Sodium nitrite eluent

Characteristics. The elution behaviour of the sodium nitrite eluent was similar to that of the solutions mentioned above. The elution power of these four eluents followed the order of sulphate > nitrate > nitrite > chloride. Nitrous acid (HNO_2) is a weak acid ($pK_a = 3.14$[22]), and these solutions are buffered with strong bases. Their pH is effectively controlled so that the charge of As(V) is probably regulated to -2.

Prevention of the oxidation of nitrite anion and lowering of eluent pH. When using sodium nitrite eluents it is important to suppress the air oxidation of nitrite anion because the eluent pH is lowered. From the reaction mechanism reported by Klemenc and Pollak[24] and Reinders and Vles[25], the overall reaction is as follows:

$$2NO_2^- + O_2 + 2H_2CO_3 \rightarrow 2NO_3^- + 2H^+ + 2HCO_3^- \tag{1}$$
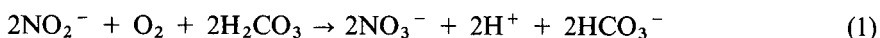
The oxidation is prevented by the depression of the absorption of carbon dioxide. Thus, for the prevention of absorption of carbon dioxide in air, a bottle filled with 100 mM potassium hydroxide solution is placed before the eluent bottle.

Moreover, in anion chromatography, the following relationship was given by Gjerde *et al.*[17].

$$\log t_s = (-y/x)\log [E] - \text{constant} \tag{2}$$

where t_s is the retention time of the sample anion, x and y are the charge numbers of the eluent anion and the sample anion, respectively, and [E] is the concentration of the eluent anion. The ratio (y/x) is given by the slope of a plot of $\log t_s$ *vs.* $\log$ [E]. The charge of the sample anion can be estimated from this ratio.

Fig. 1 shows the retention times of sample arsenic anions obtained by using sodium nitrite solutions as eluents. From the slope and the concentration of the eluent, it was estimated that the charge of As(V) is -2 and that carbon dioxide is hardly absorbed.

The use of sodium nitrite eluent

Optimum chromatographic condition. As shown in Fig. 1, the separation of arsenic(V) anion from other sample arsenic anions is possible by using concentrations lower than 3 mM, and if the concentration of eluent anion is increased the time required for separation and determination of sample anions becomes short. The concentration of the salt chosen was 2 mM and the eluent pH was regulated at 7.3.

The oven, in which the column and detector are placed, was regulated at 30°C because the oven temperature hardly influences the separation of the arsenic anions,
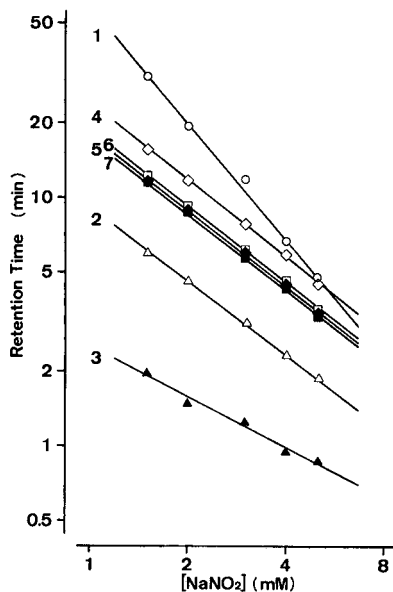
Fig. 1. Retention times of arsenic anions. Samples: 1 = As(V) (slope 1.55); 2 = MMA (slope 0.99); 3 = DMA (slope 0.69); 4 = o-APA (slope 0.94); 5 = p-APA (slope 1.01); 6 = PA (slope 1.01); 7 = o-NPA (slope 1.01). Column TSKgel IC-Anion-PW, 0.03 mequiv./g. Eluent: sodium nitrite.

and the eluent flow-rate was maintained at 1.0 ml/min after consideration of the separation of these anions and the time required.

Fig. 2 shows an ion chromatogram of an arsenic sample obtained under the above conditions.

Quantitative ranges and detection limits of arsenic anions. The quantitative ranges and the detection limits of the arsenic anions obtained by using the conditions shown in Fig. 2 are given in Table II. Better result was not obtained on the determination of As(V), because the separation of As(V) from other organoarsenic anions was prior to the determination of As(V) and the concentration of the eluent had to be lowered.

Separation of aromatic organoarsenic anions. The peaks of o-NPA, p-APA and PA anions were not separated and only the total concentration of these three arsenic anions was measured because these anions have very similar limiting equivalent ionic conductances.
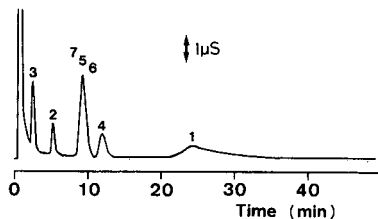
Fig. 2. Ion chromatogram of arsenic anions. Sample: 1 = As(V) (30 μg/ml as As); 2 = MMA (10 μg/ml as As); 3 = DMA (20 μg/ml as As); 4 = o-APA (10 μg/ml as As); 5 = p-APA (10 μg/ml as As); 6 = PA (10 μg/ml as As); 7 = o-NPA (10 μg/ml as As). Column: TSKgel IC-Anion-PW, 0.03 mequiv./g. Eluent: 2 mM sodium nitrite, pH 7.3

TABLE II

QUANTITATIVE RANGES AND DETECTION LIMITS OF ARSENIC ANIONS USING 2 m*M* SODIUM NITRITE AS THE ELUENT

Anion	Quantitative range (μg/ml as As)	Detection limit (μg/ml as As)
1 As(V)	20–50	5
2 MMA	1–50	0.3
3 DMA	3–50	0.3
4 o-APA	1–50	0.3
5 p-APA	1–50	0.3
6 PA	1–50	0.3
7 o-NPA	1–50	0.3

On the other hand, the peak of *o*-APA anion was separated from those of the three anions, because *o*-APA anion has a different structure, involving hydrogen bonding between an hydrogen atom of the amino-group and an oxygen atom of the arsonate-group.

Comparison between sodium nitrite eluent and basic eluent. Previously, we reported that potassium hydroxide–sodium salicylate is the preferred basic eluent in non-suppressed IC of arsenic anions[20].

For the separation of and the sensitivity towards these arsenic anions, sodium nitrite is slightly better than the mixed eluent. Moreover, the lifetime of the separator column is extended because the column is used under mild conditions.

However, in the separation of arsenic anions including arsenite [As(III)] or its derivatives, sodium nitrite is unsuitable as an eluent because these arsenic species have no charge under conditions of neutral pH.

Application to the synthetic arsenic samples. Standard solutions containing 1–20 μg/ml (as As) arsenic anions in river-water were prepared in order to evaluate the method. The recovery results are shown in Table III. Although the river-water includes many inorganic and organic anions, there was no interference with the deter-

TABLE III

RECOVERY OF ARSENIC ANIONS ADDED TO RIVER-WATER

Anion	Recovery (%)
1 As(V)	—*
2 MMA	100.8 ± 0.8
3 DMA	99.9 ± 2.2
4 o-APA	101.7 ± 2.0
5 p-APA	92.6 ± 1.4
6 PA	87.8 ± 0.5
7 o-NPA	95.8 ± 1.5

* Unsuitable for determination.

mination of the arsenic anions. It was found that sodium nitrite as the eluent is effective in controlling the pH and in separating these arsenic anions from one another and from other anions.

Thus, sodium nitrite as the eluent is effective for the separation of arsenic compounds and this chromatographic method is applicable to practical samples.

REFERENCES

1 M. Talmi and D. T. Bostic, *Anal. Chem.*, 47 (1975) 2145.
2 R. S. Braman, D. L. Johnson, C. C. Foreback, J. M. Ammons and J. L. Bricker, *Anal. Chem.*, 49 (1977) 2145.
3 M. O. Andreae, *Anal. Chem.*, 49 (1977) 820.
4 E. A. Crecelius, *Anal. Chem.*, 50 (1978) 826.
5 R. K. Elton and W. E. Geiger, Jr., *Anal. Chem.*, 50 (1978) 712.
6 D. G. Iverson, M. A. Anderson, T. R. Holm and R. R. Startorth, *Environ. Sci. Technol.*, 13 (1979) 1491.
7 H. Small, T. S. Stevens and W. C. Bauman, *Anal. Chem.*, 47 (1975) 1801.
8 L. D. Hansen, B. E. Richter, D. K. Rollins, J. D. Lamb and D. J. Eatough, *Anal. Chem.*, 51 (1979) 633.
9 F. T. Henry and M. T. Thorpe, *Anal. Chem.*, 52 (1980) 80.
10 E. A. Woolson and N. Aharonson, *J. Assoc. Off. Anal. Chem.*, 63 (1980) 523.
11 G. R. Ricci, L. S. Shepard, G. Colovos and N. E. Hester, *Anal. Chem.*, 53 (1981) 610.
12 A. A. Grabinsky, *Anal. Chem.*, 53 (1981) 966.
13 A. Y. Zolotov, O. A. Shpigun and L. A. Bubchikova, *Fresenius' Z. Anal. Chem.*, 316 (1983) 8.
14 L. K. Tan and J. E. Dutrizac, *Anal. Chem.*, 57 (1985) 2615.
15 W. D. Spall, L. G. Lynn, J. L. Anderson, J. G. Valdez and L. R. Gurley, *Anal. Chem.*, 58 (1986) 1340.
16 L. K. Tan and J. E. Dutrizac, *Anal. Chem.*, 58 (1986) 1383.
17 D. T. Gjerde, J. S. Fritz and G. Schmuckler, *J. Chromatogr.*, 186 (1979) 509.
18 D. T. Gjerde, G. Schmuckler and J. S. Fritz, *J. Chromatogr.*, 187 (1980) 35.
19 T. Okada and T. Kuwamoto, *Anal. Chem.*, 57 (1985) 829.
20 N. Hirayama and T. Kuwamoto, *J. Chromatogr.*, 447 (1988) 323.
21 A. J. Quick and R. Adams, *J. Am. Chem. Soc.*, 44 (1922) 805.
22 A. J. Dean, *Lange's Handbook of Chemistry*, McGraw-Hill, New York, 1985.
23 D. Pressman and D. H. Brown, *J. Am. Chem. Soc.*, 65 (1943) 540.
24 A. Klemenc and F. Pollak, *Z. Phys. Chem.*, 101 (1922) 150.
25 W. Reinders and S. I. Vles, *Recl. Trav. Chim. Pays-Bas*, 44 (1925) 1.

CHROM. 21 037

Note

Peak identification of amino acids in liquid chromatography by optical activity detection

KING C. CHAN and EDWARD S. YEUNG*

Ames Laboratory–USDOE and Department of Chemistry, Iowa State University, Ames, IA 50011 (U.S.A.)

(First received July 27th, 1988; revised manuscript received October 10th, 1988)

Detection in liquid chromatography (LC) has made rapid advances in the last decade[1,2]. In addition to improvements in detectability, a high degree of selectivity is offered by some types of detection schemes. The latter is useful when the separation efficiency is not sufficient to resolve all the components in a complex mixture. Information-rich detectors include infrared spectroscopy[3] and mass spectrometry[4].

A relatively new detection scheme for LC is the measurement of optical rotation[5]. As little as 1 ng of an analyte with a specific rotation ($[\alpha]$) of 100° is now detectable[6]. Much of our earlier work was centered around its selectivity, so that clinically interesting species can be monitored in biological matrices[7,8]. In the course of our work, we realized that the information content of $[\alpha]$ is actually quite high. For a group of related compounds, such as the dansylated amino acids[9], $[\alpha]$ can range from $-250°$ to $+250°$. Since one can expect to be able to determine $[\alpha]$ to the $\pm 1\%$ level, the number of resolution elements available should be better than 200. This then opens up the possibility for analyte identification based on $[\alpha]$. We note that the dansylated amino acids are spectrally very similar, and other optical detectors cannot be used for identification.

Sequential identification of phenylthiohydantoin (PTH) amino acids resulting from Edman degradation[10] in proteins or peptides sequencing requires a rapid and sensitive method. Although various methods have been used, high-performance liquid chromatography in the reversed-phase mode (RP-HPLC) has become the standard system for the separation and detection of PTH-amino acids in most of the commercial automated gas- or liquid-phase Edman protein sequencers[11–13]. A lot of papers have been published for the separation and identification of PTH-amino acids using RP-HPLC. In general, the PTH-amino acids eluted from a chromatographic column are monitored by UV absorption and are identified by their corresponding retention times. In order to have all the common PTH-amino acids well resolved in time for identification, extensive manipulation of the mobile phases (eluents) or the stationary phases or both are usually required. Furthermore, this manipulation step frequently involves some undesirable conditions for the separation system; for example, elevated temperature, high flow-rate, long analysis time and baseline drift. In addition, it is not uncommon to have some PTH-amino acids still unresolved in time, even after a lengthly manipulation of the various conditions.

The purpose of this study is to detect and identify PTH-amino acids after

chromatographic separation using polarimetric and UV absorption detection. By monitoring both the optical activity and the UV absorption, the PTH-amino acids that are not identified by retention times will readily be identified by their optical rotations or *vice versa*. This detection scheme will allow rapid identification of PTH-amino acids under simple and favorable chromatographic conditions based on isocratic elution.

EXPERIMENTAL

Chemicals

L-Phenylthiohydantoin amino acids were obtained from Fluka (Ronkonkoma, NY, U.S.A.) or Pierce (Rockford, IL, U.S.A.). Reagent-grade sodium monophosphate, phosphoric acid, sodium acetate, and HPLC-grade acetonitrile were obtained from Fisher (Fair Lawn, NJ, U.S.A.). Analytical-grade glacial acetic acid was obtained from Baker (Phillipsburg, NJ, U.S.A.). Deionized water was prepared by passing distilled water through a Nanopure water-purification system (Barnstead, Boston, MA, U.S.A.). 0.02 M Phosphate buffer (pH 3.2) was prepared by dissolving 3 g sodium monophosphate in 1 l deionized water–acetonitrile (3:2, v/v). The pH of the resulting solution was adjusted to 3.2 by adding phosphoric acid. 0.02 M Acetate buffer (pH 5.0) was prepared by dissolving 2 g sodium acetate in 1 l water–acetonitrile (3:2, v/v). The pH of the resulting solution was adjusted to 5.0 by adding glacial acetic acid.

Chromatography

A Model 2600 syringe pump (Isco, Lincoln, NE, U.S.A.) was used for eluent delivery. Injections of samples were made through a Model 7010 six-port injector (Rheodyne, Berkeley, CA, U.S.A.), equipped with a 20-μl sample injection loop. Separations of the PTH-amino acids were performed on a 100 × 4.6 mm I.D., 3-μm, C_8 Econosphere column (Alltech, Deerfield, IL, U.S.A.). All eluents were filtered through a 0.2-μm nylon membrane filter, and were degassed under vacuum using ultrasonic agitation before use. All experiments were performed at room temperature with a flow-rate of 0.67 ml/min. All the PTH-amino acid samples were freshly prepared in the eluents before use.

Detection

The system consisted of an UV absorption detector in series with a laser-based polarimeter. UV detection at 330 nm was performed on a Model 100-10 variable-wavelength spectrophotometer (Hitachi, Tokyo, Japan) equipped with a Model 155-00 analytical flow cell (Altex, Berkeley, CA, U.S.A.). The waste line of the UV detector was connected to the inlet of the flow cell of the polarimeter via a 0.007-in. I.D. PTFE tubing. The length of this tubing was kept short to minimize the extra-column band broadening. The basic arrangement of the laser-based polarimeter was reported before[5,8]. The flow cell had a volume of 100 μl and was 5 cm in length. An independent air-based Faraday rotator (d.c. coil) was placed between the polarizer and the flow cell to produce a standard optical rotation. Modulation with square wave was driven by a Model SG-1271 wave generator (Heath, Benton Harbor, MI, U.S.A.) at a voltage of 25 V and a frequency of 500 Hz. A 1-s time constant was used

at the lock-in amplifier. The outputs of the lock-in amplifier and the UV detector were displayed on a Model CR 452 dual-channel recorder (Measurement Technology, Denver; CO, U.S.A.). The two outputs were also connected to a Model 5150 personal computer (IBM/PC, Armonk, NJ, U.S.A.) for data acquisition through the Adalab interface system (Interactive Microware, State College, PA, U.S.A.). The computer took a reading every 0.1 s to allow signal averaging.

Calculations

All raw data were subjected to a 25-point moving window smooth. The peak areas from both the UV and optical activity detectors were determined by summation of the baseline corrected measurements. The optical activity peak areas and responses were normalized against the signal obtained from the d.c. coil to account for the drift in laser intensity. The d.c. coil produced a constant 0.25-millidegree rotation. These normalized peak areas were then divided by their corresponding UV peak areas to obtain the optical activity-to-UV ratios. The specific rotations [α] of the PTH-amino acids were calculated using the following formula:

$$[\alpha] = \frac{\alpha}{Cl}$$

where α is the actual rotation measured, C is the concentration of analytes at the peak maximum in g/ml solution, and l is the path length in dm. The concentration at the peak maximum can be calculated from the peak area, the area of a 1-s interval at the peak maximum, the amount of analytes injected, and the flow-rate. The retention times of the PTH-amino acids were taken as the times for the peak maximum to appear.

RESULTS AND DISCUSSION

Identification of analytes in chromatographic separations is generally based on retention times (t_R). The t_R values of the twenty PTH-amino acids for separations at pH 3.2 are shown in Table I. The conditions were chosen so that all PTH-amino acids were eluted under 10 min at a flow-rate of 0.67 ml/min. Also, we required that all PTH-amino acids were retained so that the optical activity measurement will not be affected by the refractive index disturbance present at the void volume. It is obvious that the identification of some of the PTH-amino acids based on t_R are difficult or impossible as they were poorly resolved or unresolved. For example, the PTH-amino acids within the pairs of Ser–Gln, Thr–Asp, Gly–Cmc, Val–Met, and Trp–Ile are not resolved. In addition, Asn–Ser, Glu–Thr, Asp–Glu, Glu–Gly, His–Ala, and Ile–Phe are poorly resolved. Therefore, only a few of the twenty PTH-amino acids can be identified based on t_R alone. These poor results are expected since the chromatographic conditions used were not designed for the complete separation of the PTH-amino acids.

The measured specific rotations [α] of the PTH-amino acids are also shown in Table I. Most of the PTH-amino acids show negative rotations and have small values. The [α] of some of the PTH-amino acids in methanol[14] and ethanol[15] obtained at 590 nm have been reported. Those results are similar to ours, but strict comparison can-

not be made since [α] is solvent dependent. Since the optical activity-to-UV ratios are proportional to [α][9], if the molar absorptivities are identical it will be easier in practice to monitor the optical activity-to-UV ratios rather than to calculate [α]. The optical activity-to-UV ratios of the PTH-amino acids at pH 3.2 are also shown in Table I. These ratios are approximately, but not exactly, proportional to [α]. However, they still vary substantially among the amino acids. Most of the unresolved and poorly resolved peaks mentioned above are now readily identified by their optical activity-to-UV ratios. As a result, Glu–Gly–Cmc is the only group in which the PTH-amino acids could not be identified either by the t_R or the optical activity-to-UV ratios at pH 3.2.

Since the retention and the specific rotation are expected to be pH dependent, the experiment was repeated at pH 5.0 (acetate buffer) to find out if better identification of the peaks could be achieved. The t_R, [α], and the optical activity-to-UV ratios of the PTH-amino acids separated at pH 5.0 are shown in Table II. The elution times and elution orders of most of the PTH-amino acids at pH 5.0 are similar to those at pH 3.2, except Asp and Cmc. At pH 5.0, these two compounds were not retained in the column and were eluted with the solvent front. The dependence of the rotatory power of amino acids on pH has been discussed in detail[16]. In general, the rotatory power of L-amino acids becomes more positive when the concentration of acid, [H^+], increases. This trend for the PTH-amino acids is not observed here, *i.e.*, the [α] at pH 3.2 and pH 5.0 are not significantly different. This may be because PTH derivatization changes the composition of most free amino acids to such an extent that, unlike

TABLE I

SEPARATION AND DETECTION OF PTH-AMINO ACIDS AT pH 3.2

PTH-Amino acid	Abbreviation	t_R (min)	Capacity factor k'	[α]	Optical activity-to-UV ratio
L-Asaragine	Asn	2.48 ± 0.02	0.36	−31.2 ± 0.7	−8.4 ± 0.3
L-Serine	Ser	2.67 ± 0.00	0.46	−42.1 ± 0.6	−7.0 ± 0.4
L-Glutamine	Gln	2.66 ± 0.01	0.46	−25.2 ± 0.4	−5.3 ± 0.2
L-Threonine	Thr	2.84 ± 0.01	0.56	−71.7 ± 1.8	−11.6 ± 0.5
L-Aspartic acid	Asp	2.92 ± 0.00	0.60	−14.6 ± 1.1	−3.4 ± 0.2
L-Glutamic acid	Glu	3.18 ± 0.00	0.75	≈0	≈0
Glycine	Gly	3.32 ± 0.00	0.82	≈0	≈0
Carboxymethyl-L-Cysteine	Cmc	3.36 ± 0.01	0.85	≈0	≈0
L-Histidine	His	3.86 ± 0.01	1.12	≈0	≈0
L-Alanine	Ala	4.00 ± 0.00	1.20	−13.5 ± 0.5	−2.3 ± 0.1
L-Tyrosine	Tyr	4.43 ± 0.00	1.43	−24.3 ± 1.0	−6.1 ± 0.2
L-Arginine	Arg	4.85 ± 0.02	1.66	≈0	≈0
L-Valine	Val	5.98 ± 0.01	2.29	−10.4 ± 0.6	−1.6 ± 0.1
L-Methionine	Met	5.98 ± 0.01	2.29	+14.7 ± 0.6	+2.9 ± 0.1
L-Proline	Pro	6.33 ± 0.00	2.48	−65.8 ± 1.9	−10.1 ± 0.4
L-Tryptophan	Trp	7.65 ± 0.01	3.20	≈0	≈0
L-Isoleucine	Ile	7.71 ± 0.01	3.24	−22.4 ± 0.9	−3.5 ± 0.2
L-Phenylalanine	Phe	7.84 ± 0.01	3.31	−14.2 ± 1.3	−2.8 ± 0.2
L-Leucine	Leu	8.46 ± 0.01	3.65	−34.2 ± 1.6	−7.2 ± 0.2
ε-PTC-L-lysine	Lys	8.88 ± 0.00	3.88	≈0	≈0

TABLE II

SEPARATION AND DETECTION OF PTH-AMINO ACIDS AT pH 5.0

PTH-AA	t_R (min)	k'	[α]	Optical activity-to-UV ratio
L-Aspartic acid	1.82 ± 0.04	0	⋆	−4.6 ± 0.2
Carboxylmethyl-L-cysteine	1.82 ± 0.04	0	≈0	≈0
L-Glutamic acid	2.46 ± 0.01	0.35	≈0	≈0
L-Asparagine	2.50 ± 0.00	0.37	−39.1 ± 1.0	−9.9 ± 0.3
L-Glutamine	2.61 ± 0.00	0.43	−29.1 ± 1.0	−6.9 ± 0.2
L-Serine	2.66 ± 0.03	0.46	−43.0 ± 1.5	−8.9 ± 0.3
L-Threonine	2.85 ± 0.01	0.57	−66.5 ± 3.2	−15.5 ± 0.8
Glycine	3.25 ± 0.00	0.79	≈0	≈0
L-Histidine	3.87 ± 0.01	1.13	≈0	≈0
L-Alanine	3.95 ± 0.02	1.17	−9.4 ± 0.2	−2.4 ± 0.1
L-Tyrosine	4.34 ± 0.01	1.38	−19.4 ± 0.7	−6.4 ± 0.3
L-Arginine	5.16 ± 0.06	1.84	≈0	≈0
L-Valine	6.03 ± 0.03	2.31	−8.2 ± 0.4	−1.8 ± 0.1
L-Methionine	6.25 ± 0.02	2.43	+17.5 ± 0.7	+4.8 ± 0.1
L-Proline	6.68 ± 0.00	2.67	−72.8 ± 2.8	−14.2 ± 0.6
L-Tryptophan	7.81 ± 0.01	3.29	≈0	≈0
L-Isoleucine	8.08 ± 0.03	3.44	−16.7 ± 0.1	−4.2 ± 0.1
L-Phenylalanine	8.21 ± 0.04	3.51	−8.28 ± 0.4	−2.4 ± 0.2
L-Leucine	8.70 ± 0.00	3.78	−38.3 ± 1.2	−10.3 ± 0.1
ε-PTC-L-Lysine	9.27 ± 0.00	4.09	≈0	≈0

⋆ Cannot be determined due to interference of refractive index disturbance at the void volume.

dansylation[9], they no longer behave as amino acids with respect to this acid rule. It may also be the case that a plateau has been reached such that any change in the [H$^+$] will not affect the rotatory power[17]. Another possibility is that the change in pH in this study is not large enough to cause any noticeable changes in [α].

At pH 5.0, the PTH-amino acids within the pairs of Asp–Cmc, Glu–Asn–Gln–Ser, Ser–Thr, His–Ala, Val–Met, Trp–Ile–Phe are poorly resolved or unresolved in t_R. However, all of the PTH-amino acids within these pairs can be readily identified by their optical activity-to-UV ratios. Asp and Cmc were co-eluted with the solvent front. The solvent did not affect the UV peaks much, but it produced a small disturbance in the optical activity chromatograms. This small disturbance within the peaks did not allow [α] to be calculated accurately. In fact, this is why the original conditions were chosen (at pH 3.2) to avoid interference from this disturbance. However, the irregular peak shapes for Asp and for Cmc are reproducible. An optical activity-to-UV ratio can still be derived from the chromatograms to distinguish the two. Naturally, the injection volume and the solvent for the analyte must be fixed to allow such inferences. Another way to confirm the Cmc peak is to look for the presence of an extra UV peak which is due to the degradation product of Cmc. Finally, we note that Cmc is not a naturally occurring amino acid and is produced only via certain protein degradation schemes. The implication of Table II is that, using pH 5.0 acetate eluent, all of the twenty PTH-amino acids can be identified either by the retention times or the optical activity-to-UV.

So, the combination of optical activity and UV detection has allowed simplifi-

cation of the chromatographic procedure necessary for the identification of the PTH-amino acids. A 10-min isocratic run is a substantial improvement over the normal 50–60 min gradient run, which also requires cycling the column back to the original solvent strength prior to each run. The detection limits for optical activity–UV here is in the low ng range depending on the species, which is comparable to the 10-pmol levels in the standard protein sequencing systems. Naturally, other amino acid derivatives, such as dansyl[9], can be expected to allow the same simplification. There, the $[\alpha]$ values are larger and detectability should be even better. other optical activity monitors, such as circular dichroism[18] and fluorescence detected circular dichroism[19] should also be applicable. In fact, since fluorescence–circular dichroism detectors can be miniaturized substantially to become compatible with open tubular capillary columns, one may have identification at very low mass quantities for each component. Finally, actual application to protein sequencing by Edman degradation is more complicated. This is because the coupling and cleavage steps are not 100% efficient and not 100% synchronized. It is probably possible to account for these effects by background subtraction based on the amino acids identified in the previous steps. For the worst case of Glu–Ser in Table II, one can expect to be able to tolerate up to 30% contamination before identification becomes ambiguous.

ACKNOWLEDGEMENT

REFERENCES

1 R. P. W. Scott, *Liquid Chromatography Detectors* (*Journal of Chromatography Library*, Vol. 33), Elsevier, Amsterdam, 2nd ed., 1986.
2 E. S. Yeung (Editor), *Detectors for Liquid Chromatography*, Wiley, New York, 1986.
3 K. Jinno, in E. S. Yeung (Editor), *Detectors for Liquid Chromatography*, Wiley, New York, 1986, p. 64.
4 J. B. Crowther, T. R. Covey and J. D. Henion, in E. S. Yeung (Editor), *Detectors for Liquid Chromatography*, Wiley, New York, 1986, p. 292.
5 E. S. Yeung, L. E. Steenhoek, S. D. Woodruff and J. C. Kuo, *Anal. Chem.*, 52 (1980) 1399.
6 D. R. Bobbitt and E. S. Yeung, *Appl. Spectrosc.*, 40 (1986) 407.
7 J. C. Kuo and E. S. Yeung, *J. Chromatogr.*, 223 (1981) 321.
8 J. C. Kuo and E. S. Yeung, *J. Chromatogr.*, 229 (1982) 293.
9 B. H. Reitsma and E. S. Yeung, *Anal. Chem.*, 59 (1987) 1059.
10 P. Edman, *Acta Chem. Scand.*, 4 (1950) 283.
11 H. Lu and P. Lai, *J. Chromatogr.*, 368 (1986) 215.
12 D. Hawke, P. Yuan and J. E. Shively, *Anal. Biochem.*, 120 (1982) 302.
13 C. Fonck, S. Frutiger and G. J. Hughes, *J. Chromatogr.*, 370 (1986) 339.
14 C. Djerassi, K. Undheim, R. C. Sheppard, W. G. Terry and B. Sjoberg, *Acta Chem. Scand.*, 15 (1961) 903.
15 P. Edman, *Acta Chem. Scand.*, 4 (1950) 277.
16 J. P. Greenstein and M. Winitz, *Chemistry of the Amino Acids*, Vol. I, Wiley, New York, 1961, p. 3.
17 B. Jirgensons, *Optical Activity of Proteins and other Macromolecules*, Springer, New York, 1973, p. 48.
18 R. E. Synovec and E. S. Yeung, *Anal. Chem.*, 57 (1985) 2606.
19 R. E. Synovec and E. S. Yeung, *J. Chromatogr.*, 368 (1986) 85.

CHROM. 20 953

Note

Determination of terpenic compounds in the essential oil from *Satureja thymbra* L. growing in Sardinia

WANDA CAPONE, CARLO MASCIA*, MARINELLA MELIS and LORENZO SPANEDDA

Istituto di Chimica Farmaceutica, Tossicologica ed Applicata, Universita' di Cagliari, Via Ospedale 72, 09124 Cagliari (Italy)

(First received March 11th, 1988; revised manuscript received August 9th, 1988)

The essential oils from numerous species of the *Satureja* genus have been widely investigated in the last 20 years[1–17]. Detailed studies have been carried out on *S. parvifoglia*[1], *S. odora*[2], *S. hortensis*[3–5], *S. horvatii*[6–8], *S. boliviana*[9], *S. adamovicii*[10] but, most of all, on *S. montana*[11–17], the gastrosedative and digestive properties of which are well known and appreciated in folk medicine, and whose leaves are used to spice some foods[18,19]. The essential oil from *S. montana* is also employed in liquor manufacture[20] and, recently, its antifungal and antimicrobial activities have been pointed out[21].

In the current literature a few references can be found to research on *S. thymbra* growing in Israel[22,23] and Greece[24] but, to our knowledge, data are lacking on the Italian variety, present exclusively near Cagliari in Sardinia.

For this reason, and also in view of possible pharmaceutical applications, we started our investigation aimed, as a first step, at the identification and dosage of the main components of the essential oil from Sardinian *S. thymbra*.

EXPERIMENTAL

Samples and apparatus

Branches, leaves and apeces, collected in May, June and July, that is before, during and after the blossoming season, were steam distilled for *ca.* 3 h until the complete extraction of the oil was achieved. The oil from each sampling was then separated from the water and, after its specific weight had been determined, transferred to a glass bottle and stored in the dark at 4°C until further analysis.

A Carlo Erba Model 4200 gas chromatograph was used, fitted with flame ionization detection (FID), a split–splitless injector and a linear temperature programmer; the chromatograph was connected to a recorder–integrator (Hewlett-Packard 3390 A). Two different fused-silica columns were employed, loaded respectively with Carbowax 20M liquid phase (A) (column dimensions: 25 m × 0.32 mm I.D.), and CP-Sil 5 liquid phase (B) (column dimensions: 25 m × 0.34 mm I.D.). The operating conditions were; for column A, injector, 230°C, detector, 250°C; initial column temperature 55°C for 5 min, raised at 5°C/min to 200°C and held for 5 min; carrier gas, nitrogen; split ratio 1:40; volume injected 0.2 μl; for column B, injector, 230°C; detec-

tor 250°C; initial column temperature 55°C for 12 min, raised at 5°C/min to 200°C and held for 5 min; carrier gas, nitrogen; split ratio 1:24; volume injected, 0.2 μl.

An Hewlett-Packard Model 5970 A gas chromatograph–mass spectrometer was also used, equipped with a fused-silica column packed with SE-30 liquid phase (C) (column dimensions: 12 m × 0.22 mm I.D.), under the following conditions; injector 230°C; detector 260°C; initial column temperature, 55°C for 12 min, raised at 5°/min to 200°C and held for 3 min; carrier gas, helium; split ratio 1:10; volume injected, 0.1 μl.

Procedure

A stock solution was prepared containing *ca.* 1000 mg/l in diethyl ether of the following compounds: borneol, camphene, carvacrol, β-caryophyllene, carvone, 1,8-cineole, *p*-cymene, limonene, linalool, β-mycrene, α-pinene, β-pinene, α-terpinene, γ-terpinene and thymol. Working solutions for the calibration graph were then obtained by adding 1 ml of the solution containing the internal standard (menthol) to adequate volumes of the stock solution (from 20 to 200 μl) and by diluting to 10 ml in dietyhl ether.

Each sample was injected in triplicate and analyzed according to the operating conditions listed above. The identities of the peaks were confirmed by comparison of their retention times with those of authentic samples on both column A and B and, when possible, by agreement of their mass spectra, obtained by gas chromatography–mass spectrometry (GC–MS) using column C, with those present in the literature. A mass spectrum of γ-terpinene is shown, as an example, in Fig. 1.

The quantitative analysis was performed, as indicated above, using internal standardization.

RESULTS AND DISCUSSION

The same fourteen terpenic compounds were identified either by GC–FID or by GC–MS in the samples from the three different stages of the vegetative life of *S*.
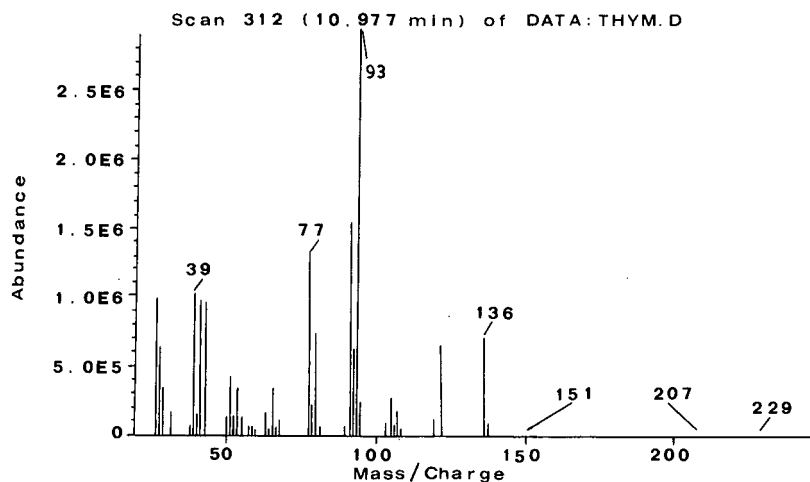
Fig. 1. Mass spectrum of γ-terpinene.

thymbra L. Constituents of the essential oils are listed in Table I according to increasing retention times on column A; this showed the best resolution power, except for limonene and 1,8-cineole which were better resolved on column B.

The concentrations and the absolute percentages (according to the specific weight of each oil) are reported for each terpene. The qualitative composition of the oils appears to be constant in the three stages, but there are notable differences in the percentages of several compounds. γ-Terpinene, thymol and p-cymene always show, in this order, the highest concentration and represent, as a whole, from 52.20 to 60.31% of the entire oil.

It must be noted that in all our samples β-caryophyllene was found in considerable amount and, on the other hand, carvone was lacking; however, in GC–MS analysis a compound was detected, with a retention time near to that of carvone and a molecular weight equal to 164, that could be an oxidized form of the same terpene.

Carvacrol, in contrast to reports by numerous authors on other species of the *Satureja* genus[5,68,11,12,15,16] and on *S. thymbra* L.[22–24] was found in low percentages.

The qualitative composition of the essential oil from Israelian *S. thymbra* L.[22,23] is similar to the Sardinian one: γ-terpinene, thymol and p-cymene are the most abundant constituents and other terpenes, not identified in the essential oil analyzed by us, are present only in traces, like terpinolene, or in very low percentages, like humulene. The same analogy exists, with regard to the main components, between the essential oil from Sardinian *S. thymbra* L. and the Grecian one which differentiates for the lack of β-pinene and limonene and for the presence of other terpenic compounds such as fenchone, cadinene, nerol, geraniol and caryophyllene oxide, though in traces or in very low amounts.

TABLE I

CONCENTRATIONS AND PERCENTAGES OF THE TERPENES IDENTIFIED IN THE ESSENTIAL OIL FROM *S. THYMBRA* L. COLLECTED BEFORE (MAY), DURING (JUNE) AND AFTER (JULY) THE BLOSSOMING SEASON

Peak	Compound	May		June		July	
		mg/ml	*%*	*mg/ml*	*%*	*mg/ml*	*%*
1	α-Pinene	19.9	2.38	48.4	5.69	21.5	2.38
2	Camphene	7.2	0.86	15.4	1.81	8.9	1.00
3	β-Pinene	12.2	1.46	28.6	3.36	13.0	1.44
4	β-Myrcene	14.1	1.69	17.8	2.09	15.1	1.68
5	α-Terpinene	24.3	2.92	22.9	2.69	25.5	2.83
6	Limonene	6.7	0.80	9.0	1.06	6.7	0.75
7	1,8-Cineole	3.9	0.47	4.4	0.52	4.3	0.48
8	γ-Terpinene	232.9	27.93	229.6	26.98	264.2	29.39
9	p-Cymene	74.6	8.94	76.5	8.99	78.7	8.76
10	Linalool	1.7	0.20	3.7	0.44	1.4	0.15
11	β-Caryophyllene	44.4	5.32	61.9	7.27	22.6	2.52
12	Borneol	9.5	1.14	16.8	1.97	9.9	1.10
13	Thymol	127.9	15.33	157.0	18.45	199.2	22.16
14	Carvacrol	8.6	1.03	16.3	1.92	12.3	1.36

In conclusion the relatively high percentage of β-caryophyllene, the absence of carvone and the low percentage of carvacrol appear to be peculiar and could be useful for the characterization of the essential oil from *S. thymbra* L. growing in Sardinia. Moreover, on the basis of the known biological activity of a number of constituents of the samples of this essential oil, it may be of pharmaceutical use.

REFERENCES

1 D. L. Acosta de Iglesias, M. E. Lalli de Viana and J. A. Retamar, *Riv. Ital. Essenze, Profumi, Piante Off., Aromat., Syndets, Saponi, Cosmet., Aerosols*, 60 (1978) 643.
2 D. L. Acosta de Iglesias and J. A. Retamar, *Riv. Ital. Essenze, Profumi, Piante Off., Aromat., Syndets, Saponi, Cosmet., Aerosols*, 60 (1978) 548.
3 G. M. Nano, A. Martelli, M. Gallino and G. Biglino, *Atto Accad. Sci. Torino*, 102 (1968) 1.
4 F. Chialva, P. A. P. Liddle, F. Ulian and P. de Smedt, *Riv. Ital. Essenze, Profumi, Piante Off., Aromat., Syndets, Saponi, Cosmet., Aerosols*, 62 (1980) 297.
5 K. S. Timchuk, *Ser. Biol. Khim. Nauk*, 6 (1981) 73.
6 M. J. Gasic and R. Palic, *Glas. Hem. Drus. Beograd.*, 48 (1983) 677.
7 S. Pavlovic, R. Ivanic, K. Savin, P. Zivanovic, R. Jancic, D. Milinkovic and S. Vujcic, *Arh. Farm.*, 33 (1983) 287.
8 S. Pavlovic, P. Zivanovic, R. Jancic, S. Vujcic, G. A. Kuznetsova and A. L. Shevarda, *Zb. Prir. Nauke*, 66 (1984) 5.
9 L. B. de Jmenez, *Rev. Boliv. Quim.*, 5 (1985) 32.
10 S. Pavlovic, P. Zivanovic, A. L. Shevarda, G. A. Kuznetsova and R. Jancic, *Arh. Farm.*, 36 (1986) 177.
11 B. Stancher and L. Poldini, *Giorn. Bot. Ital.*, 103 (1969) 65.
12 J. Garnero, P. Buil and J. Pellecuer, *Riv. Ital. Essenze, Profumi, Piante Off., Aromat., Syndets, Saponi, Cosmet., Aerosols*, 63 (1981) 344.
13 R. Palic, S. Gligorijevic and D. Pejcinovic, *Acta Biol. Med. Exp.*, 7 (1982) 9.
14 L. Coassini Lokar, V. Maurich and L. Poldini, *Webbia*, 37 (1983) 197.
15 C. Cazin, R. Jonard, P. Allain and J. Pellecuer, *C. R. Acad. Sci.*, 300 (1985) 237.
16 B. Bellomaria and G. Valentini, *Giorn. Bot. Ital.*, 119 (1985) 81.
17 A. L. Shevarda, G. A. Kuznetsova, S. Pavlovic, P. Zivanovic and R. Jancic, *Arh. Farm.*, 36 (1986) 167.
18 P. Guarrera, *Riv. Ital. Essenze, Profumi, Piante Off., Aromat., Syndets, Saponi, Cosmet., Aerosols*, 63 (1981) 222.
19 B. Bellomaria, *Giorn. Bot. Ital.*, 58 (1982) 113.
20 M. Paulet and D. Felisaz, *Riv. Ital. Essenze, Profumi, Piante Off., Aromat., Syndets, Saponi, Cosmet., Aerosols*, 53 (1971) 618.
21 M. Melgari, A. Albasini, A. Provvisionato, A. Bianchi, G. Vampa, P. Pecorari and M. Rinaldi, *Fitoterapia*, 56 (1985) 85.
22 U. Ravid and E. Putievsky, *Planta Med.*, 49 (1983) 248.
23 U. Ravid and E. Putievsky, *Planta Med.*, 53 (1985) 337.
24 S. M. Philianos, T. Andriopoulou-Athanassoula and A. Loukis, *Int. J. Crude Drug Res.*, 22 (1984) 145.

CHROM. 20 985

Note

Preparative separation by high-performance liquid chromatography of an extract of oak wood and determination of the composition of each fraction

J.-L. PUECH*, P. RABIER and M. MOUTOUNET

Laboratoire des Polymères et des Techniques Physico-chimiques, Institut des Produits de la Vigne, Institut National de la Recherche Agronomique, 9 Place Viala, 34060 Montpellier Cedex (France)

(First received August 1st, 1988; revised manuscript received September 13th, 1988)

Oak wood is used to age spirits both because of its mechanical properties, as it provides a good seal, and because of its effect on the organoleptic properties of the spirits. Among the major constituents of this type of wood, lignin and tannins play a major role in the sensory aspects of spirits[1–5]. In this context, interest is centred on extractables in the oak wood. Low-molecular-weight substances derived from oak wood tannins include gallic and ellagic acids, which are found in methanol-containing[6] or acetone–water extracts[7,8] and in ethyl acetate extracts of commercial tannins[9]. Chen[7] and Seikel *et al.*[8] noted the presence of gallotannins and ellagitannins. Monties[10] estimated that the ellagic tannin content in heartwood was 75.4 mg/g after extraction with water–methanol (20:80). Mayer and co-workers[11–14] determined the structure of these ellagitannins in *Quercus sessiliflora* and reported that they were castalin, castalagin, vescalin and vescalagin. Hydrolysis of castalagin gives ellagic acid and castalin and that of vescalagin gives ellagic acid and vescalin. Castalagin and vescalagin are isomers; isomerization involves an epimerization at the C-1 position of the sugar. In more recent work using high-performance liquid chromatography (HPLC) tannins were separated from oak wood[15].

Simple phenols connected with the biosynthesis of lignin and present in oak wood include vanillin, syringaldehyde, coniferaldehyde and sinapaldehyde[8,16–18]. A more complex group of substances referred to as lignan is found in wood; the compound identified in oak wood is lyoniresinol[8,19]. Scopoletin is dominant among the coumarins[20,21] in comparison with umbelliferone and methylumbelliferone. The use of preparative or semi-preparative HPLC has made it possible to separate the phenolic compounds found in various plants[20–25].

The purpose of the work described here was to separate oak wood extractables which were soluble in water–ethanol. The content by weight was determined in each fraction, together with the amount of methoxy groups representing the soluble lignin fraction and finally the total phenolics content. In addition, a direct injection analytical HPLC technique was used to identify and especially to determine certain phenolic compounds previously reported in the literature.

EXPERIMENTAL

Sample

Chips obtained from Limousin oak wood dried in air for 3 years were macerated for 24 h in water–ethanol (45:55, v/v) and adjusted to pH 4.25 with acetic acid. The solution was concentrated by evaporation and then freeze-dried to obtain a powder.

Determination of methoxy groups

The methoxy groups were separated by boiling in the presence of hydriodic acid, leading to the formation of alkyl iodides. These compounds were removed by a flow of carbon dioxide and trapped in toluene[26]. Determination was carried out using gas chromatograpy to separate methyl and ethyl iodides[27].

Total phenolic compounds

Folin–Ciocalteu reagent[28] was used with gallic acid as the standard. The results are expressed in milligrams gallic acid equivalent.

Preparative liquid chromatography

A Modulprep (Jobin-Yvon) system apparatus was used, fitted with a stainless-steel column (500 mm × 40 mm I.D.). The lower part of the column was fitted with a piston to permit axial compression of the stationary phase [LiChroprep RP-18 (15–25 μm) bonded silica] at 10^6 Pa. A 1-g amount of freeze-dried preparation was placed at the top of the column for each analysis. Detection was carried out at 280 nm. Elution was carried out using a step gradient with methanol–water mixtures from 10:90, increased in 10% (v/v) steps to reach absolute methanol at a flow-rate of 40 ml/min; this technique gave ten fractions (Fig. 1).
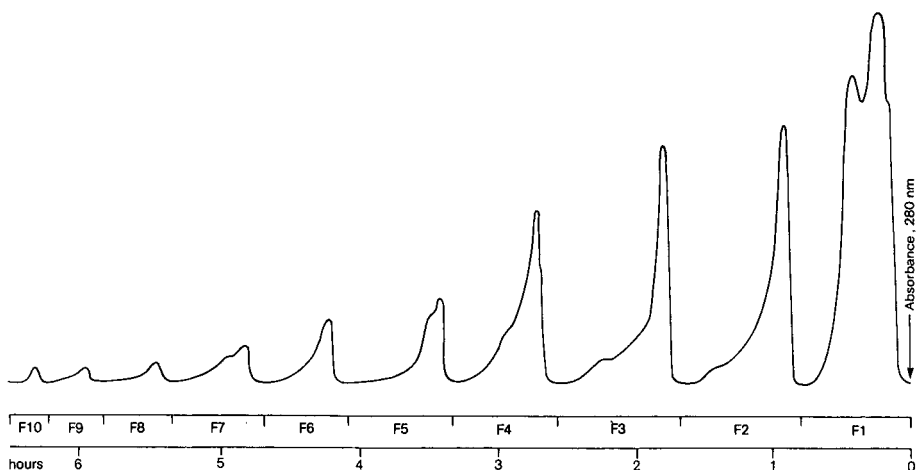
Fig. 1. Separation of ethanol–water extract of oak wood by preparative HPLC. Column, LiChroprep RP-18 (15–25 μm) (50 cm × 40 mm I.D.); mobile phase, methanol–water (10:90) for F_1, methanol–water (20:80) for F_2, etc.; Flow-rate, 40 ml min^{-1}; UV detection, 280 nm.

Analytical liquid chromatography

The fractions obtained were analysed with an apparatus consisting of a Gilson M231 automatic injector, Waters (Millipore, Bedford, MA, U.S.A.) M6000A and M510 pumps, a Waters M680 gradient programmer, a Waters M490 detector operating at two wavelengths (280 and 320 nm), a Shimadzu RF530 fluoroescence detector and an Enica 21 (Delsi) recorder–integrator. A 250 mm × 4 mm I.D. Knauer Vertex column was used packed with LiChrospher RP-18 (5 μm); it was maintained at 40°C in a Waters Model CX 4-2 oven. Solvent A was water–formic acid (98:2) and solvent B consisted of 700 ml of methanol containing 2% formic acid made up to 1000 ml with solvent A. Samples were filtered through a Millipore membrane (0.45 μm) and degassed in an ultrasonic bath; the flow-rate was 1 ml/min. Initially solvent A was used; after 3 min the proportion of B was increased to 100% over a period of 72 min using a linear gradient.

Solutes

Different samples of gallic acid, vanillic acid, syringic acid, ellagic acid, vanillin, syringaldehyde and scopoletin were purchased from Fluka (Buchs, Switzerland). Coniferaldehyde and sinapaldehyde were isolated using the method proposed by Alibert and Puech[29]. Lyoniresinol was a generous gift from Dr. Nabeta (University of Agriculture and Veterinary Medicine, Hokkaido, Japan) and castalin, castalagin and vescalagin were a generous gift from Dr. Mayer (University of Heidelberg, Heidelberg, F.R.G.).

Solvents

HPLC-grade solvents were used.

RESULTS AND DISCUSSION

Weight distribution of fractions and chemical characteristics

Preparative chromatography was used to separate into ten fractions all the

TABLE I

AMOUNTS OBTAINED FROM 5 g OF A FREEZE-DRIED PREPARATION OF ETHANOL–WATER EXTRACT OF OAK WOOD: DISTRIBUTION OF METHOXY GROUPS AND TOTAL PHENOLIC COMPOUNDS IN THE VARIOUS FRACTIONS

Fraction	Amount in each fraction (mg)	Percentage	OCH_3 in each fraction (mg)	Percentage of OCH_3	Total phenolics in each fraction (mg)	Percentage of total phenolics
F_1	2578	53.6	6.0	4.7	1425.0	64.5
F_2	543	11.3	14.1	10.9	308.9	14.0
F_3	436	9.1	30.0	23.3	199.7	9.0
F_4	324	6.8	25.2	19.6	158.0	7.1
F_5	279	5.8	23.5	18.2	90.6	4.1
F_6	263	5.4	18.7	14.6	19.5	0.5
F_7	261	5.4	9.1	7.0	7.0	0.3
F_8	53	1.1	1.8	1.4	1.7	0.07
F_9	30	0.6	0.3	0.2	0.7	0.03
F_{10}	45	0.9	0.2	0.1	1.0	0.04
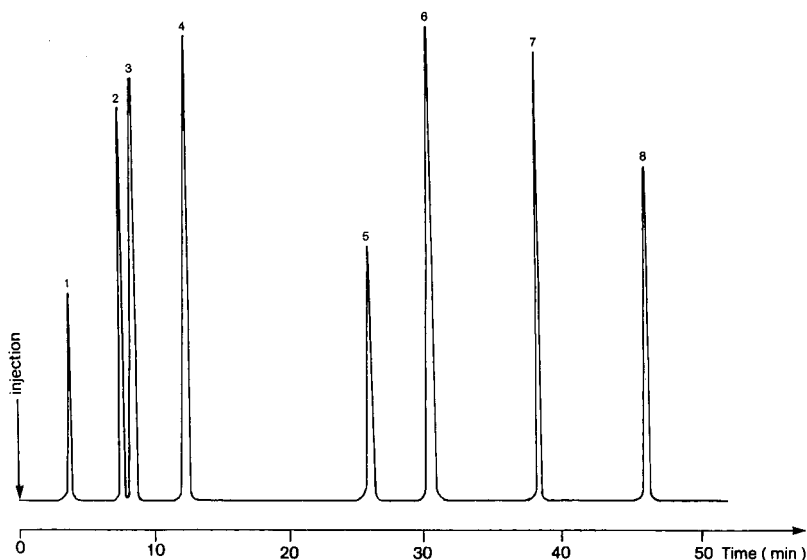
Fig. 2. HPLC resolution of a standard mixture of phenolic compounds. Column, 250 mm × 4 mm I.D.; stationary phase, LiChrospher RP-18 (5 μm); mobile phase, (A) water–formic acid (98:2) (B) 70% methanol–formic acid (98:2) + 30% A, programmed from A (3 min) to B at 75 min; flow-rate, 1 ml min^{-1}; UV detection, 280 nm. Solutes: 1 = castalin; 2 = gallic acid; 3 = vescalagin; 4 = castalagin; 5 = vanillic acid; 6 = syringic acid; 7 = lyoniresinol; 8 = ellagic acid.

compounds present in the freeze-dried preparation obtained after maceration of oak wood in ethanol–water solution. The recovery was 96.3% (Table I). Fraction F_1, the largest by weight, comprised 53.6%; the amounts in the other fractions decreased with increased methanol content in the eluent. The polarity of the substances was thus very widely distributed with eluents containing from 10 to 70% of methanol. The abundance of fraction F_1 demonstrated the predominance of polar substances.

Determination of the methoxy groups was used to assess the lignin content of the various fractions. Fraction F_3 contained the highest methoxy group content (Table I); 75% of these groups were present in the fractions obtained using solvents containing 30–60% of methanol.

With regard to total phenolic compounds, these predominated in fraction F_1; this fraction alone represented 64.5% of the phenolics (Table I). The phenolics contents of the other fractions decreased as the methanol content in the eluent increased.

All these results show that the analysis of each fraction is necessary in order to judge the chemical composition.

Phenolic compounds in the various fractions

The analytical separation of a standard mixture containing castalin, gallic acid, vescalagin, castalagin, vanillic acid, syringic acid, lyoniresinol and ellagic acid with detection at 280 nm is shown in Fig. 2. Aromatic aldehydes (vanillin, syringaldehyde, coniferaldehyde and sinapaldehyde) were detected at 320 nm. For the detection of scopoletin the excitation wavelength was 325 nm and the emission wavelength 454 nm.

TABLE II

PHENOLICS CONTENTS OF THE VARIOUS FRACTIONS OF THE ETHANOL–WATER EXTRACT

Compound	Fraction	Content (mg)
Castalin	F_1	94.1
Gallic acid	F_1	38.26
Vescalagin	F_1	799.18
Castalagin	F_1	488.78
Vanillic acid	F_2	0.85
Syringic acid	F_2	0.77
Vanillin	F_3	0.31
Syringaldehyde	F_3	0.71
Lyoniresinol	$F_3 + F_4$	23.9
Scopoletin	$F_3 + F_4$	0.091
Coniferaldehyde	F_4	0.29
Sinapaldehyde	F_4	0.51
Ellagic acid	$F_4 + F_5$	41.8

Each fraction place in ethanol–water (55:45) solution was analysed by HPLC. Fraction F_1 was found to contain mainly ellagitannins, confirming the predominance of total phenolic compounds in this fraction. Castalin, castalagin and vescalagin were identified. The vescalagin and castalagin contents in the extract were 799 and 488 mg, respectively (Table II). The castalin content was lower. In addition to these compounds, gallic acid was identified in this fraction. Subsequent fractions contained lignin derivatives consisting of phenolic acids on the one hand and aromatic aldehydes on the other. Fraction F_2 contained low concentrations of vanillic and syringic acid. The amount extracted depended on the ethanol content of the maceration solvent and also on the acidity of the medium[30]; in addition, these compounds can be found in wood in ester form [8]. The benzoic-type phenolic aldehydes vanillin and syringaldehyde were found in fraction F_3. These compounds were also identified in oak heartwood and in sapwood[8].

Both fractions F_3 and F_4 contained the lignan lyoniresinol; this was found at 23.9 mg in the ethanol–water extract of oak wood. Scopoletin were also present in these two fractions but in small amounts, necessitating spectrofluorimetric measurement. This substance was present in larger amounts in American oak wood (*Quercus alba*)[21] than in European woods (*Quercus robur and Quercus petraea*). Fraction F_4 consisted of the cinnamic-type phenolic aldehydes coniferaldehyde and sinapaldehyde identified in oak wood[8,16] and in methanol–water solutions[30]. Fractions F_4 and F_5 contained free ellagic acid[7,8,20], which is a constituent of ellagitannins. None of the substances studied was found in fractions F_6–F_{10}. Work on the identification of these compounds should therefore be undertaken.

CONCLUSION

Use of preparative HPLC made it possible to separate an ethanol–water extract of oak wood and to determine the amounts of methoxy groups in each fraction and total

phenolic compounds where then determined. In addition, new compounds were identified and quantified in these fractions, in particular ellagitannins and a lignan. This methodology makes it possible to obtain sufficient amounts for the identification and assay of a large number of phenolic compounds in oak wood extracts.

REFERENCES

1 E. M. Schpritzman and D. A. Novokhatko, *Sadovod. Vinograd. Vinodel. Mold.*, 2 (1956) 47.
2 I. M. Skourikhin, *Vinodel. Vinograd. SSSR*, 22 (1962) 17.
3 I. A. Egorov and R. Kh. Egofarova, *Prikl. Biokhim. Mikrobiol.*, 1 (1965) 680.
4 S. Baldwin and A. A. Andreasen, *J. Assoc. Off. Anal. Chem.*, 57 (1974) 940.
5 J.-L. Puech, C. Jouret and B. Goffinet, *Sci. Aliment.*, 5 (1985) 379.
6 A. Scalbert, B. Monties, J.-L. Dupouey and M. Becker, *Groupe Polyphénol*, 13 (1986) 617.
7 C.-L. Chen, *Phytochemistry*, 9 (1970) 1149.
8 M. K. Seikel, F. D. Hostettler and G. J. Niemann, *Phytochemistry*, 10 (1971) 2249.
9 M.-M. Salagoïty-Auguste, C. Tricard, F. Marsal and P. Sudraud, *Am. J. Enol. Vitic.*, 37 (1986) 301.
10 B. Monties, *Connaissance Vigne Vin*, (1987) 39.
11 W. Mayer, W. Gabler, A. Reiester and H. Korger, *Justus Liebigs Ann. Chem.*, 707 (1967) 177.
12 W. Mayer, H. Seitz and J. Jochims, *Justus Liebigs Ann. Chem.*, 721 (1969) 1986.
13 W. Mayer, H. Seitz, J. Jochims, K. Schauerte and G. Schilling, *Justus Liebigs Ann. Chem.*, 751 (1971) 60.
14 W. Mayer, *Leder*, 12 (1971) 277.
15 A. Scalbert, B. Monties and J. M. Favre, *Phytochemistry*, in press.
16 J. F. Guymon and E. A. Crowell, *Qual. Plant. Mater. Veg.*, 12 (1968) 320.
17 M. Lehtonen and H. Suomalainen, *Process Biochem.*, 14 (1979) 5.
18 J.-L. Puech, *Am. J. Enol. Vitic.*, 32 (1981) 111.
19 K. Nabeta, J. Yonekubo and M. Mikaye, *Mokuzai Gakkaishi*, 33 (1987) 408.
20 M.-H. Salagoïty-Auguste, *Connaissance Vigne Vin*, (1987) 101.
21 J.-L. Puech and M. Moutounet, *J. Assoc. Off. Anal. Chem.*, 71 (1988) 512.
22 M. A. Dubois and A. Zoll, *Groupe Polyphénols*, 11 (1982) 328.
23 J. Bakker and C. Timberlake, *J. Sci. Food Agric.*, 36 (1985) 1315.
24 D. Magnolato, R. Gujer and R. Self, *Groupe Polyphénols*, 13 (1986) 513.
25 W. Oleszek, C. Lee, A. Jaworski and K. Price, *J. Agric. Food Chem.*, 36 (1986) 430.
26 L. Deibner, C. Jouret and J.-L. Puech, *Ind. Aliment. Agric.*, 93 (1976) 401.
27 J.-L. Puech, C. Jouret and L. Deibner, *Ind. Aliment. Agric.*, 95 (1978) 13.
28 J. Blouin, L. Llorca, F. Montreau and J. Dufour, *Connaissance Vigne Vin*, 6 (1972) 405.
29 G. Alibert and J.-L. Puech, *J. Chromatogr.*, 124 (1976) 369.
30 J.-L. Puech, *Am. J. Enol. Vitic.*, 38 (1987) 236.

Note

High-performance liquid chromatographic determination of carbaryl in fruit juices

RODNEY J. BUSHWAY

Department of Food Science, 102 B Holmes Hall, University of Maine, Orono, ME 04469 (U.S.A.)

(Received September 13th, 1988)

Carbaryl (Sevin) is a broad-spectrum carbamate insecticide that is till widely applied to fruit and vegetable crops because of its low acute mammalian toxicity (the oral LD_{50} to rats is 560 mg/kg) and its effectiveness against insects. However research during the last few years has shown that carbaryl has possible chronic toxic effects[1–4]. In fact the United States Department of Agriculture has recently changed the health hazard status of carbaryl to a higher risk category[5]. Because of possible chronic toxic effects and because of it wide distribution, there is a need to know if and to what extent carbaryl may be present in process foods and in particular fruit juices.

Methods available to analyze carbaryl focus on the use of high-performance liquid chromatography (HPLC) because of the sensitivity and non-thermal porperties. Numerous HPLC methods have been developed for carbaryl analysis (reviewed by Bushway[6] and Kawai *et al.*[7]) in water, soil, biological samples and raw fruit and vegetable crops, but no procedure for fruit juices was described.

This paper describes an HPLC method that is rapid, accurate and sensitive for the determination of carbaryl in several kinds of fruit juices at the low ppb* level.

EXPERIMENTAL

Solvents and pesticides

All solvents were HPLC grade. The acetonitrile and methanol were purchased from VWR (Bridgeport, CT, U.S.A.). HPLC water was prepared by passing glass-distilled water through a Barnstead water purifying system (Fisher Scientific, Pittsburg, PA, U.S.A.). Carbaryl with a purity of 99.9% was obtained from the U.S. Environmental Protection Agency (Research Triangle Park, NC, U.S.A.).

Juice samples

All juices were commercial samples obtained from local supermarkets in Bangor, ME, U.S.A.

Standard preparation

Stock solutions of carbaryl were prepared in methanol at 0.94 mg/ml. Spiking solutions were made by removing a 0.25-ml aliquot of stock solution and placing it

---

* Throughout the article the American billion (10^9) is meant.

into a 50-ml volumetric flask. The solution was brought to volume with methanol and appropriate aliquots were removed to spike juice samples.

Apparatus

The HPLC system consisted of a Valco injector (Vici Instruments, Houston, TX, U.S.A.) with 20- and 50-μl loops, a Waters 510 pump (Waters Assoc., Milford, MA, U.S.A.), a Hewlett-Packard 1040A photodiode array detector/integrator system (Hewlett-Packard, Avondale, PA, U.S.A.). The column was an Ultremex C_{18}, 5-μm, 150 mm × 4.6 mm I.D. (Phenomenex, Palos Verdes, CA, U.S.A.). The mobile phase was methanol–water–acetonitrile (40:45:15) at a flow-rate of 1 ml/min. Detection was at 224 nm and 0.04 absorbance units full scale (a.u.f.s.). Temperature was ambient and pressure 2500 p.s.i.

Analytical procedure

Direct analysis. Juice samples as received and/or spiked were filtered (1 ml) through a 0.45-μm, 25-mm nylon filter (Gelman, Ann Arbor, MI, U.S.A.) and injected 20 or 50 μl directly into the HPLC system. Juices containing more than 70 ppb carbaryl can be analyzed by direct injection.

Trace enrichment. Juice samples (60 ml) as received and/or spiked were passed through a C_{18} Sep-Pak cartridge using a syringe. The Sep-Pak cartridge was activated by prewetting it with 4 ml of methanol followed by 5 ml of water. To elute the carbaryl adsorbed on the cartridge, 5 ml acetonitrile–water (25:75) were passed through first and discarded followed by 2 ml of acetonitrile–water (75:25). This fraction was injected (20–50 μl) into the HPLC system.

Recovery studies

Juice samples were spiked at levels ranging from 12.6 to 157.8 ppb and either passed through the C_{18} Sep-Pak cartridges or directly injected to test recovery.

Purity check

UV spectral scans from 190 to 350 nm were taken on all carbaryl peaks at three different locations on the peak to check purity.

RESULTS AND DISCUSSION

A typical chromatogram of a juice sample is shown in Fig. 1. It takes approximately 4 min for carbaryl to elute. Interferences to carbaryl were checked on all juices by taking UV spectral scans from 190 to 350 nm at three points on the peak by employing a photodiode array detector.

Table I lists the results of carbaryl spiked juice study. Juices containing no detectable amount of carbaryl were spiked at concentrations ranging from 12.6 to 157.8 ppb. Samples that contain between 5 and 70 ppb are best analyzed if they are concentrated by C_{18} Sep-Pak cartridges while direct injection works well on samples with more than 70 ppb. Average recoveries ranged from 90.4 to 100.6% with most above 96.6%. These excellent recoveries indicate that for the concentration step there was good binding of carbaryl to the Sep-Pak cartridge with very little if any irreversible binding and that for direct injection there was no juice matrix effect on peak area.
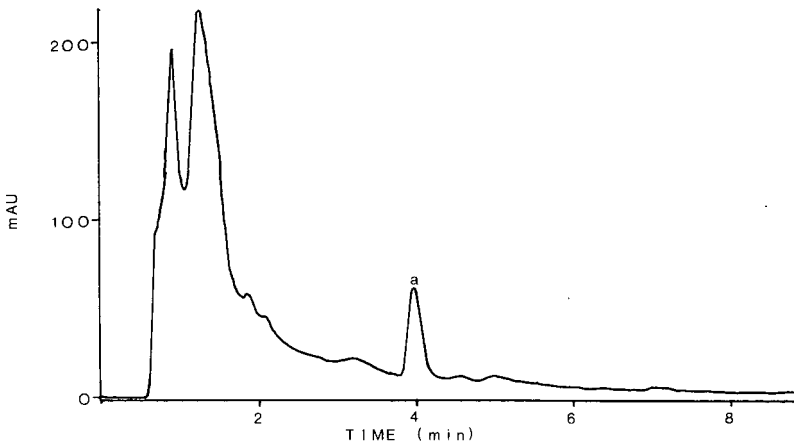
Fig. 1. Chromatogram of apple cherry juice containing 98.3 ppb carbaryl: direct injection. Solvent system, methanol–water–acetonitrile (40:45:15); flow-rate, 1 ml/min; detector sensitivity, 0.04 a.u.f.s.; 224 nm; amount injected 50 μl. Peak: a = carbaryl.

The coefficients of variation (C.V.) ranged from 13.8 to 1.7% which are good repeatable values for a residue method. Especially considering these values were obtained from samples analyzed on different days. Of course the best coefficients of variation were from direct injection which was expected since there were fewer steps.

The break-through amount for carbaryl had been determined previously for C_{18} Sep-Pak cartridges[6] and it was not repeated. However, it was demonstrated that only two 60-ml aliquots of juice could be passed through the cartridges before the recovery of carbaryl began to decrease (about 10% with the third aliquot).

The detector response for area was linear from 1 to 500 ng for carbaryl. α-Naphthol was separated from carbaryl in this method but because of the acidic conditions of the juice one would not expect to find α-naphthol present.

A survey was performed using this method to determine how much carbaryl might be present in fruit juices. Forty-seven samples were analyzed (Table II) of which twenty showed detectable levels of carbaryl (detection limit 5 ppb). Of these twenty the lowest amount found was 6.7 ppb and the highest was 175.0 ppb. Fifteen

TABLE I

CARBARYL ANALYSIS OF SPIKED JUICE SAMPLES BY HPLC

Sample	$n^{\star}$	Type of analysis	Level spiked (ppb)	Average recovery (%)	C.V. (%)
1	7	Sep-Pak	12.6	90.4	13.9
2	19	Sep-Pak	25.2	100.6	10.1
3	3	Sep-Pak	98.0	96.6	1.7
4	3	Direct injection	78.9	96.7	2.3
5	3	Direct injection	157.8	98.3	6.4

* n = Number of samples analyzed.

TABLE II

ANALYSIS OF COMMERCIAL FRUIT JUICES FOR CARBARYL

Sample	Carbaryl found (ppb)	Sample	Carbaryl found (ppb)
Apple cherry 1	ND*	Apple pineapple 2	86.7
Apple cherry 2	ND	Mixed fruit 1	8.3
Apple cherry 3	ND	Mixed fruit 2	6.7
Apple cherry 4	ND	Mixed fruit 3	ND
Apple cherry 5	98.3	Mixed fruit 4	ND
Apple cherry 6	106.7	Mixed fruit 5	ND
Apple cherry 7	118.3	Mixed fruit 6	24.2
Apple cherry 8	ND	Orange apple banana 1	74.0
Apple cherry 9	86.7	Apple apricot 1	136.7
Apple cherry 10	50.0	Apple apricot 2	175.0
Apple cherry 11	ND	Orange 1	ND
Apple cherry 12	ND	Apple 1	ND
Apple cherry 13	115.0	Apple 2	ND
Apple cherry 14	123.0	Apple 3	8.3
Apple cherry 15	113.3	Apple 4	131.7
Apple cherry 16	ND	Apple 5	118.3
Apple cherry 17	ND	Apple 6	8.3
Apple grape 1	ND	Apple 7	ND
Apple grape 2	ND	Apple banana 1	ND
Apple grape 3	ND	Cranberry 1	ND
Apple grape 4	ND	Cranraspberry	ND
Apple grape 5	ND	Fruit blend raspberry 1	ND
Apple grape 6	ND	V-8 1	ND
Apple pineapple 1	70.0		

* ND = None detected at a detection limit of 5 ppb.

had concentrations of 50 ppb or more. The levels of carbaryl found were well below the U.S.A. tolerance of 5 ppm. However, many of these juices were baby food products which may be of some concern; also, U.S.A. tolerances for carbaryl were set several years ago. All twenty juices that had detectable levels of carbaryl had some or all apple juice present. Thus this would tend to indicate that the carbaryl may be coming mostly from treated apples.

CONCLUSION

Because of the complex matrix of fruit juice compared to water, one cannot analyze carbaryl by direct injection or C_{18} Sep-Pak cartridges at as low as a concentration as water. However, carbaryl does have a large enough extinction coefficient at 223 nm that even with a complex matrix like fruit juice one can analyze for carbaryl at rather low levels with only simple clean-up.

ACKNOWLEDGEMENTS

REFERENCES

1 R. A. Branch and E. Jacqz, *Am. J. Med.*, 80 (1986) 659.
2 R. A. Branch, *Am. J. Med.*, 83 (1987) 1169.
3 Anonoymous, *J. Am. Med. Assoc.*, 260 (1988) 959.
4 L. H. Abrahamsen and M. A. Jerofsky, *Appl. Environ. Microbiol.*, 55 (1983) 1555.
5 Anonoymous, *Food Chemical News*, 30(26) (1988) 48.
6 R. J. Bushway, *J. Chromatogr.*, 211 (1981) 135.
7 S. Kawai, K. Goto, K. Kano and T. Kubota, *J. Chromaogr.*, 442 (1988) 451.

Note

Determination of isoquinoline alkaloids from *Peumus boldus by* high-performance liquid chromatography

PIERGIORGIO PIETTA* and PIERLUIGI MAURI

Dipartimento di Scienze e Tecnologie Biomediche, Sezione di Chimica Organica, Via Celoria 2, 20133 Milan (Italy)

and

ENRICO MANERA and PIERLUIGI CEVA

S.I.T., Via Cavour 70, 27035 Mede (Italy)

(Received August 12th, 1988)

Peumus boldus has long been used as a folk medicine[1] and it is still reported in many Pharmacopoeias[2]. It has been shown that its pharmacological activity is due to the isoquinoline alkaloid fraction[3] (Fig. 1).

Most published analyses of *Peumus boldus* alkaloids have involved separations by thin-layer chromatography (TLC)[4,5], while the total alkaloid content has been determined by titrimetric[6] and spectrophotometric[7] methods. The main alkaloid boldine has been determined by high-performance liquid chromatography (HPLC)[8] and by voltammetry[9].

All these procedures require time-consuming steps such as liquid–liquid partition, where the complete extraction of the alkaloids from buffered aqueous phases is difficult.

This work was undertaken to develop a rapid and reliable HPLC method for the separation of the main alkaloids bodine, isocorydine and N-methyllaurotetanine in *Peumus boldus* extracts and drugs. The method involves a combined clean-up and concentration procedure by means of a C_{18} Sep-Pak cartridge followed by isocratic reversed-phase HPLC.
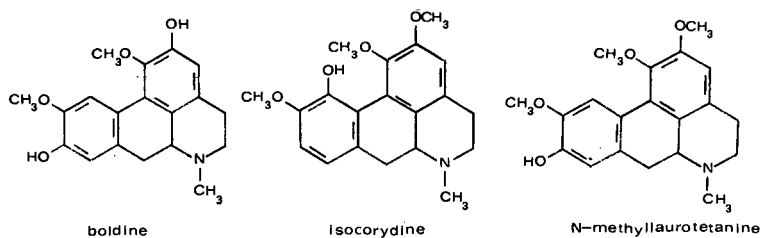
Fig. 1. Structures of boldine, isocorydine and N-methyllaurotetanine.

EXPERIMENTAL

Materials

Boldine was obtained from Sigma (St. Louis, MO, U.S.A.). Isocorydine and N-methyllaurotetanine were isolated from a commercial extract of *Peumus boldus* leaves by preparative TLC. *Peumus boldus* leaf extracts were purchased from different sources. Methanol, acetonitrile and water were of HPLC grade (Chromasolv; Riedel de Haën, Hannover, F.R.G.). Triethylamine and chloroform were of analytical-reagent grade (Carlo Erba, Milan, Italy). Sep-Pak C_{18} cartridges (Waters Assoc., Milford, MA, U.S.A.) were used for sample preparation.

Preparation of Peumus boldus samples

Peumus boldus leaf extracts (1 ml) were diluted to 5 ml with water and 2 ml were applied to a C_{18} Sep-Pak cartridge. After washing with 4 ml of 0.05 M ammonium monohydrogenphosphate buffer and 2 ml of water, the alkaloid fraction was eluted with 2 ml of methanol and the eluate diluted to 5 ml with the same solvent.

Drugs containing *Peumus boldus* extracts were treated similarly.

TLC

TLC was carried out on Merck silica gel 60 F_{254} plates. The samples were developed with chloroform–diethylamine (75:25) and the alkaloids were detected by UV irradiation at 254 nm (R_F values: boldine = 0.25; N-methyllaurotetanine = 0.35; isocorydine = 0.55).

HPLC

Alkaloids were separated using a system consisting of a Waters M-6000 pump fitted with a μBondapak C_{18} column (30 cm × 3.9 mm I.D.) and a U6K injector. A pre-column (Waters Assoc., Part No. 84550) was used to extend the column lifetime.

The mobile phase was acetonitrile–water–triethylamine (87:15:0.2, v/v) adjusted to pH 2.6 with 10% phosphoric acid. Samples were eluted isocratically at a flow-rate of 1.8 ml/min and detected at 270 nm (0.01 a.u.f.s.).

Reference solutions of boldine, isocorydine and N-methyllaurotetanine in methanol (0.07 mg/ml) were prepared and analysed by HPLC. The resulting chromatograms yielded data for the calibration graphs.

RESULTS AND DISCUSSION

In the analysis of basic substances such as alkaloids using reversed-phase HPLC, tailing peaks are obtained owing to retention by free silanol groups when aqueous methanol (acetonitrile) is used as the eluent. To improve the peak shapes and separations, acidic mobile phases or acidic amine–phosphate buffers can be useful. Various systems were therefore evaluated for their ability to resolve *Peumus boldus* alkaloids. Methanol and acetonitrile, when used as organic components of an acidic mobile phase (pH 2–3), were found to give low resolution. With acetonitrile–water–triethylamine (pH 2.6) as the eluent, the peak shapes were much improved and baseline separation of the alkaloids was achieved. Fig. 2 illustrates a chromatogram of standard boldine, isocorydine and N-methyllaurotetanine eluted with this system.
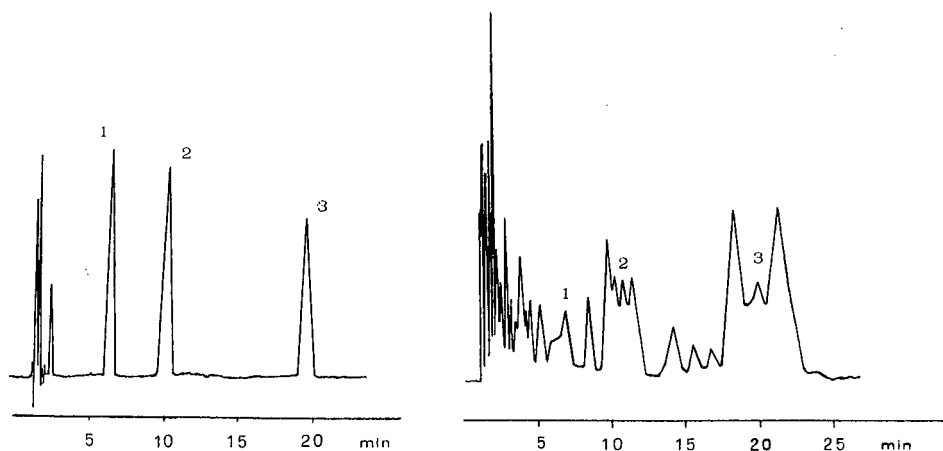
Fig. 2. Chromatogram of (1) boldine, (2) isocorydine and (3) N-methyllaurotetanine standards. Eluent, acetonitrile–water–triethylamine (87:15:0.2), pH 2.6; flow-rate, 1.8 ml/min; UV detection at 270 nm.

Fig. 3. Chromatogram of an unpurified *Peumus boldus* leaf extract. Chromatographic conditions and peaks as in Fig. 2.

However, in the analysis of *Peumus boldus* samples other constituents are coeluted with the alkaloids (Fig. 3). Hence, the identification of these compounds must be preceded by a clean-up procedure. Purification with Sep-Pak C_{18} cartridges strongly reduces the front and the impurities (Fig. 4), and provides a quantitative recovery of the alkaloids compared with extraction with chloroform. It should also be noted that neither long extraction times nor large volumes of toxic solvents are required.

Boldine, isocorydine and N-methyllaurotetanine exhibit different UV absorption maxima[10], and the determination was carried out at 270 nm, which represents the
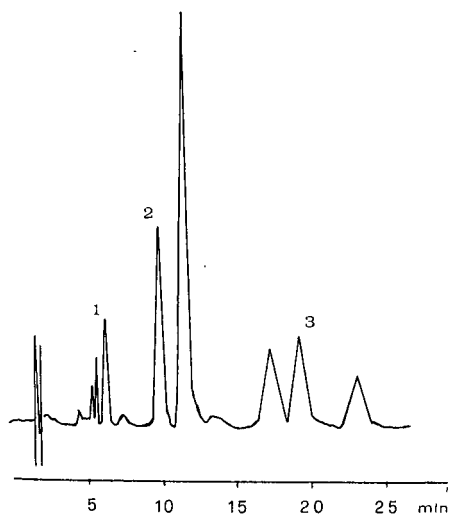
Fig. 4. Chromatogram of a purified (C_{18} Sep-Pak cartridge) *Peumus boldus* leaf extract. Chromatographic conditions and peaks as in Fig. 2.

TABLE I

CONTENTS OF BOLDINE, ISOCORYDINE AND N-METHYLLAUROTETANINE IN THREE COMMERCIAL *PEUMUS BOLDUS* LEAF EXTRACTS

Extract	Compound (%)		
	Boldine	Isocorydine	N-Methyllaurotetanine
I	0.014	0.0033	0.0029
II	0.016	0.004	0.0035
III	0.008	0.0019	0.0015

best compromise. Sets of standard alkaloids covering the range 0.5–2.5 nmol were run, and the following relationships between peak areas (y) and amount injected (nmol) (x) were obtained:

$$\text{boldine:} \qquad y = 215x + 31 \qquad r = 0.997$$
$$\text{isocorydine:} \qquad y = 181x \qquad r = 0.994$$
$$\text{N-methyllaurotetanine:} \; y = 154x + 11 \qquad r = 0.995$$

The determination of *Peumus boldus* alkaloids in commercial extracts was achieved by external standardization with a good relative standard deviation (3.3%; $n = 5$) (Table I). The procedure was successfully applied to the evaluation of commercially available preparations of *Peumus boldus* containing also other extracts, such as cascara and rhubarb.

In conclusion, the proposed method represents a useful approach to the pharmaceutical quality control of *Peumus boldus* alkaloids.

REFERENCES

1 H. Schindler, *Arzneim.-forsch.*, 7 (1957) 747.
2 *Martindale, The Extra Pharmacopoeia*, Pharmaceutical Press, London, 28th ed., 1982.
3 K. Genest and D. W. Hughes, *Can. J. Pharm. Sci.*, 3 (1968) 84.
4 F. De Lorenzi, F. Fontani and F. Morandini, *Boll. Chim. Farm.*, 108 (1969) 108.
5 P. Gorecki and H. Otta, *Herba Pol.*, 25 (1979) 285.
6 C. Van Hulle, P. Braeckman and R. Van Severen, *J. Pharm. Belg.*, 38 (1981) 97.
7 H. Washmuth and L. Van Koeckhoven, *J. Pharm. Belg.*, 49 (1967) 315.
8 V. Quercia, B. Bucci, G. Iela, M. Terracciano and N. Pierini, *Boll. Chim. Farm.*, 117 (1978) 545.
9 L. J. Nunez-Vergara, J. A. Squella and E. A. Berrios-Sagredo, *Farmaco, Ed. Prat.*, 38 (1983) 219.
10 A. Ruegger, *Helv. Chim. Acta*, 42 (1959) 754.

CHROM. 21 051

Book Review

Petroanalysis '87 — Developments in Analytical Chemistry in the Petroleum Industry (Proceedings of the Third Petro Analysis Symposium, London), edited by G. B. Crump, Wiley, New York, Brisbane, Toronto, 1988, X + 290 pp., price £ 50.00, ISBN 0-471-91946-2.

This is a typical "symposium volume" consisting of 26 articles (three of which are only summaries of papers), containing the texts of the presented contributions.

The volume is made up of "camera-ready" manuscripts, however with very clearly reproduced figures. A number of the papers are overviews and cannot in all fairness be called scientific contributions, such as "Wax chromatography — The 80's crossroads", which discusses the present situation of the chromatography of waxes, citing only one reference and that to a M.Sc thesis. No doubt this went well as an oral presentation, but why print it?

About half of the volume deals with chromatographic techniques or combinations with chromatography, all of which seem to be solid application work, with no sign of a new topic anywhere.

Taken as an account of the *Petroanalysis '87* symposium, it should prove of interest to the participants of the meeting. It should also be on the shelf of a library of laboratories dealing with petrochemistry, but may not be of interest to people outside the field.

Author Index

Adachi, K.
——, Saitoh, K. and Suzuki, N.
Reversed-phase high-performance thin-layer chromatography and column liquid chromatography of metal complexes of pheophorbide *a* 99

Anspach, B.
——, Unger, K. K., Davies, J. and Hearn, M. T. W.
Affinity chromatography with triazine dyes immobilized onto activated non-porous monodisperse silicas 195

Aoki, N., see Hamano, T. 403

Aue, W. A., see Tang, Y.-Z. 149

Baldessarini, R. J., see Trainor, T. M. 257

Berezkina, L. G.
—— and Souhodolova, V. I.
Chromatographic method for studying the hygroscopic qualities of solids 159

Bier, M., see Sloan, J. E. 137

Björkholm, E.
——, Hultman, A. and Rudling, J.
Determination of chlorine and chlorine dioxide in workplace air by impinger collection and ion-chromatographic analysis 409

Bushway, R. J.
High-performance liquid chromatographic determination of carbaryl in fruit juices 437

Buydens, L., see De Smet, M. 25

Caccamese, S.
Retention behaviour of diastereomeric truxillic and truxinic diamides and separation of an enantiomeric pair in high-performance liquid chromatography 366

Capone, W.
——, Mascia, C., Melis, M. and Spanedda, L.
Determination of terpenic compounds in the essential oil from *Satureja thymbra* L. growing in Sardinia 427

Ceva, P., see Pietta, P. 442

Chackma, A.
—— and Meisen, A.
Identification of methyl diethanolamine degradation products by gas chromatography and gas chromatography–mass spectrometry 287

Chan, K. C.
—— and Yeung, E. S.
Peak identification of amino acids in liquid chromatography by optical activity detection 421

Chawla, R. P., see Singh, P. P. 387

Davies, J., see Anspach, B. 195

De Smet, M.
——, Peeters, A., Buydens, L. and Massart, D. L.
Expert system for the selection of high-performance liquid chromatographic methods in pharmaceutical analysis. Validation of the rules for the selection of the mobile phase 25

Dorsey, J. G., see Michels, J. J. 85

Fernández-Sánchez, E.
——, Fernández-Torres, A., García-Domínguez, J. A., Santiuste, J. M. and Pertierra-Rimada, E.
Solubility parameters of gas chromatographic mixed stationary phases 55

Fernández-Torres, A., see Fernández-Sánchez, E. 55

García-Domínguez, J. A., see Fernández-Sánchez, E. 55

Gasparrini, F.
——, Misiti, D., Villani, C., La Torre, F. and Sinibaldi, M.
High-performance liquid chromatography on chiral packed microbore column with the 3,5-dinitrobenzoyl derivative of *trans*-1,2-diaminocyclohexane as selector 235

Głód, B. K.
——, Piasecki, A. and Stafiej, J.
Numerical simulation of column performance in ion-exclusion chromatography 43

Goward, C. R.
——, Stevens, G. B., Hammond, P. M. and Scawen, M. D.
Large-scale purification of the chromosomal β-lactamase from *Enterobacter cloacae* P99 317

Grob, R. L., see Loeper, J. M. 247

Guiochon, G., see Schudel, J. V. H. 1

Gupta, D., see Verma, K. K. 345

Gustavsson, J., see Johansson, B.-L. 205

Haas, J. W., III,
——, Joyce, W. F., Shyu, Y.-J. and Uden, P. C.
Phosphoric acid-modified amino bonded stationary phase for high-performance liquid chromatographic chemical class separation 215

Hamano, T.
——, Mitsuhashi, Y., Aoki, N., Yamamoto, S. and Oji, Y.
Simultaneous determination of niacin and niacinamide in meats by high-performance liquid chromatography 403

Hammond, P. M., see Goward, C. R. 317

Hearn, M. T. W., see Anspach, B. 195

INFORMATION FOR AUTHORS

(Detailed *Instructions to Authors* were published in Vol. 445, pp. 453–456. A free reprint can be obtained by application to the publisher, Elsevier Science Publishers B.V., P.O. Box 330, 1000 AH Amsterdam, The Netherlands.)

Types of Contributions. The following types of papers are published in the *Journal of Chromatography* and the section on *Biomedical Applications:* Regular research papers (Full-length papers), Notes, Review articles and Letters to the Editor. Notes are usually descriptions of short investigations and reflect the same quality of research as Full-length papers, but should preferably not exceed six printed pages. Letters to the Editor can comment on (parts of) previously published articles, or they can report minor technical improvements of previously published procedures; they should preferably not exceed two printed pages. For review articles, see inside front cover under Submission of Papers.

Submission. Every paper must be accompanied by a letter from the senior author, stating that he is submitting the paper for publication in the *Journal of Chromatography*. Please do not send a letter signed by the director of the institute or the professor unless he is one of the authors.

Manuscripts. Manuscripts should be typed in double spacing on consecutively numbered pages of uniform size. The manuscript should be preceded by a sheet of manuscript paper carrying the title of the paper and the name and full postal address of the person to whom the proofs are to be sent. Authors of papers in French or German are requested to supply an English translation of the title of the paper. As a rule, papers should be divided into sections, headed by a caption (*e.g.,* Summary, Introduction, Experimental, Results, Discussion, etc.). All illustrations, photographs, tables, etc., should be on separate sheets.

Introduction. Every paper must have a concise introduction mentioning what has been done before on the topic described, and stating clearly what is new in the paper now submitted.

Summary. Full-length papers and Review articles should have a summary of 50–100 words which clearly and briefly indicates what is new, different and significant. In the case of French or German articles an additional summary in English, headed by an English translation of the title, should also be provided. (Notes and Letters to the Editor are published without a summary.)

Illustrations. The figures should be submitted in a form suitable for reproduction, drawn in Indian ink on drawing or tracing paper. Each illustration should have a legend, all the *legends* being typed (with double spacing) together on a *separate sheet*. If structures are given in the text, the original drawings should be supplied. Coloured illustrations are reproduced at the author's expense, the cost being determined by the number of pages and by the number of colours needed. The written permission of the author and publisher must be obtained for the use of any figure already published. Its source must be indicated in the legend.

References. References should be numbered in the order in which they are cited in the text, and listed in numerical sequence on a separate sheet at the end of the article. Please check a recent issue for the layout of the reference list. Abbreviations for the titles of journals should follow the system used by *Chemical Abstracts.* Articles not yet published should be given as "in press" (journal should be specified), "submitted for publication" (journal should be specified), "in preparation" or "personal communication".

Dispatch. Before sending the manuscript to the Editor please check that the envelope contains three copies of the paper complete with references, legends and figures. One of the sets of figures must be the originals suitable for direct reproduction. Please also ensure that permission to publish has been obtained from your institute.

Proofs. One set of proofs will be sent to the author to be carefully checked for printer's errors. Corrections must be restricted to instances in which the proof is at variance with the manuscript. "Extra corrections" will be inserted at the author's expense.

Reprints. Fifty reprints of Full-length papers, Notes and Letters to the Editor will be supplied free of charge. Additional reprints can be ordered by the authors. An order form containing price quotations will be sent to the authors together with the proofs of their article.

Advertisements. Advertisement rates are available from the publisher on request. The Editors of the journal accept no responsibility for the contents of the advertisements.